



Proceeding of the 9th

Rajamangala University of Technology International Conference

RMUT Driving Innovation for Thailand 4.0

Session:

- **New Energy Innovation to make the “Future”**
- **Material Science and Engineering**
- **Smart Cities**
- **Agriculture Technology and Natural Science**

August 1-3, 2018

Rua Rasada Hotel, Trang Province, Thailand



Book Title

Proceedings of the 9th Rajamangala University of Technology International Conference

Sessions

- **New Energy Innovation to make the “Future”**
- **Material Science and Engineering**
- **Smart Cities**
- **Agriculture Technology and Natural Science**

Organized by Rajamangala University of Technology Srivijaya

Copyright Holder Rajamangala University of Technology Srivijaya

Publishing Editor Asst. Prof. Apirak Songrak

Number of pages 380

Copyright August 2018

**Designed by Research and Development Institute
Rajamangala University of Technology Srivijaya
179 M.3 Maifad Subdistrict, Sikao District,
Trang Province, 92150 Thailand**

List of Reviewer

The 9th Rajamangala University of Technology International Conference

No.	Name	Institute
1.	Assoc. Prof. Dr. Damien Guilbert	Université de Lorraine, France
2.	Dr.Faradina Merican bt. Mohd. Sidik Merican	Universiti Sains Malaysia
3.	Dr.Noor Khalidah Abdul Hamid	Universiti Sains Malaysia
4.	Asst. Prof. Dr. Thitisak Boonpramote	Chulalongkorn University
5.	Assoc. Prof. Dr. Saroj Sirisansaneeyakul	Kasetsart University
6.	Asst. Prof. Dr. Jiraporn Runglerdkriangkrai	Kasetsart University
7.	Asst. Prof. Dr. Sathaporn Chuepeng	Kasetsart University
8.	Dr.Jirawan Maneerote	Kasetsart University
9.	Dr.Jirapa Hinsui	Kasetsart University
10.	Assoc. Prof. Dr. Borwonsak Leenanon	Khon Kaen University
11.	Asst. Prof. Dr. Thanakorn Rojanakorn	Khon Kaen University
12.	Assoc. Prof. Dr. Boonyang Plangklang	Rajamangala University of Technology Thanyaburi
13.	Assoc. Prof. Dr. Suneerat Sripaoraya	Rajamangala University of Technology Srivijaya
14.	Asst. Prof. Dr. Nomchit Kaewthai Andrei	Rajamangala University of Technology Srivijaya
15.	Asst. Prof. Dr. Sirinat Srionnual	Rajamangala University of Technology Srivijaya
16.	Asst. Prof. Dr. Jaruwat Jareanjit	Rajamangala University of Technology Srivijaya
17.	Asst. Prof. Dr. Prapot Maliwan	Rajamangala University of Technology Srivijaya
18.	Asst. Prof. Dr. Laksamee Wittaya	Rajamangala University of Technology Srivijaya
19.	Dr.Sutkanung Na Ranong	Rajamangala University of Technology Srivijaya
20.	Dr.Chomson Nuntasoontron	Rajamangala University of Technology Srivijaya
21.	Assoc. Prof. Napat Watjanatepin	Rajamangala University of Technology Suvarnabhumi
22.	Asst. Prof. Dr. Sudjit Karuchit	Suranaree University of Technology
23.	Asst. Prof. Dr. Supenya Chittapun	Thammasat University
24.	Asst. Prof. Dr. Suparatchai Vorarat	Dhurakij Pundit University
25.	Dr.Jesada Kajornrit	Dhurakij Pundit University
26.	Assoc. Prof. Dr. Wiwat Meesuwan	Naresuan University
27.	Asst. Prof. Dr. Rumpai Gaensakoo	Maharakham University
28.	Asst. Prof. Dr. Tatdao Phasipol	Maharakham University
29.	Dr.Angkana Chantaraponpan	Maharakham University

30.	Asst. Prof. Dr. Narumon Sakpakornkan	Nakhon Ratchasima Rajabhat University
31.	Asst. Prof. Dr. Somrak Rodjaroen	Nakhon Si Thammarat Rajabhat University
32.	Assoc. Prof. Dr. Siseerotm Ketkaew	Ramkhamhaeng University
33.	Asst. Prof. Dr. Potjamarn Suraninpong	Walailak University
34.	Dr.Sukhumal Chitpornpun	Walailak University
35.	Asst. Prof. Dr. Cheewita Suwanchawalit	Silpakorn University
36.	Asst. Prof. Dr. Warangkana Kitpipit	Silpakorn University
37.	Assoc. Prof. Dr. Suppasil Maneerat	Prince of Songkla University
38.	Assoc. Prof. Dr. Sommai Chiayvareesajja	Prince of Songkla University
39.	Assoc. Prof. Dr. Thumronk Amornsakun	Prince of Songkla University
40.	Assoc. Prof. Dr. Kanita Nitjvarunkul	Prince of Songkla University
41.	Asst. Prof. Dr. Opas Bunkoed	Prince of Songkla University
42.	Asst. Prof. Dr. Suwaluk Wisunthorn	Prince of Songkla University
43.	Asst. Prof. Dr. Sirusa Kritsanapuntu	Prince of Songkla University
44.	Asst. Prof. Dr. Rawee Chiarawipa	Prince of Songkla University
45.	Asst. Prof. Dr. Khanchit Chuarkham	Prince of Songkla University
46.	Dr.Uraiwan Sirimahachai	Prince of Songkla University
47.	Dr.Jutarat Inthapun	Prince of Songkla University
48.	Dr. Anant Choksuriwong	Prince of Songkla University
49.	Dr.Wachirapan Boonyaputthipong	Ubon Ratchathani University
50.	Assoc. Prof. Dr. Santi Wangnipparnto	Pathumwan Institute of Technology
51.	Dr.Rujira Deewatthanawong	Thailand Institute of Scientific and Technological Research

Preface

Rajamangala University of Technology Srivijaya has been assigned to be the host for the 9th Rajamangala University of Technology International Conference (9th RMUTIC) on “RMUT Driving Innovation for Thailand 4.0” during August 1 – 3, 2018 at Rua Rasada Hotel, Muang District, Trang Province, Thailand.

The main objective of this conference is to be a forum for researchers to exchange academic idea and creative technology, focusing on the dissemination of academic innovation and technology applications. This is important knowledge that benefits society, especially in economic development throughout the region of Thailand following the government policy promoting stability, prosperity, and sustainability. We are highly honored to host the conference this year.

We would like to thank you everyone for contributing physical and mental effort, and valuable time to enable this conference. We hope that all nine Rajamangala Universities of Technology will continue to strengthen our cooperation to become the leading universities in Thailand.

The conference includes keynote speeches together with research presentations from researchers of the nine Rajamangala Universities of Technology and other researchers from higher education institutions in Thailand and abroad.

On this occasion, we would like to thank you for sharing the 9th Rajamangala University of Technology International Conference (9th RMUTIC). We hope that all of you will gain benefits and satisfaction from the exchange of knowledge from this conference.

Research and Development Institute
Rajamangala University of Technology Srivijaya

Message from the President

Rajamangala University of Technology Srivijaya has hosted the 9th Rajamangala University of Technology International Conference (9th RMUTIC) on “RMUT Driving Innovation for Thailand 4.0” during August 1 – 3, 2018 at Rua Rasada Hotel, Muang District, Trang Province, Thailand.

Research is an important tool for studying particular topics to obtain information, knowledge, technology, innovation and work. The nine Rajamangala Universities of Technology have recognized the importance of research development and support systems to acquire knowledge from each research subject to improve the quality of people's lives. As the university focuses on technology skills and creates innovation for social communication, we aim to develop research that responds to the needs of community development at all levels.

Accordingly, the 9th Rajamangala University of Technology International Conference (9th RMUTIC) on “**RMUT Driving Innovation for Thailand 4.0**” features cooperative networking between the nine Rajamangala Universities of Technology and other national research support organizations, namely, Ministry of Science and Technology, National Research Council of Thailand (NRCT), Office of the Higher Education Commission (OHEC), the Thailand Research Fund (TRF), Agricultural Research Development Agency (Public Organization), National Science Technology and Innovation Policy Office (STI) and nationwide higher education institutions. This cooperation will generate fruitful researches to develop strong and sustainable Thai society.

On behalf of Rajamangala University of Technology Srivijaya, I would like to thank all the co-hosting institutions and to thank the keynote speakers, researchers, participants, presenters, and conference committees, as well as the staff from the nine Rajamangala Universities of Technology, for participating in and organizing this conference.

Asst. Prof. Yongyuth Nuniem
Acting President
Rajamangala University of Technology Srivijaya

Conference Schedule for Oral Presentation

Code number	Title	Name	No
IO-001	Feasibility Study of a Grid-tied 60 KW Floating Solar PV Power Station for Sea in the South of Thailand	Dr.Kwanruetai Boonyasana RMUTP	2
IO-003	The Design of Pre-Charge Systems for Electric Formula Student	Mr.Sura Laptawee TNI	12
IO-004	Speed Control of Induction Motor with Over-voltages Suppression Methods for Long Cable Drive Applications	Dr.Grit Tongkhundam TSU	19
IO-005	Coin-Screening Machine Base on Digital Image Processing Technique	Mr.Ruangyos Keteruksa RMUTR	25
IO-006	Design of Data Acquisition Unit Using Arduino from a Flow Velocity Meter for Tides in the River	Mr.Sanya Samaimak RMUTR	38
IO-007	Alarm Bubble within Intra Venous Tube via Application Line	Miss Jantira Juakvont RMUTSV	44
IO-008	Design and Implement of IoT-Based Electric Slide-Up Door Control System Using Raspberry Pi 3 Model B Case Study: Department Of Electrical Engineering RMUTL NAN	Mr.Charnyut Karnjanapiboon RMUTL	54
IO-009	Development and Performance Evaluation of a Cassava Digger Namely Fork Shear Blade Type	Dr.Sahapat Chalachai RMUTTO	61
IO-010	Application of Design of Experiment (DOE) for Aluminum Wheel of Single Pulley Performance for Transmission line	Miss Bussakorn Hammachukiattikul TNI	74
IO-011	The Calculated Speed and Torque of Motor for Electric Formula Student	Miss Supaluk Prapan TNI	85
IO-012	Design of Intake Manifold for Formula Student Car	Mr.Phatsakon Phan-Ophat TNI	92
IO-013	Design and Analysis of Bias Brake for Formula Student	Mr.Wisit Songmuang TNI	100
IO-014	A C Program for The Teaching of View Factors for Heat Transfer Problems for Two and Perpendicular Planes	Dr.Marwan Affandi RMUTSV	109
IO-015	Structural Engineering Assessment for Seismic Damaged Concrete Building: A Case Study of One Storey Kindergarten School	Dr.Thanongsak Imjai RMUTTO	119
IO-017	Durable Articles and Building Repairing Informing System: A Case Study of RMUTSV Rattaphum College	Mr.Wanpracha Nuansoi RMUTSV	130
IO-018	Using Information Systems in Curriculum Management According to the Standard Framework of Vocational Education Undergraduate	Mr.Soontorn Kongsintu KMUTBN	138
IO-019	Impact Strength and Flexural Properties of Biodegradable Foams Containing Polylactic Acid and Epoxidized Natural Rubber	Assoc.Prof. Dr. Tarinee Nampitch KU	149
IO-020	Effect of Waste Tire Powder on the Properties of Natural Rubber Latex Foams	Dr.Suwat Rattanapan RMUTSV	159
IO-021	Survey Study of Current Seawater Desalination Processes	Prof.Dr.Hanshik Chung GNU	169

IO-024	Triploid Induction by the Use of 6-dimethylaminopurine (6-DMAP) for the Tropical Oyster, <i>Crassostrea belcheri</i> (Sowerby, 1871)	Dr.Supatcha Chooseangjaew RMUTSV	180
IO-025	Genetic Variability, Heritability and Genetic Advance among Yardlong Bean Lines	Assoc.Prof.Dr.Pramote Pornsuriya RMUTTO	189
IO-026	Increasing Pineapple Suckers Using 6-Benzilaminopurine Growth Regulator on F1 Hybrid Mother Pineapple [<i>Ananas comosus</i> (L.) Merr.] Plants	Assoc.Prof.Dr.Suneerat Sripaoraya RMUTSV	196
IO-027	Shoot Multiplication of HQC34 Hybrid Pineapple [<i>Ananas comosus</i> (L.)Merr.] Using Bioreactor System	Miss.Orachat Sittichan RMUTSV	203
IO-028	Increasing the Harvesting Index Efficiency for Prolonging Shelf Life of Smooth Cayenne Pineapple (<i>Ananas comosus</i> cv. 'Pattavia') Fruit	Mr.Kullawich Panichkul RMUTL	209
IO-029	Effect of Carbon Sources and Inoculation Protocols on Carissa Acetification Process	Asst.Prof.Dr.Ni-orn Chomsri RMUTL	220

Conference Schedule for Poster Presentation

Code number	Title	Name	No
IP-002	Analysis of Heavy Metals using 5-Amino Levulinic Acid (ALA)-Chitosan Modified Electrodes	Mrs.Rattiya Saradit RMUTSV	232
IP-003	Mechanical Properties and Swelling of Natural Rubber Vulcanizate Filled with Rice Bran Carbon	Asst.Prof.Darinya Moonchai MJU	239
IP-004	Strength and Strain-induced Crystallization of Vulcanized Natural Rubber	Mr.Watcharin Sainumsai SKRU	246
IP-005	Sodium Methoxide Dissolution in Various Solvents	Asst.Prof.Dr.Thirawat Mueansichai RMUTT	257
IP-006	Poisson Regression Model for Predict Dengue Haemorrhagic Fever Prevalence in Kreang Sub-District, Cha-Uat District, Nakhon Si Thammarat, Thailand	Asst.Prof.Dr.Suppawan Promprao NSTRU	263
IP-007	Exploration of Aquatic Plants and Algae in Rajamangala University of Technology Srivijaya	Dr.Akhom Khatfan RMUTSV	273
IP-008	Evaluation of Universal Pre-enrichment Medium for Multiple Foodborne Pathogen Detection in Milk by PCR Based Method	Dr.Chanida Kupradit RMUTI	279
IP-009	Potential Use of Cashew Leaf Extracts for the Quality Improvement in Chinese Sausage (Kun-Chiang)	Asst.Prof.Dr.Supasit Chooklin RMUTSV	290
IP-010	Development of Pasta from Riceberry Flour, Commercial Rice Flour and Mung Bean Flour	Asst.Prof.Dr.Arpathsra Sangnark RMUTK	302
IP-013	Harvesting Maturities Affecting Phenolic Compounds and Antioxidant Activities in “Sungyod Phatthalung” Rice Cultivated at Upland	Asst.Prof.Uraiwan Wattanakul RMUTSV	307
IP-014	Substitution of Soybean Meal with Fermented Palm Kernel Meal in Diet of Sex Reversed Red Tilapia (<i>Oreochromis niloticus</i> × <i>O. mossambicus</i>)	Asst.Prof.Wattana Wattanakul RMUTSV	316
IP-015	Gamat (<i>Stichopus horrens</i>) Pickling with Different Sugar Media and Addition into Rice Porridge	Asst.Prof.Dr.Chutnut Sujarit RMUTSV	322
IP-016	The Use of Boiled Liquid Waste as an Ingredient for Crab Sauce	Asst.Prof.Dr.Chutinut Sujarit RMUTSV	332
IP-017	Development of Shellfish Soup Enhanced with Herbs Upgraded and Nutritional Value	Asst.Prof.Chompunooch Somalee RMUTSV	340
IP-018	Effect of Fermented Bioextracts on Yield Potential and Growth of Rice RD 49 Variety	Miss Sujitra Ruengdechawiwat RMUTL	351
IP-019	<i>In vitro</i> Gas Production of <i>Leucaena</i> (<i>Leucaena leucocephala</i>) Silage Added with Xylanase and Cellulase from Dried Tomato Pomace by <i>Aspergillus niger</i>	Asst.Prof.Dr.Smerjai Bureenok RMUTI	357

IP-020	Optimization of Culture Condition for Biomass Production and Starch Accumulation of Cyanobacteria, <i>Nostoc</i> sp.	Asst.Prof.Dr.Somrak Rodjaroen NSTRU	363
IP-021	Effect of Mixed Enzyme Produced From Tomato Pomace By <i>Aspergillus niger</i> on Meat Quality Attributes of Broiler Chickens	Asst.Prof.Dr.Benya Saenmahayak RMUTI	371
IP-023	Isolation and Screening of Acetic Acid Producing Microorganisms from Fruits in the Northeastern Region (Isan) of Thailand	Dr.Nittaya Pitiwittayakul RMUTI	376

Oral Presentation

The 9th Rajamangala University of Technology

International Conference

RMUT Driving Innovation for Thailand 4.0

Feasibility Study of a Grid-tied 60 KW Floating Solar PV Power Station for Sea in the South of Thailand

Kwanruetai Boonyasana^{1*} Duanrung Chouyruang² and Suveena Rungrodruttanagorn³

ABSTRACT

Environmental protests arising in the south of Thailand face the challenge of meeting power needs. Thai government finds itself caught between pressure to meet regional power demands and backlash from citizens fearing the environmental effects of coal-fired electrical plants. However, a solution might be provided by a floating solar photovoltaic (PV) power station for sea, which is not only environment-friendly but also suitable for the geography of the southern region of Thailand. This paper considers the implementation of a floating solar pilot project at Rajamangala Beach, Trang province, focusing on the feasibility study of a grid-tied 60 KW floating solar PV power station, which will help in assessing the potential of floating solar installations to supply power to island and coastal regions in the south of Thailand in the future. For financial analysis, the floating PV system could cost USD 482,000 with a payback period of 11 years. However, for economic analysis, which includes social costs and social benefits, the payback period of this project should be significantly shorter due to the number of positive environmental side effects. In addition, a larger project may be able to adopt technologies of production, and this can lead to economies of scale, giving rise to lower per-unit cost. We envisage this renewable energy innovation as shedding light on the energy and geopolitical challenges facing the south of Thailand.

Keywords: Power plant, Floating solar photovoltaic, Grid-tied, The south of Thailand

¹ Department of Finance, Faculty of Business Administration, Rajamangala University of Technology Phra Nakhon, 86 Phitsanuloke Road, Dusit, Bangkok 10300, Thailand

² Department of General Education, Faculty of Sciences and Fisheries Technology, Rajamangala University of Technology Srivijaya, 179 M.3 Mai Fad, Sikao, Trang 92150, Thailand

³ Department of Business English, Faculty of Business Administration, Rajamangala University of Technology Phra Nakhon, 86 Phitsanuloke Road, Dusit, Bangkok 10300, Thailand

*Corresponding author, e-mail: kwnaruetai.b@rmutp.ac.th, kwanruetai@live.com

Introduction

Currently, Thailand is facing a major challenge to balance trade-offs among competing goals when designing energy, economic and environmental policies. Overall, the power sector in Thailand features characteristics similar to that of many developing countries, including such problems as high demand but limited supply, unstable power supply systems, delayed development of power distribution networks, and public enterprises in a financially fragile situation (Lamphayphan *et al.*, 2015). Furthermore, in recent years, the local people have tried every campaign tactic to urge the government not to build harmful coal-fired power plants in Krabi and Songkhla's Thepa district to protect their beloved home (Rujivanarom, 2018), drawing criticism of the Thai government from rights activists and environmentalists. As a result, the policy makers aim to increase in absolute terms electricity imports from neighbouring countries and generation from renewable energy.

The Thai government has put forward one of the most ambitious renewable energy plans in Southeast Asia setting a target of 30% of total final energy consumption by 2036 in its 2015 Alternative Energy Development Plan, and a target of 20 gigawatts (GW) of installed capacity by 2036 (International Energy Agency: IEA, 2016). Hence, this policy promotes highly efficient green alternatives for Thailand (International Renewable Energy Agency: IRENA, 2017). It would seem that this is the right way in moving forward to avoid protests against coal-fired electrical plant projects with the argument that they negatively impact the environment. In spite of this, in 2018, the Energy Regulatory Commission of Thailand (ERC) decided to stop buying electricity power from new renewable energy projects with a higher price than 2.40 baht/unit for five years. However, Thailand still needs to address electricity shortages in the south.

In 2016, the power plants in the south of Thailand generated 2,225 megawatts (MW), while another 375 MW was provided from the central region power plants (Electricity Generating Authority of Thailand: EGAT, 2016). Even though, currently, electricity supply is still sufficient for demand in southern Thailand, power consumption is rising steadily. The Thai government accepted that construction of new large-scale power plants in this region is unlikely over the next five years, believing that existing power plants are capable of meeting demand (Theparat, 2018). However, policy makers need to be concerned about sources of electricity supply in the south of Thailand, with reliable fuel diversification, for the stability of the power system.

At the present time, electricity security with low energy price and environmental sustainability is the key priority for Thailand. Because renewable energy could solve economic, environmental and social problems, this paper focuses on such energy which is suitable for the geography of the southern region of Thailand. One solution to this energy crisis might be provided by a floating solar photovoltaic (PV) power station for sea, which is not only environment-friendly, but also suitable for the geography of the southern region and other coastal areas. Because of the littoral nature of much of Thailand, with total coastal length of about 2,815 kilometres (km), including Gulf of Thailand coast of 1,873 km and Andaman Sea coast of 937 km (The Department of Mineral Resources, 2018), needless to say, floating solar PV power stations for sea should present attractive investment projects for this country.

However, to avoid possible risks to investment, a feasibility study should be completed before starting a new project. This paper considers the implementation of a floating solar pilot project at Rajamangala Beach, Trang province, focusing on the feasibility of a grid-tied 60 KW floating solar PV power station, using data to shape the project planning process. Such studies can generate crucial insight for approved projects in relation to cost-benefit analysis. Therefore, this paper will help in assessing the potential of floating solar installations to supply power to islands and coastal regions in the south of Thailand into the future.

Literature Review

Electricity is a vital infrastructure for countries, being instrumental in the provision of basic needs that serve government, businesses and industries. The General Agreement on Tariffs and Trade (GATT) has never considered electricity as a commodity since the late 1940s because of its unique characteristics (Mattoo and Sauvé, 2003). There are several such characteristics of the power generation industry: 1) Electricity cannot be stored as inventory like other merchandise; 2) Capacity expansion cannot be realized within a short period of time - thus, investment decisions require forward-looking demand projection; and 3) Electricity is both a necessity and a public utility, hence, the government plays an important role both in generation and distribution processes (Tunpaiboon, 2016). The Commission for Environmental Cooperation (CEC), in 2011, further noted that a portion of the electric energy is lost during transmission and distribution. It is clear that, when electricity has to be transmitted from the central region power plants to the south of Thailand via extensive networks, the transmission over these long distances creates power losses.

Fortunately, we can dramatically reduce transmission losses as well as carbon footprint by directly generating electricity from clean, renewable sources, like floating PV technology. Sahu *et al.* (2016) pointed out that floating PV systems have a number of advantages compared to land-based systems, including fewer obstacles to block sunlight, and higher power generation efficiency owing to lower temperature underneath the panels. In addition, Leybourne (2017) observed that floating PV technology can remove the competition for land use and potentially high rent charged by landowners. It is also suitable for off-grid locations, and an array can be assembled more quickly than for land-based systems.

On the other hand, Leybourne (2017) further noted that there are comparative drawbacks and challenges of floating PV technology, which need to be considered. Reduction of light into the water from panel obstruction can have a detrimental effect on the water's ecosystem. Movement of water can change the orientation, and therefore output of the array, and this may lead to fatigue-based micro-cracking in the panels over time. Floating PV systems might have higher direct current (DC) cable cost and associated losses in transmitting the power ashore. On large water bodies, especially the sea, with potentially long fetch lengths, the effect of locally generated waves in storms could be significant.

There are clear advantages and disadvantages of floating PV technology that need to be considered. After trying to break through the barriers of disadvantage, Swimsol, a company in Austria, launched the world's first floating solar solution for the sea in 2014. The floating solar structure of this company can increase production by 5 to 10 percent over the rooftop equivalent, perform for 30 years, be integrated into diesel power grids and complete service is provided by the company (Swimsol, 2018). This commercial renewable energy product, that employs space for solar panels on the sea surface, is suitable for the project location at Rajamangala Beach, Trang province. The latitude and longitude information of our location is: (Andaman Sea 7.536565, 99.311977) 7°32'11.6"N, 99°18'43.1"E (see Figure 1). At the project location, there is a high amount of solar irradiation, thereby making it a very attractive site for the proposal of solar PV systems.

Materials and methods

1. Methodology

The research project is a co-operative effort among eight universities in Thailand (Rajamangala University of Technology Phra Nakhon, Rajamangala University of Technology Srivijaya, Rajamangala University of Technology Thanyaburi, Rajamangala University of Technology Suvarnabhumi, King Mongkut's University of Technology Thonburi, Ratchapat Chankasem University, Naresuan University and Burapha University), Royal Thai Police and Swimsol. After Swimsol designs the grid-tied 60 KW floating solar PV power station for Rajamangala beach, a group of Thai researchers will investigate in six areas: floating solar

technology, smart grid system, environment, internet of things (IoTs), energy law and energy economics. For this paper, we focus on energy economics to study a feasibility analysis of this renewable energy system.

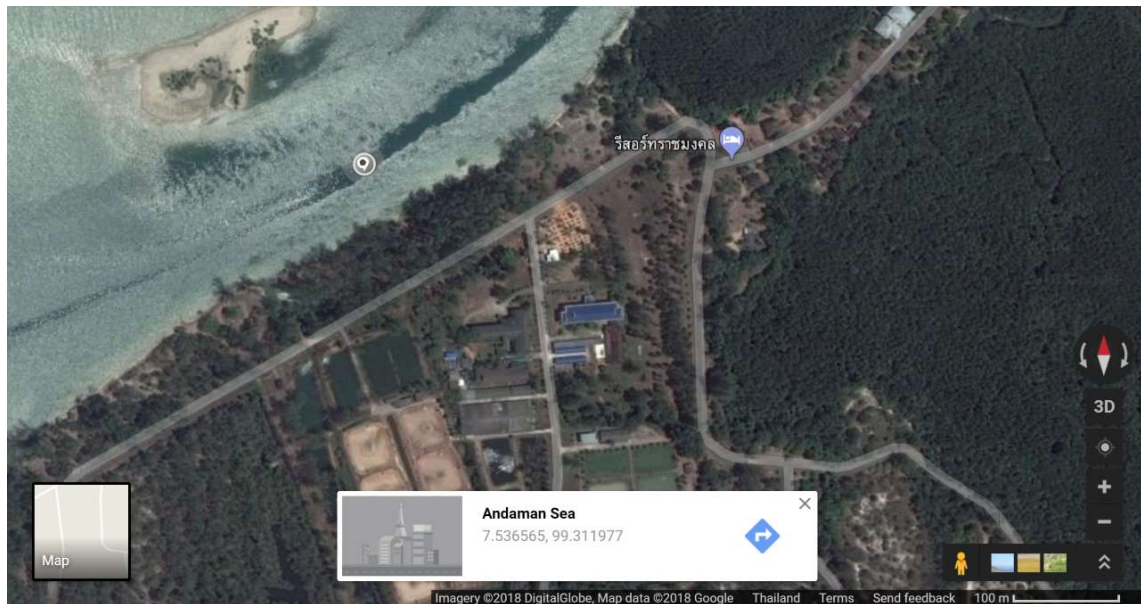


Figure 1 Map of Rajamangala Beach (Google, 2018)

Feasibility Analysis

This paper employs an economic feasibility study (EFS) to demonstrate the net benefit of the grid-tied 60 KW floating solar PV power station for sea project with a view to accepting or rejecting. EFS is the most commonly used method for determining the efficiency of a new project, which helps in identifying profit against investment expected from the project. For this analysis, cost and time are the most essential factors involved in this field of study. The EFS in this paper focuses on cost-benefit analysis (CBA), which summarizes the revenues and costs involved with the project. Once the values in the CBA have been derived, the project's results can be presented in three forms: Payback Period (PP) or Break-Even, Net Present Value (NPV), and Internal Rate of Return (IRR) (Yanga, 2012).

Data

The data for financial analysis, for example, electricity prices, diesel prices, interest rates, and costs of investment, are collected from Provincial Electricity Authority (PEA), PTT Public Company Limited (PTT), Bank of Thailand (BOT), EGAT and Swimsol. Furthermore,

Google map (see Figure 1) is used to prepare the geo-synchronized layout for the proposed water body. In addition, basic survey accessories, including sunshine hours (see Figure 2), sea temperature data (see Figure 3), rainfall (see Figure 4) and wind (see Figure 5), are used for manual survey of the site and compared with geo-synchronized layout. Finally, a manual survey on the Rajamangala Beach is performed to determine the shadow cast by the structures present around the sea of the site. There is no construction work done around the location, hence there will be no shadow formed over the sea surface.

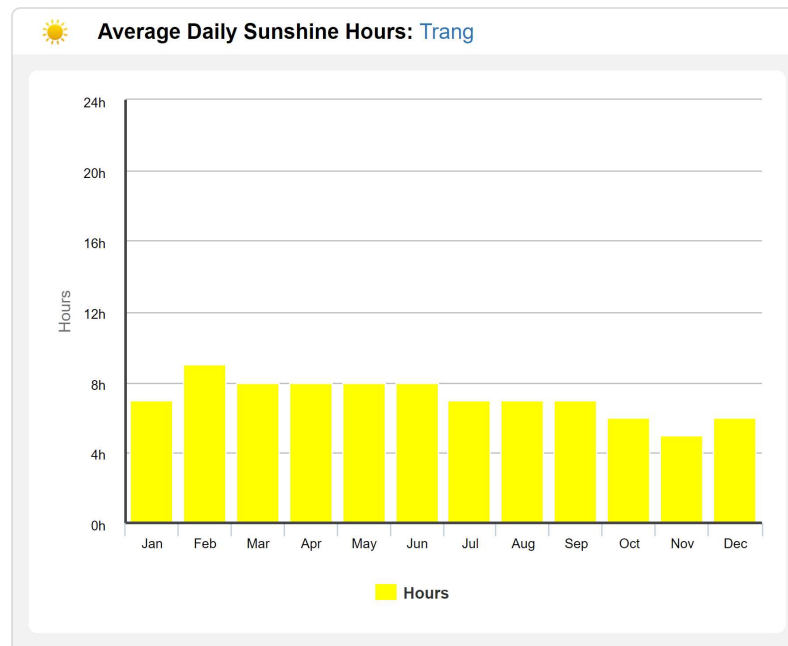


Figure 2 Average Daily Sunshine Hours in Trang in 2018 (Holiday-weather.com, 2018)

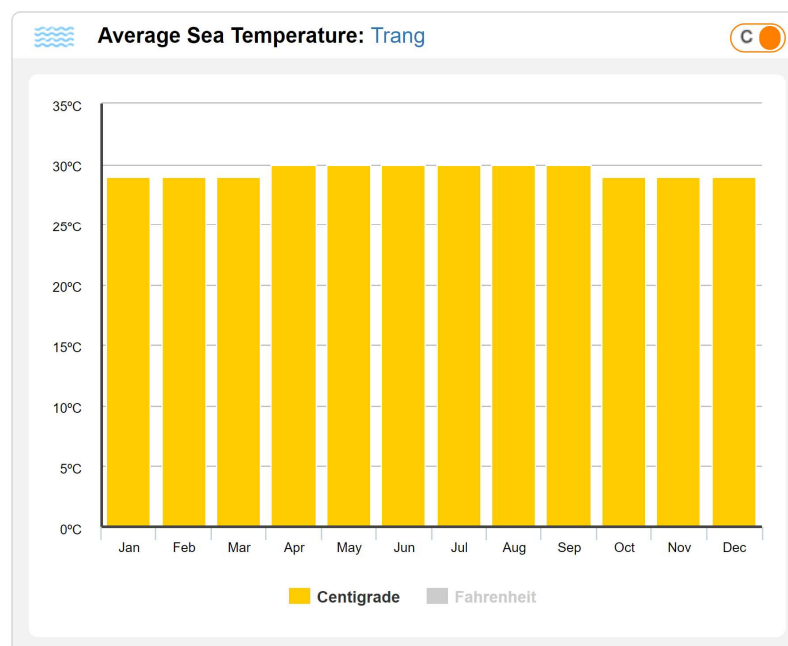


Figure 3 Average Sea Temperature in Trang in 2018 (Holiday-weather.com, 2018)

2. Materials

The main materials of the floating solar array are from Swimsol (2018) with the four key aspects regarding qualifications below (see Figure 6):

- Patent-Pending Floating Solar Structure

The development of this unique floating solar platform is from computer simulations, tests, and trials with the Thai research team. The platform can survive waves of tropical shallow water lagoons, as well as the currents, tides, extreme Ultraviolet (UV), humidity and is corrosion-proof.

- 5-10% Higher Production Than Rooftop Equivalent

The solar panels on floating solar systems give a 5-10% higher output than rooftop systems. This is due to the cooling effect of water and additional light reflections from the sea surface.

- Performance For 30 Years
With high-quality components and high-performance panel platforms developed specifically for the south of Thailand, the systems have a lifetime of around 30 years.
- Integration Into Diesel Power Grids and Complete Service
Correctly sized hybrid diesel-solar systems account for diesel generator efficiency, and can generate extra savings by allowing generator shut down during the sunny hours of the day.

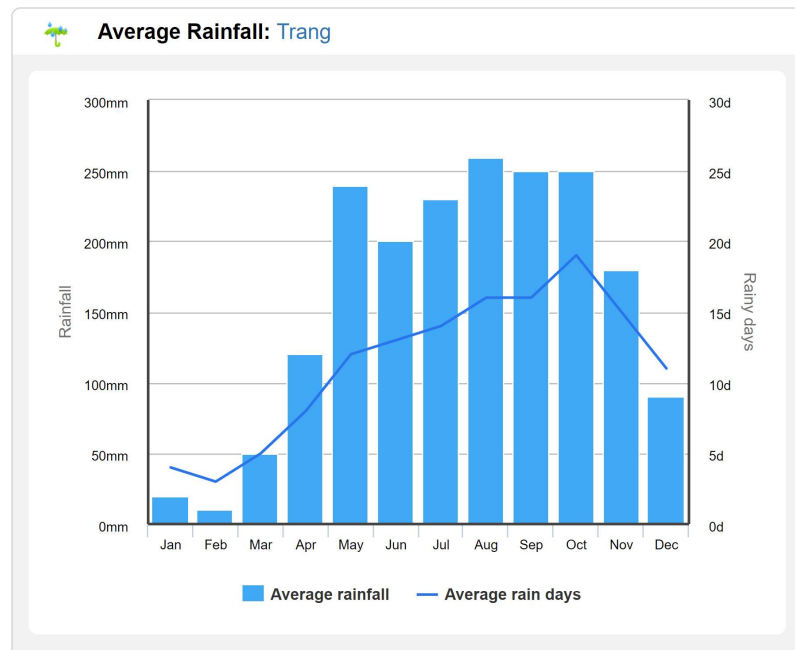


Figure 4 Average Rainfall in Trang in 2018 (Holiday-weather.com, 2018)

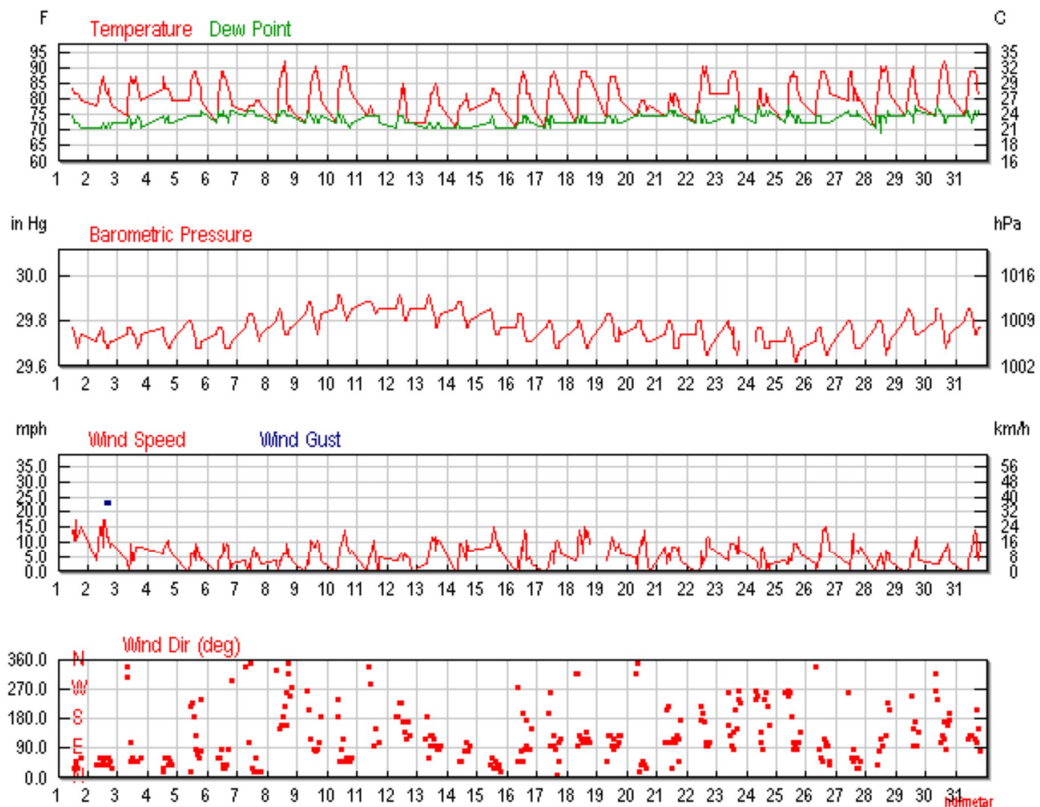


Figure 5 Monthly Weather History Graphs (Wind Speed) in January 2018 (Wunderground.com, 2018)



Figure 6 Floating Solar PV Power Station (Swimsol, 2018)

Results and discussions

According to literature review, the output of the floating system is about 1.1 times greater than the conventional land based system. The cost of the floating solar PV system can be estimated as around USD 482,000. For feasibility study with three assumptions, electricity price is 8 baht/kWh, average sunshine is 8 hours/day, and there is no tax for floating system. NPV will be USD 86,953, and IRR will be 2% (see Table 1). The payback period, which is the time span in which the cost of the yield becomes equal to the capital invested in installation, is expected to be about 11 years. Therefore, we should invest in this project. However, according to the policy of ERC in 2018, which decided to stop buying electricity power from new renewable energy projects with higher price than 2.40 baht/unit, the simulation results have changed. The payback period will be around 36.58 years, NPV will be USD -311,139, and IRR will be -12%, hence, we should avoid investing in this project. The results show that there is a marked difference, when electricity price changes.

The results from documentary research and feasibility analysis show that a policy to stop buying electricity power from new renewable energy projects with higher price than 2.40 baht/unit can have a negative effect on the floating solar PV system project. Moreover, it can have a detrimental effect on energy security in Thailand, and such policy will not be sufficient to attain Thailand's "green energy" and greenhouse gas emissions reduction goals, since there exists no incentive system for technological innovation within the electric power industry.

For financial analysis with three assumptions, electricity price is 8 baht/kWh, average sunshine is 8 hours/day, and there is no tax for floating system. The payback period is expected to be about 11 years, NPV will be USD 86,953, and IRR will be 2%. However, for economic analysis, which includes social costs and social benefits, the payback period of this project should be significantly shorter from saving the environment. Hence, for further study, the authors plan to investigate social costs and social benefits through sensitivity analysis. In addition, adoption of technologies of production by way of a larger project may lead to economies of scale, resulting in lower per-unit cost.

Conclusion

This paper investigates implementing a floating solar pilot project at Rajamangala Beach, Trang province, with a focus on the feasibility study of a grid-tied 60 KW floating solar PV Power station. This will be of assistance in determining the potential of floating solar installations in supplying power to island and coastal regions in the south of Thailand into the future. For financial analysis, the floating PV system could cost around USD 482,000 with a payback period of 11 years. With three assumptions, electricity price is 8 baht/kWh, the average sunshine is 8 hours/day, and there is no tax for floating system, NPV will be USD 86,953, and IRR will be 2%. The sensitivity analysis results show that there is a marked difference, when electricity price changes from the government policy. Through this study, we are able to gain insight into how this renewable energy innovation sheds light on the energy and geopolitical challenges facing the south of Thailand.

Acknowledgements

The authors would like to thank Swimsol for helpful advices on various technical issues examined in this paper. In addition, the authors would like to thank Mr. Robin Neill for comments and suggestions, and Rajamangala University of Technology Phra Nakhon for its support.

References

- EGAT. 2016. **Electricity Peak Demand hits 28,351.7 MW, Breaking the Peak Record for the Second Time in 2016**. EGAT (Electricity Generating Authority of Thailand). Available Source: <https://www.egat.co.th/en/news-announcement/news-release/electricity-peak-demand-hits-28-351-7-mw-breaking-the-peak-record-for-the-second-time-of-2016>, April 12, 2018.
- IEA. 2016. **Thailand Electricity Security Assessment 2016**. OECD/IEA (International Energy Agency), Paris.
- IRENA, 2017. **Much of the World's Energy Transformation Will Hinge on the Continent's Fast-growing Markets**. IRENA (International Renewable Energy Agency). Available Source: http://www.irena.org/-/media/Files/IRENA/Agency/Quarterly/IRENA_Quarterly_2017_Q4.pdf, May 1, 2018.
- Lamphayphan, T., Toyoda, T., Czerkawski, C. and Kyophilavong, P. 2015. Export Supply of Electricity from Laos to Thailand: An Econometric Analysis. **International Journal of Energy Economics and Policy** 5(2): 450–460.

- Leybourne, M. 2017. **Floatovoltaics – Thinking Beyond the Cost of Floating Solar PV**. LinkedIn.com. Available Source: <https://www.linkedin.com/pulse/floatovoltaics-thinking-beyond-cost-floating-solar-pv-mark-leybourne/>, February 23, 2018.
- Rujivanarom, P. 2018. **Anti-coal Protesters Start New Hunger Strike Demanding End to Two Projects**. The Nation. Available Source: <http://www.nationmultimedia.com/detail/national/30338680>, February 13, 2018.
- Sahua, A., Yadavb, N. andSudhakar K. 2016. Floating Photovoltaic Power Plant: A Review. **Renewable and Sustainable Energy Reviews** 66(2016): 815–824.
- Swimsol. 2018. **SolarSea® Solar Power Beyond the Land Limitations**. Available Source: <https://swimsol.com/#lagoon>, January 3, 2018.
- The Department of Mineral Resources. 2018. **Status of Coastal Geo-environment in Thailand**. Available Source: http://www.dmr.go.th/ewtadmin/ewt/dmr_web/main.php?filename=coastal_En, May 4, 2018.
- Theparat, C. 2018. **Ministry Downplays Need for Southern Power Plants**. Bangkokpost.com. Available Source: <https://www.bangkokpost.com/business/news/1416722/ministry-downplays-need-for-southern-power-plants>, April 10, 2018.
- Tunpaiboon, N. 2016. **THAILAND INDUSTRY OUTLOOK 2016-18 Power Generation Industry**. krungsri.com. Available Source: https://www.krungsri.com/bank/getmedia/4911f203-6f38-4a9a-acf6-d6bf744eb185/IO_Power_2016_EN.aspx, February 5, 2018.
- Yanga, J., Chenb, W., Chena, B. and Jiab, Y. 2012. Economic Feasibility Analysis of a Renewable Energy Project in the Rural China. **Procedia Environmental Sciences** 13(2012): 2280–2283.

The Design of Pre-charge Systems for Electric Formula Student

Sura Laptawee^{1*}, Boonyakorn Rakthanyakarn² and Kiattisak Sunan¹

ABSTRACT

Motor controllers in electric vehicle typically have a large internal bank of capacitors with very low Equivalent Series Resistance (ESR). As a result, when initially connecting a battery to the motor controllers, there is an inrush of current, which can easily reach over 1000A, followed by a voltage surge due to battery and cabling inductance. Both current spikes and voltage surges may cause problems for various components, such as damaging motor controllers or other capacitive loads, damaging accumulator packs that are not rated for the inrush of current, blowing the main fuse before the vehicle can even run, and most commonly, welding the contactor's contacts. Problems such as welded contacts cannot be detected by just visually inspecting components. A pre-charge circuit will solve these problems without limiting the operating current of the tractive system. The Battery Management System (BMS) has a pre-charge circuit built into the system. The pre-charge circuit of the BMS works in the following sequence: when the vehicle is initially powered; the pre-charge circuit first enables the pre-charge relay. Then, after approximately 1-2 sec of pre-charging, it will detect a sufficiently low current flowing through the pre-charge resistors. At that point, the circuit enables the main contractor, and current can now pass through the less resistive pathway.

Keywords: Pre-charge, Electric vehicle, Electric formula car

¹ Department of Electrical Engineering, Faculty of Engineer, University of Thai-Nichi Institute of Technology, 1771/1, Suanluang, Bangkok 10250, Thailand

² Department of Automotive Engineering, Faculty of Engineer, University of Thai-Nichi Institute of Technology, 1771/1, Suanluang, Bangkok 10250, Thailand

* Corresponding author, e-mail: sura.l@tni.ac.th

Introduction

Fossil fuels contribute a significant percentage of global energy consumption and play an important role in our daily life, as they are used for powering vehicles, generating electricity, and many other uses. (Campbell and Laherrere, 1998) As with any non-renewable resource; the continued consumption of fossil fuel has increased prices considerably over the last decade. In addition, fossil fuels contribute significantly to greenhouse gas emissions as well as pollution. All of the above makes the use of renewable energy attractive and has prompted scientists and researchers to start looking towards alternative energy sources and other technological innovations to reduce the carbon footprint.

Technology innovations such as electric vehicles (EV) and the installation of renewable energy, namely solar and wind farms, have become prominent to the public. Government incentives for clean energy that are currently in place are helping to accelerate this. Particularly in the automotive field, vehicles using hybrid or electric propulsion systems have been actively developed (Pisu *et al.*, 2006; Hashimoto *et al.*, 2010). Currently, electric vehicles are gaining much attention. These electric propulsion systems use electric power to drive the vehicles, so energy storage devices such as batteries have an essential role in these systems.

Consequently, the Thai Society Automotive Engineer (TSAE) competition has focused on promoting engineering principles for design and research with Electric Formula Student cars. The Electric Formula Student competition has designed the following rules for the electrical systems: the vehicles must have Electric Safety Systems with Brake System Encoders, Electric Accelerators, Insulation Monitoring Devices, Battery Chargers, Discharge, and Pre-charge.

In this paper, we present a design for pre-charge for the Electric Formula Student vehicle of the CarreraZ Racing Team from Thai-Nichi Institute of Technology. This pre-charge is designed to prevent voltage surges that may cause severe problems and damage the motor controller or other capacitive load.

Analysis of Resistor and Capacitor

Analysis of resistor and capacitor for pre-charge circuit calculated failure resistors and analyzed the motor controller capacitances.

1. Calculation of failure resistors

During the pre-charge stage, the circuit could be modeled as a simple RC circuit. According to the RC constant, $\tau = R \times C$, the capacitor increases in charge by 63.2%. As a rule of thumb, the capacitor is fully charged after an approximate time. Therefore, the power dissipated by the pre-charge resistor is then equal to the energy in the charged capacitor divided by the time taken to fully charge the capacitor.

Table 1 Specifications of Resistors

Groups	Pre-Test
Resistance	100 Ohm
Temperature Coefficient	± 100 ppm/ $^{\circ}\text{C}$
Dimensions	24.1 x 72 x 47.5mm
Package/Case	Aluminum Housed
power resistors	75 Watts
Tolerance	$\pm 5\%$

Given that the accumulator packs are 96 V maximum and resistors are rated at 100 Ω , the power dissipated in the pre-charge resistor is therefore equal to 22.5 W. This is only 30%

of what the pre-charge resistor could take (Table 1). The instantaneous power, which is ten times the power dissipated, will not be an issue, as the resistors used can handle peaks up to ten times of their continuous rating. Therefore, they are less likely to fail from overheating.

$$P = \frac{E}{T} = \frac{CV^2}{2(5RC)} = \frac{V^2}{2(5R)} = \frac{V^2}{10R} \quad (1)$$

2. The motor controller capacitances

To charge the capacitor up to 95% state of charge, the time required to pre-charge is at least 3τ (Dear *et al.*, 2012). With the given information on the min pre-charging time (1s) and the rating of the resistor used, the maximum capacitance that the pre-charge circuit can take is given by

$$T = 3\tau = 3RC \quad (2)$$

From this, Equation (3) and $R=100 \, \Omega$ Capacitor follow as:

$$C = \frac{1}{300} = 3.33 \times 10^{-3} \, \text{F} \quad (3)$$

Due to a lack of available information on the motor controller's capacitances and the inaccuracy of measuring capacitance with a multimeter, it is impossible to determine whether the capacitances in the motor controller will be charged to 95% state of charge.

3. Simulation of the RC circuit

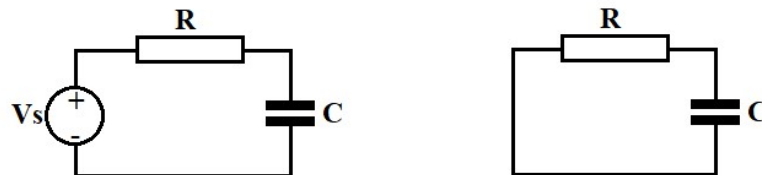


Figure 1 The charging and discharge RC circuits

Figure 1 shows the schematics of charging and discharging RC circuits. The component's value was set at $R = 1 \, \text{k}\Omega$, $C = 3.33 \times 10^{-3} \, \text{F}$ and $V_s = 96 \, \text{V}$. Figure 2 shows the result of simulation for charging, with the time required to pre-charge set at 1 second, and Figure 3 shows the result of simulation for discharging, with the time required for discharge set at 2 seconds.

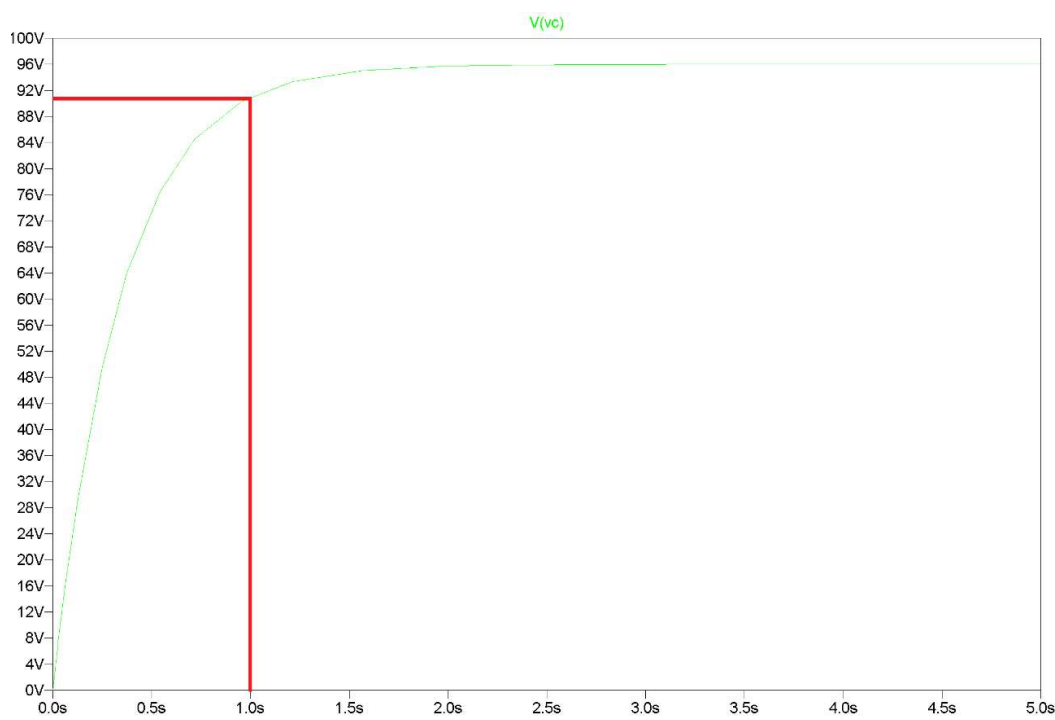


Figure 2 The simulation of charging

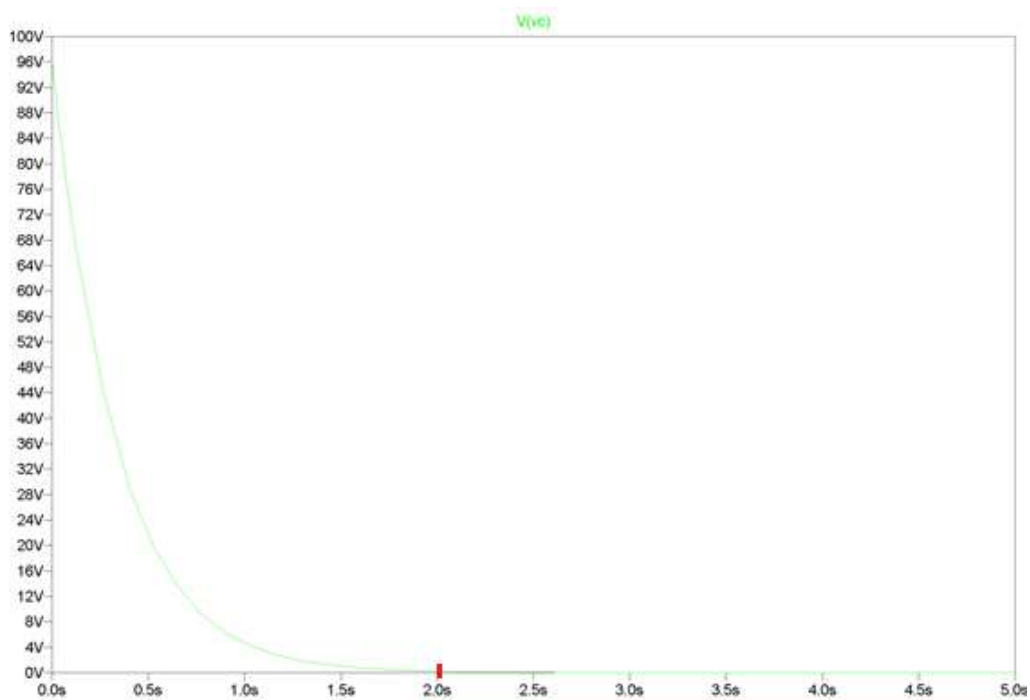


Figure 3 The simulation of discharging

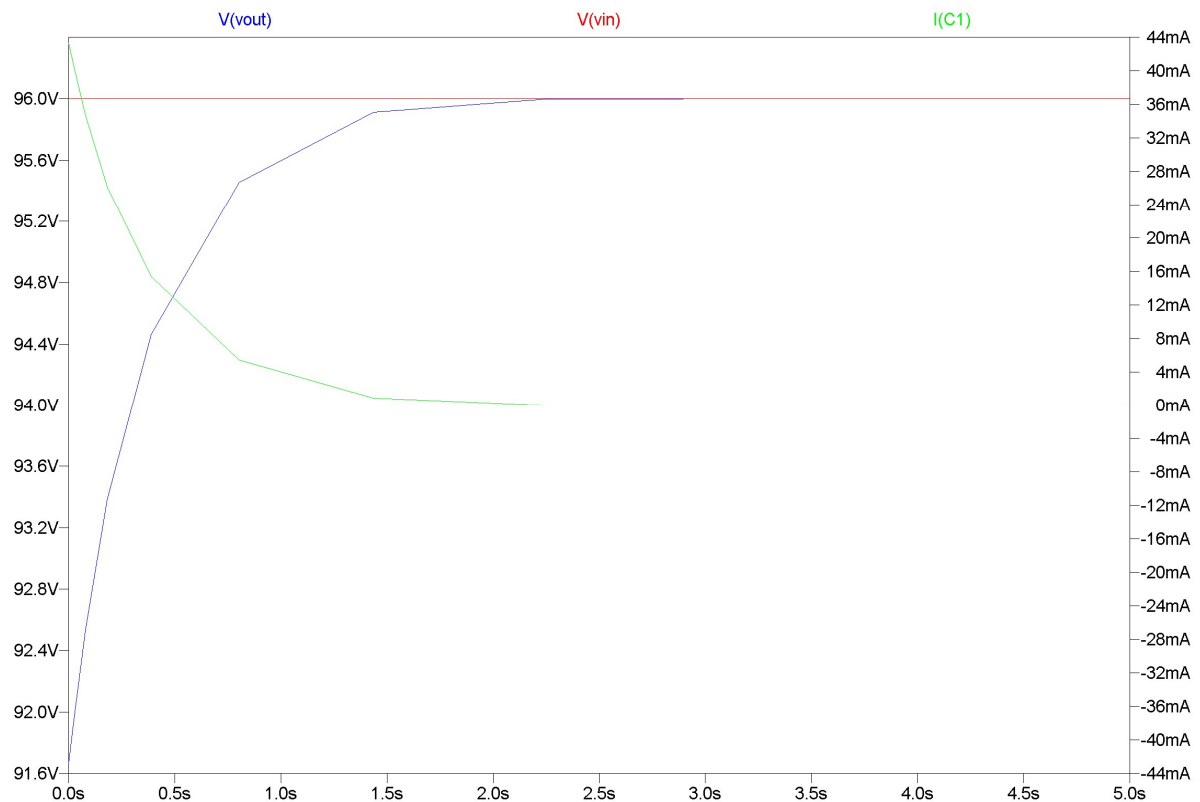


Figure 5 The simulation of the pre-charge circuit

3. Experimental results

The pre-charge function was complete in 1 second. After that, normal operation of a pre-charge circuit is to terminate pre-charge mode when the circuit voltage is about 91.2 Volt. Upon completion of pre-charging, the pre-charge resistance is switched out of the power supply circuit and returns to a low impedance power source for normal mode. The high voltage loads are then powered up sequentially. Table 2 shows the test of the operation of the circuit. That found the pre-charge circuit worked normally.

Table 2 Testing the pre-charge circuit

SW1	Timer Delay	Relay K1	Relay K2	LED 1	LED 2	AIRs
ON	OFF	ON	OFF	OFF	ON	OFF
	After 1s	ON	ON	ON	OFF	ON
OFF	OFF	OFF	OFF	OFF	OFF	OFF

Conclusion

The capacitive loads of motor controllers can be exposed to high electric current during the initial turn-on. It can cause considerable stress and damage to the system components. In some applications, occasions to activate the system are rare occurrences, such as in commercial utility power distribution. In other systems such as vehicle applications, pre-charge will occur with each use of the system, multiple times per day. Pre-charge is implemented to increase the lifespan of electronic components and increase reliability of the

high voltage system. As the circuit voltage approaches near steady state, then the pre-charge function is complete in 1 second. Normal operation of a pre-charge circuit is to terminate pre-

charge mode when the circuit voltage is 95% of the operating voltage. Upon completion of pre-charging, the pre-charge resistance is switched out of the power supply circuit and returns to a low impedance power source for normal mode. The high voltage loads are then powered up sequentially.

Acknowledgement

I would like to express my special thanks to Thai-Nichi Institute of Technology for funding, equipment and tool support.

References

- Campbell, C.J. and Laherrere, J.H. 1998. The end of cheap oil. **Scientific American**. 273: 78 - 83.
- Hashimoto, T. , Yamaguchi, K, Matsubara, T., Yaguchi, H. and Takaoka, T. 2010. Development of new hybrid system for compact class vehicles. **Transactions of Society of Automotive Engineers of Japan**. 41: 43–47.
- Li, P. and Bashirullah, R. 2007. A Wireless Power Interface for Rechargeable Battery Operated Medical Implants. **IEEE Transactions on circuits and systems—II: express briefs**. 54(10): 912 - 916.
- Pisu, P., Serrao, L., Cantemir, C.G. and Rizzoni, G. 2006. Hybrid-Electric Powertrain Design Evaluation for Future Tactical Truck Vehicle Systems, pp. 271–278. **In Proceeding of the ASME International Mechanical Engineering Congress and Exposition**, Chicago, IL, USA.
- Society of Automotive Engineers. **Formula SAE Rules 2018**. Available Source: <https://www.fsaeonline.com>, March 27, 2018.

Speed Control of Induction Motor with Over-Voltages Suppression Methods for Long Cable Drive Applications

Grit Tongkhundam^{1*}

ABSTRACT

This paper presents V/F drives of induction motors using a single voltage source inverter through long feeding cables. As known, when the cable length is long, over-voltages at the motor terminal could be doubled from the pulsed output voltage at the inverter terminal. In this paper, a half DC-link inverter is implemented to drive three motors simultaneously for different configurations of cable lengths. The implemented inverter drastically reduces the over-voltage at three motor terminals with a proper duration time of $V_{dc}/2$ level (β). Simulation and experimental results are provided to show the effectiveness of over-voltage reduction by using this inverter. According to the results for three motors with series multiple drives configuration, this β should be calculated based on the cable length closed to the longest.

Keywords: V/F drives, Long Cable Applications

¹ Department of Computer, Faculty of Science, Thaksin University, Banpraw, Papayom, Phattalung 93210, Thailand

*Corresponding author, e-mail: grit_tsu@hotmail.com

Introduction

Normally, all variable-speed motor drives use pulse width-modulated voltage-source inverters (PWM). Switching devices used in inverters are usually the insulated gate bipolar transistors (IGBT). A high switching frequency of the power switching devices is required to improve the current waveform quality. Switching frequencies of 2-20 kHz and a rise time of 0.1µs are typical specifications in the modern IGBT module. As known, the cable delay transport is increased as the cable distance increases. When the cable transport delay is higher than the critical rising or falling time of inverter terminal voltages, the motor terminal voltage could increase to double and eventually attribute to motor starter winding failures and eventually it will reduce the lifetime of motor (Marc *et al.*, 1998; Hanigovszki *et al.*, 2004; Rodriguez *et al.*, 2006). Significant damage to the motor insulation can occur if these overshoots are greater than the maximum rated voltage of the motor. As defined by NEMA MG1, Part 30, general-purpose motors should be limited to voltage overshoots of less than 1000 volts. General-purpose motors that operate at 220 volts (rms) due not produce overshoots of this magnitude. Motors with voltages of 380 volts (rms) (dc-bus 537 volts) or greater may require filters or reactors to reduce the amount of overshoot to an acceptable level.

An Over Voltage Suppression Method Analysis

An Over Voltage Suppression Method with the 2 level inverter is called half-dc link inverter (Lee and Nam, 2002). When imputed $u(t)$ into the inverter, the cable and the motor model will be shown as in figure 1. The voltage at the motor terminal is equal to $V(l,s)$. This causes over voltage as shown in the figure 1. If we change the input to $u(t)/2$, the voltage at the motor terminal

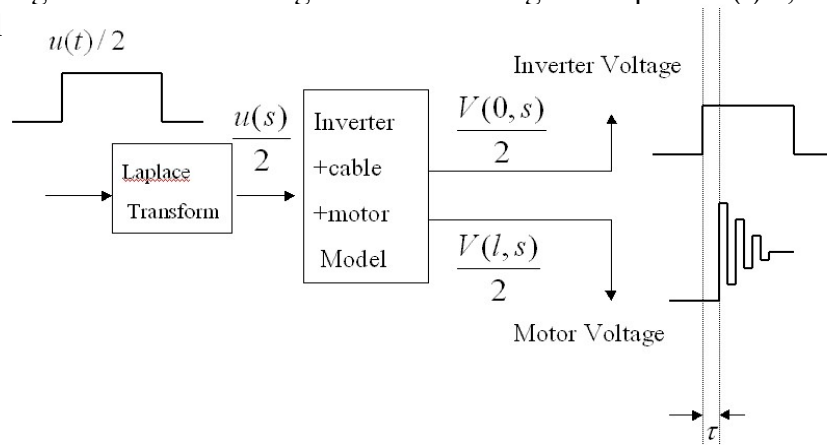


Figure 1 The motor and the inverter terminal voltage with input $u(t/2)$ to the cable and motor model.

When input $\frac{u(t - \beta)}{2}$ into the cable and the motor model, the voltage at the motor terminal equals to $V(l,s)$. This causes the double over voltage with the delay time = β as shown in Figure 2. [4].

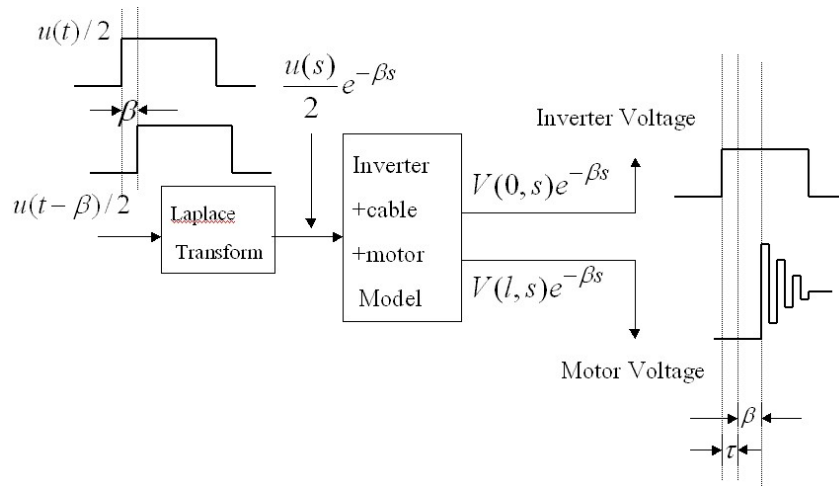


Figure 2 The motor and the inverter terminal voltage with input $u(t - \beta)/2$ attached to the cable and the motor model.

The signal $u(t)/2$ plus $u(t - \beta)/2$ equals $V_u(t) = \frac{u(t) + u(t - \beta)}{2}$ and then we use this as an input of the cable and the motor model in the equation (24) and (25). When we analyze by using the laplace transform, we have:

When $V_u(t) = \frac{u(t) + u(t - \beta)}{2}$ take Laplace, $V_u(s) = \frac{u(s) + u(s)e^{-\beta s}}{2}$

Replace $u(t)$ into equation (24) and (25) with $V_u(t)$ therefore

$$V_u(l, s) = u(s) \frac{1 + e^{-\beta s}}{2} \left[\frac{(1 + K_L)e^{-\tau s}}{1 - K_L K_G e^{-2\tau s}} \right] \quad (1)$$

When we expand the equation (26) into series, we have.

$$V_u(l, s) = \frac{1 + K_L}{2} u(s) \left[e^{-\tau s} + e^{-(\tau + \beta)s} + K_L K_G e^{-3\tau s} + K_L K_G^{-(3\tau + \beta)s} + \dots \right] \quad (2)$$

Replace β in equation (27) with 2τ , we have

$$V_u(l, s) = \frac{1 + K_L}{2} u(s) \left[e^{-\tau s} + (1 + K_L K_G) e^{-3\tau s} + K_L K_G (1 + K_L K_G) e^{-5\tau s} + \dots \right] \quad (3)$$

The cable and the motor model are written by using the equation (28). The input is $V_u(t) = \frac{u(t) + u(t - \beta)}{2}$. The over voltage at the motor terminal will be dropped as shown in Figure 3.

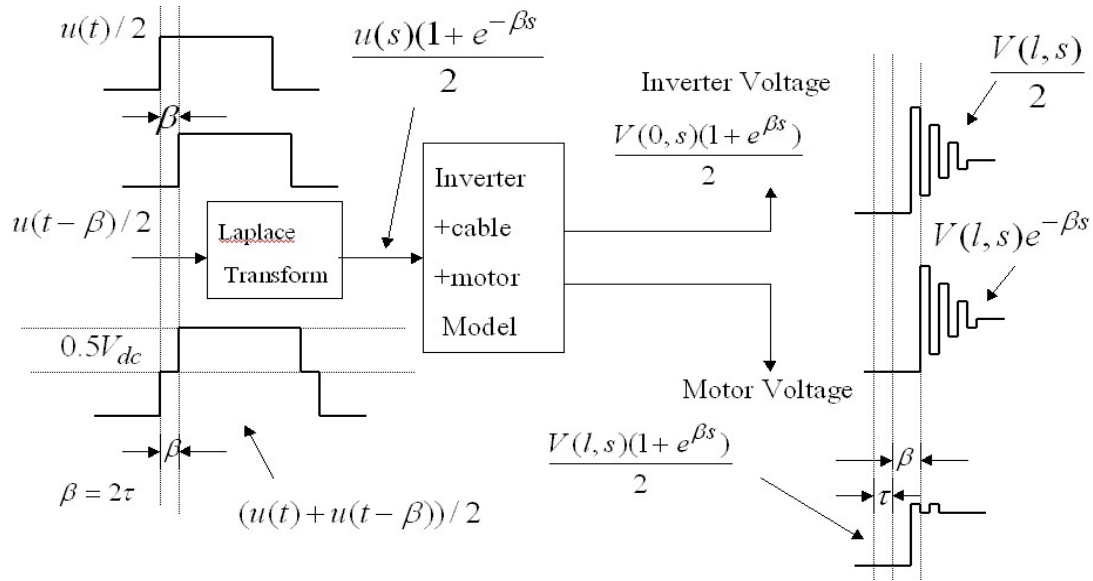


Figure 3 The motor and the inverter terminal voltage with input

$$V_u(t) = \frac{u(t) + u(t - \beta)}{2} \quad \text{to the cable and the motor model.}$$

From the equation (3), when we calculate the motor terminal voltage maximum, we are only interested in $t = 0$ to 2τ because the over voltage will have the maximum value of $t = 2\tau$. Thus, when other terms in the equation (3) are eliminated, we have:

$$V_u(l, s) = \frac{K_G + (K_G + 2)K_L}{2} \times 100\% \quad (4)$$

Experimental Results

Figures 2 and 3 show overall system and actual pictures of the Speed Control of Induction Motor with Over-voltages Suppression Methods for Long Cable Drive Applications, respectively. Overall hardware is implemented on MC3PHAC monolithic intelligent motor control, MCS-51 8-bit microcontroller and gate driver circuit. For additional six auxiliary switches (Q7-Q12). In this inverter, their switching signals are implemented by mono-stable circuitry and their controls are from the same microcontroller. The inverter is designed to use MOSFET (IRG4PH40UD) which has the switching characteristic rising time = 35 ns and falling time = 240 ns.

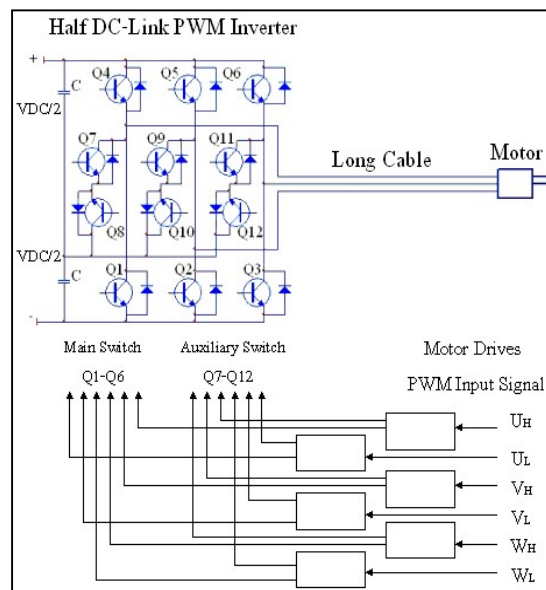


Figure 4 Speed control of Induction motor with over-voltages suppression methods circuit

The cable is 1.5-mm² PVC type 67 m. Its parameters are $L=16.5\mu\text{H}/\text{m}$, $C=4.45\text{pF}/\text{m}$, and $R=4\Omega$. The motor parameters are $C_{hf}=750\text{pF}$, $R_{hf}=300\Omega$, and $R_{lf}=2.5\Omega$, $L_{lf}=500\mu\text{H}$. The inverter is modeled as an ideal PWM voltage source with a source resistance ($R_S=7\Omega$).

Figure. 5.3-5.8 and 5.9-5.17 show the simulation and experimental results, respectively.

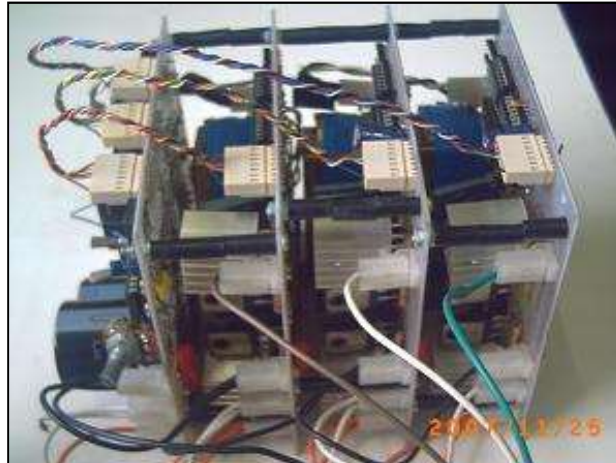


Figure 5 Speed control of induction motor with over-voltages suppression prototype

Figures 4 and 5 show overall system and actual pictures of the speed control of the induction motor with over-voltages suppression methods circuit, respectively. Overall hardware is implemented on MC3PHAC monolithic intelligent motor control, MCS-51 8-bit microcontroller and gate driver circuit. An additional six auxiliary switches (Q7-Q12) are in this inverter and their switching signals are complemented by mono-stable circuitry and their controls are from the same microcontroller. The inverter is designed to use MOSFET (IRG4PH40UD) which has the switching characteristic rising time = 35 ns and falling time = ?

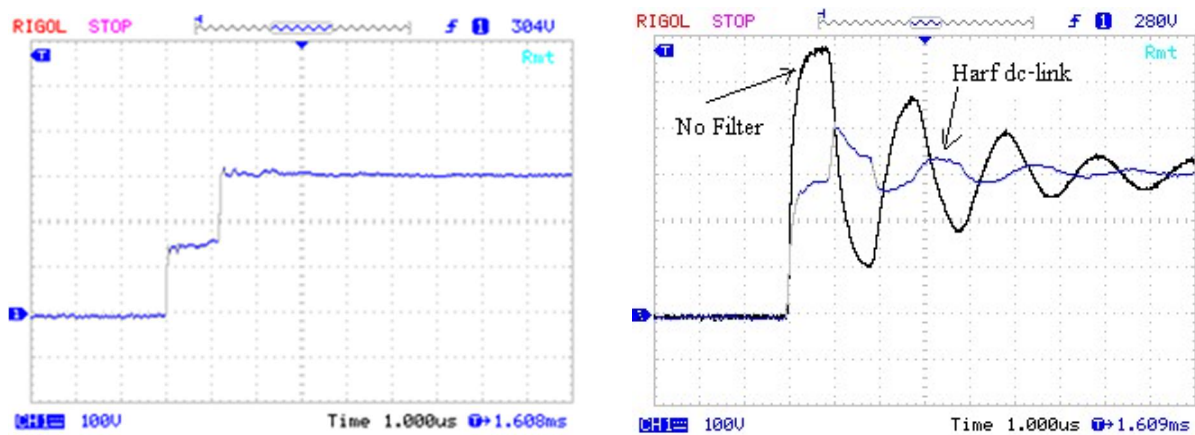


Figure 6 inverter and terminal voltage of hardware prototype

Conclusion

This thesis proposes over-voltage suppression methods for PWM inverter in long cable applications by using filters and half dc-link solutions. The main issue of this proposed research is to analyze the efficiency and loss of half dc-link in inverter and filters solution with the optimum design half dc link inverter as the function of cable length.

References

- Hanigovszki, N., Poulsen, J. and Blaabjerg, F. 2004. A Novel Output Filter Topology to Reduce Motor Overvoltage. **IEEE Transactions on Industry Applications** 40 (3): 845-852, May/June.
- Lee, S. and Nam, K. 2002. An Overvoltage Suppression Scheme for AC Motor Drives Using a Half DC-Link Voltage Level at Each EM Transition. **IEEE Transactions on Industrial Electronics** 49 (3): 549-557, June.
- Marc, F., Taylor, P.E. 1998. Conceptual Design for Sub-Sea Power Supplies for Extremely Long Motor Lead Applications. Copyright Material IEEE, Paper no. PCIC-98-14, pp. 119-128.
- Rodriguez, J., Pontt, J., Silva, C., Musalem, R., Newman, P., Vargas, R. and Fuentes, S. 2006. Resonances and Overvoltages in a Medium-Voltage Fan Motor Drive with Long Cables in an Underground Mine. **IEEE Transactions on Industry Applications** 42(3): 856-863, May/June.

Coin-Screening Machine Base on Digital Image Processing Technique

Ruangyos Keteruksa^{1*}, Suthee Rukkaphan¹ and Fusak Cheevasuvit¹

ABSTRACT

This paper presents a coin-screening machine with digital image processing technique. The structure of machine consists of a webcam, personal computer (PC), coin-screening equipment, and micro-controller Arduino board. The PC, which was designed as digital image processor, was developed by the MATLAB program. The coins under consideration feed into the coin-screening equipment by means of a conveyor belt. The webcam captures the picture, which is the image file and sends them to the digital image processor. The digital image processor performs an analysis with the Sobel edge detection method and compares it with the original image data. Then the digital image processor sends a command to the microcontroller Arduino board to control the coin-screening equipment. The experimental coins have five sets: 1 baht coin, 2 baht coin, 5 baht coin, 10 baht coin, as well as others. The experimental results showed that a coin-screening machine with digital image processing technique can sort coins for particular purposes.

Keywords: Coin-screening, Digital image processing, Sobel edge detection method

¹Department of Instrumentation, Faculty of Engineering, Rajamangala University of Technology Rattanakosin
96 Moo 3 Thanon Phutthamonthon Sai 5 Salaya Phutthamonthon Nakhon Pathom 73170, Thailand.

*Corresponding author, e-mail : ruangyos.k@rmutr.ac.th

Introduction

In this paper, we address how technology has played a greater role in human life with respect to an increase in comfort, less time spent on the job, and reduced labour costs. This results in less error as well as reduced risks and hazards to workers. It can also drive the economy, investment and trade practices of a country. One of the major roles for technology is in the financial sector. In Banking Finance for Deposits and Loans the main problems are: identifying the huge amount of coins that bankers must count and sort out each day. This also includes sales people who count the number of coins each day. The coin sorting machine with its image processing technique is a very accurate and fast means to facilitate the separation of coins. To summarize: this paper begins with the structure of the machine which consists of a webcam, personal computer (PC), coin-screening equipment, and microcontroller Arduino board. The PC, which was designed as a digital image processor and was developed by the MATLAB program. The coins under consideration feed into the coin-screening equipment by a conveyor belt. The webcam captures the picture, which is an image file and sends them to the digital image processor. The digital image processor performs an analysis with the Sobel edge detection method. Then compares it with the original image data. Then, the digital image processor sends a command to the microcontroller Arduino board to control the coin-screening equipment.

Materials and methods

Gonzalez and Woods (2002) discuss the edge by checking the border drag across, or near any point. This is measured by the change in intensity at positions close to that point. They are able to find the edge by the Gradient method and Laplacian method. This research paper is interested in the Gradient method as a way to find the edge by finding the lowest point and the highest in the form of the first derivative of the image. The edge points are located above the threshold, so the border is thick. Examples of ways to find the edges of this group are: Prewitt, Sobel, Roberts, Candy, etc.

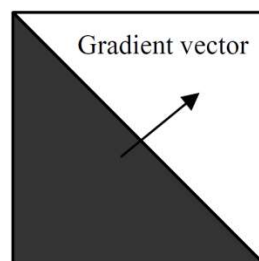


Figure 1 Finding the edge Gradient Method

Finding the edge (Edge Detection Methods). There are many algorithms for finding the edges. Based on relevant research, the algorithm of Canny edge detection is highly accepted for its good edge finding capabilities but cannot be used because of previous algorithms. The result is much more complex than the other algorithms, which makes the generated circuit too big.

Therefore, in this research, attention was paid to the Sobel method, because of the sharp outer borders.

Sobel edge detector for use in edge finding (Gonzalez and Woods. 2002).

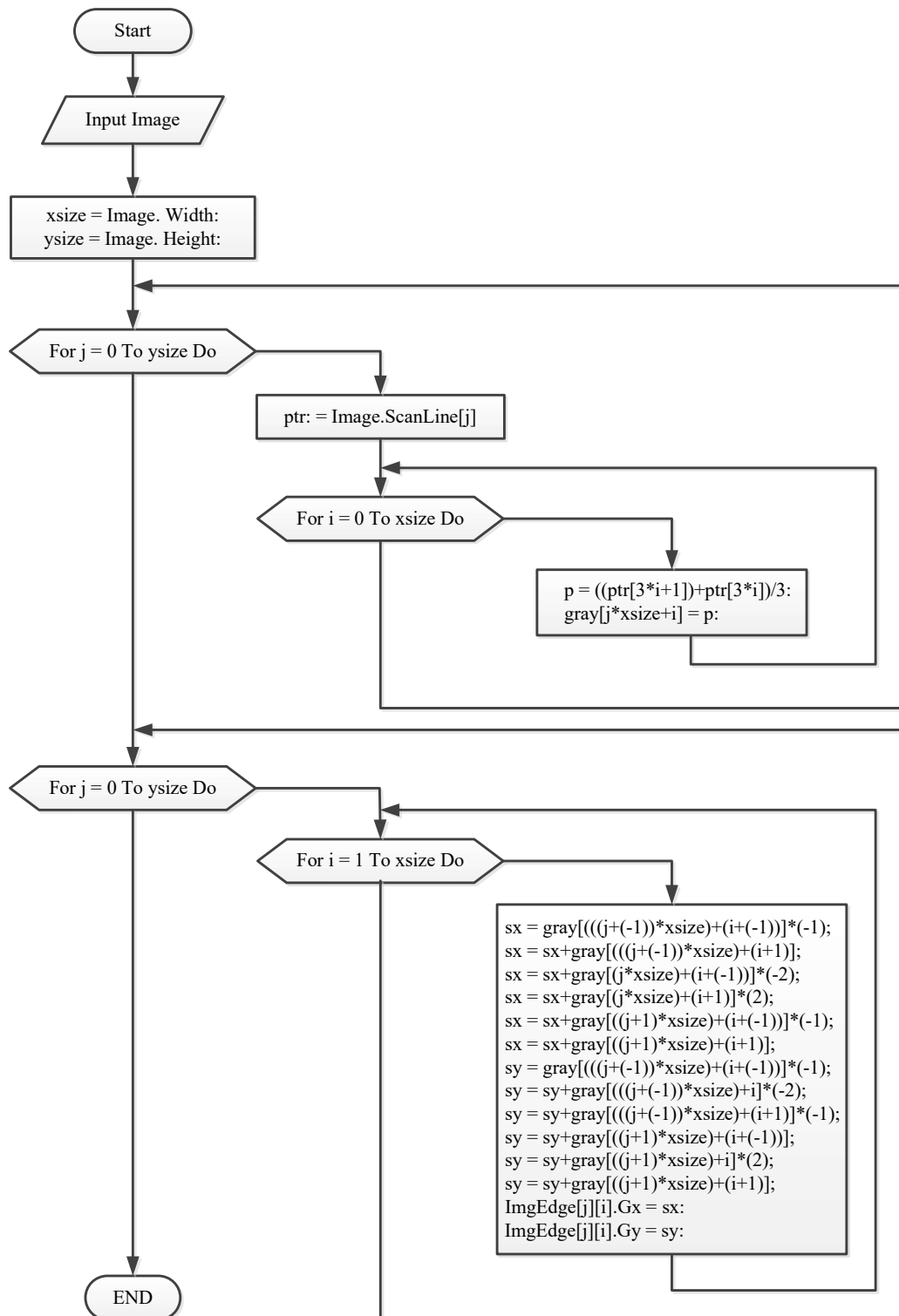


Figure 2 Flow Chart of Sobel edge detectors for use in edge finding.

Sobel uses gradient operators by applying the first derivative to the two-dimensional image. The gradient of the image is represented by the position determined by the vector as follows:

$$\text{Determined} \quad \nabla f = \begin{bmatrix} G_x \\ G_y \end{bmatrix} \begin{bmatrix} \frac{\partial f}{\partial x} \\ \frac{\partial f}{\partial y} \end{bmatrix} \quad (1)$$

The results obtained from the vector analysis yields the value derived from the change in the maximum level of the gradient vector in the various directions at the location (x, y) and the most important quantitative way to find the border is the value. Determined ∇f

$$\nabla f = \text{mag}(\nabla f) = \sqrt{(G_x^2 + G_y^2)} \quad (2)$$

Direction of the gradient vector can be calculated by assigning $\alpha(x, y)$ represented by the angular direction of the vector ∇f at (x, y) using the equation

$$\alpha(x, y) = \tan^{-1} \left[\frac{G_y}{G_x} \right] \quad (3)$$

When the angle is the distance of the x-axis, the direction of the edge at (x, y) is the perpendicular to the direction of the gradient vector at that point. Sobel work to find nonlinear edges. Discrepancies can be changed by adjusting the margin $R \in T^x$ of the original image by working on the gradient vector and using a mask size $3 * 3$ for the algorithm.

Determined

G_z = Mask of the action at various positions.

G_x = Mask of the action at the axial position x

G_y = Mask of the action at the axial position y

$$G_z = \begin{bmatrix} R_1 & R_2 & R_3 \\ R_4 & R_5 & R_6 \\ R_7 & R_8 & R_9 \end{bmatrix} \quad G_x = \begin{bmatrix} +1 & 2 & +1 \\ 0 & 0 & 0 \\ -1 & -2 & -1 \end{bmatrix} \quad G_y = \begin{bmatrix} -1 & 0 & +1 \\ -2 & 0 & +2 \\ -1 & 0 & +1 \end{bmatrix}$$

When a mask size $3 * 3$ is obtained, it will be replaced by the value and can be calculated from the following equation:

$$G_x = (R_7 + 2R_8 + R_9) - (R_1 + 2R_2 + R_3) \quad (4)$$

$$G_y = (R_3 + 2R_6 + R_9) - (R_1 + 2R_4 + R_7) \quad (5)$$

Convolution is the implementation of values G_x and G_y mark where actions are multiplied by the image.

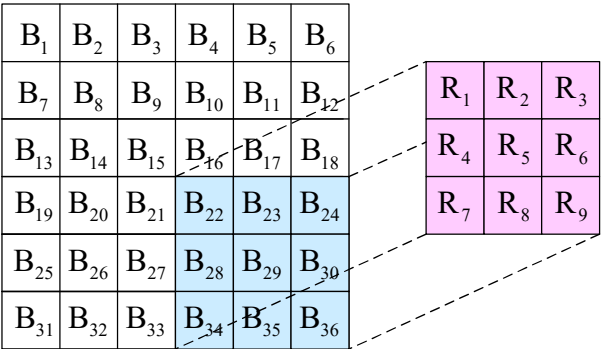


Figure 3. Convolution add Mark



Figure 4 The example of finding edge by the Sobel method (Gonzalez and Woods 2002)

Figure 5. The coin-screening machine with image processing technique starts by screening the mechanical devices. Then, the measurement and display devices are sorted by the number shown and the positions in sequence are described.

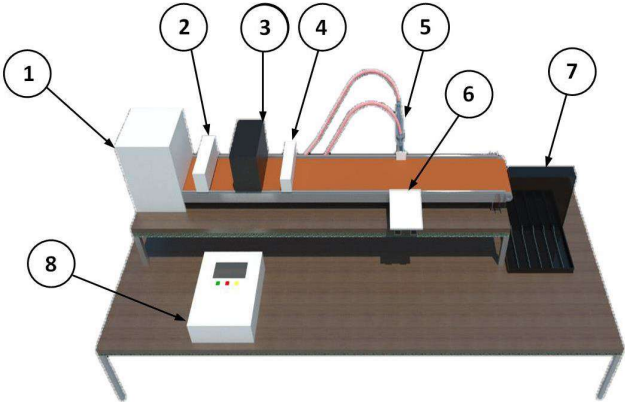


Figure 5 Structures for Coin-Screening Machine

- Position 1 = Install the coins into the conveyor belt.
- Position 2 = Sensor mount, point 1 is used to detect objects to shoot.
- Position 3 = A Webcam is set up for coin shooting from top to bottom.
- Position 4 = Sensor mount point 2 is used for metal detection.
- Position 5 = Cylinder mounting point for coin pressure.
- Position 6 = Where coins are pushed out.
- Position 7 = These are different coin sorting locations.
- Position 8 = An interior workstation installation point consists of a microcontroller modular relay power supply and motor driver modules. The external workstation installation is composed of a monitoring display.

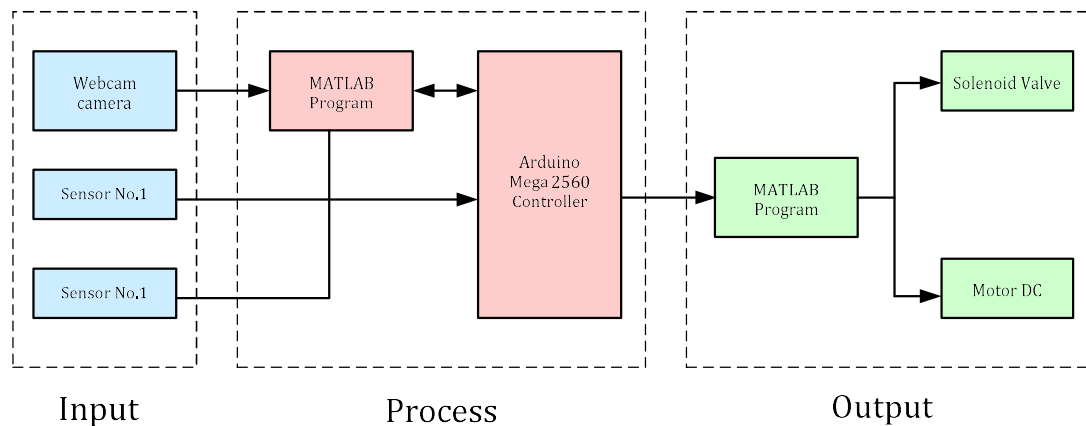


Figure 6 Structures for control unit

Figure 6. Structures for control unit. Arduino Mega 2560 microcontrollers can be divided into three main areas.

- (1) The input sector acts as a data input by receiving values from both sensor sensors and images from the webcam to send for processing in the processor.
- (2) The processing sector is responsible for processing input data from the input sector. The image to sort the coins is processed in the following way: the MATLAB program receives images from the Webcam and uses the microcontroller to connect the sensor with the MATLAB program in order to read the sensor object 1 which controls the image, and to read the sensor object 2 which controls the operation of the solenoid to open-close the wind in the program. Then, the MATLAB will process the image to sort the coins. And the output will work.
- (3) The output sector is responsible for receiving orders from the processing sector and in executing the orders received. The processor will instruct the relay module to run.

Results and Discussion

In the reign of the His Majesty King Bhumibol Adulyadej (King Rama IX of Thailand); the Government issued coins consisting of copper and tin coin with the coat of arms of Thailand. In 1950, it produced 5 Baht coins for the first time and in 1972, it produced 10 Baht coins for the first time. In 1988, with coin production in circulation, commemorative coins were also issued and a commemorative medal was developed. The following coins have been in

circulation up to the present time. There are six sets: 25 Satang coin, 50 Satang coin, 1 Baht coin, 2 Baht coin, 5 Baht coin, and 10 Baht coin.

Table 1 Circulated coins: Data from Bank of THAILAND








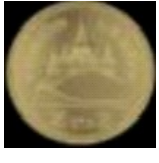
Circulated coins					
Image		Cost	Data		
Front	Back		Diameter	Weight	Material
		25 Satang	16 mm.	1.9 g.	Copper Plated Steel
		50 Satang	18 mm.	2.4 g.	Copper Plated Steel

Table 1 Circulated coins: Data from Bank of THAILAND (continued)

Circulated coins					
Image		Cost	Data		
Front	Back		Diameter	Weight	Material
		1 Bath	22 mm.	3 g.	Nickel steel
		2 Bath	21.75 mm.	4 g.	Aluminum bronze

		5 Bath	24 mm.	6 g.	Cu Nickel Copper Filled
		10 Bath	26 mm.	8.5 g.	Ring: Cu Nickel Central: Aluminum bronze

(3.1) The procedure of the coin-screening test with image processing techniques.

Figure 7. There is a coin to be conveyed. Then proceed to insert the coin into the conveyor and send the coin to the belt in order be to sort in the next step.



Figure 7 The coin-screening machine.

Figure 8. Sensor No.1 stands by and detects moving coins. When the coins move through the sensor moves, the MATLAB program will take a picture. The image is processed according to the following conditions.



Figure 8 Sensor No.1 stand by detects moving coins.

Figure 9. This shows the process command window, and conditions with image processing techniques using the Sobel way to sort the coins according to the conditions.

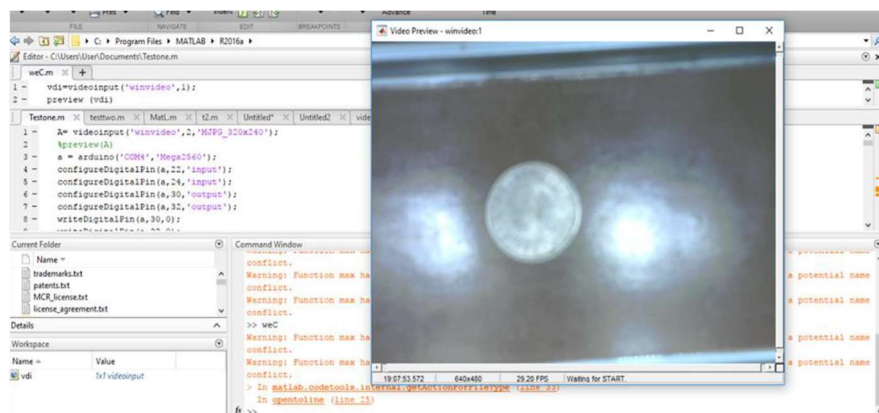


Figure 9 The process command window.

Figure 10. Sensor No.2 stands by to detect moving coins. When the coin moves through the sensor, the MATLAB program will compare it with the original image, and the work is processed by the microcontroller which controls the next condition.

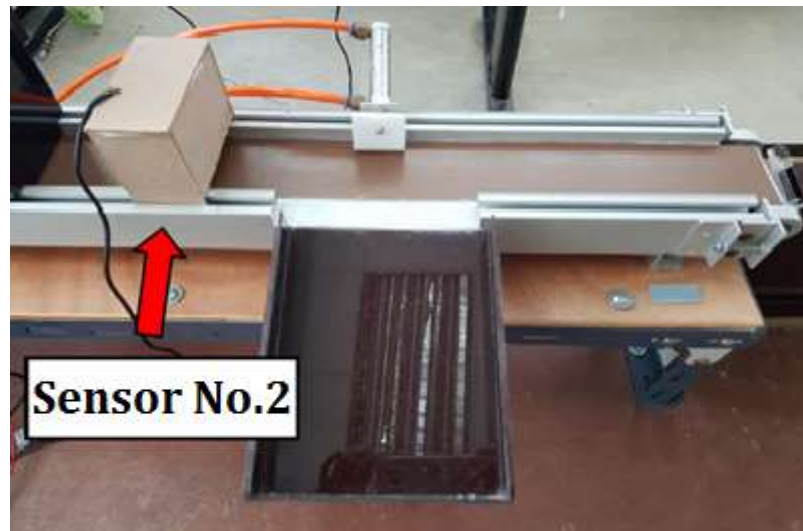


Figure 10 The sensor No.2 stands by to detect moving coins.

Figure 11. The process of sorting coins is different. The second sensor sends the data to the microcontroller operator for the cylinder to work out the different coils from the conveyor belt.



Figure 11 The process of sorting coins is different.

Figure 12. The processed coin and the tossed-out coin will continue to flow down to the coin sorting machine.



Figure 12 The coin into the sorting machine.

Experimental topics

- (1) Coin-screening by coin processing technique 25 Satang, 50 Satang, 1 Baht, 2 Baht, 5 Baht and 10 Baht up to 50 times. 5
- (2) Coin-screening using 50 different coin processing techniques.
- (3) Coin-screening by coin processing technique 25 Satang, 50 Satang, 1 Baht, 2 Baht, 5 Baht and 10 Baht and 50 different random coin types. 5
- (1) Coin-screening by coin processing technique: 25 Satang, 50 Satang, 1 Baht, 2 Baht, 5 Baht and 10 Baht to 50 times. 5

Category Sorting	Number of images Tested	Accuracy	
		Number of images	Percent
25 Satang	50	50	100
50 Satang	50	50	100
1 Baht	50	50	100
2 Baht	50	50	100
5 Baht	50	50	100
10 Baht	50	50	100
Average	50	50	100

(2) Coin-screening using 50 different coin processing techniques.

Category Sorting	Number of images Tested	Accuracy	
		Number of images	Percent
25 Satang	50	46	92
50 Satang	50	48	96
1 Baht	50	49	98
2 Baht	50	49	98
5 Baht	50	49	98
10 Baht	50	49	98
Average	50	48.34	96.67

(3) Coin-screened by coin processing technique 25 Satang, 50 Satang, 1 Baht, 2 Baht, Baht and 10 Baht and 50 different random coin types.

5

Category Sorting	Number of images Tested	Accuracy	
		Number of images	Percent
25 Satang	50	46	92
50 Satang	50	49	96
1 Baht	50	50	100
2 Baht	50	50	100
5 Baht	50	50	100
10 Baht	50	50	100
Average	50	49.17	98

Conclusion

The simulation results showed the coin sorting machine with the image patching technique. Starting from the input, it takes a picture from a webcam that processes it using the MATLAB program which analyses the conditions with edge detection technique. The Arduino Mega 2560 microcontroller is compatible with the object sensor, to coin the coins according to conditions. The next step is to get input and output data. The Arduino Mega 2560

microcontroller is the final condition. If the object is processed as correct, it sends information about the object being conveyed to the end of the conveyor belt. If the object is processed as incorrect, the program will send data to remove the object from the belt.

Acknowledgement

The research for this project has been carried out by Associate Professor Dr. Fusak Cheevasuwit, The Digital Image Processing Laboratory in Instrumentation Engineering Faculty of Engineering Rajamangala University of Technology Rattanakosin. Mr. Adisorn Thiansawang and Miss. Wipada Jewbumrung for providing excellent lab facilities that make this work possible.

References

- Achalakul, T. and Madarasmi, S. 2002. A concurrent modified algorithm for Generalized Hough Transform, pp. 965-969. **Proceedings of IEEE International Conference on Industrial Technology 2**.
- Gao, W., Yang, L., Zhang, X. and Liu, H. 2010. An Improved Sobel Edge Detection. **The 3rd IEEE International Conference on Computer Science and Information Technology**, 978-1-4244- 5540-9/10.
- Gonzalez, R. C. and Woods, R. E. 2003. **Digital Image Processing** (2nd ed). Pearson Education, India.
- Haralick, R. M. 1984. Digital step edges from zero crossing of the second directional derivatives. **IEEE Transactions on Pattern Analysis and Machine Intelligence** PAMI-6(1):58-68.
- Heath, M. D., Sarkar, S., Sanocki, T. and Bowyer, K. W. 1997. A Robust Visual Method for Assessing the Relative Performance of Edge Detection Algorithms. **IEEE Transactions on Pattern Analysis and Machine Intelligence** 19(12): 1338-1359.
- Hueckel, M. H. 1973. A local visual operator which recognizes edges and line. **Journal of the ACM** 20(4): 634-647.
- Kirsch, R. A. 1971. Computer determination of the constituent structure of biomedical images. **Comput. Electron. Res.** 4:315-328.
- Marr, D. and Hildreth, E. 1980. Theory of Edge Detection. **Proceedings of the Royal Society of London. Series B, Biological Sciences** 207 (1167): 187-217.
- Nadernejad, E., Hassanpour, H. and Sharifzadeh, S. 2008. Edge Detection Techniques: Evaluations and Comparisons. **Applied Mathematical Sciences** 2(31):1507 – 1520.
- Peli, T. and Malah, D. 1982. A Study of Edge Detection Algorithms. **Computer Graphics and Image Processing** 20: 1-21.
- Raju, C.N., Naga Mani, S., Rakesh Prasad, G and Sunitha, S. 2011. Morphological Edge Detection Algorithm Based on Multi Structure Elements of Different Directions. **International Journal of Information and Communication Technology Research** 1 (1):37-43.
- Shin, M. C., Goldgof, D. and Bowyer, K.W. 2001. Comparison of Edge Detector Performance through Use in an Object Recognition Task. **Computer Vision and Image Understanding** 84(1): 160-178.
- Yang, H. and Zhang, J. 2005. Mathematical Morphology in Edge Detection Application. **Journal of Liaoning University (Natural Science Edition)** 32(1): 50-53.

- Zheng, Y., Rao, J. and Wu, L. 2010. Edge Detection Methods in Digital Image Processing. **The 5th IEEE International Conference on Computer Science & Education**, 978-1-4244-6005-2/10.
- Zhengyao, W. 2003. Edge detection of digital image. **Master paper**, Xi'an: Xi'an Jiaotong University.

Design of Data Acquisition Unit Using Arduino from a Flow Velocity Meter for Tides in the River

Sanya Samaimak^{1*} and Shanin Harnnarong¹

ABSTRACT

The Royal Irrigation Department is responsible for managing water availability in Thailand. Many instruments are used to read the data to obtain the needed hydrological data. The instruments that it has applied to measure the velocity of the tide are the flow velocity meters A-OTT C31 that compatible with the audio and numerical displayer Z 41-00. They have been used for 30 years, (1988 - 2018).

Design of Data Acquisition Unit Using Arduino from a Flow Velocity Meter for Tides in the River was presented in this paper. It was designed to use as a substitute for the audio and numerical displayer Z 41-00 that were broken. The result of the design and the experimentation show the ability of working together with the flow velocity meters A-OTT C31 and the accuracy of the data acquired from this designed instrument are satisfactory.

Keywords: The Royal Irrigation Department, Flow Velocity Meter, Arduino

¹ Department of Instrumentation Engineering, Faculty of Engineering, Rajamangala University of Technology Rattanakosin, 96 Moo 3 Salaya Phutthamonthon NakhonPathom 73170, Thailand

*Corresponding author, e-mail: sanya.sam@rmutr.ac.th

Introduction

1. Current meters

The water current velocities are measured by the tools that measure the speed of the tide and they are classified into two types (Leevajanakul, 2000; Polpananavee, 2011).

1.1 Mechanical current meters

Mechanical current meters are mechanical devices that are the main components. The tools will move when the current flows and there are three types.

1.1.1 Vertical axis current meters

1.1.2 Horizontal axis current meters

1.1.3 Pendulum current meters

1.2 Electronic current meters

Electronic current meters are electronic devices that work primarily on electronic devices. These tools work better than mechanical current meters and there are three types.

1.2.1 Electromagnetic velocity meters

1.2.2 Doppler velocity meters

1.2.3 Optical strobe velocity meters

The tools that have been used by the Irrigation Department are A-OTT C31, the current flow meters, with Z 41-00, audio and numerical indicators. The A-OTT C31 current flow meter is mechanical current meter that is the type of horizontal axis current meter.

2. Arduino

Arduino is an open-source electronics platform based on easy-to-use hardware and software (Makarn, 2009; Arduino Language Reference, 2018). In this paper, we use Arduino Due which is one of the Arduino family.

Arduino Due can be obtained signals in square wave form via digital pin. After that interrupt service function is called to count the incoming waveforms. The obtained values are stored in *p_count* variable and those values will be managed in various processes later.

Materials and Methods

1. Signal form A-OTT C31

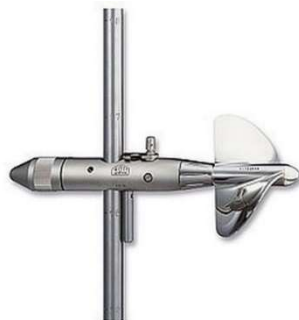


Figure 1 A-OTT C31

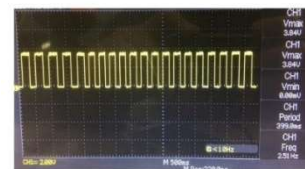


Figure 2 A-OTT C31 Signal

The A-OTT C31, the original universal current meter for flow velocity measurement in rivers and open waterways. It has proven quality, precision and reliability (OTT Hydromet, 2017)

Water flow causes rotation of the current meter propeller. Once per revolution, a magnet attached to the current meter propeller operates a water-tight sealed reed contact. The contact sequence is proportional to the velocity of the water at the measuring point. The sequence is captured by an attached counter and used for calculating flow velocity at the measuring point, based on the current meter equation (OTT Hydromet, 2017)

The relationship between propeller revolution and flow velocity is determined by the following formula

$$v = k \cdot n + \Delta \quad 1$$

Wherein:

k : Hydraulic pitch of the current meter propeller [m/rev] which was determined by towing tests carried out in a rating tank.

n : Propeller rotation per second [rps].

Δ : Current meter constant [m/s] which was determined by towing tests carried out in a rating tank.

Since there are mechanical differences between the propellers caused by manufacturing tolerances and differences in bearing, the constants k and Δ are precisely determined individually for each current meter in the OTT rating tank (BARGO Test Certificate and BAREL Velocity Table) [5].

2. Block diagram

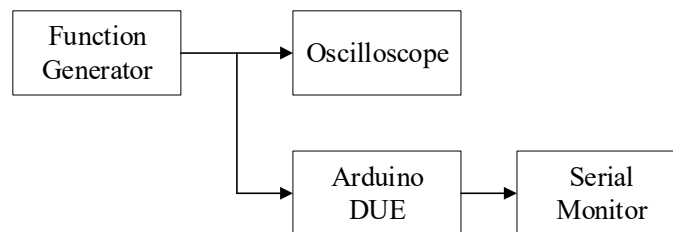


Figure 3 Block Diagram

The block diagram consists of 4 parts:

2.1 Function Generator that can supply the square wave form in many frequencies. It has the signal form which is similar to the signal that can be measured from the A-OTT C31 universal current meter.

2.2 Oscilloscope is used to measure the supplied signal from the function generator. The results of the oscilloscope measurements are used to calculate the errors and uncertainties of the designed instrument.

2.3 Arduino Due is used to measure the supplied signal from the function generator at the same time with the oscilloscope. The results of the Arduino Due measurements are used to calculate the errors and uncertainties for comparisons with the results of the oscilloscope measurements.

2.4 Serial Monitor is used to display the results of the Arduino Due measurements. As Arduino starts to measure the signal, the frequency results of the measurements are sent out to the serial port. Then the frequency results will be displayed on the serial monitor.

3. Flowchart

To show the workflow of the designed process in this paper was presented in flowchart. When the program starts, it manages the hardware in its initial state and then it resets all of the variables before it enters the main loop. The main loop is controlled for a fixed time of 1 second per work cycle. In this way, the main loop period is constant so that the frequency can be determined by reading the value obtained from the interrupt routine. Every time an interrupt occurs, the value of the *p_count* variable is updated at runtime. When the program reaches the cycle of reading in the main loop, the value of the *p_count* variable will be taken to the *p_store* variable. This value will be calculated to frequency values and then the *p_count* variable is reset to 0. The program run in loop continuously.

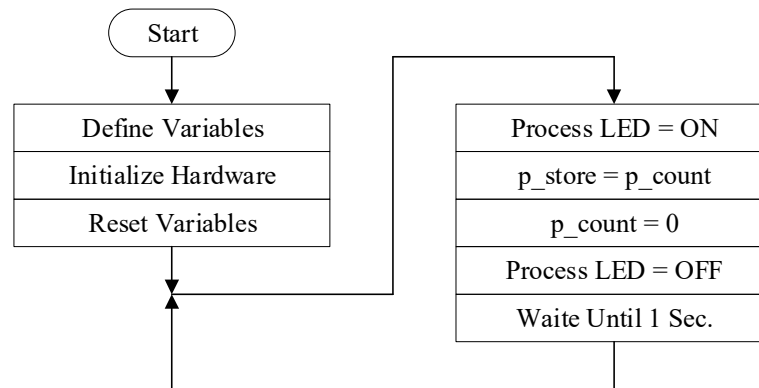


Figure 4 Flowchart

Results and Discussion

1. Testing at 20 Hz, 200 Hz, 1 kHz and 2 kHz

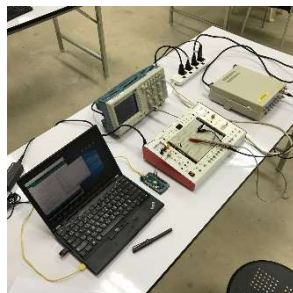


Figure 5 Test bench.

Experimented by frequency input with a function generator at frequencies of 20 Hz, 200 Hz, 1 kHz and 2 kHz. Then measure the output signal with oscilloscope and Arduino to compare results.

Determine the number of random variant $n = 15$. To keep all raw data from a serial monitor. The results of all experiments are shown in Tables 1 to 4.

Table 1 Test results at 20 Hz

Oscilloscope	Serial Monitor	Summary
		Oscilloscope = 20.0564 Hz $n = 15$ Average = 20.0000 Hz SD = 0.0000 Ua = 0.0000

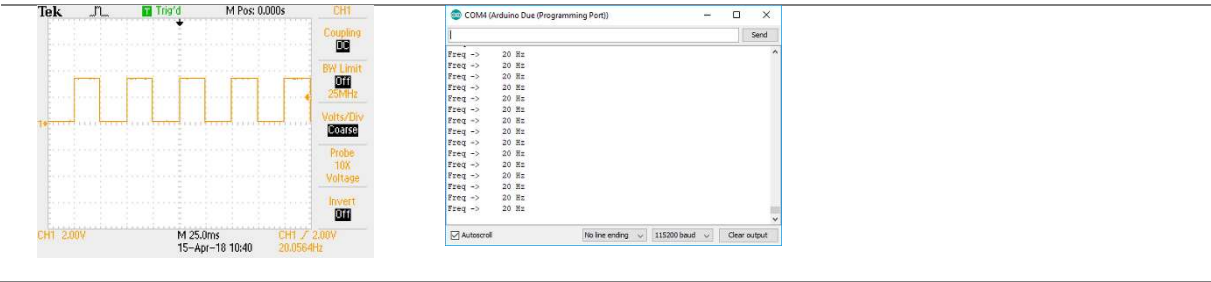


Table 2 Test results at 200 Hz

Oscilloscope	Serial Monitor	Summary
		<p>Oscilloscope = 200.044 Hz n = 15 Average = 200.0667 Hz SD = 0.2582 Ua = 0.0667</p>

Table 3 Test results at 1 kHz

Oscilloscope	Serial Monitor	Summary
		<p>Oscilloscope = 1004.19 Hz n = 15 Average = 1004.2000 Hz SD = 0.4140 Ua = 0.1069</p>

Table 4 Test results at 2 kHz

Oscilloscope	Serial Monitor	Summary
		<p>Oscilloscope = 2006.27 Hz n = 15 Average = 2006.3333 Hz SD = 0.4880 Ua = 0.1260</p>

Conclusion

The experimental results show that this designed prototype can read four tested areas of the frequency range properly well. The application of this prototype will be applied to the A-OTT c31, the current flow meter, for replacing the damaged Z 41-00, the counter which is used to display as an audio and numerical output. It can be done simply by connecting only two

wires. The prototype of this research will be developed as a tool to be used in fieldwork in the future.

Acknowledgement

This research was supported by the Institute of Research and Development, Rajamangala University of Technology Rattanakosin. In addition, the authors would like to thank Mr.Voravot Boontong, Hydrologic Instrument Standards Branch Chief, working in Hydrology Division, Bureau of Water Management and Hydrology for all his help and suggestions. Thankfulness to the supporters : Mr.Jetsdaporn Satansup, Mr.Ruangsimon Jamkrajang and Mr.Pawaritsorn Chaisong for all their support throughout the period of this research.

References

- Arduino Language Reference. 2018. Available Source: <https://www.arduino.cc/reference/en>.
- Leevajanakul, Kirati. 2000. **Hydrology**. Bangkok: Rangsit University Press. (in Thai)
- Makarn, Eakachai. 2009. **Learn Understand and Use the AVR Micro controller family with Arduino**. Bangkok: ETT Co., Ltd. (in Thai)
- OTT Hydromet. 2017. **A-OTT C31**. Available Source: <http://www.ott.com/products>.
- Polpananavee, Pramohit. 2011. **Principle of Water Flow calculation through Irrigation Structures**. Bangkok: Regional Irrigation Office 8. (in Thai)

Alarm Bubble within Intra Venous Tube via Application Line.

Jantira Juakvont^{1*}, Jiraphong Kongpeng¹ and Thanusak Jankaew¹

ABSTRACT

Currently medical treatment is necessary to use infusion pump for controlling solution flow intravenous tube. And infusion pump in the market can protect patient from air bubble within the intravenous tube by alarm sound, thus nursing staffs have to stand by within area that can hear sound from alarm system of the infusion pump. This paper presents a method to increase area of warning air bubble within the intravenous tube of the infusion pump by using application Line. And nursing staffs will get warning message via smart phone or tablet. From tested result found that the alarm bubble within the intravenous tube system can detect air bubble, then send alerted information through network and the warning message was displayed on mobile device. The alarm bubble within the intravenous tube system spent more time in sending warning message through network internet. While time for processing the detected signal till sending message to sever is about 1.37 seconds. In conclusion the alarm bubble within the intra venous tube system can be applied with the infusion pump to protect the patient from air bubble within the intravenous tube.

Keywords: Alarm bubble system, Intravenous tube, Infusion pump, LINE application

¹Department of Engineering, Faculty of Engineering and Technology, Rajamangala University of Technology Srivijaya, Maifad, Sikao District, Trang 92150, Thailand

*Corresponding author, e-mail: jantira.j@rmutsv.ac.th

Introduction

An air embolism occurs when one or more air bubbles enter a vein or artery and block it. These air bubbles can move to brain, heart, or lung and cause stroke, heart attack, or respiratory failure. A syringe or IV can accidentally inject air into veins while intravenous therapy. *Intravenous therapy (IV)* is a *therapy* that delivers liquid substances directly into a vein. And can be done by injection or infusion by using an infusion pump to control deliver of liquid substances into patient's body. One method to protect patient from air embolism is detecting air bubble in intravenous tube and alerting nursing staff to assist the patient before the air bubble will enter to vein of the patient. In general, air bubble detection function also equipped with many infusion pumps that included in safety features, and alert user by sound alarm. Because of alerting air bubble in the intravenous tube by sound alarm, thus there must be nursing staffs stand by in area that the alarm sound can be heard for assisting the patient. For more convenient of nursing staff in assisting the patient can be done by increasing distance or area of alerting air bubble. Thus this paper introduced application of internet of thing technology to increase alerting area by using LINE application to inform the air bubble in the intravenous tube instead of sound alarm. That is more convenient for the nursing staff to work and can assist the patients in larger area. Concept of alerting air bubble in the intravenous tube by LINE application begins when sensor detected air bubble in the intravenous tube and the sensor generated signal, then the signal from the sensor is sent to processor for processing. And output of the processor is alerted message that is sent to communication module, the communication module upload the alerted message to server via Wi-Fi. Then the server sends the alerted message to mobile device or computer of the nursing staff through LINE Notify. Thus the nursing staff can assist or service the patient in larger area on time. Concept of alerting air in the intravenous tube via LINE application is shown in **Figure 1**.

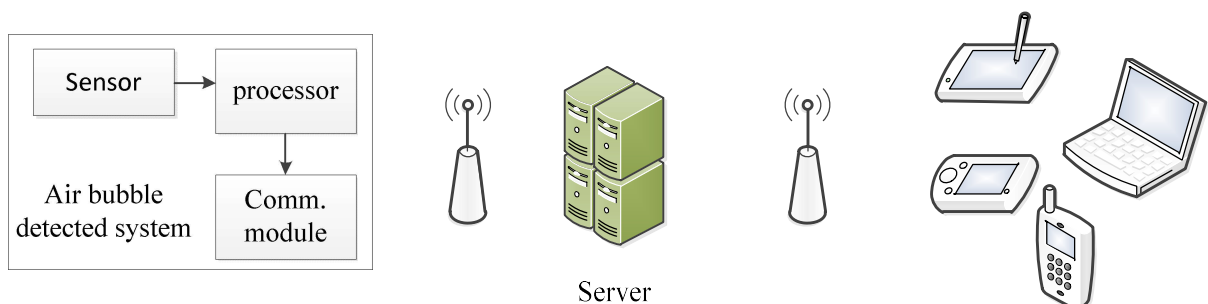


Figure1 Concept of alerting air bubble in the intravenous tube via LINE application

Materials and Methods

1. Air bubble sensor

From the concept of alerting air bubble in the intravenous tube, first of all, air bubble detected system was developed by using domestic material. The air bubble detected system consists of sensor, processor, and communication module. There are many air-in-line sensors in market that can detect air bubble by using ultrasonic technology or capacitive technology, but this project tried to use photodiode to detect air bubble instead. The air bubble sensor by photodiode was developed by M-Care Engineering Ltd. With concept of the photodiode generates current when received light on other side of the intravenous tube and the light can travel through the intravenous tube when there is air in the intravenous tube. The air bubble sensor is shown in **Figure 2**.



Figure 2 Air bubble sensor

2. Processor

Current from the photodiode is sent to transimpedance amplifier circuit that converts current signal to voltage signal that is appropriate for Arduino UNO board to process later. Processor of the air bubble detected system that is installed on the Arduino UNO board is ATmega328P microcontroller. The ATmega328P microcontroller processes the voltage signal follow program that developed and downloaded into the Arduino board. After the

ATmega328P finished processing the voltage signal, then alerted message is generated. The alerted message can be read on LCD monitor of the air bubble detected system case whether there is air bubble as shown in **Figure 3**.



Figure 3 Alerted information on the air bubble detected system case

3. Communication module

To increase distance or area of alerting the air bubble in the intravenous tube, the alerted message must be sent to ESPino 32 board that contain ESP32 chip. The ESP32 chip is a single 2.4 GHz Wi-Fi and Bluetooth combo that is designed for mobile, wearable electronics, and Internet-of-Things (IoT) applications. The ESPino32 board is connected to the Arduino UNO board provide Wi-Fi and Bluetooth functionality through I2C interfaces as shown in Figure 4. Function of the ESP32 chip is processes the alerted message for uploading to server via Wi-Fi. And the server sends warning message through application LINE Notify on mobile device as shown in **Figure 5**.

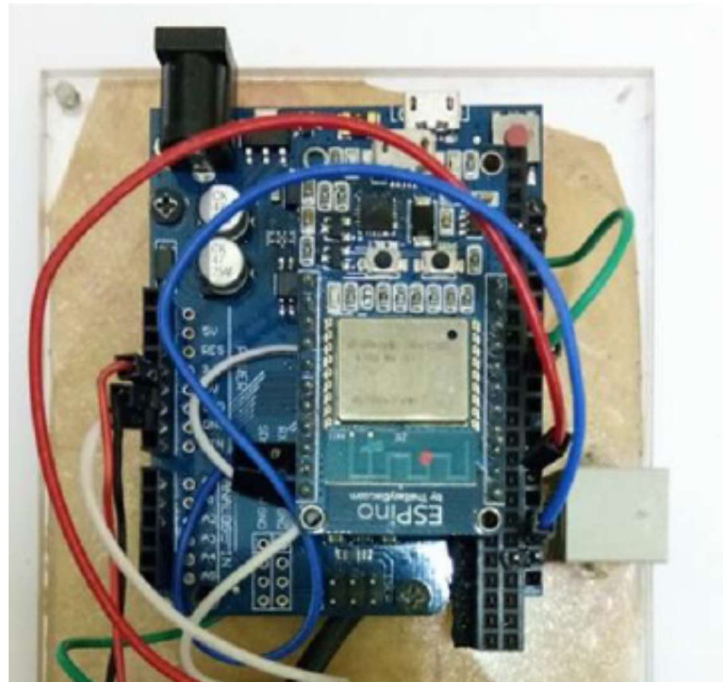


Figure 4 ESPino32 and Arduino UNO are connected



Figure 5 LINE application shown warning message that there is air bubble in IV tube.

4. LINE application

LINE Notify is a service of LINE that prepared in form of application programming interface (API) for developer to develop project that require sending notification message

depended on condition to group or personal account. This project applied LINE Notify to send warning message of the air bubble in the intravenous tube as shown in **Figure 5**. To use application LINE Notify, both sender and receiver have to create LINE account, and register to the LINE Notify website for using service. Then open Line application and add LINE Notify as friend, the receiver can get warning message after finished this step. While the sender has to request the LINE Notify website for token and use the token for sending message. Developer had created code and programmed into the air bubble detected system for sending the warning message in Thai language as shown in Figure 5.

Results and Discussion

The Alarm bubble in the intravenous tube system was tested by setting saline bag, the air bubble sensor, the detected air bubble case, the mobile device, and air bubble generator as shown in **Figure 6**.

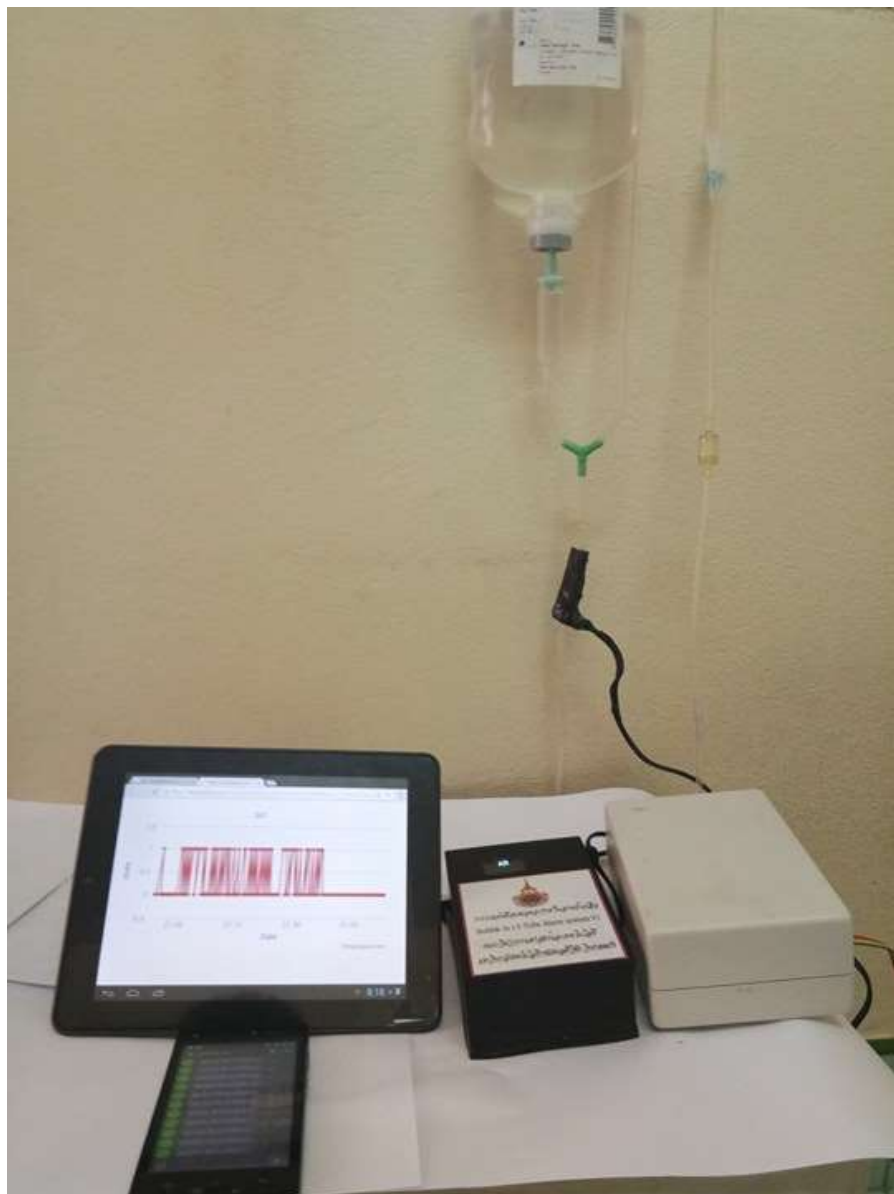


Figure 6 Testing setup of the alarm bubble in IV tube system

This alarm bubble system was tested to ensure that can detect air bubble and send the warning message corresponded to message received on mobile device. The testing used Srivijaya Wifi network for sending the warning message to server and receiving the warning message by the mobile device. The air bubble generator generated air bubble in the intravenous tube varies by:

1. Generated air bubble every 10 minutes for 1 hour and checked number of warning messages in the mobile device.
2. Generated air bubble every 5 minutes for 1 hour and checked number of warning messages in the mobile device.
3. Generated air bubble every 2 minutes for 1 hour and checked number of warning messages on mobile device.

Tested result found number of the warning message that arrive the mobile device presented as graph in **Figure 7** to **Figure 9**. When set up the air bubble generator to generate air bubble every 10 minutes, graph in **Figure 7** shows 5 warning messages of air bubble in the intravenous tube within 1 hour. That presents the alarm bubble system can detect and send the warning message for all air bubbles that generated. Seems the system worked well with period 10 minutes of the air bubble generated.

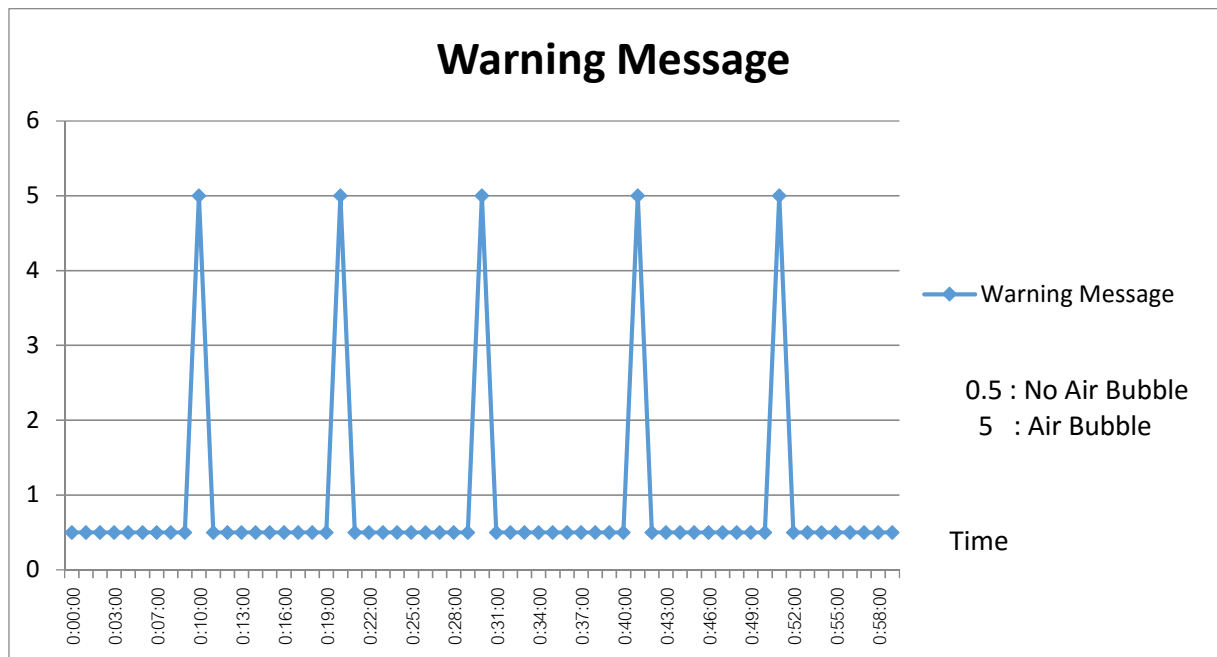


Figure 7 Number of warning messages that displayed on the mobile device when generated air bubbles every 10 minutes.

Then changed period of generating air bubble to be 5 minutes, graph in **Figure 8** shows the mobile device received air bubble warning message every 5 minutes within 1 hour, except at 30-33 minutes seems there is delay of sending message. That occurred one time within 1 hour. Performance in working of the alarm bubble system decrease about 10 percent when there is air bubble every 5 minutes.

After that still decreased the period of generating air bubble to be 2 minutes and got result in **Figure 9**. The graph displays there is delay on updating warning message in the mobile device 11 times within 1 hour. That means the alarm bubble system cannot detect and send the warning message for all air bubbles that occur every 2 minutes. On the other hand, this testing

exhibited time that the alarm bubble system needed to work since detected the air bubble until the warning message was displayed on the mobile device is less than 2 minutes on sometimes and more than 2 minutes on sometimes.

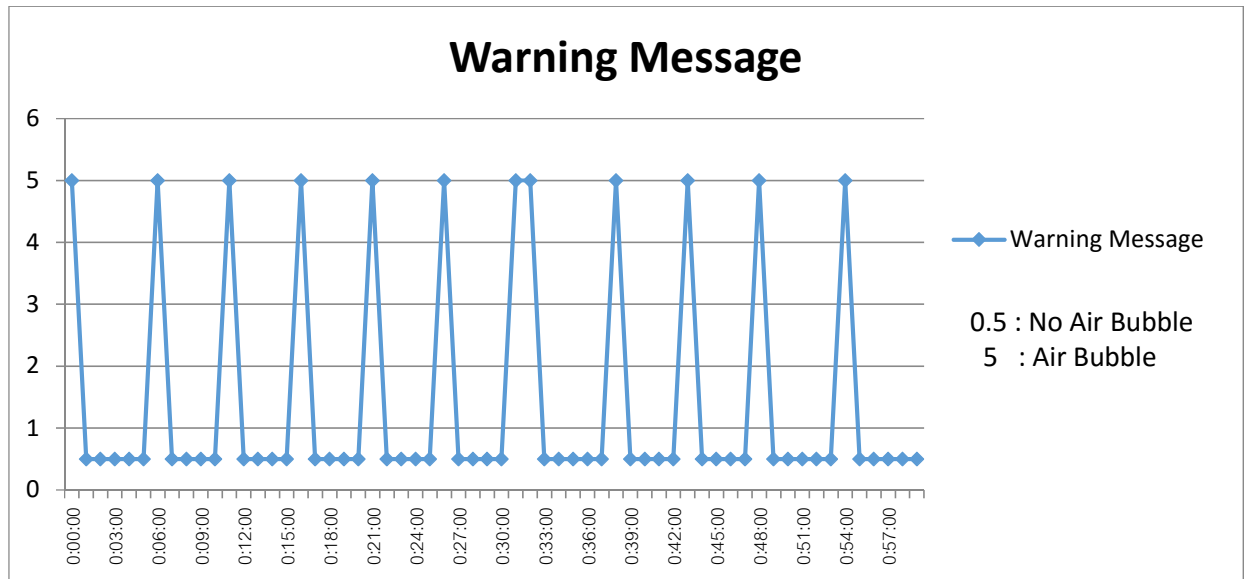


Figure 8 Number of warning messages that displayed on the mobile device when generated air bubbles every 5 minutes.

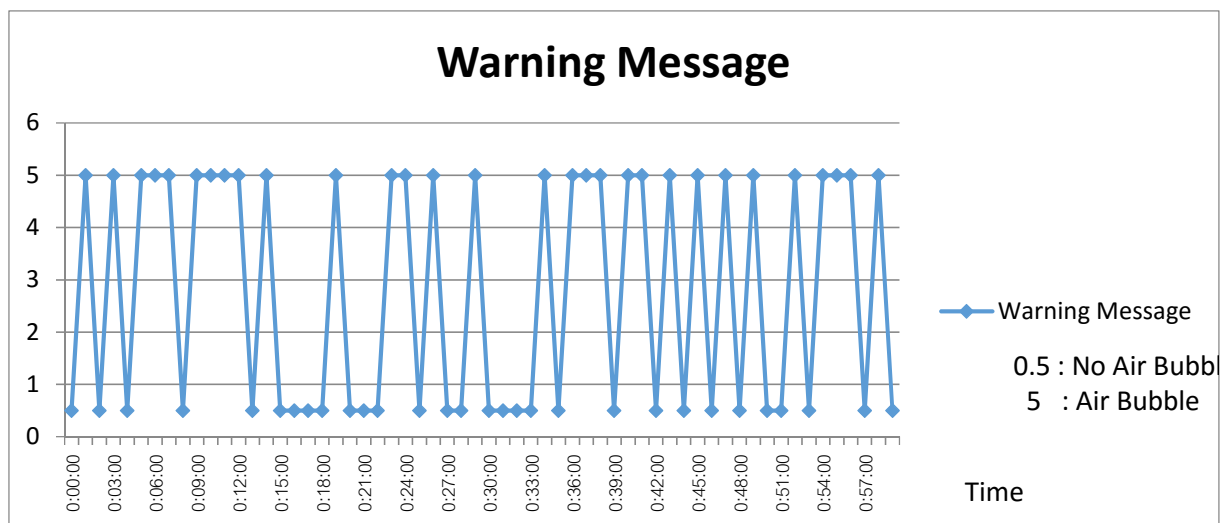


Figure 9 Number of warning messages that displayed on the mobile device when generated air bubbles every 2 minutes.

Then developer had investigated the delay of the system by separating delay time into delay on network and delay on hardware. Since delay on network depends on many variables, thus checking delay of hardware is easier. Developer had measured delay of hardware since the sensor detected the air bubble until the ESPino32 module sent the warning message to server, spent time for 1.37 second that displayed in **Figure 10**.

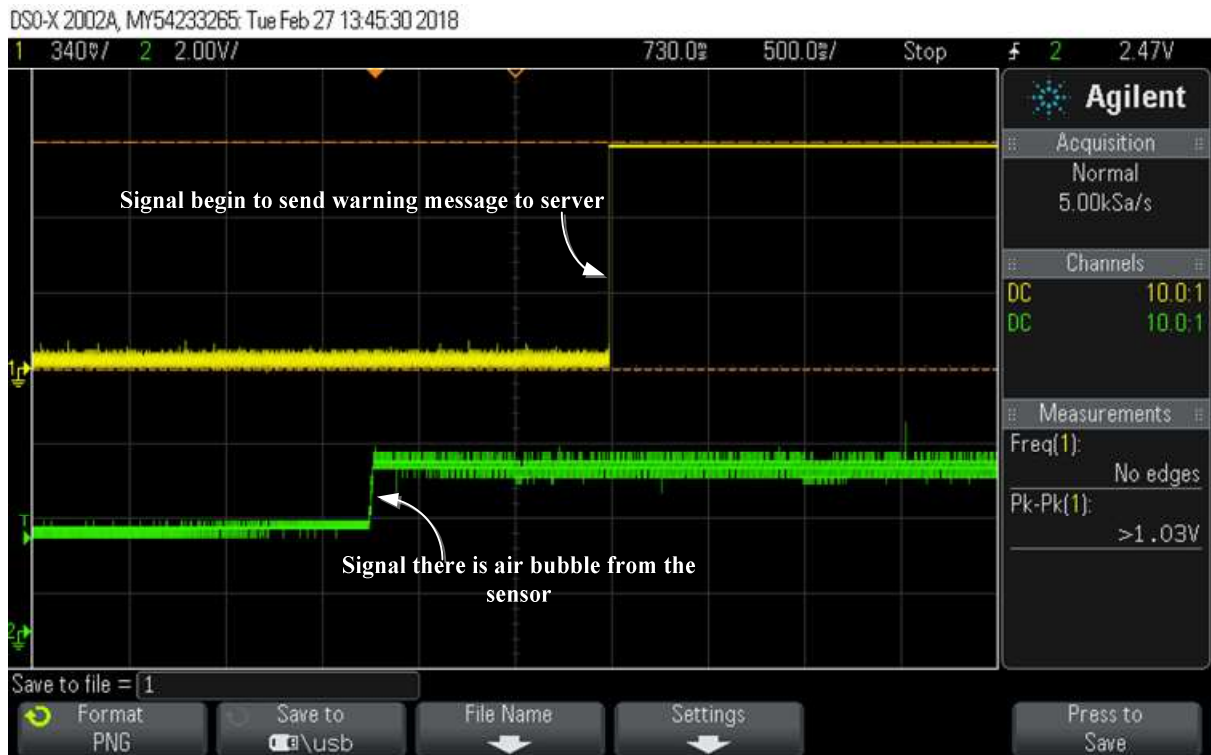


Figure 10 Processing time of the air bubble system since detected air bubble till sent warning message to server is 1.37 second.

Result of the investigated delay indicated that the warning message was delayed in internet network. Imply that delay of the alarm bubble system depends on delay of the internet network. So the alarm bubble system can work well with period of 2 minutes air bubble generated if speed of the internet network is increased.

Conclusion

The alarm air bubble system can work well to protect the patient from air embolism because the system spends time less than 2 second in detecting air bubble and sending alerted message to server. But time to receive the warning message is depended on speed of the internet network. Thus the alarm air bubble system will work exactly if speed of the internet network is increased. And the alarm air bubble system work separately from deliver fluids system into a patient's body, thus the alarm air bubble system do not disturb operation of any intravenous therapy and support nursing staff for more convenience on assisting the patient. Furthermore, using the alarm air bubble system can increase area of alerted air bubble in intravenous tube when compared with alerted by sound alarm, because the alarm air bubble system can be applied with infusion pump everywhere that can access the internet network.

Acknowledgement

We would like to express our very great appreciation to M-Care Engineering Ltd. for providing the air bubble sensor including suggestion during developed this project.

References

- Atmel. 2009. 8-Bit Avr® Microcontroller With 4/8/16/32k Bytes In-System Programmable Flash. Atmel Corporation.
- CNXSOF.T. 2017. **Getting Started With Espruino & Javascript On Esp32 With Espino32 Board**. Available Source:<https://www.cnx-software.com/2017/09/11/Getting-Started-With-Espruino-Javascript-On-Esp32-With-Espino32-Board/>
- Cook, L. S. 2013. Infusion-Related Air Embolism. **Journal of Infusion Nursing** 36(1): 26-36.
- Espressif Systems. 2018. **Esp32 Datasheet Version 2.1**. Copyright © 2018 Espressif Inc.
- Line Corporation, 2016. **LINE Notify API Document**. Available Source:<https://notify-bot.line.me/doc/en/>
- LINE Corporation. **Messaging API**. Available Source:<https://developers.line.me/en/docs/messaging-api/overview/>
- LINE Engineering. 2016. **Using LINE Notify to send stickers and upload images**. Available Source: <https://engineering.linecorp.com/en/blog/detail/94>
- Martina O'Toole and Dermot Diamond. 2008. Absorbance Based Light Emitting Diode Optical Sensors and Sensing Devices. SENSORS ISSN 1424-8220
- McCarthy, C. J., Behraves, S., Naidu, S. G. and Oklu, R. 2016. Air Embolism: Practical Tips for Prevention and Treatment. **Journal of Clinical Medicine** 5(11), 93. <http://doi.org/10.3390/jcm5110093>
- Pant, D., Narani, K. K. and Sood, J. 2010. Significant air embolism: A possibility even with collapsible intravenous fluid containers when used with rapid infuser system. **Indian Journal of Anaesthesia** 54(1), 49–51. <http://doi.org/10.4103/0019-5049.60498>
- Quer, J.C. 2014. **Arduino UNO**. Available Source:<https://datasheet.octopart.com/a000066-arduino-datasheet-38879526.Pdf>
- Thai Easyelec. 2016. **Espino32 User Manual Version 1.0**. Available Source: https://Thaieasyelec.Com/Downloads/Etee061/Espino32_User_Manual_Th.Pdf
- U.S. Food And Drug Administration, 2018. **Infusion Pumps**. Available Source: <https://www.fda.gov/medicaldevices/productsandmedicalprocedures/generalhospitaldevicesandsupplies/infusionpumps/>

Design and Implement of IoT-Based Electric Slide-Up Door Control System Using Raspberry Pi 3 Model B Case Study: Department Of Electrical Engineering RMUTL NAN

Charnyut Karnjanapiboon^{1*}, Aunnon Buasre¹ and Pairoj Piyarungsan¹

ABSTRACT

The building of electrical engineering department at RMUTL NAN has a traditional electric slide-up door in the front of the building. The routine task of every official day, is that the users have to open the door at 7:30 am and close the door at 5:30 pm by using a key to access a door control box, then press a switch for commanding the door. The use of internet of thing (IoT) technology that is widely used in the world can bring the convenient way to the users. There are 8.4 billion embedded IoT devices around the world operated now. To take the advantages of IoT technology, this paper proposes a design and implementation of the internet of thing based electric slide-up door control system using Raspberry Pi 3 model B. The Raspberry Pi is a credit-card-size and low-cost system on chip microcomputer that was developed for children to learn a computer programming skill. Blynk is a free mobile phone software for android and ios system that is used for assisting the beginners to develop their first rapid prototype of IoT system with easy procedure. The users can control this prototype system by personal mobile phone using Blynk application or by a computer using web application. The experiment with the electric slide-up door has shown that after the users command the door up via Blynk application, the time when the door moves up from fully-closed to fully-opened takes 10.58 seconds and after the users command the door down via Blynk application the time when the door moves down from fully-opened to fully-closed takes 8.73 seconds.

Keywords: Blynk Application, Internet of Thing (IoT), Raspberry Pi 3

¹ Department of Electrical Engineering, Faculty of Engineering, Rajamangala University of Technology Lanna NAN, 59 Moo13, Fai Kaeo, Meuang, Nan, 55000, Thailand

*Corresponding author, e-mail : charnyutk@gmail.com

Introduction

It is the fact that every building has a door for allowing people to access it or not. Currently, there is a remote control door that can be controlled remotely, mostly are electrical doors. While raining the users not wet because they do not need to walk in the rain to open the door. The door will lock itself when it's turn off so the user does not waste time for locking the door. The remote control door acts as a key in itself. Of course, the installation of remote doors, safety devices are also required, such as emergency backup power source, when the door is opened or closed. So, the motor can be used even if the power outage. The electric door system can be used manually if the users do not want to use the remote control. At present, there are many brands of the electric door seller are available in the market. Usually, the door was controlled using radio frequency (RF) remote control. The electric door package included one or two RF remote controls. For large buildings with more than two officer, a safety box must be built near the door in function to keep the RF remote control in as shown in Figure 1. To open the electric door, the user first unlocks the safety box and press the button of the RF remote to command the door to open or close. This routine is inconvenient to use. Nowadays, Internet technology is growing and online in almost every area in the world.

To utilize the benefit of Internet and IoT technology with electrical doors. This article proposed Design And Implementation Of Internet Of Thing Based Electric Slide-Up Door Control System Using Raspberry Pi 3 Model B Case Study: Department Of Electrical Engineering RMUTL NAN. In order to demonstrate the ability of IoT technology that affected the modern lifestyle of human era.



Figure 1 The RF-remote control box

An Internet of Things (IoT) is a technology that discusses a thing has been connected to the internet (Jitphomma and Lyimpornjitvilai, n.d.). IoT has been proposed since 1999 by kelvin Ashton, MIT's Media Center. IoT connects to the Internet network to report the status of the device, an important data of the device, and send control commands for the device. IoT may have different names, such as Machine to Machine (M2M), Ubiquitous Computing, Embedded Computing, Smart Services or Industrial Internet. The key to creating an IoT system is an embedded system. This system is interfaced to a sensor and send data forward to the server in a cloud through the Internet network. By implementing embedded devices into things, the device will work as a genius.

Home appliances use more embedded systems, enabling them to work on their own and can be integrated into a larger system. The connection between things is working systematically, making things work together over the Internet. The data transmission can be sent anywhere and anytime. It is an automated system that can be Person to thing P2T or thing to thing t2t IoT technology is an application and service on the high Economic value added

affair that grown considerably. IoT is a technology that the world needs to pay attention to the machine based on the intelligent system started from Machine to Machine M2M. The connection between the device and the device is a main important part of the IoT system.

Examples benefit of IoT, the user is allowed to use the mobile devices to monitor the energy environment, to control their infrastructure at anywhere anytime. The cooperation between IoT developers and farmer can develop an IoT equipment that appropriates with the farming tasks. IoT equipment also providing a reliable data and leads to high accuracy decision making in the production process of the agriculture.

In Smart City, The People will require more convenient service such as traveling with smart vehicles that need to be built with basic infrastructure to provide connectivity in a V2I (vehicle to infrastructure) protocol such as a signaling device and traffic information. The vehicle needs to communicate with each other in order to make it travel faster and safer. An intelligent city is involved many technologies, such as wireless communication and wire communication, internet technology, embedded system, Intelligent Wireless Networking Technology, Home automation, Office automation and Industrial automation.

Components of IoT system are 1) Things, 2) Device controller, an input device, an output device, 3) the wireless internet connection or wired internet connection, 4) Data, 5) Database management System, Cloud Server. The thing in an IoT system can be anything that has an embedded system to connect the Internet. In modern IoT technology, the connection of the devices should be wireless communication. There are many operators offers a wide range of cloud server services, some of them charge and some of them free of charge.

Blynk is one of the IoT platforms for smartphone and computer applications that make it easy to create the IoT system for a beginner (Tuhm-nahk, n.d.). The Blynk is connected to a remote device over the Internet network using smartphones, the developer does not need to provide anything whether it be a web server, a web page, a display and a control software. The website www.blynk.cc is the work of a new generation of people who propose a project into Kick Starter. The founder is Pavel Baiborodin. Blynk first launched in May 2015. It provides the tools to develop the IoT system for the beginner. The Blynk application is compatible with all popular hardware including the Arduino board, ESP8266, ESP32, Raspberry Pi, Orange Pi and etc. The strength of Blynk is to provide a highly scalable cloud computer server to users. It also allows users to create their own Blynk server on a PC or Raspberry Pi that can store everything on your own computer. Internet of things for planting in smart farm hydroponics style (Pitakphongmetha *et al.*, 2006) is an example of a research topic that uses Blynk application to monitor temperature and humidity and control relay for hydroponic systems.

Raspberry Pi (Sirikarnchit-tavorn *et al.*, n.d.), a single board microcomputer, was created under the concept that wants the kids to write programs with cheap tools. Eben Upton and his team at the Raspberry Pi Foundation are distributed to students in the computer science field at the University of Cambridge, UK, for learning and brainstorming aimed to help children get interested in programming. But it limited in the field of university education. Back in the year 2006, the first prototype of Raspberry Pi was implemented based on the Atmega644 microcontroller. It was chipped by ATMEL, with the release of a schematic circuit and a PCB circuit board. With this approach, a team of academics and computer science experts in the field of software and hardware can be assembled to exchange information and learn from each other, leading to design with a new processor chip. Inspired by Acorn's BBC Micro, the original ARM chip maker, the raspberry pi was named as ABC Computer because it wanted to convey that it was a startup computer that could be compared to the English textbook ABC.

Then, Eben Upton produced a motherboard board that came out with the ARM processor chip as the USB Flash Drive size. There is only one USB port and one HDMI port. He has to wait for 5 years until the end of August 2011. The Alpha version of the 50 prototype board was produced for testing and presentation to interested users. In the same year, Raspberry

Pi Model B in the beta version of 25 boards was tested again, this time with Linux operating system. It can play HD video with 1080p resolution. The whole world is turning the spotlights of the embedded system focused on Raspberry Pi. Raspberry Pi can do everything that computers can. But more flexible when used in embedded systems project. Because the mainboard is much smaller and has many GPIO ports for interfacing with another device. An internet access makes Raspberry Pi easy to send and receive signals to control its system efficiently. The user just has a basic programming knowledge.

Principles of system design

In the proposed systems, there are two main controllers. The first controller is an RF Door Controller and Motor Drive System. It receives a door command signal from RF remote controller and push-button switch then supplied the electrical power to the motor of the Electric door. Another controller is Raspberry Pi 3 Model B function as the main IoT controller. This controller connects to the internet network in order to receive the user command and communicated a data to the user via the internet network. This two controller is linked together by an electrical interfacing circuit. The interfacing circuit consists of three 330 ohm resistors act as a Current limit for the Light emitting diode in optocoupler and three optocoupler act as the electrical isolating circuit between two controllers. There are three acts of the push button switches for commanded the door: UP, STOP and DOWN command. The diagram of the proposed Internet of Thing Based Electric Slide-Up Door Control System is shown in Figure 2. The wiring diagram is shown in Figure 3. In an RF Door Controller and Motor Drive System: a switch S1 function as a UP command, a switch S2 function as a STOP command and a switch S3 function as a DOWN command.

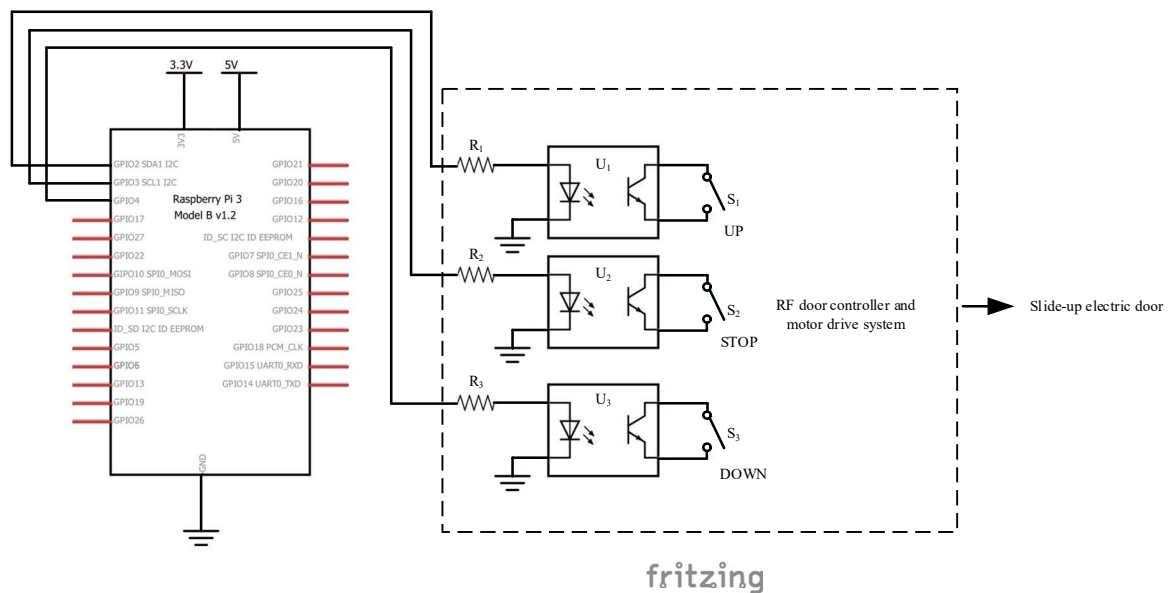


Figure 2 The diagram of the proposed slide-up electric door control system

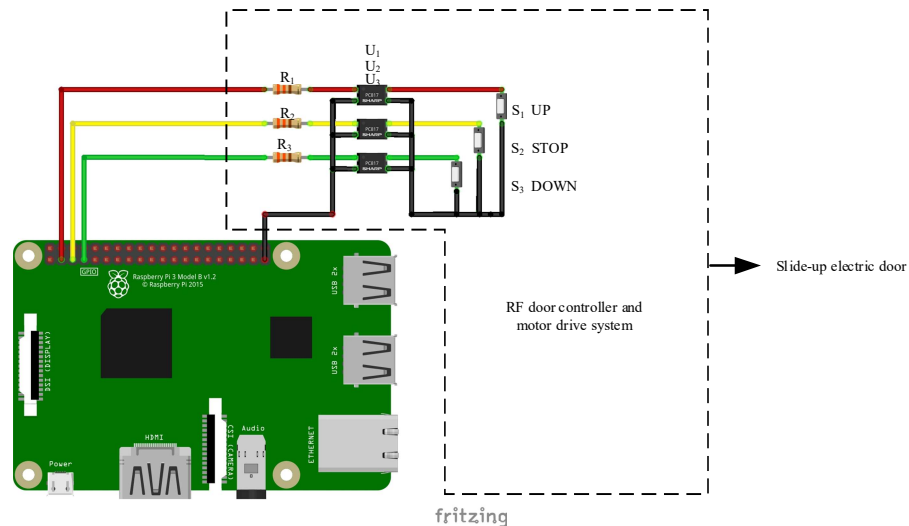


Figure 3 The wiring diagram of the proposed slide-up electric door control system

System operation principle

The operation principle of this proposed system can be described as follow: the user login to Blynk application on iOS or Android system as shown in Figure 4(a) then create the “Front door” project act as a user interfaces for the user as shown in Figure 4(b). The user interface consists of three button command: UP, STOP and DOWN. When the user wants to open the door, the user presses the UP button. When the user wants to stop the door, the user presses the STOP button. When the user wants to close the door, the user presses the DOWN button. The communication software between Blynk application and Raspberry Pi is shown in Figure 5. The user interface of Blynk application in this article is present only ios system. On the other hand, for android system, the 95 percent of the procedure is similar to ios system. The protocol TCP/IP is a communication channel between Blynk application and Raspberry Pi.

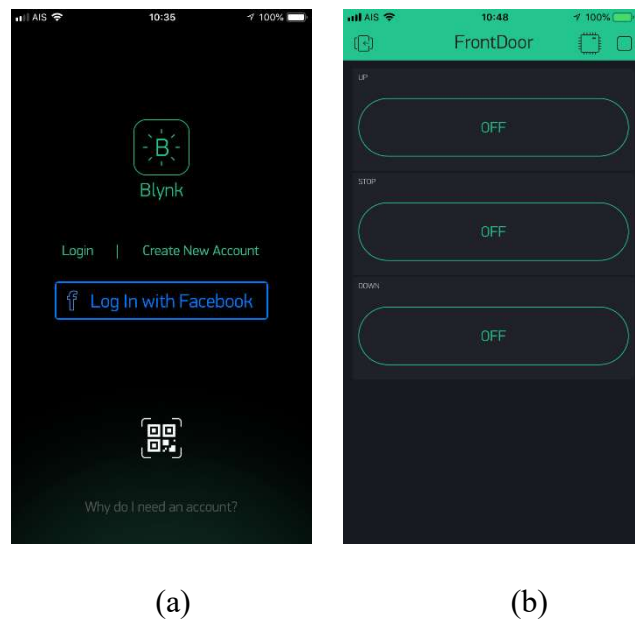


Figure 4 Blynk login page and Blynk project page.

```

var Blynk = require('blynk-library');
const Gpio = require('onoff').Gpio;
const btn_up = new Gpio(2, 'out');
const btn_stop = new Gpio(3, 'out');
const btn_down = new Gpio(4, 'out');

var AUTH = '8af4da176d054e6996e5d902ad54175d';

var blynk = new Blynk.Blynk(AUTH);

var v0 = new blynk.VirtualPin(0);
var v1 = new blynk.VirtualPin(1);
var v2 = new blynk.VirtualPin(2);

v0.on('write', function(param) {
  btn_up.writeSync(parseInt(param[0]));
});

v1.on('write', function(param) {
  btn_stop.writeSync(parseInt(param[0]));
});

v2.on('write', function(param) {
  btn_down.writeSync(parseInt(param[0]));
});

blynk.on('connect', function() { console.log("Blynk ready."); });
blynk.on('disconnect', function() { console.log("DISCONNECT"); });

```

Figure 5 the Node.js source code for Raspberry Pi

Experimental Results

The backside view of traditional electric slide-up door control system is shown in Figure 6(a). The control box of the RF door controller and motor drive system is installed at the right side of the door. The detail the RF door controller and motor drive system is shown in Figure 6(b). The inside detail the RF door controller with a modified circuit using Raspberry Pi 3 is shown in Figure 6(c).

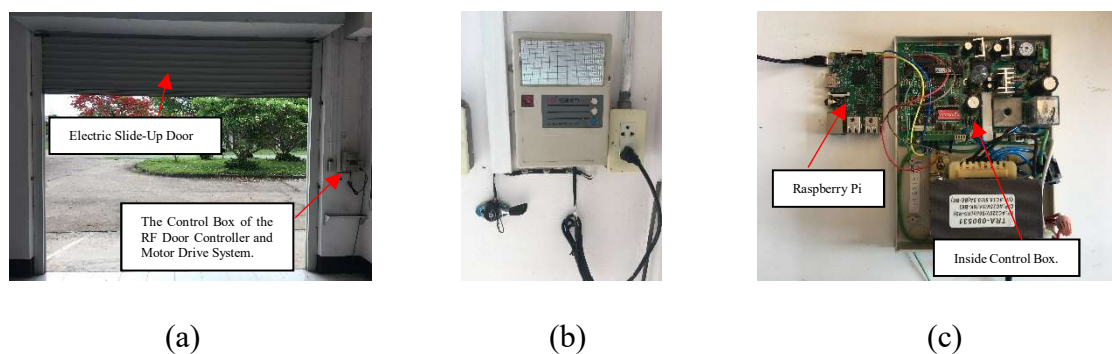


Figure 6 The inside detail the RF door controller with a modified circuit using Raspberry Pi 3

After the Raspberry Pi single board computer receive the command data from the user By Blynk application, the Raspberry Pi send the digital logic to appropriate the command type of the user to the RF door controller and motor drive system in order to slide the electric door up, to slide the electric door down or stop moving the door. To experimental with the door, first, command the door to fully-closed as shown in Figure 7(a). Second command the door to move up. The half-opened door is shown in Figure 7(b). The fully-opened door is shown in Figure 7(c). it was found that the time that the door moves up from fully-closed to fully-opened is taken 10.58 seconds (six samples 10.83, 10.62, 10.53, 10.43, 10.42 and 10.65 seconds) and the time that the door moves down from fully-opened to fully-closed is take 8.73 seconds (six samples 8.52, 9.15, 8.78, 8.54, 8.72 and 8.64 seconds).



Figure 7 the position of the electric slide-up door while operated

Conclusion

The Internet of Thing Based Electric Slide-Up Door Control System Using Raspberry Pi 3 Model B shows a good performance. It serves a convenient way to opened or closed the door for the user with response time less than 100 ms. The Raspberry Pi using in this article is used to demonstrate the ability of IoT system that effect to a modern lifestyle of the people. But there are many Iot chips that cheaper than Raspberry Pi such as ESP32, ESP8266, and Arduino Wifi module. In the future work, a different platform must be studied in order to provide a broad solution for the smart IoT system. The cost of the proposed system is approximately 1,800 baht.

Acknowledgment

The authors would like to express their sincere thanks to the RMUTL and Smart Farm Research and Development Laboratory for providing the necessary tools.

References

- Jitphromma, T. and Lyimpornjitvilai, C. n.d., **Experiment in Internet of Things (IoT) Devices**. (C) Innovative Experiment Co., Ltd.
- Jitphromma, T. and Lyimpornjitvilai, C. n.d., **Internet of Things (IoT) with NodeMCU**. (C) Innovative Experiment Co., Ltd.
- Jitphromma, T. and Lyimpornjitvilai, C. n.d., **Raspberry Pi 3 Basic Device Control using Internet**. (C) Innovative Experiment Co., Ltd.
- Pitakphongmetha, J., Boonnam, N., Wongkoon, S., Horanont, T., Somkiadcharoen, D., &Prapakornpilai, J., 2016, **Internet of things for planting in smart farm hydroponics style**. International Computer Science and Engineering Conference (ICSEC), pp. 1–5.
- Sirikarnchit-tavorn, O., Jaiyen, K., Kornkaew-wattanakul, V., laio-wattanatum, N. and Jitphromma, T. n.d., **Raspberry Pi 3 Interfacing with GPIO**. (C) Innovative Experiment Co., Ltd.
- Sirikarnchit-tavorn, O., Jaiyen, K., Kornkaew-wattanakul, V., and Jitphromma, T. n.d., **Raspberry Pi 3 Interfacing with GPIO 2nd**. (C) Innovative Experiment Co., Ltd.
- Sirikarnchit-tavorn, O., Jaiyen, K., Kornkaew-wattanakul, V., laio-wattanatum, N. and Jitphromma, T. n.d., **The Basic Usage of Raspberry Pi 3**. (C) Innovative Experiment Co., Ltd.
- Tuhm-nahk, S. n.d., **Easy Internet of Things (IoT) with Blynk**. (C) Innovative Experiment Co., Ltd.

Development and Performance Evaluation of a Cassava Digger Namely Fork Shear Blade Type

Sahapat Chalachai^{1*}, Kritsana Naoprakhon¹, Rangsak Koodsamrong¹, Peeyush Soni² and
Anuchit Chamsing³

ABSTRACT

The study designed and tested a digging unit for collecting data for the design of a cassava harvester that is suitable for Thai farms. The development of a cassava digger was suitable for a 36 hp tractor for continuous working. After designed, the cassava digging unit was functional tested on fork shear blade type at three different digging angles of 20°, 25° and 30° and three different speeds of 1.3, 1.9 and 2.6 km/h respectively. After modifying the cassava digging unit prototype, the field performance test of the prototype machine was evaluated. The scope of testing was improvement, mainly to reduce draft force, fuel consumption, and harvesting loss to increase harvesting capacity and field efficiency. The main features in the proposed design is it Fork shear blade (55 cm) which can be adjustable in length and angle of the blade for versatile use in vivid planted areas. The results indicated that the best digging efficiency was obtained when digging with 20 degree digging angles of the blade and the speeds of 1.9 km/h (gears Low-3). The results showed that the capacity was 0.22 ha/hr, fuel consumption per hectare was 25.37 L/ha, field efficiency was 87.18% and a cassava loss in soil was around 7.11%. This loss is fairly low as compared to the other existing designs. This developed cassava digger is accepted by private sector for its commercial production.

Keywords: Cassava, Cassava digger, Harvesting, Fork shear blade type, Thailand

¹ Department of Agricultural Engineering and Technology, Faculty of Agriculture and Natural Resources, Rajamangala University of Technology Tawan-ok, Bangphra, Sriracha, Chonburi Province 11120, Thailand

² Department of Food Engineering and Bioprocess Technology, School of Environment Resources and Development, Asian Institute of Technology, P.O. Box 4 58 Moo 9, Km. 42, Paholyothin Highway, Klong Luang, Pathum Thani 12120, Thailand

³ Agricultural Engineering Research Institute, Department of Agriculture, Bangkok 10900, Thailand

*Corresponding author, e-mail : sahapat@hotmail.com

Introduction

Cassava was originated in the tropical areas of America, particularly in South America. Mexico, Peru, Guatemala and Honduras are regions where cassava was found before three to five thousand years back, and then the plant was circulated across America and elsewhere. The transport of cassava to the African continent was accomplished by the slave brokers and Portuguese in the 15th period (TTSA, 2004). Between 2006 and 2010, the world's cassava output grew 1.93% per year because producing countries Congo, Mozambique, Ghana, Vietnam and Indonesia expanded to increase production to meet consumer demand and the increasing demand for renewable energy production. Cassava is considered as a highly economic crop for a country like Thailand. It is used basically as raw material for several industries. It is also used for two purposes, firstly as energy crop for ethanol production which is needed for gasohol production, and secondly as substitute for Methyl Tertiary Butyl Ether (MTBE) in bio diesel production. (Kongsawat, 2004). Thailand is a major world exporter of cassava worth 2 billion USD (65 billion THB) per year. It is the fourth largest cassava maker after Nigeria, Brazil and Indonesia. In Thailand, the planted area for cassava is 7,905,056 rai which is the fourth largest area after rice, maize and rubber with a total production of 30 million tons (FAO, 2014). The total area used for cassava cultivation is 1.34 million hectares, which is 5% of the total area used for cultivation (FAO, 2016). Thailand uses about 50% of cassava root production, around 18 million tons in 2006, to extract about two million tons of starch. Half of this is destined for the domestic food market and supplied to industries, while the rest is exported in the form of a higher-value modified starch (FAO, 2006). Cassava can also be processed into pellets and chips. Furthermore, the price of cassava is guaranteed by the Thai Government, which is also encouraging farmers to increase land used to cultivate the root and switch from other crops to cassava.

In Thailand, there are two common harvesting practice patterns: a) mostly using human labor with simple tools; and b) using of cassava digger attached to a tractor and then processed by human labor (Chamsing, 2012). However, the rate of harvesting shows that about 37% of the labor cost and 10% of the harvesting cost could be saved by using the second pattern. Currently, labor shortage is a major constraint for cassava production in Thailand, especially for harvesting. Because of the growing economy, and in particular industrial growth, there has been a shift of labor from the agricultural sector to the industrial sector, influenced by more comfortable working conditions, as well as higher wages.

Harvesting cost is the largest contributor to cassava production cost due to the high labor requirement and labor shortage problems (Jarernrat *et al.*, 2007). Like other important economic crops of the country, except for rice where rice combine harvester is available and popularly used (Chamsing, 2007), cassava do not yet enjoy luxury of adequate mechanization. Despite several designs of cassava diggers have been developed since over 30 years, yet at present, cassava diggers are not popularly used as expected. However, researchers continuously attempted to bring about necessary modifications in existing designs (Mongkol tanatas *et al.*, 1992; Mongkol and Chamsing, 2007). Lacks of adequate cooperation among cassava producers, farmers, researchers and extension officers as well as technical complexity of cassava digger itself are possible the prime causes of current challenge. Therefore, in this research, to lower the harvest cost and address the labor shortage problems in cassava production, study on the current situation and resulting development of a suitable cassava digger to address current problems was felt necessary.

Materials and Methods

The methodology used to achieve the objectives of this research is detailed in this topic.

Conceptual framework

The conceptual framework is present by schematic show in **Figure 1**.

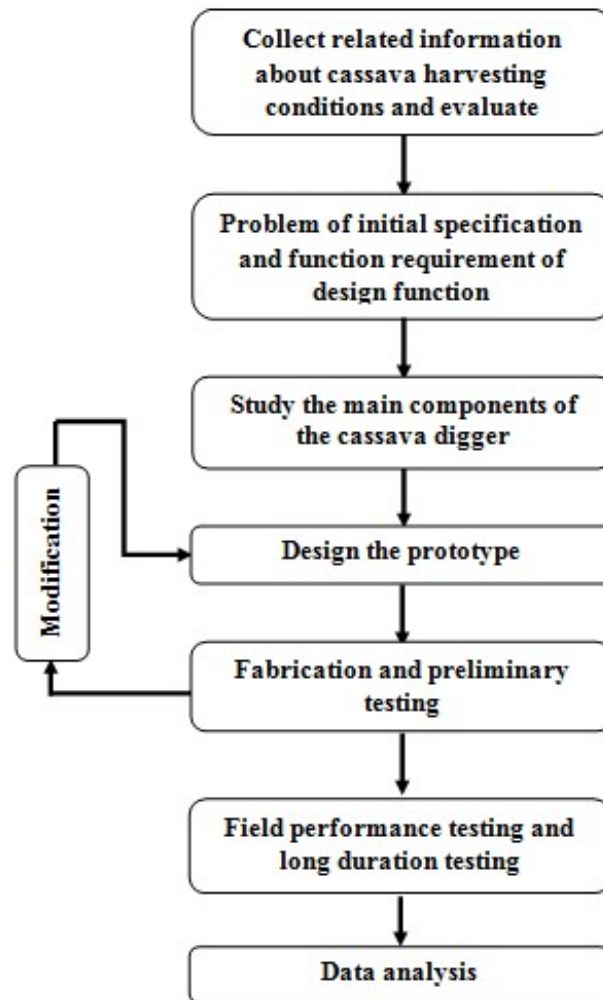


Figure 1 Schematic block diagram of the conceptual framework.

Study current harvesting methods and some physical properties of cassava

This study will collect necessary data for develop and evaluate a cassava harvester suitable for Thai farms and designing the various components of prototype. Sufficient information of harvesting conditions will obtain from previous research. Burirum province is the larger area of planting cassava was selected for field survey and testing. Issues in the study of current situation of cassava harvesting and use of existing available cassava diggers included the problem, constraints and farmer's perceptions.

Soil properties measured

While conducting research, it is very important to characterize the soil in the experimental field. So in order to be specific in the characterization of soil, the following soil properties will be measured. The resistance of soil is the ones effect of lifting force for cassava root, so measurement of soil properties around the root is a key factor in this research study. Some of the soil properties will be measured in laboratory prior to the field experiments while other soil properties will be measure during the field experiments. The experiments were conducted in the field at Buriram province, Thailand. **Table 1** shows the properties of the soil at the test site.

Table 1 Soil properties measured before the experiments at Buriram province

Item	Detail
1) Type of soil	Buriram sandy loam rad color and have contaminated gravel
2) Mean soil clod dimension	1.35 mm
3) Soil moisture content	16.16 %wb
4) Bulk density of soil	1.22 g/cm ³
5) Consistency limits	
Plastic limit (w.b.)	42.20%
Liquid limit (w.b.)	86.2%
Plasticity Index (I _p)	44.06
6) Penetrometer profile and cone index (15 places)	
at 50 mm	0.53 MPa
at 100 mm	0.90 MPa
at 150 mm	1.09 MPa
at 200 mm	2.24 MPa
at 250 mm	2.58 MPa
at 300 mm	3.70 MPa

Design and Fabrication of the Prototype

A much-reported constraint of cassava harvesting by using a cassava digger attached to a 50 hp tractor of larger is its limitation in continuous operation and the tractor is too large. Main reason for this limitation is because the cassava roots that were dug in previous pass are pressed by tractor wheel in the following pass – causing to increase damage and yield losses. As a current practice, a number of laborers are required to wait along the digging rows to collect the dug root out immediately after digging before continue with the next row. Retain link operation; harvesting loss and high fuel consumption are thus very commonly reported problems in the current situation.

To develop and evaluate a cassava digger attached to 36 hp tractors a testing unit was developed for examining related components including Fork shear blade (size and blade angle). Harvesting loss, produce damage, fuel consumption and field capacity were among the major assessment indicators.

Experiment Parameter

The prototype of the digging unit was used to study the performance on a cassava field in the Northeast of Thailand (Buriram province). Three different blade angles (20°, 25° and 30°) were used at three different tractor speeds (low-2, low-3, and high-1) (**Fig. 2**). The dynamometer was used to measure the draft force requirement. The soil condition was measured. A comparison between treatment means were done by least significant difference (LSD) at $P < 0.05$. The relationships between dependent and independent variables were considered by simple linear regression and/or non-linear regression

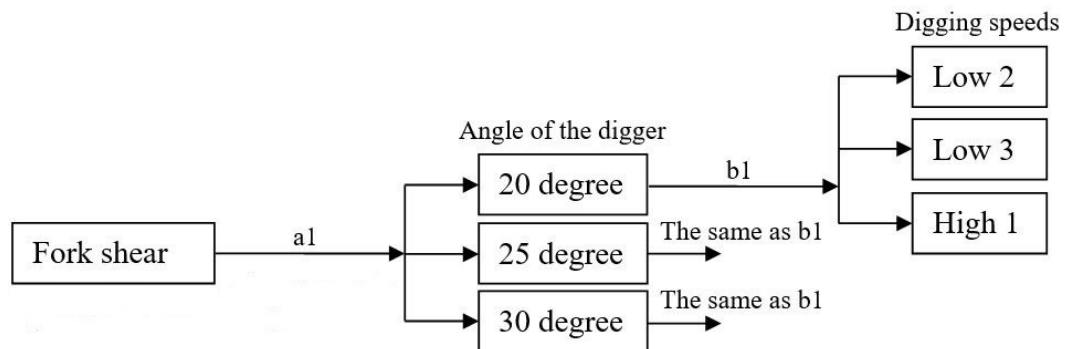


Figure 2 Experimental designs for digging unit

Results and Discussions

Current status of cassava harvesting and use of cassava digger

Recommended age of cassava harvesting is 8-14 months; survey revealed that in the study area harvesting in range of 10-12 months is commonly practiced. Usually cassava harvesting in Thailand is done throughout the year. Over 10% of cassava in a year was harvested during November to March of the next year (OAE, 2010).

Harvesting system:

a) Manual harvesting: In Thailand cassava is ready for harvest starting from 8 to 12 MAP. The method of harvesting by small scale farmers in Thailand using specific hand tools are shown in **Figure 3** (Klanarong and Kuakoon, 2007).

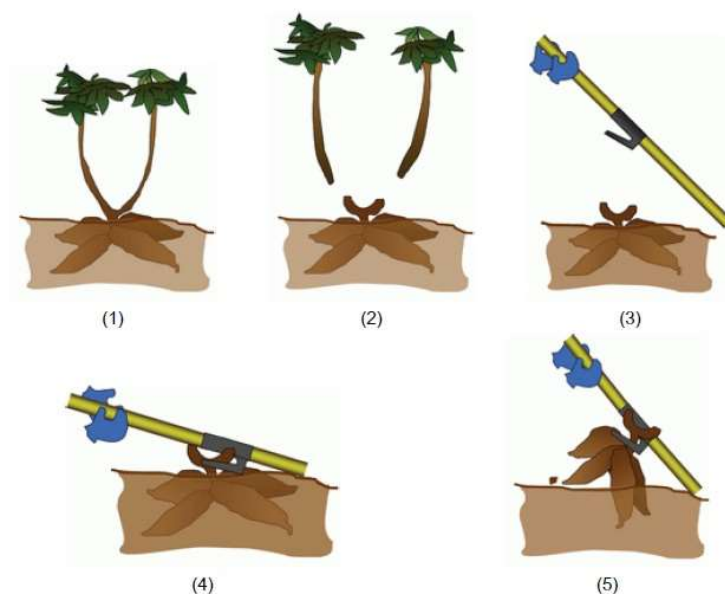


Figure 3 Procedural steps of harvesting cassava by small-scale Thai farmers using locally made hand tool called-Mac hoe (Klanarong, 2007)

There are four steps in harvesting. The first step is to cut stem before harvesting; cassava stems are both cut and collected for using as stock for the next crop planting (**Fig. 4**), or some farmers just remove it from field (Sirikun, 2009). Second step is digging or pulling cassava root from the soil; using a cassava lifter indigenously developed by Thai farmers that is known as “Mac hoe” (**Fig. 5**) (Mongkol *et al.*, 2007). Third, collect and cutting cassava root from the stem, and eventually carrying it to truck for transportation and sale (**Fig.6**) (Wongpichet *et al.*, 2003).



Figure 4 Thai farmers: a) cutting, and b)collecting cassava stems before root harvesting (Sirikun, 2009)



Figure 5 An indigenously developed Cassava lifter by Thai farmers (Mac hoe). (Mongkol *et al.*, 2007)



Figure 6 Activities done after digging cassava root (Wongpichet *et al.*, 2003).

b) Tractor-mouthed cassava digger: Mechanical harvesting of cassava involves the use of a harvesting implement integrally hitched to a prime mover, usually tractor, to uproot the cassava roots. However, manual effort is still required after the uprooting has been completed to collect and separate the cassava root from stem. The field is also required to be in good condition for an optimum mechanical cassava harvesting operation such as: a) a field free from hidden obstructions (rocks, roots, stumps etc. down to 40 cm deep) of sizes that can interfere with lifting the root; b) having good weed control as weeds block the lifters; and c) cutting down (coppicing) the cassava plant to a stalk height of about 30 cm prior to harvesting (USDA and NRCS, 2003).

Presently, majority of large-scale cassava farmers in Thailand employ tractor-mounted cassava digger. Ironically, harvesting cost constitutes the largest share in cassava production due to the high labor requirement and high wages especially during months of labor shortage (Jarernrat *et al.*, 2007). Given the importance of mechanization in cassava production, cassava diggers have been developed since over 30 years. **Figure 7** shows the cassava diggers that are available in Thailand, and **Table 2** compares the salient features of tractor-mounted cassava diggers available in Thailand. Based on the shear blade used, the existing cassava diggers can be broadly grouped as fork shear blade type and curve shear blade type (Chamsing *et al.*, 2012).



a. Fork shear blade type



b. Curve shear blade type

Figure 7 Type of cassava diggers available in Thailand (Chamsing *et al.*, 2012).

The fork shear blade type is popularly used at Sakeaw, Prajin Buri and Chachoengsao and Buriram provinces. Both turning and non-turning (only lift up) soil with cassava root types are available during digging operation (Fig. 8). In case of turning type, two designs are available namely, turning both left and right sides, and only one side of the digging bottom (Fig. 9). The former type (both sides turning) may cause problems of unable to continuous working, especially when attached to medium and large size of tractors. This is due to wheel pressing on dug cassava root that causes to increase damage and harvesting loss as well as requires additional labor to collect and move out cassava root from the previously dug row. Although cassava diggers are commercial produced and accepted for use by some farmers, some modification/adjustment after buying still needed. Moreover, results showed that by fabrication structure and working operation trend to require high draft force, difficult for depth control and may cause damage to hydraulic system of tractor. Over turning of soil and cassava root also caused high harvesting loss and labor requirement. Therefore, improvement over existing designs was required.



(a)



(b)

Figure 8 Harvesting by (a) turning type cassava digger and (b) by non-turning type (Chamsing *et al.*, 2012)



Figure 9 Turning soil and cassava root for (a) both sides and (b) turning only one side (Chamsing *et al.*,2012)

Table 2 Comparison of tractor-mounted cassava diggers available in the Thai market

Type	Popular Use In	Advantage	Disadvantage
Fork shear blade	Rayong and Prachinburi	<ul style="list-style-type: none"> - Do not turn over the soil - Can keep the root for 2-3 day - Tractor not breaking the root for next row - Can work in the hard soil 	<ul style="list-style-type: none"> - More cassava loss in the soil - Working width to small - Need more power
Curve shear blade	Nakhonratchasima, Kampkaengphet, Nakhonpathom, Ralchaburi and Kanchanaburi, etc.	<ul style="list-style-type: none"> - Easy to maintenances - Easy to collect the cassava root - Not much about the cassava loss in the soil - Can use in every soil and small tractor 	<ul style="list-style-type: none"> - Tractor breaking the root for next row - More breaking loss - Need more labor to collect the root

Source: Field survey from Chamsing *et al.* (2012)

Table 3 Man-hour requirement of traditional harvesting method

Item	Man-hour requirement
Grading quality of stem, man-h/ha	0.0
Number of operator	1
Man-hour requirement	
a) Stem cutting, man-h/ha	36.75
b) Stem collecting, man-h/ha	8.75
c) Storage, man-h/ha	4.88
Total process, man-h/ha	50.33

Sources: Sirikun, (2009)

From **Table 3** show the efficiency of the manual cutting stem harvesting method. The capacity of manual harvesting was 0.16 ha/man-day, or the man-hour requirement was 50.33 man-h/ha.

Research and development a cassava digger

Fabrication of testing unit and primary test: The digging unit is design to meet the current cassava root harvesting practices. Before designing the cassava unit, the type and problem of cassava digger that is available to sell in the market has to be studied. In this study, fork shear blade type (**Figure 10a**) is used. All this information will be used for analysis of the problem and to guide the design and development of the prototype of cassava root digging unit. The knowledge and technology used for fabrication of digging unit is simple so that the local workshops can manufacture it without difficulty. The prototype of the digging unit is shown in **Figure 10b**. A cassava digging in from of testing unit was developed to study the important factors. It was able to adjust and replace of some component (blade and angle of the blade, distant between bottom set to tractor and adjustable of cross beam). The results show that the testing unit was capable to work continuously. However, size of main structure need to be increased.

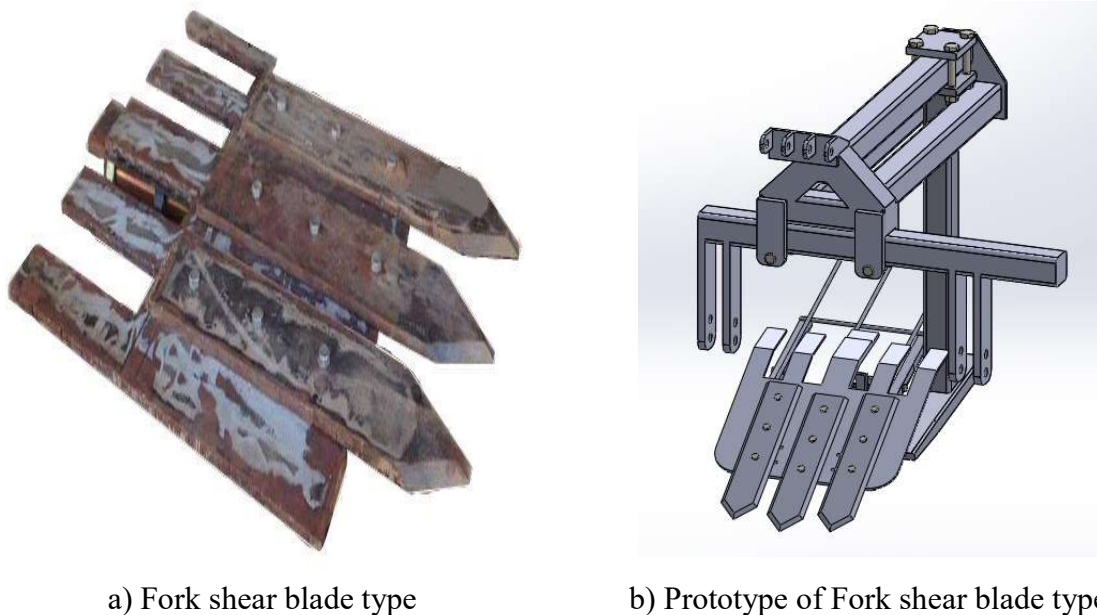


Figure 10 The prototype of cassava digger

Effect of type and angle of the blade on draught force: The draft requirement of the cassava digger at Fork shear blade type with different angles was determined in the field. The drafts of digger with different angles at the same traveling speeds of 1.3 km/hr are presented in **Table 4**. The results indicate that the draft of the whole digger increased rapidly with increasing blade angle at a given speed. The average drafts of the digger with fork shear blade type it was 5.56 to 9.88 kN/row. So, the blade angle at 20° was select.

Table 4 Average draft requirement and wheel slip at the same traveling speeds of 1.3 km/hr

Angle of blade	Draft per unit width (kN/row)	Wheel slip (%)
20°	5.56±0.71	7.50±0.37
25°	6.70±0.47	8.80±0.31
30°	9.88±0.28	9.48±0.53

(Mean± standard deviation, n=5)

After obtaining the results of draft requirement of cassava digger, the Equations 1 was calculate Drawbar Power (kW) and the Equations 2 was calculate Brake Horse Power (kW)

$$\text{Draught Force (kN)} \times \text{Average Speed (m/s)} \quad (1)$$

$$\text{Drawbar Power (kW)} / 0.19 \quad (2)$$

Table 5 Average power requirement for digging at Buriram province

Type	Speed (m/s)	Drawbar Power (kW)	Brake Hp (kW)	Hp
Fork	1.3	2.22±0.36	11.70±1.87	10.39±1.66
	1.9	4.11±0.35	21.65±1.84	19.22±1.63
	2.6	7.88±0.36	41.46±1.91	36.80±1.69

(Mean± standard deviation, n=5)

Table 5 shows the drawbar power, brake horse power and horse power at different traveling speeds (1.3, 1.9 and 2.6 km/h) observed for cassava digger. The results for fork shear blade type show the average drawbar power ranges from 2.22 to 7.88 kW, brake horse power from 11.70 to 41.46 kW and horse power from 10.37 to 36.80 hp. Therefore, the 36 hp of tractor available to use in this test

Field performance evaluation of digger: The designed cassava digger was evaluated for its performance on indicators, such as: working width, depth of digging, actual travelling speed, fuel consumption per hectare, field capacity, field efficiency and cassava losses in the soil. The three different gears of tractor - Low-2 (1.3 km/h), Low-3 (1.9 km/h) and High-1 (2.6 km/h) - were used in this study. The blade angle was selected at 20 deg and the engine speed was 1200 rpm.

The results shown in **Tables 6 and 7** indicate that the type of the digging blade was the most significant factor affecting digging depth, field efficiency, and cassava losses in the soil, but had little effect on fuel consumption. The operating speeds significantly affected the fuel consumption and field capacity, but had little effect on digging depth and field efficiency. The test results revealed that the performance of the digger depended on the type of the digging blade and traveling speed.

This study showed that the Fork shear type blade with gear L3 had the highest field efficiency and the least cassava losses in the soil and fuel consumption per hectare. Therefore, the Fork shear type blade with gear L3 is deemed suitable for this area. **Figure 11 and 12** shows the cassava digger testing in the field. The operating depth was about 30 cm.

Table 6 Performance evaluation for cassava digger testing at Buriram province

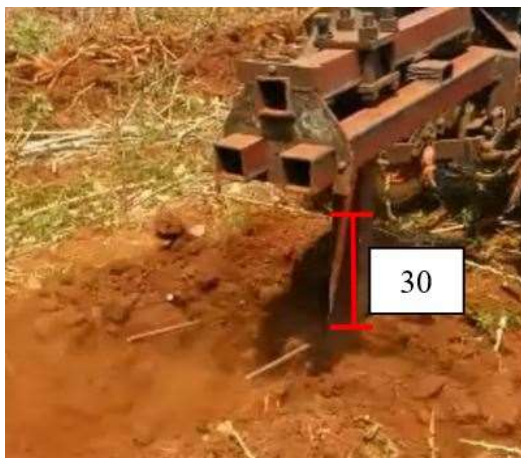
Item	Digger type		
	FL2	FL3	FH1
a) Working width, m	0.80	0.80	0.80
b) Depth of digger, m	0.28	0.28	0.27
c) Actual travelling speed, km/h	1.30	1.90	2.60
d) Fuel consumption per hectare, L/ha	25.36	25.32	26.67
e) Field capacity, ha/h	0.18	0.22	0.24
f) Field efficiency, %	85.55	87.18	84.20
g) Cassava losses in soil %	7.32	7.11	7.21

(FL2 = Fork shear blade type with gear low – 2, FL3 = Fork shear blade type with gear low – 3, FH1 = Fork shear blade type with gear high – 1, n = 9)

Table 7 Summary of ANOVA results for the field performance of digger

Source of variable	P-value				
	Digging depth	Fuel consumption	Field capacity	Field efficiency	Cassava losses
Type of blade (A)	0.000	0.020	0.095	0.000	0.000
Operating speeds (B)	0.001	0.000	0.000	0.001	0.038
Interaction (A *B)	0.383	0.586	0.139	0.785	0.040

The results shown in Tables 4 showed that the fork shear blade type with gears Low-3 had the highest field efficiency and least cassava losses in the soil and fuel consumption per hectare. Therefore, the fork shear blade type with gears L3 is suitable for this area.

**Figure 11** The 30 cm height of the soil**Figure 12** The cassava root after digging

Conclusions

Literature review and primary field survey showed that four harvesting operations are commonly practiced: a) stem cutting before harvesting; b) digging or pulling cassava root from the soil; c) collecting and cutting of cassava root from the stem; and d) carrying to truck for transporting and sale. Two harvesting patterns were categorized, which are a) employing laborers for all harvesting operations, and b) using cassava digger attached to tractor combined with employing laborers after digging operation. About 37% of labor requirement and 10% of harvesting cost were saved by using of the latter pattern. The existing cassava diggers used in Thailand had various types and sizes depending on geographical planted areas, socio economic characteristics and tractor size (50-70 hp). However, existing cassava digger designs still required to reduce draft, fuel consumption, wearing of tractor and harvesting loss. A new design of cassava digger capable of continuous working was developed. The main features were Fork type blade with adjustable, and angle of the blade for versatile use in wide soil condition.

The results indicate that the 36 hp of tractor can used and the best digging efficiency was obtained when testing on 20 degree digging angles of the blade and the speeds of tractor around 1.9 km/hr (gears Low-3). The information shows that the capacity was 0.22 ha/h, Fuel consumption per hectare was 25.37 L/ha, field efficiency was 87.18% and a cassava loss in soil around 7.11%. This loss is fairly low as compared to the other existing designs. This developed

cassava digger is accepted by private sector for its commercial production. However, the prototype needs to be testing in different area for approve the performance of machine.

References

- Chamsing, Anuchit. 2007. Agricultural Mechanization Status and Energy Consumption for Crop Production in Thailand. AIT Diss No. AE-07-01, Asian Institute of Technology, Pathum Thani, Thailand.
- Chamsing, A, Akkapol, S, Suphasit, S, Phakwipha, S, Yuttana, K, Khanit, W, Prasat, S. 2012. Research and Development of a Cassava Digger Attached to 50 hp Tractor. Agricultural Engineering Research Institute, Department of Agriculture. Proceeding of International Symposium on Agricultural and Bio-Systems Engineering for ASIA Sustainability: Opportunity and Channenge. Nong Lam University, Ho Chi Minh city – Vietnam, March 29-30, 2012.
- FAO. 2006. Food and Agriculture Organization of the United Nation. Available online at URL: <http://www.fao.org>
- FAO. 2014. Food and Agriculture Organization of the United Nation. Available online at URL: <http://www.fao.org>
- FAO. 2016. Food and Agriculture Organization of the United Nation. Available online at URL: <http://www.fao.org>
- Jarernrat, S., Sarongbol, N., Klannurak, K., Pokprasert, A., Tangsakul, S., Limsila, J. and Laebwan, U. 2007. Activity of Study on Opportunity and Constraints of Important Economic Crops, Experiment of the Worthiness and Farmer Risk from the Production and Pricing of Cassava and Sugarcane Production. In Proceeding of the Seminar on Research and Development Trend for Increasing of Cassava Productivity. pp. 135-139.
- TTSA 2004. Thai Tapioca Starch Association. Bangkok, Thailand. Tapioca Background. Available online at URL: <http://www.thaitapiocastarch.org/background.asp>
- Kongsawat, W. 2004. **Thailand's recorded in the End of 2004: Energy Situation of Thailand 2005-2008**. Post Today Newspaper. Available Source: <http://www.posttoday.com/thailand2547/plang.html>
- Klanarong S. and Kuakoon, P. 2007. **Utility of Cassava**. Thailand Tapioca Starch (TTSA), Bangkok. Available Source: [http:// www. Thailandtapiocastarch.net](http://www.Thailandtapiocastarch.net)
- Mongkol, T, Jaruwat, Wenujun, Satit, Jearaniku, Kanungsak and Jutasuwan, Sutin. 1992. **Analysis of using of cassava digger. AED Final Research Report 1992**, Research Register Number 3508006008. Agricultural Engineering Division, Department of Agriculture.
- Mongkol, T. and Chamsing, A. 2007. Cassava Digger. **Kasikorn Newspaper**, 80(5): 89-102.
- Office of Agricultural Economic (OAE). 2010. **Agricultural Statistic of Thailand Crop year 2008/2009**. Ministry of Agricultural and Co-Operative.
- Sirikun, C. 2009. Development of A Cassava stem Harvester. AIT Thesis No. AE-09-09, Asian Institute of Technology, Pathum Thaina, Thailand.
- USDA and NRCS. 2003. **Plant Guide – Cassava: Manihot esculenta Crantz**. National Plant Data Centre, Baton Rouge, Louisiana and Pacific Islands, Mongmong, Guam. Available Source: [http:// plants.usda.gov/plantguide/pdf/cs_maes.pdf](http://plants.usda.gov/plantguide/pdf/cs_maes.pdf)
- Wongpichet, S., Chusilp, S., Luenam, L., and Thangdee, W. 2003. **Development of Cassava Harvesting Process with Cassava Digger**. Department of Agricultural Engineering, Faculty of Engineering, Khon Kaen University, 40002

Application of Design of Experiment (DOE) for Aluminum Wheel of Single Pulley Performance for Transmission Line

Bussakorn Hammachukiattikul^{1*} and Sanga Kongkaew²

ABSTRACT

The single pulley is one of the major pieces of equipment used in the installation of transmission lines that are connected with towers. To carry out the structural analysis; therefore, the aluminum wheel is considered as the external forces acting on the groove inside wheel for structural analysis of the aluminum wheel is performed for carrying conductor. By this simulation is an effective to aluminum wheel; consequently, statistics principles combined with a simulation model were able to significantly reduce the von Mises stress. The distribution of stress in the aluminum wheel was also obtained. In this study, modeling design, analysis and mathematical model of aluminum wheel were carried out based on a design using Finite Element Analysis. Furthermore, Solidworks has been used for modeling, and Solidworks Simulations has been used for obtaining analysis results. We estimated 80 kN as the working load capacity to be gradually applied. Eventually, we observed the von Mises stresses that developed were less than the yield strength. For these results, von Mises stresses were compared with DOE's array for specific results. The design of experiments will be obtained through mathematical model and the integration of system Solidworks Simulation with Minitab solved. The simulation results proved the validation and effectiveness of the presented modeling approach for simulation of Minitab as well. Thus, the geometry which will obtain at the end of the simulation and the dimension will be considered and the prototype will be manufactured. Finally, Actual testing has been done by applying the load 80 kN to the wheel of single pulley. The aluminum wheel was assembled with a tool called dynamometer on the upper part by using rope to hook around the aluminum wheel for 180° while the lower part, the eye bolt was connected by the top of the experiment table base.

Keyword: CAD method, Aluminum wheel, Finite element analysis, Stress analysis, Design of experiment

¹ Department of Engineer, University of Thai-Nichi Institute of Technology, 1771/1, Suanluang, Bangkok 10250, Thailand

² Department of Engineering ,Zeck TSE International Ltd., 88/53 Ramkamhaeng 174 Minburi, Bangkok, Thailand, 10510

* Corresponding author, e-mail: bussakorn@tni.ac.th

Introduction

Pulleys are simple machines in the form of a wheel mounted on a fixed axis and supported by a frame. The wheel, or disk, is normally grooved to accommodate a rope. The wheel is sometimes referred as a “sheave” (sometimes “sheaf”). The frame that supports the wheel is called a block. A block and tackle consist of a pair of blocks. Each block contains one or more pulleys and a rope connecting the pulley(s) of each block. Single Fixed Pulley A single fixed pulley is really the first-class lever with equal arms. The arm from point “R” to point “F” is equal to the arm from point “F” to point “E” (both distances being equal to the radius of the pulley). When the first-class lever has equal arms. Thus, the force of the pull on the rope must be equal to the weight of the object being lifted. The only advantage of a single fixed pulley is to change the direction of the force, or pull on the rope.

Different types of pulley systems:

A. Fixed

A fixed pulley has an axle mounted in bearings attached to a supporting structure. A fixed pulley changes the direction of the force on a rope or a belt that moves along its circumference. Mechanical advantage is gained by combining a fixed pulley with a movable pulley or another fixed pulley of a different diameter.

B. Movable

A movable pulley has an axle in a movable block. A single movable pulley is supported by two parts of the same rope and has a mechanical advantage of two.

C. Compound

A combination of fixed and movable pulleys forms a block and tackle. A block and tackle can have several pulleys.

Modeling of Single Pulley Block

2.1 Geometric Dimension of Single Pulley Block

Engineering drawings of parts and assemblies were created in Solidworks. These drawings were fully associative with 3D solid models. All components of a single pulley block are shown in Figure 1.

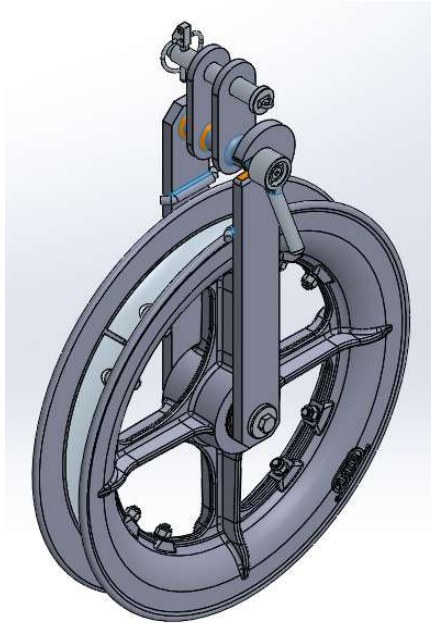


Figure 1 Single Pulley Block

An aluminum wheel was simulated by Solidworks Simulations as shown in Figure 2.

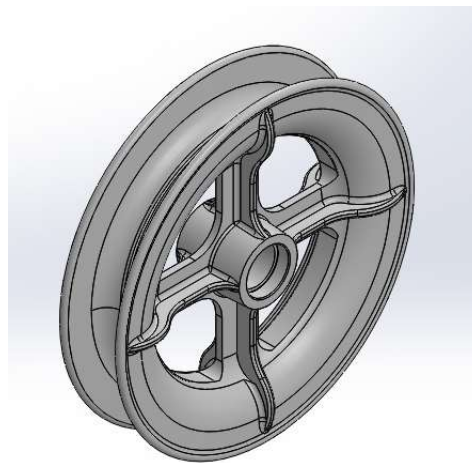


Figure 2 Aluminum Wheel

2.2 Analysis of Design of Experiments

The factors levels key parameter input variable (KPIV) have been defined in the design of experiment. Seven design factors were defined: R1, R2, R3, R4, R5, D1 and D2. The 2 levels were Min and Max, as shown in Table 1, for solving the mathematical model. Consequently, DOE's Minitab has generated a simulation with 128 scenarios.

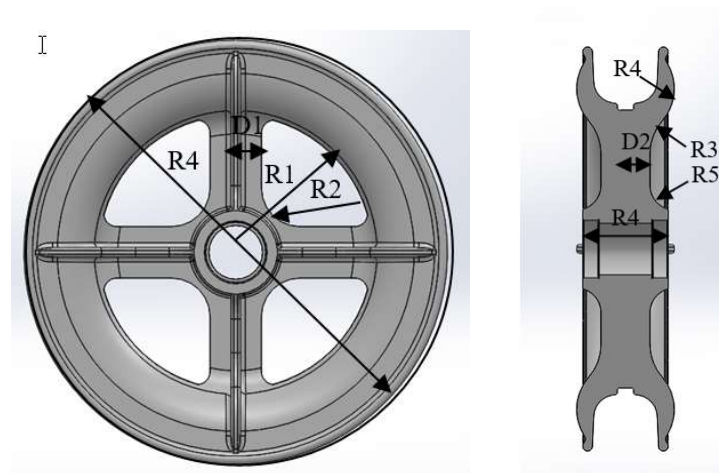


Figure 3 Aluminum Wheel, Front and Right Views

Table 1 Factors levels key parameter input variable for design of experiments

Parameter Constraint	Unit	MIN	MAX
D1	mm	10	20
R1	mm	97.5	107.5
R2	mm	20	30
D2	mm	10	20
R3	mm	30	40
R4	mm	70	80
R5	mm	10	20

3.

Numerical Procedures

Here is a reminder of the main steps involved in the FEA of structural problems. It shows the estimated proportions of time and effort that are spent in the various phases of preprocessing, solution and post processing.



Preprocessing

- Define the geometric domain of the problem.
- Define the element type.
- Define the material properties of elements.
- Define the geometric properties of the elements.
- Define the element connectivity.
- Define the physical constraints.
- Define the loading.

Solution

- Compute the unknown values of primary field variables.

Post processing

Postprocessor software contains sophisticated routines used for sorting, printing, and plotting selected results from a finite element solution.

The statics analysis for the aluminum wheel was executed by Solidworks Simulation. For Case Studies 1 and 2, the Von Mises stress was analyzed after simulations.

3.1 Material properties: Aluminum wheel was 7075, Modulus of Elasticity was 7200 MPa, Tensile Strength was 570 MPa and Yield Strength was 505 MPa.

3.2 Fixtures: All translational and all rotational degrees of freedom were restrained at bearing positions as shown in Figure 4.

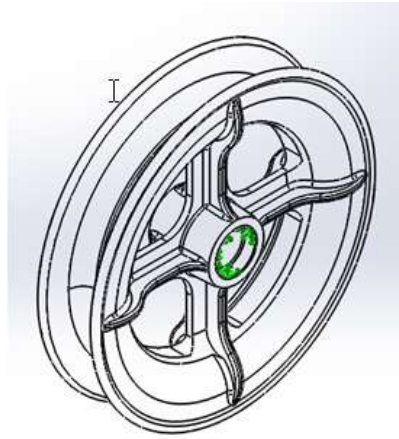
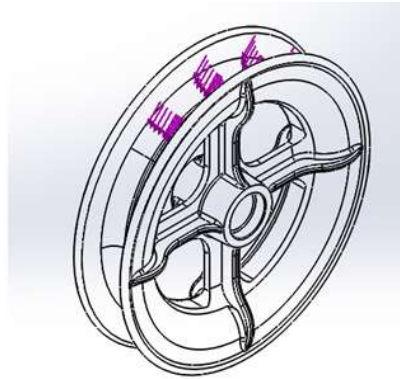
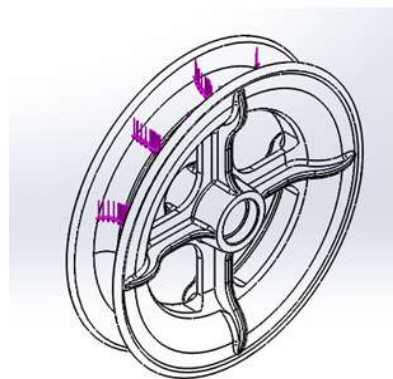


Figure 4 Fixture support in bearing

3.3 External loads: Apply load was 80 kN to aluminum wheel in vertical direction as two case studies shown in Figure 5. Case Study 1 was to apply load to aluminum wheel at the center rib and Case Study 2 was to apply load to aluminum wheel at middle between rib to rib.



Case Study 1



Case Study 2

Figure 5 External load 80 kN

3.4 Meshing method: Meshing density is carried out generally based on the fineness of the mesh. The tester selected the mesh parameters to make them fit the curvature-based mesh as shown in Figure 6.

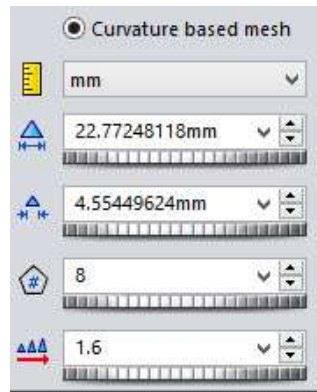


Figure 6 Meshing method

3.5 Meshed aluminum wheel model: The solid model's mesh consisted of 62,519 elements and 109,252 nodes as shown in Figure 7.

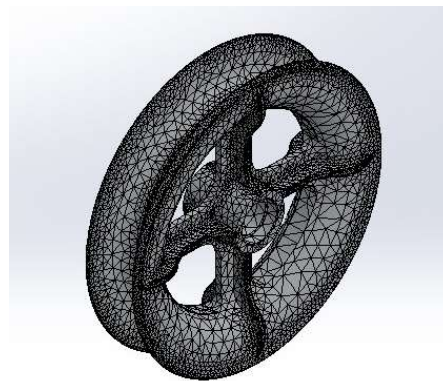
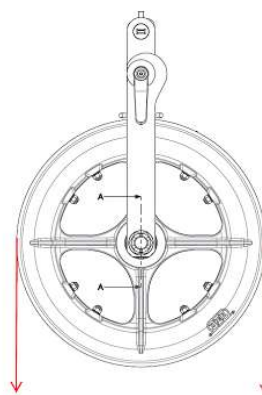


Figure 7 Meshed aluminum wheel model

3.6 Result option: von Mises stresses

Testing Method

The single pulley was put in straight position, one suitable rope was wound around the aluminum wheel for 180° and it was connected with the rope eyes to the table base.



External load 80 kN

Figure 8 External load

The value to be reached, 80 kN, was the designed working load. A small pull on the crane was given to check whether one rope was balanced and the frame was not tilted. The requested pull valve operation on the crane was reached very softly and pulling speed was lower than 2000 N/sec. As soon as the value of 80 kN was reached, measured by reading the load at the dynamometer, the lift was stopped and the pull was continued for three minutes.

Results and Discussion

5.1 Numerical Results

The problem solved linear static structural solution for two case studies of results for an aluminum wheel are shown in Figures 9-10 (Case Study 1) and Figures 11-12 (Case Study 2).

5.1.1 Case Study 1: von Mises stress

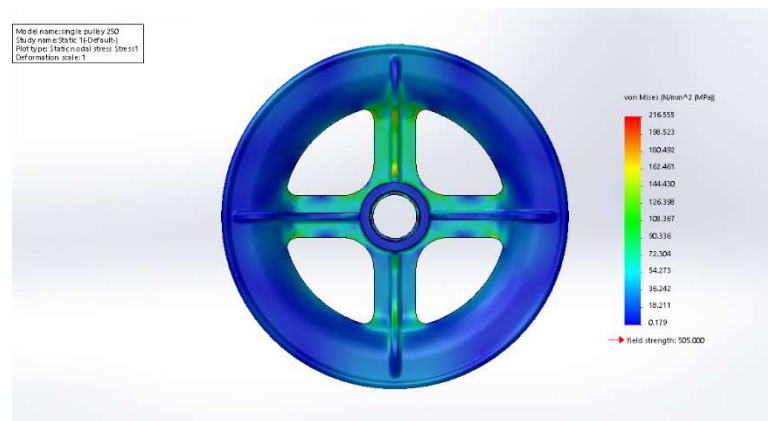


Figure 9 von Mises stress Case Study 1, Front View

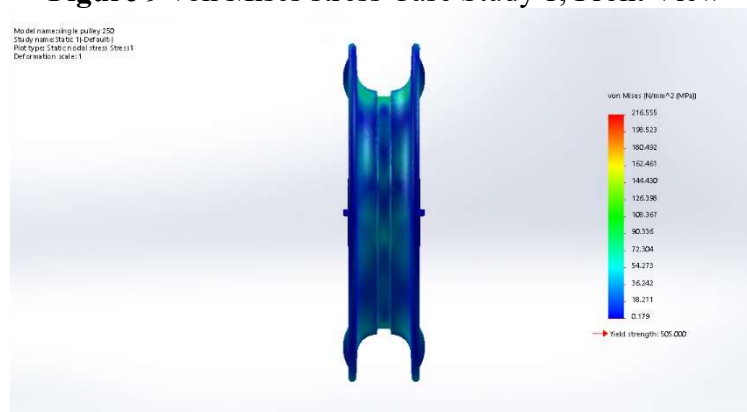


Figure 10 von Mises stress Case Study 1, Right View

The results from Figures 9 and 10 suggest that there is a maximum von Mises stress in the center rib. From 128 scenarios, Case Study 1 found that the minimum von Mises stress was 216.55 MPa, based on the parameters shown in Table 2.

5.2.2 Case Study 2: von Mises stress



Figure 11 von Mises stress Case Study 2, Front View



Figure 12 von Mises stress Case Study 2, Right View

The results from Figures 11 and 12 suggest that there is a maximum von Mises stress beside the ribs. From 128 scenarios, Case Study 2 found that the minimum von Mises stress was 323.52 MPa based on the parameters shown in Table 2.

Table 2 The proposed solution methods of 128 scenarios showing von Mises stress

Case Study	D1	R1	R2	D2	R3	R4	R5	von Mises stress (MPa)
Case Study 1	20	107.5	30	20	40	80	20	216.55
Case Study 2	20	107.5	30	20	30	70	20	323.52

5.2 Results of Analysis Design of Experiments

Experiment results were analyzed by Minitab Release and showed significant findings as shown in Figure 13.

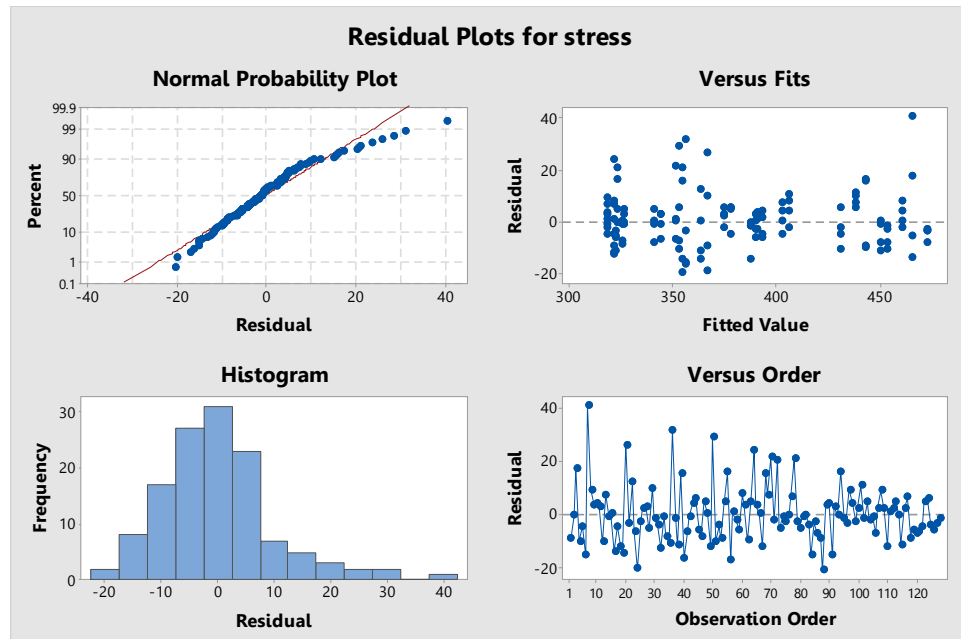


Figure 13 Residual Plot for Stress Data.

Consideration of the residual pattern, shown on Figure13, found that distribution was along a straight line. Residual data with normal distribution and residual plot with order of experiment found that the graph did not have a trend. Hence, the experiment was independent, correct and reliable.

Table 3 Analysis of Variance for Case Study 2

Source	DF	Adj SS	Adj MS	F-Value	P-Value
Model	11	310910	28265	241.30	0.000
Linear	5	299551	59910	511.46	0.000
D1	1	222319	222319	1897.95	0.000
R1	1	1218	1218	10.40	0.002
D2	1	69924	69924	596.95	0.000
R4	1	4196	4196	35.82	0.000
R5	1	1894	1894	16.17	0.000
2-Way Interactions	6	11359	1893	16.16	0.000
D1*R1	1	988	988	8.43	0.004
D1*D2	1	7271	7271	62.07	0.000
D1*R4	1	1243	1243	10.61	0.001
R1*D2	1	482	482	4.12	0.045
D2*R4	1	767	767	6.55	0.012
D2*R5	1	608	608	5.19	0.025
Error	116	13588	117		
Total	127	324498			

The analysis results showed that seven factors and cofactors influenced the response variable at the significance level of 0.05.

Table 4 Model Summary

R-sq	R-sq(adj)	R-sq(pred)
95.81%	95.42%	94.90%

Consider decision coefficient value (R-sq and R-sq(adj)) measure equation that suitable data. Results found that R-sq(adj) as 95.81% showed regression equation is a good suitable for data.

Therefore, suitable model for this research could show regression model. This model is the relationship between factor that have effects on stress follow as

$$\text{von Mises stress} = 1124 - 33.59 D1 - 1.119 R1 - 9.89 D2 - 4.484 R4 - 2.077 R5 + 0.1111 D1 * R1 + 0.3015 D1 * D2 + 0.1246 D1 * R4 - 0.0776 R1 * D2 + 0.0979 D2 * R4 + 0.0872 D2 * R5$$

5.3 Actual testing

The conditions were to apply an 80 kN working load to the aluminum wheel, and then to check the geometry of the aluminum wheel. After applying the load, we found that the model is strong enough as shown in Figure 14.



Figure 14 Actual testing

Conclusion

This project has aimed to design and analyze the aluminum wheel, which happens to be the main part of a single pulley in installations for the erection of transmission line. Observation of the analysis results of two case studies showed the Von Mises stress to be less than the yield strength. The result indicated that from total 128 scenarios, Case Study 1 got a minimum value at 216.55 MPa. of the von Mises stress. The value is from factors - D1: 20 mm, R1: 107.5 mm, R2: 30 mm, D2: 20 mm, R3: 40 mm, R4: 80 mm and R5: 20 mm. From total 128 scenarios, Case Study 2 got a minimum value at 323.52 MPa of the von Misses stress. The value is from factors - D1: 20 mm, R1: 107.5 mm, R2: 30 mm, D2: 20 mm, R3: 30 mm, R4: 70 mm and R5: 20 mm. From the simulations results, Case Study 2 got higher value

of von Misses stress than Case Study 1. von Mises stress value is related to Factors of Safety (FoS). Case Study 2's load capacity is lower than Case Study 1. Therefore, the study showed that Case Study 2 has greater critical points than Case Study 1. Hence, we can conclude that the new design of aluminum wheel without any failure matches the company's requirements.

Acknowledgements

The authors would like to thank the Design Engineering Department of Zeck TSE International for its financial support of this project.

References

- Bawane, S.G. 2012. Analysis and optimization of flywheel. **International Journal of Mechanical Engineering and Robotics Research** 1(2): 272-276.
- Chou, I.N., and Hung, C. 1999. **Finite element analysis and optimization on spring back reduction**. National Chiao Tung University Institutional Repository. Available at <http://hdl.handle.net/11536/31470>.
- Choudhary, M. 2012. Design and Optimization of Flywheel - A Past Review. **International of Mechanical Engineering and Robotics Research** 1(12): 1-4.
- Dhenge, M. Investigation of stresses in arm type rotating flywheel. **International Journal of Engineering Science and Technology** 4: 641-650.
- Kanade, P.R. 2017. Design optimization of flywheel using FEM. **International Journal Scientific Research & Development** 5(4) 1894-1896.
- Krishna, Y.M. 2017. Fatigue analysis of diesel engine flywheel by using s-glass composite material. **International Journal of Emerging Technology in Engineering Research** 5(5): 1-11.
- Mohsin M.K. 2016. Performance evaluation of pulley arm design. **International journal for scientific research and development** 3(11): 2321-0613.
- Sudipta, S. Computer aided design & analysis on flywheel for greater efficiency. **International Journal of Advanced Engineering Research and Studies** 1: 299-301.
- Third Class Lever. n.d. Available Source: http://avstop.com/ac/Aviation_Maintenance_Technician_Handbook_General/3-10.html
- Xu, X. and Yu, Z. 2005. Failure analysis of diesel engine flywheel. **Engineering Failure Analysis** 12(1): 25-34.
- Yilmaz, D. 2009. Finite element analysis of failure in rear mounted mower pulley. **Journal of food agriculture and environment** 7(3, 4): 856-868.

The Calculated Speed and Torque of Motor for Electric Formula Student

Supaluk Prapan^{1*} and Chawannat Chaichumporn¹

ABSTRACT

The Formula SAE Electric competition is designed to create a Formula Student at the university level. Formula Student is the foremost educational motorsport competition in the world. In the competition, there are four types of events: autocross event, skid pad event, acceleration event and endurance event. Each event measures how well the vehicle is designed and how well it performs based on these design decisions. At the TSAE formula student 2017-2018 competition, there was only one race with an internal combustion engine. The electric vehicle was just a prototype. In this research, attention is paid to the acceleration competition. The acceleration event evaluates the car's acceleration in a straight line on flat pavement. The length will be 75 m from starting line to finish line. At the TSAE race in Thailand, the best time of the internal combustion engine was 3.84 s. In the next competition, the Carreraz Racing team has a goal to achieve the best acceleration. In this paper, vehicle dynamics is considered for selecting the proper electric motor that would provide required traction force, torque power and speed of motor. The results showed that the factors affecting the racing car were torque and speed of motor. The optimal value of torque and speed is 130 Nm and 10162 rpm respectively. We found a suitable motor by calculating real torque and speed. As a result, the Emrax-208 had the best acceleration and the HPEVS AC-23 had the best velocity and running time.

Keywords: Formula Electric, Motor Power, Motor Torque

¹ Faculty of Engineer, University of Thai-Nichi Institute of Technology, 1771/1, Suanluang, Bangkok 10250, Thailand 10250, Thailand

* Corresponding author, e-mail: supaluk@tni.ac.th

Introduction

At present, the demand for energy across the world is constantly rising from population growth and economic development. This is especially true in the transport sector which has the highest energy consumption due to the use of internal combustion engines (ICE). The impact of fossil fuels and carbon dioxide emissions on the environment has led to dangerous global warming and climate change. As a result, there has been a development of renewable energy or high efficiency technologies in order to reduce fossil fuel emissions. Electric vehicle technology is one development designed to lower fossil fuel consumption and reduce air pollution. (Larminie and Lowry, 2012)

Formula SAE Electric vehicle competition is an engineering design competition for undergraduate and graduate students. The goal for engineering is to develop and improve a racing car in overall design, construction, performance and cost. In the dynamic events of Formula SAE competition, points are scored to determine how the car performs. These events have 4 race types which consist of Skid-Pad, Acceleration, Autocross and Endurance events. This research focused on the acceleration event which evaluates the car's acceleration in a straight line on flat pavement at a length of 75 m from starting line to finish line. (SAE International, 2016) In the TSAE formula student 2017-2018 competition, the best time in the acceleration event by the internal combustion engine was 3.84 s. Our goal is to make the acceleration event time better.

In this paper, we present the calculation of factors affecting the Electric Formula Student of Team Carreraz Racing form Thai-Nichi Institute of Technology and analyze the most suitable motors by calculating the actual values.

Table 1 Requirements of Formula student competition

Competition	Max. admissible different of potentials between any two points of system (V)	Total peak power motor
Formula SAE Electric	300 VDC	80 kW
Formula SAE Brazil	300 VDC	
Formula SAE Australasia	600 VDC	
Formula SAE Italy	600 VDC	
Formula Student	600 VDC	

Vehicle Dynamics

In the TSAE formula student 2017-2018 competition, the acceleration event will have a distance of 75 m from starting line to finish line. We intend to design the car to equal the best time from the last competition. We have taken a time of 3.84 s to calculate a maximum velocity and acceleration by fundamental equation.

Table 2 Calculation of maximum velocity and acceleration.

Parameter	Symbol	Value
Distance	s	75 m
Time	t	3.84 s
Maximum velocity in 75 m	v_{\max}	140.6 km/h
Acceleration	a	10.2 m/s ²

Tractive Force

1. Rolling resistance force (F_{rr})

The rolling resistance is the resistance that the vehicle encounters due to the contact of tires with road. (Larminie and Lowry, 2012) The equation is

$$F_{rr} = C_{rr}mg\cos\theta \quad (1)$$

where, C_{rr} is the coefficient of rolling resistance

m is mass in kg

g is acceleration due to gravity 9.81 m/s^2

θ is slope angle

2. Aerodynamic drag force (F_{ad})

The aerodynamic force drag is caused by the friction of the vehicle body moving through the air. It is determined by the shape of the vehicle. The formula for calculating is given by

$$F_{ad} = \frac{1}{2}\rho AC_d v^2 \quad (2)$$

where, ρ is the density of the air in kg/m^3

A is the frontal area of car in m^2

v is the relative velocity with the wind in m/s

C_d is a constant called the drag coefficient

3. Hill climbing force (F_{hc})

The hill climbing force of the vehicle is the resistance offered to the vehicle while climbing a hill or traveling in downward slope. The formula for calculating is given by

$$F_{hc} = \pm mg\sin\theta \quad (3)$$

4. Linear acceleration force (F_{la})

The linear acceleration force of the vehicle is given by

$$F_{la} = ma \quad (4)$$

Total tractive force is sum of all these forces (F_{tf})

$$F_{tf} = F_{rr} + F_{ad} + F_{hc} + F_{la} \quad (5)$$

Table 3 Vehicle parameter dynamics

Parameter	Symbol	Value
Coefficient of rolling resistance	C_{rr}	0.01
Vehicle mass with driver	m	280 kg
Slope angle	θ	0
Air density at 30°C	ρ	1.1644 kg/m ³
Frontal Area of car	A	1 m ²
Gear ratio	G	3.46
Aerodynamic drag coefficient	C_d	0.75
Tyre radius	r	0.127 m
Gravitational acceleration	g	9.81 m/s ²

We calculated all of the tractive force from equation (1) to (5) shown in table 4.

Table 4 Result of tractive force

Resistive Force	Value (N)
Rolling resistance force(F_{rr})	27.5
Aerodynamic drag force (F_{ad})	666.3
Hill climbing force (F_{hc})	0
Linear Acceleration force (F_{la})	2848.3
	3542.1

Based on formula (5), we get the maximum torque for the electric motor

$$\tau = \frac{F_{tf}r}{G} \quad (6)$$

Where, G is the gear ratio of the system connecting the motor to the axle.

In order to calculate the motor speed (ω) on the shaft under maximum speed, we used the following formula:

$$\omega = \frac{v_{max} \cdot G}{r} \quad (7)$$

We calculated torque and motor speed from equation (6) and (7) using 3.46 of gear ratio for our car design as shown in table 5

Table 5 Calculation of maximum torque and speed of motor

Factor	Value
Maximum torque motor	130 Nm
Maximum speed motor	10163 rpm

Comparison of different motors

According the rules of TSAE competition, the traction motor has a capacity of up to 80 kW. We compared four motors that pass the rule: Golden motor, Emrax-208, HPEVS AC-23 and Kostov K13. Then, we compared the values obtained from table 5. The torque, speed and power of the various motors are shown in table 6, figure 1.

Table 6 Comparison of different motors

Motor name	Speed motor (rpm)	Motor Torque (Nm)	Power (kW)
Golden Motor	5000	160	50
Emrax-208	6000	150	80
HPEVS AC-23	8000	120	55
Kostov K13	4500	140	65

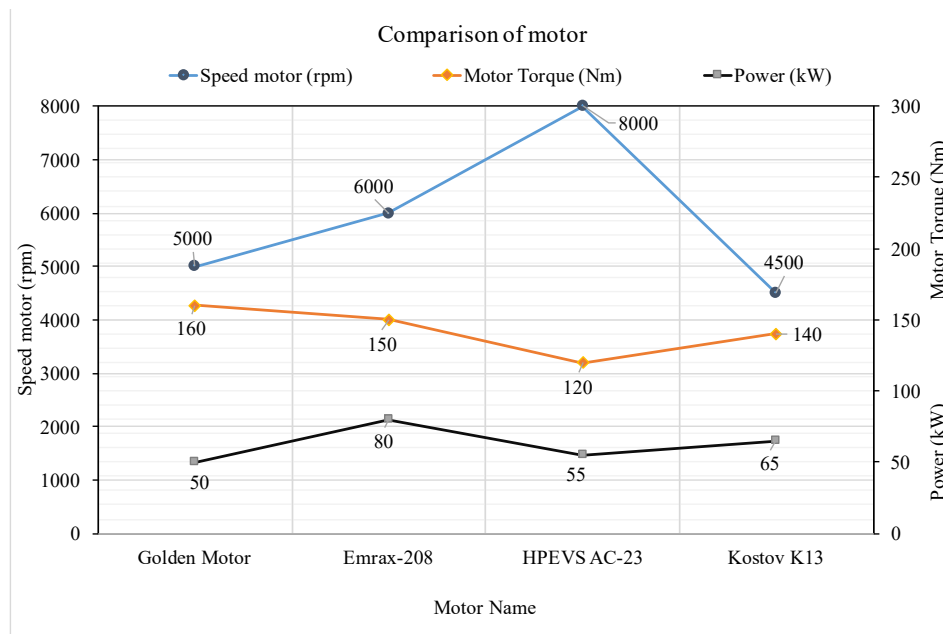


Figure 1 Comparison of Golden motor, Emrax-208, HPEVS AC-23 and Kostov K13

The torque and speed value of the various motor are calculated from equations (5), (6) and (7). The values from table 3, used to find maximum velocities, accelerations and running times of 75 m. are shown in table 7

Table 7 The real value from various motor

Motor name	Max Velocities (km/h)	Accelerations (m/s ²)	Running times (s)
Golden Motor	83.0	13.7	4.10
Emrax-208	69.2	14.9	4.55
HPEVS AC-23	110.7	10.1	3.96
Kostov K13	62.3	13.1	5.00

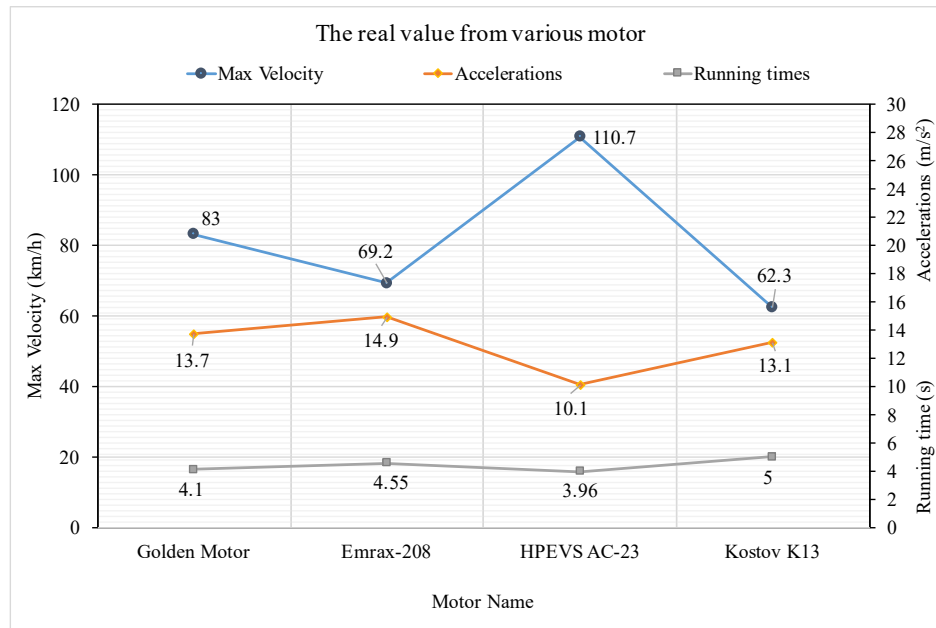


Figure 2 The real value of Golden motor, Emrax-208, HPEVS AC-23 and Kostov K13

In figure 2, a comparison of the four motors indicates that Emrax-208 has the best acceleration and HPEVS AC-23 has the best velocity and running time.

Conclusion

The purpose of this research is to design motors for the Formula SAE Electric competition. The time of acceleration event must be less than 3.84 seconds. We are interested in motors with similar specifications. This is determined by the torque and the speed of motor at 130 Nm and 10162 rpm respectively. The motors torque is considered close to the designed speed but less than 8000 rpm. The HPEVS AC-23 has the best running time of 75 m in 3.96 s. We found that the maximum velocity of each motor is related to the running time. However, additional factors such as cost and gear ratio for each motor type should be taken into consideration. This requires further study.

Acknowledgement

We would like to express our special thanks to the Thai-nichi Institute of Technology for funding, equipment and tools support.

References

- Ahmed, A. and Bhutia, D.D. 2015. Propulsion System Design and Sizing of an Electric Vehicle. **International Journal of Electronics and Electrical Engineering** 3(1):14-18.
- Chauhan, S. 2015. Motor Torque Calculations for Electric Vehicle. **International Journal of Scientific & Technology Research** 4(8): 126 – 127.
- Korobkov, D.S. and Ufimtseva, O.V. 2016. Choice of the Traction Motor for the Electric Racing Car “Formula Student”. **Science Direct Procedia Engineering** 150: 283 – 288.
- Larminie, J. and Lowry, J. 2012. Electric Vehicle Technology Explained. **Hoboken, John Wiley & Sons.**

- Patidar, L. and Bhamidipati, S. R. 2014. Parametric Study of Drag Force on a Formula Student Electric Race Car Using CFD. **Applied Mechanics and Materials** 57 : 300 – 305.
- Porselvi, T., Srihariharan, M. K. Ashok, J. , Ajith Kumar, S. 2017. Selection of Power Rating of an Electric Motor for Electric Vehicles. **International Journal of Engineering Science and Computing** 7(4):6469-6472.
- Society Automotive Engineer. 2018. Formula SAE Rules 2018. Available Source: <https://www.Fsaeonline.com>, March 27, 2018.

Design of Intake Manifold for Formula Student Car

Phatsakon Phan-Ophat^{1*} and Sutthipong Rattanawijit¹

ABSTRACT

The intake manifold is a key feature in a powertrain as it controls the amount of air that is allowed into the engine. The more air that can make it into the cylinder, the more power the engine can make. There are four main components to the intake manifold: the throttle body, restrictor, plenum, and runner. Each of these effects different properties of the manifold and must all be packaged and balanced in a way to provide maximum airflow under the designed RPM range. Analysis of the runner length of 160 mm and plenum volume of 2.1 liters is the most suitable for CBR 500. The study of airflow within the intake manifold used the ANSYS program to model air flow. The simulation result air pressure was measured in the intake Plenum of 11.77 kPa and the measurement of torque and power are 44 Nm and 53 HP, respectively.

Keywords: Formula Student, Intake Manifold, Plenum

¹Department of Automotive Engineering, Faculty of Engineer, University of Thai-Nichi Institute of Technology, 1771/1, Suanluang, Bangkok 10250, Thailand

^{1*} Corresponding author, e-mail: paskorn@tni.ac.th

Introduction

The Society of Automotive Engineers (SAE) is a global association of aerospace, automotive and commercial-vehicle related engineer and experts association which organizes a series of events including FSAE. This is a series of competitions of formula-style vehicles called Formula Student. The Thailand Society of Automotive Engineers competition has been active since 2008 for cultivating the skills of self-motivated students. The Carrera Z Racing 2017 (CRZ 10) team from Thai-Nichi Institute of Technology has participated in the Student Formula SAE Competition. This year, the team aims to increase the efficiency of the car in terms of torque and engine power.

The intake manifold is a key feature in a powertrain as it controls the amount of air that is allowed into the engine. The more air that can make it into the cylinder, the more power the engine can make. There are four main components to the intake manifold, the throttle body, restrictor, plenum, and runner. Each of these effects different properties of the manifold and must all be packaged and balanced in a way to provide maximum airflow under the designed RPM range (Merkel, 2013). In order to limit the power of competition vehicles, Formula SAE requires a 20-millimeter circular restrictor to be placed between the throttle plate and the intake port (Society Automotive Engineer, 2018). The study included research on the intake manifold and investigated the effects of internal geometry on flow through an intake manifold by means of Computational Fluid Dynamics Package Fluent (Porter, 2008). The study later investigated the effects of intake plenum length and volume on the performance characteristics of a spark-ignited engine with electronically controlled fuel injectors (Ceviz, 2007). In addition, it examined the design, analyses and testing of a new air intake system for a single seat race car using CFD analyses (Kennedy, 2011) and studied and modified the engine manifold system for high torque and power at mid-range speed engines (8,000–12,000 rpm) (Sutthisong, 2011). Therefore, the torque and power of the engine is mainly determined by the intake manifold. With a focus on intake manifold design and analysis, we investigated the effects of intake plenum volume variation on engine performance and emissions to constitute a base study for variable intake plenum.

This paper therefore presents the optimization of an engine intake manifold with runners and restrictor. This optimization aims to obtain the maximum torque and the maximum power at desired engine speeds.

Numerical Analysis

In design of plenum volumes has initially set to 1.5, 1.8, and 2.1 liters and runner lengths are 160, 200, and 240 millimeters.

Table 1 Specifications of the engine model CBR500 [8].

Specifications	Description
Cylinder	2
Displacement	471 cc.
Bore	67.0 mm
Stroke	66.8 mm
Compression Ratio	10.7:1
Cooling	Liquid
Engine Type	4-stroke
Valve configuration	DOHC
Valves per cylinder	4

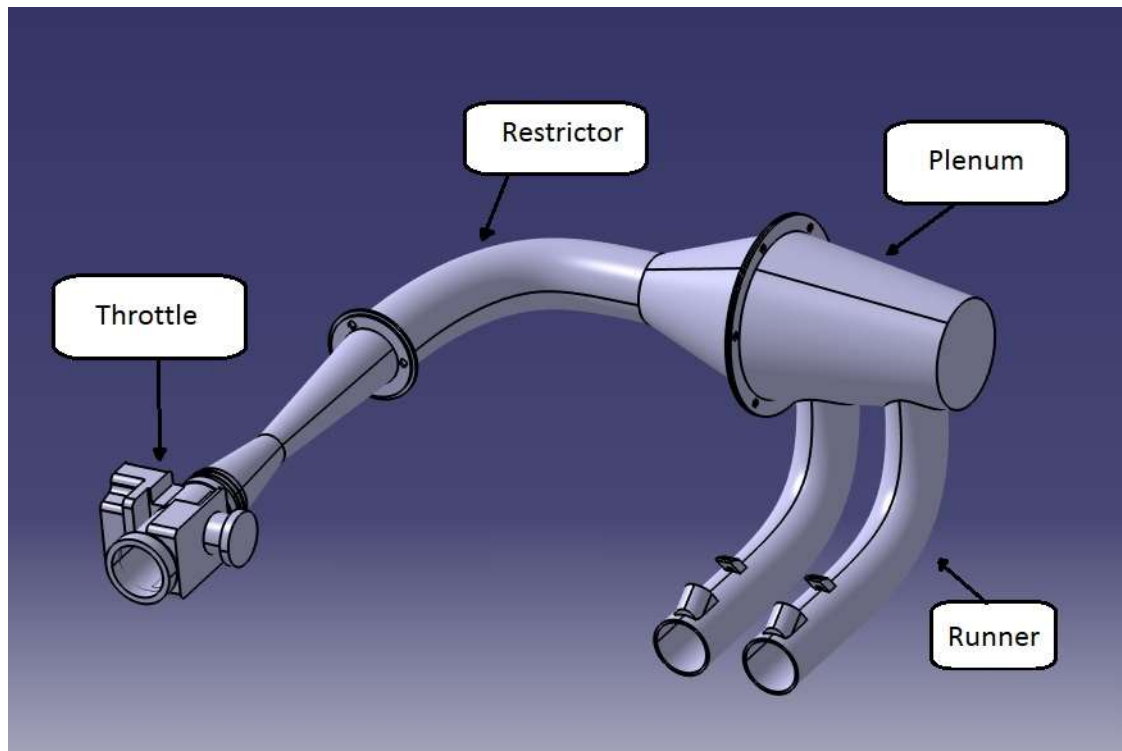


Figure 1. The designed engine intake manifold in CATIA, showing filter, throttle, restrictor, plenum, runner, and engine.

With a particular emphasis on the engine intake manifold, the engine model CBR500 has been utilized. This model is manufactured in Thailand and provides higher torque which is suitable for a racing car. This CBR500 2-cylinder engine and its specifications are summarized in Table 1. As described in Table 1, the displacement, bore, stroke, and compression ratio are 471 cc., 67.0 mm., 66.8 mm., and 10.7:1, respectively.

The engine intake manifold has been designed using CATIA as illustrated in Figure 1 and shows filter, throttle, restrictor, plenum, runner, and engine. Based on fundamental calculations corresponding to engine displacements, the optimization procedures are as follows: the plenum volumes were initially set to 1.5, 1.8, and 2.1 liters. For each case of plenum volumes, the runner lengths are 160, 200, and 240 millimeters. Figure 2 shows the schematic diagram of the overall engine airflow system using Lotus Engineering Software. It can be shown from Figure 2 that the air flows through the throttle, restrictor, and finally the plenum. The air flow is divided into the two runners prior to engine.

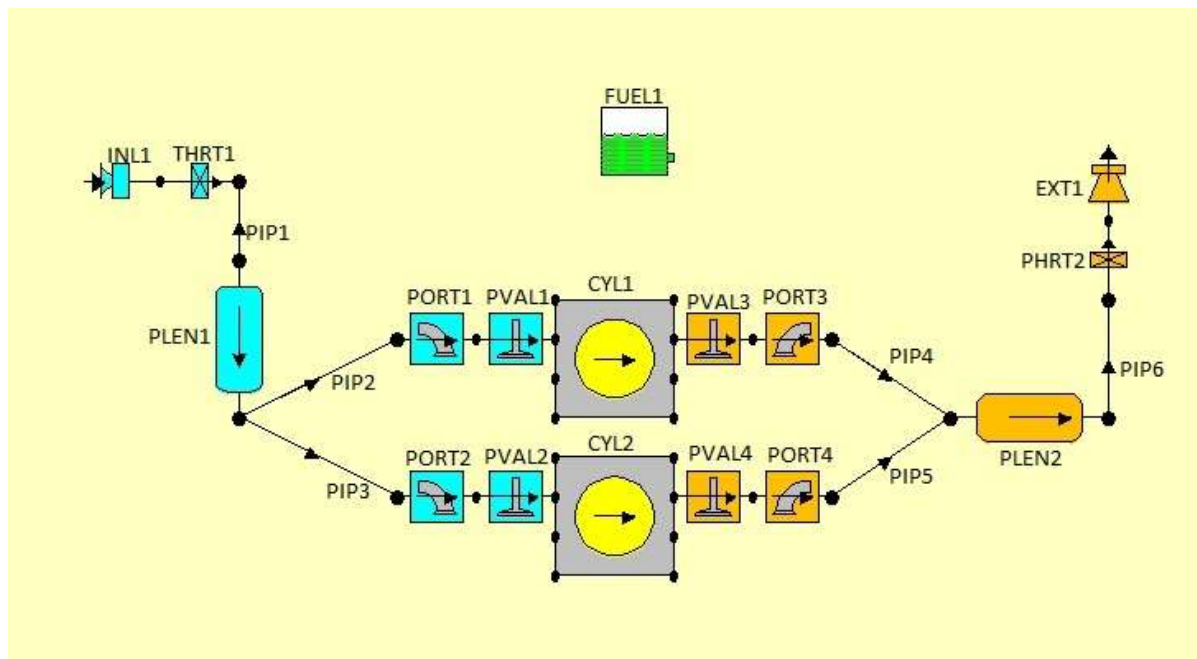


Figure 2 The schematic diagram of the overall engine airflow system using Lotus Engineering Software.

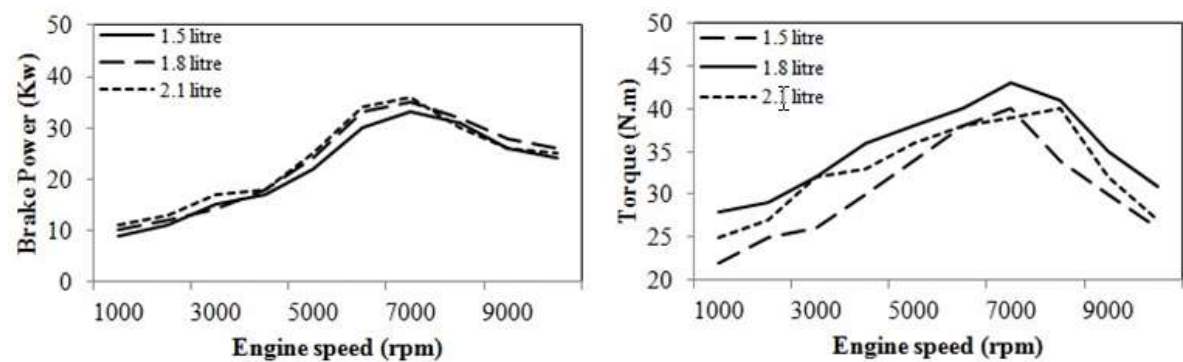


Figure 3 Simulation results of runner length of 160 mm

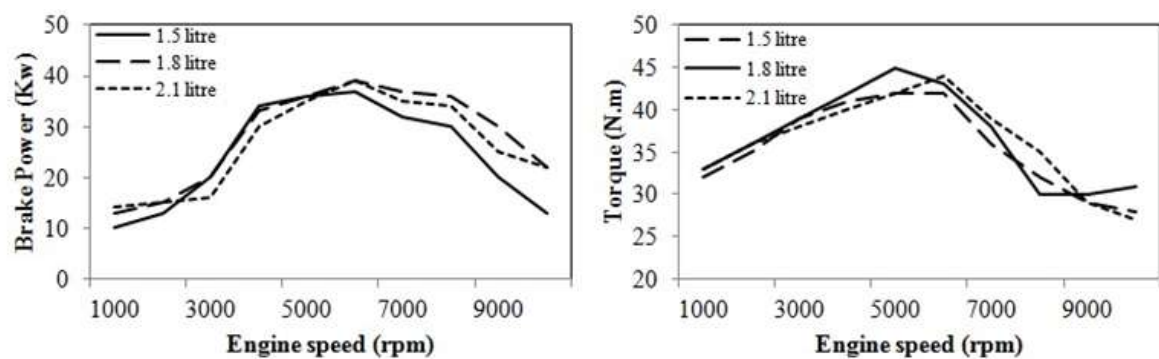


Figure 4 Simulation results of runner length of 200 mm

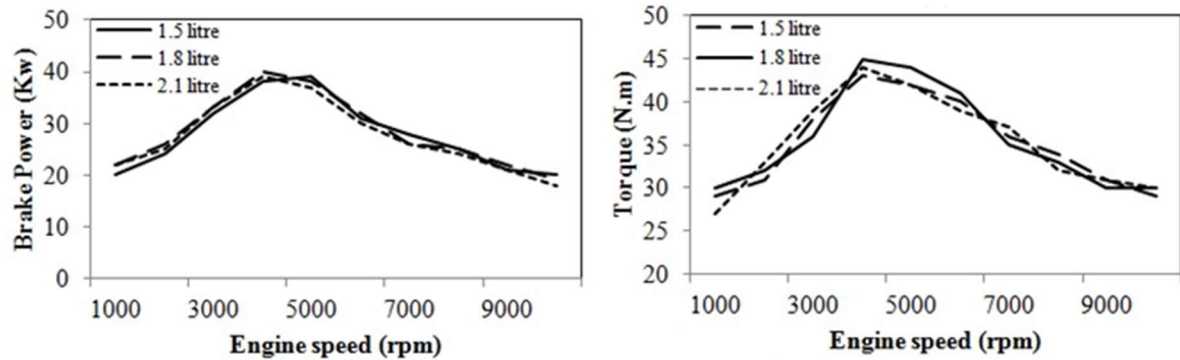


Figure 5 Simulation results of runner length of 240 mm

Figure 3 - 5 shows the simulation results from Lotus Engineering Software at various speed engines and different plenum volumes. Figure 3 shows the simulated results of the power and torque at the runner length of 160 mm and different plenum volume of 1.5, 1.8, and 2.1 liters. Figure 4 shows the simulated results of the power and torque at the runner length of 200 mm and different plenum volume of 1.5, 1.8, and 2.1 liters and Figure 5 shows the simulated results of the power and torque at the runner length of 240 mm and different plenum volume of 1.5, 1.8, and 2.1 liters.

The engine model CBR500 has a maximum torque with an engine speed of 8500 rpm. Thus, a runner length of 160 mm and plenum volume of 2.1 liters is the most suitable.

Design of the intake manifold

Figure 5 shows the design of the engine intake manifold. The engine intake manifold was designed with a runner of 160-millimeter and a plenum volume of 2.1 liters. The intake plenum was designed around the runner size, restrictor position, and the packaging with in the engine bay. Due to the position and orientation of the intake port on the engine, it was not possible to create an intake manifold that was completely linear. While this would be the most efficient way to reduce turbulence and pressure loss through the intake manifold, it would not fit within the packaging of the car. Since an efficient restrictor requires the lowest diverging angle possible, it was decided to mount the restrictor and throttle body above the intake port and use the plenum volume to efficiently provide air to the runner entrance. Since the plenum has the highest cross-section throughout the intake manifold, the sharpest turns can be made along the cross-section centerline with the least energy loss.

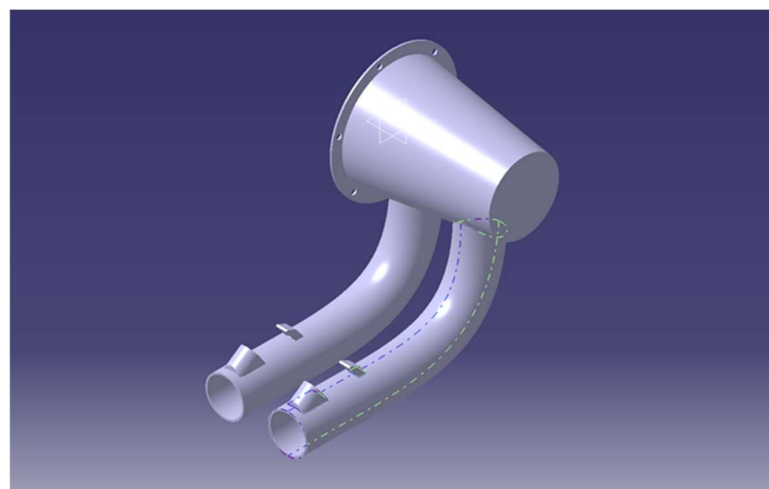


Figure 6 Design of intake manifold obtained from CATIA V5-6 R 2015

Figure 7 shows the simulated results of the intake manifold obtained from ANSYS Workbench. It was found that the internal air intake system was moving at an average speed of 35.26 m/s and the average pressure is 13.05 kPa. The inlet pressure was set at 1 atmosphere or 101.325 kPa and when the air pressure was measured in the intake manifold at the Plenum, it was equal to 11.77 kPa. The velocity streamlines showed an effective air flow which was orderly and well-balanced in to the two runners. Moreover, the simulated pressure contour h indicated that this case has the lowest pressure compared to other cases.

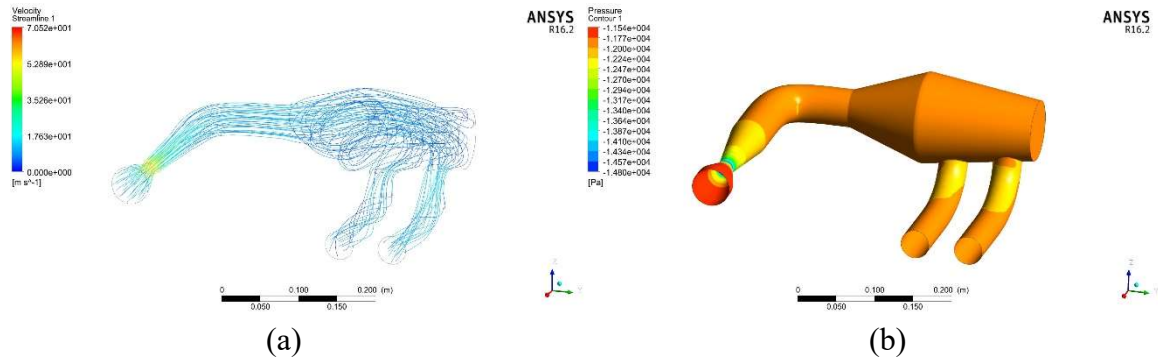


Figure 7 Simulated results of intake manifold obtained from ANSYS Workbench; (a) velocity streamlines and (b) pressure contour.

Results



Figure 8 Final implementation of the engine intake manifold in the racing car.

Figure 8 shows the final implementation of the engine intake manifold in the racing car and figure 9 shows the result of measurement torque and power of the racing car. This found that the racing car has a maximum power of 52.0 HP and a maximum torque of 44 N·m.

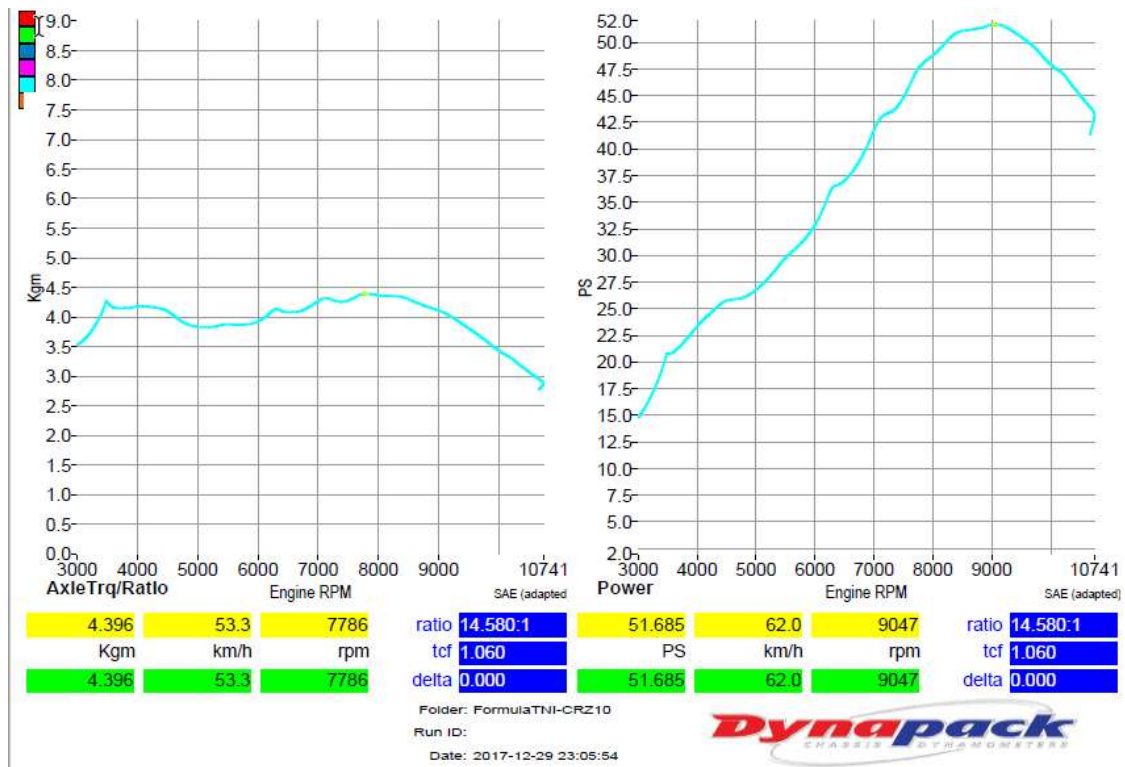


Figure 9. The result of measurement torque and power form Dynamo meter Test

Conclusion

This paper has presented an analysis of the engine intake manifold including plenum volume and lengths of runners as well as design and simulation of plenum volume and lengths. The implementation of the engine intake manifold and measurement of the torque and power of the racing car found a plenum volume of 2.1-liters and a runner length of 160-millimeters. The simulation resultant air pressure was measured in the intake Plenum of 11.77 kPa and the measurement of torque and power was 44 Nm and 53 HP, respectively.

Acknowledgement

The authors are grateful to The Society of Automotive Engineers Thailand (TSAE) and Thai-Nichi Institute of Technology for financial and equipment support.

References

- Ceviz, M.A. 2007. Intake plenum volume and its influence on the engine performance, cyclic variability and emissions: **Energy Conversion and Management** 48(3): 961-966.
- Ceviz, M.A. 2010. Design of a new SI engine intake manifold with variable length plenum: **Energy Conversion and Management** 51(11): 2239–2244.
- Damien K. 2011. Development of a New Air Intake and Exhaust System for a Single Seat Race Car: **Proceedings of the Irish Transport Research Network (ITRN2011)**. Irish Transport Research Network, University College Cork, Cork.
- Kinkead, W., Morette, C., Pickering, A., Sears, Z., and Waldo, J. 2016. Design and Optimization of a Formula SAE Vehicle. **Worcester Polytechnic Institute**.

- Porter, M. A. 2008. Intake Manifold Design using Computational Fluid Dynamics: **The UNSW Canberra at ADFA Journal of Undergraduate Engineering Research** 1(2):1-31.
- Merkel, J. 2013. Development of Multi-Element Active Aerodynamics for the Formula SAE Car. **The University of Texas at Arlington**
- Milliken, W. F. and Douglas, L. 1995. Race Car Vehicle Dynamics. **Warrendale, PA, U.S.A.: SAE International,**
- Ronnachai, S. 2011. Optimization of Runner Length for High Torque and Power at Mid-Range Speed engines. **International Conference of Automotive Technology for Young Engineers.**
- Society Automotive Engineer. **Formula SAE Rules 2018.** Available Source: <https://www.Fsaeonline.com>, March 27, 2018

Design and Analysis of Bias Brake for Formula Student

Wisit Songmuang^{1*} and Suppachok Singha¹

ABSTRACT

The brake system of the Formula Student race car is extremely important because a good braking system makes the car easier to control. In the competition, each station needs to calibrate the difference between the brake force of the front and the rear wheels. The bias brake allows the braking force on the front and rear wheels to be adjusted to the required braking force. Balance-bars are used to distribute the force from the driver to the front and rear wheel pumps. They can move the clevis range to 31.2 millimeters and be adjustable from the center of each side to 15.6 millimeters. It can also adjust the ratio of brake force between front wheels and rear wheels up to a ratio of 80: 20. The brake force ratio can be adjusted to suit for the event. In case of a braking test, the position of the balance-bar was center. An adjustment of the balance-bar to the middle position will make the front wheel brake and the rear wheel brake with the same force. The front and rear wheels have a braking ratio of 60% and 40% for Endurance and Autocross events. The pressure on the front of the car makes it easy to control the vehicle. The balance-bars can be adjusted easily and consume less time. It can be done during or between each event.

Keywords: Balance-bars, Formula Student, Brake System

¹ Department of Automotive Engineer, Faculty of Engineer, University of Thai-Nichi Institute of Technology, 1771/1, Suanluang, Bangkok 10250, Thailand

*Corresponding author, e-mail: wisit@tni.ac.th

Introduction

Formula Student Competition is a popular competition among student groups. The competition is accredited by the International Association of Automotive Engineers (SAE), competing both in Thailand and abroad. There are many competitions in engineering design. Business presentation and competition to test the efficiency of the car, such as the speed of the car, acceleration, autocross, endurance, and skid pad. Brake pressure must be adjusted to suit the competition.

Another key aspect which is incorporated in the front-rear split is a controlled balance bar that is easy to use and can change the braking characteristics on the track (Bulsara *et al.*, 2017). Different pressures are obtained at various positions of the balance bar which gives the correct setup of the system as per the required biasing. Pushrod position is decided as per theoretical knowledge and experience (Puranik *et al.*, 2017).

The brake system is designed for reducing the speed of the car. The master cylinder delivers the oil pressure to the brake caliper to push a brake pad that clamps against the disc. When the brake pad is pressed against the disc, the speed of the car is reduced. Normally, the front brakes work before the rear brakes. Thus, the front wheels adhere to the road to allow for better control of the vehicle. In the Formula Student race car, there are many competitions that require strong brakes in both the front and rear wheels. The overall performance of the car and the racing test require a 60% function of the front wheel brakes, 40% function of the rear axle, to ensure good steering.

The factors that result in more braking force are as follows.

To brake the front wheel or rear wheel with different braking force. This can be done by modifying the braking system.

1. The size of the brake disc is bigger.
2. A change in brake pads with more friction coefficient.
3. Increase the piston size of the master cylinder.

These factors can make the brake force of the front wheel and rear wheel to change as desired. If these factors cannot be done during the competition or if it is changed during the competition, each item cannot be completed immediately. It takes a long time to change and may require replacement.

The purpose of this research is to design and analyze the mechanisms that allow the braking force of the front and rear wheels to be adjusted according to the needs of each station.

Study Method

In the study, design and analysis of the mechanism to adjust the braking force of the front wheel and rear wheel during each race is as follows.

1. Learn the brake system of Student Formulas

The brake system of the formula student car is as follows:

- 1.1 The brake pedal from the driver transfers force to the brake pedal, front wheel and rear wheel.
- 1.2 The balance bar transfers force to the master cylinder. Then it exerts pressure on the front and rear brake. It can be tilted by the resistance of the mother pump brake.
- 1.3 The brake pump builds a hydraulic oil pressure on the brake caliper by the brake lines.
- 1.4 The brake calipers press the brake onto the brake pads to create friction between the brake pads and the brake discs.

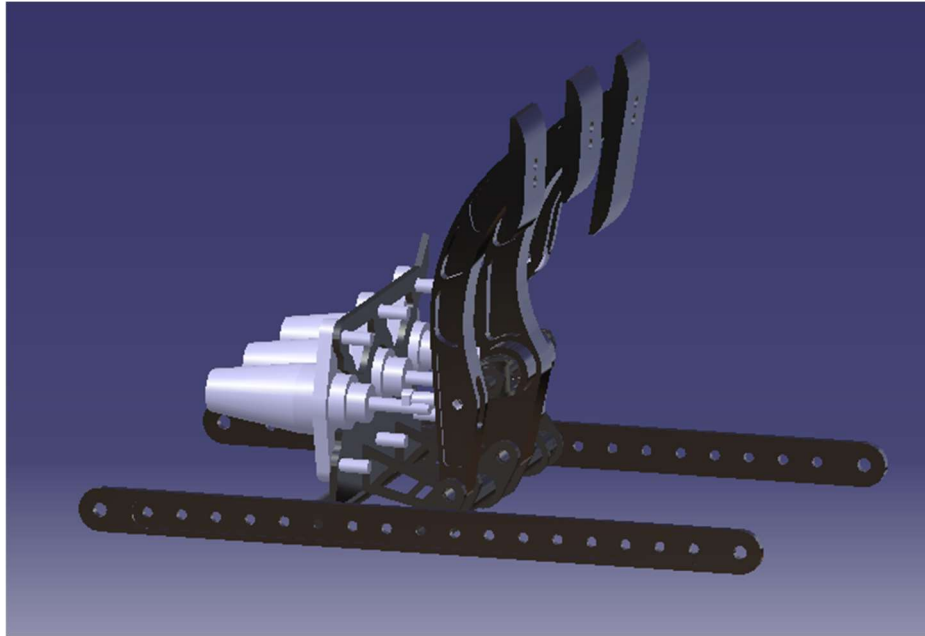


Figure 1 Brake system of formula student.

2. Bias brake design

In the brake system, the design of the Carreraz Racing team is composed of the master cylinder, brake caliper, brake pads and brake discs on both front and rear. By leveraging the braking force between the front and rear brakes, the brake is controlled by the balance bar.

2.1 Brake paddle and clamp design

The brake pedal is made of 6061-T6 aluminum with a tube for the balance bar.



Figure 2 brake paddle design

2.2 Balance bar design

The force applied to the master cylinder, front and rear can be calculated.

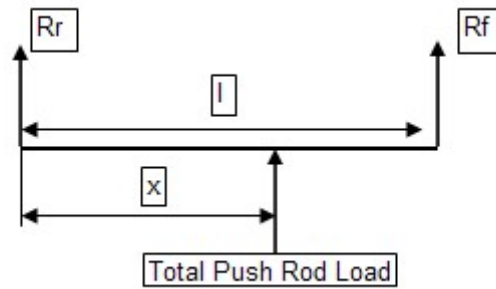


Figure 3 force when position X changes.

Figure 3 shows the force applied to the bar. The balance bars can be shifted in different positions within the l-range, which will cause the distance X to shift to the front and rear axles.

Rr is the force that acts on the rear master cylinder brake

Rf is the force that acts on the front master cylinder brake

l is the total distance that the bar can move

x is the reference distance from the rear brake pump

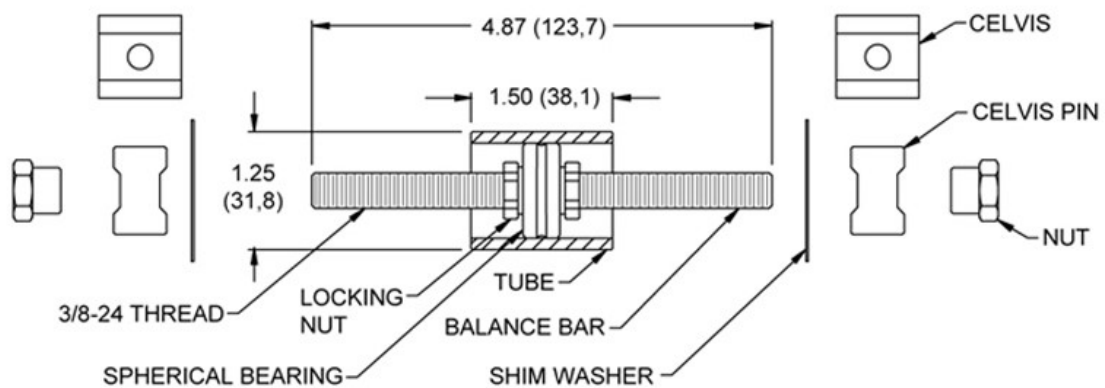


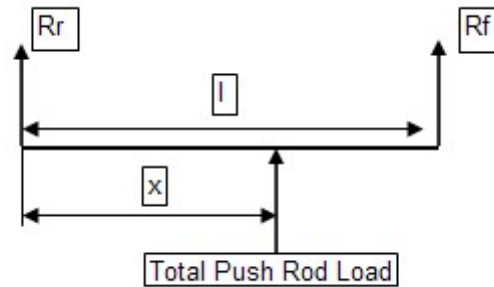
Figure 4 All components of the balance bar

Components of the balance bar are

1. Spherical Bearing
2. Locking Nut
3. 3/8-24 thread
4. Housing Tube
5. Celvis set

3. Analysis of the force transfers from the driver to the front and rear brake with the calculation method.

3.1 Calculate the force on the mother cylinder front and rear.



The equation

$$R_f = \frac{\text{Input Force} \times x}{l} \quad (1)$$

$$R_r = \text{Input Force} - R_f \quad (2)$$

where R_r is the force that acts on the rear master cylinder brake
 R_f is the force that acts on the front master cylinder brake
 l is the total distance that the bar can move
 x is the reference distance from the rear brake pump

3.2 Internal pressure calculations for front and rear brake.

The equation

$$P = \frac{F}{A} \quad (2)$$

$$F = \text{Input Force} \times \text{Pedal Ratio} \quad (3)$$

where P is the pressure of the master cylinder
 F is the force on the mother cylinder
 A is the area of the piston of the master cylinder
 Input force is the force that the driver acts on the brake
 Pedal ratio is the ratio of the distance between the pivot point to the axis of the master cylinder and the distance between the pivot point and the driving force as shown in figure 5

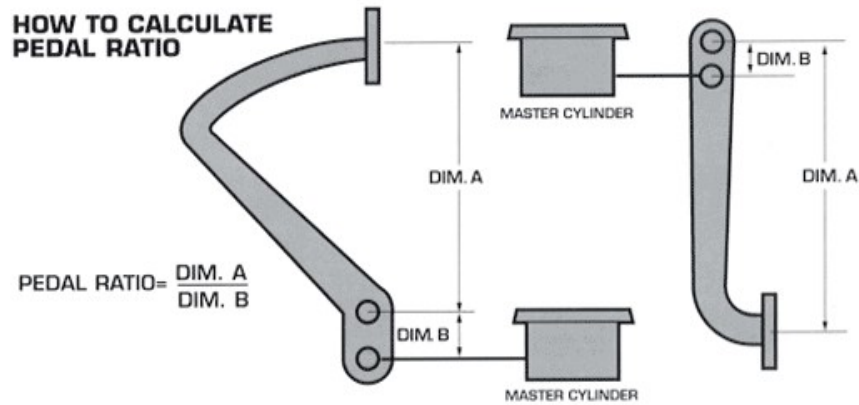


Figure 5 The pedal ratio of the brake pedal

The diameter of Toyota Hilux Vigo clutch master cylinder is 5/8". It is small in size and gives maximum pressure suitable for use.

$$\text{Pedle Ratio} = \frac{\text{Dim.A}}{\text{Dim.B}} = \frac{186}{30} = 6.2 \quad (4)$$

$$\text{Bore Aera} = \frac{\pi D^2}{4} = \frac{\pi (15.875)^2}{4} = 197.93 \text{ mm}^2 \quad (5)$$

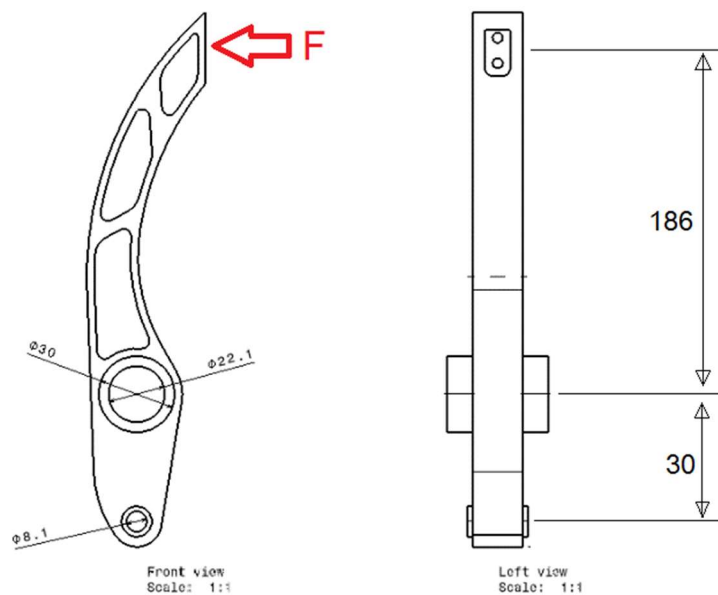


Figure 6 Distance to calculate the pedal ratio of the brake pedal

Results

1. Design balance bar results

The balance bar function divides the pressure distribution from the driver to the front and rear master cylinder. The force applied to the front and rear brakes varies according to the adjustment. It can move the space of the celvis to 31.2 mm, moving from the middle position of 15.6 mm per side, which can be divided into the required braking force.

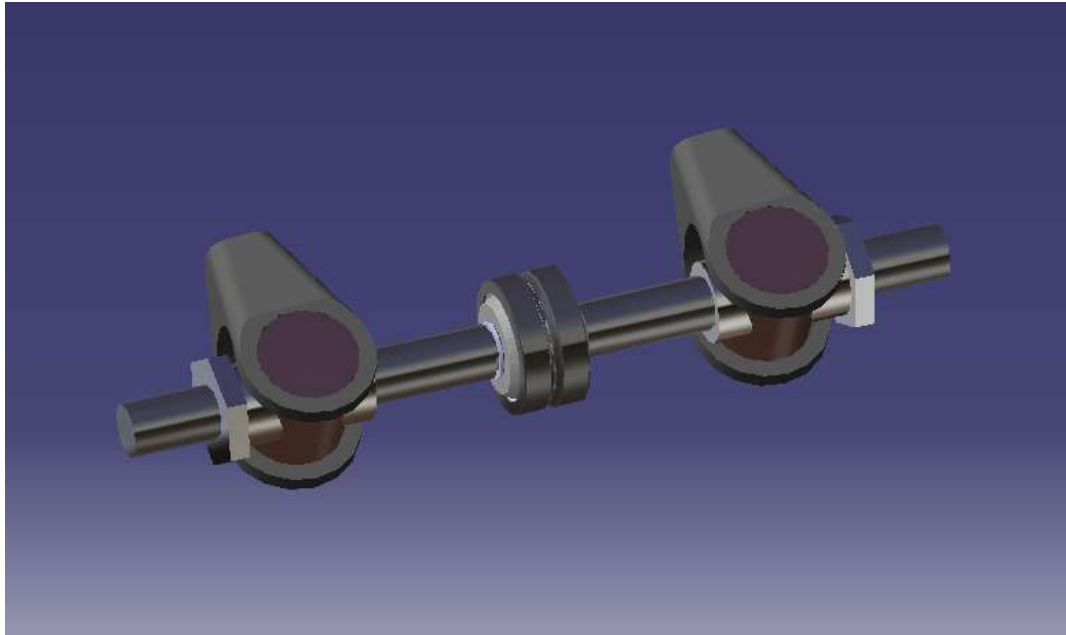


Figure 7 Brake balance bar

2. Analysis of force and pressure on the front and rear master cylinders.

2.1 The force on the master cylinder when the bearing position changes.

The force applied to the front and rear brakes is 400 N. This value was determined from the experiment. In the case of the bearing position balance in the middle, the braking force on the front and rear wheels is equal to 200 N. The result shows that the brakes have the same ratio in both front and rear wheels. When moving the bearing to the left or right, the force acting on the master cylinder shifted the front and rear brake. If a ball bearing is pushed to the right at 5.2 mm, it will have a force acting on the front wheel brakes of 240 N. It is 60% of the total force. The rear axle brake has a force of 160 N. It represents 40% of the total force.

Table 1 Force when changing the length (X)

Input (N)	X (mm)	From Center (mm)	L (mm)	Rf (N)	Rr (N)	%Rf	%Rr
400	10.4	-15.6	52	80	320	20%	80%
400	15.6	-10.4	52	120	280	30%	70%
400	20.8	-5.2	52	160	240	40%	60%
400	26	0	52	200	200	50%	50%
400	31.2	5.2	52	240	160	60%	40%
400	36.4	10.4	52	280	120	70%	30%
400	41.6	15.6	52	320	80	80%	20%

2.2 Pressure on front and rear brakes

It can be seen that the force applied to the front and rear brakes is 400 N. This was determined from the experiment. In the case of the bearing position balance in the middle, the pressure applied to the front and rear brakes is 62.8 bar. The result is same in both front and rear wheels. When moving the bearing to the left or right, the pressure acting on the front and rear axles is shifted to the next stage. If you move the balance ball to the right 5.2 mm, the pressure in the front wheel brake cylinder is 75.22 bar or 60%, the rear wheel cylinder will have a force of 50.14 bar, equivalent to 40%

By calculating the maximum pressure at the bearing position to the right or left at 15.6 mm from the center, the pressure is equal to 100.29 bar when the brake force acts on 400 N.

Table 2 Front and rear brake cylinder pressure when the bearing is rotated

Input (N)	From center	Rf	Rr	Fr _f	Fr _r	Pr _f (bar)	Pr _r (bar)
400	-15.6	80	320	496	1984	25.07	100.29
400	-10.4	120	280	744	1736	37.61	87.55
400	-5.2	160	240	992	1488	50.14	75.22
400	0	200	200	1240	1240	62.68	62.68
400	5.2	240	160	1488	992	75.22	50.14
400	10.4	280	120	1736	744	87.55	37.61
400	15.6	320	80	1984	496	100.29	25.07

Summary

With the bias brake design using a balanced bar, the team can adjust a suitable braking force of the front and rear wheels. For a brake test, the braking system will position the bearing in the middle position, thus the pressure applied to the front and rear brakes has the same braking force. The Endurance and Autocross competitions require a front and rear grip ratio of 60% and 40% respectively. Exerting weight transfer on the front of the vehicle makes it possible to control the car. To adjust the balance bar to the front wheel master cylinder, the length is 5.2 mm. The bar can be easily adjusted and as a result less time can be achieved during each race.

References

- AP Racing Limited. **Race Brake Actuation System Set Up**. Available Source: <http://www.apracing.com/>, March 3, 2018.
- Bulsara, A., Lakhani, D., Agarwal, Y. and Agiwa.Y. 2017. Design and testing of an adjustable braking system for an FSAE vehicle. **International Journal of Research in Engineering and Technology** 06 (10): 25-29.
- Puranik, A., Jaju, H. and Karambelkar, T. 2017. Brake Bias Bar Design and Simulation on a Formula Student Car. **International Conference on Ideas, Impact and Innovation in Mechanical Engineering**. 05(06): 852-855.
- Tilton Engineering. **Installation Instructions Balance Bars**. Available Source: <http://tiltonracing.com/wp-content/uploads/2013/07/98-1250-600-Series-Balance-Bars.pdf>, March 3, 2018.
- Tom McCready and James Walker, **Brake Bias and Performance Why Brake Balance Matters**. Available Source: <http://www.stoptech.com/technical-support/technical-white-papers/white-paper---brake-bias-and-performance-why-brake-balance-matters>, March 3, 2018.
- Wilwood Engineering **“Tru-Bar Balance Bar Brake Pedal Installation and Adjustment Guide**. Available Source: <http://www.wilwood.com/PDF/DataSheets/ds1102.pdf>, March 3, 2018.

A C-Program for the Teaching of View Factors for Heat Transfer Problems for Two Perpendicular Planes

Marwan Affandi^{1*}, Suhaidee Sani¹, Ranggita Dwi Affandi²

ABSTRACT

Radiation is one of the three modes of heat transfer which is very important for high temperatures. Heat exchange between two planes can be computed if the view factor between them is known. This paper discusses view factors for two perpendicular planes. The graph for this view factor is available in all heat transfer textbooks. However, the use of graphs is prone to error and inaccurate. An explicit formulas for the view factor of the geometry is available. However, it is quite complicated for the purpose of teaching. While view factor calculators are available for the internet, their use is commonly restricted to simple cases. The C-program developed in this paper can be used to compute view factors for 12 cases for the concerned geometry. Students can use the program to enhance their knowledge of heat transfer while lecturers or instructors will benefit it from creating problems and getting answers quickly.

Keywords: Radiation, View Factor, Heat Transfer, C-Program

¹ Department of Mechanical Engineering, Faculty of Engineering, RMUTSV, Songkhla 90000, Thailand

² School of Environmental Engineering, Universiti Malaysia Perlis, Arau 02600, Malaysia

*Corresponding author, e-mail : Marwan Affandi, khun.fandi@gmail.com

Introduction

Heat transfer is one of core subjects taught at all Mechanical Engineering departments. There are three modes of heat transfer: conduction, convection and radiation. This paper is only concerned with radiation heat transfer, which is very important at high temperatures. There are many applications of radiation heat transfer such as in combustion of fuels, solar power plants and space vehicles. Radiation heat transfer exists between two or more surfaces. Analysis is based on two surfaces which is then extended to more surfaces. When analyzing heat transfer between two surfaces, one must consider the shape factor between them. Shape factor, view factor or configuration factor are similar terms and they will be used freely in this paper. There are various configurations for real applications which need different shape factors; extensive lists can be found in Howell and Siegel (2010). This paper will discuss the computation of shape factors between two perpendicular planes touching each other for all possible situations. At first, three theorems which are useful to determine the shape factor will be briefly discussed. Full descriptions of those theorems are given in most heat transfer text books; see Cengel (2002), Holman (2010) and Incropera (2007), for example. Figure 1 shows two surfaces with areas of A_1 and A_2 , respectively. The reciprocity theorem states that

$$A_1 F_{1-2} = A_2 F_{2-1} \quad (1)$$

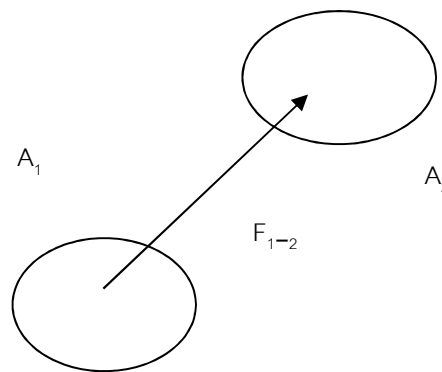


Figure 1 Reciprocity theorem

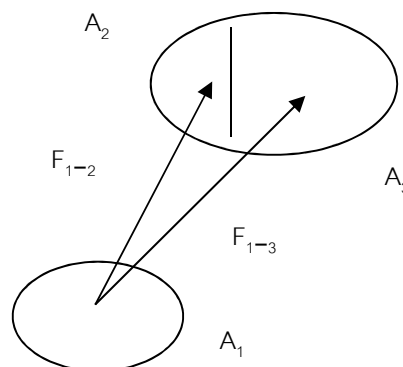


Figure 2 Addition theorem

Figure 2 shows three surfaces with areas of A_1 , A_2 , and A_3 , respectively. Heat radiates from surface 1 to surfaces 2 and 3. The addition theorem states that

$$F_{1,2-3} = F_{1-2} + F_{1-3} \quad (2)$$

Figure 3 shows three surfaces where one surface receives heat radiation from two others. Combining reciprocity and addition theorems we then have

$$A_{1,2}F_{1,2-3} = A_1F_{1-3} + A_2F_{2-3} \quad (3)$$

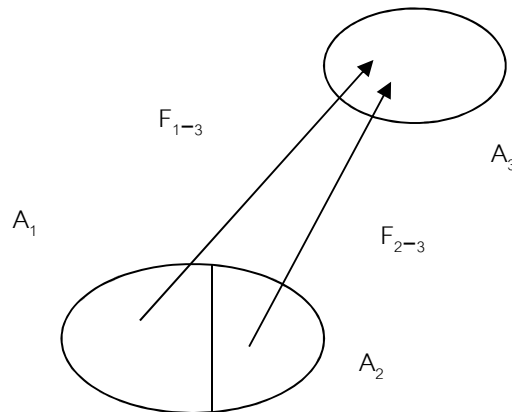


Figure 3 Combination of reciprocity and addition theorems

Armed with these three theorems we will determine all possible shape factors between two planes or surfaces for the given configuration.

Figure 1.

Two perpendicular rectangles with common edge

Figure 4 shows two perpendicular rectangles with common edge. The shape factor for this configuration can be found from the graph which is given in most heat transfer textbooks; see for example Cengel (2002), Holman (2010), Incropera (2007) and Kreith (2011).

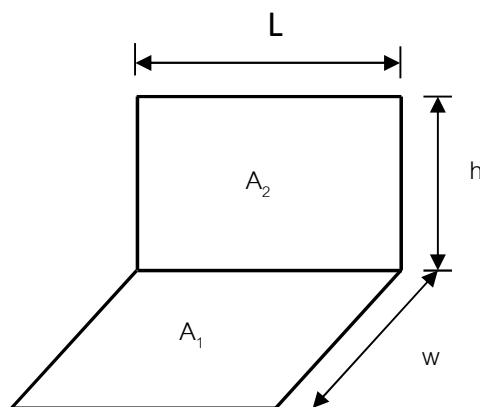


Figure 4 Two perpendicular rectangles with common edge

The analytical formula for the shape factor is given in most heat transfer text books. When the shape factor must be computed several times, it is better to use analytical formula

rather than using a graph which is usually done in the class. Reading a graph is prone to error and inaccurate, particularly when the parameters must be interpolated. The graph for the geometry discussed in this paper is shown in Figure 5. An extensive list of formulas for various configurations is given by Howell (1982) and Howell et. al., (2011). The analytical formula for the configuration shown in Figure 4 is given here but with different notations; the formula is separated into three parts because the original one is quite long.

$$F_{1-2} = (1/\pi)(A + B/4 + C/4 + D/4) \quad (4)$$

where

$$A = W \tan^{-1}(1/W) + H \tan^{-1}(1/H) - (H^2 + W^2)^{1/2} \tan [1/(H^2 + W^2)^{1/2}] \quad (4a)$$

$$B = \ln [(1 + W^2)(1 + H^2)/(1 + H^2 + W^2)] \quad (4b)$$

$$C = W^2 \ln [W^2(1 + H^2 + W^2)/[(1 + W^2)(H^2 + W^2)]] \quad (4c)$$

$$D = H^2 \ln [H^2(1 + H^2 + W^2)/[(1 + H^2)(H^2 + W^2)]] \quad (4d)$$

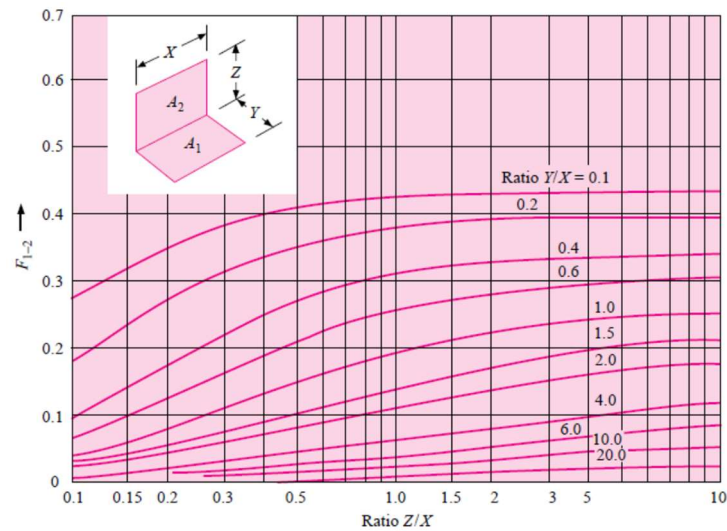


Figure 5 View factor between perpendicular rectangles with a common edge

Generalized perpendicular-rectangle arrangement

Figure 6 shows a generalized perpendicular-rectangle arrangement. Figure 6 is slightly different from the usual or conventional arrangement given in heat transfer textbooks; see Figure 7 as taken from Holman (2010). The current arrangement makes it easier for developing a computer program since the symbols used can be readily translated into codes for any programming languages.

There are six subplanes in the horizontal plane and six subplanes in the vertical plane. We wish to determine radiation shape factor from any surface (subplane) in the horizontal plane (1,2, ..., 6) to any surface in the vertical plane (a, b, ..., f).

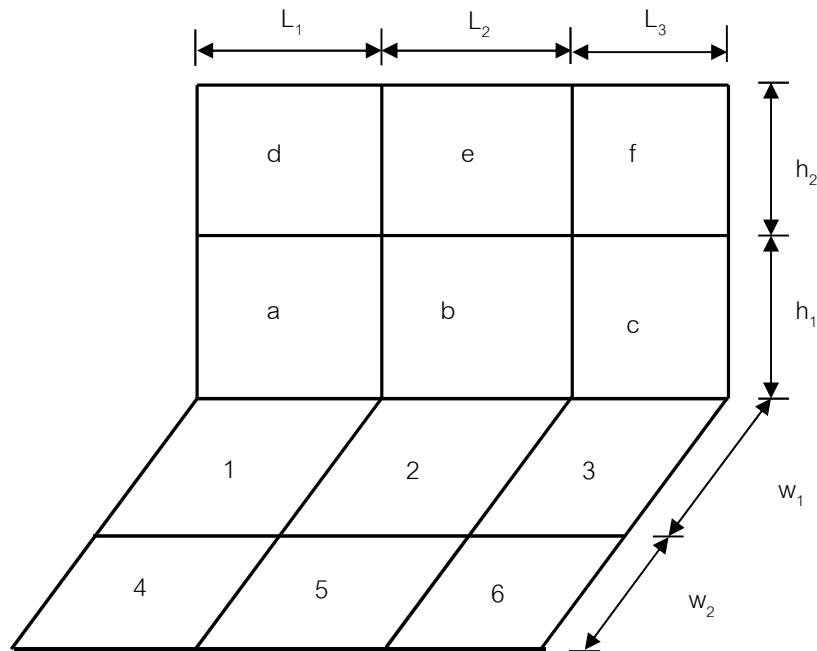


Figure 6 Generalized perpendicular-rectangle arrangement

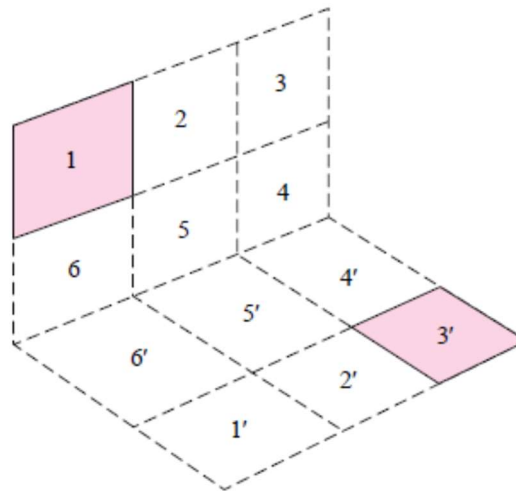


Figure 7 Usual arrangement given in heat transfer textbooks

The shape factors from the vertical plane to the horizontal plane can be found from reciprocity theorem. The shape factors for all possible configurations are grouped in the following cases. The division of the cases is based on the similarity of geometry pattern among the members of each case. For example, F_{1-a} is similar to $F_{1,4-a,d}$ and $F_{2,3-b,c}$ while F_{4-b} is similar to F_{4-be} and $F_{5-c,f}$. For simple notation, we will remove the comma and hyphen from the shape factor symbols. So, $F_{1,4-a,d}$ is just written as F_{14ad} .

Derivations of all 12 shape factors

There are 12 basic cases for the generalized arrangement as shown in Figure 6; they are F_{1a} , F_{1d} , F_{4a} , F_{4d} , F_{1b} , F_{1c} , F_{1e} , F_{1f} , F_{4b} , F_{4c} , F_{4e} , and F_{4f} . Except for Case 12 (to find F_{4f}), there are at least two possible arrangements for each case. Table 1 shows all basic cases and the number of possible arrangement for each case.

Table 1 All possible basic cases

Case No.	1	2	3	4	5	6
Basic	F_{1a}	F_{1d}	F_{4a}	F_{4d}	F_{1b}	F_{1c}
Total	24	12	12	6	16	6

Case No.	7	8	9	10	11	12
Basic	F_{1e}	F_{1f}	F_{4b}	F_{4c}	F_{4e}	F_{4f}
Total	5	2	6	2	2	1

The description of all possible basic cases is mentioned as follow.

Case 1: F_{1a} is the very basic case; the shape factor is computed using Equation 4.

Case 2: From (2) we have $F_{1ad} = F_{1a} + F_{1d}$, from which we have

$$F_{1d} = F_{1ad} - F_{1a}.$$

Both F_{1ad} and F_{1a} are from Case 1.

Case 3: From (3) we have $A_{14}F_{14a} = A_1F_{1a} + A_4F_{4a}$. We then have

$$A_4F_{4a} = A_{14}F_{14a} - A_1F_{1a}.$$

Case 4: From (3) we have after arranging the terms $A_4F_{4a,d} = A_{14}F_{14ad} - A_1F_{1ad}$. But from (2),

$$A_4F_{4ad} = A_4F_{4a} + A_4F_{4d}.$$

So, we then have

$$A_4F_{4d} = A_{14}F_{14ad} - A_1F_{1ad} - A_4F_{4a}$$

F_{4-a} is computed based on Case 3. So, A_4F_{4-d} can be written in terms of Case 1:

$$A_4F_{4d} = (A_{14}F_{14ad} - A_1F_{1ad}) - (A_{14}F_{14a} - A_1F_{1a})$$

Case 5: For Case 5 we need another theorem; see Chapman (1960) for the proof. Figure 8 shows the configuration for the theorem.

$$A_1F_{1b} = A_2F_{2a} \quad (5)$$

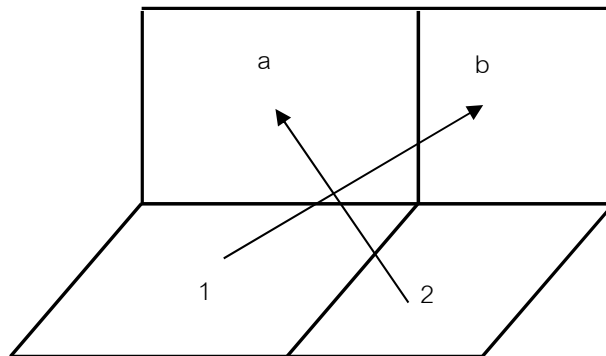


Figure 8 Case for two skewed planes

We can determine A_1F_{1b} as follow. From (3) we have

$$A_{12}F_{12a} = A_1F_{1a} + A_2F_{2a}$$

$$A_{12}F_{12b} = A_1F_{1b} + A_2F_{2b}$$

So, $A_{12}(F_{12a} + F_{12b}) = A_1F_{1a} + A_2F_{2a} + A_1F_{1b} + A_2F_{2b}$

Or $A_{12}F_{12a,b} = A_1F_{1a} + 2A_1F_{1b} + A_2F_{2b}$

$$F_{1b} = (A_{12}F_{12ab} - A_1F_{1a} - A_2F_{2b}) / 2A_1 \quad (6)$$

Now, all cases from 6 to 10 can be determined.

Case 6: Here, $F_{1c} = F_{1bc} - F_{1b}$. From the similarity of F_{1bc} with F_{1b} (Case 5), it can be seen that $F_{1bc} = (A_{123}F_{123abc} - A_1F_{1a} - A_{23}F_{23bc}) / 2A_1$. So, F_{1c} can be found.

Case 7: Here, $F_{1e} = F_{1be} - F_{1b}$. From the similarity of F_{1be} with F_{1b} (Case 5), it can be seen that $F_{1be} = (A_{12}F_{12abde} - A_1F_{1ad} - A_2F_{2be}) / 2A_1$. So, F_{1e} can be found.

Case 8: Here, $F_{1f} = F_{1cf} - F_{1c}$. F_{1cf} is similar to F_{1cf} (Case 6). But F_{1f} can also be found from $F_{1f} = F_{1ef} - F_{1e}$ where F_{1ef} is similar to F_{1e} (Case 7). Here, $F_{1ef} = (A_{12}F_{12abde} - A_1F_{1a} - A_2F_{2b}) / 2A_1$.

Case 9: F_{4b} is found from $A_4F_{4b} = A_{14}F_{14b} - A_1F_{1b}$. But F_{14b} is similar to F_{1b} (Case 5). Here, $F_{14b} = (A_{1245}F_{1245ab} - A_{14}F_{14a} - A_{25}F_{25b}) / 2A_{14}$.

Case 10: Here, $F_{4c} = F_{4bc} - F_{4b}$. F_{4bc} is just similar to F_{4b} (Case 9); $F_{4bc} = (A_{14}F_{14bc} - A_1F_{4bc}) / 2A_4$.

Case 11: Here, $F_{4e} = F_{4be} - F_{4b}$ where both terms in the right-hand side are of Case 9.

Case 12: This is the last case to discuss where $F_{4f} = F_{4cf} - F_{4c}$ where both terms of the right-hand side are of Case 10. However, we have $F_{4f} = F_{4ef} - F_{4e}$ where both terms of the right-hand side are of Case 11. We can verify if the value of from the two equations are the same.

Derivation of F_{4f} using the very basic case

Now, we wish to determine F_{4f} from only the very basic case i.e., Case 1. We proceed backward as follow:

$$A_4F_{4f} = A_4F_{4cf} - A_4F_{4c}$$

$$A_4F_{4c} = A_{14}F_{14c} - A_1F_{1c}$$

$$F_{1c} = F_{1bc} - F_{1b}$$

$$2A_1F_{1b} = A_{12}F_{12ab} - A_1F_{1a} - A_2F_{2b}$$

$$2A_1F_{1bc} = A_{123}F_{123abc} - A_1F_{1a} - A_{23}F_{23bc}$$

So,

$$2A_1F_{1c} = (A_{123}F_{123abc} - A_{12}F_{12ab}) - (A_{23}F_{23bc} - A_2F_{2b})$$

Similarly,

$$2A_{14}F_{14c} = (A_{123456}F_{123456abc} - A_{1245}F_{1245ab}) - (A_{2356}F_{2356bc} - A_{25}F_{25b})$$

So,

$$2A_4F_{4c} = [(A_{123456}F_{123456abc} - A_{1245}F_{1245ab}) - (A_{2356}F_{2356bc} - A_{25}F_{25b})] - [(A_{123}F_{123abc} - A_{12}F_{12ab}) - (A_{23}F_{23bc} - A_2F_{2b})]$$

Similarly,

$$2A_4F_{4cf} = \{[(A_{123456}F_{123456abcdef} - A_{1245}F_{1245abde}) - (A_{2356}F_{2356bcef} - A_{25}F_{25be})] - [(A_{123}F_{123abcdef} - A_{12}F_{12abde}) - (A_{23}F_{23bcef} - A_2F_{2be})]\}$$

So,

$$2A_4F_{4f} = 2A_4F_{4cf} - 2A_4F_{4c} = [(A_{123456}F_{123456abcdef} - A_{1245}F_{1245abde}) - (A_{2356}F_{2356bcef} - A_{25}F_{25be})] - [(A_{123}F_{123abcdef} - A_{12}F_{12abde}) - (A_{23}F_{23bcef} - A_2F_{2be})] - \{[(A_{123456}F_{123456abc} - A_{1245}F_{1245ab}) - (A_{2356}F_{2356bc} - A_{25}F_{25b})] - [(A_{123}F_{123abc} - A_{12}F_{12ab}) - (A_{23}F_{23bc} - A_2F_{2b})]\}$$

Or,

$$2A_4F_{4f} = A_{123456}F_{123456abcdef} - A_{1245}F_{1245abde} - A_{2356}F_{2356bcef} + A_{25}F_{25be} - A_{123}F_{123abcdef} + A_{12}F_{12abde} + A_{23}F_{23bcef} - A_2F_{2be} - A_{123456}F_{123456abc} + A_{1245}F_{1245ab} + A_{2356}F_{2356bc} - A_{25}F_{25b} + A_{123}F_{123abc} - A_{12}F_{12ab} - A_{23}F_{23bc} + A_2F_{2b}$$

So, F_{4f} can be found by evaluating 16 shape factors from Case 1 only. Chapman (1960) and Holman (2010) also give a formula to compute F_{4f} directly without any derivation. The formula is slightly different due to the different symbols used.

Results and Discussion

As an example, the program was run using the following numerical values: $L_1 = 1$, $L_2 = 2$, $L_3 = 3$, $w_1 = 1$, $w_2 = 2$, $h_1 = 2$ and $h_2 = 5$. Table 2 gives the values of the shape factors for all cases as computed using program written in C. The output of the display in the screen for Case 6 is shown below.

```

Enter the dimensions of the planes along the X-axis (L1,L2 and L3): 1 2 3
Enter the dimensions of the planes along the Y-axis (W1 and W2): 1 2
Enter the dimensions of the planes along the Z-axis (h1 and h2): 2 5
Case 6: F1c.
      F1c = F1bc - F1b
      F1bc = (A123.F123abc - A1.F1a - A23.F23bc)/(2A1)
      F1a = 0.232853, F23bc = 0.342947, F123abc = 0.349254
      F1b = 0.069695, F1bc = 0.073968
      F1bc = (A123.F123abc - A1.F1a - A23.F23bc)/(2A1)
      = (6.00*0.349254 - 1.00*0.232853 - 5.00*0.342947)/(2*1.00)
      = 0.073968
      F1c = F1bc - F1b
      = 0.073968 - 0.069695
      = 0.004272
*****
Computed directly:
      F1bc = 0.073968, F1b = 0.069695
      F1c = F1bc - F1b
      = 0.073968 - 0.069695
      = 0.004272
Press any key to continue:
    
```

Table 2 Values of the shape factors for all cases

Case No.	1	2	3	4	5	6
Symbol	F_{1a}	F_{1d}	F_{4a}	F_{4d}	F_{1b}	F_{1c}
Value	0.232853	0.015545	0.045268	0.031357	0.069695	0.004272

Case No.	7	8	9	10	11	12
Symbol	F_{1e}	F_{1f}	F_{4b}	F_{4c}	F_{4e}	F_{4f}
Value	0.020844	0.009062	0.044450	0.009710	0.047526	0.027014

Computations of the shape factors for all cases are done by a program written in C language. C is chosen because it is widely available and some of them is free. Furthermore, C is offered in many engineering faculties in their computer programming courses. Students can learn it quickly, enabling them to solve their problems easily. There are 12 functions that have been developed to compute a shape factor for each case. For all cases except the very basic one

(Case 1) intermediate results are shown so that the students can compare the results with their own calculation done manually. Of course the students must understand the theory of the shape factor first before they can use the programs. C is only a tool so it may not fully benefit the students if they do not have enough background for the problems they want to solve. Apart from C, Excel can also be used to compute the problems of heat transfer such as done in Becker (1986) and Holman (2010). However, while Excel can give very quick results by just copy and paste the formula it cannot be so conveniently used for complicated shape factors such as cases 10 and 12.

By using this program, a lecturer or instructor who teaches radiation heat transfer to the students can create examples and solve problems easily. Since intermediate values are shown in the output of the program, it is relatively easy to check if there are mistakes in the solution. For simple cases, the students can check their answers by using the usual graph as shown in Figure 5. The use of computer in solving difficult problems in radiation heat transfer will enhance their knowledge of the students. Most heat transfer textbooks only give problems up to case 9. Case 12 is the most difficult one and no example is ever mentioned in any heat transfer textbooks. Nowadays, most university students have their own computers or they can access them in their faculties. Accordingly, the teaching-learning process for the Heat Transfer course can be conducted better by using computers. Here, both lecturers and students will benefit by using the program which can solve quite difficult problems.

Many “view factor calculators” are available in the internet; they can be easily found by searching them. However, they can only compute the very basic view factor that is F_{1a} . If we want to compute other cases such as F_{1f} or F_{4f} we must run those programs several times using the very basic view factors and compute the required view factor manually. Howell (2018) has a site dedicated for computing view factors for various configurations. Actually there is a section in the site which will compute all 12 cases mentioned here. However, the approach used is very general and rather awkward to use; see Figure 9. It requires eight inputs instead of seven as required by our program. Moreover, its analytical formula is quite complicated; see Howell (2018). To check the validity of our program, the outputs have been verified using the Howell’s program.

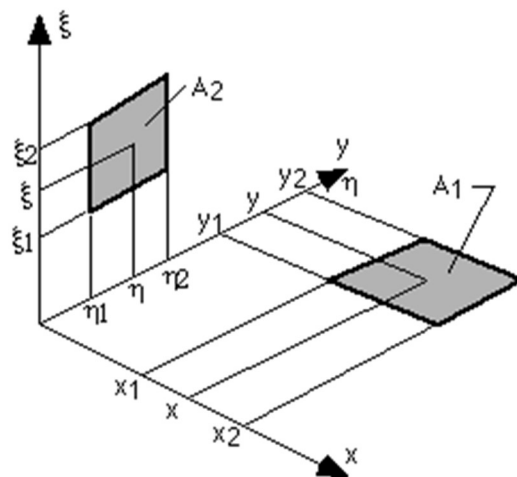


Figure 9 View factor from finite area to finite area

Conclusion

Descriptions for all 12 different shape factors have been completed. Case 12, F_{4f} , is very complicated. It needs 16 evaluation of shape factors from Case 1. For most cases intermediate values are shown; this makes it easier to check if there are mistakes in the solution. The computation is facilitated by using C language, which is widely available. The program will benefit both lecturers and students.

Acknowledgement

The authors wanted to convey their thanks to Assoc. Prof. Charoon Charoennetkul and Dr. Keerati Inthavisas who had facilitated the first author to submit this paper to the RMUTCON 2018.

References

- Becker, M. 1986. **Heat Transfer A Modern Approach**. Plenum Press, New York.
- Cengel, Y. 2002. **Heat Transfer A Practical Approach**. 2nd Ed. McGraw-Hill. New York.
- Chapman, A.J. 1960. **Heat Transfer**. The Macmillan Company, New York.
- Holman, J.P. 2010. **Heat Transfer**, 10th Ed. McGraw-Hill, New York.
- Howell, J.R. 1982. **A Catalog of Radiation Configuration Factors**. McGraw-Hill, New York.
- Howell, J.R. 2018. **A Catalog of Radiation Configuration Factors**. Available Source: <http://www.thermalradiation.net/tablecon.html#C1>, April 10, 2018.
- Howell, J.R., Siegel, R. and Mengüç, M.P. 2011. **Thermal radiation Heat Transfer**. CRC Press, Boca Raton.
- Incropera, F.P., Dewitt, D.P., Bergman, T.L. and Levine, A.S. 2007. **Fundamentals of Heat and Mass Transfer, 6th Ed**. John Wiley & Sons.
- Keith, F., Maglik, R.M and Bohn, M.S. 2011. **Principles of Heat Transfer**. Cengage Learning, Inc. Stamford.

Structural Engineering Assessment for Seismic Damaged Concrete Building: A Case Study of One Storey Kindergarten School

Thanongsak Imjai ^{1*}, Surin Suthiprabha ¹ and Thaworn Thirawetchayan ¹

ABSTRACT

Partial and total collapses of existing buildings during strong earthquakes in developing countries are responsible for heavy losses and numerous casualties. In Northern Thailand, many substandard reinforced concrete buildings were subjected earthquake on June 5, 2014 in Chaingrai province and many of these damages are attributed to the collapse of numerous ductile reinforced concrete (RC) frame buildings built before the introduction of modern seismic design guidelines. Many of such collapses occurred due to structural failures of inadequately detailed critical structural elements, such as columns and beam-column joints. Structural engineering assessment performed in this project is divided into two steps: 1) Initial structural assessment that will involve recording the history of the building from its inception to completion and subsequent lift and mapping of abnormalities, defects as to the type, magnitude, locations and severity and 2) in the second step, Detail Engineering Assessment (DEA) will then follow. The DEA process deals with making field measuring to obtain accurate information on member properties, dimensions, and position and loading that imposed on the working area. Following information and discussion was made during the DEA process. This article reports a case study of a structural engineering assessment on one storey-concrete building in kindergarten school which is located in Ampor Pan, Chaingrai province. The building is partially damaged as several cracks were formed along the wall and beam-column joints. As part of initial assessment, innovative and repair solutions are introduced to minimize the construction time and labour and material cost.

Keywords: Structural engineering assessment, Seismic assessment, Strengthening, Ductility

¹ Construction Innovation Research Unit (CIRU), Department of Civil Engineering, Rajamangala University of Technology Tawan-Ok, Bangkok, 10310, Thailand

*Corresponding author, e-mail : thanongsak_im@rmutto.ac.th

Introduction

High human and economic losses in recent major earthquakes in developing countries in Asia (Pakistan 2005, Indonesia 2008, Nepal 2015) have highlighted the seismic vulnerability of many existing reinforced concrete (RC) structures. Whilst Thailand is located in a region of moderate seismic hazard, the 2011 Burma and 2014 Mae Lao earthquakes exposed the vulnerability of the existing RC building stock. Many collapses in buildings were attributed to inadequate reinforcement detailing of beam-column joints and to the use of low strength concrete (Ornthammarath, 2015; Lukkunaprasit *et al.*, 2015). For instance, Figure 1a shows a partial collapse of a building due to beam-column joint failure during the 2014 Mae Lao earthquake (Chaeng-rai, Thailand), whereas Figure 1b shows typical substandard detailing observed in such beam-column joints. Although an up-to-date seismic design code was enforced in Thailand in 2007 (EIT 1302-52), the code does not provide guidance on vulnerability assessment of existing deficient buildings. Moreover, it is necessary to find suitable strengthening solutions to reduce the vulnerability of these buildings.

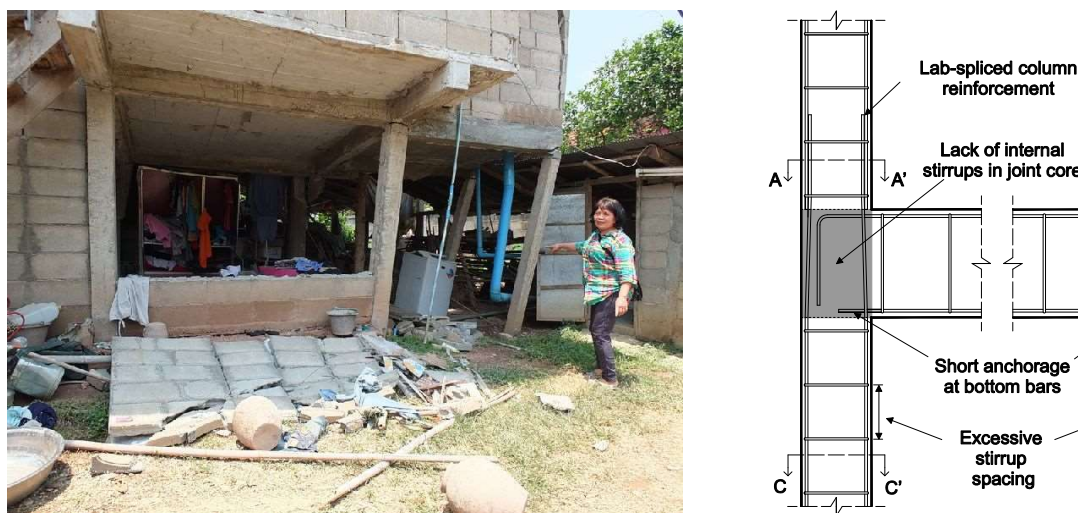


Figure 1 (a) Building partial collapse during the 2014 Mae Lao earthquake (Chaing-rai, Thailand) due to failure of exterior beam-column joints, and (b) typical substandard detailing of beam-column joints in Thailand

As part of the Academic Engineering Consultancy Service that the Construction Innovation Research Unit (CIRU) team from Rajamangala University of Technology Tawan-Ok has been requested to perform structural integrity investigation of one story reinforced concrete (RC) building that was damaged during the 2014 Mae Lao earthquake. The team consists of a local chief engineer and academic experts (CIRU) to perform a visual inspection to preliminary assess building structural safety based on Engineering Institute of Thailand Building Code (EIT 1302-52). The project is divided into two phases; phase 1 deals with structural engineering assessment of damaged building and 2) results from phase 1 will be used to design repair/strengthening solutions in phase 2.

This paper describes the results from structural engineering assessment thorough visual inspection of every structural element in the building performed in Phase 1. Non-Destructive

Tests (NDT) were also used and followed by software analysis of concrete strength. Such assessment was used to decide whether further in-depth assessment with Destructive Tests or Strengthening is required. The outcome from phase 1 contributes towards promoting the use of innovative strengthening techniques such as EBR FRP (Imjai and Garcia 2016) and Post-Tensioned Metal Strapping (PTMS) (Ma *et al.*, 2016; Imjai *et al.* 2018) as strengthening solutions in the seismic zone of South East Asia as proposed in the rehabilitation work in phase 2.

Project facts

The investigated RC building is the public primary school (Sanchangtai School) located in Northern of Thailand (Ampor Pan, Chiang Rai province). The one story RC building has 7 teaching rooms (13 bays in X and 3 bays in Y directions having a typical span of 3 m - see Figure 1). The building was built in 1998. The cross-section of column is 20x20 cm, 3 m height, reinforced with main reinforcement of 4-DB 12 and RB6@0.20 as steel stirrup. The wall is made from concrete block. The ground slab is 12 cm thick. Before performing the visual inspection, no drawing/material data were available and the averaged concrete compressive strength were obtained from NDT test as $f'_c = 175$ ksc. With such a limit information from the construction drawings, detailed engineering assessment (DEA) was subsequently performed by the design team to re-check structural capacity of the as-built concrete members.



Figure 1 Overview of one story kindergarten school

Structural Condition Assessment and Damage level

During work performed in phase 1, the visual inspection is limited to those areas and sections of the damaged RC building that is fully accessible and visible to the inspector teams at the time of inspection. Nothing contained in this article implies that any inaccessible or partly inaccessible area(s) or section(s) of the damaged RC building being inspected by the assessor on the date of the inspection were free from defects latent or otherwise. There could be some difficulties in the conduct of a visual inspection as some of the main structural elements in a building may have been covered up by architectural finishes. It is therefore important that professional judgment is exercised by the structural engineer to determine which areas that are covered up should be exposed for inspection. Reference to structural layout plans to determine the presence of critical structural elements would be crucial under such circumstances. In order to investigate the damage rank of the building as a whole, design checks on load bearing capacity with the actual material properties needs to be considered. The flow chart from preliminary inspection to solution can be shown in Figure 2.

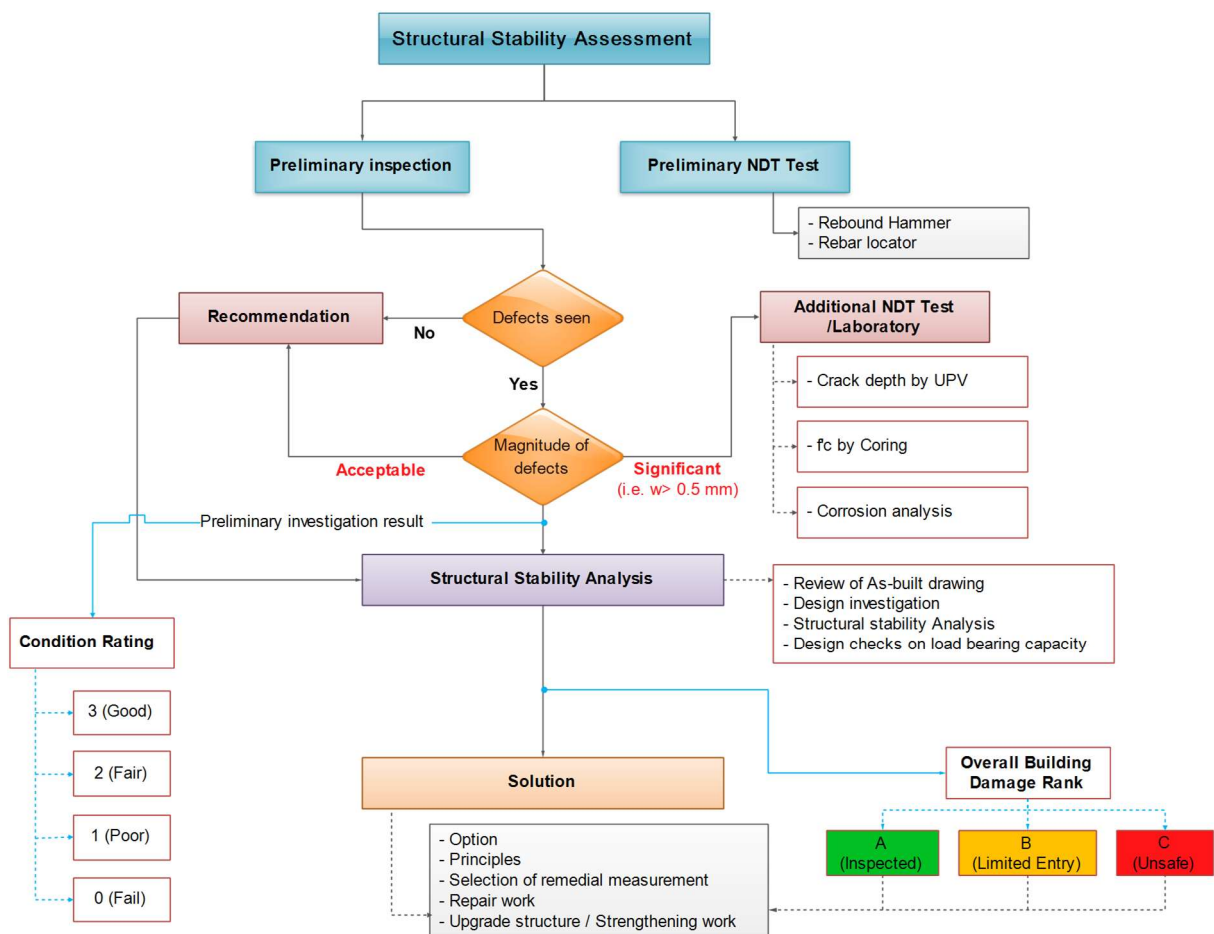




Figure 2 Flow chart from structural condition assessment to solution

For damages as a result of current loading, repair or replacement terms will be added to the criteria for the structure at present condition, i.e. a structural element that shows small defects, well maintenance and good construction practice will have condition rating of 2 or “Fair condition”. If the same element has some effects/damages from current loading to the level that replacement of the element will be of more benefit to the whole structure than rehabilitation, then the term “Replacement” shall be recommended for “Fair condition”

(adopted from ACI 364.1 R-94, USACIERL Technical Report M-91/18, RILEM Technical Committee 104). No responsibility can be accepted for defects, which are latent or otherwise not reasonably detected on a visual inspection without interference with or removal of any of the structure including fixtures or fittings on the inspected building (e.g. Figure 3). For the purpose of this inspection, the following definitions, an element rating system is developed to properly assess the current condition against the originally intended function of the existing structure. From the field inspection, Inspectors have classified the conditions of the structural components into four groups as listed in Table 1 and Table 2 adopted from RILEM Technical Committee 104 (1991).

Table 1 Structural condition rating, action requires and equivalent floor damaged rank

Condition Rating	Descriptions	Required Action	Building Damage Rank*
3 (Good)	Element performs intended function with high degree of reliability. The item or area inspected appears to be in sound condition without any significant visible defects.	None	 Rank A
2 (Fair)	Element performs intended function with small reduction in reliability. No effects on structural performance and/or instability.	May require some minor repairs of maintenance, and /or increase inspection frequency.	Rank A or Rank B
1 (Poor)	Element does not perform intended function with any degree of reliability. The item or area inspected exhibits some minor defects, minor damage or deterioration due to age or lack of maintenance.	Immediate repair or replacement of Element.	Rank B
0 (Fail)	Element does not perform intended function at all	Immediate replacement or Provision of immediate temporary support.	 Rank B or Rank C

* Note: Equivalent building damage rank is given to the individual floor inspected and the design checks and current loading condition will be accounted for. Damage Rank is shown as

 Rank A	 Rank B	 Rank C
INSPECTED	LIMITED ENTRY	UNSAFE



Figure 3 Walk-through preliminary inspection of damaged building (photo no. F-01)

Table 2 Damage conditions for reinforced concrete member

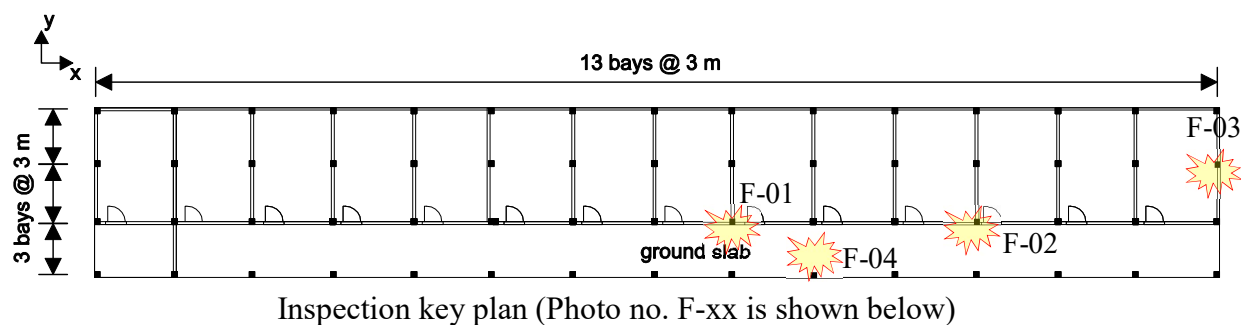
Rating level	Condition state of RC Components			
	Column width > 40cm	Beam-Column Joint	Beam	Slab
3 (Good)	<ul style="list-style-type: none"> Visibly narrow shear cracks Superficial cracking Shrinkage cracks 	<ul style="list-style-type: none"> No shear cracks 	<ul style="list-style-type: none"> Visibly narrow shear or flexural cracks Superficial cracking Shrinkage cracks 	<ul style="list-style-type: none"> Visibly narrow cracks Superficial cracking Shrinkage cracks
2 (Fair)	<i>(w < 0.2 mm)</i>		<i>(w < 0.2 mm)</i>	<i>(w < 0.2 mm)</i>
	<ul style="list-style-type: none"> Visibly clear shear cracks 	<ul style="list-style-type: none"> No shear cracks Spalling of column corner concrete 	<ul style="list-style-type: none"> Visibly clear shear/flexural cracks 	<ul style="list-style-type: none"> Visibly clear shear/flexural cracks
1 (Poor)	<i>(0.2 < w < 1 mm)</i>		<i>(0.2 < w < 1 mm)</i>	<i>(0.2 < w < 1 mm)</i>
	<ul style="list-style-type: none"> Minor cracks Local crush of cover concrete Small exposure of reinforcing bars may be observed. 	<ul style="list-style-type: none"> No shear cracks Spalling of cover concrete of joint 	<ul style="list-style-type: none"> Minor shear/flexural cracks Local crush of core concrete Small exposure of reinforcing bars may be observed. 	<ul style="list-style-type: none"> Minor shear/flexural cracks Local crush of core concrete Small exposure of reinforcing bars may be observed.
0 (Failed)	<i>(1 < w < 2 mm)</i>		<i>(1 < w < 2 mm)</i>	<i>(1 < w < 2 mm)</i>
	<ul style="list-style-type: none"> Buckling and/or breaking of reinforcing bars. 	<ul style="list-style-type: none"> Buckling of reinforcing bars 	<ul style="list-style-type: none"> Buckling and/or breaking of 	<ul style="list-style-type: none"> Buckling and/or breaking of

<ul style="list-style-type: none"> • Crush of core concrete • Visible settlement and/or inclination of floor 	<ul style="list-style-type: none"> • Crush of core concrete • Visible vertical deformation of joint 	<ul style="list-style-type: none"> reinforcing bars. • Crush of core concrete • Visible settlement and/or inclination of floor 	<ul style="list-style-type: none"> reinforcing bars. • Crush of core concrete • Visible settlement and/or inclination of floor
<i>(w > 2 mm)</i>		<i>(w > 2 mm)</i>	<i>(w > 2 mm)</i>

Key Areas to inspect for any cracking, spall, leaching, signs of corrosion etc:

1. Shear zones near supports (likely diagonal cracks), 2. Beam-column joint, and 3. Mid-span of beams

It is, however, noted that a preliminary walk-round condition survey (Figure 3) is essential and during the walk-round there may be an opportunity to obtain samples of defects / loose concrete or cracks from spalled area that may be easily detached. At this stage, opportunities to view all the structure may be limited, for example, high parts of the structure or hidden areas behind false ceilings. During the visual inspection, structural condition rating (i.e. Table 1) will be given to the inspected structural components such as column, beam and slab of the building. This rating condition is given according to the damages observed during the walk-round survey only. Damages such as concrete spalls, cracks, pop-outs are classified according to the degree of damages and rating level ranged from 0 (Fail) to 3 (Good). This condition rating for individual structural components shall not use as representative damage rank for the whole building. It is intended to use as conditional rating for only inspected structural members and thus required action can be specified for those members once the rating condition is given. Results from structural engineering assessment performed during phase 1 is shown in Figure 4.



F-01: Vertical crack ($w=0.2$ mm),
condition rating = “Fair”



F-02: Vertical crack ($w=0.15$ mm),
condition rating = “Fair”



F-03: Vertical crack on wall ($w=0.2$ mm),
condition rating = “Fair”



F-04: floor crack ($w > 2$ mm),
condition rating = “Poor”

Figure 4 Photos from visual inspection

Structural analysis and design checks according to ACI 318

A preliminary structural assessment and detailed engineering analysis of the RC building according to ACI 318 (2005) indicated that the flexural capacity of the existing RC concrete building was sufficient to sustain the original design live load. Since there is no detailed drawing/material information available at the time of inspection, concrete strength was determined using rebound hammer and yield strength of steel reinforcement was assumed to steel grade SD30 and SR24 for flexural and shear reinforcement respectively. Concrete covering and reinforcement details were also measured using Ferro scan techniques. This NDT technique gives enough information for further structural analysis. The design of the original RC members required that the design flexural strength exceeded the required factored moment

using original design live load of 300 kg/m² (public school) (i.e. $\phi M_n > M_u$). However, the ground concrete slab (thickness = 10 cm) should have sufficient strength (although without risk of collapse) to resist a certain level of seismic load in case the compact soil underneath the slab failed. It is evident that detailed reinforcement of original design was not complied with the modern seismic design guidelines and therefore, strengthening work is required to improve overall structural seismic performance. The use of innovative composite materials and novel metal strapping methods was proposed in phase 2, as discussed in the following.

Concrete crack repair and Innovative strengthening technique

According to recent strengthening techniques developed at the Rajamangala University of Technology Tawan-Ok (RMUTTO), Imjai and Garcia (2016) carried out a series of tests to verify the effectiveness and applicability of the Post-tensioned Metal Strapping (PTMS) technique at different scale levels led to the development of a novel technique for retrofitting RC beams and columns using thin Post-Tensioned Metal Straps (PTMS). The technique uses ductile high-strength steel straps post-tensioned around RC elements using strapping tools as those used in the packaging industry (see Figure 5a Metal straps are commercially available in various thicknesses, widths and strengths. The ease of handling and strengthening objective determine the strap dimensions. Typical metal strap yield strengths vary between 300 and 1,000 MPa. Two types of tensioning machines exist i) pneumatic, in which the tension force is regulated accurately by applied air/hydraulic pressure (see Figure 5b), or ii) manual, in which the tension force is controlled by the operator. A cylindrical specimen confined using an air-powered tensioning machine is shown in Figure 5c.

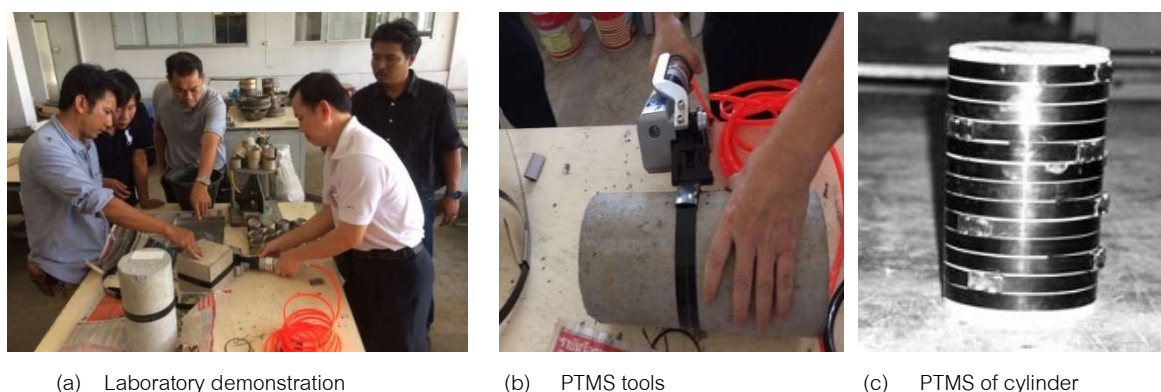


Figure 5 (a)-(b) Post-tensioning strapping, and (c) view of PTMS-confined cylinder (After Imjai *et al.*, 2018)

At the time of inspection, the building was damaged during the 2014 Mae Lao earthquake and the inspection team performed a preliminary and detailed engineering assessment on the building during 26-30 March 2018. As seen in Figure 4, several vertical cracks were found along the wall of the building, the crack widths ranged from 0.2-0.3 mm. No cracks were found on the main structural members such as column or beam. Only non-structural members such as wall or ceiling were damaged. The vertical cracks found along the concrete wall adjacent to the column face, was attributed to the lack of sufficient dowel reinforcement and the low concrete strength. It was proposed to repair the cracked concrete wall using epoxy injections prior to carrying out any strengthening work of the columns. Several strengthening schemes were proposed including traditional solutions, such as externally bonded steel plate (EBS), concrete sectional enlargement and post-tensioned metal strapping (PTMS) for main structural members to resist the actual, increased seismic load. A novel PTMS technique was chosen as a repair / strengthening solution to increase the seismic resistant capacity of buildings.

The strengthening design and construction procedure were in accordance to current ACI 318. The strengthening work is being planned and will be carried out in phase 2.

Concluding Remarks

The task performed in this project is divided into two steps: 1) Initial structural assessment that will involve recording the history of the building from its inception to completion and subsequent lift and mapping of abnormalities, defects as to the type, magnitude, locations and severity and 2) in the second step, Detail Engineering Assessment (DEA) will then follow. The DEA process deals with making field measuring to obtain accurate information on member properties, dimensions, and position and loading that imposed on the working area. Following information and discussion was made during the DEA process. Based on the case study discussed in this paper, the following conclusions can be drawn:

- Design verifications based on ACI 318 showed that the flexural and shear capacity of the original concrete members were sufficient to resist original design live loads. Externally bonded CFRP systems was successfully to increase the total flexural capacity of original post-tensioned concrete slabs by up to 120% compared to their original design capacity.
- During the visual inspection, vertical cracks found on the concrete wall with a maximum crack width of 0.2 mm which is rated as “Fair” condition. Thus this damaged wall required repair work. For ground slab, it was found that a 2 mm crack width occurred at the columns and thus was rated as “Poor”, required urgent repair work.
- It is recommended that crack repair and strengthening techniques such the use of externally bonded carbon fiber composites and post-tensioned metal strapping could be used to upgrade existing/damaged RC building for future seismic occurrence.

Acknowledgement

The authors acknowledge the financial supports provided by the National Research Council of Thailand (NRCT 2017-18) through the Research and Development Institute of Rajamangala University of Technology Tawan-Ok (RMUTTO). The authors are also thankful to Mr. Sunan Somsrida, director of the Sanchangtai School, Ampor Pan, Chiang Rai province, for providing access to the field inspection work during the first phase of the project.

References

- ACI 318. 2005. **Building Code Requirements for Structural concrete and Commentary**, B.M Johnson and A.H. Wilson, Terminology of Building Conservation Industry, Division of Building Research, NRC Canada.
- ACI 364.1. 1999. **Guide for Evaluation of Concrete Structures Prior to Rehabilitation**. 22 pp.
- Ellsworth, D. E. and Ginnado, K. 1991. **Guide for Visual Inspection of Structural Concrete Building Components**. USACIERL Technical Report M-91/18. 76 pp.
- Frangou, M., Pilakoutas, K., Dritsos, S., 1995. Structural repair strengthening of RC columns. **Construction Building Materials**, 9(5):259–266.
- Imjai , T., Garcia , R. and Pilakoutas, K. 2018. Strengthening of RC members using Post-Tensioned Metal Straps: state of the research. Lowland Technology International 2018; Special Issue on: **Green Technology for Sustainable Infrastructure Development** 19 (1): 1-10 ISSN 1344-9656.

- Imjai, T. and Garcia, R., 2016. Performance of damaged RC beams repaired and/or strengthened with FRP sheets: an experimental investigation. In **24th Australasian Conference on the Mechanics of Structures and Materials (ACMSM24)**. 7-9 December 2016 Perth, Western Australia.
- Lukkunaprasit, P., Ruangrassamee, A., Boonyatee, T., Chintanapakdee, C., Jankaew, K., Thanasisathit, N., and Chandrangsue, T. 2015. Performance of structures in the Mw 6.1 Mae Lao earthquake in Thailand on May 5, 2014 and implications for future construction. **Journal of Earthquake Engineering** DOI: 10.1080/13632469.2015.1051636
- Ornthammarath, T. 2015. Seismic Performance of Non-Engineered Residential Buildings in the 2014 Mae Lao Earthquake. In **Proceedings of the Tenth Pacific Conference on Earthquake Engineering**, 6-8 November 2015, Sydney, Australia
- Ma, C. K., Awang, A. Z., Omar, W., Liang, M., Jaw, S. W. and Azimi, M. 2016. Flexural capacity enhancement of rectangular high-strength concrete columns confined with post-tensioned steel straps. **Structural Concrete** 4:668-676.
- RILEM Technical Committee 104. 1991. Damage classification of concrete structures. **Materials and Structures** 24(4): 253-259.

Durable Articles and Building Repairing Informing System: A Case Study of RMUTSV Rattaphum College

Wanpracha Nuansoi ^{1*}, Supawadee Mak-on¹, Suppachai Maduea¹,
Sivadol Noulnoypadol¹ and Wandee Nuansoi ²

ABSTRACT

Due to the problem of durable articles and building repairing informing system in RMUTSV, Rattaphum College still used the paper in step of informing to the repairing section. It caused several belated operations such as taking long time to inform the repairing, knowing the results of repairing difficultly, taking time to check and search for the informing repairing data, and losing the data. The researchers developed the durable articles and building repairing informing system, a case study of RMUTSV, Rattaphum College, by using the software development life cycle (SDLC). The Data Flow Diagram (DFD) was used to design of data following, and E-R Diagram was used to design the database. System development was employed with PHP language and MySQL was used for the database. The results of development was presented as 2 sectors, administrator and user. The administrator was able to log in, add members, edit data, add and delete the informing repairing data, and view the report of the informing repairing. Meanwhile, the user was able to log in, inform the repairing and view the report of informing repairing only.

The results of satisfaction on presenting the system showed that the users were satisfied with the system at a good level ($\bar{x} = 4.47$, $SD. = .52$) and the results of satisfaction on using the system showed that the users were satisfied with the system at a very good level ($\bar{x}=4.56$, $SD. = .49$).

Keywords: Informing, Repairing, PHP, MySQL

¹ Department of Industrial Rattaphum College, Rajamangala University of Technology Srivijaya, Thachamuang, Rattaphum, Songkhla 90180, Thailand

² Department of General Education Rattaphum College, Rajamangala University of Technology Srivijaya, Thachamuang, Rattaphum, Songkhla 90180, Thailand

*Corresponding author, e-mail : wanpracha.n@rmuts.ac.th

Introduction

Rajamangala University of Technology Srivijaya (RMUTSV) Rattaphum College had a durable articles and building repairing informing system through paper forms and send them to the repair department in sequence, it caused several belated operations such as informing repairing, informing result of operation, checking and searching informing repairing, loss of data and waste of resources as a fishbone chart.

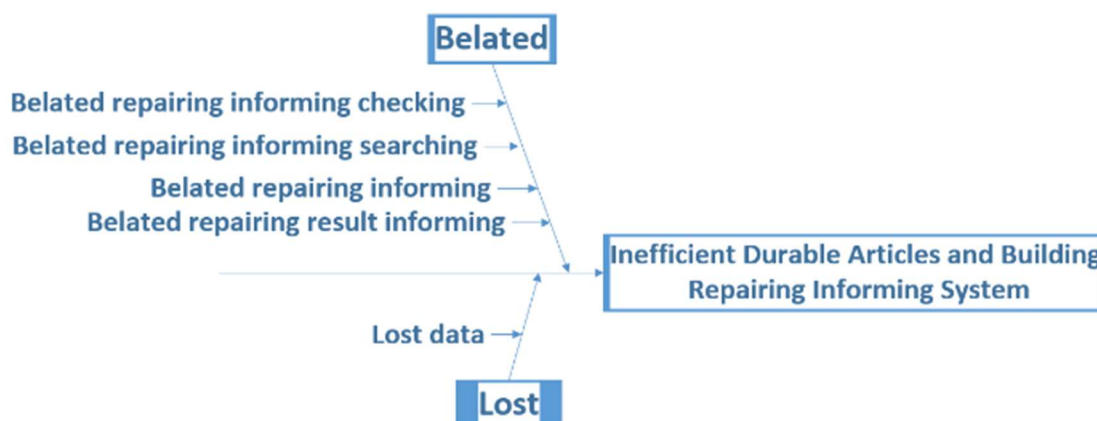


Figure 1 fishbone chart shows inefficient durable articles and building repairing informing system

To solve this problem, the research team has developed a durable articles and building repairing informing system through the web application. In this article, the first part is the introduction, the second part is related work, the third part is the system design, the fourth part is the experimental results and finally the conclusion.

Materials and Methods

1. Durable Articles

Durable articles (Durable Articles, 2017) is an asset that is intended for use in operations, is durable and has a useful life more than 1 year, with a record of durable articles having value more than 5,000 baht. They are purchased by procurement, hiring consultants, Hiring design and controlling and the lease to obtain the use of the organization and control the distribution of the regulation.

2. Software Development Life Cycle (SDLC)

It is a software development process (Vanshika, 2015). The traditional software development lifecycle includes the following processes: 1) planning 2) analysis 3) software design 4) programming 5) user manual 6) testing 7) implementation and maintenance

3. Data Flow Diagram (DFD)

A diagram (Rosziati, 2010) that shows the direction of the flow of data in the system. The DFD provides an overview of the system and show the process in the system. The data in the diagram presents data come from, where it went, where it was stored and what happened to the data on the way.

4. Entity Relationship Diagram (E-R Diagram)

E-R Diagram (Song *et al.*, 1995) shows the relationship between the data including entity, attribute and relationship, entity as objects or things that we do in the event, attribute is a property of the object that we are interested, relationship is a relationship between entity. There are several types, such as one-to-one, one-to-many, and many to many.

5. Hypertext Preprocessor (PHP)

PHP (PHP, 2017) is a popular general-purpose scripting language that is especially suited to web development. Fast, flexible and pragmatic, PHP powers everything from your blog to the most popular websites in the world.

6. MySQL

MySQL (MySQL, 2017) is the world's most popular open source database. With its proven performance, reliability and ease-of-use, MySQL has become the leading database choice for web-based applications, used by high profile web properties including Facebook, Twitter, YouTube, Yahoo! and many more.

7. phpMyAdmin

phpMyAdmin (phpMyAdmin, 2017) is a free software tool written in PHP, intended to handle the administration of MySQL over the Web. phpMyAdmin supports a wide range of operations on MySQL and MariaDB. Frequently used operations (managing databases, tables, columns, relations, indexes, users, permissions, etc) can be performed via the user interface, while you still have the ability to directly execute any SQL statement.

8. System Design

E-R Diagram level 0 or context diagram consists two entities, user and administrator. Administrator can login, adding member, editing data, adding deleting and view report informing repairing. The user is able to login, informing repairing and view report informing repairing only.

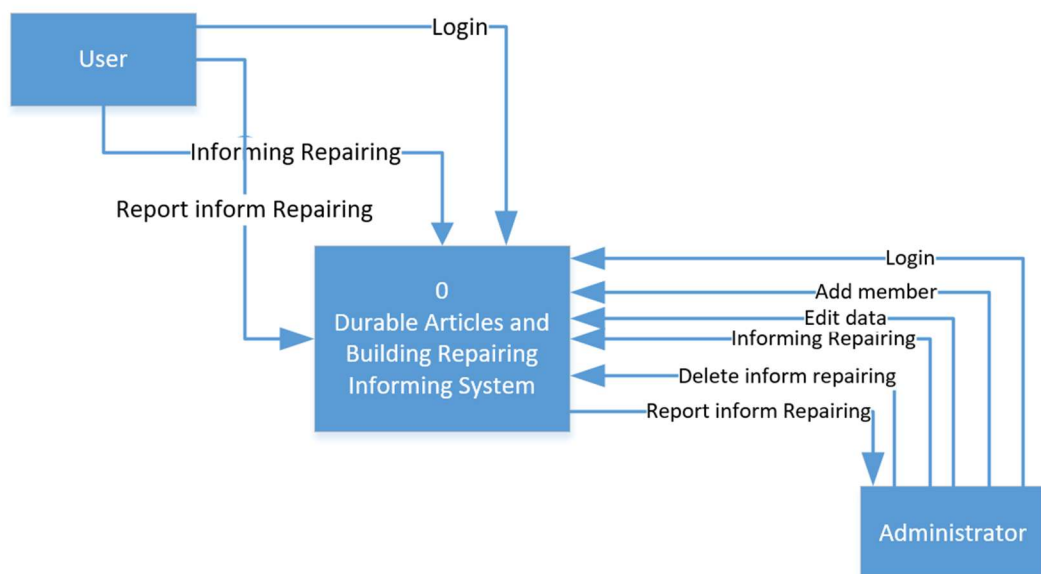


Figure 2 DFD level 0 or context diagram.

E-R Diagram level 1 shows all process in the system, it consisted six process including login, adding user, editing data, informing repairing, delete inform repairing and report informing repairing. All process had three part that is sending data to process, process getting data or putting data to database and process sending report to entity.

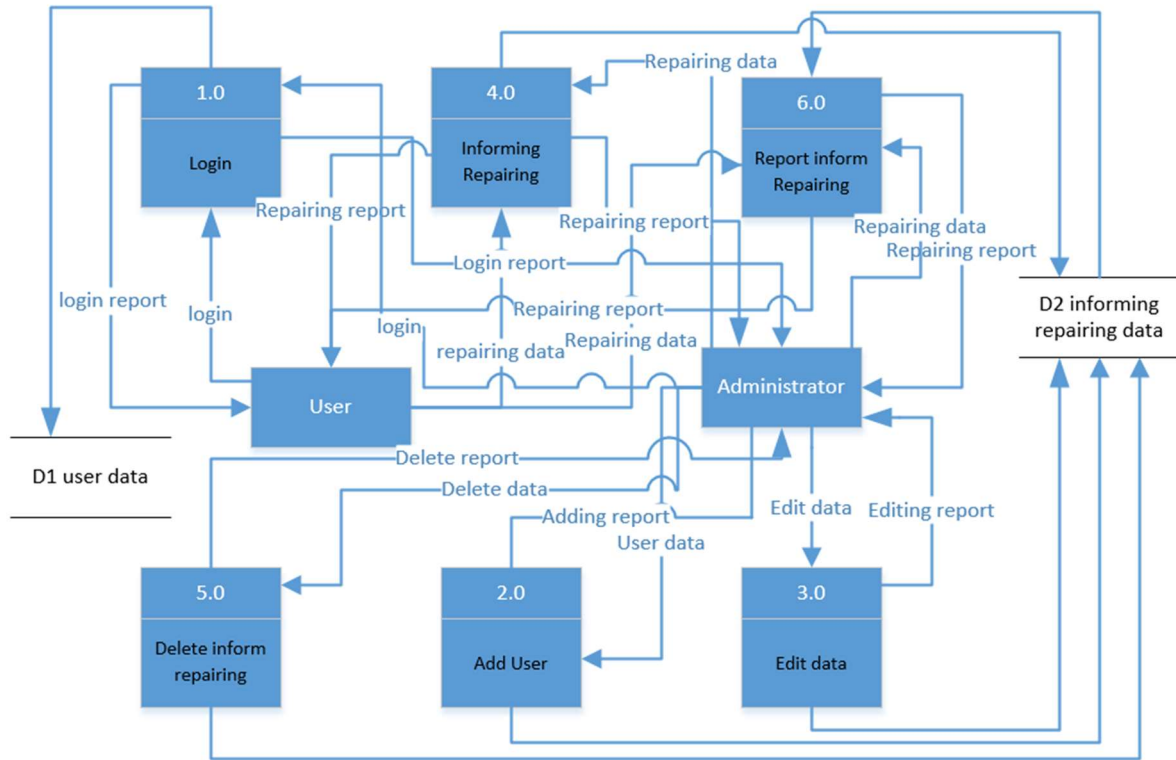


Figure 3 DFD level 1.

Database design using E-R Diagram

E-R Diagram consists three entities, user, durable articles repairing informing data and building repairing informing data. The user has attribute including ID, password, name, and status. Informing repairing building data has attribute enclosing building ID, informer name, defective item, defective, place and department. The last entity is informing repairing durable articles data which has attribute comprising durable articles ID, durable articles name, symptoms and informer name.

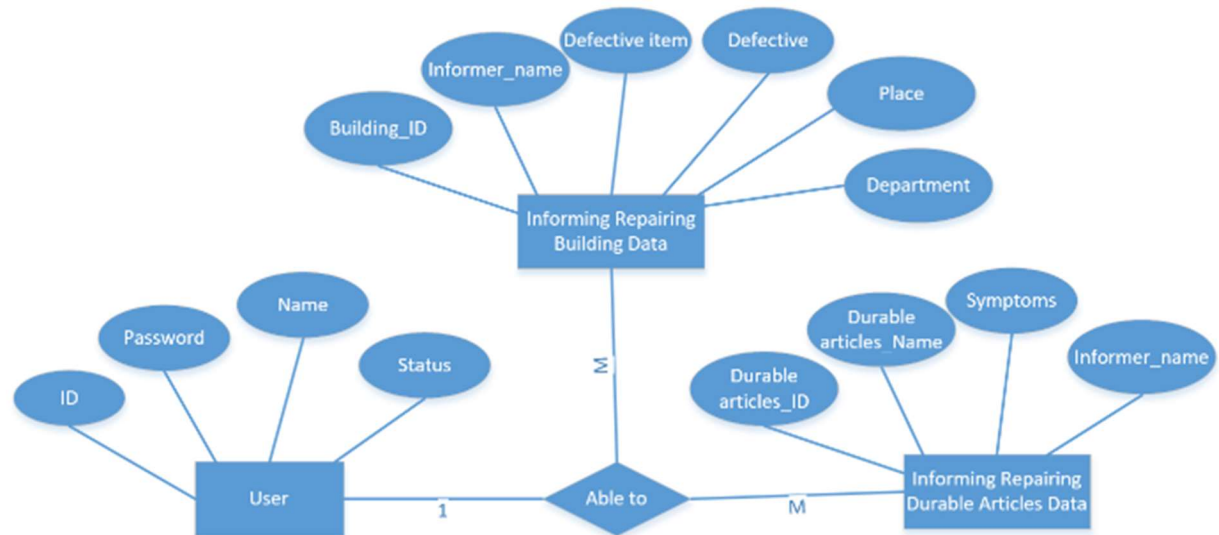


Figure 4 E-R Diagram.

When design E-R Diagram completion then we can convert form E-R Diagram to relational database table including user entity can be converted to relational database table as table 1, informing repairing building data entity can be converted to relational database table as table 2 and informing repairing durable articles data can be converted to relational database table as table 3.

Table 1 user table

<u>User ID</u>	Password	Name	Status	<u>Building ID</u>	<u>Durable articles ID</u>

Table 2 informing repairing building data table

<u>Building ID</u>	Informer_name	Defective item	Defective	Place	Department	<u>User ID</u>

Table3 informing repairing durable articles data table

<u>Durable articles ID</u>	Durable articles Name	Symptoms	Informer Name	<u>User ID</u>

Satisfied Evaluation of the system

We used Likert Scale having a five-level as follows.

5 means efficiency and satisfaction is very good.

4 means efficiency and satisfaction is good.

3 means efficiency and satisfaction is a moderate.

2 means efficiency and satisfaction is low.

1 means efficiency and satisfaction is lowest.

Satisfaction assessment test of users have two kinds that lecturer and officer amount twenty-five person. There are criteria for assessing the satisfaction of the system five levels of rating scales.

4.50-5.00 means efficiency and satisfaction is very good.

3.50-4.49 means efficiency and satisfaction is good.

2.50-3.49 means efficiency and satisfaction is a moderate.

1.50-2.49 means efficiency and satisfaction is low.

1.00-1.49 means efficiency and satisfaction is lowest.

Statistical Methods

Descriptive statistics were used to describe the characteristics of the data such as mean (X) and standard deviation (SD)

Acceptance criteria of the test group

The average score is better to recognize that the system is efficient and satisfying to use.

Results and Discussions

There are two types of users: administrators and users. Administrators can login, adding user, editing data, adding deleting and viewing report informing repairing. The users are able to login, informing repairing and view report informing repairing only. Users can view their repair logs without login that the latest update will be displayed. If they log in with your username and password that get from administrator, are able to informing repairing both durable articles and building, can find a list of informing repairing for a specific date range, can also specify the search status, such as completed and in progress status.



Figure 5 the home page of system on website.

Forms of durable articles informing repairing consist four part, informer name, durable articles ID, durable articles name and symptom when users filled complete and press the submit button to save. The system will notify to confirm for saving data.

แบบฟอร์มแจ้งซ่อมครุภัณฑ์

ผู้แจ้ง:

หมายเลขครุภัณฑ์:

ชื่อครุภัณฑ์:

อาการเสีย:

บันทึกแจ้งซ่อม

Figure 6 Forms of durable articles informing repairing.

Forms of building informing repairing consist five part, informer name, department, defective item, place and defective when users filled complete and press the submit button to save. The system will notify to confirm for saving data.

แบบฟอร์มแจ้งอาคารสถานที่

ผู้แจ้ง:

หน่วยงาน:

รายการชำรุด:

สถานที่:

ลักษณะการชำรุด:

บันทึกแจ้งซ่อม

Figure 7 Forms of building informing repairing.

Table 4 the results of satisfaction on presenting the system.

No.	Acceptation Statement	\bar{X}	SD	Degree
1	Accuracy in content arrangement.	4.52	0.50	Very much
2	Accuracy in using the media or images in the display.	4.28	0.54	much
3	Quick to use.	4.72	0.45	Very much
4	Appropriate use of symbols or images in the media.	4.36	0.48	much
Total		4.47	0.52	much

Table 5 the results of satisfaction on using the system.

No.	Acceptation Statement	\bar{X}	SD	Degree
1	Easy to use system.	4.64	0.48	Very much
2	Appropriate to choose font type.	4.32	0.47	much
3	System suitability.	4.52	0.50	Very much
4	Accuracy in data validation through the system.	4.68	0.47	Very much
5	The correctness of the data through the system.	4.52	0.50	Very much
6	The speed to use the system.	4.72	0.45	Very much
	Total	4.56	0.49	Very much

Conclusions

Durable articles and building repairing informing system development in part of data flow design is used DFD that consisted DFD level 0 and 1 for showing overview of the system and all system process. The another design is database design which is used E-R Diagram comprising three entities, user, durable articles repairing informing data and building repairing informing data. The software development on website is used PHP language and database is used MySQL. The result of development consisted login, adding user, editing data, adding deleting and viewing report informing repairing. The system had two user, user and administrator, user could use three systems, login, adding and viewing report informing repairing, and administrator could use all systems.

The results of satisfaction on presenting the system showed that the users were satisfied with the system at a good level ($x = 4.47$, $SD = .52$) and the results of satisfaction on using the system showed that the users were satisfied with the system at a very good level ($x = 4.56$, $SD = .49$).

Acknowledgements

Thank you for the research assistant is Mr. Sathaporn Naratho

References

- Durable Articles. n.d. Available Source: <http://www.vcharkarn.com>, November 1, 2017.
- Hypertext Preprocessor (PHP). 2017. Available Source: <http://php.net>, November 1, 2017.
- Ibrahim, R. and Yen, S. Y. 2010. Formalization of the data flow diagram rules for consistency check. **International Journal of Software Engineering & Application** 1(4):95-111.
- MySQL. 2017. Available Source: <https://www.mysql.com>, November 1, 2017.
- phpMyAdmin. 2017. Available Source: <https://www.phpmyadmin.net>, November 1, 2017.
- Rastogi, V. 2015. Software Development Life Cycle Models-Comparison, Consequences. **International Journal of Computer Science and Information Technologies** 6(1): 168-172.
- Song, I. Y., Evans M. and Park, E.K. 1995. A Comparative Analysis of Entity-Relationship Diagram. **Journal of Computer and Software Engineering** 3(4): 427-459.

Using Information Systems in Curriculum Management According to the Standard Framework of Vocational Education Undergraduate

Soontorn Kongsintu^{1*}, Piya Korakotjintanakarn² and Nudthee Srisawa³

ABSTRACT

This research aims (1) to analyze the opinion about using information system in curriculum management according to the standard framework of vocational education undergraduate and (2) to develop information system in curriculum management tools to the standard framework of vocational education undergraduate created by the researchers. The sample group of this research was the representative teachers from 23 institutes of vocational education. 52 respondents who have experienced in using TQF: HEd. 3-7 or TQF: VEd. 2-6. were as a sample group the participants who were chosen by a purposive sampling. The instruments used in this research were information system in curriculum management and a questionnaire of experts' opinion on using information system in curriculum management with 5 rating scales. Statistical analysis used was Mean and Standard Deviation.

The results found that the teachers in institutes of vocational education agreed with using information system in curriculum management at the mean level of 4.17. The standard deviation (S.D.) was at 0.70. When considering each item, it was found that the teachers in institutes of vocational education agreed with using information system in curriculum management on efficiency and usage of the system was at high level ($\bar{x} = 4.19$, S.D.= 0.72). According to the item of designing was at high level ($\bar{x} = 4.20$, S.D.= 0.64), for the item of user supporting and service was at the high level ($\bar{x} = 4.11$, S.D.= 0.73). The research found that the mentor and developer of the system should focus on building up confidence to the users in data connection of the system, system connection in using, beauty, modernity, and interesting homepage. The minor importance was the speed of the display, letter, and information.

Keywords: curriculum management, information systems, curriculum Management Tools

¹Technical Pedagogic Research and Development Program, Department of Teacher Training in Mechanical Engineering, Faculty of Industrial Education, King Mongkut's University of Technology North Bangkok, Khwaeng Wong

Sawang, Khet Bang Sue, Krung Thep Maha Nakhon 10800, Thailand

²Department of Teacher Training in Mechanical Engineering, Faculty of Industrial Education, King Mongkut's University of Technology North Bangkok, Khwaeng Wong Sawang, Khet Bang Sue, Krung Thep Maha Nakhon 10800, Thailand

³Institute of Vocational Education Coordination Center. Office of Vocational Education Commission, 319 Ratchadamnoen Nok Road, Khwaeng Dusit, Khet Dusit, Krung Thep Maha Nakhon 10300, Thailand

*Corresponding author, e-mail : Soonwa4@gmail.com, piya.ko@fte.kmutnb.ac.th

Introduction

National Education Act, BE 2542 (1999) and Amendment 2002, Part 2, Section 9, Technology for Education, Section 65 states that "To have the development of people, both the producers and users of technology for education, is to make people have knowledge and skills in producing and using a proper, qualitative, and efficient technology (Office of the Education Council, 2006) as well as the process of information systems for searching, analyzing, storing, management, and dissemination of information to enhance the effectiveness of course management. The efficient course exercise should use the information system as a tool to reduce working time and it is precise. The use of information systems in teaching plan helps teachers analyze the original data clearer. It is counted as an important factor to develop higher learning achievement (Changlom, and Sigkabundit, 2016). In a school exercise, it is too necessary that the teachers and administrators must have a broad vision and see the importance and benefits of information systems using it as a tool for management. They must have a Self-development, change the way of thinking and methodology, change the attitude to work, keep up self-improvement to be modern and ready to cope with the world of changes, accept any new changes always occur including with promoting and developing people in the institutions able to use information system efficiently and effectively in teaching management (Reece, and Brandt, 2005; Snell, and Bohlander, 2010). The suggestions from the external quality assurance committee, round 3 (Public Organization) appraised by the Office of Standards and Quality Assessment, mentioned that teachers lacked of using information systems to provide teaching activities to continually develop students catching up technology. It is also suggested that technology should be applied in the teaching and learning activities and assesses the development of learners, improve teaching management and methodology to continually develop the effectiveness of teaching and learning activities (The Office for Standards and Quality Assessment of Education (Public Organization), 2012). Using information technology is necessary and very important because the planning and decision-making process require using information systems as a central element of every stage of management. How successful the development of education is depends on a good information system. The information system used must be accurate and valid prompt in the present and future and direct to the needs. For this reason, information systems must be developed to use in planning and decision making with efficiency and effectiveness in course management. For the reason mentioned, the researcher is interested in studying the level of teachers' opinion in institutes of vocational education about using information system in the curriculum management to use as data for analyzing and guideline for development of management systems using information systems. If the institutes of vocational education use the information system in their management, it will effect on the performance of teachers and educational persons. The institutes of vocational education also thrive in the era of society of learning toward the ASEAN community. It drives Thai education better and acceptable in society.

Materials and Methods

1. Research Objectives

1. To analyze the opinion on using information system in curriculum management according to the standard framework of vocational education undergraduate.
2. To develop information system using in curriculum management tools according to the standard framework of vocational education undergraduate.

2. Research Methodology

In this study, the researcher used the methodology of research and development (Theresa, and Donald, 2012) which had the following steps shown in Figure 1.

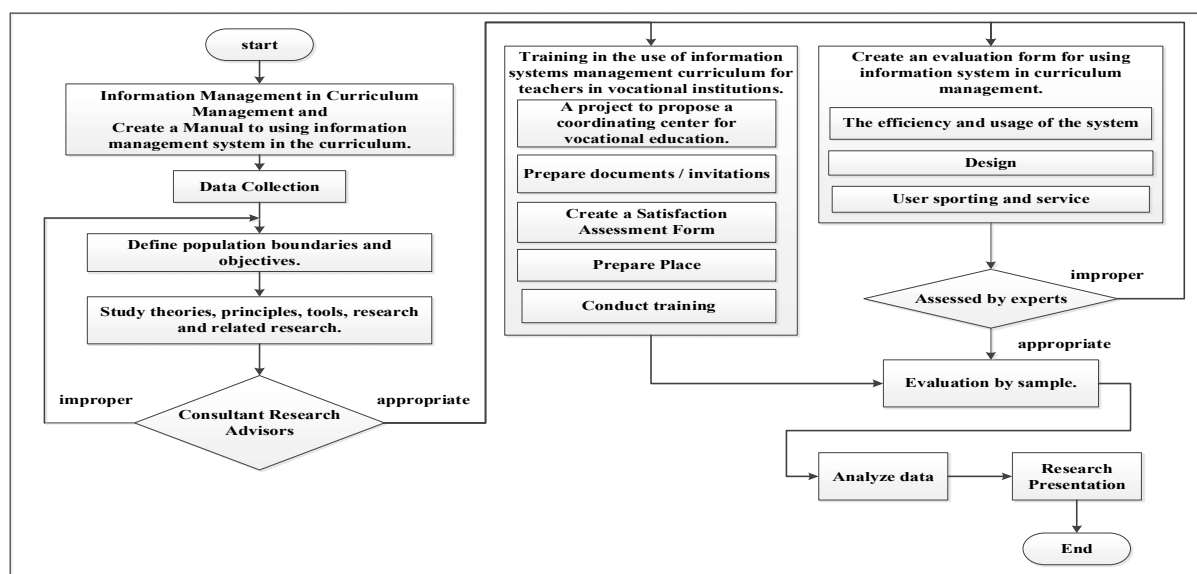


Figure 1. The process of the training of using information systems in curriculum management

The researcher brought the developed website to try out its using in institutes of vocational education. Testing from the actual using of the developer, the teachers in institutes of vocational education tested its using and evaluated the effectiveness of the website. After testing by the teachers in the institutes of vocational education, the teachers gave some suggestions on the developed website. The researcher took the various suggestions to improve the working system to mostly meet the needs of the users. The system is classified into 3 kinds of users: 1. System Mentor, 2. Teachers in institutes of vocational education, and 3. Chief Executives. The users' privilege are; 1. The system mentor can manage the data in the system, 2. The teachers in the institutes of vocational education could manage the information of TQF: VEd. 2-6, and 3. The chief executives could access all sections and can see reports of the teachers in institutes of vocational education. In research exercise, the researcher began with studying the original document recording or form for submission. The researcher had taken the data to analyze and design the system. It was to support the performance of the teachers in institutes of vocational education and the chief executives to mostly meet the needs of the using.

The research instrument used to analysis and design the information system was Context Flow Diagram, Decomposition Flow Diagram, Data Flow Diagram, Entity Relationship Diagram, and Data 5 Dictionary. Then, it was developed the system using the Visual Studio Professional 2012 language together ASP.NET web form with Visual Basic .NET that is compatible with the apache webserver and connected to Microsoft SQL SERVER 2008 R2. It is a technological application to develop the effectiveness of the system well serving to the needs of users. After developing of the system was complete, the researcher tested the system using to measure the quality and efficiency of the prepared system with the opinion evaluation form on information system in the curriculum management.

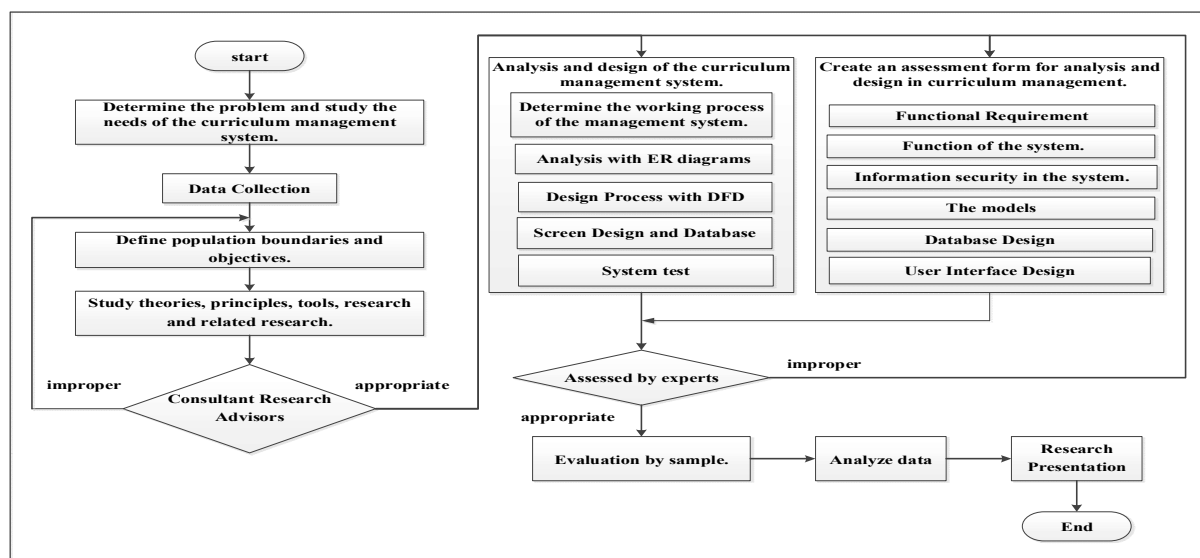


Figure 2. The process of analyzing and designing information systems in curriculum management

2.1 Research sample

The sample of this study were 52 representative teachers in 23 institutes of vocational education who had previous experience in using the TQF: HEd. 3-7 or TQF: VEd. 2-6 chosen by a purposive sampling.

2.2 Research tools

This research used information system in curriculum management shown in Figure 3. And a questionnaire of opinion on using the information system in curriculum management according to the standard framework of vocational education undergraduate developed by the researcher shown in Figure 3 and 4.

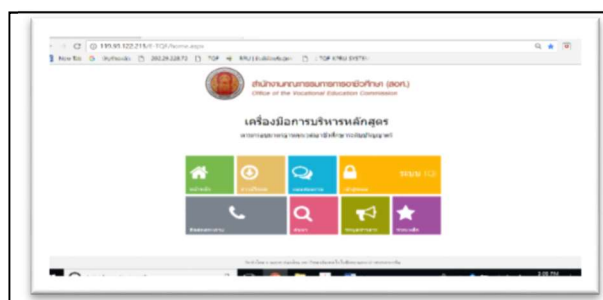


Figure 3. Website Information System in curriculum Management (<http://119.59.122.215>)



Figure 4. The training in the using information systems in curriculum management.

2.3 Quality Assessment of Research Instruments

The quality assessment of the research instruments was evaluated by 5 experts. The index of consistency (IOC) was 0.50-1.00 and the reliability value, reliability coefficient, of evaluation form on using the information system in curriculum management was 0.95.

2.4 Data Analysis

Statistics used in data analysis were mean (\bar{X}) and standard deviation (S.D.). The questionnaire was an open-ended questionnaires and 5-point rating scale. The scores began from 1 to 5, the lowest score was 1 meant strongly disagree and the highest score was 5 meant strongly agree. Then found the average score for each level. They were divided into intervals. The interpretation of the calculated mean was divided in to 5 levels.

Average score of 4.51 - 5.00 meant Strongly agree

Average score of 3.51 - 4.50 meant Agree

Average score of 2.51 - 3.50 meant Neither agree or Disagree.

Average score is 1.51 - 2.50 meant Disagree.

Average score is 1.00 - 1.50 meant Strongly disagree

Results and Discussion

1. Results

Research on using information systems in curriculum management according to the standard framework of vocational education undergraduate. The results of this research are as follows;

1.1. Results of data analysis from the questionnaire of respondents' opinion on the efficiency and usage of the system

From Figure 5 shows that most respondents had an opinion on using information systems in curriculum management according to the standard framework of vocational education undergraduate that the overall score in the efficiency and usage of the system is at a high level (\bar{X} = 4.19, S.D. = 0.72). When considering each item, the highest score is in item 1.11. The systems can reduce the amount of using paper, it is at the highest level (\bar{X} = 4.73, S.D. = 0.49). Secondly, item 1.10. The systems support to work faster, it is at a high level (\bar{X} = 4.39, S.D. = 0.68). Item 1.12. The language used in the system is formal, pertinent, and clearly meaningful. 1.14. The administrators can take advantage of the system to control their workings according to any components, it is at a high level (\bar{X} = 4.37, S.D. = 0.68). The lowest score is in item 1.8. System connection is efficient for using (the frequency of failed connection, recording, uploading photos, transmitting data), it is at a high level (\bar{X} = 3.71, S.D. = 0.82).

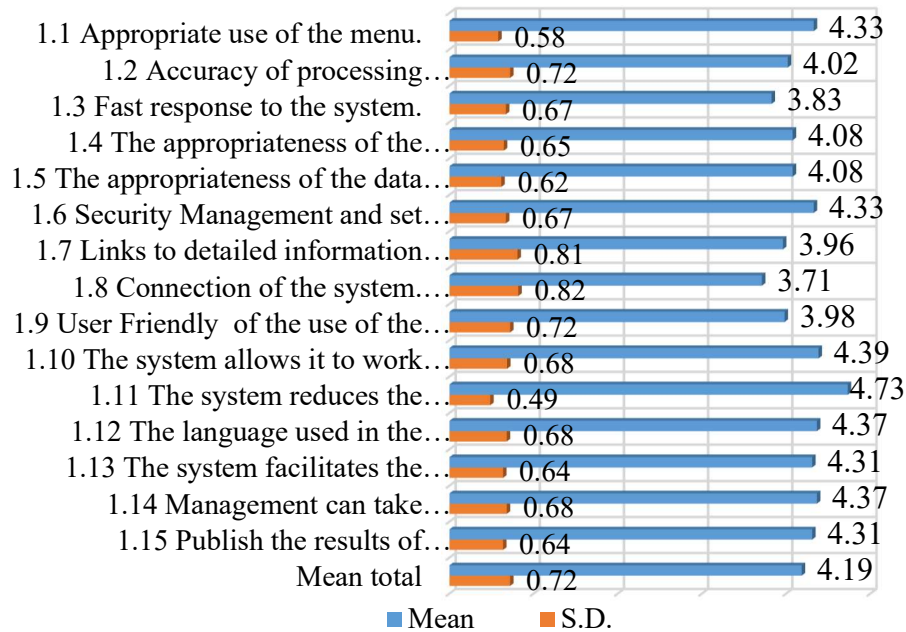


Figure 5 Mean and Standard Deviation of the efficiency and usage of the system

1.2. Results of data analysis from the questionnaire of respondents' opinion on designing

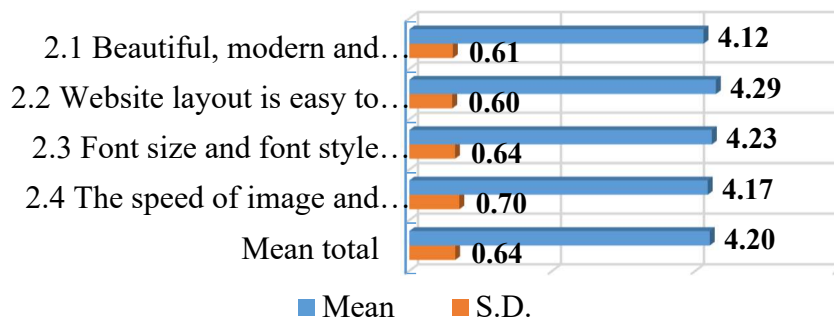


Figure 6 Mean and Standard Deviation in designing

From Figure 6 shows that most respondents had an opinion on using information systems in curriculum management according to the standard framework of vocational education undergraduate that in designing, the overall score is at a high level ($\bar{X} = 4.20$, S.D. = 0.64). When considering each item, the highest score is in item 2.2. Website layout is easy to read and use, it is at a high level ($\bar{X} = 4.29$, S.D. = 0.60), Secondly, item 2.3. Font size and font style are easily readable and beautiful, it is at a high level ($\bar{X} = 4.23$, S.D. = 0.64). Item 2.4. The speed of showing image, letters, and any information, it is at a high level ($\bar{X} = 4.17$, S.D. = 0.70). The lowest score is item 2.1. Beauty, modernity, and attractive home page, it is at a high level ($\bar{X} = 4.12$, S.D. = 0.61).

1.3. Results of data analysis from the questionnaire of respondents' opinion on user support and service

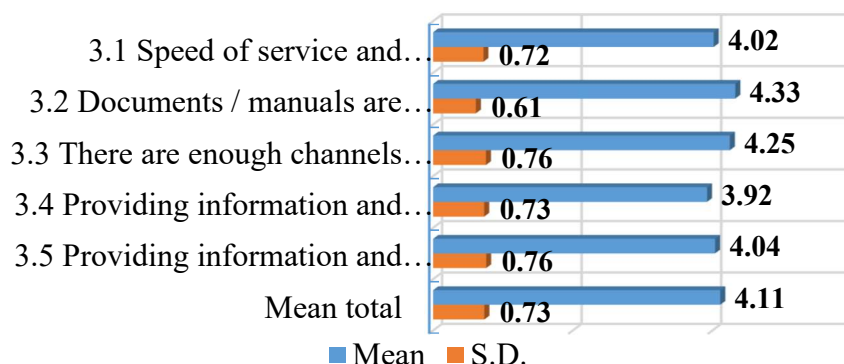


Figure 7 Mean and Standard Deviation in user support and service

From Figure 7 shows that most respondents had an opinion on using information systems in curriculum management according to the standard framework of vocational education undergraduate that in user support and service, the overall score is at a high level ($\bar{X}=4.11$, S.D.=0.73). When considering each item, the highest score is in item 3.2. Documents / manuals are clear and easy to understand, it is at the high level ($\bar{X}=4.33$, S.D.=0.61), Secondly, item 3.3. There are enough channels to contact / inquire about the problems, it is at a high level ($\bar{X}=4.25$, S.D.=0.76). Item 3.5. Information and troubleshooting services of the Institute of Vocational Education is at a high level ($\bar{X}=4.04$, S.D.=0.76). The lowest score is item 3.4. Information and troubleshooting service of VEC, it is at a high level ($\bar{X}=3.92$, S.D.=0.73).

2. Discussion

From the results of the research on using information systems in curriculum management according to the standard framework of vocational education undergraduate, it leads to important issues for discussing about the teachers in the institutes of vocation education who agreed with using information systems in curriculum management as follows.

1. The efficiency and usage of the system, the teachers in the institutes of vocational education agreed with using information systems in curriculum management, it is at a high level ($\bar{X}=4.19$, S.D. = 0.72). This corresponds to the research conducted by Nonthaphet, (2017) studied on "Using Information Technology for Secondary School Administration, Kalasin Secondary Educational Service Area Office 2. ", the overall picture was at a high level and the research of Sangthong, (2010) on "Information System for Workload Management of Instructors, Case Study, Faculty of Science and Technology, Phetchabun Rajabhat University", the results showed that most of the employees were satisfied at the high level, the mean was 4.17, and the standard deviation was 0.26, and Khamphad, (2010) studied on "Information System for Advisor Management, Case Study, Phrae Technical College", the results found that the efficiency and effectiveness of the overall application was very effective and the data was complete, modern, not complicate. It promptly reacted to the needs of the users. The results of this research show that system mentors and developers should focus on and ensure the users in

the information linking system in the system and the system connection in using, such as the frequency of a failed connection, recording, uploading photos, and transmitting information.

2. Design, the teachers in institutes of vocational education agreed with using information systems in curriculum management. It is at a high level ($\bar{X} = 4.20$, S.D. = 0.64). It is coherent with the research conducted by Sihawat, (2011) "Study of the Use of Information Technology for School Administration in Chaiyaphum Educational Service Area, Region 1, the overall picture is at a high level. And the research by Khumtita, (2009) studied on Computer Information System for Fang School Network, the results of the evaluation showed that the system security design and the benefits to the students were at a high level. The administrators, system mentor, and teachers were satisfied with the design, system security, and the accuracy of processing is a highest level. It is also consistent with Tabnoi, (2009) Said that, the design of the system or website is easy to use, fast to complete the transaction, accurate, valid, reliable, always modern, can be checked, safe, worth and thrift, and flexible. It can be found from the research that the system mentor and developer should focus on and ensure the user in beauty, modernity, and attractive homepage. Minor focusing are the speed of showing images, text, and any information.

3. User support and service, the teachers in the institutes of vocational education agreed with using information systems in curriculum management, it is at a high level ($\bar{X} = 4.11$, S.D. = 0.73). It corresponds to the research of Kreuasri and et al., (2015) on using information technology in the administration of school administrators under the Office of the Secondary Education Region 32, the overall picture was at a high level. The research studied by Jantarasomboon, (2010) found that supporting for applications or services would well satisfy the system using. Besides, a good support and service also effected on the effort on building up skills in using and developing information systems. The results of this research shows that the system mentors and developers should focus on the development of the system and promote using such as information and troubleshooting service of OVEC (Office of the Vocational Education Commission), followed by the speed of service and solving problems. Creating adequate communication channels for asking about the problems. And most important needs of the users are the format of the document / manual should be clear, the users can self-study and be in a position where the user can easily search.

Conclusion

The research on using information systems in course management according to the standard framework of vocational education undergraduate can be summarized as follows;

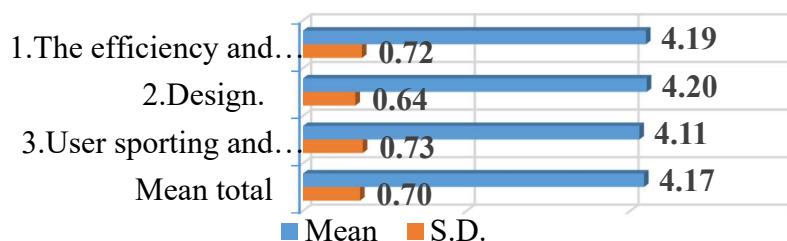


Figure 8 Mean and Standard Deviation of the overall picture on using information systems

From Figure 8 the evaluation results of the teachers' opinion from 23 institutes of vocational education on using information systems in course management shows that the agreement from the teachers is at a high level ($\bar{x} = 4.17$, S.D.= 0.70). When considering each item, the agreement from the teachers on using information system in the efficiency and usage of the system, it is at high level ($\bar{x} = 4.19$, S.D.= 0.72). In designing, it is at high level ($\bar{x} = 4.20$, S.D.= 0.64). In user support and service is at high level ($\bar{x} = 4.11$, S.D.= 0.73).

Recommendation

Due to the development of information systems has some limitations, the next study should improve this information system in reporting which should be well documented in PDF format for being easy used, website design should be based on Website Development Standards to reduce obstacles in accessing and using i.e. font colors and sizes.

Acknowledgement

Thanks to the director Institute of Vocational Education Coordination Center, Director of Vocational Institute of Southern 1, and Director of Vocational Institute of Bangkok who supported the cost of various projects in this research.

References

- Changlom, K. and Sigkabundit, S. 2016. A problem and needs Analysis for Information Technology application, Based upon the Opinions of Administrators and Teachers from the Local Authority Organisation of Pathum Thani Province. **EAU Heritage Journal of Social Science and Humanity** 6(2): 66-78.
- Jantarasomboon, A. 2010. **Factors Affecting Satisfaction of employee of using system application (ERP-SAP) of accountants – case study of the provincial electricity authority**. Master's thesis in Business Administration, Thammasat University
- Khamphad, K. 2010. **Information Management System for teachers in Phrae Technical College**. Master's thesis in Information Technology, Naresuan University.
- Khumtita, K. 2009. **Computer management information system for fangchanupathum school network**. Master's thesis in Computer Science, Chiang Mai University.
- Kreuasri, E., Vajintharangkul, K. and Sringan, K. 2015. Using Information Technology for Administration of School Administrators Under the secondary educational service area office 32, pp. 202-210. In **The National Conference and Research Presentation “Create and Development to Approach ASEAN Community II” June 18-19, 2015 at Nakhonratchasima College**. Mueang Nakhonratchasima, Nakhonratchasima.
- Nonthaphet, T 2017. The Information Technology Usage for Administration of Academic Institutions under Nakhon Si Thammarat Primary Educational Service Area Office 3. **Princess of Naradhiwas University Journal of Humanities and Social Science** 3(1): 47-56.
- Office of the Education Council. 2006. **The National Education Act, BE 2542 (1999) and the Amendments (No. 2) BE 2545**. Bangkok, Office.

- Reece, B.L. and Brandt, R. 2005. **Effective human relations: personal and organizational applications**. Houghton Mifflin Company, New York.
- Sangthong, N. 2010. **Information Management for Workload Management of Faculty Members, Faculty of Science and Technology** Phetchabun Rajabhat University. Master's thesis in Information Technology, Naresuan University.
- Sihawat, A. 2011. **The Study of Information Technology Uses for the School Administration of the Schools under the Jurisdiction of Chaiyaphum Educational Service Area Office 1**. Master's thesis in Educational Administration, Chaiyaphum Rajabhat University.
- Snell, S and Bohlander, G. 2010. **Principles of Human Resource Management** (15thed). China Translation & Printing Services Limited, China.
- Tabnoi, S. 2009. **The operation of information system of elementary schools: primary school ratchaburi province**. Master's thesis in Education Management, Srinakharinwirot University.
- The Office for Standards and Quality Assessment of Education (Public Organization). 2012. **The results of the evaluation. Third Round External Quality (2011-2015)**. Bangkok. Office.
- Theresa L. W. and Donald H. M. 2012. **Research Methods**. Wadsworth Publishing Company, United States of America.

Impact Strength and Flexural Properties of Biodegradable Foams Containing Polylactic Acid and Epoxidized Natural Rubber

Suttasinee Puttajan¹, Tarinee Nampitch^{1*}

ABSTRACT

Biodegradable foams containing polylactic acid (PLA) and epoxidized natural rubber (ENR50) are prepared using various chemical foaming agents (CFAs), which are factors that affect the properties and characteristics of biodegradable foams. In this research, ENR50 was employed as a toughening agent for blending with PLA by twin screw extruder followed by compression moulding. As a result, the impact strength of PLA/ENR50 foams tended to increase as a result of the ENR50 molecules generating hydrogen bonds with the carbonyl groups of PLA, leading to interaction between ENR50 and PLA, whereas the flexural strength of PLA/ENR foams tended to decrease with an increase in ENR content. In addition, the effect of chemical foaming agent content on the properties of biodegradable foams was investigated.

Keywords: Foam, Flexural strength, Polylactic acid, Epoxidized natural rubber, Chemical foaming agent

¹ Department of Packaging and Materials, Faculty Agro-Industry, Kasetsart University, Lat Yao, Jatujak, Bangkok 10900, Thailand

*Corresponding author, e-mail : fagitnn@ku.ac.th

Introduction

At the present, due to competitive material and processing costs and mechanical properties, this environmentally friendly biopolymer is being considered as a replacement for polystyrene. Polystyrene foam products are used for commodity applications such as packaging, cushioning, construction, and thermal and sound insulation. However, the foam waste obtained from polystyrene (PS), which is a petroleum-based plastic, has been a serious global concern due to harmful effects on people's health and the accumulation of waste in the environment. Consequently, biodegradable materials such as polylactic acid (PLA) have been investigated for development as biodegradable foams in order to replace PS (Ariff *et al.*, 2008; Li & Matuana, 2003; Julien *et al.*, 2015; Najib *et al.*, 2009; Luo *et al.*, 2013; Matuana, *et al.*, 2009).

Polylactic acid (PLA) is a biodegradable and biocompatible polymer that is produced from renewable resources such as corn starch and sugarcane. With a wide range of applications, PLA possesses excellent physical properties combined with biocompatibility and biodegradability properties. PLA has a high potential for employment in food packaging because of its transparency, good mechanical properties and acceptable moisture processability for dry food stuff. However, some PLA applications are limited for use in food packaging due to its low elongation at break, high brittleness, poor crystallization behavior and low melt strength (Auras *et al.*, 2004; Nampoothiri *et al.*, 2010; Resal *et al.*, 2010; Lim *et al.*, 2008). Attempts to increase the toughness of PLA have employed methods such as adding plasticizer or polymer, including controlled stereomistry. Blending of PLA with epoxidized natural rubber (ENR) as an effective toughening agent in plastic has been extensively carried out (Tanjung *et al.*, 2015; Ouipanich *et al.*, 2017; Kaisone *et al.*, 2016; Lee *et al.*, 2010; Suganuma *et al.*, 2011; Pilla *et al.*, 2009; Pilla *et al.*, 2009; Zhang *et al.*, 2013; Zhai *et al.*, 2009; Jaratrokarnjorn *et al.*, 2012; Wang *et al.*, 2016; Raps *et al.*, 2015; Yuan *et al.*, 2014; Dechatiwong Na Ayutthaya and Poompradub, 2014; Masek *et al.*, 2016; Tham *et al.*, 2016; Wang *et al.*, 2015; Sukpuang *et al.*, 2014).

ENR is a renewable resource obtained from *Hevea brasiliensis* (Nawamawat *et al.*, 2011). It has many advantages, such as abundant availability, biodegradability, high toughness and outstanding mechanical strength. ENR is polar because there are epoxy groups contained on the backbone chain, which can improve the polarity of NR and hence promote compatibility with PLA (Nampoothiri *et al.*, 2010). There are only a few research studies examining NR-toughened PLA and PLA foam. In 2013, Zhang and others investigated the use of ENR as a toughening agent for PLA (Zimmermann *et al.*, 2013). This report revealed that the incorporation of ENR in blends could reduce the tensile modulus and strength but enhance the elongation and impact strength of PLA, including strong shear thinning behavior. Tanjung *et al.*, 2015 investigated the effects of rubber polarity, rubber viscosity and molecular weight on the mechanical properties of the PLA/ENR and PLA/NR-g-PMMA blends. It was found that all blends showed higher strength than PLA and NR because of the addition of an effective toughening agent. This study also focused on the effects of ENR and chemical foaming agents on the properties of biodegradable foams.

Materials and Methods

1. Materials

Poly lactide polymer 2003D in pellet form with melt flow rate of 5 – 7 g/10 min (2.16 kg, 210 °C) was purchased from Natureworks LLC (USA). Epoxidized natural rubber (ENR50) contained 50 mol% epoxidation was kindly supplied by the Key Laboratory of Tropical Crop Products Processing (Ministry of Agriculture, China).

2. Methods

The PLA and ENR50 were separately dried at 80 °C and 50 °C, respectively for 8 hours in a hot air oven, prior to the blending. The polymer blends between PLA and ENR50 were prepared with various ENR50 contents ranging from 0 to 40% by weight. The well-mixed blends were carried out in twin screw extruders (types LTE-20-32 and LTE-20-40, Rheocord 90, Germany), at a rotor speed of 45 rpm and temperature of 190 °C for 10 min, followed by cutting them into small granules. Prior to foaming, the ENR50/PLA foams were prepared with various CFA contents ranging from 0.5 to 2.0 phr. The fabricated specimens were carried out by using compression moulding (Wabash model labtech) at 210 °C for 14 min. The designations and formulations of the PLA/ENR50 foams are mentioned in Table 1.

Table 1 Designation of PLA/ENR-50 foams

Sample name	PLA (wt%)	ENR50 (wt%)	CFAs (wt%)
P100/B0.5	100	-	0.5
P100/B1.0	100	-	1.0
P100/B1.5	100	-	1.5
P100/B2.0	100	-	2.0
P90/E10/B0.5	90	10	0.5
P90/E10/B1.0	90	10	1.0
P90/E10/B1.5	90	10	1.5
P90/E10/B2.0	90	10	2.0
P80/E20/B0.5	80	20	0.5
P80/E20/B1.0	80	20	1.0
P80/E20/B1.5	80	20	1.5
P80/E20/B2.0	80	20	2.0
P70/E30/B0.5	70	30	0.5
P70/E30/B1.0	70	30	1.0
P70/E30/B1.5	70	30	1.5
P70/E30/B2.0	70	30	2.0
P60/E40/B0.5	60	40	0.5
P60/E40/B1.0	60	40	1.0
P60/E40/B1.5	60	40	1.5
P60/E40/B2.0	60	40	2.0

PLA: Polylactic acid; ENR-50: Epoxidized natural rubber with 50 mol% epoxidation; CFAs: Chemical foaming agents

All samples for the Izod impact test were prepared by compression moulding (Wabash model labtech) at 200 °C for 14 min. Then the specimens were cut into 12.7 mm x 63.7 mm x 12.7 mm sections and a V notch was made to a 2.5 mm depth in accordance with ASTM D256. The Izod impact test (Notched Izod) was evaluated by using the QC-639 impact testing machine.

Samples for the flexural test were prepared by compression moulding (Wabash model labtech) at 200 °C for 14 min. Then the specimens were cut into 13 mm x 190 mm x 9.6 mm sections in accordance with ASTM D790. The flexural test was performed by using three-point

bending tests in a testing machine (Lloyd Instruments Ltd. A structuring experiment for data to use in SPSS (Statistical Package for the Social Science) was carried out. The SPSS19 was used to optimize and determine the significance of factors affecting the impact strength and flexural strength of PLA/ENR50 foams. The experimental results were examined by repeating the experiment five times.

Results and Discussion

1. Mechanical properties of PLA/ENR50 foams

1.1 Impact strength of PLA/ENR50 foams

The impact strength of PLA/ENR50 foams is shown in Figure 1 and Table 2. The results, it can be seen that the impact strength of blend foams was improved via the addition of ENR because the ENR50 molecules could generate hydrogen bonds with the carbonyl groups of PLA. ENR was shown to be a very effective substance for increasing the impact strength of blend foam containing PLA. In addition, these results revealed that the presence of more stress transfer from brittle matrix to tough ENR50 and ENR50 acts as an impact modifier, hence increasing the energy absorption capacity of the blend foams (Akbari *et al.*, 2014; Wahit *et al.*, 2015).

Table 2 Impact strength and flexural strength of PLA/ENR50 foams

Sample name	Impact strength (J/m ²)	flexural strength (J/m ²)
P100/B0.5	0.3861 ± 0.14 ^{b,c,d}	14.9840 ± 2.14 ⁱ
P100/B1.0	0.4403 ± 0.09 ^{d,e}	21.0180 ± 2.77 ^j
P100/B1.5	0.3009 ± 0.06 ^{a,b}	12.5682 ± 3.33 ^h
P100/B2.0	0.2889 ± 0.04 ^{a,b}	12.2644 ± 2.96 ^h
P90/E10/B0.5	0.3045 ± 0.04 ^{a,b}	10.4208 ± 2.71 ^{g,h}
P90/E10/B1.0	0.2740 ± 0.06 ^{a,b}	7.3416 ± 1.16 ^{e,f}
P90/E10/B1.5	0.3290 ± 0.13 ^{a,b,c}	6.7763 ± 0.69 ^{d,e,f}
P90/E10/B2.0	0.2546 ± 0.04 ^a	8.3900 ± 0.84 ^{f,g}
P80/E20/B0.5	0.3607 ± 0.06 ^{a,b,c,d}	5.6522 ± 0.44 ^{c,d,e}
P80/E20/B1.0	0.2785 ± 0.03 ^{a,b}	2.8223 ± 0.44 ^{a,b}
P80/E20/B1.5	0.2859 ± 0.04 ^{a,b}	2.8245 ± 0.58 ^{a,b}
P80/E20/B2.0	0.2661 ± 0.04 ^a	2.6863 ± 0.35 ^{a,b}
P70/E30/B0.5	0.4271 ± 0.07 ^{c,d,e}	4.9222 ± 0.27 ^{b,c,d}
P70/E30/B1.0	0.5264 ± 0.13 ^{e,f}	4.4618 ± 0.53 ^{a,b,c}
P70/E30/B1.5	0.5361 ± 0.06 ^{e,f}	3.8500 ± 0.11 ^{a,b,c}
P70/E30/B2.0	0.5235 ± 0.06 ^{e,f}	3.4733 ± 0.50 ^{a,b,c}
P60/E40/B0.5	0.4706 ± 0.10 ^{d,e}	3.2216 ± 0.60 ^{a,b}
P60/E40/B1.0	0.5219 ± 0.02 ^{e,f}	3.2030 ± 0.53 ^{a,b}
P60/E40/B1.5	0.4351 ± 0.07 ^{c,d,e}	2.5074 ± 0.28 ^{a,b}
P60/E40/B2.0	0.6155 ± 0.11 ^f	2.0944 ± 0.54 ^a

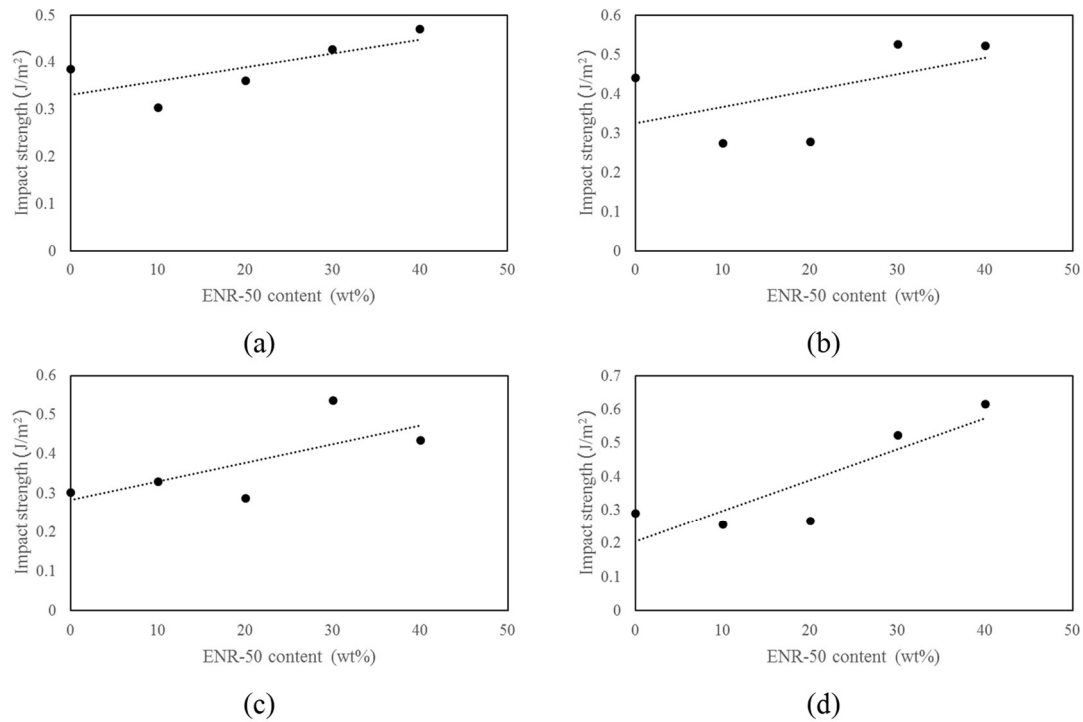


Figure 1 Impact strength of PLA/ENR-50 foams as blowing agent (a) 0.5 phr, (b) 1.0 phr, (c) 1.5 phr and (d) 2.0 phr.

1.2 Flexural strength of PLA/ENR50 foams

Flexural strength of PLA/ENR-50 foams is shown in Figure 2. In Figure 2, the effect of ENR50 content on the flexural properties of blend foams is shown. The results showed that the flexural strength of PLA/ENR foams tended to decrease with an increase in ENR content ranging from 0 to 40 wt%. This was due to the reduction in stiffness of the blend foams. The results exhibited lower flexural properties of blend foams with an increase of the ENR content as a result of large ENR50 particle sizes forming in blend foams that contained PLA and ENR50, and there was an increase of non-uniformity of cell structure, with open cell content, while decreasing skin thickness was shown in SEM images (Wahit *et al.*, 2015). In addition, the reduction in the flexural properties of blend foams with the increase of ENR50 content was attributed to the low modulus of the ENR50 contained in blend foams (Wahit *et al.*, 2015).

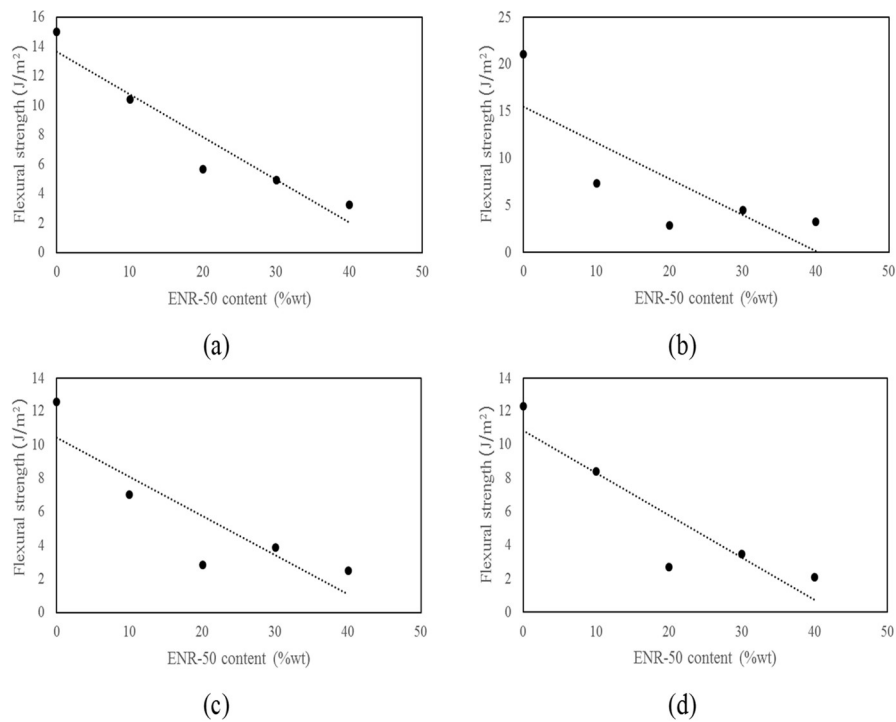


Figure 2 Flexural strength of PLA/ENR-50 foams as blowing agent (a) 0.5 phr, (b) 1.0 phr, (c) 1.5 phr and (d) 2.0 phr.

1.3. Morphology of blend foams

One of the important parameters is the morphology of foam because many mechanical properties depend on the dimension, organization, and distribution of cells (Carvalho and Frollini, 1999; Bledzki and Faruk, 2006). The SEM images exhibited the difference in the morphology and the sizes and numbers of the cells obtained with the different amount of blowing agent (Zimmermann *et al.*, 2013). In this experiment, the morphology of specimens for P100/B0.5, P100B1.5, P90/E10/B0.5, P90/E10/B1.5, P90/E10/B2.0, and P80/E20/B1.0 was investigated by scanning electron microscopy (SEM), as shown in Figure 3. These results exhibited that the NR domain are dispersed in the PLA matrix. This is consistent with the previous reports of Juntuek *et al.* (2012). The porosity of foams was exhibited in the SEM images at 25 times magnification. The addition of chemical foaming agents in blended foams lead to the increment of pore size and pore numbers of foams. In addition, PLA foam showed homogeneous pore size distributions, whereas Figure 3 (C) - (F) showed *non-homogenous pore size* distributions of the matrix with the addition of ENR (Zimmermann *et al.*, 2013). In addition, after CFAs were heated, those CFAs degraded to CO₂ and water (Ariff *et al.*, 2008; Li *et al.*, 2003; Zimmermann *et al.*, 2013), and nucleation of cells was formed at the polymer matrix (Nofar and Park, 2014).

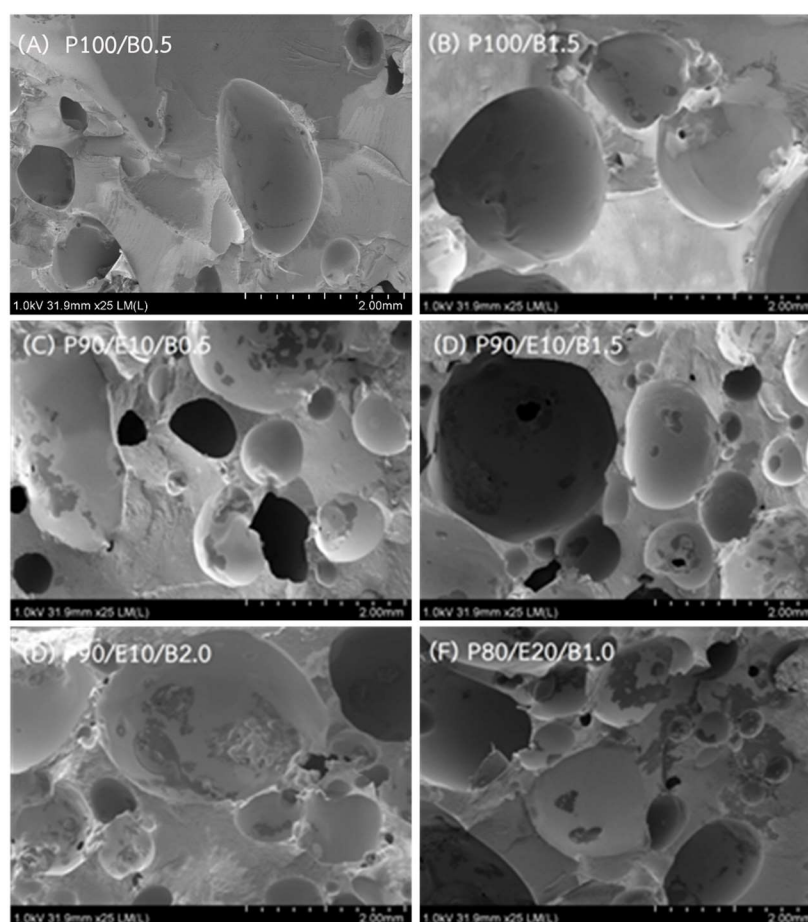


Figure 3 SEM images (x25 magnifications) of (A) P100B0.5, (B) P100B1.5, (C) P90/E10/B0.5, (D) P90/E10/B1.5, (E) P90/E10/B2.0 and (F) P80/E20/B1.0

Conclusion

In this study, the impact strength and flexural strength of PLA/ENR-50 foams were studied. The ENR-50 was employed as a toughening agent for blending with PLA. It was revealed that there are several factors which may influence the effectiveness of a rubber toughening polymer, such as the amount and composition of rubber employed. In addition, the size and shape of the particle and the interfacial adhesion between the matrix and rubber particles also influence the effectiveness (Juntuek *et al.*, 2012). The impact strength of PLA/ENR-50 foams tended to increase because the epoxy groups in ENR could react with the carboxyl groups in PLA, whereas the flexural strength of PLA/ENR foams tended to decrease with an increase in ENR content.

Acknowledgment

The writers gratefully acknowledge the Thailand Research Fund (TRF) for financial support under Grant Number MSD5810098. In addition, the authors are also grateful to the Graduate School of Kasetsart University for financial support for this project.

References

- Akbari, A., Jawaid, M., Hassan, A. and Balakrishnan, H. 2014. Epoxidized natural rubber toughened polylactic acid/talc composites: Mechanical, thermal, and morphological properties. **Journal of Composite Materials** 48(7): 769-781.
- Ariff, Z.M., Rahim, N.A.A. and Low, L.C. 2008. Effect of compound formulation on the production and properties of epoxidised natural rubber (Enr-25) foams. **Polymer Processing Society 24th Annual Meeting (PPS-24)**. Salerno, Italy.
- Auras, R., Harte, B. and Selke, S. 2004. An overview of polylactides as packaging materials. **Macromolecular bioscience** 4(9): 835–864.
- Bledzki, A.K. and Faruk, O. 2006. Injection moulded microcellular wood fibre-polypropylene composites. **Composites Part A: Applied Science and Manufacturing** 37(9): 1358-1367.
- Carvalho, G. and Frollini, E. 1999. Lignin in phenolic foams 66. **Polímeros** 9(1): 66-75.
- Dechatiwong Na Ayutthaya, W. and Poompradub, S. 2014. Thermal and mechanical properties of poly(lactic acid)/natural rubber blend using epoxidized natural rubber and poly(methyl methacrylate) as co-compatibilizers. **Macromolecular Research** 22(7): 686–692.
- Jaratrotkamjorn, R., Khaokong, C. and Tanrattanakul, V. 2012. Toughness enhancement of poly(lactic acid) by melt blending with natural rubber. **Journal of Applied Polymer Science** 124(6): 5027–5036.
- Julien, J.M., Quantin, J.-C., Bénézet, J.-C., Bergeret, A., Lacrampe M.F. and Krawczak, P. 2015. Chemical foaming extrusion of poly(lactic acid) with chain extenders: Physical and morphological characterizations. **European Polymer Journal** 67:40-49.
- Juntuek, P., Ruksakulpiwat, C., Chumsamrong, P. and Ruksakulpiwat, Y. 2012. Effect of glycidyl methacrylate-grafted natural rubber on physical properties of polylactic acid and natural rubber blends. **Journal of Applied Polymer Science** 125(1): 745-754.
- Kaisone, T., Harnkarnsujarit, N., Leejarkpai, T. and Nampitch, T. 2016. Mechanical and thermal properties of toughened PLA composite foams with modified coconut fiber. **Applied Mechanics and Materials** 851:179-185.
- Lee, S.Y., Hassan, A., Tan, I.K.P., Terakawa, K., Ichikawa, N. and Gan, S.N. 2010. Reactions of palm oil-based mcl-PHAs with epoxidized natural rubber. **Journal of Applied Polymer Science** 115(4): 2039–2043.
- Li, Q. and Matuana, L.M. 2003. Foam extrusion of high density polyethylene/wood-flour composites using chemical foaming agents. **Journal of Applied Polymer Science** 88: 3139–3150.
- Lim, L.-T., Auras, R. and Rubino, M. 2008. Processing technologies for poly (lactic acid). **Progress in Polymer Science** 33(8): 820-852.
- Luo, Y., Zhang, J., Qi, R., Lu, J., Hub, X. and Jiang, P. 2013. Polylactide foams prepared by a traditional chemical compression-molding method. **Journal of Applied Polymer Science** 130(1): 330-337.
- Masek, A., Diakowska, K. and Zaborski, M. 2016. Physico-mechanical and thermal properties of epoxidized natural rubber/polylactide (ENR/PLA) composites reinforced with lignocellulose. **Journal of Thermal Analysis and Calorimetry** 125(3): 1467–1476.
- Matuana, L.M., Faruk, O. and Diaz, C.A. 2009. Cell morphology of extrusion foamed poly(lactic acid) using endothermic chemical foaming agent. **Bioresource Technology** 100(23): 5947-5954.
- Najib, N.N., Ariff, Z.M., Manan, N.A., Bakar, A.A. and Sipaut, C.S. 2009. Effect of blowing agent concentration on cell morphology and impact properties of natural rubber foam. **Journal of Physical Science** 20(1):13–25.

- Nampoothiri, K.M., Nair, N.R. and John, R.P. 2010. An overview of the recent developments in polylactide (PLA) research. **Bioresource technology** 101(22): 8493-8501.
- Nawamawat, K., Sakdapipanich, J.T., Ho, C.C., Ma, Y. and Song, J. 2011. Surface nanostructure of *Hevea brasiliensis* natural rubber latex particles. **Colloids and Surfaces A: Physicochemical and Engineering Aspects** 390(1-3): 157-166.
- Nofar, M. and Park, C.B. 2014. Poly (lactic acid) foaming. **Progress in Polymer Science** 39(10): 1721-1741.
- Ouippanich, S., Kaisone, T., Hanthanon, P., Wiphanurat, C., Thongjun, Y. and Nampitch, T. 2017. Effect of the citric acid as blowing agent on the compressive properties and morphology of PLA/ENR blend foams. **Applied Mechanics and Materials** 873: 95-100.
- Pilla, S., Kim, S.G., Auer, G.K., Gong, S. and Park, C.B. 2009. Microcellular extrusion-foaming of polylactide with chain-extender. **Polymer Engineering & Science** 49(8): 1653-1660.
- Pilla, S., Kramschuster, A., Yang, L., Lee, J., Gong, S. and Turng, L.H. 2009. Microcellular injection-molding of polylactide with chain-extender. **Materials Science and Engineering: C** 29(4): 1258-1265.
- Raps, D., Hossieny, N., Park, C.B. and Altstädt, V. 2015. Past and present developments in polymer bead foams and bead foaming technology. **Polymer** 56: 5-19.
- Rasal, R.M., Janorkar, A.V. and Hirt, D.E. 2010. Poly (lactic acid) modifications. **Progress in Polymer Science** 35(3): 338-356.
- Suganuma, K., Horiuchi, K., Matsuda, H., Cheng, H. N., Aoki, A. and Asakura, T. 2011. Stereoregularity of poly(lactic acid) and their model compounds as studied by NMR and quantum chemical calculations. **Macromolecules** 44(23): 9247-9253.
- Sukpuang, P., Opaprakasit, M., Petchsuk, A., Tangboriboonrat, P., Sojikul, P. and Opaprakasit, P. 2014. Polylactic acid glycolysate as a cross-linker for epoxidized natural rubber: Effect of cross-linker molecular weight. **Journal of Elastomers and Plastics** 48(2): 105-121.
- Tanjung, F.A., Hassan, A. and Hasan, M. 2015. Use of epoxidized natural rubber as a toughening agent in plastics. **Journal of Applied Polymer Science** 132(29): 42270.
- Tham, W.L., Poh, B.T., Mohd Ishak, Z.A. and Chow, W.S. 2016. Epoxidized natural rubber toughened poly(lactic acid)/halloysite nanocomposites with high activation energy of water diffusion. **Journal of Applied Polymer Science** 133(3): 42850.
- Wahit, M.U., Hassan, A., Ibrahim, A.N., Zawawi, N.A. and Kunasegeran, K. 2015. Mechanical, thermal and chemical resistance of epoxidized natural rubber toughened polylactic acid blends. **Sains Malaysiana** 44(11): 1615-1623.
- Wang, Y., Chen, K., Xu, C. and Chen, Y. 2015. Supertoughened biobased poly(lactic acid)-epoxidized natural rubber thermoplastic vulcanizates: Fabrication, co-continuous phase structure, interfacial in situ compatibilization, and toughening mechanism. **The Journal of Physical Chemistry** 119(36): 12138-12146.
- Wang, Y., Wei, Z., Leng, X., Shen, K. and Li, Y. 2016. Highly toughened polylactide with epoxidized polybutadiene by in-situ reactive compatibilization. **Polymer** 92: 74-83.
- Yuan, D., Xu, C., Chen, Z. and Chen, Y. 2014. Crosslinked bicontinuous biobased polylactide/natural rubber materials: Super toughness, “net-like”-structure of NR phase and excellent interfacial adhesion. **Polymer Testing** 38: 73-80.
- Zhai, W., Ko, Y., Zhu, W., Wong, A. and Park, C.B. 2009. A study of the crystallization, melting, and foaming behaviors of polylactic acid in compressed CO₂. **International Journal of Molecular Sciences** 10(12): 5381-5397.
- Zhang, C., Huang, Y., Luo, C., Jiang, L. and Dan, Y. 2013. Enhanced ductility of polylactide materials: Reactive blending with pre-hot sheared natural rubber. **Journal of Polymer Research** 20: 121.

Zimmermann, M.V.G., Brambilla, V.C., Brandalise, R.N. and Zattera, A.J. 2013.
 Observations of the effects of different chemical blowing agents on the degradation of
 poly (lactic acid) foams in simulated soil. **Materials Research** 16(6): 1266-1273.

Effect of Waste Tire Powder on the Properties of Natural Rubber Latex Foams

Suwat Rattanapan^{1*} Jutatip Artchomphoo¹ and Anuchit Wichianchom¹

ABSTRACT

Waste tire powder (WTP) was incorporated with natural rubber latex (NRL) compound and foamed to make natural rubber latex foam (NRLF) by using a well-known technique called the Dunlop method. The purpose of this study was to use WTP as a filler for NRLF. Different amount and size of WTP were added to NRL compound and was foamed to make NRLF. The mechanical properties, density and compression set of NRLF were studied. The properties was performed on WTP-Filled NRLFs, and they were compared with silica (Si) and calcium carbonate (CaCO₃) filler. Decreasing size of WTP increased the tensile strength, elongation at break and shrinkage of NRLF. The tensile strength and density of the NRLF increased with an increase in WTP loading. Smaller WTP size indicated higher elasticity of WTP-filled NRLF, but the recovery of WTP-filled NRLF decreased with increasing WTP loading. Addition Si and CaCO₃ into the NRL together with WTP would also decreased the properties of NRLF. The foams observed by optical microscopy revealed to have open cells.

Keywords: Waste Tire Powder, Natural Rubber, Latex, Foam

¹ Department of Rubber and Polymer Technology, Faculty of Science and Technology, Rajamangala University of Technology Srivijaya Nakhon Si Thammarat Campus (Sai Yai), Tham Yai Sub-district, Thung Song District, Nakhon Si Thammarat Province 80110, Thailand

*Corresponding author, e-mail) : suwat.r@rmuts.ac.th

Introduction

Recently, environmental considerations and public concern have become increasingly important as the world strives toward environmental quality and preservation through sustainable development and cleaner technology (Li *et al.* 2011). Waste tire powder (WTP) have been widely used as fillers in rubber, thermoplastic and polymer composite materials (Kim and Burford, 1998). WTPs are a major concern as they cause environmental problems. Although some recycling methods of used tires do exist, they are not sufficient to consume all the amount of accumulated ones. The dispersion of tires in the natural environment is the cause of a huge pollution phenomenon as the materials that constitute a tire are not biodegradable and produce toxic smokes when incinerated. Therefore, new methods of reusing waste tires are needed, especially if they aim at transforming this waste into a cheap resource. There are many methods to manage waste tires such as reclamation, recycling, devulcanization, high pressure and high temperature sintering, burning for energy recovery or use as fuel, pyrolysis to produce carbon black and others. With regard to generating an environmental friendly and economical aspect, one of the preferred methods is recycling by grinding followed by use of the rubber crumbs as raw materials. However, although rubber is the major component of tires (41–48%), there are other components to consider: carbon black, metal, textiles, curing agents, and other additives but the rubber recovered from waste tires is the main target of this recycling. The recovered rubber can be classified into four types according to its composition, shape, density, and size: shredded tires, tire chips, ground rubber, and WTP. WTPs can be produced by two major technologies: ambient mechanical grinding and cryogenic grinding. There are several grades of WTPs depending on the quality and granule size. Generally the granule size is ≤ 6.35 mm.

Natural rubber latex (NRL), the first latex to be used industrially. NRL is also defined as the dispersion of natural rubber particles in water (Hossain *et al.* 2010). NRL is a stable colloidal dispersion of polymeric particles in an essentially aqueous medium (Hamza *et al.* 2008). The colloidal stability of the latex is extremely sensitive to pH and the ionic environment of the dispersing medium (Nawamawat *et al.* 2011). Schidrowitz and Goldsbrough (Blackley 1966) made an attempt in 1914 to produce a porous rubber product from natural latex concentrates, called “latex foam” (Madge 1962). Addition of any kind of foreign material with different pH can easily cause agglomeration of latex. Latex foam rubber is defined as a cellular rubber that has been made directly from liquid latex. The Dunlop process is particularly well adapted to the manufacturing of thick molded latex foam rubber products, such as pillows, cushions, mattresses, and upholstery foam. Various applications of latex foam include carpet underlay material, mattresses, pillows, cushioning seats at concert halls, theaters, hotels, houses, vehicles, and factories.

General principles can be given for the preparation of aqueous solutions, dispersions, or emulsions for addition to aqueous latices. The particle size of dispersion and colloid stability should be comparable to that of the latex to which they are added. Also, the pH and ionic strength of the aqueous phase of the dispersion should be similar to that of the latex aqueous phase. Few attempts have been made to incorporate fibers into natural rubber latex foam. The use of glass fiber to reinforce natural latex foam rubber has been studied in some detail, and such an approach is claimed to reduce shrinkage and increase tensile strength. Mineral fillers such as kaolinite clays, calcium carbonate and silica have also been added as fillers for latex foam. Improvements in properties of high styrene-butadiene lattices have also been claimed by

addition of mineral fillers. In general, however, the addition of any normal type of compounding ingredient gives little advantage with respect to the load-weight ratio. Despite that, there have been no research studies that have incorporated WTP as filler in natural rubber latex foam. So far, there have been no reports of adding WTP to natural rubber latex foam.

Goals of the present study are to understand the effect of WTP on the mechanical of latex foam, as well as to reduce the overall compounding cost of the NRLF. The compression properties of silica, CaCO₃ and WTP incorporated NRLF were analyzed. WTP filler is expected to enhance the mechanical properties and also reduce the material cost of natural rubber latex foam. Usage of WTP is also expected to reduce land fill pollution and contribute as an asset to the waste tire industry rather than being waste material.

Materials and Methods

1. Materials and Formulation

The formulation and materials of the NRLF is as shown in Table 1. High ammonia natural rubber latex (LNR) with a dry rubber content of approximately 60 wt %, manufactured by the T.T. Latex&Products Co., Ltd., (Nakorn Sri Thammarat, Thailand), was used as the raw material for the preparation of natural rubber latex foam (NRLF). Latex chemicals (sulfur, wingstay L, potassium oleate, Zinc diethyldithiocarbamate (ZDEC), Zinc 2-mercaptobenzthiozolate (ZMBT), Diphenylguanidine (DPG) and Sodium silicofluoride (SSF) from Bayer. Waste tire powder (WTP) supplied by Saeng Thai Rubber Co., Ltd.

Table 1 Formulation of natural rubber latex foam filled with waste tire powder

Ingredients	Total Solid Content (%)	Formulation (phr)
Natural rubber latex	60	100
K-Oleate	20	1.0
Sulphur	50	5.0
ZDEC	50	1.0
ZMBT	50	1.0
Wingstay L	50	1.0
ZnO	50	5.0
DPG	33	1.0
SSF	25	0.4
WTP-20, WTP-30, WTP-40	100	10, 20 , 30

Particle size of WTP-20, WTP-30, WTP-40 were 20, 30 and 40 mesh, respectively.

2. Sample Preparation

Firstly, high ammonia natural rubber latex (LNR) was filtered and weighed according to the formulation. Then, latex and latex chemical (ZMBT, ZDEC, Sulphur, Wingstay L and potassium oleate) were stirred for about 16 hours (hr) by using a mechanical stirrer at low speed. After 16 hr of continuous stirring, the NRLF compound was foamed using the stand mixer (OTTO Mixer HM-273). WTP was slowly added to NRLF compound and the mixture was beaten by using stand mixer for about 4 min until the homogenized compound was obtained. After that, The NRLF compound was beaten intensively for about 2 min until the volume of the compound increased up to three times its initial volume. Foaming speed was lowered to obtain

a fine and even foam once the desired volume was obtained. Next, the primary gelling agent (zinc oxide, ZnO) together with diphenyl guanidine (DPG) was added to the foam, and beating was continued for another 1 min. Then, the secondary gelling agent (sodium silicofluoride, SSF) was added and the foam was beaten for 1 min. Finally, the ungelled foam was obtained and the ungelled foam was quickly poured into the desired aluminum mould and allowed to gel for 3 min at ambient temperature. Gelled foam was then cured in a steam cure at 100 °C for 30 min. The WTP powder filled NRLF foam (WNRLF) was stripped from the mould and washed thoroughly with distilled water to remove the excessive non-reacted materials. After washing, the cured WNRLF was dried in a hot air oven at 70 °C for 4 hr. The well dried foam will appear to be off white in color.

3. Measurement of foams

Tensile Properties

Tensile tests were carried out according to ASTM D 412 by using a universal testing machine Hounsfield-H10 KS. Dumbbell shaped samples were cut from the WNRLF sample by using a Pneumatic Shape Cutting Device 403S-S Series. Five samples were required from each loading of WTP. The tensile test was performed at ambient temperature with a crosshead speed of 500 mm/min. Samples of WTP (WTP-20, WTP-30 and WTP-40) filled NRLF with 10 phr, 20 phr and 30 phr filler loading were tested. Tensile properties such as tensile strength and elongation at break were obtained from tensile testing and the average results were reported.

Density

The density of WTP filled NRLF was determined by calculation from the mass and volume of a specimen as shown in Eq. 1. Samples used in this test method were in a regular shape not less than 1000 mm³ in volume (according to ASTM D3574). Five samples of each WTP loading were measured, and an average of three results was reported.

$$\text{Density (kg/m}^3\text{)} = (M/V) \times 10^6 \quad (1)$$

where M is the mass of the specimen (g) and V is the volume of the specimen (mm)³.

Compression Set

Compression set properties of WTP filled NRLF were evaluated according to ASTM D3574. Samples used were in regular shape of 50 mm x 50 mm x 25 mm with parallel top and bottom surface and essentially perpendicular sides. Three specimens per samples were tested. Specimens were placed in the test apparatus and deflected to 50 ± 1 % of their original thickness. Within 15 min, deflected specimens and the apparatus were placed in mechanically convected air oven for 22 hr with a test temperature of 70 ± 2 °C. Specimens were immediately removed from apparatus and measured after 30 minutes recovery. Compression set and recovery percentage were obtained from this testing. Three samples of each WTP loading were tested. Calculate the compression set, expressed as a percentage of the original thickness, as shown in Eq. 2.

$$C_t = [(t_o - t_f) / t_o] \times 100 \quad (2)$$

where:

C_t = compression set expressed as a percentage of the original thickness,

t_o = original thickness of test specimen, and

t_f = final thickness of test specimen.

Results and Discussion

1. The effect of waste tire powder on properties of NRLF

Mechanical Properties

Results related to the mechanical properties of WTP-filled NRLF are shown in Figure 1, Figure 2 and Figure 3. The tensile strength and density of the NRLF increased with an increase in WTP loading, but the elongation at break of WTP-filled NRLF decreased with increasing WTP loading. Decreasing size of WTP increased the tensile strength and elongation at break of NRLF. The strength of a composite is expected to depend on the filler-matrix interfacial interactions. Considering that the WTP surface was not treated and that no compatibilizer or coupling agents were used in this work, but WTP surface was the rubber. It was reasonable to find that the strength was improved significantly. The filler content increases there is more filler surface that needs to be wetted by the polymer in order to have good contact and sufficient stress transfer, and less polymer that is available to wet the WTPs, so the strength started to decrease upon further addition of fillers (Karim *et al.*, 2016). The elasticity of foam was reduced, resulting in a stiffer and more rigid foam. This led to lower resistance to break (Muniandy *et al.*, 2012). A reducing trend in elongation at break was attributed to the addition of WTP powder, introduced more flaws to the WTP filled NRLF resulting from the low WTP-rubber interaction.

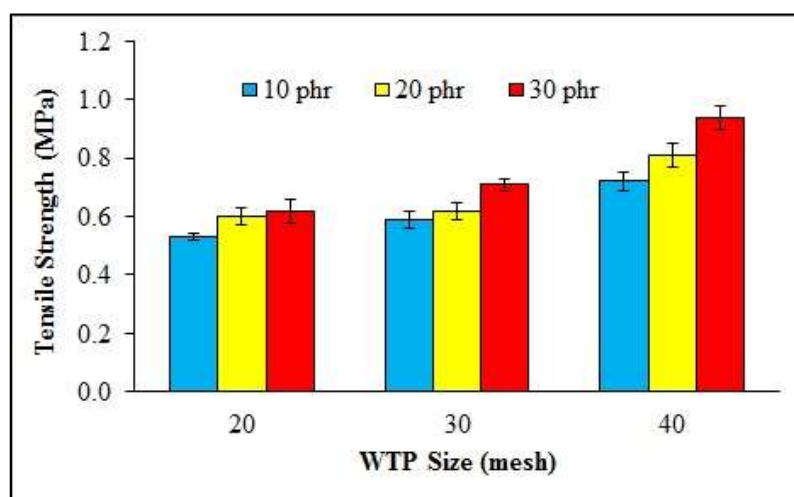


Figure 1 The effect of amount and size of WTP on tensile strength of WTP-filled NRLF

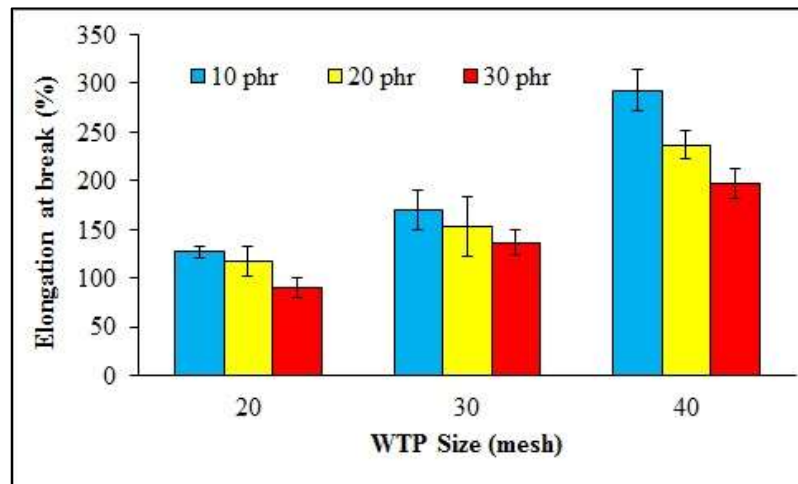


Figure 2 The effect of amount and size of WTP on elongation at break of WTP-filled NRLF

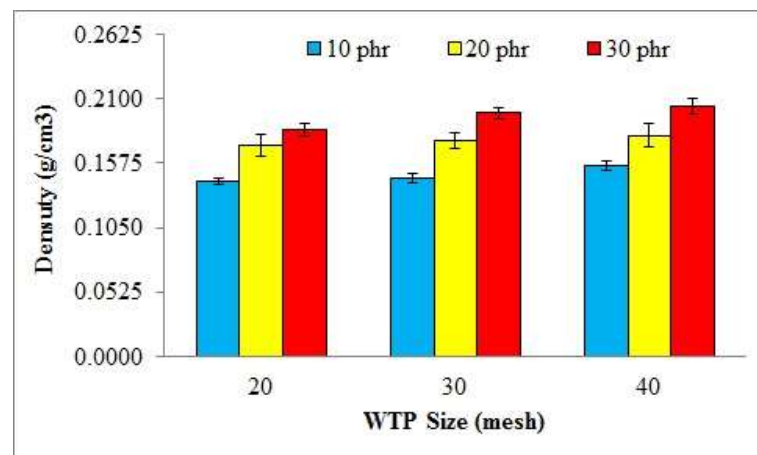


Figure 3 The effect of amount and size of WTP on density of WTP-filled NRLF

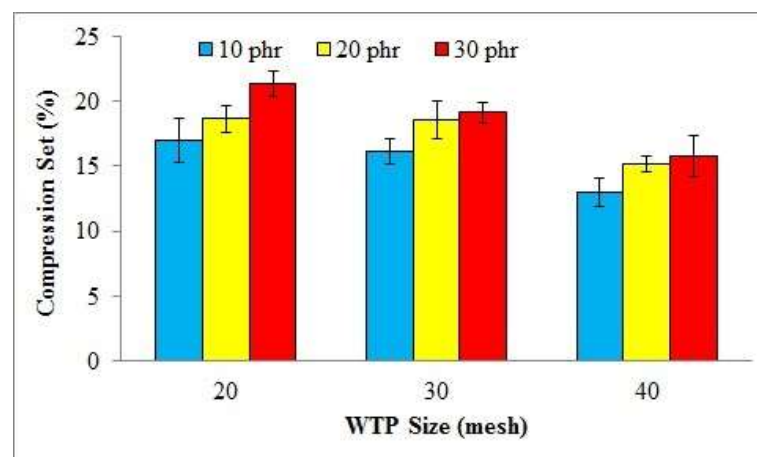


Figure 4 The effect of amount and size of WTP on compression set of WTP-filled NRLF

The compression set is a measure of the elastic behavior of the material. Figure 4 shows that the WTP-filled NRLF (with 40 mesh, 10 phr) had the lowest compression set. Low compression sets indicate a high elasticity. The NRLFs with higher WTP loadings had higher compression sets. Figure 4 reveals that the control NRLF (with 10 phr WTP) had the highest

and fastest recovery percentage. The recovery percentage of WTP incorporated NRLF decreased with decreased WTP size. The recovery percentage of WTP-filled NRLF decreased with increasing WTP loading. Non elastic deformation was mainly due to the deformation of the hard phase of which more WTP is present (Bashir *et al.*, 2015). These results are shown in Figure 5.



Figure 5 Photographs of WTP-filled NRLF

2. The effect of filler loading on properties of NRLF

Figure 6 and Figure 7 show the effect of silica (10 phr), calcium carbonate (CaCO_3) (10 phr), Silica, CaCO_3 /WTP (10 phr) blend on tensile properties of NRLF. The Silica, CaCO_3 /WTP blend NRLF caused a decrease in the tensile strength and elongation at break. In general the tensile strength of foam strongly depends on the foam density (Rattanapan *et al.*, 2016). Figure 8 clearly shows that density of NRLF decreased with added Silica, CaCO_3 /WTP blend into the NRLF.

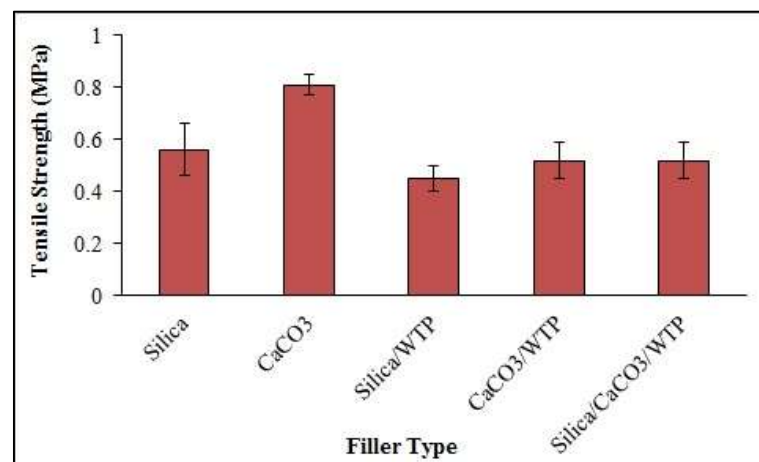


Figure 6 The effect of filler and WTP on tensile strength of NRLF

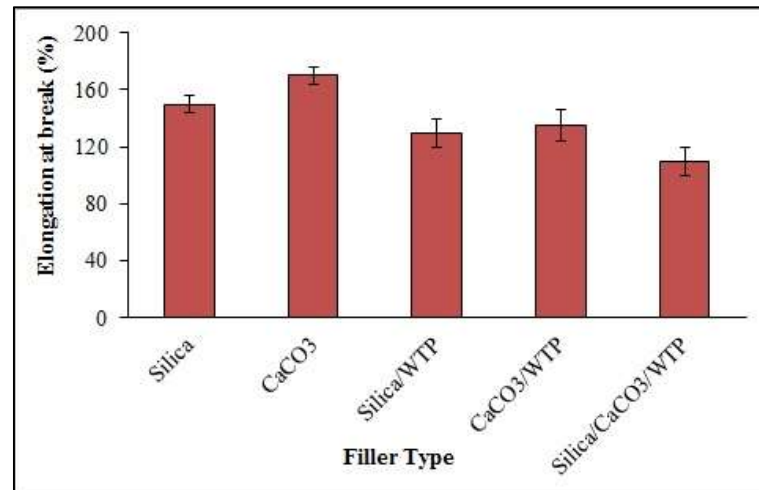


Figure 7 The effect of filler and WTP on elongation at break of NRLF

The compression set was performed to study the dimensional durability of foam under stress (Zhang *et al.*, 1998). A low compression set indicates that the foam is more flexible or has a high elasticity, i.e., it can recover better its original shape after deformation. The addition of Silica, CaCO₃ and WTP into the foam influenced the compression set of NRLF. Silica/CaCO₃/WTP blend showed the lowest value (13 %) whereas Silica-NRLF and Silica/WTP-NRLF showed a higher value than CaCO₃-NRLF and CaCO₃/WTP-NRLF. However, the compression set value of all NRLFs was relatively low (Figure 9). This might be due to the effect of cellular structure which contained lots of open cells making it more flexible. These results are shown in Figure 10.

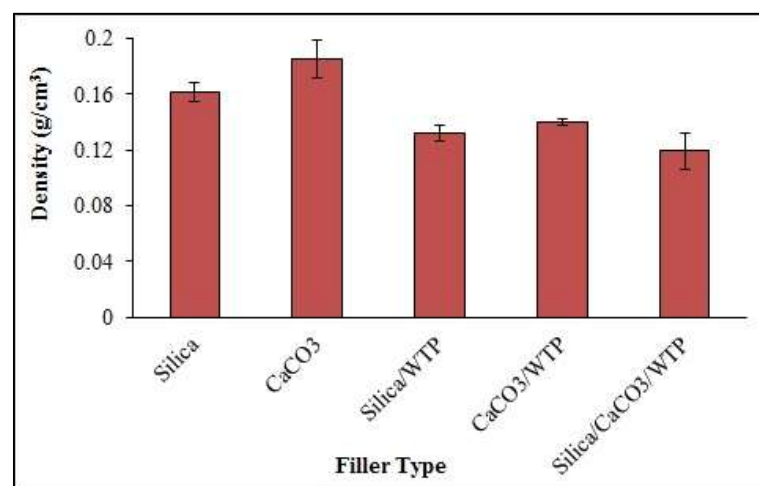


Figure 8 The effect of filler and WTP on density of NRLF

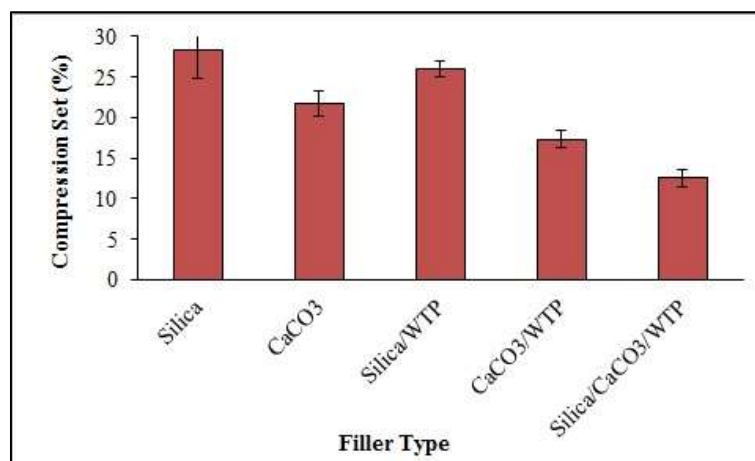


Figure 9 The effect of filler and WTP on compression set of NRLF



Figure 10 Photographs of filler and WTP - filled NRLF

Conclusion

The tensile strength and density of the NRLF increased with an increase in WTP loading, but the elongation at break of WTP-filled NRLF decreased with increasing WTP loading. Decreasing size of WTP increased the tensile strength and elongation at break of NRLF. Smaller WTP size indicated higher elasticity of WTP-filled NRLF, but the recovery of WTP-filled NRLF decreased with increasing WTP loading. Addition Si and CaCO₃ into the NRL together with WTP would also decreased the properties of NRLF. The foams observed by optical microscopy revealed to have open cells.

Acknowledgement

The authors gratefully acknowledge the National Research Council of Thailand for its financial support of this work.

References

- Bashir, A.S.M., Manusamy, Y., Chew, T.L., Ismail, H. and Ramasamy, S. 2015. Mechanical, Thermal, and Morphological Properties of (Eggshell Powder)-Filled Natural Rubber Latex Foam. **Journal of vinyl & additive technology** 23(1): 1-12.
- Blackley, D.C. 1966. Polymer Lattices Science and Technology. **Springer**. London.

- Hamza, Z.P., Difi, K.F.A., Muralidharan, M.N. and Kurian, T. 2008. Microwave oven for the rapid determination of total solids content of natural rubber latex. **International Journal of Polymeric Materials and Polymeric Biomaterials** 57(9): 918-923.
- Hossain, K.M., Sarwaruddin, A.M., Haque, M.E., Dafader, N.C. and Akhtar, F. 2010. Effect of natural antioxidant (*Diospyros peregrina*) on the aging properties of radiation vulcanized (γ -radiation) natural rubber latex film. **Polymer-Plastics Technology and Engineering** 49(2): 136-140.
- Karim, A.F.A., Ismail, H. and Ariff, Z.M. 2016. Properties and Characterization of Kenaf-Filled Natural Rubber Latex Foam. *BioResources* 11(1): 1080-1091.
- Li, Y., Ding, X., Guo, Y., Rong, C., Wang, L., Qu, Y., Ma, X. and Wang, Z. 2011. A new method of comprehensive utilization of rice husk. **Journal of Hazardous Materials** 186(2-3): 2151-2156.
- Madge, E.W. 1962. Latex Foam Rubber. **Maclaren & Sons**. London.
- Muniandy, K., Ismail, H. and Othman, N. 2012. Fatigue life, morphological studies, and thermal aging of rattan powder-filled natural rubber composites as a function of filler loading and a silane coupling agent. **BioResources** 7(1): 841-858.
- Nawamawat, K.S., Jitladda, T. H., Chee, C., Yujie Song, M., Vancso, J. and Julius, G. 2011. Surface nanostructure of Hevea brasiliensis natural rubber latex particles. **Grishpoll Bay (Coll) Surf Forecast and Surf Reports** 390(1-3): 157-166.
- Rattanapan, S., Pasetto, P., Pilard, J.-F. and Tanrattanakul, V. 2016. Preparation and properties of bio-based polyurethane foams from natural rubber and polycaprolactone diol. **Journal of Polymer Research**. 23(9): 1-12.
- Zhang, X.D., Bertsch, L.M. and Macosko, C.W. 1998. Effect of amine additives on flexible, molded foam properties. **Cellular Polymers** 17:327-349.

Survey Study of Current Seawater Desalination Processes

Hanshik Chung^{1*}, Napat Watjanatepin², Chalermopol Ruangpattanawiwat² and Soon-Ho Choi¹

ABSTRACT

Considering that nearly 1 billion people in the developing world don't have access to clean and safe drinking water at present, the water resource can be the cause of a global conflict in the near future. Realistically, breaking through such a global water shortage would be to acquire freshwater from abundant seawater on the earth. Commercially, seawater desalination is classified into a membrane process and a thermal process. Although the thermal process, which simply evaporates seawater and condenses the evaporated steam for obtaining freshwater, was the main (method) in the past, the membrane process has dominated the seawater desalination market at present. The main reason to change the seawater desalination market transit is the specific energy consumption (SEC), which means that the energy consumption required to produce the freshwater of a unit mass. This review thoroughly investigated the current seawater desalination technologies and compared the SEC of each process. Especially, this review focused on the mechanism of how to reduce the SEC of a thermal type seawater desalination process from the survey of the reported studies. Furthermore, in the case of a thermal type seawater desalination process, the mechanism of why the SEC can be reduced was described on the basis of thermodynamics.

Keywords: Desalination, Global Water Shortage, Reverse Osmosis, Specific Energy Consumption, Thermal Type Desalination

¹Department of Energy and Mech. Eng., Institute of Marine Industry, Gyeongsang National University, Tongyoung, 650-160, Republic of Korea

²Rajamangala Univ. of Technology Suvarnabhumi, Nonthaburi 1, Suan-Yai, Muang-Nonthaburi, 11000, Thailand

*Corresponding author, e-mail : hschung@gnu.ac.kr

Introduction

As well known, both human population and water resources are unevenly distributed across the globe. In many areas, densely populated regions do not overlap with those that are water rich (Kummu *et al.*, 2010). Due to the rapidly increasing population and water use per capita in many areas of the world, nearly one third of the world's population currently lives under physical water scarcity. Figure 1 shows the global water stress map that is the average exposure of water users in each country to baseline water stress (Amber and Matlock, 2011).

Despite the abundance of water resource on the earth, the cause of water shortage comes from the fact that most water on the earth is seawater. Of the total water resource on the earth, freshwater available to humans is extremely restricted as shown in Figure 2 (Chung *et al.*, 2014). Water shortage can be overcome by developing unutilized water resource and the easiest way would be underground development. However, underground water development brings about the adverse effects such as a reduction of river flowrate, a depletion of lakes or sink holes.

Certainly, the most realistic breakthrough to solve water shortage is seawater desalination and various processes have been used to obtain freshwater from seawater. Commercially, Seawater desalination process is classified into two processes called membrane and thermal process (Van der Bruggen and Vandecasteele, 2002). However, seawater desalination is a process that consumes a lot of energy no matter what process is adopted for seawater desalination. At present, the economics of seawater desalination process is generally evaluated by the concept of specific energy consumption (SEC), which means the energy required to produce 1 kg of freshwater from seawater (Chung *et al.*, 2016; Choi, 2016).

Although many new technologies for seawater desalination such as membrane distillation, reverse osmosis using carbon nanotube and graphene or freshwater extraction from methane hydrate would be appeared in future (Chung *et al.*, 2014), only commercial seawater desalination processes used in the present market are reviewed in the viewpoint of SEC. Furthermore, the reverse osmosis process for brackish water (BWRO) will not mentioned SEC in this review article since BWRO system obtains freshwater from the very low salinity water, not from seawater nearly with the salinity of 35,000 ppm. Since this review is concerned with SECs of the commercial seawater desalination processes, the characteristics of multi-stage flashing (MSF), multi-effect distillation (MED) and reverse osmosis of seawater (SWRO) were evaluated from the viewpoint of SEC.

In principle, thermal process for seawater desalination evaporates seawater and condenses the evaporated steam to obtain freshwater. Therefore, thermal process requires the thermal and electrical energies simultaneously. The former is for heating seawater and for maintaining the evaporating chambers in a vacuum state; the latter is mainly for transporting seawater and freshwater

Unlike thermal process, the reverse osmosis (RO) process can be simply referred as a mechanical filtration. In the RO process, the salty components are removed while seawater is passing through the molecular size holes formed on the membrane surface, which requires a very high pressure.

Although thermal process was dominant in seawater desalination market in the past, the RO desalination system has widely and broadly expands its influence on the market. Therefore, taking into account changes in seawater desalination market, it is very important to correctly analyze the strengths and weaknesses of each process and SEC at the planning stage of the project to construct seawater desalination plant.

In this review article, the characteristics of seawater desalination processes to be used at present were evaluated. Additionally, the operating principles of each process were also

described and so the authors are sure that this review is helpful to the engineers related with seawater desalination.

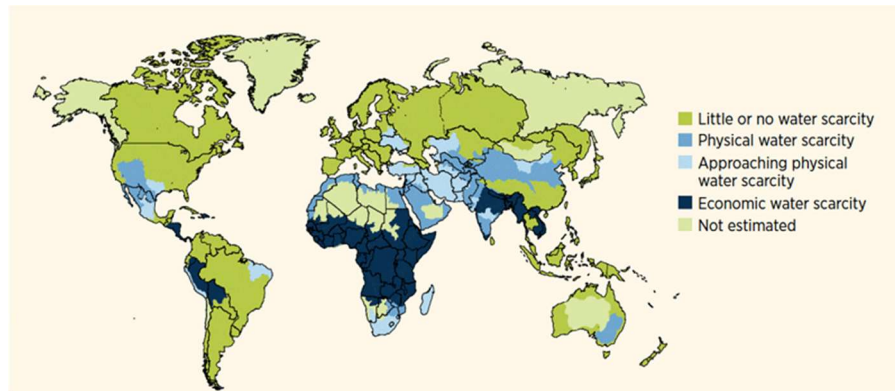


Figure 1 Global physical and economic water scarcity. This figure was cited from the reference of Amber and Matlock (2011).

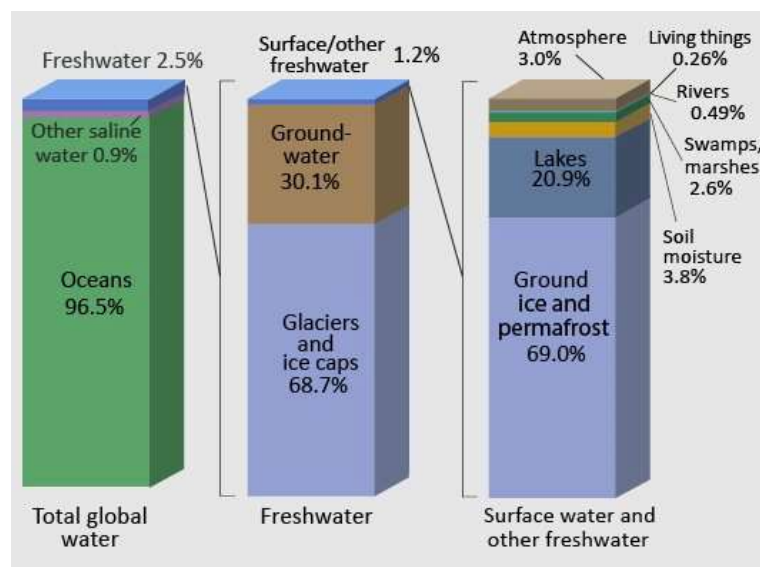


Figure 2 Freshwater ratio to total water resource on the earth. This figure was cited from the reference of Chung *et al.* (2014).

Thermal Process

As described briefly in the previous section, the typical thermal processes are MSF and MED shown in Figure 3 and Figure 4. Although the evaporating section consist of a few evaporating chambers, the MSF system is over 20 stages and the MED system is over ten stages in general. For the easy understanding of this review, it will be appropriate to mention the operating principles of each thermal process.

1. Multi-stage Flashing (MSF) Process

The MSF system plant is shown in Figure 3 has a series of evaporators called stages, each evaporator is actually the heat exchanger coupled with an evaporator and a condenser. The brine heater, which is for heating seawater, is called a hot end and the last stage is a cold end while the intermediate stages have intermediate temperatures. Each stage has a different pressure corresponding to the boiling points of water at the stage temperatures.

When the plant is operating in steady state, feeding seawater at the cold inlet temperature is pumped through the condenser tube banks installed at the top section of the stages and warms up. When it reaches the brine heater, it already has nearly the maximum temperature. In the brine heater, an amount of additional heat is added. After the heater, the seawater flows into the stages that have ever lower pressure and temperature. As it flows back through the stages the seawater is now called brine, to distinguish it from the inlet seawater. In each stage, as the brine enters, its temperature is above the boiling point at the operating pressure of the stage, and a small fraction of the brine boils (“flashes”) to steam thereby reducing the temperature until a thermal equilibrium is reached. The resulting steam is a little hotter than the feeding seawater in the condenser. The steam cools and condenses on the condenser tubes, thereby heating the feeding seawater as described earlier.

The total evaporation in all the stages is up to approximately 15% of the seawater supplied to the system, depending on the range of temperatures and the stage number used. With increasing temperature there are growing difficulties of scale formation and corrosion. 120 °C appears to be a maximum, although scale avoidance may require temperatures below 70 °C (Chung *et al.*, 2014; Chung *et al.*, 2016; Choi, 2016).

The feed water carries away the latent heat of the condensed steam, maintaining the low temperature of the stage. The pressure in each chamber remains constant as equal amounts of steam is formed when new warm brine enters the stage and steam is removed as it condenses on the condenser tubes.

In the final stage, the brine and the condensate has a temperature near the inlet temperature. Then the brine and condensate are pumped out from the low pressure in the stage to the ambient pressure. The brine and condensate still carry a small amount of heat that is lost from the system when they are discharged. As seen in Figure 3, the thermal energy and electrical energies are required for operating the MSF plant.

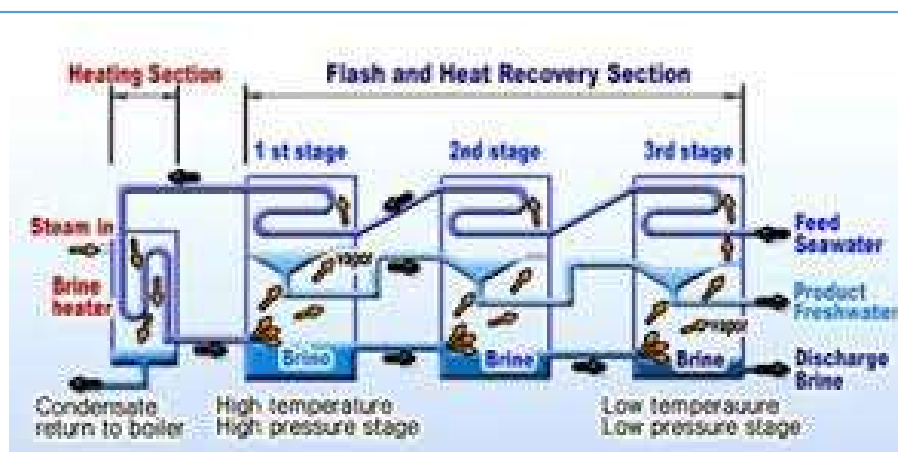


Figure 3 Schematic diagram of multi-stage flashing desalination system. This figure was cited from the reference of Chung *et al.* (2014).

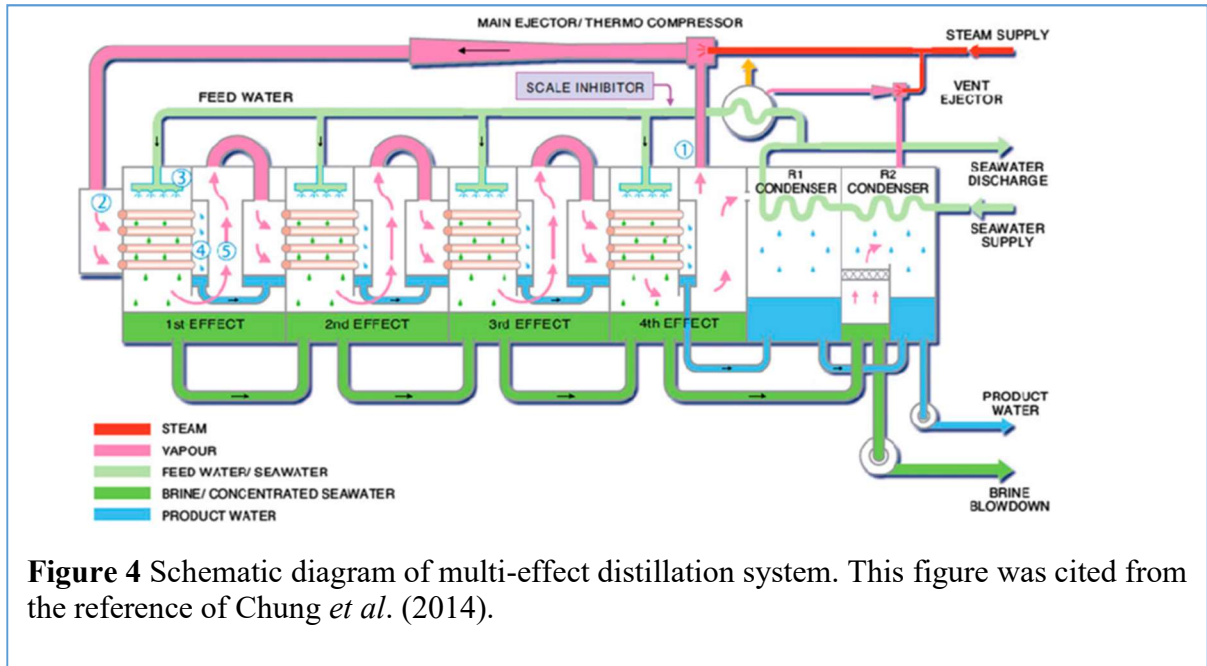
2. Multi-effect Distillation (MED) Process

The MED process has been used since the late 1950s and early 1960s. Multi-effect distillation occurs in a series of vessels (effects) and uses the principles of evaporation and condensation at reduced ambient pressure. The schematic of a horizontal tube Multi-Effect MED unit is presented in FIGURE 4. The steam enters into the plant through the first stage and is used to evaporate heated seawater. Unlike the MSF, the steam flows into the tube side in the MED system and the seawater is sprayed on the tube bank. The vapor evaporated on the tube outside is used for the heating source of the next stage and this skim is repeated from the first stage to the last stage.

The MED technique is based on double-film heat transfer. Latent heat of steam is transferred at each stage by steam condensation through the heat transfer surfaces to the evaporated falling film of seawater. The process is repeated up to 16 times or more in existing plants between the upper possible temperature and the lower possible cooling water, which depends on seawater temperature used for cooling the water. The produced freshwater is the condensate that accumulates from stage to stage. A vacuum pump/compressor is used to maintain the gradual pressure gradient inside the vessel by removing the accumulated non-condensable gases (NCGs) together with the remaining steam after the final condensation stage.

The pressure gradient along the MED effects is dictated by the saturation pressure of the feed stream and the saturation pressure of the condensing steam exiting the last stage and is condensed by cooling seawater. The most distinct feature in the MED system is a thermos-vapor compressor (TVC). As seen in Figure 4, the TVC is a steam ejector operated by the high pressure and high temperature steam supplied from a power plant. Its role is to make a suction of the steam from the final condenser and then mixing it with the high pressure and high temperature steam. By keeping that the mixed steam temperature is higher than the first effect operating temperature, the mixed steam can be used as the heating medium for the first effect. Since a part of steam is reutilized in the MED system, the MED system has generally higher thermal efficiency than the MSF system

1.



In the MED system, the vapor compression can be achieved by adopting a mechanical vapor compressor (MVC) instead of the TVC. In such case, the energy efficiency can be more increased. However, the MED-MVC has a demerit due to a reduced stage number. Currently, three stages is a maximum application in the MED-MVC.

3. Membrane Process-Reverse Osmosis

The membrane processes for seawater desalination can be regarded as a filtration or separation basically. In general the membrane process has some advantages compared to thermal process.

Firstly, freshwater separation is achieved on the basis of molecular size, shape and charge; it can be carried out at ambient or modest temperatures and therefore damage to heat.

Secondly, since no change of phase is required, energy requirements are modest.

Thirdly, the equipment used for desalination is modular and hence capacity is scaled up by using multiple units.

Fourthly, the equipment is compact and system size is directly related to membrane surface area and therefore the space requirement is small.

Fifthly, membrane process is not significantly affected by the feeding seawater temperature while the thermal processes are greatly affected by the feeding seawater temperature.

Although already mentioned in the previous section, this review does not include the electro dialysis (ED) and the BWRO. Those two processes are not for seawater but for low salinity water such as brackish water. Since the purpose of this review is to compare the performances of the current desalination processes on the market, the SWRO system is only considered and described.

As seen in Figure 5, the SWRO system consists of pre-treatment module, RO module and post-treatment module. The pre-treatment module has a role to transfer seawater, to settling it and to remove some suspended materials through the micro-filter (MF) module. Since the MF module removes micro-sized impurities from seawater, it protects the RO module

contamination and eventually plays a role to extend the operating lifetime of the RO membranes. In the SWRO system, water molecules are forcibly penetrated through the molecular sized holes on the membrane surface. Therefore, the high pressure pump over about 80 bar·g should be used. The post-treatment module is for sterilizing the produced freshwater.

Unlike the thermal process, the required power in the SWRO system is only electricity for operating various pumps; the intake pump, the high pressure pump and service pump. At the current technology of SWRO membrane, 50 % of the seawater supplied to the SWRO module can be passing through the membrane, which is referred to the recovery ratio of 50 %.

The produced freshwater is a little bit higher than the atmospheric due to a very high flow resistance when passing through the membrane. However, the rejected seawater not permeated through the membrane has the same pressure supplied by a high pressure pump. The high pressure held by the rejected seawater is high quality energy. Therefore, the recent SWRO system recovers the pressure energy from the rejected seawater by using energy recovery device, which is for reducing the energy to produce freshwater.

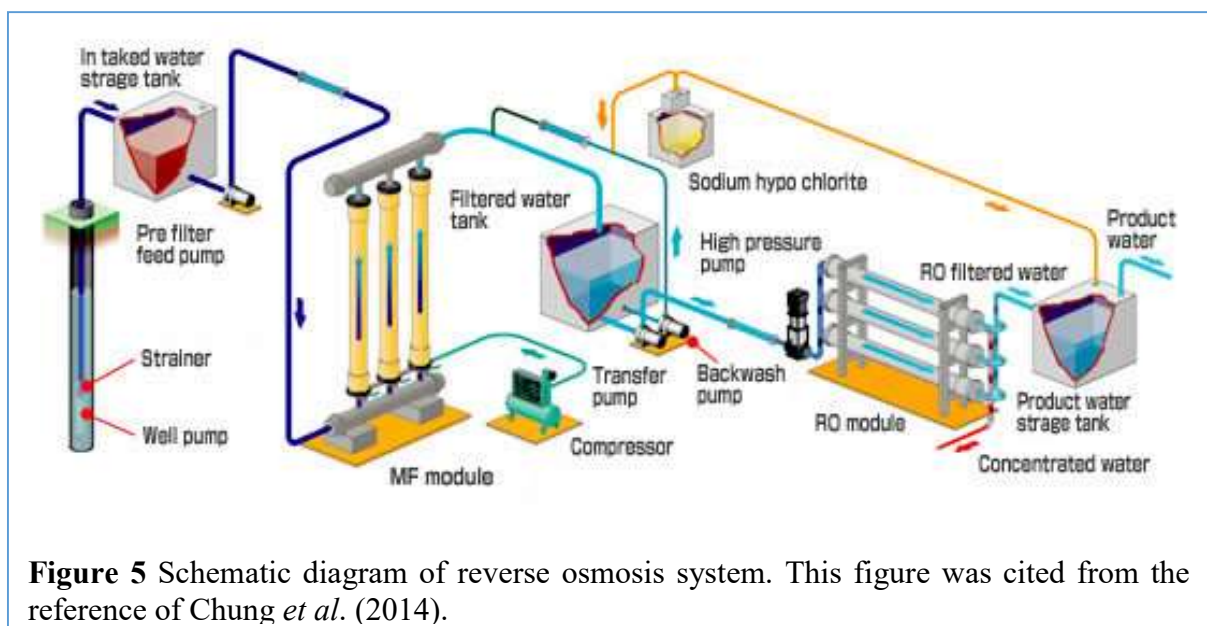


Figure 5 Schematic diagram of reverse osmosis system. This figure was cited from the reference of Chung *et al.* (2014).

Features of Seawater Desalination Processes

For comparing each seawater desalination processes, the plant performance of seawater desalination has been evaluated by using various concepts. In the past, the concept of gained output ratio (GOR) was used in the thermal process. GOR is a measure of how much thermal energy is consumed in a desalination process. In other words, how many kilograms of distilled water are produced per 1 kg of steam consumed? However, the concept of GOR considers only the thermal energy. Considering even if the thermal process uses the thermal and electrical energies simultaneously for producing freshwater, GOR cannot be adequate standard to compare a plant efficient.

Recently, Chung *et al.* (2016) and Choi (2016) introduce the concept of specific energy consumption (SEC) in the SI unit. According to their definition, the SEC means the energy expressed in Joule to produce 1kg of freshwater from seawater. Therefore, the concept of SEC can be applied not only the thermal process but also the membrane process.

Table 1 shows the features of each seawater desalination process and the SECs of commercial seawater desalination processes that are surveyed in some typical researches (Glueckstern, 1982; Uche *et al.*, 2001; Miller, 2003; National Water Commission, 2008; Chung *et al.*, 2014).

Table 1 Typical features of seawater desalination processes.

Description	MED-TVC	MSF	SWRO
Capacity (MIGD) ^[1]	18 MIGD	8 MIGD	5 MIGD
Plant expandability	Not good	Not good	Good
Allowable TDS (ppm)	30000-50000	30000-50000	30000-45000
Raw water pre-treatment	Low requirement	Low requirement	Very high requirement
Operating temperature (°C)	< 70	< 120	Ambient
Raw water utilization efficiency ^[2]	15-40 %	12-25 %	35-40 %
Produced water quality in TDS (mg/liter)	5-10	5-10	300-500
Main energy source ^[3]	Heat and Electricity	Heat and Electricity	Electricity
Specific energy consumption (kWh/m ³)	10-16	6-12	4-5
Construction cost (US\$/m ³ /day)	1200-1500	900-1000	700-900
Operating cost (US\$/m ³)	1.1-1.25	0.8-0.9	0.7-0.9

[1] 1 MIGD=4,542 m³/day.

[2] The ratio of produced freshwater to supplied seawater.

[3] Heat means the thermal energy and the electrical energy is required to operate the pumps, instrumentation and control room.

Results and Discussion

As seen in Table 1 of the previous section, the thermal processes are inferior to the SWRO system in all aspect even though the MSF system is still major seawater desalination in the Gulf countries. In the past, the RO membrane was highly expensive and the production rate of freshwater was low. For increasing the production rate of freshwater, a more high pressure should be applied to seawater, which causes the rapid contamination of SWRO membrane. The high procurement cost and the short period of SWRO membrane replacement bring about the

construction and operating costs, which resulted in a low competitiveness compared to the thermal process up to early 1990s.

However, with the advancement of nano technologies, the unit price to purchase the RO membrane has been sharply decreased from the end of 1990s. Furthermore, the increased porosity formed on the membrane surface makes it possible to increase the freshwater production rate with a lower discharge pressure of a high pressure pump. Due to the reduced membrane cost and the increased freshwater productivity, the SWRO system had been dominant in seawater desalination market from the mid of 1990s as shown in Figure 6. Furthermore, since the energy recovery device for recovering the high pressure energy from the rejected seawater is still improved, there is a room for further reduction of SEC in the SWRO system.

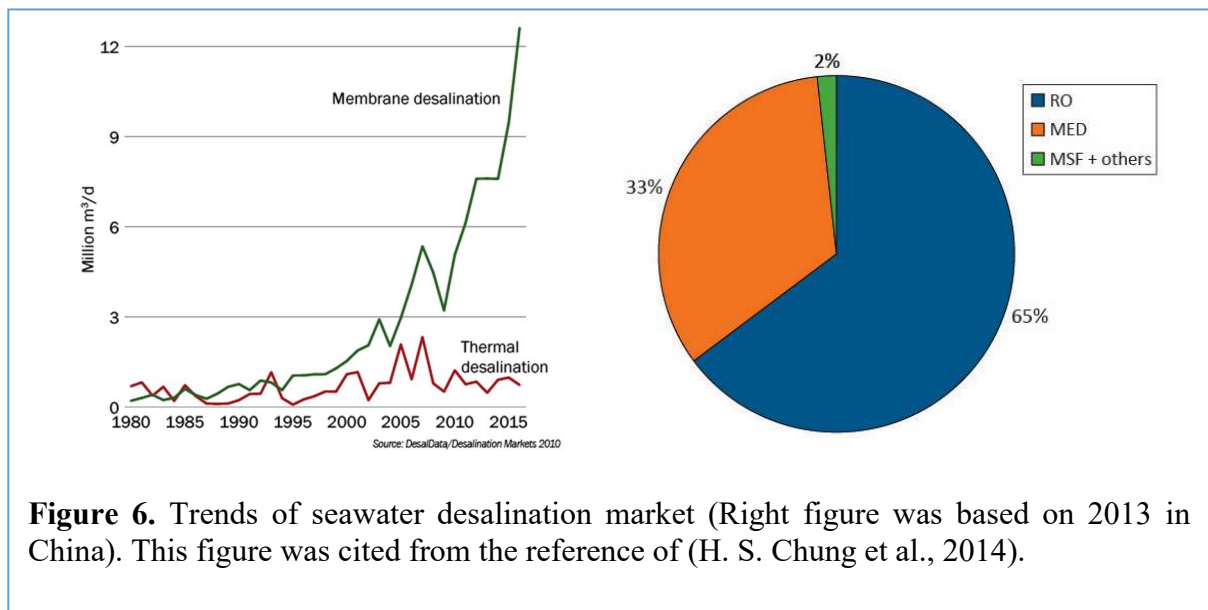


Figure 6. Trends of seawater desalination market (Right figure was based on 2013 in China). This figure was cited from the reference of (H. S. Chung et al., 2014).

Although it can be confirmed that the SWRO system is the most efficient among various seawater desalination processes at present, the engineers should pay attention to the characteristics of SWRO. The weak point of SWRO is sensitive to the quality of raw seawater. If raw seawater quality is bad, the SWRO module is rapidly contaminated and the module replacement period is shortened. This would be the cause of the increased operating cost. Additionally, the produced seawater quality from SWRO is much lower than that of the thermal process as seen in Table 1. The quality over 100 ppm cannot be used for demineralized cooling water or boiler make-up water of mechanical equipment, which means that the freshwater produced from SWRO is not proper for the plant operation.

At present, the temperature effect of raw seawater on SWRO membrane is not investigated in detail. If the temperature of raw seawater is high, the porous hole size formed on the membrane certainly gets larger. The increased hole size facilitates the penetration of seawater through SWRO membrane and increases freshwater production rate. This will make the produced freshwater quality degrade and reduce the power of a high pressure pump at the same time. If mentioning more specifically, the freshwater quality produced from SWRO is declined, the freshwater production rate is increased and the pump power is reduced with the raw seawater temperature.

Therefore, the engineers related to seawater desalination deeply consider raw seawater quality, the usage of the produced freshwater, the capacity, available energy sources, future

expandability and so on. The authors are sure that Table 1 provides highly useful information with the engineers when they begin the project for constructing a seawater desalination plant.

Acknowledgment

This research was supported by Basic Science Research Program through the National Research Foundation of Korea (NRF) funded by the Ministry of Education (No.2015R1D1A1A01058030) and Gyeongsang National University Fund for Professors on Sabbatical Leave, 2018

References

- Amber, B. and Matlock, M. D. 2011. A Review of Water Scarcity Indices and Methodologies, **Sustainability Consortium**, White paper 106.
- Choi, S. H. 2016. On the brine re-utilization of a multi-stage flashing (MSF) desalination plant. **Desalination** 398: 64-76.
- Chung, H. S. *et al.* 2014. **KAERI/RR-KAERI/CM-1878**.
- Chung, H. S., Jeong, H. M., Jeong, K. W., Choi, S. H. 2016. Improved productivity of the MSF (multi- stage Flashing) desalination plant by increasing the TBT (top brine temperature). **Energy** 107: 683-692.
- Glueckstern, P. 1982. Comparative energy requirements and economics of desalting processes based on current and advanced technology. **Desalination** 40: 63-74.
- Kummu, M., Ward, P.J., de Moel, H., and Varis, O. 2010. Is physical water scarcity a new phenomenon? Global assessment of water shortage over the last two millennia. **Environmental Research Letters** 5: 034006.
- Miller, J. E. 2003. Review of water resources and desalination technologies. **SAND** 2003-0800.
- National Water Commission. 2008. **Waterlines Report Series** 9.
- Uche, J., Serra, L. and Valero, A. 2001. Hybrid desalting systems for avoiding water shortage in Spain. **Desalination** 138: 329-334.
- Van der Bruggen, B. and Vandecasteele, C. 2002. Distillation vs. membrane filtration: overview of process evolutions in seawater desalination. **Desalination** 143(3): 207-218.

Triploid Induction by the Use of 6-dimethylaminopurine (6-DMAP) for the Tropical Oyster, *Crassostrea belcheri* (Sowerby, 1871)

Supatcha Chooeangjaew^{1,2,*}, Suwat Tanyaros¹, Worawut Koedprang² and Alongklod Tanomtong³

ABSTRACT

Currently, numerous methods for triploid induction both physical and chemical such as pressure, caffeine, CB and 6-DMAP were used and successful in bivalves. In this study, triploidy oysters were induced by chemical treatment with 6-dimethylaminopurine (6-DMAP). 6-DMAP was carried out on strip-spawned method of the tropical oyster, *C. belcheri*. Three levels of 6-DMAP concentration (100, 200 and 300 µM), three levels of time after fertilization (30, 40 and 50 min), and two levels of exposure duration (5 and 10 min) were operated. Triploid percentage, survival rate, and yields of triploid were examined in the short term at trochophore stage. The result showed that the highest triploid percentage at 100 µM 6-DMAP, 30 min after fertilization and 10 min exposure was 86.99±2.45% ($P < 0.05$). Moreover, the highest survival rate was recorded for the control (54.00±7.45%) and 100 µM 6-DMAP, 50 min after fertilization and 5 min exposure (54.00±2.74%) while the survival rates in other experimental unit ranging from 34.13±5.11- 53.25±16.27 %. The highest triploid yield was found at 100 µM 6-DMAP, 50 min after fertilization and 5 min exposure (43.68±2.44%). Moreover, tetraploid and pentaploid can be detected from triploid induction with 6-DMAP. In addition, 6-DMAP is safer to handle and easily used. This research enables the future consideration of the triploid performance and improves survival rate and growth rate in commercial aquaculture of oyster and other shellfish.

Keywords: *Crassostrea belcheri*, Tropical oyster, Triploid, 6-DMAP

¹ Marine Shellfish Breeding Research Unit, Department of Marine Science, Faculty of Science and Fisheries Technology, Rajamangala University of Technology Srivijaya, Trang campus, Trang 92150, Thailand.

² Department of Fisheries Technology, Faculty of Science and Fisheries Technology, Rajamangala University of Technology Srivijaya, Trang campus, Trang 92150, Thailand.

³ Cytology and Ecotoxicology Research Group, Department of Biology, Faculty of Science, KhonKaen University, Muang, KhonKaen 40002, Thailand.

*Corresponding author, e-mail : sumarine2545@gmail.com

Introduction

Chromosome manipulations are useful in mollusk aquaculture because of their faster growth, improved meat quality and reduced sexual maturation. In oysters, triploidy has been induced and evaluated in *Crassostrea gigas*, (Allen and Downing, 1986; Downing and Allen, 1987; Guo *et al.*, 1996) *C. virginica* (Stanley *et al.*, 1981; 1984), *Saccostrea* sp. (Nell *et al.*, 1994; Cox *et al.*, 1996; Hand *et al.*, 1998), *Ostrea edulis* (Gendreau and Grizel, 1990; Hawkins *et al.*, 1994) and *C. madrasensis* (Mallia *et al.*, 2006). Triploid oyster can be produced by two methods as inhibiting first or second polar body formation after fertilization and used the tetraploid broodstock. Inhibiting polar body formation utilized by chemical treatment during meiosis lead to the retention of the maternal chromosome set. Successful induced triploidy using cytochalasin-B (CB) in *C. gigas*, *C. virginica*, *S. glomerata* and *O. edulis* and clams (Allen *et al.*, 1989; Dufy and Diter, 1990; Nell, 2002). There are two problems in producing triploids by this method. The first is that it does not produce 100% triploids. The second is that the chemical cytochalasin B is carcinogenic and although it is only used in the fertilization of the animals and hence poses little possibility of carrying over a toxic effect, there has been concern of repercussions from the public (Guo, *et al.*, 1996). The puromycin analog 6-dimethylaminopurine (6-DMAP) is less frequently used, but has been revealed to highly efficiency for triploid induction in *C. gigas*, *Mytilus edulis* and *Argopecten magellanicus* confirmed in this chemical (Desrosiers *et al.* 1993). The activity of 6-DMAP is meiotic block of microtubule formation within the metaphase spindle (Neant and Guerrier, 1988). These agents have advantages of being water-soluble which can be easily washed off from the embryo after treatment, safer to use than CB and is not a carcinogen (Hand *et al.*, 2004; Thomas *et al.*, 2006). Moreover, It is easy to handle which 6-DMAP treatment process can be carried out without any additional facilities, even at room temperature.

Tropical oyster, *C. belcheri*, is one of the most commercially important bivalves in Thailand. The majority of spat for grow-out farms are collected from natural sources, but the amount of oyster seed produced from those sources is limited and insufficient. Oyster seed production from hatcheries is being developed and is the subject of great interest in Thailand. This study describes further experiments conducted to suitable technique for the triploid production of *C. belcheri* by examining the dosage, timing and duration of embryo treatment with 6-DMAP.

Materials and Methods

1. Broodstock collection, fertilization and gamete handling

The broodstocks of *C. belcheri* were collected from oyster farm at Kantang district, Trang province, southern of Thailand for induction experiment. The oysters were cleaned and acclimated in sand-filtered seawater (30 psu) in the hatchery. Gametes were obtained from sacrificed oysters and sex was determined under compound microscope. Male and female gametes were separately stripped into 30 psu filtered (1 µm) and UV-treated seawater. The eggs were filtered through screen at pore size 70-90 µm, while sperms were filtered by 20-30 µm to remove debris and meat prior to fertilized using 1 male: 4 females. After 10 minutes, fertilized

eggs were filtered by 20-30 μm to remove excess sperm and prevent polyspermy. The fertilized eggs were stocked for further development in filtered (1 μm) and UV-treated seawater in 10 L plastic container before experiment.

2. Triploid induction

The bottom off plastic vial (35 ml) and closed by screen at pore size 20/30 μm was designed to use as the sample container. The 100,000 fertilized eggs were taken to each sample container after fertilization for 15 mins. The samples were kept in filtered sea water (30 psu) at room temperature and gently aeration to prevent eggs settles to the bottom. The samples were exposed to three concentrations of 6-DMAP (100, 200 and 300 μM), three times post fertilization (30, 40 and 50 min) and two levels of duration (5 and 10 min). After treatment, the samples were then moved into filtered sea water as same as the previous condition. The $3 \times 3 \times 2$ factorial in completely randomized design (CRD) was set up as experimental design. Each treatment was triplicates. When the embryo was reached to trochophore stage or 6 hr after fertilization, the larval sample in each vial was randomized to count and then the survival rate was calculated.

3. Chromosome preparation and ploidy determination

The larval sample at swimming trochophores stage from each treatment in sea water was moved, and soaked in 0.02 % colchicine for 90 minutes. Then, the samples were rinsed with clean filtered sea water about 2-3 times for cleared out of the colchicines, and followed by hypotonic treatment in 0.075% KCl for 40 min at room temperature and continuously shaken for prevent cell sedimentation. Next, the samples were transferred to Carnoy's fixative solution (3:1, absolute methanol and glacial acetic acid) for 5-10 minutes. Afterwards, 15-20 drops of 50% glacial acetic acid was added to 0.2 ml of sample on plate for 10-20 minutes. The cell suspensions were dropped by pipette on a clean and warm slide at 50-60°C. The slides were air dried and stained using 20% giemsa in phosphate buffer (pH 6.8) for 40 minutes. Later, the slide was gently rinsed with fresh water, and was air dried at room temperature. Finally, the chromosomes both control and treated batch were examined and counted in metaphase plates for determination the ratio of triploid under compound microscope at magnification 400 (Olympus, CH30, Japan). In this study, the number of ploidys was classified follow by Yamamoto *et al.* (1988), diploid ($2n$) = 18-21 chromosome, triploid ($3n$) = 25-34 chromosome, tetraploid ($4n$) = 35-44 chromosome, pentaploid ($5n$) = 45-64 chromosome.

4. Statistical Analysis

The data of triploid percentages, survival rate, yields and polyploidy percentage of trochophore stage were performed to analysis of variance ANOVA. When the ANOVA presented significant differences among means, the Duncan's New Multiple Range Test (DMRT) was applied. Significance level was set at $P < 0.05$ for all tests. The analyses were performed using the IBM SPSS Statistics 20.

Results

Significant differences ($P < 0.05$) were found in triploid percentage, survival rate, and yields of triploidy (Table 1.). The result of triploid percentage reported that highest triploid

percentage at 100 μ M of 6-DMAP, 30 min after fertilization and 10 min exposure duration ($86.99 \pm 2.45\%$) while there was no difference ($P > 0.05$) with 100 μ M, 30 min after fertilization and 5 min exposure duration ($83.01 \pm 1.52\%$) and 100 μ M, 50 min after fertilization and 5 min exposure duration ($81.00 \pm 5.29\%$). The lowest percentage of triploid was presented in 300 μ M 30 min after fertilization and 10 min exposure duration ($43.85 \pm 12.28\%$). Moreover, triploid percentage in trochophore stage was slightly decreased when high concentration ($P < 0.05$).

The highest survival rate of the trochophore stage presented in control batch ($54.00 \pm 7.45\%$), and no significant difference ($P > 0.05$) with 5 treatment including 100 μ M, 50 min after fertilization and 5 min duration exposure ($54.00 \pm 2.74\%$), 200 μ M, 30 min after fertilization and 5 min duration exposure ($53.25 \pm 16.27\%$), 200 μ M, 30 min after fertilization and 10 min duration exposure ($53.25 \pm 6.76\%$), 200 μ M, 40 min after fertilization and 10 min duration exposure ($52.50 \pm 7.65\%$), and 300 μ M, 30 min after fertilization and 5 min duration exposure ($52.87 \pm 3.75\%$) and lowest was showed in 300 μ M, 50 min after fertilization and 5 min duration exposure ($34.13 \pm 5.11\%$).

The highest triploid yields of trochophore stage was achieved at 100 μ M, 50 min after fertilization and 5 min exposure duration ($43.68 \pm 2.44\%$), and lowest at 300 μ M, 50 min after fertilization and 5 min exposure duration ($21.12 \pm 6.80\%$). Moreover, the trend of yield of triploid was declined when concentration increased. In addition, the triploid yields at 100 μ M 6-DMAP (35.61%) was showed higher average than those of 200 (29.72%) and 300 μ M (26.03%). There was no significant of average triploid yield between concentration of 6-DMAP at 200 and 300 μ M.

Moreover, the effect of triploid induction with 6-DMAP can induce another polyploidy as; tetraploid and pentaploid in the all experiment units. Highest production of tetraploid was revealed in 200 μ M, 40 min after fertilization and 10 min duration exposure ($31.94 \pm 13.86\%$) and the high result of pentaploid from triploid induction was found at 300 μ M, 30 min after fertilization and 10 min duration exposure ($26.73 \pm 7.86\%$). All results from triploid induction with 6-DMAP was shown in Table 1.

Table 1 Triploidy percentage, survival rate, yields and percentage of polyploidy of the Tropical oyster *C. belcheri* induced by 6-DMAP.

6-DMAP conc. (μM)	TAF (min)	Exposure duration (min)	3n (%)	Survival rate (%)	Yields of 3n (%)	4n (%)	5n (%)
Control	-	-	-	54.00±7.45 ^a	-	-	-
100	30	5	83.01±1.52 ^{ab}	43.88±16.99 ^{abc}	36.4±14.13 ^{ab}	15.92±0.56 ^{cd}	1.06±1.25 ^d
		10	86.99±2.45 ^a	35.63±6.29 ^{bc}	31.05±5.92 ^{bc}	11.89±1.90 ^d	1.11±1.48 ^d
	40	5	74.1±12.85 ^{cd}	48.00±10.03 ^{abc}	36.05±12.4 ^{ab}	23.32±9.83 ^{abcd}	2.62±3.40 ^{cd}
		10	79.52±4.59 ^{bc}	45.00±6.36 ^{abc}	35.63±3.94 ^{ab}	17.51±4.72 ^{bcd}	2.96±4.19 ^{cd}
	50	5	81.00±5.29 ^{ab}	54.00±2.74 ^a	43.68±2.44 ^a	15.99±4.12 ^{cd}	3.00±2.97 ^{cd}
		10	67.09±3.63 ^{de}	46.60±13.96 ^{abc}	30.85±7.84 ^{bc}	21.55±1.37 ^{abcd}	11.35±4.12 ^{bcd}
	200	30	63.16±4.54 ^{de}	53.25±16.27 ^a	33.9±11.91 ^{abc}	23.82±3.93 ^{abc}	13.02±4.65 ^{bc}
		10	65.10±6.24 ^{de}	53.25±6.76 ^a	34.51±3.63 ^{abc}	24.22±5.63 ^{abc}	10.67±2.75 ^{bcd}
	40	5	58.39±10.73 ^e	40.13±9.20 ^{abc}	24.13±9.51 ^{bc}	30.18±10.36 ^a	11.43±9.31 ^{bcd}
		10	56.81±11.80 ^e	52.50±7.65 ^a	29.58±6.63 ^{bc}	31.94±13.86 ^a	11.25±5.37 ^{bcd}
	50	5	61.57±6.71 ^e	49.50±9.41 ^{ab}	30.85±8.93 ^{bc}	28.00±4.65 ^{ab}	10.42±2.90 ^{bcd}
		10	63.75±5.54 ^{de}	40.13±8.43 ^{abc}	25.33±4.01 ^{bc}	27.50±3.76 ^{abc}	8.74±7.21 ^{bcd}
300	30	5	64.97±5.19 ^{de}	52.87±3.75 ^a	34.25±1.94 ^{abc}	26.91±3.36 ^{abc}	8.11±5.98 ^{cd}
		10	43.85±12.28 ^f	50.63±6.41 ^{ab}	22.29±6.97 ^c	29.42±5.57 ^a	26.73±7.86 ^a
	40	5	56.91±9.01 ^e	46.88±7.39 ^{abc}	26.36±3.58 ^{bc}	30.47±11.58 ^a	12.61±3.71 ^{bc}
		10	56.85±8.69 ^e	45.00±4.24 ^{abc}	25.65±5.14 ^{bc}	30.10±5.39 ^a	13.04±7.91 ^{bc}
	50	5	63.8±12.45 ^{de}	34.13±5.11 ^c	21.12±6.80 ^c	16.98±12.9 ^{bcd}	19.1±15.85 ^{ab}
		10	68.58±4.72 ^{cde}	37.13±4.31 ^{bc}	25.52±3.88 ^{bc}	28.03±2.57 ^{ab}	3.39±3.99 ^{cd}

* $\bar{X} \pm \text{SD}$, values with the superscript are not significant different ($P > 0.05$),

TAF= Time after fertilization

Effect of one factor of concentration, two interaction of concentration and time after fertilization, three interaction of concentration, time after fertilization and exposure duration were revealed that significant different ($P < 0.05$) on triploid percentage, while the result showed that two interaction of concentration and time after fertilization had significant main effect on survival rate ($P < 0.05$). Only one factor of concentration was presented that significant different ($P < 0.05$) on triploid yields. All results from three-way ANOVA were shown in Table 2.

Table 2 Analysis of variance for the effect of concentration, time after fertilization and Exposure duration on triploid percentage, survival rate, and yields of polyploidy of the Tropical oyster *C.belcheri* induced by 6-DMAP.

Three-way ANOVA					
	3n (%)	Survival rate (%)	Yields of 3n (%)	4n (%)	5n (%)
Conc	$P<0.05$	$P>0.05$	$P<0.05$	$P<0.05$	$P<0.05$
Time AF	$P>0.05$	$P>0.05$	$P>0.05$	$P<0.05$	$P>0.05$
Duration	$P>0.05$	$P>0.05$	$P>0.05$	$P>0.05$	$P>0.05$
Conc* Time AF	$P<0.05$	$P<0.05$	$P>0.05$	$P>0.05$	$P>0.05$
Conc* Duration	$P>0.05$	$P>0.05$	$P>0.05$	$P>0.05$	$P>0.05$
Time AF* Duration	$P>0.05$	$P>0.05$	$P>0.05$	$P>0.05$	$P>0.05$
Conc* Time AF* Duration	$P<0.05$	$P>0.05$	$P>0.05$	$P>0.05$	$P<0.05$

Discussion

This study is first reported of triploid induction in Tropical oyster *C.belcheri* using 6-DMAP in Thailand. Numerous studies on the triploid induction in bivalves such as abalone, clam, oyster and scallop have shown that many methods both physical and chemical can be used and shown that resulted in different percentage, survival rate and yield of triploids. Successfully triploid induction in bivalves using 6-DMAP showed in many researches. This chemical have been inhibited extrusion of PB I, PB II and first cleavage. Moreover, the performance of 6-DMAP was similar with other chemical as CB for triploid induction. This study shows optimal treatment for triploid percentage is 100 μ M 6-DMAP, 30 min after fertilization and 10 min exposure duration, which shown highest triploid (86.99%) in *C. belcheri*. However, the result showed higher triploid percentage than in *C. madrasensis* at 100 μ M of 6-DMAP (Thomas *et al.*, 2006). Moreover, the study on *C.gigas* have yielded 56.49 -99% triploidy at tests range 300-450 μ M of 6-DMAP (Desrosiers *et al.*, 1993; Gerard *et al.*, 1994; Gerard *et al.*, 1999; Melo *et al.*, 2015). In addition, the study on triploid induction in other bivalves species with 6-DMAP induction at 400 μ M on scallop *P.magellanicus* showed 95% triploid (Desrosiers *et al.*, 1993). While, triploid level about 92% was reported for geoduck clam *P.abrupta* at 600 μ M 6-DMAP (Vadopalas and Davis, 2004).

This study showed that highest survival rate were recorded for the control group and 100 μ M 6-DMAP to induce triploidy (54%) at trochophore stage in the tropical oyster, *C.belcheri*. While, the study by Thomas *et al.* (2006), the survival rate of *C. madrasensis* of the larvae in the first day was 59.52% at 100 μ M 6-DMAP. Moreover, a study on geoduck clam *P.abrupta* at 3-day-old (Vadopalas and Davis, 2004) and abalone, *Haliotis rubra* at 7-day-old was 30% at 600 and 150 μ M 6-DMAP, respectively (Liu *et al.*, 2004). However, this study showed that lower survival rate than some previously research probably due to gamete from stripped method were

used, the quality of gamete was incomplete and led to eggs were not well-synchronized and the techniques in handling the gamete should be repeated rinsing with sea water after soak in chemical treatment to prevent the residues from this agent.

The analysis of variance indicated that the concentration of 6-DMAP was increased from 100-300 μM 6-DMAP, level of triploid percentage decreased from 78.62 to 59.18%, while concentration of 6-DMAP was increased from 150-600 μM 6-DMAP showed that triploid percentage have been increased from 40% to 83% (Gerard *et al.*, 1994). Moreover, reduction of exposure duration consistent increased survival larvae (Vadopalas and Davis, 2004).

Moreover, triploid induction using 6-DMAP showed that the performance of 6-DMAP depends on the synchrony of meiosis in the eggs (Downing and Allen Jr, 1987), duration of time after fertilization and duration of exposure, so accurate time at which 6-DMAP should be related with meiosis process in bivalve eggs. Furthermore, the period to development meiosis process of oyster from strip method was not well synchronized led to meiosis I and meiosis II have been overlapped. So, increases duration of exposure of 6-DMAP get better the production of triploid in eggs bivalves.

In addition, these results agree with Gerard *et al.* (1994) reported that, triploid percentage depends on 6-DMAP dosage, time after fertilization and duration treatment. So, main factor for induce triploidy as low cost, high production achieved almost 100%. Melo *et al.* (2015), reported that high mortality induce triploid using 6-DMAP when compared with other chemical as CB. However, CB is higher cost, higher hazard and high toxicity to human and environment.

Although caffeine, CB and 6-DMAP are toxic and carcinogen for induce triploidy in bivalves, only 10-40 min for treated duration of fertilization eggs to these chemical, so that, no chemical residues need to be considered for the adult bivalves used for human consumption (Nell *et al.*, 1996). Moreover, triploid production in marine bivalves was 90-95% using 6-DMAP; this chemical showed high performance and safe alternative method for induce triploid in commercial aquaculture (Desrosiers *et al.*, 1993).

In this study we estimated triploid percentage, survival rate, and yield production in trochophore stage by chromosome counting. Further studies need to examine the growth rate and each stage of survival for guidelines to improved commercial aquaculture in oyster and other shellfish.

Acknowledgement

This work was supported by the Faculty of Science and Fisheries Technology, Rajamangala University of Technology Srivijaya and Cytology and Ecotoxicology Research Group, KhonKaen University. The authors wish to thank Pimjai Uttama and Thirawi Pitichotworawat who helped for sampling.

References

- Allen Jr, S.K. and Downing, S.L. 1986. Performance of triploid Pacific oysters, *Crassostrea gigas* (Thunberg). I. Survival, growth, glycogen content, and sexual maturation in yearlings. **Journal of Experimental Marine Biology and Ecology** 102(2-3): 197-208.

- Allen, S.K., Downing, S.L., Chew, K.K. and Program, W.S.G. 1989. **Hatchery Manual for Producing Triploid Oysters**: Washington Sea Grant Program.
- Cox, E.S., Smith, M.S.R., Nell, J.A. and Maguire, G.B. 1996. Studies on triploid oysters in Australia. VI. Gonad development in diploid and triploid Sydney rock oysters *Saccostrea commercialis* (Iredale and Roughley). **Journal of Experimental Marine Biology and Ecology** 197(1): 101-120.
- Desrosiers, R.R., Gerard, A., Peignon, J.-M., Naciri, Y., Dufresne, L., Morasse, J., Ledu, C., Phelipot, P., Guerrier, P. and Dube, F. 1993. A novel method to produce triploids in bivalve molluscs by the use of 6-dimethylaminopurine. **Journal of Experimental Marine Biology and Ecology** 170(1): 29-43.
- Downing, S.L. and Allen Jr, S.K. 1987. Induced triploidy in the Pacific oyster, *Crassostrea gigas*: Optimal treatments with cytochalasin B depend on temperature. **Aquaculture** 61(1): 1-15.
- Dufy, C. and Diter, A. 1990. Polyploidy in the Manila clam, *Ruditapes philippinarum*. I-Chemical induction and larval performances of triploids. **Aquatic Living Resources** 3(1): 55-60.
- Gendreau, S. and Grizel, H. 1990. Induced triploidy and tetraploidy in the European flat oyster, *Ostrea edulis* L. **Aquaculture** 90(3-4): 229-238.
- Gerard, A., Ledu, C., Phelipot, P. and Naciri-Graven, Y. 1999. The induction of MI and MII triploids in the Pacific oyster *Crassostrea gigas* with 6-DMAP or CB. **Aquaculture** 174(3-4): 229-242.
- Gerard, A., Naciri, Y., Peignon, J.M., Ledu, C. and Phelipot, P. 1994. Optimization of triploid induction by the use of 6-DMAP for the oyster *Crassostrea gigas* (Thunberg). **Aquaculture Research** 25(7): 709-719.
- Guo, X., DeBrosse, G.A. and Allen Jr, S.K. 1996. All-triploid Pacific oysters (*Crassostrea gigas* Thunberg) produced by mating tetraploids and diploids. **Aquaculture** 142(3-4): 149-161.
- Hand, R.E., Nell, J.A. and Maguire, G.B. 1998. Studies on triploid oysters in Australia. X. Growth and mortality of diploid and triploid Sydney rock oysters *Saccostrea commercialis* (Iredale and Roughley). **Journal of Shellfish Research** 17(4): 1115-1118.
- Hand, R.E., Nell, J.A. and Thompson, P.A. 2004. Studies on triploid oysters in Australia: XIII. Performance of diploid and triploid Sydney rock oyster, *Saccostrea glomerata* (Gould, 1850), progeny from a third generation breeding line. **Aquaculture** 233(1-4): 93-107.
- Hawkins, A., Day, A., Gerard, A., Naciri, Y., Ledu, C., Bayne, B. and Heral, M. 1994. A genetic and metabolic basis for faster growth among triploids induced by blocking meiosis I but not meiosis II in the larviparous European flat oyster, *Ostrea edulis* L. **Journal of Experimental Marine Biology and Ecology** 184(1): 21-40.
- Liu, W., Heasman, M. and Simpson, R. 2004. Induction and evaluation of triploidy in the Australian blacklip abalone, *Haliotis rubra*: a preliminary study. **Aquaculture** 233(1-4): 79-92.

- Mallia, J.V., Thomas, P. and Muthiah, P. 2006. Induced triploidy in the edible oyster, *Crassostrea madrasensis* by temperature shock. **Journal of the Marine Biological Association of India** 48(2): 249-152.
- Melo, E.M.C., Gomes, C., Silva, F., Suhnel, S. and Melo, C. 2015. Chemical and physical methods of triploidy induction in *Crassostrea gigas* (Thunberg, 1793). **Boletim do Instituto de Pesca** 414: 889-898.
- Nell, J.A., Cox, E., Smith, I.R. and Maguire, G.B. 1994. Studies on triploid oysters in Australia. I. The farming potential of triploid Sydney rock oysters, *Saccostrea commercialis* (Iredale and Roughley). **Aquaculture** 126(3-4): 243-255.
- Nell, J., Hand, R., Goard, L., McAdam, S. and Maguire, G. 1996. Studies on triploid oysters in Australia: Evaluation of cytochalasin B and 6-dimethylaminopurine for triploidy induction in Sydney rock oysters *Saccostrea commercialis* (Iredale and Roughley). **Aquaculture Research** 27(9): 689-698.
- Neant, I. and Guerrier, P. 1988. 6-Dimethylaminopurine blocks starfish oocyte maturation by inhibiting a relevant protein kinase activity. **Experimental Cell Research** 176(1): 68-79.
- Nell, J.A. 2002. Farming triploid oysters. **Aquaculture** 210(1-4): 69-88.
- Stanley, J.G., Allen Jr, S.K. and Hidu, H. 1981. Polyploidy induced in the American oyster, *Crassostrea virginica*, with cytochalasin B. **Aquaculture** 23(1-4): 1-10.
- Stanley, J.G., Hidu, H. and Allen Jr, S.K. 1984. Growth of American oysters increased by polyploidy induced by blocking meiosis I but not meiosis II. **Aquaculture** 37(2): 147-155.
- Thomas, P., Mallia, J.V. and Muthiah, P. 2006. Induction of triploidy in Indian edible oyster *Crassostrea madrasensis* (Preston) using 6-Dimethylaminopurine. **Asian Fisheries Science** 19(1): 15-20.
- Vadopalas, B. and Davis, J.P. 2004. Optimal chemical triploid induction in geoduck clams, *Panopea abrupta*, by 6-dimethylaminopurine. **Aquaculture** 230(1-4): 29-40
- Yamamoto, S., Sugawara, Y., Nomura, T. and Oshino, A. 1988. Induced triploidy in Pacific oyster *Crassostrea gigas*, and performance of triploid larvae. **Tohoku Journal of Agricultural Research** 39(1): 47-59.

Genetic Variability, Heritability and Genetic Advance among Yardlong Bean Lines

Pramote Pornsuriya^{1*} Pornthip Pornsuriya¹ and Anucha Julakasewee¹

ABSTRACT

Yardlong bean is one of the most important vegetable cultivated in Thailand. Better understanding on the variability existing in a yardlong bean base population is significant to crop improvement and for plant breeders to exploit in breeding program. This study aimed to estimate the magnitude of genetic variability, heritability and genetic advance for yields and pod characters of 30 yardlong bean F₃-lines selected from the cross of 2 parental lines (Bangpra#2 x Bangpra Purple). The experiment was laid out in a randomized complete block design with 2 replications. The results revealed that there was no significant difference ($P > 0.05$) among the F₃-lines tested for yield, seeds per pod and pod weight, but significant difference ($P < 0.05$) obtained for pod width and pod length. Genotypic coefficient of variance (GCV) was much lower than phenotypic coefficient of variance (PCV) for all these characters, corresponding with their low broad-sense heritability values, indicating high environment effect on the expression of these characters. The values of genetic advance as percent of the mean (GAM) for pod width, pod length, seeds per pod, pod weight and yields were 4.23, 4.80, 0.37, 6.12 and 2.15 %, respectively (at 5% selection intensity). However, yields among the 30 F₃-lines ranging from 9.49 to 15.65 ton/hectare signified the phenotypic variability available for elite line selection.

Keywords: Yardlong Bean, Heritability, Genetic Gain

¹ Department of Plant Production Technology, Faculty of Agriculture and Natural Resources, Rajamangala University of Technology Tawan-ok, Bangpra, Sriracha, Chonburi 20110, Thailand

*Corresponding author, e-mail : pornsuriya@hotmail.com

Introduction

Yardlong bean (*Vigna unguiculata* (L.) Walp. subsp. *sesquipedalis* (L.) Verdc.) (Stephens, 2003; Porcher, 2005) is belonging to a member of the Fabaceae family (United States Department of Agriculture, 2007). It is one of the most important vegetable crops widely grown in all seasons throughout Thailand. Yardlong bean is a highly nutritive vegetable containing digestible protein, thiamin, riboflavin, calcium, phosphorus, sodium, potassium, magnesium, iron and a very good source of Vitamin A and C (National Research Council, 2006). It is considered promising good income to farmers so that it is commonly cultivated by many vegetable farmers in Thailand.

To select new elite lines from a parental cultivar in a self-pollinated crop as yardlong bean is hardly successful because of its homozygosity. Hybridization of two or more appropriate parental cultivars to create genetic variability for selecting better genotypes is one of the effective methods in self-pollinated crops. The variability existing in a base population of crop is significant so that it can be exploited by plant breeders for crop improvement. The apparent variation, known as phenotypic variation, depends upon the genotypic composition of the population and the environment in which it is raised. Variation arising due to differences in genotypic composition of individuals in a population is known as genotypic variation (Agrawal, 1998). Moreover, to achieve the goal of breeding program depends not only on the amount of variation existing in a crop but also on the magnitude of genetic variation which is heritable from the parent to the progeny (Bello *et al.*, 2014). Heritability estimate of a character is important for plant breeders since it provides information on the extent to which a particular character can be transmitted from the parent to the progeny (Poehlman and Sleper, 1995). In view of these, the present study aimed to estimate the variability, heritability and genetic advance for yield and pod characters in 30 F₃-family lines of yardlong bean. This yardlong bean study was based on the previous breeding program of the department, which obtained some elite lines properly used for crossing in order to make use for the next breeding program.

Materials and Methods

Experimental Procedures: The study was carried out at Department of Plant Production Technology, Faculty of Agriculture and Natural Resources, Rajamangala University of Technology Tawan-ok, Chonburi, Thailand, during February – April 2017. Thirty genotypes of F₃-family lines selected from the cross of 2 parental elite lines of the breeding program (Bangpra#2 x Bangpra Purple). The experimental design was randomized complete block design with 2 replications. The experimental plot unit was 1 m x 3 m in size having 0.5 m wide drains between 2 adjacent beds and 0.75 m wide drain between blocks. Plants were grown in a 2-row bed using plastic mulch, with 50 cm hill spacing and 75 cm row spacing, 2 plants per hill, totally 24 plants per plot, under trellising system using bamboo stakes. Manures and fertilizers were applied as per recommended dose. Recommend practices were followed to raise a good crop. Data on the pod characters (fresh marketable pod), namely pod width (cm), pod length (cm), seed number per pod and pod weight (g) were recorded from 10 selected pods of each plot. Yield per plot was collected from fresh pod weight of each plot for 5 weeks and it was calculated to yield per hectare (ton/hectare).

Estimation of Genetic Parameters: The recorded data were subjected to analysis of variance in RCBD and means were compared using Duncan's new multiple range test (DMRT) (Gomez and Gomez, 1984). The mean squares were used to estimate genotypic and phenotypic variances according to Sharma (2008) as the following formulas.

$$\text{Genotypic variance } (\sigma_G^2) = \frac{\text{MS (genotype)} - \text{MS(error)}}{\text{Number of replications}}$$

$$\text{Phenotypic variance } (\sigma_P^2) = \sigma_G^2 + (\text{MS(error)}/r)$$

$$\text{Genotypic Coefficient of Variability (GCV)} = [(\sqrt{\sigma_G^2})/\bar{x}] \times 100$$

$$\text{Phenotypic Coefficient of Variability (PCV)} = [(\sqrt{\sigma_P^2})/\bar{x}] \times 100$$

Estimation of Heritability in Broad Sense (H_{bs}^2): Heritability in broad sense was estimated and expressed in percentage according to Falconer and Mackay (1996).

$$\text{Heritability in Broad Sense } (H_{bs}^2) = \frac{\sigma_G^2}{\sigma_P^2} \times 100$$

Estimation of Genetic Advance (GA) and Genetic Advance as Percentage of the Mean (GAM): Genetic Advance (GA) and Genetic Advance as Percentage of the Mean (GAM) at 5% selection intensity were determined as described by Allard (1960):

$$\text{GA} = K (\sigma_P) H_{bs}^2$$

$$\text{GAM (\%)} = \frac{\text{GA}}{\bar{x}} \times 100$$

Where: K = 2.06 at 5% selection intensity; σ_P = the phenotypic standard deviation of the character; \bar{x} = grand mean of a character.

Results and Discussion

Analysis of variance and mean comparison

The analysis of variance revealed significant differences ($P < 0.05$) for pod width and pod length, but no significant difference for seed number per pod, pod weight and yield (Table 1), suggesting the adequate amount of genetic variability for pod width and pod length among F_3 -lines that may be helpful for improvement these characters. The highest pod length was recorded from line F3-2/8 (67.55 cm), while, the minimum was observed from line F3-5/25 (51.85 cm). Number of seed per pod was observed from 14.70 seeds/pod of F3-2/3 line to 19.45 seeds/pod of F3-1/34 line. Pod weight ranked from 20.00 g/pod of line F3-1/17 to 39.00 g/pod of line F3-1/26 and had an average of 26.15 g/pod. Pod length was the important character that positively correlated to yield of yardlong bean according to the study of Kanhong and Pornsuriya (2014). Yield data ranging from 9.49 to 15.65 t/ha signified the phenotypic variability available for elite line selection. The first and second highest yield was recorded for lines F3-4/33 and F3-5/14 (15.65 and 14.44 t/ha, respectively), whereas the lowest was observed for line F3-5/25 (9.49 t/ha).

Estimates of variance components

Genotypic variance (σ_G^2), phenotypic variance (σ_P^2), genotypic coefficient of variation (GCV) and phenotypic coefficient of variance (PCV) were estimated and shown in Table 2. Genotypic variance value is the inherent or genetic variability which is more useful to a plant breeder for exploitation in selection or hybridization (Singh and Narayanan, 2013). To compare the magnitude of variance among characters, GCV and PCV were the appropriate values to be used instead of variance values because they were adjusted to the same unit as percent. As expected, PCV was greater than GCV for all characters. The estimates of GCV for all characters were low as indicated by Sivasubramanian and Menon (1973) ranging from 1.48% of number of seed per pod to 8.44 % of pod weight. PCV estimates ranged from 10.65% of pod width to 23.98% of pod weight.

Heritability

Heritability in broad sense is the ration of genotypic variance to the phenotypic variance or total variance, and it is generally expressed in percent. It is a good index of the transmission of characters from parents to their offspring (Falconer, 1981). As comparison among these 5 characters, pod length possessed the highest heritability value (20.17%) followed by pod width (19.26%), whereas the lowest heritability value was recorded for number of seed per pod (1.48%). However, heritability values of all characters were classified as low heritability according to Singh (2001) that heritability values greater than 80% were high, values from 60-79% were moderately high, values from 40-59% were medium and values less than 40% were low. From the study, heritability values were low because the base population studied was the F₃ generation that genetic variability was lower than that of F₂. Moreover, the heritability values estimated in this study calculated from the mean of all plants from each plot unit, where an individual plant still had more variability. From this reason, the selection in this generation should be conducted from the individual plant instead of each family line. The low heritability values in this study conformed to the results of Sarutayophat and Nualsri (2010) which reported that low heritability for pod yield per plant was found in F₄ populations. The previous studies of Vidya *et al.* (2002) and Rambabu *et al.* (2016) reported the high heritability for all studied characters because the populations they studied were various local cultivars that generally possessed high genetic diversity. High broad sense heritability only may not be reliable for selection, because it is based on total genetic variance which includes both fixable (additive) and non-fixable (dominance and epistatic) variances (Singh and Narayanan, 2013). However, genetic effects of self-pollinated crop as yardlong bean should be mostly influenced by additive genes under the assumption of this study thus heritability in broad sense might be primary used for the breeding program.

Table 1 Performance mean of 30 F₃-progeny lines for pod characters and yield

Treatment/ F ₃ -progeny line	Pod width (cm)	Pod length (cm)	Seed/pod (seed)	Pod weight (g)	Yield (t/ha)
T1 F3-4/1	0.62 a-e	55.28 b-e	17.35	22.00	11.88
T2 F3-3/20	0.71 ab	52.48 de	16.20	24.50	11.06
T3 F3-3/33	0.62 b-e	54.95 b-e	15.45	22.50	11.24
T4 F3-1/22	0.63 a-e	63.45 abc	16.50	28.00	12.69
T5 F3-4/33	0.62 b-e	60.50 a-e	17.30	27.50	15.65
T6 F3-1/26	0.69 abc	66.80 a	19.10	39.00	12.62
T7 F3-4/13	0.64 a-e	62.50 a-d	18.70	27.00	11.77
T8 F3-3/3	0.57 de	60.25 a-e	18.95	24.50	14.10

T9	F3-3/30	0.64 a-e	58.75 a-e	16.55	28.50	11.52
T10	F3-5/14	0.64 a-e	64.93 ab	17.80	32.00	14.44
T11	F3-1/17	0.58 de	55.08 b-e	15.50	20.00	11.94
T12	F3-1/23	0.62 a-e	55.53 b-e	17.80	23.50	13.26
T13	F3-4/15	0.66 a-d	59.55 a-e	18.30	27.50	12.99
T14	F3-3/29	0.55 e	54.95 b-e	17.60	21.50	12.57
T15	F3-1/7	0.63 a-e	54.30 cde	16.85	24.00	12.61
T16	F3-1/34	0.63 a-e	62.43 a-d	19.45	28.50	14.13
T17	F3-2/8	0.59 cde	67.55 a	16.80	29.00	13.32
T18	F3-3/32	0.61 b-e	57.70 a-e	18.25	27.50	10.86
T19	F3-2/26	0.61 b-e	53.73 cde	17.20	24.00	11.20
T20	F3-3/26	0.63 a-e	58.30 a-e	15.50	24.50	10.32
T21	F3-5/17	0.72 a	56.20 b-e	15.95	28.50	9.90
T22	F3-5/26	0.61 b-e	61.20 a-e	17.05	27.00	12.47
T23	F3-2/6	0.59 cde	60.45 a-e	18.30	29.50	11.97
T24	F3-2/3	0.60 cde	53.43 cde	14.70	24.00	12.25
T25	F3-5/32	0.63 a-e	61.75 a-e	17.75	28.00	9.98
T26	F3-5/13	0.62 a-e	57.28 a-e	17.35	26.00	13.34
T27	F3-5/31	0.57 de	62.38 a-d	17.40	25.50	11.63
T28	F3-5/25	0.54 e	51.85 e	14.90	21.00	9.49
T29	F3-5/1	0.56 de	53.53 cde	17.20	21.00	11.94
T30	F3-5/5	0.64 a-e	60.65 a-e	16.90	28.50	12.29
Mean ± S.E.						12.18
		0.62± 0.007	58.59±0.782	17.16±0.222	26.15±0.701	±0.255
Minimum		0.54	51.85	14.70	20.00	9.49
Maximum		0.72	67.55	19.45	39.00	15.65
F-test		*	*	ns	ns	ns
CV (%)		6.82	7.29	9.81	16.98	14.94

ns and * = not significant and significant at P < 0.05, respectively

Table 2 Estimates of variance and genetic parameters for pod characters and yield in 30 F₃-progeny lines

Genetic parameters	Pod width (cm)	Pod length (cm)	Seed/pod	Pod weight (g)	Yield (t/ha)
σ_G^2	0.001	9.24	0.06	4.87	0.30
σ_P^2	0.004	45.83	4.38	39.31	5.57
GCV (%)	4.68	5.19	1.48	8.44	4.50
PCV (%)	10.65	11.55	12.20	23.98	19.37
H_{bs}^2 (%)	19.26	20.17	1.48	12.39	5.39
GA	0.03	2.81	0.06	1.60	0.26
GAM (%)	4.23	4.80	0.37	6.12	2.15

Note: σ_A^2 : Genotypic variation, σ_P^2 : Phenotypic variation, GCV: Genotypic coefficient of variation, PCV: Phenotypic coefficient of variation, H_{bs}^2 : Heritability in broad sense, GA: Genetic advance, GAM: Genetic advance as percentage of the mean

Genetic advance

Genetic advance is the measure of genetic gain under selection. It refers to the improvement of characters in genotypic value for the new population compared with the base population under one cycle of selection at given selection intensity (Singh, 2001). Genetic advance values for all studied characters were displayed in Table 2. Estimates of genetic advance for pod width, pod length, number of seed per pod, pod weight and yield were 0.03 cm, 2.81 cm, 0.06 seeds/pod, 1.60 g and 0.26 t/ha, respectively, hence, the next generation at 5% selection intensity would possess 0.65 cm of pod width, 61.40 cm of pod length, 17.12 seeds/pod, 27.75 g of pod weight and 12.44 t/ha of yield. Genetic advance as percent of the mean (GAM) of these characters were 4.23, 4.80, 0.37, 6.12 and 2.15 %, respectively. All GAM values were categorized as low according to Singh and Narayanan (2013) that GAM values less than 10% were low. Genetic advance under selection depends on heritability. Thus from this study low heritability values gave the low genetic advance values.

Conclusion

Significant differences were observed among the 30 F₃-family lines for pod width and pod length. Yield of fresh pod ranged from 9.49 to 15.65 t/ha that signified the variability available for a promising line selection. The estimates of genotypic coefficient of variation for all characters were low ranging from 1.48% of number of seed per pod to 8.44 % of pod weight. Phenotypic coefficient of variation estimates ranged from 10.65% of pod width to 23.98% of pod weight. Heritability in broad sense estimates for pod width, pod length, seed/pod, pod weight and fresh pod yield were 19.26, 20.17, 1.48, 12.39 and 5.39 %, respectively. Genetic advance as percent of the mean of these characters were 4.23, 4.80, 0.37, 6.12 and 2.15 %, respectively. In conclusion, selection in this generation should be based on an individual plant which might give more genetic gain than that on a family line.

References

- Agrawal, R. L. 1998. **Fundamentals of Plant Breeding and Hybrid Seed Production**. Science Publishers, Inc., New Hampshire.
- Allard, R.W. 1960. **Principles of Plant Breeding**. John Wiley & Sons Inc., New York.
- Bello, O.B., S.a. Ige, M.A. Azeez, M.S. Afolabi, S.Y. Abdulmalik and J. Mahamood. 2012. Heritability and genetic advance for grain yield and its component character in maize (*Zea mays* L.) **International Journal of Plant Research** 2: 138-145.
- Falconer, D.S. 1981. **Introduction to Quantitative Genetics** (2nd ed.). Longmans Green, London/New York.
- Falconer, D.S. and T.F.C. Mackay. 1996. **Introduction to Quantitative Genetics** (4th ed.). Addison Wesley Longman, Harlow.
- Gomez, K.A. and A.A. Gomez. 1984. **Statistical procedures for agricultural research** (2nd ed.). John Wiley and sons, New York.
- Kanhong, A. and P. Pornsuriya. 2014. Yield trial of 40 yard long bean lines. **Khon Kaen Agr.J.** 42 Suppl.1: 634-640.
- National Research Council. 2006. **Lost Crops of Africa, Vol. II: Vegetables**. The National Academies Press, Washington, DC.
- Poehlman, J.M. and D.A. Sleper. 1995. **Breeding Field Crops** (4th ed.). Iowa State University Press, Ames.
- Porcher, M. H. 2005. **Sorting Vigna names**. The University of Melbourne. Available Source: <http://www.plantnames.unimelb.edu.au/Sorting/Vigna.html>. March 10, 2007.

- Rambabu, E., K. Ravinder Reddy, V. Kamala, P. Saidaiah and S.R. Pandravada. 2016. Genetic variability and heritability for quality, yield and yield components in yardlong bean (*Vigna unguiculata* (L.) Walp. ssp. *sesquipedalis* Verdc.). **Green Farming** 7: 311-315.
- Sarutayophat T. and C. Nualsri. 2010. The efficiency of pedigree and single seed descent selections for yield improvement at generation 4 (F₄) of two yardlong bean populations. **Kasetsart J. (Nat. Sci.)** 44: 343-352.
- Sharma, J.R. 2008. **Statistical and Biometrical Techniques in Plant Breeding**. New Age International Publishers, New Delhi.
- Singh, B. 2001. **Plant Breeding: Principles and Methods** (6th ed.). Kalyani Publishers, New Delhi.
- Singh, P. and S.S. Narayanan. 2013. **Biometrical Techniques in Plant Breeding** (5th ed.). Kalyani Publishers, New Delhi.
- Sivassubramanian, S. and P. Madhava Menon. 1973. Genotypic and phenotypic variability in rice. **Madras Agric. J.** 60: 1093-1096.
- Stephens, J. M. 2003.** Bean, Yard-Long -- *Vigna unguiculata* subsp. *sesquipedalis* (L.) Verdc. **University of Florida IFAS Extension, Publication #HS562.** Available Source: <http://edis.ifas.ufl.edu/MV029>. November 21, 2013.
- United States Department of Agriculture. 2007. *Vigna unguiculata* (L.) Walp. subsp. *sesquipedalis* (L.) Verdc. Available Source: <http://www.ars-grin.gov/cgi-bin/npgs/html/taxon.pl?41646>. March 10, 2007.
- Vidya, C., S.K. Oommen and V. Kumar. 2002. Genetic variability and heritability of yield and related characters in yard-long bean. **Journal of Tropical Agriculture** 40: 11-13.

Increasing Pineapple Suckers Using 6-Benzilaminopurine Growth Regulator on F₁ Hybrid Mother Pineapple [*Ananas comosus* (L.) Merr.] Plants

Fatah Ridwan¹, Hasan Ma'arif¹, Orachat Sittichan¹, Sommai Kaewmanee¹ and Suneerat Sriporaya^{1*}

ABSTRACT

The effect of 6-benzylaminopurine (BA) on F₁ hybrid pineapple sucker multiplication, was investigated at Rajamangala University of Technology Srivijaya, Thungyai, Nakhon Si Thammarat from September 2017 to February 2018. 140 F₁ hybrid pineapple harvested mother plants were selected and current pineapple suckers were separated from mother plant. All mother plants were treated with BA hormone by spraying nearly into pineapple stem. Seven treatments following BA concentrations 20, 30 and 40 ppm for one-time spraying, then BA concentrations 20, 30 and 40 ppm for two times spraying and treatment control (no BA spraying) was experimented using Completely Randomize Design with four replications. Number and height of sucker were recorded at 10, 14 and 16 weeks after BA spraying. The result for number of sucker, BA 40 ppm two-time spraying gave highest 2.68 suckers at week 16. For the result of sucker height, using BA 30 ppm one-time spraying gave the highest of sucker obtaining 73.48 centimeters at week 16. With economic and sucker productivity reasons, the research can conclude that BA 30 ppm one-time spraying was the most effective for sucker increasing and shoot development. Moreover, BA 30 ppm one-time spraying gave the cheapest cost to produce number of sucker from harvested mother plants.

Keywords: Pineapple, F₁ hybrid, Mother plants, 6-Benzylaminopurine, *Ananas comosus*

¹Plant Science Division, Faculty of Agriculture, Rajamangala University of Technology Srivijaya, Thungyai, Nakhon Si Thammarat Province, 80240, Thailand

*Corresponding author, e-mail: suneerats@gmail.com

Introduction

Pineapple [*Ananas comosus* (L.) Merr.] is one of the most important and is an economic fruit crop of Bromeliaceae family. In general, pineapple production is in tropical and sub-tropical areas. Pineapple gives some benefits for human that is used to contribute in keeping ideal weight and gastrointestinal system and nutrition stability because pineapple comprise many substantial amounts such as calcium, potassium, vitamin C, carbohydrates, crude fiber, water and different minerals (Popluechai *et al.*, 2007). With pH rates from 4,5 to 6,5 of sandy grounds, pineapple can accept dry condition and better adapt in tropical area. Pineapple propagation can produce from their crowns which produce at the top of the stem or from their suckers (Baruwa, 2013).

The main pineapple distributor is Thailand (Srivichien *et al.*, 2015). Most commercial variety of pineapple production is Smooth Cayenne group (Srivichien, 2014). Bartholomew and Malezieux observed Thai pineapple and grouped it into five groups. They are: “Tradsithong”, ‘Phuket’ and ‘Shawee’ in Queen’s Group, ‘Pattavia’ and ‘Nanglae’ in Cayenne, and ‘Intrachitdang’ in the Spanish Group, Abaxaci and Maipure or Perolera group” (Popluechai *et al.*, 2007). New pineapple variety was bred by Sripaoraya (2009), HQC34 F₁ hybrid variety was crossed from Phuket and Pattavia groups. It shows high fruit quality and resistant to heart rot and wilt diseases (Sripaoraya, 2009). However, this new variety still has limits for number of suckers to propagate and mass growing for farmers. With conventional propagation of mother plant, it gives less number of suckers. Using 6-Benzylaminopurine growth regulator may increase amounts and height of F₁ hybrid pineapple suckers and then make sufficiency for farmers to grow new F₁ Hybrid pineapple variety. Therefore, it is necessary to study how to rapidly multiple the number of suckers.

Materials and Methods

1. Preparing for BA growth regulator stock solution

To prepare a 50 ml stock solution, add 0.05 g of the 6-benzylaminopurine to a 50-ml volumetric flask and add 2 ml NaOH 1 N to dissolve the BA. Once completely dissolved, adjust volume distilled water until 48 ml to reach 50 ml of stock solution. Stirring the solution while adding water to keep the material in solution. Store the stock solution at 4°C. To prepare BA different concentrations, take 1, 1.5, and 2.0 ml from stock solution and make 50 ml fully volumetric flask volume by adding 49, 48.5, and 48 ml distilled water respectively. Then, take 25 ml for each mother plant spraying.

2. Selection pineapple harvested mother plants

140 F₁ hybrid pineapple mother plants were selected from pineapple field. The current pineapple suckers were separated first from mother plant. This method was used to make sure that pineapple mother plants were obliterated from current suckers.

3. Spraying BA growth regulator on pineapple mother plants

Each collected pineapple mother plants were sprayed with 6-Benzylaminopurine hormone nearly into pineapple stem. The experiment used Completely Randomized Design,

seven treatments with four replications, the experimental unit which used in this experiment were five pineapple mother plants. Seven treatments; Treatment 1: 20 ppm, one-time spraying; 2: 30 ppm, one-time spraying; 3: 40 ppm, one-time spraying; 4: 20 ppm, two times spraying; 5: 30 ppm, two times spraying; 6: 40 ppm, two times spraying, and 7 for control (no BA spraying). The volume of BA spraying is 25 ml per mother plant. The second spraying was the day after the first spraying.

4. Data collection and data analysis

The number of suckers (sucker) and sucker height (cm.) were recorded at week 10, 14, and 16 after BA spraying. Analysis of variance (ANOVA) was analyzed as CRD experimental design. Duncan Multiple Range Test was used to mean different analysis in this study.

Results and Discussion

1. Number of sucker

The number of suckers of F₁ hybrid pineapple mother plants sprayed with BA growth regulator were recorded at week 10. The result demonstrated that concentrations of BA were highly significant different for number of sucker. BA 40 ppm two times spraying showed highest number of sucker giving 2.62 suckers. Treatment 2, 3, 4, 5, 7 and 1 gave 2.5, 2.25, 2.12, 1.38, 1.5 and 1.25 suckers respectively as **Table 1** and **Figure 1**.

Table 1 The average of number of suckers at week 10-16 after spraying different concentrations of BA in F₁ hybrid pineapple mother plants experimented at RMUTSV, Thungyai, Nakhon Si Thammarat, Thailand in 2017

BA concentrations	Number of sucker (sucker)		
	week 10	week 12	week 16
20 ppm, one-time spraying	1.25 ^c	1.25 ^d	1.56 ^c
30 ppm, one-time spraying	2.5 ^{ab}	2.56 ^a	2.56 ^a
40 ppm, one-time spraying	2.25 ^{ab}	2.42 ^{ab}	2.50 ^a
20 ppm, two times spraying	2.12 ^{ab}	2.16 ^{ab}	2.16 ^{ab}
30 ppm, two times spraying	1.38 ^{cd}	1.50 ^{bc}	1.62 ^c
40 ppm, two times spraying	2.62 ^a	2.62 ^a	2.68 ^a
Control (no BA spraying)	1.5 ^{bc}	1.67 ^{cd}	1.67 ^{bc}
F-test	**	**	**
CV%	13.92	23.61	14.43

Means of the same category followed by different letters are significantly different from each other using Duncan test at 0.05 level of probability

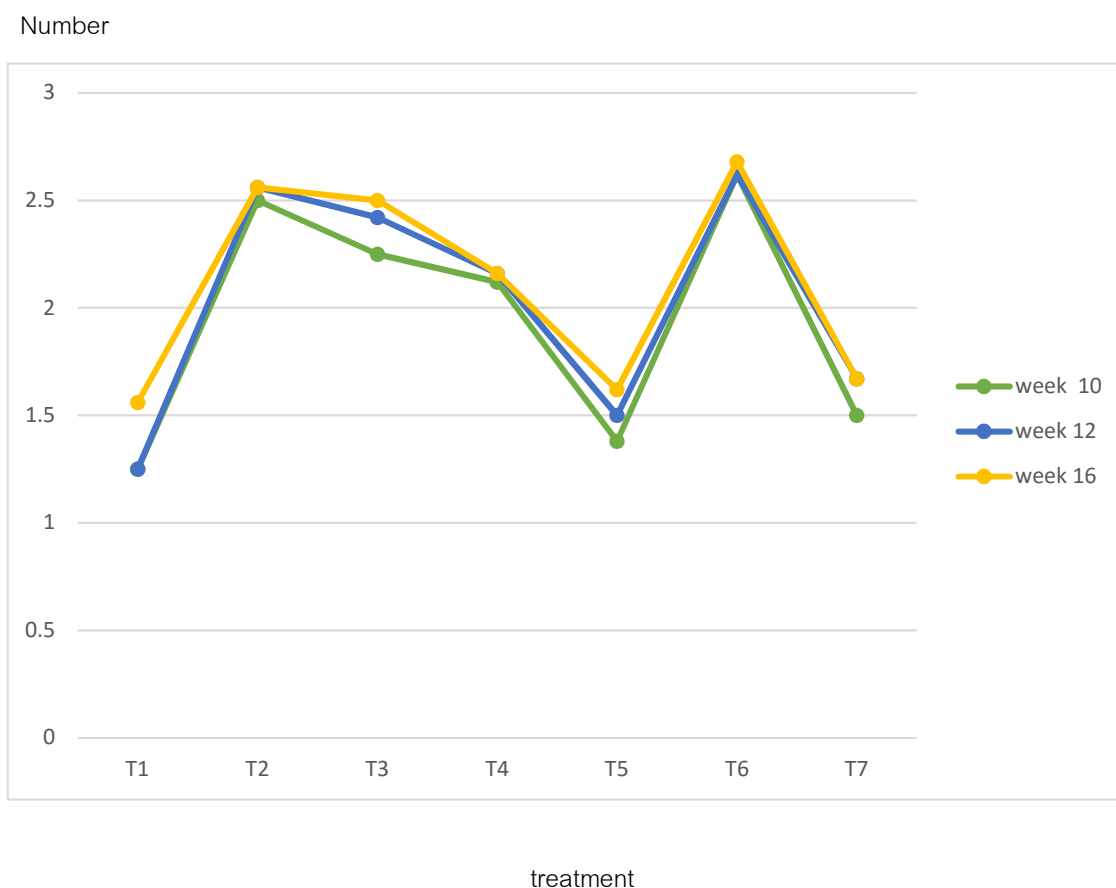


Figure 1 Number of sucker after spraying different concentrations of BA in F₁ hybrid pineapple mother plants with T1: BA 20 ppm one-time spraying, T2: BA 30 ppm one-time spraying, T3: 40 ppm one-time spraying, T4: BA 20 ppm two times spraying, T5: BA 30 ppm two times spraying, T6: BA 40 ppm two times spraying and T7: control (no BA spraying).

The research indicated that high BA concentration trends in high number of sucker. BA 40 ppm, two times spraying presented high result because it used more hormone concentration. At the meantime, it spent more cost for buying BA hormone as well.

At week 12 and week 16, F₁ hybrid pineapple mother plants sprayed with BA growth regulator were recorded. The result demonstrated that both week 12 and week 16, BA 40 ppm, 2 times spraying gave highest for number of sucker giving 2.62 and 2.68 suckers respectively. Treatments 2, 3, 4, 5, 7 and 1 showed 2.56, 2.42, 2.16, 1.50, 1.67, and 1.25 suckers respectively in week 12 as **Table 1** and **Figure 1**. The result showed that BA 30 ppm, one-time spraying gave the same number of sucker in week 12 and week 16 giving 2.56 suckers and was not significant difference with using 40 ppm, 2 times spraying. In contrast, 40 ppm, 2 times spraying used more BA hormone volume. It therefore need to pay more money for BA cost.

2. Height of sucker

Different concentrations of BA showed highly significant different for height of sucker at week 10. BA 30 ppm, one-time spraying showed highest suckers giving 42.025 cm. Treatment 3, 4, 5, 6, 7 and 1 gave 21.58, 25.89, 16.89, 30.31, 38.36, and 16.69 cm respectively as **Table 2**. Treatment 2 or BA 30 ppm, one-time spraying had good outcome with lower concentration than treatment 6 (BA 40 ppm, two times spraying) with high amount of number, treatment 6 did not have the highest of height because suckers from treatment 6 may divide nutrients for more suckers.

At week 12, BA 30 ppm, 1 time spraying gave the highest showing 52.65 centimeters and was significantly difference from treatment 3, 4, 5, 6, 7 and 1 giving 28.81, 33.65, 21.81, 39.10, 40.91, and 21.41 cm respectively shown as **Table 2**. Finally at week 16, BA 30 ppm, one-time spraying gave the highest sucker giving 73.48 centimeters and was significantly difference in sucker height from other BA concentrations. Treatment 3, 4, 5, 6, 7 and 1 gave 43.73, 48.46, 33.80, 58.81, 43.78, and 33.59 cm. respectively following as **Table 2**.

Table 2 The average of height of suckers at week 10-16 after spraying different concentrations of BA in F₁ hybrid pineapple mother plants experimented at RMUTSV, Thungyai, Nakhon Si Thammarat, Thailand in 2017

Treatments	Height of sucker (cm.)		
	week10	week12	week16
20 ppm, one-time spraying	16.69 ^c	21.41 ^b	33.59 ^c
30 ppm, one-time spraying	42.02 ^a	52.65 ^a	73.48 ^a
40 ppm, one-time spraying	21.58 ^c	28.81 ^b	43.73 ^{bc}
20 ppm, two times spraying	25.89 ^c	33.65 ^{ab}	48.46 ^{bc}
30 ppm, two times spraying	16.88 ^c	21.81 ^b	33.80 ^c
40 ppm, two times spraying)	30.31 ^{abc}	39.10 ^{ab}	58.81 ^{ab}
Control (no BA spraying)	38.36 ^{ab}	40.91 ^{ad}	43.78 ^{bc}
F-test	**	**	**
CV%	36.66	35.62	31.19

Means of the same category followed by different letters are significantly different from each other using Duncan test at 0.05 level of probability.

After spraying BA as designed concentrations to pineapple mother plants for increasing number of suckers, the results showed that the number of sucker gave highly significant all weeks that collected data. Finally result showed that 1) number of sucker increasing significantly every week when threatened by BA hormone, 2) lowest concentration of BA hormone gave lowest result in number of sucker, 3) best result in number of sucker was BA 40 ppm, 2 times spraying with 2.64 suckers but it was not significant difference in number of sucker with BA 30 ppm, one-time spraying compared average mean by DMRT giving 2.56 suckers.

According to research, data demonstrated that pineapple mother plants gave various in height of sucker. The result defined respectively that 1.) Different concentrations showed different results for the height of sucker, 2.) BA 30 ppm, one-time spraying had highest sucker in every single week, the highest sucker was 73.48 cm. This research result gave the same result with Crosby *et al.* (1981). They reported that BA was successfully used highly increasing on number of fruit.

3. Cost of BA and economic use

Price for 1 g 6-Benzylaminopurine (BA) approximately is 1,730 baht. For this study, BA was used 0.05 g per 10 ppm for making stock solution (20, 30 and 40 ppm). Then, price per sucker after been threatened by BA is 2 baht for 20 and 30 ppm one spraying, 5 baht for 40 ppm one-time spraying, 4 baht for 20 and 30 two times spraying and 10 baht for 40 ppm two times spraying.

Conclusion

Investigation reported that application of 6-Benzylaminopurine on pineapple F₁ hybrid pineapple mother plant variety increased in height and number of pineapple suckers. This happen because 6-Benzilaminopurine act as growth regulator and stimulate for shoot meristem, plant regeneration and highly proliferate in cell division better than when not applied any growth hormone in pineapple. Authors of this research recommended using 30 ppm one spray is the best treatment. It had the best and highest result in number and height of sucker, likewise, 30 ppm and only one-time spraying was the cheapest choice to produce high number of sucker and is better for farmers to grow new good pineapple variety. Hopefully this investigation will support on pineapple sustainable and research base for pineapple cultivation and productivity, especially for pineapple producers or farmers.

Acknowledgement

This research was supported by Plant Science Division, Faculty of Agriculture, RMUTSV Thungyai, Nakhon Si Thammarat, Thailand. We also would like to thanks SBPAC (Southern Border Province Administrative Centre) for financial support.

References

- Baruwa, O. I. 2013. Profitability and constraints of pineapple production in Osun State, Nigeria. **Journal of Horticultural Research** 21(2), 59–64. <https://doi.org/10.2478/johr-2013-0022>
- Bashan, Y., & de-Bashan, L. E. 2010. How the plant growth-promoting bacterium azospirillum promotes plant growth-a critical assessment. **Advances in Agronomy** 108. [https://doi.org/10.1016/S0065-2113\(10\)08002-8](https://doi.org/10.1016/S0065-2113(10)08002-8)
- Crosby, K. E., Aung, L. H., and Buss, G. R. 1981. Influence of 6-benzylaminopurine on fruit-set and seed development in two soybeans, *Glycine max* (L.) Merr. genotypes. **Plant Physiology**, 68(5), 985-988.
- Popluechai, S., Onto, S., and Eungwanichayapant, P. D. 2007. Relationships between some Thai cultivars of pineapple (*Ananas comosus*) revealed by RAPD analysis. **Songklanakarin Journal of Science and Technology** 29(6), 1491–1497.
- Sripaoraya, S. 2009. Pineapple hybridization and selection in Thailand. In **Acta Horticulturae** 822, 57–62.
- Srivichien, S. 2014. Comparison of Nitrate Content in “Smooth Cayenne” Pineapple Flesh Related to Its Different Cut Sections, Maturity and Crop Season. **Journal of Advanced Agricultural Technologies** 1(1), 65–68. <https://doi.org/10.12720/joaat.1.1.65-68>
- Srivichien, S., Terdwongworakul, A., and Teerachaichayut, S. 2015. Quantitative prediction of nitrate level in intact pineapple using Vis-NIRS. **Journal of Food Engineering** 150, 29–34. <https://doi.org/10.1016/j.jfoodeng.2014.11.004>

Shoot Multiplication of HQC34 Hybrid Pineapple [*Ananas comosus* (L.) Merr.] Using Bioreactor System

Suneerat Sripaoraya¹, Yuenyong Vanichpakorn¹, Pimol Tiengtum¹ and Orachat Sittichan^{1*}

ABSTRACT

With conventional pineapple propagation, it takes time and obtained less of suckers or plantlets. Tissue culture technique is used for increasing pineapple suckers particularly in new pineapple variety. This research aims to increase suckers of new pineapple variety use bioreactor system. Kind of media and explants were investigated in order to increase HQC34 hybrid pineapple shoots as a mass multiplication using bioreactor system. Completely Randomized Design was used with 4 treatments and 2 replications following as 1) MS+BA 2 mg/L+ callus 2) MS+BA 3 mg/L + young shoot 3) MS+CPPU 2 mg/L+ callus and 4) MS+CPPU 2 mg/L + young shoot. Media were fed 3 times daily for 2 minutes each time. Number and height of shoots were recorded at 4, 6, 8 and 10 week. The results showed that different explants were not significant difference for giving shoot number. For media, MS+BA 2 mg/L gave the highest number of shoot and was highly significant difference compared to MS+CPPU 2 mg/L. Number of shoots were 62.67, 64.00, 18.33 and 20.00 shoots in the treatment 1 to 4 respectively at week 10. The best medium, MS+BA 2 mg/L, was further investigated number of daily feeding as 6 or 8 times per day. Number and height of shoots were recorded at week 4. It was clearly found that 8 times per day medium feeding could produce the most numbers of HQC34 hybrid pineapple shoots giving 233.10 shoots compared to 126.70 shoots in 6 times per day feeding treatment. However, for shoot height, with 6 times/day of medium feeding gave higher and was significant difference showing 2.40 and 1.73 cm. for 6 and 8 times per day feeding respectively. In conclusion, both callus and young shoot can be use an explant for multiple mass shoots of HQC34 hybrid pineapple variety used MS+BA 2 mg/L as a medium in bioreactor system.

Keywords: Pineapple, *Ananas comosus*, Bioreactor, Shoot Multiplication, Hybrid

¹ Plant Science Division, Faculty of Agriculture, Rajamangala University of Technology Srivijaya, Thungyai, Nakhon Si Thammarat Province, 80240, Thailand

*Corresponding author, e-mail: orachatsittichan@gmail.com

Introduction

Thailand is the world largest producer and exporter of pineapple with 1,942,508 tons producing and 511,846 acres harvesting area (Agricultural economic office, 2015). 70-80 percents pineapple products are used in the industry for canning and processing pineapple such as pineapple juice. 20-30 percents was used for domestic fresh consumption. Thailand is a producer and exporter of pineapple in the world however yield is still very low mainly causing of cultivars and management. Many pineapple cultivars are grown in Thailand but there are only two commercial cultivars; a Smooth cayenne known as Pattavia and a Queen known as Phuket. Pattavia cultivar is grown for fresh and processing while Phuket is grown only for fresh consumption. Both cultivars have different fruit quality and agronomic characters. Pattavia variety has a large and cylindrical fruit with wide flat eyes. Their leaves are spineless except near the tip which is considered a desirable characteristic. However, it is susceptible to wilt heart and root rot diseases. In contrast, Phuket is resistant to these diseases but it has smaller with either conical or cylindrical shape. It has crisp, good smelling and sweet flesh. However, it has narrow and prominent eyes, spiny leaf which consumers complain when they peel the fruit for fresh consumption. In order to have a better fruit quality and better agronomic traits, Sripaoraya (2009) have bred pineapple by crossing between Phuket and Pattavia cultivars both direct and reciprocal cross. From those crossing and selection, HQC34 hybrid was obtained. This hybrid gave better fruit quality such as sweet, crispy and good smell flesh and resistant to wilt, root rot diseases. Pineapple generally propagates using sucker, crown or slip. With normal propagation method, suckers are slowly produced and obtain less amount of sucker. It is necessary to rapidly multiple shoot and to generate to plantlets and finally suckers.

The current technology allows tissue culture propagation. This technology can produce large amount number of suckers and take shorter time, it can also reduce production costs. This research aims to multiple shoot in shorter time and obtain a large number of suckers using bioreactor system technology.

Materials and Methods

1. Medium preparation and explant study for bioreactor system

1.1 Medium preparation

Prepare MS (Murashige and Skoog) medium stock as report of Murashige and Skoog (1962). Two media, MS + BA 2 mg/l and MS + CPPU 2 mg/l were used for this study. Each medium is volume with distilled water, add sugar 30 g and adjust pH 5.8. Put 150 ml of each medium in bottle. Equipment and medium were sterilized by autoclave at temperature 121 °C , and pressure 15 pound/in² for 20 minutes.

1.2 Media and explant studies

Two kinds of explant were used for investigation. They were callus and young shoot. Put the 5 pieces of each explant of HQC34 hybrid pineapple in to the empty sterilized bottle set. All processes worked in sterile cabinet. Two kinds of media and explants were set to study shoot multiplication. Four treatments; MS + BA 2 mg/l + callus, MS + BA 2 mg/l + young shoot, MS + CPPU 2 mg/l + callus and MS + CPPU 2 mg/l + young shoot with 2 replications. All treatments were fed three times a day with 2 minutes each. The number and height of shoot were record at 4, 6, 8 and 10 weeks after culture.

2. Number of feeding study

Take the best result from the first investigation, it was BA 2 mg/l medium + young shoot explant. The number of feeding; 6 and 8 times per day was set to invest the best increasing for shoot. The number and height of shoot were recorded. Cut a piece of pineapple hybrid HQC34 and put 20 young shoot explants in the empty sterile bottle. Number of plantlets and the plantlet height were recorded at week 4 after culture.

3. Compare HQC34 pineapple hybrid increasing using bioreactor and shaker

Trim parts of HQC34 hybrid and put 10 pieces of young shoot explant in the sterile empty bottle. Two treatments; using bioreactor system feed 8 times / day and using shaker. Pineapple young shoot were placed in a shaker. Explants were fed all the time. Number of plantlets and the height of plantlets were observed at week 4.

Results and Discussions

1. Kinds of media and explants

This result compared media and explants *in vitro* of hybrid HQC34 pineapple using bioreactor during 10 weeks by collecting data for 4 times in week 4,6,8 and 10. The results showed that BA 2 mg/l with callus and young shoot explants gave better than medium CPPU 2 mg/l. Media gave statistically significant difference for number of shoot. BA 2 mg/l both callus and young shoot showed higher number of shoot for all week records compared to CPPU 2 mg/l. During weeks 4-10, BA 2 mg/l with callus gave 60.00; 62.00; 62.00 and 62.67 shoots respectively. For BA 2mg/l with young shoot showed 59.67, 62.00; 62.33, and 64.00 shoots respectively. For using CPPU 2 mg/l with both explants gave number of shoot lower than using BA 2mg/l in all weeks of recording. MS + CPPU 2 mg/l with young shoot explant gave 16.67, 19.00, 19.33 and 20.00 shoots in week 4, 6, 8 and 10 respectively. **(Table 1)**

For the height of shoot of HQC34 hybrid at 10 weeks, medium MS + BA 2 mg / l with young shoot increase best the amount and height of shoot. It demonstrated 2.50, 2.73, 2.73 and 2.83 cm. in week 4, 6, 8 and 10 respectively, compared to 1.00, 1.40, 1.40 and 1.40 cm for MS+CPPU 2 mg/l with young shoot showing as Table 2. The kinds of explant in the research gave no effect on creasing shoot number and was not significant different both height and number of shoot. This result gives the same results of Srichuay and Te-chato (2014) who studied the effects of MS medium with NAA and BA in Phulae variety. BA is a growth regulator which is cytokine in. It plays a role in cell division and expansion.

And a feeding every 2 hours, 2 minutes/ time results showed that increasing the concentration of BA results more increase for pineapple shoots. Escalona *et al.*, 1999 cited by Boonmanee (2007) studied on the induction of pineapple explants under bioreactor. Received feeding 8 times / day for a period of 2 minutes/time, inducing new shoot moreover cultured in solid and liquid (Fangmuang and Kongbangkerd, 2012) studied the effect of growth regulators. The development of seedlings *Dendrobium lamellatum* Lindl in sterile conditions by raising seedlings on MS media with BA at a concentration of between 1.0 - 2.0 mg per liter can induce birth to a new well.

The height of HQC34 hybrid pineapple from tissue culture found that week 4 treatment 1 and 2 have higher than treatment 3 and 4 statistically was 2.17, 2.50, 1.17 and 1.00 centimeters respectively, at week 6 found that treatment 1 and 2 were still higher and better than treatment 3 and 4 as follows 2.50, 2.73, 1.58 and 1.40 respectively. **(Table 2)**

The height of HQC34 hybrid pineapple from tissue culture found that week 4 treatment 1 and 2 have higher than treatment 3 and 4 statistically was 2.17; 2.50; 1.17; and 1.00 centimeters respectively, at week 6 found that treatment 1 and 2 were still higher and better than treatment 3 and 4 as follows 2.50, 2.73, 1.58 and 1.40 respectively. Treatment 1 and treatment 2 continue to provide better result than treatment 3 and 4 at week 8, significantly was 2.50, 2.73, 1.58 and 1.40 respectively. As result from another week, week 10 also showed that treatment 1 and 2 have higher result than treatment 3 and 4 significantly was 2.56, 2.83, 1.57 and 1.40 respectively.

Studies in the feed between 6 and 8 time/day

Used formula feed MS + BA 2 mg/l by piece early HQC34 pineapple hybrid beneath bioreactor system. Study time feeding compare 6 and 8 time/day found that 8 time/day increase seedling pineapple to 233.1 which more than feeding 6 time/day (126.7 shoot) statistically highly significant. However the height of the seedling that is inversely proportional to the amount of the increase that is feeding total 8 time/day seedling with a height of 1.73 cm. while feeding 6 time/day height of 2.40 cm. **(Table 3)**

The number of feeding cause the shoot of additional. This is consistent with the results of (Sumkaew *et al.*, 2010) reported the production of seedlings of eucalyptus species Carr's Lane Sea by means of tissue culture systems Temporary immersion a couple bottles that frequency in feeding the enrichment plant eucalyptus maximum is 8 hours / 1 time (Berthoule *et al.*, 1995 cited by Boonmanee, 2550) studied the increasing number of coffee trees under the Bioreactor system found that The feeding 6 times / day for 15 minutes each time can increase the amount of coffee the most.

Increase HQC34 pineapple hybrid using bioreactor and Shaker.

When taken recipes MS + BA 2 mg /l. The early parts is best to try to increase the amount of pineapple HQC34 plantlets under bioreactor system. The study compared the amount sprout between bioreactor and shaker. Which is controlled feeding 8 times / day for 5 minutes and the liquid is placed on a shaker for 4 weeks showed that the use of bioreactor increase sapling pineapple hybrid HQC34 at 152.00. The more cultured in liquid placed on a shaker has increased shoot 64.8 statistically significant. However, the height of the tender to be inversely proportional to the increases, the use of bioreactor has average height of 1.94 cm, while cultured in liquid placed on the shaker 3.33 cm. **(Table 4)**

The results indicated that the use of bioreactor systems to control and shaker feeding affect the amount of hybrid pineapple plantlets HQC34 well can actually reduce the cost of production. And can increase pineapple plantlets than farmed meat. And cultured in a liquid using a shaker (Srichuy *et al.*, 2014).

Table 1 Effect of media and types of explant on shoot number of HQC34 hybrid using Bioreactor system

Treatments	No. of shoot ^{1/}			
	4 th week	6 th week	8 th week	10 th week
MS + BA 2 mg/l (callus)	60.00 ^a	62.00 ^a	62.00 ^a	62.67 ^a
MS+ BA 2 mg/l (plant)	59.67 ^a	62.00 ^a	62.33 ^a	64.00 ^a
MS+ CPPU 2 mg/l (callus)	13.00 ^b	16.33 ^b	17.67 ^b	18.33 ^b
MS+ CPPU 2 mg/l (plant)	16.67 ^b	19.00 ^b	19.33 ^b	20.00 ^b
C.V. (%)	5.63	5.83	3.726	3.96

^{1/} Means within a column followed by the same letter are not significantly different at P< 0.01 by DMRT

Table 2 Effect of media and types of explant on shoot length of HQC34 hybrid using bioreactor system.

Treatment	Shoot length(cm) ^{1/}			
	4 th week	6 th week	8 th week	10 th week
MS + BA 2 mg/l (callus)	2.17 ^a	2.50 ^a	2.50 ^a	2.56 ^a
MS+ BA 2 mg/l (plant)	2.50 ^a	2.73 ^a	2.73 ^a	2.83 ^a
MS+ CPPU 2 mg/l (callus)	1.17 ^b	1.58 ^b	1.58 ^b	1.57 ^b
MS+ CPPU 2 mg/l (plant)	1.00 ^b	1.40 ^b	1.40 ^b	1.40 ^b
C.V. (%)	18.66	11.79	11.79	12.25

^{1/} Means within a column followed by the same letter are not significantly different at P< 0.01 by DMRT

Table 3 Effect of feeding time of MS + BA 2 mg/l on shoot number and shoot length of HQC34 hybrid using bioreactor system

Feeding time/day	No. of shoot	Shoot length (cm)
6	126.73 ^b	2.40 ^a
8	233.14 ^a	1.73 ^b

Table 4 Effect of feeding MS + BA 2 mg/l on shoots number and shoot length of HQC34 hybrid between use bioreactor system and shaker

Treatment	No. of shoot	Shoot length (cm)
Bioreactor	152.00 ^a	1.94 ^b
Shaker	64.80 ^b	3.33 ^a

Conclusion

Bioreactor system can produce mass shoots for provide to farmers for increase production. Compare medium formula, Part and time feeding (time/day) in bioreactor system, compare bioreactor and shaker. Conclude that MS+BA 2 mg/l increase the shoot and height was better MS+CPPU 2 mg/l. part and callus HQC34 pineapple hybrid non-significant. and tissue culture system bioreactor increase shoot more shaker system Conclude that the medium MS + BA 2 mg / L. with bioreactor 8 times / day increase the shoot pineapple hybrid HQC34 better feeding 6 times / day but a sapling from feeding 6 times / day are higher than that.

Acknowledgement

This research was supported by Rajamangala University of Technology (RMUTSV), Thungyai, Nakhon Si Thammarat Province, Thailand. We would like to acknowledge heartily our Advisor, Assoc. Prof. Dr. Suneerat Sriporaya and her assistances for their guidance to finish this paper.

References

- Agricultural economic office. 2015. **Agricultural statistics in Thailand**. Available Source : http://www.oae.go.th/download/download_journal/2560/yearbook59.pdf.
- Boonmanee, P. 2007. Improvement of Low Cost Temporary Immersion Bioreactor for *Curcuma alismatifolia* Gagnep Micropropagation. **Master of Science in Biotechnology**. Maejo University, Chingmai.
- Fangmuang, W. and Kongbangkerd, A. 2012. Effect of plant growth regulators on development of in vitro shoot culture of *Dendrobium Lindl*, pp.96-102. **In Proceedings of the 1st Phayao Research Conference**. University of Phayao.
- Murashige, T. and Skoog, F. 1962. A Revised medium for rapid growth and bioassays with tobacco tissue cultures. **Physiol Plantarum**. 15: 473-497.
- Sriporaya, S. 2009. Pineapple Hybridization and Selection in Thailand. **ActaHort**. 822: 57-62.
- Srichuay, W. and Te-chato, S. 2014. Effect of chlorine dioxide (ClO₂) on sterilization in micropropagation of pineapple cv. Phulae by bioreactor system. **Khon kaen Agriculture**. 42(3) : 75-80.

Increasing the Harvesting Index Efficiency for Prolonging Shelf Life of Smooth Cayenne Pineapple (*Ananas comosus* cv. 'Pattavia') Fruit

Kullawich Panichkul^{1*}

ABSTRACT

This work aimed to study the appropriate harvesting index of Smooth Cayenne pineapple (*Ananas comosus* cv. 'Pattavia') to enhance the shelf life. Three stages of pineapple were selected for study which were stage 0 (center of eyes beginning to show yellow color), stage 1 (10% of the eyes yellow) and stage 2 (20-30% of the eyes yellow). Pineapples were harvested from Baan-Sa sub-district, Chae Hom district, Lampang province in the same day. The harvested fruits were kept in controlled temperature chamber at 34 degree celsius. To analyze the chemical properties and qualities of pineapple in each stage, tritatable acidity (TA), total soluble solids (TSS) and firmness were investigated in all samples. The results showed that fruit's tritatable acidity and firmness decreased as the storage time increased while as the total soluble solids slightly increased over the time in every stage. For shelf life assessment, the shelf life of pineapple at stage 1 and stage 2 with the acceptable sensory quality for consumers were 5 and 4 days respectively while as the shelf life of pineapple at stage 0 were 5, 6 and 7 days. The model of shelf life was estimated, which was $y = 0.63x + 6.894$ by using the firmness and the sensory quality. From the model, the shelf life of pineapple at stage 0 was estimated at 8 days.

Keyword: Pineapple, Harvesting Index, Quality and Shelf life

¹Department of Plant Science, Faculty of Sciences and Agricultural Technology, Rajamangala University of Technology Lanna Lampang, Pichai Sub-district, Muang District, Lampang Province 52000, Thailand
E-mail: Kullawich@hotmail.com

Introduction

Pineapple is one of important economic crops in Thailand. In the northern part of Thailand, Lampang province is the major pineapple producer, which could create income about 70 million baht annually. Chae Hom district is one of the main pineapple plantation areas, especially in Baan Samakkee. In this area, the land has been degrading due to deforestation, but the location is appropriated for pineapple cultivation. Therefore, the Smooth Cayenne pineapple (*Ananas comosus* cv. 'Pattavia') produced from this area is high quality with sweet, juicy and bright yellow color. Currently, there are about 70 pineapple farmers in this area and it keeps expanding. Now, pineapple production has been expanded to about 1,280 rai. In some years, the price of pineapple can be 8-15 baht/kg (price of 2015-2016), generating income for farmers more than 100,000 baht per year. However, the expansion could create problems such as over production and low price resulting further social problems such as family debts, family affair and bad local environment.

Generally, fresh pineapple sold in the market has different quality and maturity. There has been no study to test and confirm the perfect quality of fresh pineapple for consumers yet. It is common to observe some sellers sold low quality or over ripen fruits (Chaithip and Rattanapanon, 1997). Moreover, quality of pineapple always change while they are on shelf such as weight loss, physical change, degrading nutrition value (vitamin C), lower sugar content due to respiration process after harvest, and increasing organic acids, which all makes change in taste and sensory (Siripanich, 2001). Low qualities fresh pineapple might create consumers' rejection, reducing in consumption and declining market. Therefore postharvest technology is very important for solving problems such as appropriate maturity stage for harvest and effective storage methods. There has been no study yet about the relation between the physical harvesting index and fruit quality after harvest for Smooth cayenne pineapple. Nevertheless the maturity level used for harvest index must have no effect on fruit quality especially the unique taste of smooth cayenne pineapple. Therefore, this work aimed to study the appropriate harvest index of pineapple to enhance the shelf life and quality for fresh pineapple. Moreover, good harvest index would allow the farmers to predict and make plans to avoid loss from harvest and postharvest process.

Materials and methods

Pineapple samples were collected from pineapple plantation in Baan-Sa sub-district, Chae Hom district, Lampang province. There were 3 maturity stages studied in this work, which were stage 0 (center of eyes beginning to show yellow color), stage 1 (10% of the eyes yellow) and stage 2 (20-30% of the eyes yellow). The pineapple samples were harvested in the same day and stored at 34 degree Celsius (relative humidity $65 \pm 3.9\%$). For chemical change in each maturity stage, total soluble solids (TSS) was measured by using Pocket Refractometer (PAL-3, Atago, Japan) and titratable acidity (TA) measurement was followed by AOAC protocol (AOAC, 1990). The firmness was analyzed by texture analyzer (TA.XT.Plus; Stable Micro System) to investigate the physical change. The sensory evaluation was performed by a panel of pineapple experts (10 persons) and 5-hedonic scale was used for the evaluation. Shelf life assessment was also performed. The study was continued until tested fruits were not appropriated for consumption. The experimental design in this work was 3×7 factorial in Completely Randomized Design (CRD). There were 3 replicates for each treatment.

Results and Discussion

The temperature in Lampang is quite high all year (average of 24-38 degree Celsius). However, the temperature may be varied in different areas and seasons. Therefore the temperature used in this experiment must be the temperature that was the representative for all seasons in Lampang. Thus, 34 degree Celsius (relative humidity $65 \pm 3.9\%$) was chosen for the storage temperature because it was the average maximum temperature in the year of 2017 (Figure 1).

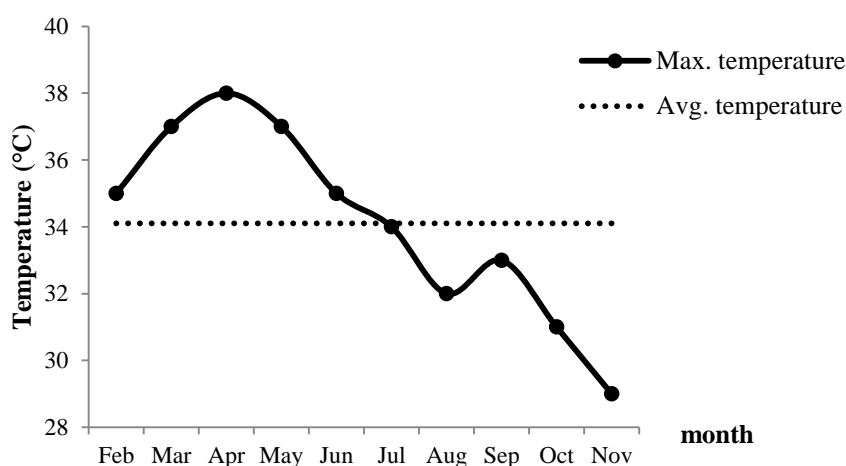


Figure 1 The average maximum temperature of the weather in Lampang province in 2017
Source: Department of Meteorological (2560) and Wunderground.com (2560)

Chemical quality

Titratable acidity (TA): There were significant differences ($p < 0.05$) for maturity factor, storage time factor and their interaction (Table 1). The TA values of the 3 stages were range from 1.39-1.97 percent. Fruit at stage 1 had the highest TA value (1.97%), while stage 1 and stage 2 have the TA value of 1.67% and 1.39% respectively. This result was in accordant with Panyamongkol (2017), which showing that the TA of Phu Lae pineapple at the early maturity stage was higher than the late maturity stage, and the TA was decreased over the time of maturation. In this experiment, the result showed that the TA of all stages decreased as the storage time increased (Figure 2). Paull (1993) reported that the TA content reached the highest at the early stage of maturity and it declined over the time when stored at 7 degree Celsius. In addition, Joomwong (2005) reported that the TA decreased as the maturity developed at the rate of 0.0014 per day. However, those studies were performed with the intact fruits. This experiment was done with the fruits removed from the plant. Pineapple was non-climacteric fruits (Siripanich, 2003) which had non to minimal change in chemical contents after maturity.

Total soluble solids (TSS): The maturity factor show statistical difference ($p < 0.05$). The TSS content of fruits in stage 0, stage 1 and stage 2 were 12.73, 13.86 and 14.54 °brix accordingly (Table 1). The storage time factor also showed statistical difference ($p < 0.05$). For all 3 stages, the TSS content increased as the storage time increased. At 7th day of storage time, fruit at stage 2 had the highest TSS content (16.03 °brix). Normally, pineapple was non-climacteric fruit with the slow respiration process, and the respiration rate would not be increased when the fruit fully ripen. Therefore this kind of fruit could not be incubated for ripening because of the minimal chemical change inside the fruits (Weerawoot, 1998). This

result was similar to report from Chaithip and Rattanapanon (1996) stating that at 5, 10 and 20 degree Celsius, the TSS content of the pineapple was not stable and it fluctuated in the range of 14.2-15.1 °brix. Raiphuttha *et al.* (2011) also reported that the Phu Lae pineapple had a slight change during the storage (14.3-16.0 °brix). In addition, Joomwong (2006) reported that the TSS of pineapple increased as the maturity stage increased at the rate of 0.375 °brix because the starch inside was changed into sugar as the maturity stage developed which made the fruit sweeter and less sour (Pongjanta *et al.*, 2010).

Table 1 Chemical quality of pineapple samples during storage for 7 days

Treatments	Titrateable acidity (%)	Total soluble solids (°Brix)
Maturity stage levels		
Stage 0	1.97 ± 0.58 ^a	12.73 ± 1.21 ^c
Stage 1	1.67 ± 0.57 ^b	13.86 ± 0.91 ^b
Stage 2	1.39 ± 0.52 ^c	14.54 ± 0.93 ^a
Storage time		
Day 1	2.50 ± 0.31 ^a	12.41 ± 1.14 ^g
Day 2	2.70 ± 0.29 ^b	12.69 ± 0.92 ^f
Day 3	1.94 ± 0.28 ^c	13.14 ± 0.82 ^e
Day 4	1.73 ± 0.22 ^d	13.60 ± 0.62 ^d
Day 5	1.42 ± 0.22 ^e	14.12 ± 0.68 ^c
Day 6	1.10 ± 0.28 ^f	14.71 ± 0.74 ^b
Day 7	0.87 ± 0.21 ^g	15.28 ± 0.73 ^a
Maturity stage level × Storage time		
Stage 0 × Day 1	2.80 ± 0.00 ^a	10.93 ± 0.06 ^u
Stage 0 × Day 2	2.50 ± 0.00 ^c	11.53 ± 0.06 ^t
Stage 0 × Day 3	2.30 ± 0.00 ^d	12.10 ± 0.10 ^s
Stage 0 × Day 4	2.00 ± 0.00 ^g	12.87 ± 0.06 ^q
Stage 0 × Day 5	1.70 ± 0.00 ⁱ	13.33 ± 0.06 ^o
Stage 0 × Day 6	1.40 ± 0.00 ⁱ	13.90 ± 0.00 ^j
Stage 0 × Day 7	1.10 ± 0.00 ^p	14.43 ± 0.06 ^f
Stage 1 × Day 1	2.60 ± 0.00 ^b	12.83 ± 0.06 ^r
Stage 1 × Day 2	2.13 ± 0.06 ^e	12.90 ± 0.00 ^p
Stage 1 × Day 3	1.87 ± 0.06 ^h	13.40 ± 0.00 ^m
Stage 1 × Day 4	1.70 ± 0.00 ⁱ	13.67 ± 0.23 ^k
Stage 1 × Day 5	1.37 ± 0.06 ^m	14.17 ± 0.23 ^h
Stage 1 × Day 6	1.13 ± 0.06 ^o	14.67 ± 0.32 ^e
Stage 1 × Day 7	0.87 ± 0.06 ^q	15.37 ± 0.40 ^c
Stage 2 × Day 1	2.10 ± 0.00 ^f	13.47 ± 0.06 ⁿ
Stage 2 × Day 2	1.87 ± 0.06 ^h	13.63 ± 0.06 ^l
Stage 2 × Day 3	1.67 ± 0.06 ^j	13.93 ± 0.06 ⁱ
Stage 2 × Day 4	1.50 ± 0.00 ^k	14.27 ± 0.06 ^g
Stage 2 × Day 5	1.20 ± 0.00 ⁿ	14.87 ± 0.06 ^d
Stage 2 × Day 6	0.77 ± 0.06 ^r	15.57 ± 0.06 ^b
Stage 2 × Day 7	0.66 ± 0.06 ^s	16.03 ± 0.06 ^a

Note: ^{a-u} letters in the same column show statistically significant difference (p<0.05)

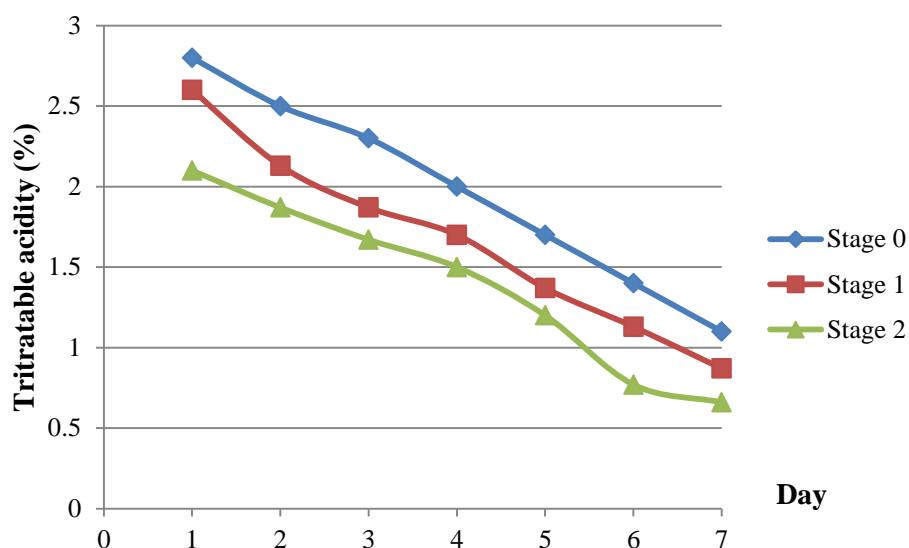


Figure 2 Relationship between storage times and titratable acidity of pineapple

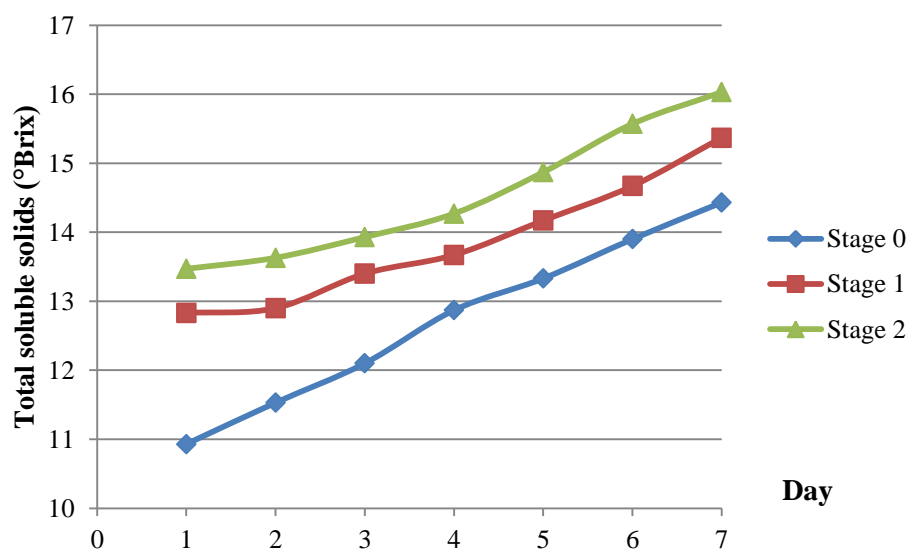


Figure 3 Relationship between storage times and total soluble solid contents of pineapple

Physical quality

The firmness of fruits at stage 0, stage 1 and stage 2 were 4.38, 3.83 and 3.35 N/mm. The maturity stage and the storage time had effect on the firmness (Table 2). The firmness of fruit of 3 stages decreased as the storage time increased. On the 1st day of storage, the fruit at stage 0 has the highest firmness value (6.09 N/mm), whereas the lowest firmness value was belonged to the fruit at stage 2 at the 7th day of storage (1.51 N/mm) (Figure 4). The result was similar to the previous report stating that the fruit firmness would decrease as the storage time increased (Trairongjitmoh and Somboon, 2011). Moreover, Panyamongkol (2017) had tested the pineapple firmness with fruit penetrometer and reported that the firmness slowly decreased as the maturity developed. For smooth cayenne pineapple, fruits harvested after 140 days after flowering in every season would have declining firmness (Joomwong and Sornsrivichai, 2005) because the fruit body was composed with starch and pectin, which would be degraded as the maturity increased, resulting in the decreased firmness and when

storing for a period of time, lose of water from the cell, resulting in the decreased in turgidity. This would affect the texture decreasing in hardness and crispness (Riquelme *et al.*, 1994).

Table 2 Physical quality of pineapple samples during storage for 7 days

Treatments	Firmness (N/mm)
Maturity stage levels	
Stage 0	4.38 ± 1.31 ^a
Stage 1	3.83 ± 1.16 ^b
Stage 2	3.35 ± 1.12 ^c
Storage times	
Day 1	5.42 ± 0.57 ^a
Day 2	4.96 ± 0.61 ^b
Day 3	4.54 ± 0.52 ^c
Day 4	4.12 ± 0.51 ^d
Day 5	3.26 ± 0.27 ^e
Day 6	2.64 ± 0.31 ^f
Day 7	2.03 ± 0.47 ^g
Maturity stage level × Storage time	
Stage 0 × Day 1	6.09 ± 0.14 ^a
Stage 0 × Day 2	5.71 ± 0.16 ^b
Stage 0 × Day 3	5.14 ± 0.08 ^d
Stage 0 × Day 4	4.63 ± 0.09 ^g
Stage 0 × Day 5	3.50 ± 0.13 ^l
Stage 0 × Day 6	2.96 ± 0.07 ^o
Stage 0 × Day 7	2.59 ± 0.05 ^q
Stage 1 × Day 1	5.31 ± 0.22 ^c
Stage 1 × Day 2	4.80 ± 0.22 ^f
Stage 1 × Day 3	4.51 ± 0.17 ^h
Stage 1 × Day 4	4.23 ± 0.08 ^j
Stage 1 × Day 5	3.32 ± 0.10 ⁿ
Stage 1 × Day 6	2.66 ± 0.17 ^p
Stage 1 × Day 7	1.97 ± 0.08 ^s
Stage 2 × Day 1	4.85 ± 0.20 ^e
Stage 2 × Day 2	4.36 ± 0.18 ⁱ
Stage 2 × Day 3	3.96 ± 0.06 ^k
Stage 2 × Day 4	3.50 ± 0.14 ^m
Stage 2 × Day 5	2.96 ± 0.08 ^o
Stage 2 × Day 6	2.29 ± 0.16 ^r
Stage 2 × Day 7	1.51 ± 0.06 ^t

Note: ^{a-t} letters in the same column show statistically significant difference (p<0.05)

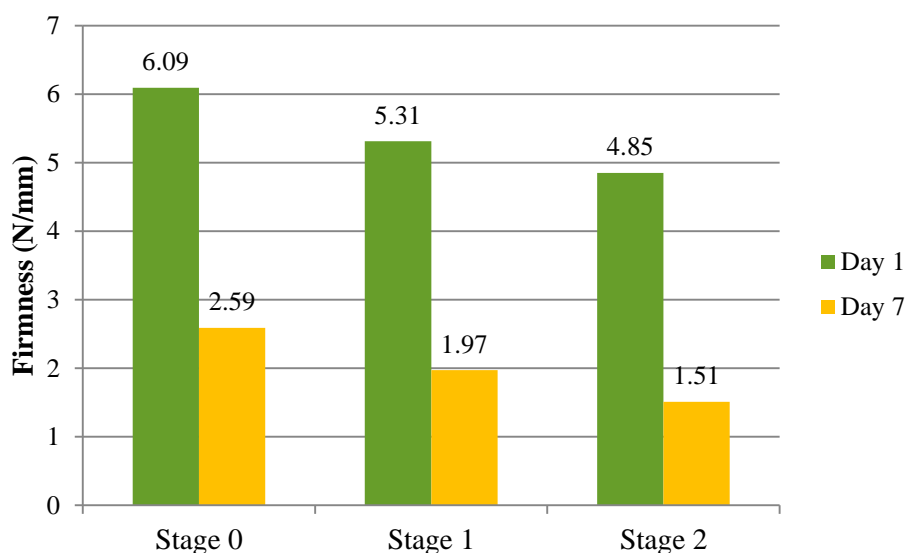


Figure 4 Interaction between maturity stage and storage times of pineapple samples affected the change in the firmness

Sensory quality

For sensory test, 5 Point Hedonic Scaling Test was employed (1 for dislike the most and 5 for like the most) with 10 professional evaluators. The characteristics investigated were appearance, color, smell, taste and texture. Fruit at stage 1 had the highest score for appearance and color, while fruit at stage 0 and stage 2 had the highest score for aroma. The fruits at all stage had similar score for the taste (2.56, 3.20 and 3.30 for stage 0, stage 1 and stage 2 accordingly). The fruit at stage 0 has the highest score for texture (3.20) (Table 3).

For maturity factor and storage factor affected the appearance, color, aroma, taste and texture differently ($p < 0.05$). For appearance and color, fruit at all stages gained higher score as the storage time increased. The shell color was confirmed with color measurement and the result was in accordance with color observed by eyes of evaluators. For the taste, the evaluators gave higher score to fruit at stage 0 at 5th, 6th and 7th day of storage (4.50), while fruit at stage 2 received high score for 2nd, 3rd, 4th and 5th day of storage. However, the texture of fruits at those stages during 1st - 4th day of storage were not statistically different, and the evaluators gave score to those fruits in the “like” level (4.00-4.40) (Table 3).

Pothisawat (2001) reported that good quality of fresh pineapple must has high sugar content and good aroma. Similarly, Smith (1998) also reported that the eating quality of pineapple highly related to TSS, which meant pineapple at late maturity stage would have high TSS resulted in high sensory score. The results of the work will be found the maturity stage level at stage 0 of storage was 5, 6 and 7 days, TSS content was higher for the storage period also increased the taste score as well.

In this work, fruit at stage 0 at 5th, 6th and 7th day of storage had high TSS content when the storage time increased. Moreover, fruit at stage 1 and stage 2, at 5th and 4th day of storage got the least score for taste and texture (1.00-2.30) from the evaluators and the score was lower as the storage time increase. This was because the abnormality in texture color such as browning and becoming mushy, and the appearance showed sign of senescence with disliked taste for the evaluators, which caused by the biochemical and physiological change affecting the sensory assessment (Watada *et al.*, 1994). After the experiment period, all samples became senescent stage, which the shelf life was expired. This observe was similar to Panichkul (2011) work showing that smooth cayenne pineapple harvested during summer (April-May) had 7 days before the sensory quality become deteriorated.

From the sensory assessment, all pineapple samples received score in the level of “so-so” to “like a little” (3-5) from the evaluators in every characteristics, and the evaluators also gave comments that those pineapple samples were not different enough to be distinguished from each other in the sensory evaluation, which reflected in similar score for each different samples.

Table 3 Sensory quality of pineapple samples during storage for 7 days

Treatments	appearance	color	aroma	taste	texture
Maturity stage level × Storage					
Stage 0	3.71 ± 1.16 ^b	2.61 ± 0.89 ^c	3.31 ± 1.52 ^a	2.56 ± 0.93 ^b	3.20 ± 1.22 ^a
Stage 1	3.64 ± 0.98 ^a	3.44 ± 1.24 ^a	3.00 ± 1.05 ^b	3.20 ± 1.36 ^a	2.56 ± 0.91 ^c
Stage 2	3.89 ± 1.52 ^b	3.30 ± 1.15 ^b	3.26 ± 1.67 ^a	3.30 ± 1.72 ^a	2.93 ± 1.42 ^b
Stage 0 × Day 1	2.60 ± 0.52 ^e	2.00 ± 0.00 ^d	1.60 ± 0.52 ^g	1.50 ± 0.53 ^{fg}	1.70 ± 0.48 ^c
Stage 0 × Day 2	2.80 ± 0.42 ^e	2.20 ± 0.00 ^d	1.60 ± 0.52 ^g	1.70 ± 0.48 ^f	1.90 ± 0.32 ^c
Stage 0 × Day 3	2.90 ± 0.32 ^e	2.50 ± 0.00 ^c	2.10 ± 0.32 ^g	2.30 ± 0.48 ^e	2.60 ± 0.52 ^b
Stage 0 × Day 4	3.40 ± 0.52 ^e	3.30 ± 0.48 ^b	3.20 ± 0.42 ^e	3.40 ± 0.52 ^c	2.90 ± 0.32 ^b
Stage 0 × Day 5	4.40 ± 0.52 ^d	4.50 ± 0.48 ^a	4.70 ± 0.48 ^a	4.50 ± 0.53 ^a	4.20 ± 0.42 ^a
Stage 0 × Day 6	4.60 ± 0.52 ^c	4.70 ± 0.00 ^a	4.80 ± 0.42 ^a	4.50 ± 0.53 ^a	4.50 ± 0.53 ^a
Stage 0 × Day 7	4.80 ± 0.42 ^b	4.90 ± 0.32 ^a	4.80 ± 0.42 ^a	4.50 ± 0.53 ^a	4.60 ± 0.52 ^a
Stage 1 × Day 1	4.00 ± 0.00 ^d	3.00 ± 0.00 ^c	3.30 ± 0.48 ^d	2.30 ± 0.48 ^e	2.50 ± 0.53 ^b
Stage 1 × Day 2	4.30 ± 0.48 ^d	3.00 ± 0.00 ^c	3.50 ± 0.53 ^b	2.50 ± 0.53 ^e	2.80 ± 0.63 ^b
Stage 1 × Day 3	4.40 ± 0.52 ^d	3.00 ± 0.00 ^c	3.70 ± 0.48 ^b	3.40 ± 0.52 ^c	3.20 ± 0.63 ^b
Stage 1 × Day 4	4.80 ± 0.42 ^b	3.30 ± 0.48 ^b	4.00 ± 0.00 ^b	3.70 ± 0.48 ^b	3.50 ± 0.53 ^a
Stage 1 × Day 5	4.30 ± 0.48 ^d	3.30 ± 0.48 ^b	3.40 ± 0.52 ^c	3.20 ± 0.42 ^d	3.00 ± 0.00 ^b
Stage 1 × Day 6	2.50 ± 0.53 ^e	1.70 ± 0.48 ^e	1.60 ± 0.52 ^g	1.50 ± 0.53 ^{fg}	1.60 ± 0.52 ^c
Stage 1 × Day 7	1.70 ± 0.48 ^f	1.00 ± 0.00 ^f	1.50 ± 0.53 ^g	1.50 ± 0.53 ^{fg}	1.30 ± 0.48 ^c
Stage 2 × Day 1	4.80 ± 0.42 ^a	4.00 ± 0.00 ^a	4.40 ± 0.52 ^a	4.40 ± 0.52 ^{ab}	4.00 ± 0.00 ^a
Stage 2 × Day 2	4.80 ± 0.42 ^a	4.00 ± 0.00 ^a	4.40 ± 0.52 ^a	4.60 ± 0.52 ^a	4.00 ± 0.00 ^a
Stage 2 × Day 3	4.80 ± 0.42 ^a	4.10 ± 0.57 ^a	4.80 ± 0.42 ^a	4.80 ± 0.42 ^a	4.00 ± 0.00 ^a
Stage 2 × Day 4	4.80 ± 0.42 ^a	4.20 ± 0.63 ^a	4.80 ± 0.42 ^a	4.80 ± 0.42 ^a	4.40 ± 0.52 ^a
Stage 2 × Day 5	4.00 ± 0.00 ^d	3.40 ± 0.52 ^b	2.40 ± 0.52 ^f	2.30 ± 0.48 ^e	2.10 ± 0.32 ^c
Stage 2 × Day 6	1.90 ± 0.32 ^f	1.50 ± 0.53 ^d	1.60 ± 0.00 ^h	1.00 ± 0.00 ^g	1.00 ± 0.00 ^d
Stage 2 × Day 7	1.30 ± 0.48 ^f	1.90 ± 0.32 ^d	1.00 ± 0.00 ⁱ	1.00 ± 0.00 ^g	1.00 ± 0.00 ^d

Note: ^{a-i} letters in the same column show statistically significant difference (p<0.05)

Evaluation of shelf-life of pineapple samples: For fruit at stage 0, after 7th day of storage, its sensory level was still good (4.00-4.50). Therefore, its' shelf life needed to be assessed by using accelerating condition. From equation, $y = 0.63x + 6.894$ (Figure 5), which was to determine the senescence of the fruits by using texture characteristic as the main factor because texture was a unique characteristic for this kind of pineapple. The consumer would noticed this character first when they tried, and they would reject if the texture was abnormal (Shamberger *et al.*, 1997). However, fruit at stage 1 and stage 2 from 6th and 7th day of storage received low score on sensory quality (below 2.50) (Table 3), which was in the “rejection” level for the evaluators. These scores were varied to the firmness (Table 2) at 6th and 7th day of storage, and it kept declining as the storage time increase. Although there were many criteria for senescence analysis, Shamberger *et al.* (1997) had reported the firmness

was the most important factor for senescence in consumer's point of view. Therefore the firmness value of 2.29 N/mm was used as the criteria for senescence in this work. This study showed that 8 days was the maximum storage time that still yielded acceptable firmness for the consumers. However, other chemical change may be interfering with the acceptance from the consumers. Therefore, other characteristics such as specific aroma should be applied along with the sensory assessment, and the relationship should be studied to get the appropriate index.

Harvesting pineapple fruit at stage 0 will yield the most firmness and very crisp texture during consumption but the taste was not acceptable for the consumers when it kept less than 5 days. However fruit at stage 0 can be kept for as long as 8 days. Therefore, for short storage time fruit at late maturity should be harvested, so that the taste and texture would be accepted by the consumers.

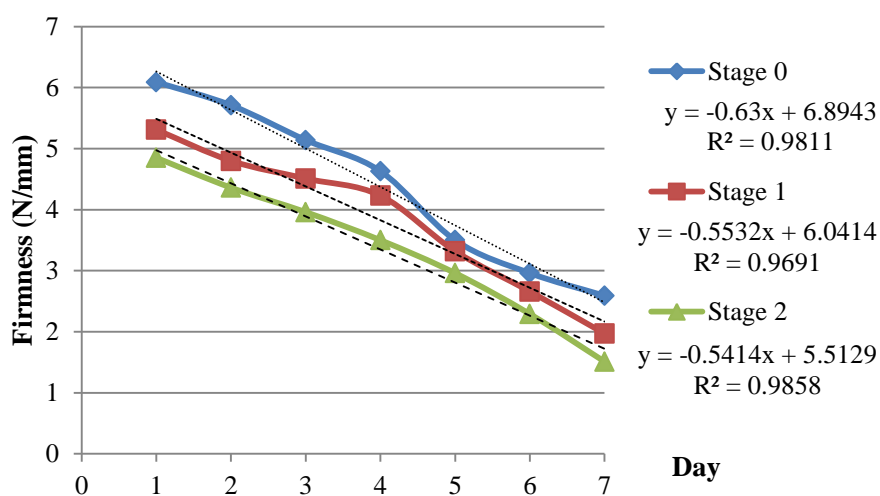


Figure 5 Relationship between shelf-life and firmness of pineapple after storage

Conclusions

The experiment was a study of appropriate maturity stage of Smooth cayenne pineapple cultivated from Baan-Sa sub-district, Chae Hom district, Lampang province to find suitable harvest index for shelf-life. It was found that maturity stage factors and storage time factors of all the maturity stage levels of pineapple affected to the titratable acidity content and the firmness decreased throughout the shelf life while as the amount of total soluble solids tended to change slightly over the shelf life.

The shelf life assessment of Smooth cayenne pineapple showed that fruit at stage 1 and stage 2 at 5th day and 4th day of storage respectively gained the acceptance from the consumers, after those times, the fruits became senescent stage. However fruit at stage 0 gained the acceptance at 5th, 6th and 7th day of storage, and the shelf-life assessment by using the equation of $y = 0.63x + 6.894$ with the texture characteristic related to the firmness as the criteria for determination showed that the appropriate shelf-life for fruit at stage 0 was 8 days.

Acknowledgements

Thank you for the Thailand Research Fund, the research team and Department of Agro-industry, Faculty of Sciences and Agricultural Technology, Rajamangala University of Technology Lanna Lampang.

References

- AOAC. 1990. Official Methods of Analysis of the Association of Official Analytical Chemists. Vol. 2, 15th ed. K. Helrich (Ed.), pp. 910-930, 1045-1114. U.S.A. Association of Official Analytical Chemists, Inc.
- Chaithip, S. and Rattanapanon, N. 1996. Effect of temperature and coating on the quality and shelf-life of fresh and ready-to-eat pineapple. Full Research Report. Chiang Mai University
- Department of Meteorological. 2560. **Thai Meteorological Department: Meteorological information**. Available Source:<https://www.tmd.go.th/services/services.php> (January 1, 2018)
- Joomwong, A. 2005. Assessment of quality in relation to maturity and cropping season of pineapple (*Ananas comosus* cv. Smooth Cayenne) fruit growing in northern Thailand. Doctor of philosophy (Biology) Chiang Mai university.
- Joomwong, A. 2006. Changes in chemical properties and sugars in pineapple berry fruit during ripening. **Journal of Agricultural Science** Vol. 37 No. 6 (Special) November-December 2006. The 6th National Horticultural Congress, Chiang Mai.
- Joomwong, A. and SornSriwichai, J. 2006. Effect of harvesting time on translucency and chemical properties of pineapple (*Ananas comosus* cv. Smooth Cayenne) fruit. **Journal of Agricultural Science** Vol. 37 No. 5 (Special): 152-155.
- Panichkul, K. 2011. Changes in postharvest quality of pineapple (*Ananas comosus* cv. Smooth Cayenne) in market system. Full research reports. Rajamangala University of Technology LannaLampang, Lampang
- Panyamongkol, S. 2017. The relation between Physical and chemical properties in poolae pineapple with maturity stage among number 0-7. **Kasalongkham Research Journal**. Issue 11, Volume 3, Special Issue Chiang Rai Rajabhat University.
- Paull, R.E. 1993. **Pineapple and papaya in Biochemistry of Fruit Ripening**. G. Seymour, J. Taylor., and G. Tucker (Eds.), pp. 291-323. Chapman & Hall, London
- Pothisawat, P. 2011. Comparative study on growth and quality of pineapple (*Ananas comosus* cv. Smooth Cayenne) varieties. Master Thesis. Kasetsart university, Bangkok.
- Pongjanta, J., Nuanboonreuang, A., Parnjai, L. and Buaphan, T. 2010. Changes in organic acids and sugars in pineapple juices (*Ananas comosus* cv. Smooth Cayenne) at different planting sites and ripening levels. Full research reports. Agricultural Technology Research Institute. Rajamangala University of Technology Lanna.
- Raiphuttha, J., Sritao, S., Chaiwong, S. and Suttalak, P. 2011. Effect of packaging types on the quality of PhuLae pineapple. **Journal of Agricultural Science** Vol. 42 No. 3 (Special). 673 p.
- Riquelme, F., Pretel, M.T., Martinez, G., Serrano, M., Amoros, A., and Romo Jaro, F. 1994. Packaging of fruits and vegetables: recent result. *In Food packaging and preservation*. M. Mathlouthi (Ed.), pp. 141-168. U.K. Blackie Academic and Professional.
- Shamberger, R.J., B.A. Shamberger and C.E. Willis 1977. **Malonaldehyde content of food**. **Journal of Nutrition** 107: 1404-1409.

- Siripanich, J. 2001. **Physiology and postharvest technology of fruits and vegetables**. 4th: Kasetsart University Press. Bangkok., 396 p.
- Siripanich, J. 2003. **Physiology and postharvest technology of fruits and vegetables**. 5th: Kasetsart University press. Bangkok., 369 p.
- Smith, L.G. 1988. Indices of physiological maturity and eating quality in Smooth Cayenne pineapples. 2. Indices of eating quality. **Queensland Journal Agriculture and Animal Science**. 45: 219-228
- Trairongjitmoh, S. and Somboon, P. 2011. Postharvest day assessment of pineapple using electronics noses. **34th Electrical Engineering Symposium (EECON-34)**, Siam University.
- Watada, A.E., Abe, K., and Yamuchi, N. 1994. Physiological activities of partially processed fruits and vegetables. **Food Technol.**, 44: 116-122
- Weerawoot, J. 1998. **Pineapple and the physiology of pineapple growth**. Kasetsart University, Bangkok Press. 196 p.
- Wunderground. 2560. **Weather underground: Historical weather**. Available Source: <https://www.wunderground.com/history/> (January 1, 2018)

Effects of Carbon Sources And Inoculation Protocols On Carissa Acetification Process

Ni-orn Chomsri^{1*}, Jutharat Yangprasert¹, Punwika Wongkeaw¹ and Kamonwan Manowan¹

ABSTRACT

Acetification is an oxidative activity of ethanol to acetic acid performed by bacteria genera *Acetobacter* and *Gluconobacter*. The aim of the present study was to assess factors affecting carissa acetification process. Two factors of carbon sources at two levels and inoculation protocols of yeast culture for alcoholic fermentation at 3 levels were designated. Results revealed that L* color values of the final vinegars obtained from consecutive fermentation were significantly different in the range of 31.30-38.19 ($p \leq 0.05$) and a* and b* values were in the ranges of 2.88-4.21 and 3.61-6.07, respectively ($p > 0.05$). The turbidity and conductivity properties of the vinegars were between 12.45-14.70 NTU and 1.61-1.84 mS/m, respectively. The chemical properties of total acidity content, total anthocyanin content, total phenolic content and antioxidant activity were in the ranges of 2.63-4.16 %, 10.25-1.63 mg/L, 280.00-327.73 mg/L and 20.97-36.09 (% ABTS scavenging effect), respectively. Sensory evaluation indicated that the panelists were satisfied with the carissa vinegars at the average score levels of 6.63-7.25 scores.

Keywords: Acetification, Carissa, Vinegar

¹ Agricultural Technology Research Institute, Rajamangala University of Technology Lanna, 202 Moo 17, Pichai District, Amphur Muang, Lampang 52000

*Corresponding author, e-mail : niornchomsri@rmutl.ac.th

Introduction

Carissa carandas L. is an evergreen and spiny shrub belonging to Apocynaceae family. It is commonly known in many local names, e.g. Carandas (Bansal, 2014), Karanda and Carunda (Kubola *et al.*, 2011), Karaunda (Mehmood *et al.*, 2014) Namdaeng (Yuenyongphuthakal *et al.*, 2012) Karamcha (Khatun *et al.*, 2017). Karanda is a good source of phytochemicals with excellent health benefits (Chomsri *et al.*, 2017). In recent years, the interest in Karanda has increased because of its pharmacological characteristics, e.g. treatment of constipation and diarrhea, stomachic, anorexia, intermittent fever, mouth ulcer and sore throat, syphilitic pain, burning sensation, scabies and epilepsy (Mehmood *et al.*, 2014, Khatun *et al.*, 2017; Bahdane and Pati, 2017). Karanda is widely studied in various areas as medicinal and dietary aspects. The fruit contains an astringent taste and it is claimed to be useful for cure of anemia, to improve female libido and to remove worms from the intestinal tract (Wani *et al.*, 2013). It is a common herb used in traditional system of medicine in Bangladesh (Khatun *et al.*, 2017). Bhadane and Patil (2017) reported the ripened Karanda fruits were rich of flavonoids, e.g. rutin, epicatechin, quercetin and kaemferol including phenolics, e.g. syringic acid, vanillic acid and caffeic acid. Research of drying of Karanda pomace revealed its alternative use of the tablet product (Yuenyongphuthakal *et al.*, 2012). Maturity stage on the fruit quality and shelf-life of Karanda were also studied to promote its utilization (Joomwong, 2014; Siritrakulsak *et al.*, 2016).

Acetification is a typical two-stage fermentation process. In the first stage, fermentable sugars are converted into ethanol by the action of yeasts, normally strains of *Saccharomyces cerevisiae*, while in the second stage, acetic acid bacteria (AAB) oxidize the ethanol to acetic acid (Baena-Ruano *et al.*, 2016). This fermentation process is used for vinegar production. AAB are in family Acetobacteraceae and currently classified into twelve genera (Mounir *et al.*, 2016). Although these bacteria members can produce acetic acid, the AAB recovered from vinegar fermentation are mainly distributed in the genera *Acetobacter*, *Gluconobacter*, and *Gluconacetobacter* (Sengun and Karabiyikli, 2011). These species have a relevant importance in vinegar production for their ability to oxidize ethanol to acetic acid which is an active component. Generally, there is 5-15.5 g acetic acid in 100 g of vinegar (Belitz *et al.*, 2009). Vinegar is the most important single flavoring in food to give or enhance the sour, acidic taste of food. It is commonly used in a wide variety of food products, including mayonnaises, ketchups, sauces, chopped pickles, fermented beverage and brined vegetables (Pure *et al.*, 2017). Vinegar, diluted with water, was commonly used as a refreshing, non-intoxicating drink in Roman times (Wood, 1998). Vinegar was used as medicine to fight infections and other acute conditions in Hippocrates's time, but recent research suggests that vinegar ingestion favorably influences biomarkers for ulcerative colitis heart disease, cancer and diabetes (Johnston, 2009; Shen *et al.*, 2016). Moreover, it can be used for inactivation of harmful bacteria (Park *et al.*, 2016). Vinegar can be produced from many fruits such as grape, raspberry, apple, strawberry, pineapple, apricot (Chomsri *et al.*, 2010, 2015; Hidalgo *et al.*, 2013; Mounir *et al.*, 2016; Trček *et al.*, 2016; Pure *et al.*, 2017).

The aim of the present study was to investigate the influence of different carbon sources and inoculation protocols of yeast culture on carissa juice acetification process.

Materials and Methods

1. Microorganism strains and growth medium

Saccharomyces cerevisiae strain E, *S.cerevisiae* strain V and acetic acid bacteria were derived from the collection of the Section of Food Science and Technology, Agricultural Technology Research Institute, Rajamangala University of Technology Lanna, Lampang Province Thailand. Yeasts and bacteria were grown at 25 and 30°C on YPD and GY media, respectively.

2. Carissa juice

Carissa fruits were obtained from carissa trees grown in Agricultural Technology Research Institute, Lampang Province, Thailand in 2009. The carissa fruits were harvested and sorted out to eliminate defective units and washed. The seeds were taken out from the carissa fruits by hands. Then carissa flesh was crushed and pressed to obtain juice.

3. Fermentation conditions

Two factors of carbon sources at two levels, i.e. fructose syrup and longan honey and inoculation protocols of yeast culture for alcoholic fermentation at 3 levels, i.e. *S. cerevisiae* strain E, *S.cerevisiae* strain V and mixed culture of *S. cerevisiae* strain E and *S.cerevisiae* strain V at the ratio of 1:1, were designated. Triplicate experiments were conducted using 750 ml sterile bottles (650 ml carissa juice per bottle) at 20 °C for the first step of alcoholic fermentation. The yeast inoculum was aseptically transferred to the fermentation vessel to achieve the initial population of 1×10^6 cells/ml. The fermentation trial was terminated after 21 days. Then, the acetic acid fermentation was introduced to substrates (alcohol) which were obtained from the first step of fermentation. The 2nd step fermentation was performed in 250-ml flasks with a substrate volume of 100 ml. The substrate employed in this fermentation contained alcohol concentration of 6 % (v/v). An amount of 10 ml of acetic acid bacteria inoculum was added to the fermentation flask. The fermentation was performed at 30 °C for 14 days.

4. Chemical analysis

pH was measured by a pH meter (Model C831, Belgium). Total acidity was determined by diluting each 5 ml aliquot of sample in 50 ml distilled water and then titrating to pH 8.2 using 0.1 N NaOH (Iland *et al.*, 2000). Titratable acidity was expressed as acetic acid percentage. Total soluble solid content was determined on an Atago hand-held refractometer. Ethanol concentration was measured by ebulliometer (Dujardin – Salleron, Noizay, France) according to Iland *et al.* (2000). Free alpha amino nitrogen (FAN) was quantified by spectrophotometric method (Intaramoree and Chomsri, 2014). Total anthocyanin content was evaluated by the method of Giusti and Wrolstad (2005). The modified method of Spinola *et al.* (2015) was used to evaluate total phenolic content. The antioxidant activity was determined by modified method of Wongputtisri *et al.* (2007).

4. Sensory analysis

Sensory descriptive analysis was used for the intensity of vinegar odors (Meilgaard *et al.*, 2006). The vinegar products were assessed for odor attributes of ethyl acetate, pungent sensation, honey, fruit wine, complex and overall acceptance. A sensory panel of 20 trained individuals was selected internally. Intensities were scored on a 10-cm-line scale; data were statistically analyzed and visually represented in the form of spider diagrams.

5. Statistical analysis

All the experiments were carried out with replications. Analysis of variance (ANOVA) was used to compare mean differences of the samples. Significant differences between treatments were analyzed by Duncan's new multiple range test (DNMRT) at a 0.95 significance level. Values were expressed as the mean of all replicate determinations standard deviation.

Results and Discussion

1. Effect of carbon sources and inoculation protocols of yeast culture on physical and conductivity parameters of end products

In this study, end products of acetic acid fermentation process of carissa juice were analyzed for physical properties and conductivity. Results showed that two carbon sources, i.e. syrup and honey and three inoculation protocols of yeast culture for alcoholic fermentation, i.e. *S. cerevisiae* strain E, *S. cerevisiae* strain V and mixed cultures of *S. cerevisiae* strain E and *S. cerevisiae* strain V affected the color values, turbidity and conductivity of vinegar products. The use of syrup as carbon source produced higher lightness of L* value compared to honey whereas different yeast protocols did not show a substantial difference on L* color value. However, acetification products, i.e. vinegar obtained from different yeast inoculation protocols exhibited significant difference values redness (a*) and yellowness (b*) as shown in Table 1 ($p \leq 0.05$). Vinegar products obtained from 6 treatments showed L*, a* and b* color values in the ranges of 31.30 to 38.19, 2.88 to 4.21 and 3.61 to 6.58, respectively (Table 1).

The turbidity and conductivity parameters of the final vinegar products were in the ranges of 13.20-61.00 NTU and 1.03-1.89 mS/m, respectively. The use of different carbon sources and inoculation protocols of yeast culture in acetification fermentation process of carissa juice had an impact on turbidity and conductivity of end products. The vinegars obtained from alcoholic substrates with honey as carbon source had greater values of turbidity and conductivity ($p \leq 0.05$). These different fermentation behaviors affected by different alcoholic substrates and inoculum cultures were also observed by Chomsri *et al.* (2010, 2015), Thepkaew and Chomsri (2013), Chomsri and Thepkaew (2016). Additionally, different compounds, e.g. amino acids, proteins, sugars, existing in syrup and honey including metabolites produced during fermentation could also substantially influence the values of turbidity and conductivity (Vaclavik and Christian, 2008; Miranda *et al.*, 2016; Deng *et al.*, 2018).

Table 1 Color, turbidity and conductivity of end products from fermentation with different carbon sources and inoculation protocols of yeast culture

Factors	L*	a*	b*	Turbidity NTU	Conductivity mS/m
Factor A	*	ns	ns	*	*
Syrup (S)	37.51±0.80 ^a	3.80±0.46	5.42±1.45	32.30±19.18 ^b	1.24±0.19 ^b
Honey (H)	32.48±1.18 ^b	3.35±0.53	5.28±1.28	43.90±20.88 ^a	1.65±0.33 ^a
Factor B	ns	*	*	*	*
<i>S. cerevisiae</i> strain E (E)	34.74±4.05	3.04±0.27 ^b	3.79±0.60 ^b	22.75±6.29 ^c	1.56±0.37 ^a
<i>S. cerevisiae</i> strain V (V)	34.72±2.16	3.98±0.48 ^a	6.25±0.95 ^a	58.25±3.17 ^a	1.34±0.14 ^c

E + V	35.51±2.65	3.70±0.34 ^a	6.01±0.39 ^a	33.30±23.21 ^b	1.44±0.46 ^b
Interaction	*	ns	ns	*	*
S-E	38.19±0.12 ^a	3.21±0.03	3.61±0.07	28.20±0.28 ^d	1.24±0.00 ^d
S-V	36.52±0.32 ^a	4.21±0.08	6.58±0.71	55.50±0.00 ^b	1.46±0.00 ^c
S-E+V	37.81±0.14 ^a	3.97±0.03	6.07±0.04	13.20±0.00 ^f	1.03±0.07 ^f
H-E	31.30±1.28 ^c	2.88±0.32	3.98±0.97	17.30±0.00 ^e	1.89±0.00 ^a
H-V	32.92±1.02 ^{bc}	3.75±0.70	5.92±1.32	61.00±0.00 ^a	1.22±0.01 ^e
H-E+V	33.21±0.20 ^b	3.43±0.26	5.95±0.67	53.40±0.42 ^c	1.84±0.00 ^b

ns denotes means are not significantly different ($p>0.05$); fructose syrup with *S. cerevisiae* strain E (S-E), fructose syrup with *S. cerevisiae* strain V (S-V), fructose syrup with *S. cerevisiae* strain E and V (S-E+V), honey with *S. cerevisiae* strain E (H-E), honey with *S. cerevisiae* strain V (H-V) and honey with *S. cerevisiae* strain E and V (H-E+V)

* Means in a column with the different letters represent significant differences ($p\leq 0.05$)

2. Effect of carbon sources and inoculation protocols of yeast culture on chemical parameters of the final vinegars

Chemical analyses of pH, total acidity and total soluble solids in end products, i.e. vinegar of acetic acid fermentation process of carissa juice were in ranges of 2.64-2.69, 2.63-4.16% and 3.80-4.40 °Brix (Figure 1), respectively. It has been reported that a high concentration of acids during acetous fermentation is mainly related acetic acid produced by acetic acid bacteria (Song, 2016). The highest concentration of acetic acid was detected in the final vinegar product with honey as a carbon source and mixed yeast inoculum protocol, although the values of acidity were different depending on carbon sources and inoculation protocols used for fermentations. This could be possibly described by some nutrients found in honey might support microbial growth during alcoholic fermentation better than nutrients found in syrup (Mendes-Ferreira *et al.*, 2010), hence greater amount of acids was obtained. The yield of acids reached 87% in this study which could be improved via various tactics such as nutrient feeding strategy (Qi *et al.*, 2017), species selection (Treck *et al.*, 2016; Yuan *et al.*, 2017). The acetic acid concentration of 4.16% in the end product with honey and mixed yeast achieved the required standard of the Thai legislation as vinegar, in agreement with previous report (Viana *et al.*, 2017).

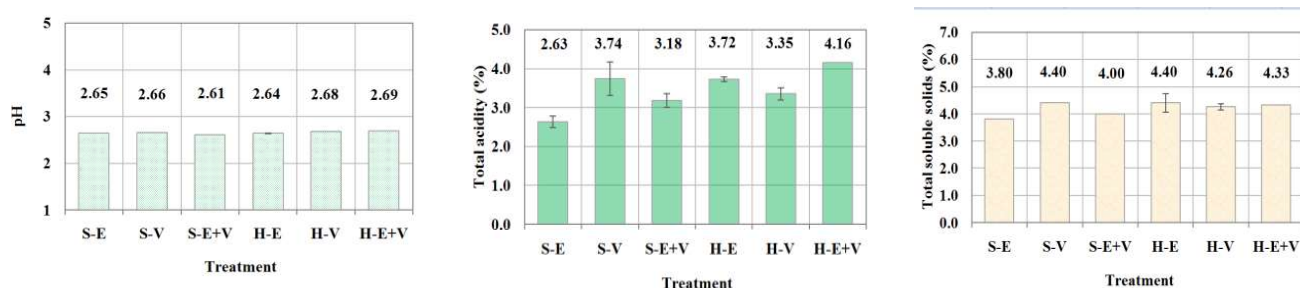


Figure 1 pH, total acidity and total soluble solid content of end products fermented by different carbon sources and inoculation protocols; fructose syrup with *S. cerevisiae* strain E (S-E), fructose syrup with *S. cerevisiae* strain V (S-V), fructose syrup with *S. cerevisiae* strain E and V (S-E+V), honey with *S. cerevisiae* strain E (H-E), honey with *S. cerevisiae* strain V (H-V) and honey with *S. cerevisiae* strain E and V (H-E+V)

Utilization of syrup and honey as carbon sources with different inoculation protocols of yeast culture for acetic acid fermentation process of carissa juice resulted in variation of chemical properties of free alpha amino nitrogen content, total anthocyanin content, total phenolic content and antioxidant activity in vinegars (Table 2). Considering FAN measurements in vinegars of this study, the values remained between 1.19-2.24 mg/L. It is generally agreed that a concentration exceeding 140 mg N/L is adequate for a low risk of sluggish or stuck fermentation (Ugliano *et al.*, 2007; Torrea *et al.*, 2011). This means that substrates used in this trial might not be a sufficient and efficient source of assimilable nitrogen to support yeast growth during its fermentation. However, many factors such as pH, temperature, oxygen, fermentation techniques could influence final constituents in the end products of alcoholic and acetous fermentation (Sengun and Karabiyikli, 2011; Krusong *et al.*, 2014).

Measurements of total anthocyanin content, total phenolic content and antioxidant activity were performed to understand the influence of fermentation conditions on compounds related health concern in vinegars. Little amounts of total phenolic were detected in the vinegars of this study in comparison to other reports (Cerezo *et al.*, 2010; Hidalgo *et al.*, 2013), whereas total phenolic contents were in ranges as previously reported (Andlauer *et al.*, 2000; Ubeda *et al.*, 2013). Antioxidant activity of vinegars were between 20.97 and 36.09 % ABTS scavenging effect which decreased approximately 30% compared to the carissa juice (Chomsri *et al.*, 2017). This reduction could be caused by many factors such as degradation during fermentation, substrate preparation and fermentation condition (Andlauer *et al.*, 2000; Ubeda *et al.*, 2013; Chomsri *et al.*, 2015).

Table 2 Chemical properties of vinegars fermented by different added carbon sources and inoculation protocols of yeast culture

Factors	FAN [†]	TAC [†]	TPC [†]	AOA [†]
Factor A	*	ns	*	*
Syrup (S)	1.63±0.36 ^b	0.57 ± 0.32	318.56 ± 7.37 ^a	32.40±3.10 ^a
Honey (H)	1.96±0.23 ^a	0.92 ± 0.68	307.65 ± 21.59 ^b	29.64±6.75 ^b
Factor B	*	ns	*	*
<i>S. cerevisiae</i> strain E (E)	1.55±0.41 ^c	0.69 ± 0.29	318.07 ± 6.35 ^b	35.27±1.39 ^a
<i>S. cerevisiae</i> strain V (V)	1.74±0.03 ^b	0.60 ± 0.37	297.50 ± 20.38 ^c	31.52±2.37 ^b
E + V	2.10±0.21 ^a	0.94 ± 0.88	323.75 ± 4.74 ^a	26.28±6.14 ^c
Interaction	*	*	*	*
S-E	1.19±0.02 ^c	0.57 ± 0.12 ^c	312.95 ± 3.53 ^d	36.09±1.61 ^a
S-V	1.75±0.05 ^b	0.90 ± 0.08 ^{ab}	315.00 ± 1.28 ^{cd}	29.53±0.60 ^d
S-E+V	1.96±0.19 ^b	0.25 ± 0.31 ^c	327.73± 1.28 ^a	31.59±0.30 ^{cd}
H-E	1.91±0.01 ^b	0.81 ± 0.42 ^{ab}	323.18 ± 1.93 ^{ab}	34.45±0.70 ^{ab}
H-V	1.75±0.03 ^b	0.31 ± 0.27 ^c	280.00 ± 4.49 ^c	33.52±0.80 ^{bc}
H-E+V	2.24±0.14 ^a	1.63 ± 0.57 ^a	319.78 ± 1.60 ^{bc}	20.97±0.60 ^c

ns denotes means are not significantly different ($p>0.05$); fructose syrup with *S. cerevisiae* strain E (S-E), fructose syrup with *S. cerevisiae* strain V (S-V), fructose syrup with *S. cerevisiae* strain E and V (S-E+V), honey with *S. cerevisiae* strain E (H-E), honey with *S. cerevisiae* strain V (H-V) and honey with *S. cerevisiae* strain E and V (H-E+V)

* Means in a column with the different letters represent significant differences ($p\leq0.05$)

[†] FAN = free alpha amino nitrogen content (mg/L), TAC = total anthocyanin content (mg/L),

TPC = total phenolic content (mg/L), AOA = antioxidant activity (% ABTS scavenging effect)

Sensory descriptive analysis revealed diversity of odor intensities as shown in Figure 2. Panelists evaluated pungent intensity of acetic acid to be a scale value of 4.88–7.36. This high intensity indicated the vinegar characteristics. There were no significant differences between the two carbon sources and the three inoculation protocols of yeast culture which might be due to a strong odor of acetic acid existing in the end products. However, the overall impression scale was rated at high scale value of 6.63-7.25 indicating desirable quality of carissa vinegars.

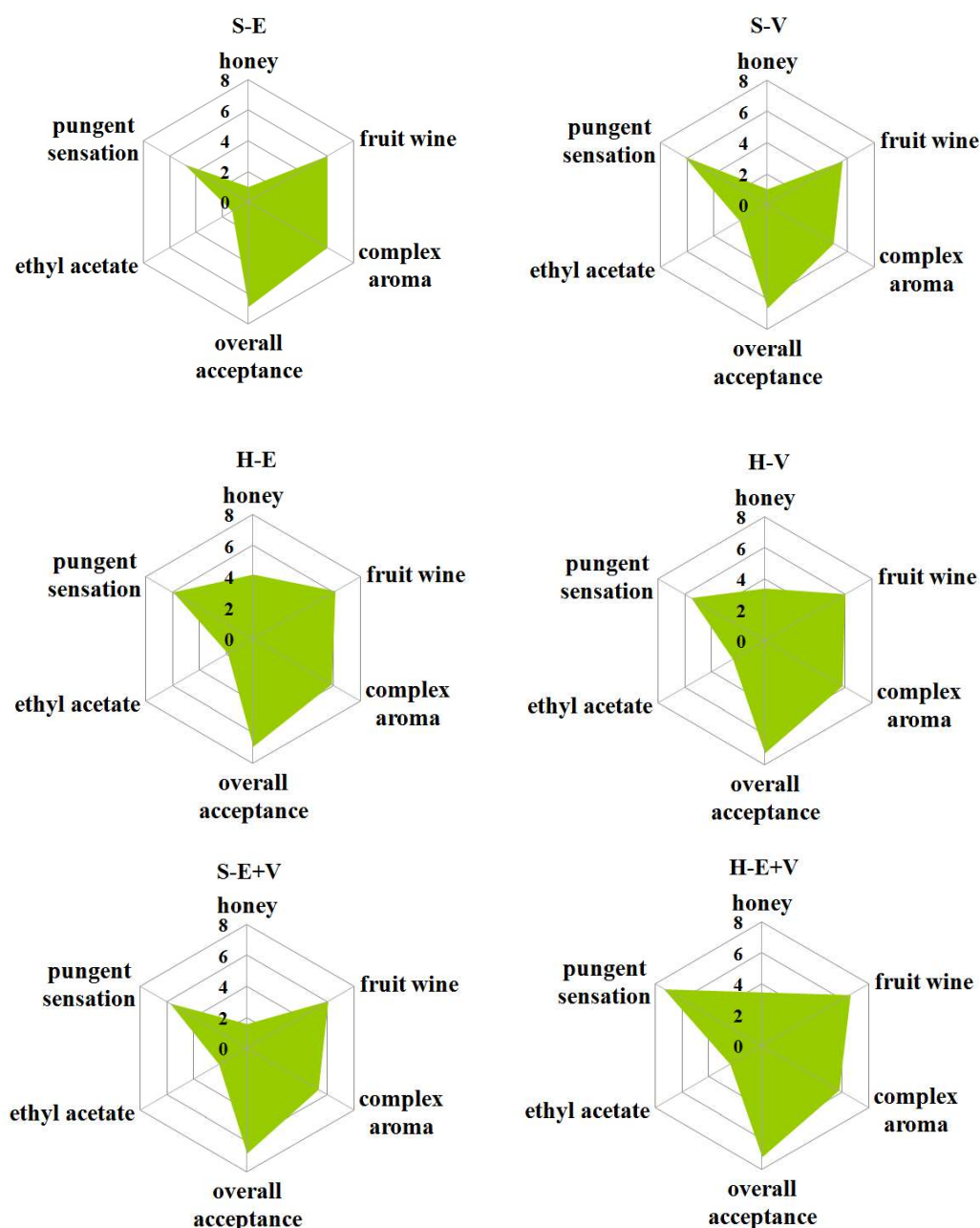


Figure 2 Sensory analysis of end products fermented by different added carbon sources and inoculation protocols of yeast culture; fructose syrup with *S. cerevisiae* strain E (S-E), fructose syrup with *S. cerevisiae* strain V (S-V), fructose syrup with *S. cerevisiae* strain E and V (S-E+V), honey with *S. cerevisiae* strain E (H-E), honey with *S. cerevisiae* strain V (H-V) and honey with *S. cerevisiae* strain E and V (H-E+V)

Conclusion

Utilization of syrup and honey as carbon sources with different yeast inoculation protocols of yeast culture for acetic acid fermentation process of carissa juice produced end products of vinegar with diversity of physicochemical and sensorial properties.

Acknowledgement

This present work was financed by Rajamangala University of Technology Lanna.

References

- Andlauer, W., Stumpf, C. and Furst, P. 2000. Influence of the acetification process on phenolic compounds. **Journal of Agricultural and Food Chemistry** 48: 3533-3536.
- Baena-Ruano, S., Jimenez-Ot, C., Santos-Duenas, I.M., Cantero-Moreno, D., Barja, F. and Garcia-Garcia, I. 2006. Rapid method for total, viable and non-viable acetic acid bacteria determination during acetification process. **Process Biochemistry** 41: 1160–1164.
- Bansal, L. 2014. *Carissa carandas* as a natural colourant and its effect on physical and fastness properties of silk. **An International Quarterly Journal of Biology & Life Sciences** 2 (2): 470-474.
- Belitz, H.D., Grosch, W. and Schieberle, P. 2009. **Food Chemistry**. Springer. Heidenberg.
- Bhadane, B.S. and Pati, R.S. 2017. Isolation, purification and characterization of antioxidative steroid derivative from methanolic extract of *Carissa carandas* (L.) leaves. **Biocatalysis and Agricultural Biotechnology** 10: 216–223.
- Cerezo, A.B., Cuevas, E., Winterhalter, P., Garcia-Parrilla, M.C. and Troncoso, A.M. 2010. Anthocyanin composition in Cabernet Sauvignon red wine vinegar obtained by submerged acetification. **Food Research International** 43: 1577–1584.
- Chomsri, N., Chanrittisen, T. and Thepkaew, N. 2010. Fermentation of pineapple juice to vinegar with different Inoculation protocols and its use for beverage production. **In The 2nd RMUTIC on Science and Technology Development in Creative Economy**. Bangkok, Thailand.
- Chomsri, N., Kampok, N. and Intaramoree, S. 2015. Supplementation of pineapple juice as co-substrate for apricot vinegar fermentation. **King Mongkut's Agricultural Journal** 33(Special Issue 1): 105-111.
- Chomsri, N. and Thepkaew, N. 2016. Co-cultures of non-conventional yeasts and *Saccharomyces cerevisiae* impact fermentation dynamics of pineapple wine. pp. 73-75. RMUTIC Proceeding: Creative Technology for All, **In The 7th Rajamangala University of Technology International Conference (7th RMUTIC)**. Rajamangala University of Technology Krungthep, Bangkok, Thailand.
- Chomsri, N., Yangprasert, J., Wongkeaw, P. and Manowan, K. 2017. Morphological and physicochemical properties of karanda (*Carissa carandas* L.) at the ripening stage based on different clones. pp. 135-141. **The 8th Rajamangala University of Technology International Conference (8th RMUTIC) “Creative RMUT and Sustainable Innovation for Thailand 4.0”**. IMPACT Muang Thong Thani Exhibition and Convention during 7-9 August 2017, Bangkok, Thailand.

- Deng, J., Liu, R., Lu, Q., Hao, P., Xu, A., Zhang, J. and Tan, J. 2018. Biochemical properties, antibacterial and cellular antioxidant activities of buckwheat honey in comparison to manuka honey. **Food Chemistry** 252: 243–249.
- Giusti, M.M. and Wrolstad, R.E. 2005. Characterization and Measurement of Anthocyanins by UV-Visible Spectroscopy, pp. 19-31, In: Wrolstad, R.E., ed. **Handbook of food analytical chemistry (Vol 2): pigment, flavors, texture and bioactive food components**. John Wiley and Sons. Inc., New Jersey.
- Hidalgo, C., Torija, M.J., Mas, A. and Mateo, E. 2013. Effect of inoculation on strawberry fermentation and acetification processes using native strains of yeast and acetic acid bacteria. **Food Microbiology** 34: 88-94.
- Iland, P., Ewart, A., Markides, A., Sitters, J. and Bruer, N. 2000. **Techniques for chemical analysis and quality monitoring during winemaking**. Patrick Iland Wine Promotions, Adelaide.
- Intaramoree, S. and Chomsri, N. 2014. Miso produced from different Thai rice cultivars: physicochemical and sensory characteristics. pp. 487-495. In K. Boonlertnirun, ed., **The 5th Rajamangala University of Technology International Conference: The Technology and Innovation toward ASEAN**. Rajamangala University of Technology Suvarnabhumi, Phranakhon Si Ayutthaya, Thailand.
- Johnston, C.S. 2009. **Medicinal Uses of Vinegar**. Complementary and Alternative Therapies and the Aging Population. Academic Press. Amsterdam.
- Joomwong, A. 2014. Effect of maturity stages on physical and chemical quality of *Carissa carandas* Linn. **Agricultural Science Journal** 45(3/1): 229-232.
- Khatun, M., Habib, M.R., Rabbi, M.A., Amin, R., Islam, M.F., Nurujjaman, M., Karim, M.R. and Rahman, M.H. 2017. Antioxidant, cytotoxic and antineoplastic effects of *Carissa carandas* Linn. Leaves. **Experimental and Toxicologic Pathology** 69(7): 469-476.
- Kubola, J., Siriamornpun, S. and Meeso, M. 2011. Phytochemicals, vitamin C and sugar content of Thai wild fruits. **Food Chemistry** 126: 972–981.
- Krusong, W., Pornpukdeewatana, S., Kerdpi boon, S. and Tantratian, S. 2014. Prediction of influence of stepwise increment of initial acetic acid concentration in charging medium on acetification rate of semicontinuous process by artificial neural network. **LWT - Food Science and Technology** 56: 383-389.
- Mehmood, M.H., Anila, N., Begum, S., Syed, S.A., Siddiqui, B. S. and Gilani, A.H. 2014. Pharmacological basis for the medicinal use of *Carissa carandas* in constipation and diarrhea. **Journal of Ethnopharmacology** 153: 359 – 367.
- Meilgaard, H., Civille, G.V. and Carr, B.T. 2006. **Sensory evaluation techniques**. CRC Press. Boca Raton.
- Mendes-Ferreira, A., Cosme, F., Barbosa, C., Falco, V., Inês, A. and Mendes-Faia, A. 2010. Optimization of honey-must preparation and alcoholic fermentation by *Saccharomyces cerevisiae* for mead production. **International Journal of Food Microbiology** 144: 193–198.
- Miranda, B., Lawton, N.M., Tachibana, S.R., Swartz, N.A. and Hall, W.P. 2016. Titration and HPLC characterization of Kombucha fermentation: a laboratory experiment in food analysis. **Journal of Chemical Education** 93: 1770–1775.
- Mounir, M., Shafiei, R., Zarmehrkhorsid, R., Hamouda, A., Alaoui, M.I. and Thonart, P. 2016. Simultaneous production of acetic and gluconic acids by a thermotolerant *Acetobacter* strain during acetous fermentation in a bioreactor. **Journal of Bioscience and Bioengineering** 121(2): 166-171.

- Pure, A.E., Mofidi, S.M.G., Keyghobadi, F. and Pure, M.E. 2017. Chemical composition of garlic fermented in red grape vinegar and kombucha. **Journal of Functional Foods** 34: 347–355.
- Park, S.Y., Kang, S. and Ha, S. 2016. Antimicrobial effects of vinegar against norovirus and *Escherichia coli* in the traditional Korean vinegared green laver (*Enteromorpha intestinalis*) salad during refrigerated storage. **International Journal of Food Microbiology** 238: 208–214.
- Qi, Z., Dong, D., Yang, H. and Xia, X. 2017. Improving fermented quality of cider vinegar via rational nutrient feeding strategy. **Food Chemistry** 224: 312–319.
- Sengun, I.Y. and Karabiyikli, S. 2011. Importance of acetic acid bacteria in food industry. **Food Control** 22: 647–656.
- Shen, F., Feng, J., Wang, X., Qi, Z., Shi, X., An, Y., Zhang, Q., Wang, C., Liu, M., Liu, B. and Yu, L. 2016. Vinegar treatment prevents the development of murine experimental colitis via inhibition of inflammation and apoptosis. **Journal of Agricultural and Food Chemistry** 64: 1111–1121.
- Siritrakulsak, P., Ounmahong, C., Simla, S., Kunlanit, B. and Benchasri, S. 2016. Storage life extension of karandas (*Carissa carandas* L.) fruits. **Songklanakarin Journal of Plant Science** 3(Suppl. I): M07/33–39.
- Song, N., Cho, H. and Baik, S. 2016. Bacteria isolated from Korean black raspberry vinegar with low biogenic amine production in wine. **Brazilian journal of microbiology** 47: 452–460.
- Spínola, V., Pinto, J. and Castilho, P.C. 2015. Identification and quantification of phenolic compounds of selected fruits from Madeira Island by HPLC-DAD–ESI–MSn and screening for their antioxidant activity. **Food Chemistry** 173: 14–30.
- Thepkaw, N. and Chomsri, N. 2013. Fermentation of pineapple juice using wine yeasts: kinetics and characteristics. **Asian Journal of Food and Agro-Industry** 6(1): 1–10.
- Torrea, D., Varela, C., Ugliano, M., Ancin-Azpilicueta, C., Francis, L. and Henschke, P.A. 2011. Comparison of inorganic and organic nitrogen supplementation of grape juice—effect on volatile composition and aroma profile of a Chardonnay wine fermented with *Saccharomyces cerevisiae* yeast. **Food Chemistry** 127: 1072–1083.
- Trček, J., Mahnič, A. and Rupnik, M. 2016. Diversity of the microbiota involved in wine and organic apple cider submerged vinegar production as revealed by DHPLC analysis and next-generation sequencing. 2016. **International Journal of Food Microbiology** 223: 57–62.
- Ubeda, C., Callejón, R.M., Hidalgo, C., Torija, M.J., Troncoso, A.M. and Morales, M.L. 2013. Employment of different processes for the production of strawberry vinegars: effects on antioxidant activity, total phenols and monomeric anthocyanins. **LWT - Food Science and Technology** 52: 139–145.
- Ugliano, M., Henschke, P.A., Herderich, M.J. and Pretorius, I.S. 2007. Nitrogen management is critical for wine flavour and style. **Wine Industry Journal** 22(6): 24–30.
- Vaclavik, V.A. and Christian, E.W. 2008. **Essentials of Food Science**. Springer. Dallas.
- Viana, R.O., Magalhães-Guedes, K.T., Braga Jr., R.A., Dias, D.R. and Schwan, R.F. 2017. Fermentation process for production of apple-based kefir vinegar: microbiological, chemical and sensory analysis. **Brazilian journal of microbiology** 48: 592–601.
- Wani, R.A., Prasad, V.M., Hakeem, S.A., Sheema, S., Angchuk, S. and Dixit, A. 2013. Shelf life of Karonda jams (*Carissa carandas* L.) under ambient temperature. **African Journal of Agricultural Research** 8(21): 2447–2449.

- Wongputtisris, P., Khanongnuch, C., Pongpiachan, P. and Lumyoung, S. 2007. Antioxidant activity improvement of soybean meal by microbial fermentation. **Research Journal of Microbiology** 2(7): 577-583.
- Wood, B.J.B. 1998. **Microbiology of fermented foods**. Blackie Academic and Professional. London.
- Yuan, H., Tan, L., Chen, H., Sun, Y., Tang, Y. and Kida, K. 2017. Vinegar production from post-distillation slurry deriving from rice *shochu* production with the addition of caproic acid-producing bacteria consortium and lactic acid bacterium. **Journal of Bioscience and Bioengineering** 124(6): 653-659.
- Yuenyongphutthakal, W., Khongsomphet, S. and Weeraphae, P. 2012. Drying of Karanda (*Carissa carandas*) pomace and its tablet product. **KKU Science Journal** 40(3): 877-889.

Poster Presentation

The 9th Rajamangala University of Technology
International Conference
RMUT Driving Innovation for Thailand 4.0

Analysis of Heavy Metals Using 5-amino Levulinic Acid (ALA)-Chitosan Modified Electrodes

Rattiya Saradit^{1*}

ABSTRACT

This research describes the preparation and modification of electrodes with 5-amino levulinic acid (ALA)-chitosan. The electrochemical characterization and optimum parameters of ALA-chitosan modified electrodes were investigated by cyclic voltammetry. The results show that the ALA-chitosan modified electrode is effective in measuring lead due to the high current and stable voltage. The optimal conditions were sodium acetate solution at pH 7 as supporting electrolyte, a scan rate of 0.6 V/s, a deposition time of 80 s, an equilibration time of 20 s. and a correlation coefficient of 0.995.

Keywords: Modified electrode, Chitosan, 5-amino levulinic acid

¹ Department of Science, Faculty of Science and Technology, Rajamangala University of Technology Srivijaya, Thungsong, Nakhon Si Thammarat, 80110, Thailand

*Corresponding author e-mail: kek315@hotmail.com

Introduction

The techniques that have been employed for the determination of trace metal ions include atomic absorption spectrometry (AAS), inductively coupled plasma-mass spectrometry (ICP-MS), and inductively coupled plasma-optical emission spectrometry (ICP-OES) and electrochemical techniques. Spectroscopic techniques are very expensive and require preconcentration. Electroanalytical techniques can be considered the most powerful techniques due to their excellent detection limits, high sensitivity, capacity for multielement determination, high speed, simplicity, and relatively low cost. Mercury has been the most commonly used electrode material in various configurations for electrochemical determination of trace metal ions. Despite advantages such as the formation of amalgam and high overvoltage for gases, among others, there have been numerous attempts to replace mercury, which is well-known for its toxicity, with a nontoxic or less-toxic electrode material (Pipat, 2017).

In recent years, researchers in electrochemical method applications of chemically modified electrodes (CMEs) have shown great interest in various areas of research and development for electrocatalysis, electronics, biosensors and electroanalysis (Martínez-Huitle *et al.*, 2010). CMEs are electrodes with chemically active species, resulting from the immobilization of a modifying agent on the surface of a base electrode in order to preset and control the physical-chemical nature of the electrode-solution interface as a means of altering the reactivity and selectivity of the base sensor (Souza, 1997). The modification of these electrodes can be performed in several ways and using different materials. Chitosan has been identified as an effective reactant for chemical extraction and determination of metals. The NH₂ groups of chitosan can react with aldehydes or ketones to form imines (Nuriye *et al.*, 2012). It has been reported that chitosan Schiff bases have excellent chelation ability with heavy metal ions. Multidentate Schiff bases have been widely used as ligands, because they can be easily attached to metal ions due to the formation of highly stable coordination compounds. In addition, these compounds have been recently used as ionophores in metal sensors (Kucukkolbasi *et al.*, 2013).

Carbon paste electrodes (CPE) have drawn the attention of researchers in recent years for their desirable properties, including the ease of preparation and the detection applications (Lu *et al.*, 2001). Therefore, the aim of this work was to prepare and modify electrodes with 5-amino levulinic acid (ALA). Cyclic voltammetry was used to investigate the optimum parameters and determine trace amounts of heavy metals.

Materials and methods

1. Preparation of 5-amino levulinic acid-Chitosan particles (ALA-C)

Chitosan (150 mg) was dissolved in 10 ml of 2% acetic acid and added to 990 ml of ALA solvent, following sonicate for 40 seconds at 120 watts on an ice bath. The reaction mixture was then magnetic stirred for 4 hours and centrifuged to precipitate at a speed of 12,000 rpm and 4 °C for 15 minutes. The nanoparticles were collected in clear 15% mannitol before being freeze dried.

2. Preparation of carbon paste modified by ALA-chitosan (ALA-CCPE)

The modified carbon paste electrode (ALA-CCPE) was prepared by hand-mixing 73.7% graphite powder and 5.3% ALA-C, followed by mixing with 21% paraffin oil in a mortar for approximately 10 min to form a homogeneous solution. The mixture was placed in the inner hole of the working electrode body. The electrode surface was polished with a weight paper

until shiny. It was used directly for voltammetric measurements without preconditioning. The electrodes were only washed with distilled water and stored in a refrigerator at +4 °C when not in use (Kucukkolbasi *et al.*, 2013).

3. Analytical Procedure

25 ml of 0.2 mol/L sodium acetate solution and 3 ml of standard solution (1×10^{-3} mol/L) were added in a measuring vessel. The three-electrode system consisted of ALA-CCPE as a working electrode, platinum wire as a counter electrode and Ag/AgCl electrode as a reference electrode. Nitrogen gas was purged for 3 min to eliminate interfering oxygen. The electrochemical behavior of ALA-CCPE was examined by cyclic voltammetry (CV). The optimum conditions for the modified electrode, including electrolyte solution, pH, scan rate, deposition time and equilibration time, were studied with the same method.

Results and Discussion

1. Electrochemical behaviors of copper and lead

The electrochemical behaviors of the Cu(II) and Pb(II) ions on the carbon paste electrode modified with 5-amino levulinic acid-chitosan were studied in terms of the effect on cyclic voltammetry.

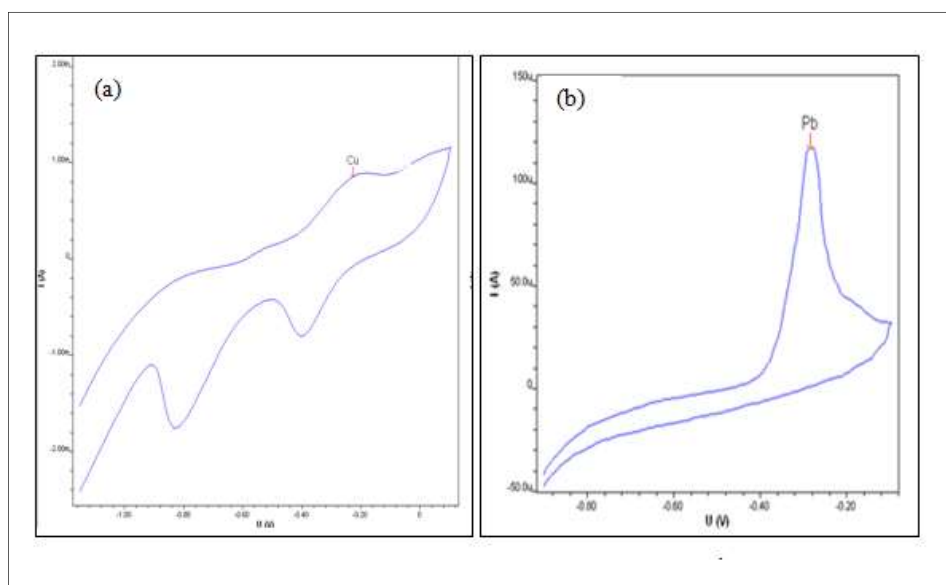
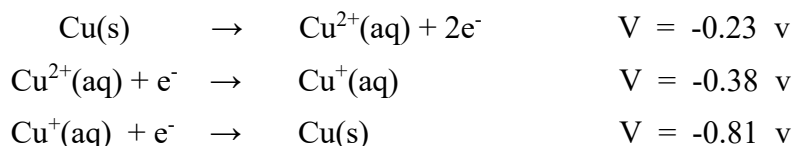


Figure 1 Cyclic voltammograms of (a) Cu(II) and (b) Pb(II) at ALA-chitosan modified electrode

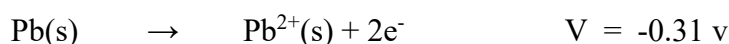
ALA-Chitosan Carbon Paste Electrode (ALA-CCPE) was used for the study of electrochemical behavior of the copper content by using Cyclic Voltammetry. The oxidation peak was carried out at -0.23 V and the current was 0.78 μ A. The reduction peak, carried out at -0.38 and -0.81 V, gave currents of -107 mA and -185 mA, respectively. The electrochemical behavior of lead showed the oxidation peak at -0.31 V, giving a current of 140 mA, as shown in Figure 1.

The voltammetric peak of Pb (II) was observed to be higher than Cu(II) at the modified carbon paste electrode. The result indicates that CNSB can greatly promote the preconcentration of Pb(II) and significant increase the sensitivity of the determination of Pb(II). The results show that the modified carbon paste electrode is an efficient sensor for the sensitive determination of Pb(II) ions.

The redox reaction of Cu(II) on ALA-CCPE



The oxidation reaction of Pb(II) on ALA-CCPE



2. Optimization of analytical conditions

2.1 pH and supporting electrolyte

The influence of pH of the solutions on the Pb(II) signal was investigated in the range of 3.0-10.0 in the presence of 1000 mg/L Pb(II). The peak current increased with an increase of pH from 3 to 7 and decreased above pH 8 (Figure 2). At lower pH (pH<5) and higher pH (pH>8) the modifier loses its ability to complex with Pb(II), and the peak current decreases because the degradation of ALA-C takes place and the ability to immobilize Pb(II) is lost (Martínez-Huitle *et al.*, 2010). Furthermore, at higher pH, the peak current decreased and the peak shape was deformed due to the hydrolysis of Pb(II) in basic solution (Rong *et al.*, 2009). The peak current reached a maximum value around pH of 7.0. To achieve maximum sensitivity, the pH 7.0 was used in all subsequent experiments.

The supporting electrolyte can greatly affect the voltammetric response of the sensor. The effect of various supporting electrolytes (HCl, NaNO₃, KNO₃ and NaAc solutions) on the stripping peak currents of Pb(II) was investigated at pH 7.0. The best voltammetric results were obtained in NaAc solution including HCl, NaNO₃, KNO₃ and NaAc, solutions.

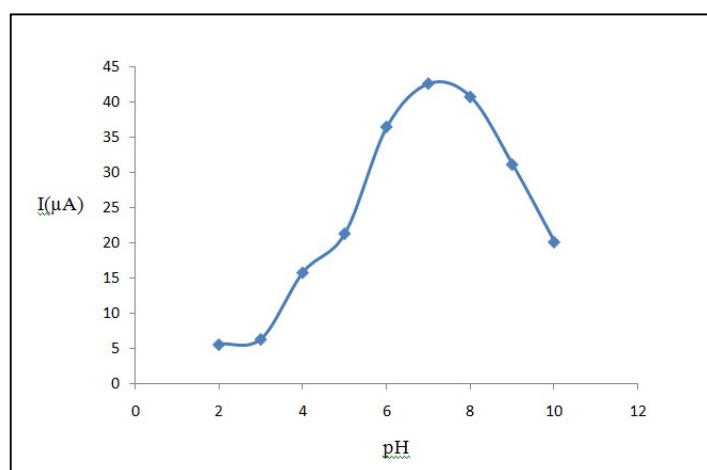


Figure 2 The relationship of peak current and pH of Pb(II) standard solution in NaAc (pH 7) as electrolyte solution at ALA-Chitosan modified electrode

2.2 Scan rate

The influence of the scan rate of the solutions on the Pb(II) signal was investigated in the range of 0.1-1 V/s. in the presence of 1000 mg/L Pb(II). The peak current increased with the increase of the scan rate to 0.6 V/s (Figure 3). The scan rate at 0.6 V/s was used in all subsequent experiments.

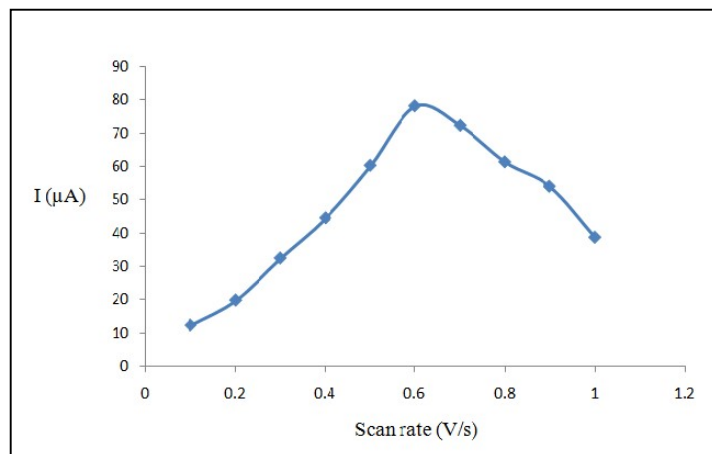


Figure 3 The relationship of peak current and scan rate of of Pb(II) standard solution in NaAc (pH 7) as electrolyte solution at ALA-Chitosan modified electrode

2.3 Deposition time and Equilibration time

Deposition time can apparently influence the determination of Pb(II). The peak current was investigated in the range of 0-100 s in the presence of 1000 mg/L Pb(II). The peak current increased with the increase of deposition time to 80 s, after which the current decreased (Figure 4). The surface of the modified electrode was completely covered by Pb(II), which resulted in distortions of observed peaks. Taking into account sensitivity, repeatability and efficiency, the accumulation time of 80 s was used in all following experiments.

Equilibration time was investigated in the range of 5-30 s. in the presence of 1000 mg/L Pb(II). The peak current increased with the increase of equilibration time to 20 s (Figure 5). The equilibration time at 20 s was used in all subsequent experiments.

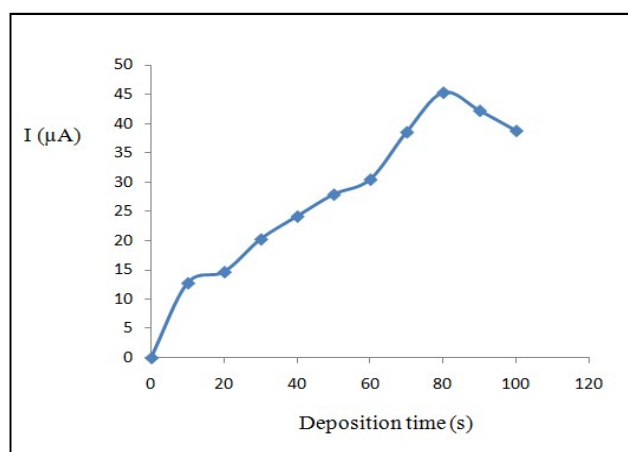


Figure 4. The relationship of peak current and deposition time of Pb(II) standard solution in NaAc (pH 7) as electrolyte solution at ALA-Chitosan modified electrode

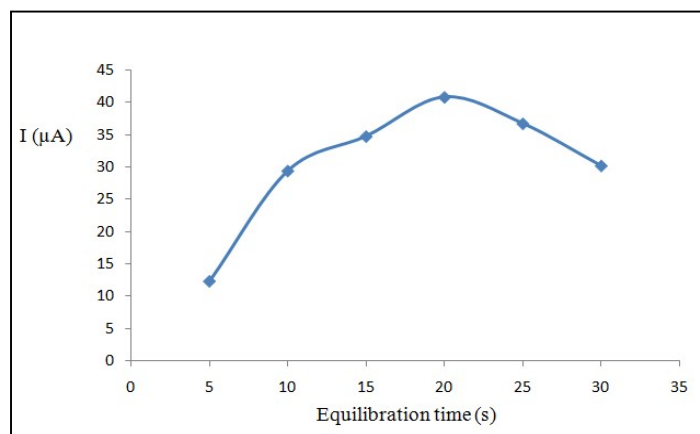


Figure 5. The relationship of peak current and equilibration time of Pb(II) standard solution in NaAc (pH 7) as electrolyte solution at ALA-Chitosan modified electrode

2.4 Linear range and detection limit

The peak current is related to Pb(II) concentration over the range of 1 to 100 $\mu\text{g/l}$ with a linear regression correlation coefficient of 0.995. The detection limit of Pb(II) by developed method under the optimized conditions is 40 $\mu\text{g/l}$.

Conclusion

Chitosan was successfully synthesized by ionotropic gelation of chitosan and 5-amino levulinic acid. Chitosan-bound Schiff bases of 5-amino levulinic acid were then prepared. The synthesized compound can be used as a modifier in carbon paste electrodes (CPE). The most successful aspect of this work was to prepare a simple and selective sensor for Pb(II) by using a chitosan-modified carbon paste electrode.

Acknowledgement

The author would like to thank the Department of Science of the Faculty of Science and Technology, Rajamangala University of Technology Srivijaya, Nakhon Si Thammarat Campus for supporting this research by providing funds and laboratory facilities.

References

- Deng, P., Xu, Z., Feng, Y. and Li, J. 2012. Electrocatalytic reduction and determination of p-nitrophenol on acetylene black paste electrode coated with salicylaldehyde-modified chitosan, pp. 381-389. **Sensors and Actuators**.
- Hiroshi, I., Maiko, M., Boonma, L. and Tomoyo, I. 1994. Synthesis of chitosan-amino acid conjugates and their use in heavy metal uptake. *International Journal of Biological Macromolecules*. 17: 21-23.
- Kucukkolbasi, S., Erdogan, Z.Ö., Barek, J., Sahin, M., and Kocak, N. 2013. A novel chitosan nanoparticle-Schiff base modified carbon paste electrode as a sensor for the determination of Pb(II) in waste water. **International Journal of Electrochemical Science**. 8: 2164-2181.

- Lu, G., Yao, X., Wu, X. and Zhan, T. 2001. Determination of the total iron by chitosan-modified glassy carbon electrode. **Microchemical Journal**. 69: 81-87.
- Martínez-Huitle, C. A., Suely, F. N., Cerro-Lopez, M., Quiroz, M. A. 2010. Determination of trace metals by differential pulse voltammetry at chitosan modified electrodes, pp. 39-49. **Portugaliae Electrochimica Acta**.
- Nuriye, K., Mustafa, S., Semahat, K. and Zehra, O. E. 2012. Synthesis and characterization of novel nano-chitosan Schiff base and use of lead(II) sensor. **International Journal of Biological Macromolecules**. 51: 1159-1166.
- Ng, J. C. Y., Cheung, W. H., and McKay, G. 2002. Equilibrium studies of the sorption of Cu(II) ions onto chitosan. **Journal of Colloid and Interface Science**. 255: 64-74.
- Pipat, C. 2017. Modified electrodes for determining trace metal ions, pp. 129-152. *In* Roumen, Z. and Stoytcheva, M., eds. **Applications of the Voltammetry**. Available at IntechOpen. DOI: 10.5772/intechopen.68193.
- Rong, M.W., Nai, P.H., Peng, F.S., Yu, F.H., Lan, D. and Zi, Q. L. 2009. Preparation of nano-chitosan Schiff-base copper complexes and their anticancer activity. **Polymers Advanced Technologies**. 20(12): 959-964.
- Souza, M.F.B., 1997. Eletrodos quimicamente modificados aplicados à eletroanálise: Uma breve abordagem. **Quimica Nova**. 20: 191-195.
- Ye, X., Yang, Q., Wang, Y. and Li, N. 1998. Electrochemical behaviour of gold, silver, platinum and palladium on the glassy carbon electrode modified by chitosan and its application. **Talanta**. 47: 1099-1106.
- Zheng, M., Gao, F., Wang, Q., Cai, X., Jiang, S., Huang, L. and Gao, F. 2013. Electrocatalytical oxidation and sensitive determination of acetaminophen on glassy carbon electrode modified with grapheme–chitosan composite. **Materials Science and Engineering C**. 33:1514-1520.

Mechanical Properties and Swelling of Natural Rubber Vulcanizate Filled with Rice Bran Carbon

Darinya Moonchai^{1*}, Philaiwan Pornprasit¹, Vimol Donmoon¹, and Sasidhorn Chanputdha¹

ABSTRACT

In this research, rice bran carbon (RBC) was used as a filler in natural rubber. The effects of RBC on swelling and mechanical properties of natural rubber vulcanizate were investigated. RBC was prepared using a carbonization temperature of 600 °C for 60 min. The particle size of RBC was 74-102 µm. Filler content was varied at 0, 10, 20, 30, 40 50 and 60 phr (parts per hundred of rubber). The results indicated that an increased RBC loading caused an increase in hardness, modulus and swelling resistance. In addition, increasing the RBC loading caused a decrease in tensile strength, elongation at break and rebound resilience. The properties of the RBC-filled natural rubber vulcanizate were also compared with industrial grade carbon black (N330)-filled natural rubber vulcanizate. At similar filler loading, carbon black (N330) gave higher tensile strength, modulus, hardness and swelling resistance. However, RBC-filled natural rubber vulcanizate showed higher elongation at break and gave higher rebound resilience at 30-60 phr of filler.

Keywords: Natural rubber, Rice bran carbon, Carbon black, Swelling, Mechanical properties

¹Rubber and Polymer Technology Program, Faculty of Engineering and Agricultural Industry, Maejo University, Chiang Mai 50290, Thailand

*Corresponding author e-mail: darinyamoonchai@gmail.com

Introduction

Carbon black is known as the most effective reinforcing filler for rubbers. The incorporation of carbon black normally increases tensile strength, tear strength, modulus and abrasion resistance of rubber compounds (Li *et al.*, 2014). However, carbon black is a non-renewable material. The use of renewable materials as fillers for natural rubber (NR) compounds by several natural resources such as rice husk ash, fiber, starch, chitin and defatted rice bran has become an issue of major interest (Sai-Oui *et al.*, 2002; Gopalan and Dufresne, 2003; Lin *et al.*, 2004; Arayaprane and Rempel, 2008; Mondragon *et al.*, 2009; Kanking *et al.*, 2012; Moonchai *et al.*, 2012; Moonchai and Moonchai, 2013; Moonchai *et al.*, 2016). Fillers derived from renewable materials have attracted interest because of their low cost, renewability and environment-friendly nature. However, most renewable materials have no reinforcement ability.

Rice bran, a low-value agriculture waste, is a by-product of the rice-milling process. It is also the source of high quality edible oil. Rice bran oil is extracted from rice bran, leaving defatted rice bran (DRB) as a by-product. DRB still contains significant amounts of protein, carbohydrate, dietary fibre and phenolic substances (Wiboonsirikul *et al.*, 2007). Moonchai *et al.* (2012) studied the use of DRB as a filler in NR. According to the results, DRB exhibited no reinforcement ability on the rubber compounds because of its large particle size. The particle size has a strong influence on the reinforcement ability of fillers (Kumar and Gupta, 1998).

In this work, carbonization was used to reduce the particle size of DRB in order to improve the reinforcement ability of DRB. RBC was produced from the carbonization of DRB at 600°C for 60 min. The effects of RBC on swelling, and mechanical properties of vulcanized NR were investigated. The properties of the RBC-filled natural rubber vulcanizate were also compared with industrial grade carbon black (N330)-filled natural rubber vulcanizate.

Materials and Methods

1. Preparation of rice bran carbon

RBC was obtained from the carbonization of DRB at 600°C for 60 min using an electrically heated furnace (model TNF-66-3, TCR-TYPE PY-55, Paragon). The DRB was passed through a 40-mesh screen before the carbonization. The particle size obtained by particle analyzer laser (Malvern, Mastersizer) was 74-102 µm. The chemical compositions of RBC were determined by X-ray fluorescence spectrometer (JEOL, JSX-340). It was found that the RBC consisted of MgO, SiO₂, P₂O₅, K₂O, CaO, MnO, Fe₂O₃ and ZnO.

2. Materials and preparation of rubber compounds

All mixing ingredients were used as received. NR (STR 20), elemental sulphur (2.5 phr), stearic acid (2 phr), zinc oxide (4 phr), accelerators, paraffinic oil (3 phr), and antioxidant (Lowinox® CPL, 1 phr) were purchased from Lucky Four Co. Ltd. (Thailand). Two types of accelerators were used: dibenzothiozyl disulphide (Vulkacit® MBTS, 1 phr) and tetramethylthiuram disulphide (Vulkacit® TMTD, 0.5 phr). Stearic acid and zinc oxide were of rubber grade. Two fillers were used: RBC (varied; 0-60 phr) and carbon black (N330, varied; 0-60 phr). N330 was purchased from Lucky Four Co. Ltd.

Mixing was carried out in a two-roll mill (model YFTR-8). The rubber compounds were then compression-moulded at 150°C using a hydraulic hot press (OOMN semi-automatic

moulding press model HPC-100(D)) according to their respective cure times (t_{90}) from the cure curves. The cure time (t_{90}) was measured using a moving die rheometer (model UR-2010) that was operated at 150°C with 3° arc for 60 min, following ISO 6502.

3. Swelling test

The swelling test was performed to determine the swelling behavior of vulcanized rubber samples when immersed in toluene. The samples with 1 x 1 x 0.2 cm³ were used to study the swelling behavior. Swelling behavior was determined by the change in mass. The rubber vulcanized test pieces of known weight (W_1) were immersed in toluene in test bottles and kept at room temperature for 96 hours until values with ± 0.0001 g precision were obtained. Samples were removed from the bottles and the wet surfaces were quickly wiped using tissue paper and re-weighted (W_2). The swelling of filled-NR vulcanizates was calculated as following: Percentage swelling = $(W_2 - W_1 / W_1) \times 100$, where, W_1 is the initial weight and W_2 is the swollen weight.

4. Mechanical properties test

The tensile properties were determined using an Instron universal testing machine (model 5569, Instron Corp., USA) with a crosshead speed of 500 mm/min., and 1-kN load cell. The specimens were stamp-cut from a 2-mm-thick compression-moulded sheet. The dimension of the test specimens used was type I according to ISO 37. The specimens were symmetrically placed at the grips of the testing machine to achieve uniform tension distribution over the cross section. The tensile strength was determined from stress at rupture while the modulus at 100% strain was evaluated from the tensile stress at 100% elongation. The elongation at break was also determined. The sample hardness was determined using a Shore A durometer (model HPE-A, Bareiss, Germany) in accordance with ASTM D2240-05. It was determined at three different positions on the specimens (about 6-mm thick) and the median value was indicated. The rebound resilience was determined according to DIN 53512 using a rebound tester (Rebound Check-Pendolo Shob). The rebound resilience was calculated as follows: Percentage resilience = $(1 - \cos \alpha) \times 100$, where α is the maximum rebound angle.

Results and Discussion

1. Swelling

Figure 1 shows the swelling values of natural rubber vulcanizates filled with RBC and N330. It was observed that the swelling decreased with an increase in filler loading. The swelling is affected by several factors, including crosslink density, filler dispersion in the NR and nature of the filler (Ekebafe *et al.*, 2010). The crosslink density of the NR vulcanizates is related to the swelling; higher swelling means a lower crosslink density. Decreasing the swelling values and increasing the filler content showed the extent of crosslinking of the filled-NR vulcanizates. Moreover, the swelling decreased with increasing filler content because each filler particle acted as an obstacle to the diffusion molecules and thus reduced the amount of penetrant solvent (Ekebafe *et al.*, 2010). Compared to N330-filled NR vulcanizate, RBC-filled NR vulcanizate exhibited lower swelling resistance. Therefore, it can be concluded that N330 gave higher crosslink density. The additional crosslinks are formed on the filler surface and the carbon black particles acted as giant crosslinks, resulting in the swelling restriction of N330-filled NR vulcanizate.

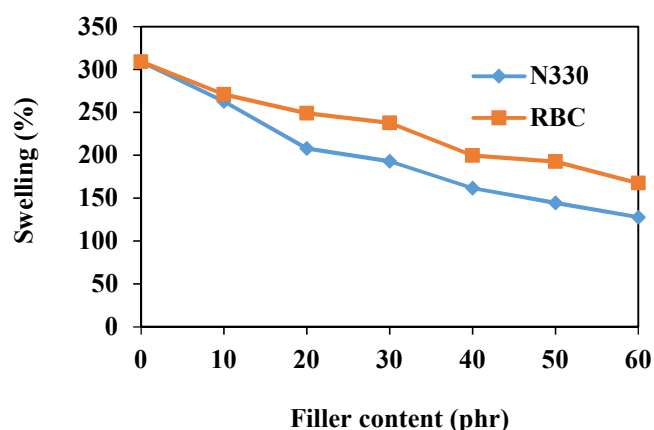


Figure 1. Swelling of NR vulcanizates with different fillers

2. Mechanical properties

In this study, the effects of RBC on the mechanical properties were studied. The mechanical properties were also compared with industrial grade carbon black (N330). The results are shown in Figure 2-6. It was observed that the filler loading affected the most of mechanical properties of NR vulcanizates for both the RBC and N330. An increasing of filler loading of RBC caused a decrease in the tensile strength, elongation at break and rebound resilience while hardness and modulus increased. The addition of N330 in the NR vulcanizate caused an increase in the tensile strength, hardness, modulus and a decrease in the elongation at break and rebound resilience. The increase of tensile strength of N330-filled NR vulcanizate is due to the reinforcing effect of carbon black. The elongation at break decreased with an increasing of filler content. This trend may be attributed to the fact that both crosslink density and rigid filler-rubber interface increase with the increasing of filler content. This can be also observed by an increasing of modulus and hardness. The rebound resilience dropped with an increasing of filler content. This is simply attributed to the dilution effect, because it is well known that the rubber portion gives an elastic property as measured in term of the rebound resilience (Sae-Oui *et al.*, 2009).

Compared to N330-filled NR vulcanizate, the RBC-filled NR vulcanizate showed lower tensile strength, modulus and hardness but it gave higher elongation at break and higher rebound resilience at 30-60 phr of filler loading. From the results, the improvement of the tensile strength of N330-filled NR vulcanizate is due to the reinforcement ability of N330. This observation could be attributed to the fact that apart from filler loading, other factors, such as particle size, structure and nature of filler play significant roles in determining the reinforcement ability of the fillers. The improved reinforcement which is given by N330 may be attributed to the small particle size and its surface properties. N330 is an industrial grade carbon black which has a small particle size (83 nm). RBC exhibited a large particle size with 74-102 μm , which may contribute to the lower-reinforcement ability of RBC. Aguele and Madufo (2012) also reported that the modulus of carbon black NR vulcanizate was higher than that of carbonized coir NR vulcanizate. This behavior can be explained by the fact that adhesion occurred between the carbon black and the rubber matrix, which led to the increase in stiffness, rigidity, and hence the modulus. Generally, the hardness is related to the rebound resilience of NR vulcanizates: highly stiff materials show lower rebound resilience (Moonchai and Moonchai, 2013). Therefore, the RBC-filled NR vulcanizate with lower hardness showed higher rebound resilience.

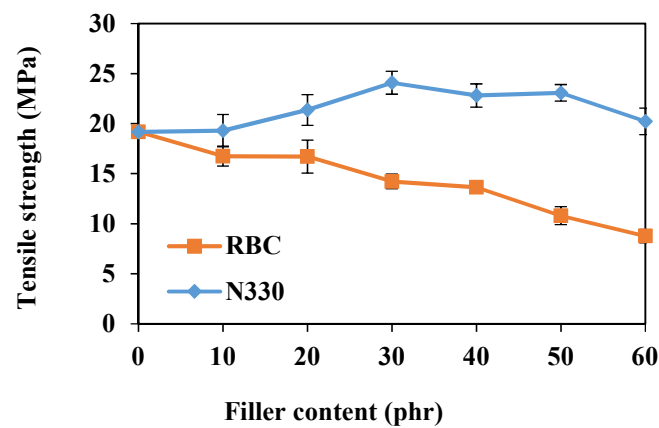


Figure 2. Tensile strength of NR vulcanizates with different fillers

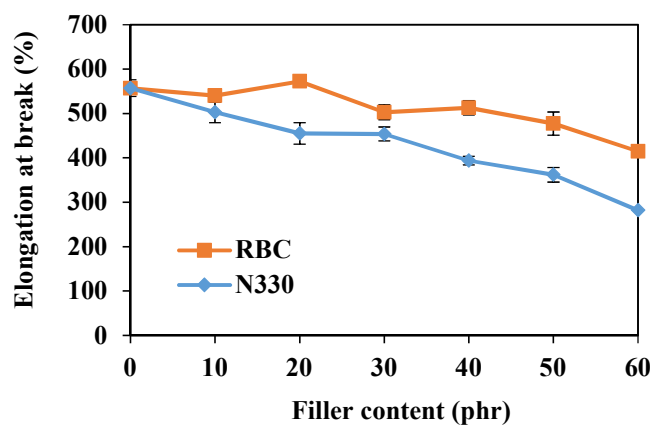


Figure 3. Elongation at break of NR vulcanizates with different fillers

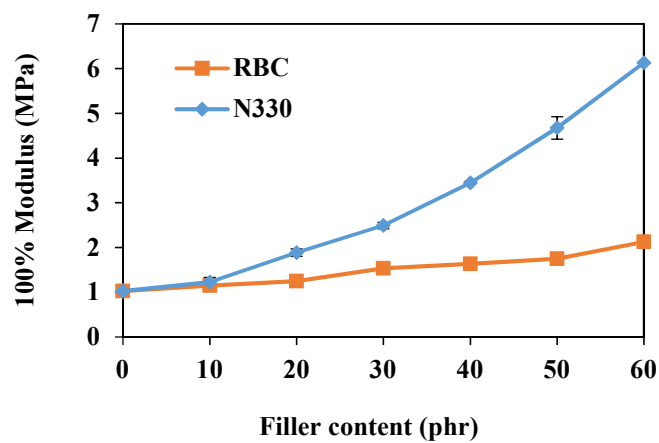


Figure 4. 100% Modulus of NR vulcanizates with different fillers

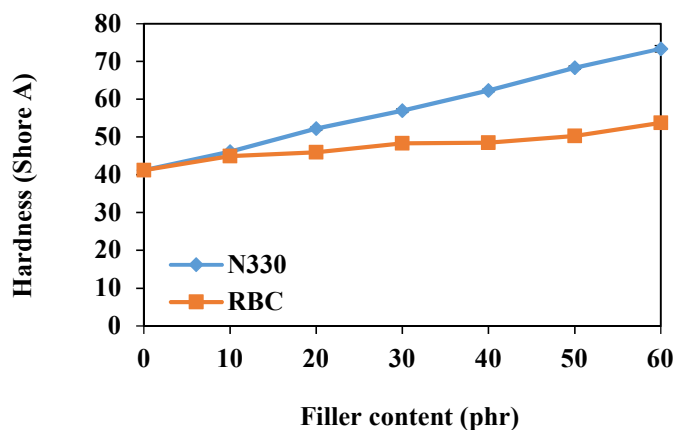


Figure 5. Hardness of NR vulcanizates with different fillers

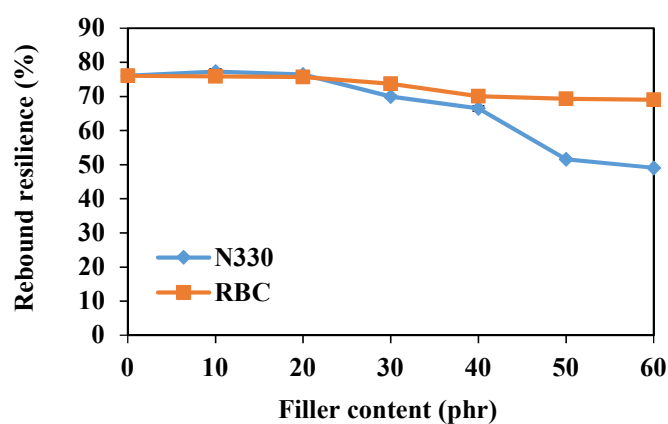


Figure 6. Rebound resilience of NR vulcanizates with different fillers

Conclusion

This work explored the use of RBC as a filler in NR vulcanizate. RBC was prepared by carbonization at 600 °C. The properties of the RBC-filled NR vulcanizate were also compared with industrial grade carbon black (N330)-filled NR vulcanizate. It was found that N330 gave higher reinforcement ability. Compared to N330-filled NR vulcanizate, the RBC-filled NR vulcanizate showed higher elongation at break and higher rebound resilience at 30-60 phr of filler loading. From the results, the RBC was classified as a non-reinforcing filler for natural rubber because of its large particle size and deterioration of mechanical properties. Thus, RBC can potentially be used as a cheaper and more environment-friendly natural filler.

Acknowledgement

The authors gratefully acknowledge the Faculty of Engineering and Agricultural Industry, Maejo University, for their research grant.

References

- Aguele, F.O. and Madufor, C.I. 2012. Effects of carbonised coir on physical properties of natural rubber composites. **American Journal of Polymer Science** 2(3): 28-34.
- Arayaprane, W. and Rempel, G.L.. 2008. A comparison of the properties of rice husk ash, silica, and calcium carbonate filled 75:25 NR/EPDM blends. **Journal of Applied Polymer Science** 110: 1165-1174.
- Ekebaf, L.O., Imanah, J.E. and Okieimen, F.E. 2010. The influence of carbonization temperature on vulcanization behavior and cross-link density of filled NR compounds. **Nigerian Journal of Chemical Research** 15: 12-21.
- Gopalan, N.K. and Dufresne, A. 2003. Crab shell chitin whisker reinforced natural rubber nanocomposites, processing and swelling behavior. **Biomacromolecules** 4: 657-665.
- Kanking, S., Niltui, P. and Wimolmala, E. 2012. Use of bagasse fiber ash as secondary filler in silica or carbon black filled natural rubber compound. **Materials and Design** 41: 74-82.
- Kumar, A. Anil. and Gupta, K.R. Rakesh. 1998. **Fundamentals of Polymers**. International Edition, McGraw Hill, Singapore.
- Li, M.C., Zhang, Y. and Cho, U.R. 2014. Mechanical, thermal and friction properties of rice bran carbon/nitrile rubber composites: Influence of particle size and loading. **Materials and Design** 63: 565-574.
- Lin, G., Zhang, X.J., Liu, L., Zhang, J.C., Chen, Q.M. and Zhang, L.Q. 2004. Study on microstructure and mechanical properties relationship of short fibers/rubber foam composites. **European Polymer Journal** 40: 1733-1742.
- Mondragon, M., Hernandez, E.M., Rivera-Armenta, J.L. and Rodriguez-Gonzalez, F.J. 2009. Injection molded thermoplastic starch/natural rubber/clay nanocomposites: Morphology and mechanical properties. **Carbohydrate Polymer** 77: 80-86.
- Moonchai, D., Moryadee, N. and Poosodsang, N. 2012. Comparative properties of natural rubber vulcanisates filled with defatted rice bran, clay and calcium carbonate. **Maejo International Journal of Science and Technology** 6(2): 249-258.
- Moonchai, S. and Moonchai, D. 2013. Modelling and optimization of rebound resilience and hardness of defatted rice bran/calcium carbonate-filled NR vulcanisates. **Polymer Testing** 32: 1472-1478.
- Moonchai, D., Juntamui, P. and Ruankum, R. 2016. Effect of defatted rice bran, calcium carbonate and clay on properties of cellular natural rubber. **Silpakorn University Science and Technology Journal** 10(4): 10-14.
- Sai-Oui, P., Rakdee, C. and Thanmathorn, P. 2002. Use of rice husk ash as filler in natural rubber vulcanizates: In comparison with other commercial fillers. **Journal of Applied Polymer Science** 83: 2485-2493.
- Sae-oui, P., Sirisinha, C. and Thaptong, P. 2009. Utilization of limestone dust waste as filler in natural rubber. **Journal of Material Cycles and Waste Management** 11:166-171.
- Wiboonsirikul, J., Kimura, Y., Kadota, M., Morita, H., Tsuno, T. and Adachi, S. 2007. Properties of extracts from defatted rice bran by its subcritical water treatment. **Journal of Agricultural Food and Chemistry** 55: 8759-8765.

Strength and Strain-induced Crystallization of Vulcanized Natural Rubber

Watcharin Sainumsai^{1, 2*}, Krisda Suchiva^{2, 3}, and Shigeyuki Toki^{2, 3, 4}

ABSTRACT

The present work is concerned with the study of the effect of crosslink density of sulphur-vulcanized natural rubber (NR) on strain-induced crystallization (SIC) and tensile strength of NR vulcanizate. SIC of varied crosslink densities of vulcanized NR are compared using a synchrotron wide-angle X-ray diffraction (WAXD). It was found that the crosslink density has almost no effect on the onset of SIC for low crosslink density, but for high crosslink density (above 8×10^{-5} mole/cm³), the onset of SIC showed slight decrease. The strain-induced crystallinity index was found to increase with increasing crosslink density then decreased. Tensile strength showed similar dependence on the crosslink density. The crystallinity index developed reaches a constant value of about 1.5 even at high strain. Since the stress still continues to rise even after the degree of crystallinity reaches a constant value, it was proposed that the high tensile strength of NR vulcanizate is not the direct consequence of SIC as is widely believed but is due to orientation of the molecular segments, particularly those connected to the crystalline structures.

Keywords: Natural rubber, Strain-induced crystallization, Mechanical properties, WAXD

¹Program in Rubber and Polymer Technology, Faculty of Science and Technology, Songkhla Rajabhat University, Khao-Roob-Chang, Muang District, Songkhla 90000, Thailand

²Department of Chemistry, Faculty of Science, Mahidol University, Salaya, Nakorn Pathom, 73170 Thailand

³National Metal and Materials Technology Center, National Science and Technology Department Agency, Pathum Thani 12120, Thailand

⁴Department of Chemistry, State University of New York at Stony Brook, NY, 11794-3400, USA

*Corresponding author, e-mail : watcharin.sa@skru.ac.th Phone: +668 9599 7455

Introduction

Natural rubber (NR, cis-1,4-polyisoprene) vulcanizates show great physical and mechanical properties in tensile strength and fatigue resistance, together with high hysteresis energy (Gent, 1992). Since these characteristics take place without addition of any filler. In particular, its high tensile strength (20-30 MPa) and large strain at break (8.0-10.0) are excellent in comparison with the case of unfilled SBR (Styrene Butadiene Rubber) vulcanizate where the tensile strength is about 1.5-2.0 MPa and the strain at break is 4.0-5.0. These superior properties of NR have been assumed to be due to its strain-induced crystallization (SIC) ability (Roberts, 1988; Mark *et al.*, 1994; Murakami *et al.*, 2002; Toki *et al.*, 2002). Therefore, the study on SIC behavior of crosslinked NR is the most importance for elucidating the mechanical characteristics of NR.

The strain-induced crystallization in NR has been observed and studied by X-ray since 1925 (Katz, 1925). The increase of strain-induced crystallization in NR with strain had been studied extensively (Gehman and Field, 1939; Bunn, 1941; Luch and Yeh, 1973; Shimomura and White, 1982; Mitchell, 1984). The simultaneous measurements of the stress-strain relation and the strain-induced crystallization by wide angle X-ray diffraction (WAXD) using a conventional X-ray instrument (Toki *et al.*, 2000) revealed that the hysteresis of stress-strain relation is caused by the strain-induced crystallization. The results show that the strain-induced crystallization decreases the stress since the length of amorphous molecule along the stretching direction increases due to its crystallization.

Synchrotron X-ray and modified stretching machine make it clear to show the both hysteresis in the stress-strain relation and in the strain-induced crystallization in rubbers and to elucidate the stress decrease by the onset of strain-induced crystallization (Murakami *et al.*, 2002; Tosaka *et al.*, 2004; Toki *et al.*, 2004b). The experimental results agree with classical thermo-mechanical theories on strain-induced crystallization (Bekkedahl and Wood, 1941; Flory, 1947) that suggested the onset of strain-induced crystallization decrease the stress before the upturn of stress.

Sulphur vulcanized rubbers have network structures that are mainly composed of monosulphidic, disulphidic, and polysulphidic crosslinks. The structures including the crosslink densities and types of vulcanizates are very important parameters because of their dominant effects on the mechanical properties. The ratio of polysulphidic, disulphidic and monosulphidic crosslinks depends on the ratio of sulphur to the accelerators, cure time and the kind of accelerator in the formulation. The crosslink has been considered to be vital for SIC since the theory of rubber elasticity of polymer crosslink network has applied to elucidate SIC at thermo-mechanical equilibrium state. In this paper, we focus on the role of crosslink. Five levels of crosslink density are studied.

Materials and Methods

1. Materials

Commercial grade of Standard Thai Natural Rubber, 5L grade (STR-5L) was used for this research activity. The compositions of several natural rubber compounds tested in this study are shown in Table 1. All the ingredients including sulphur and accelerator were mixed on a laboratory-scale 6-in. roll mill. Vulcanization was carried out in an electrically heated hydraulic press at 150°C using the optimum cure time (T_c90) previously determined with a moving die rheometer (TechPro MD+) at 150°C following ASTM D-5289.

Table 1 Composition and sample preparation conditions of the samples

Ingredients	Quantity (phr)				
	CV1	CV2	CV3	CV4	CV5
STR-5L	100	100	100	100	100
Zinc Oxide	5	5	5	5	5
Stearic acid	1	1	1	1	1
CBS ^a	0.19	0.56	0.75	0.94	1.31
Sulphur	0.50	1.50	2.00	2.50	3.50
Cure time ^b [min]	31	16	13	12	11

^aCBS (N-cyclohexyl-2-benzothiazole sulphenamide), ^bCuring temperature 150°C

2. Determination of crosslink density

Equilibrium swelling in toluene was used to determine the crosslink densities of the rubber vulcanizates. The Crosslink density was determined using the method described by Cunneen and Russell (1970). The molecular weight of the network chain between chemical crosslinks for a phantom network, M_c ; is expressed by the Flory-Rehner relationship (Flory and Rehner, 1943; Flory, 1950):

$$M_c = \frac{-2\rho_r V_s (V_r^{1/3} - V_r / 2)}{[\ln(1 - V_r) + V_r + \chi V_r^2]} \quad (1)$$

where V_r is the volume fraction of rubber in the swollen sample, V_s is the molar volume of the swelling solvent, ρ_r is the density of the rubber sample, and χ is the rubber-solvent interaction parameter. The values of the constant used in the above calculation were $V_s = 107 \text{ cm}^3/\text{mole}$ and $\chi = 0.393$ (Brydson, 1978). The crosslink density (ν) (Blow, 1975) is given by:

$$\nu = \frac{1}{2M_c} \quad (2)$$

3. Measurements of stress-strain curves and tensile strength

Tensile properties of NR vulcanizates were measured according to ASTM D-412 using a universal testing machine (Instron 5569 series, Norwood, USA) at 25°C. The rate of deformation was 500 mm/min.

4. Strain-induced crystallization measurement

In-situ wide-angle X-ray diffraction (WAXD) measurements were carried out at the X27C beamline in the National Synchrotron Light Source (NSLS), Brookhaven National Laboratory (BNL). The wavelength of X-ray was 0.1371 nm. An MAR-CCD X-ray detector (made by MAR, USA) was used to record the two-dimensional WAXD patterns for quantitative image analyses. The typical image acquisition time for each scan was 30 sec. The data analysis software package (POLAR) used was developed by Stony brook Technology and Applied Research at Stony Brook, New York. The tensile machines allowed the symmetric stretching of the sample, permitting the focused X-ray to illuminate the same sample position during deformation. The chosen deformation rate was 10 mm/min. The stress-strain curves during extension were collected at 25°C in the uniaxial deformation mode.

Results and Discussion

Stress-strain curves of NR vulcanizates with various crosslink densities are shown in Figure 1. The sample with the larger crosslink density showed the higher modulus in the tensile measurements of this study (Table 2). In the lower strain region, the modulus is low and slowly increases with the increase in strain; when the strain is larger, the upturn in stress. The sample with the larger crosslink density showed the upturn in stress at lower strain.

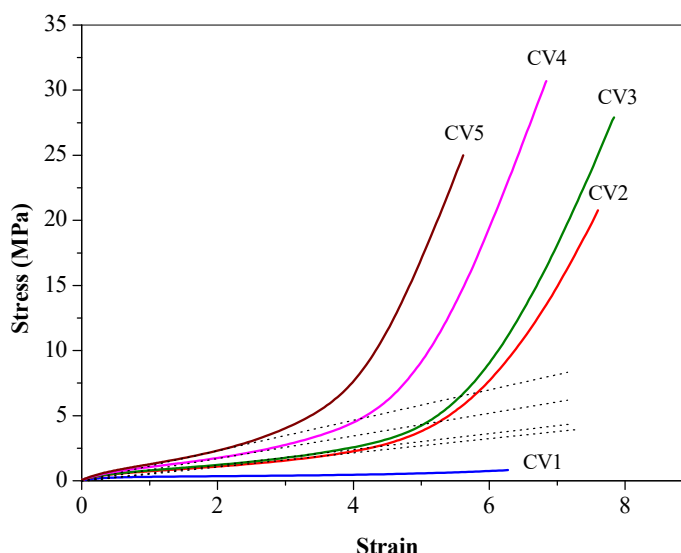


Figure 1 Tensile stress-strain curves of NR vulcanizates with various crosslink densities

Table 2 Total crosslink densities and mechanical properties of the samples

Properties	CV1	CV2	CV3	CV4	CV5
Total crosslink density [$\times 10^{-5}$ mol/cm ³]	0.5	5.6	7.8	8.7	11.3
Modulus at strain 1.0 [MPa]	0.3	0.7	0.8	1.0	1.3
Modulus at strain 3.0 [MPa]	0.4	1.5	1.9	2.7	4.1
Tensile strength [MPa]	0.9	20.5	28.7	30.6	24.9
Strain at break	6.2	7.6	7.5	6.9	5.8

The stress-strain curve and selected 3D WAXD patterns during deformation (at a 10 mm/min rate) of sample CV3 at 25°C are shown in Figure 2. Each WAXD image is taken at the strain indicated by the arrow. The high intensity of synchrotron X-rays made it possible to collect the WAXD patterns during deformation in real time without holding the sample still. It was seen that stress generally increased with strain. In Figure 2, it is seen that 3D WAXD patterns exhibited an amorphous halo below strain 3.0, while its intensity distribution shifted slightly toward the equator with increasing strain (e.g., strain 3.0). At strain 4.0, the deformation of the halo pattern became more intense, and several weak but distinct crystalline reflections are seen. These reflections are sharp and highly oriented and appeared in smaller numbers than those in fully crystallized patterns (e.g., at strains 5 and more). These reflections are caused by the first-formed strain-induced crystallites, which are defective in crystalline ordering or registration but highly oriented with respect to the stretching direction. This finding is consistent with the fringemicelle crystal model induced by strain during deformation of rubber recently proposed by Toki and coworkers (Toki *et al.*, 2002; Toki *et al.*, 2003; Toki and Hsiao, 2003; Toki *et al.*, 2004b). In contrast, at strains above 4 (e.g., strains 5.0 and more), the WAXD patterns exhibited well oriented crystalline reflections from a monoclinic unit cell with parameters similar to $a = 1.25$ nm, $b = 0.89$ nm, $c = 0.81$ nm, and $\gamma = 92^\circ$, as previously reported by Bunn (1941). It is interesting to see that, even at strains 5.0 and more, one can observe the persistence of the unoriented amorphous halo, which is consistent with the finding that a substantial amount of amorphous chains remain unstretched at high extension (Toki *et al.*, 2002; Toki *et al.*, 2003; Toki *et al.*, 2004a).

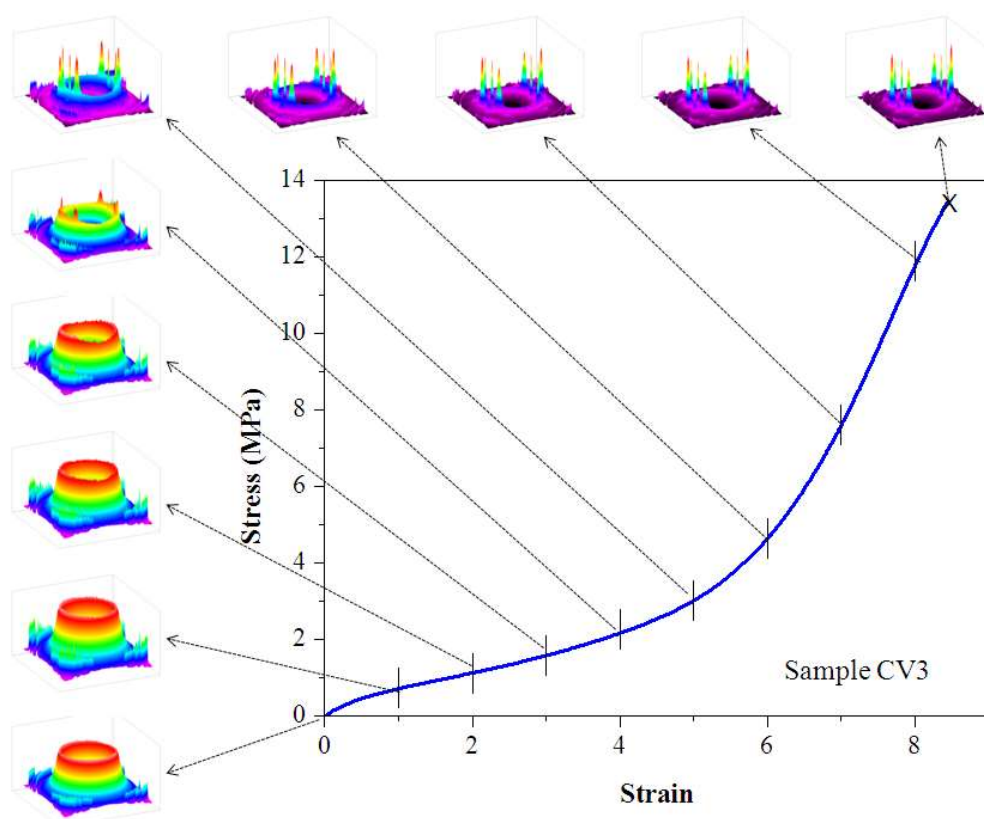


Figure 2 The stress-strain relationship and selected WAXD patterns in 3D expression of the sample CV3. Each image was taken at the average strain indicated by the arrows.

WAXD patterns can be analyzed into three fractions such as crystal, oriented amorphous and unoriented amorphous. The procedure to analyze the data is mentioned elsewhere (Toki *et al.*, 2002; Toki *et al.*, 2003; Toki *et al.*, 2004b). The integral intensities as a function of scattering vector “s” at each strain are shown in Figure 3. It is clear that the anisotropic fraction increases with strain smoothly.

From the integrated intensity patterns, we can evaluate crystallinity index and oriented amorphous index as shown in Figure 4. Crystallinity index increases with strain during deformation. The oriented amorphous index does not increase significantly and seems to be a precursor of strain-induced crystallization. The tendencies are similarly observed in pure vulcanized NR and pure vulcanized IR (Toki *et al.*, 2002; Tosaka *et al.*, 2004; Toki *et al.*, 2005). From the above observation, we can conclude that the oriented amorphous chains are precursors to the induced crystals. The crystallization rate from the oriented chains must be very fast, probably in the order of 60 m/s, as reported by Mitchell and Meier (1968). In addition, it is reasonable to rationalize that the strain-induced crystallites are in the extended chain crystal form having a microfibrillar structure. As only a small fraction of chains are oriented and crystallized, this suggests that the strain-induced crystallites form an additional physical crosslinking network, carrying most of the applied load. The above results indicate that even

under a very high deformation state, the majority of the chains remain unoriented. This behavior seems to be very universal in rubbery materials.

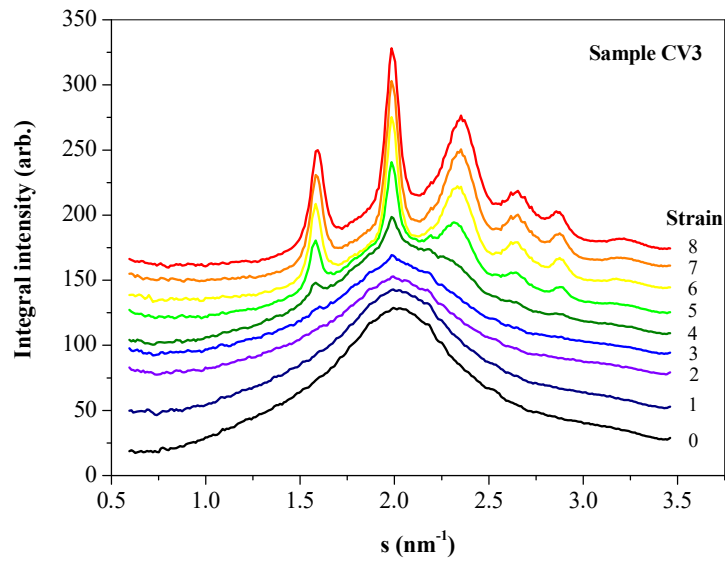


Figure 3 1D cylindrical intensity profiles as a function of scattering vector “s” of the sample CV3.

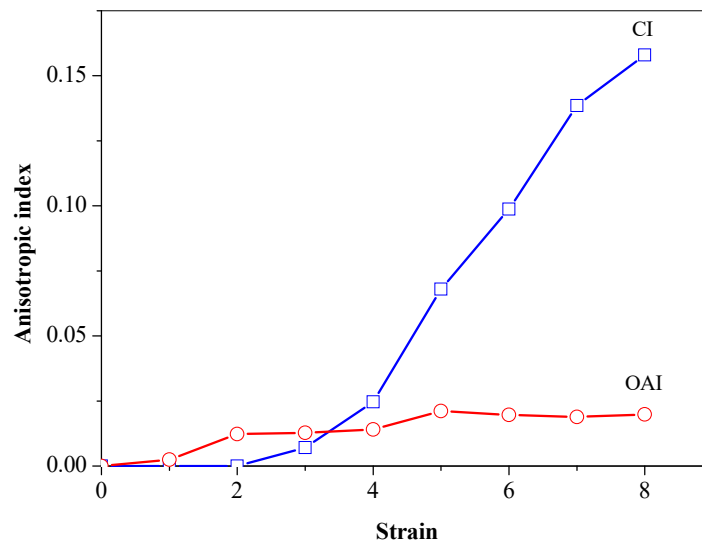


Figure 4 The anisotropic fractions (oriented amorphous and crystal) of the sample CV3 at each strain during deformation.

The variations of the crystallinity index of NR vulcanizates with various crosslink densities during deformation at 25°C are shown in Figure 5. It is found that the crystallinity index starts to increase at strain around 2.5 in all samples. The crosslink density had only negligible influence on the onset strain of crystallization (Table 3). At strain = 3.0, the crystallinity index is almost identical. At strain larger than 3, the crystallinity index becomes

dominant. NR vulcanizates with various crosslink densities showed similar trends. The crystallization started after the sample is elongated to some extent. The sample with the larger crosslink density typically exhibited a steeper slope in the plot. It is interesting to find that the rate of SIC is the faster for the samples with the higher crosslink density.

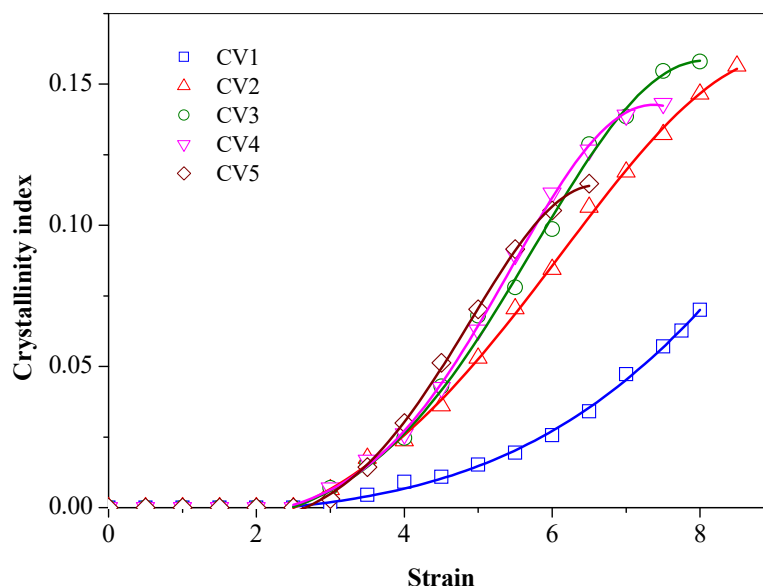


Figure 5 Relationship between crystallinity index and tensile strain of NR vulcanizates with various crosslink densities.

Table 3 Crystallization rate, incipient strain of crystallization and strain at upturn stress of the samples

Sample	Crystallization rate [min ⁻¹]	Onset strain of crystallization	Strain at upturn stress
CV1	0.014	2.45	-
CV2	0.029	2.55	3.9
CV3	0.035	2.55	3.6
CV4	0.036	2.63	2.9
CV5	0.036	2.37	2.3

The crystallization rate reflects a relative SIC rate and was obtained from the slope of linearly increasing part of the curve in Figure 5 (slope in the strain dependence of anisotropic fraction). In contrast to the almost no effect of crosslink density on the onset of SIC, the crosslink density was found to have definite influence on the rate of SIC as shown in Figure 6. The rate of SIC showed linearly increases with increasing crosslink density up to the value of 8×10^{-5} mole/cm³. Further increasing of the crosslink density resulted in a nearly constant of the rate of crystallization.

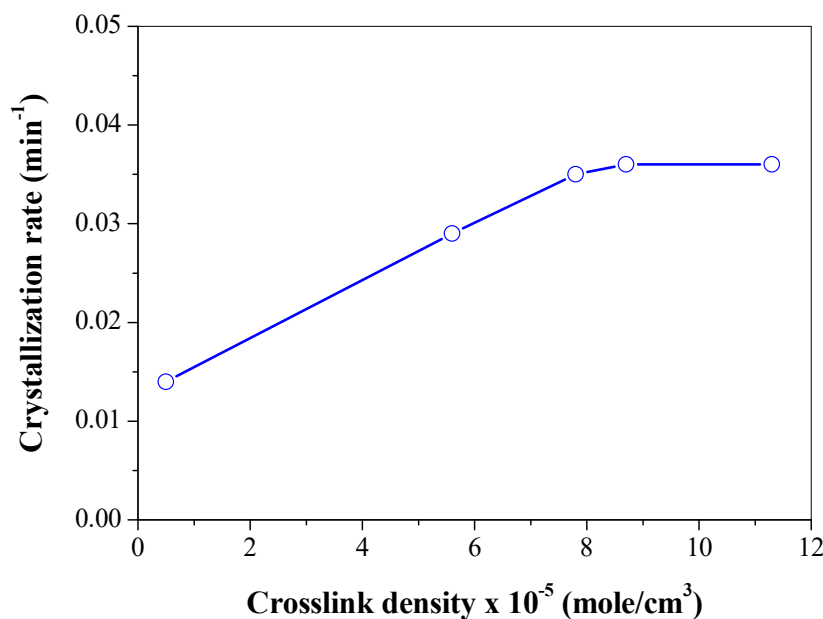


Figure 6 Dependence of rate of SIC on crosslink density.

The upturn of stress in the stress-strain curve of NR vulcanizate has popularly been attributed to SIC (Versloot *et al.*, 1992). Results of the present study suggest otherwise. It can be seen that the crystallinity index developed approximately reaches a constant value at about 1.5 even at the large strain at which stress-upturn is observed. The results of the present study, thus, indicate that stress-upturn and the high tensile strength of NR vulcanizate are not the direct consequence of SIC. For rubbery materials, this stress-upturn is generally associated with the stress at which the smallest chains reach their critical extensibility (Chenal *et al.*, 2007). Therefore, it appears that molecular orientation along the applied stress is responsible for the observed upturn of stress at a certain strain and also the final strength of the vulcanized rubber. SIC may contribute to the high strength by facilitating the formation of orientation of either molecules or crystals, increasing the rubber's ability to bear force. Thus, further studies on SIC and orientation of sulphur-vulcanized NR samples are necessary in order to understand better the factors that are responsible for high strength of strain-crystallizable rubbers.

Conclusion

1. In the NR samples vulcanizates with CV curing system an increase in the total crosslink densities, tensile strength and crystallinity index are increased up to maximum, then decreased.
2. The NR vulcanizates with the larger crosslink density showed the upturn in stress at lower strain.
3. The crosslink density had only negligible influence on the onset strain of crystallization. The rate of SIC is the faster for the samples with the higher crosslink density.
4. Crosslink types do not change the crystallization behavior of the NR vulcanizates under deformation at 25°C.

Acknowledgement

The author would like to express his gratitude to SKRU and MU for financial support throughout this work and the National Synchrotron Light Source (NSLS), Brookhaven National Laboratory (BNL), New York, USA for synchrotron WAXD measurement facility.

References

- Bekkedahl, N. and Wood, L.A. 1941. Crystallization of vulcanized rubber. **Industrial & Engineering Chemistry**. 33(3): 381-384.
- Blow, C.M. (Ed.). 1975. **Rubber Technology and Manufacture**. Newness Butterworths, London.
- Brydson, J.A. 1978. **Rubber Chemistry**. Applied Science Publishers Ltd., London.
- Bunn, C.W. 1941. Molecular structure and rubber-like elasticity I. The crystal structures of β gutta-percha, rubber and polychloroprene. **Proceedings of the Royal Society A**. 180: 40-66.
- Chenal, J.M., Chazeau, L., Guy, L., Bomal, Y. and Gauthier, C. 2007. Molecular weight between physical entanglements in natural rubber: A critical parameter during strain-induced crystallization. **Polymer**. 48(4): 1042-1046.
- Cunneen, J.I. and Russell, R.M. 1970. Occurrence and prevention of changes in the chemical structure of natural rubber tire tread vulcanizates during service. **Rubber Chemistry and Technology**. 43(5): 1215-1224.
- Flory, P.J. 1947. Thermodynamics of crystallization in high polymers. I. Crystallization induced by stretching. **The Journal of Chemical Physics**. 15: 397-408.
- Flory, P.J. 1950. Statistical mechanics of swelling of network structures. **The Journal of Chemical Physics**. 18: 108-111.
- Flory, P.J. and Rehner, J. 1943. Statistical mechanics of cross-linked polymer networks II. Swelling. **The Journal of Chemical Physics**. 11: 521-526.
- Gehman, S.D. and Field, J.E. 1939. An X-Ray investigation of crystallinity in rubber. **Journal of Applied Physics**. 10(8): 564-572.
- Gent, A.N. 1992. **Engineering with rubber**. Oxford University Press, Oxford, U.K.
- Katz, J.R. 1925. Röntgenspektrographische Untersuchungen am gedehnten Kautschuk und ihre mögliche Bedeutung für das Problem der Dehnungseigenschaften dieser Substanz. **Naturwissenschaften**. 13(19): 410-416.
- Luch, D. and Yeh, G.S.Y. 1973. Morphology of strain-induced crystallization of natural rubber. Part II. X-Ray studies on cross-linked vulcanizates. **Journal of Macromolecular Science, Part B**. 7(1): 121-155.
- Mark, J.E., Erman, B. and Eirich F.R. (Eds.). 1994. **Science and Technology of rubber**, second ed., Academic Press, San Diego.
- Mitchell, G.R. 1984. A wide-angle X-ray study of the development of molecular orientation in crosslinked natural rubber. **Polymer**. 25(11): 1562-1572.
- Mitchell, J.C. and Meier, D.J. 1968. Rapid stress-induced crystallization in natural rubber. **Journal of Polymer Science Part A-2: Polymer Physics**. 6(10): 1689-1703.

- Murakami, S., Senoo, K., Toki, S. and Kohjiya, S. 2002. Structural development of natural rubber during uniaxial stretching by in situ wide angle X-ray diffraction using a synchrotron radiation. **Polymer**, 43(7): 2117-2120.
- Roberts, A.D. 1988. **Natural Rubber Science and Technology**. Oxford University Press, Oxford, U.K.
- Shimomura, Y. and White, J.L. 1982. A comparative study of stress-induced crystallization of guayule, hevea, and synthetic polyisoprenes. **Journal of Applied Polymer Science**. 27(9): 3553-3567.
- Toki, S. and Hsiao, B.S. 2003. Nature of strain-induced structures in natural and synthetic rubbers under stretching. **Macromolecules**. 36(16): 5915-5917.
- Toki, S., Fujimaki, T. and Okuyama, M. 2000. Strain-induced crystallization of natural rubber as detected real-time by wide-angle X-ray diffraction technique. **Polymer**. 41(14): 5423-5429.
- Toki, S., Sics, I., Hsiao, B.S., Murakami, S., Tosaka, M., Poompradub, S., Kohjiya, S. and Ikeda, Y. 2004a. Structural developments in synthetic rubbers during uniaxial deformation by in situ synchrotron X-ray diffraction. **Journal of Polymer Science Part B: Polymer Physics**. 42(6): 956-964.
- Toki, S., Sics, I., Hsiao, B.S., Murakami, S., Tosaka, M., Poompradub, S., Kohjiya, S. and Ikeda, Y. 2004b. Strain-induced molecular orientation and crystallization in natural and synthetic rubbers under uniaxial deformation by in-situ synchrotron X-ray study. **Rubber Chemistry and Technology**. 77(2): 317-335.
- Toki, S., Sics, I., Hsiao, B.S., Murakami, S., Tosaka, M., Poompradub, S., Kohjiya, S. and Ikeda, Y. 2005. Probing the nature of strain-induced crystallization in polyisoprene rubber by combined thermomechanical and in situ X-ray diffraction techniques. **Macromolecules**. 38(16): 7064-7073.
- Toki, S., Sics, I., Ran, S., Liu, L. and Hsiao, B.S. 2003. Molecular orientation and structural development in vulcanized polyisoprene rubbers during uniaxial deformation by in situ synchrotron X-ray diffraction. **Polymer**. 44(19): 6003-6011.
- Toki, S., Sics, I., Ran, S., Liu, L., Hsiao, B.S., Murakami, S., Senoo, K. and Kohjiya, S. 2002. New insights into structural development in natural rubber during uniaxial deformation by in situ synchrotron X-ray diffraction. **Macromolecules**, 35(17): 6578-6584.
- Tosaka, M., Kohjiya, S., Murakami, S., Poompradub, S., Ikeda, Y., Toki, S., Sics, I. and Hsiao, B.S. 2004. Effect of network-chain length on strain-induced crystallization of NR and IR vulcanizates. **Rubber Chemistry and Technology**. 77(4): 711-723.
- Tosaka, M., Murakami, S., Poompradub, S., Kohjiya, S., Ikeda, Y., Toki, S., Sics, I. and Hsiao, B.S. 2004. Orientation and crystallization of natural rubber network as revealed by WAXD using synchrotron radiation. **Macromolecules**. 37(9): 3299-3309.
- Versloot, P., Haasnoot, J.G., Reedijk, J., van Duin, M., Duynstee, E.F.J. and Put, J. 1992. Sulfur vulcanization of simple model olefins, Part I: Characterization of vulcanization products of 2,3-dimethyl-2-butene. **Rubber Chemistry and Technology**. 65(2): 343-349.

Sodium Methoxide Dissolution in Various Solvents

Thirawat Mueansichai^{1*}, Benjaphorn Kaewsubdejsiri¹, Panupong Limsongtham¹, Yarachanee Moomuangsong¹ and Weerinda Appamana¹

ABSTRACT

Sodium methoxide (CH_3ONa), a catalyst base, is generally used in biodiesel production and pharmaceuticals industry. It dissolves more quickly than sodium hydroxide (NaOH) in methanol (CH_3OH). This work investigated the dissolution of sodium methoxide in various solvents like acetone, benzyl alcohol, 2-butanol, cyclohexane, dicloromethane, ethanol, ethyl acetate, formic acid, glycerol, hexane, methanol and phenol. The experiments performed at room temperature by adding sodium methoxide in the various solvents then shaking and observed the dissolution of sodium methoxide. The results show that sodium methoxide was dissolved in most solvents except hexane, cyclohexane and ethyl acetate. From these results, it was found that sodium methoxide can be dissolved in acid substances, alcohol, and phenol. Therefore, hexane, cyclohexane and ethyl acetate are suitable to use as anti-solvent for crystallization process of sodium methoxide.

Keywords: sodium methoxide, dissolution, solvent, hexane

¹ Department of Chemical and Materials Engineering, Faculty of Engineering, Rajamangala University of Technology Thanyaburi, Klong 6, Thanyaburi, Pathum Thani 12110, Thailand

*Corresponding author, e-mail: thirawat.m@en.rmutt.ac.th

Introduction

Sodium methoxide or sodium methylate is a metal alkoxides which synthesized since 1955 (Wardlaw 1955; Wardlaw 1956; Bradley 1958). Nowadays, it is used as a catalyst for production of biodiesel by the transesterification of triglycerides with methanol (Kai *et al.*, 2014; Karnis and Chilari, 2013). As a catalyst, sodium methoxide showed better results when compared to sodium hydroxide (Karnis and Chilari, 2013). The size of catalyst is also important factor for the transesterification reaction. The study of sodium methoxide preparation by crystallization which reduced the size of sodium methoxide gave a conversion higher than 96% for the production of biodiesel from canola oil (Kai *et al.*, 2014).

The manufacture of sodium methoxide in the industry has many methods for example the manufacturing sodium methoxide from sodium metal or from sodium hydroxide (Granjo and Oliveira 2016). There are many investigators proposed methods for production of sodium methoxide such as preparation of alkali metal methoxides from aqueous alkali metal hydroxide and methanol (Guth *et al.*, 2004). The most popular method for producing sodium methoxide is reactive distillation (Granjo and Oliveira, 2016). In the past, sodium methoxide produced from sodium and an excess of methanol. This process consists of a reactor and follow by distillation column for separation of sodium methoxide (Tse, 1997). The main problem of the present process of sodium methoxide production is high energy consumption (Granjo and Oliveira, 2016). Therefore, we need a novel method to produce sodium methoxide which is low energy consumption. As mention above, the crystallization is the process that we can use to produce sodium methoxide with high conversion of biodiesel production (Kai *et al.*, 2014).

Crystallization is one of the most popular separation process in pharmaceuticals because the crystal products have high purity and easy to operate (Nowee *et al.*, 2008; Gao *et al.*, 2017). There are a lot of methods for separation of crystalline product process. For example, cooling, evaporation, and non-solvent addition (Flood, 2009). The important information for design of crystallization process is the properties of the substances such as solubility, supersaturation, and the dissolution in various solvents. Therefore, this study aim to investigate the dissolution property of sodium methoxide in various solvents. These results will be used for selection of anti-solvent in crystallization process design.

Materials and Methods

Chemicals: Methanol (CH_3OH), acetone (CH_3COCH_3), benzyl alcohol ($\text{C}_6\text{H}_5\text{CH}_2\text{OHC}_7\text{H}_8\text{O}$), 2-butanol ($\text{C}_4\text{H}_{10}\text{O}$), cyclohexane (C_6H_{12}), dicloromethane (CH_2Cl_2), ethanol ($\text{C}_2\text{H}_6\text{O}$), ethyl acetate ($\text{CH}_3\text{CH}_2\text{COOCH}_3$), formic acid (CH_2O_2), glycerol ($\text{C}_3\text{H}_8\text{O}_3$), hexane (C_6H_{14}), and phenol ($\text{C}_6\text{H}_5\text{OH}$) were selected as a solvent. Sodium methoxide (CH_3ONa) is a solute for study the dissolution in all solvents.

Equipment: Test tube, test tube rack, spatula, stirring rod, graduated cylinder, beaker, stopwatch, pH meter, and balance

Procedure: The dissolution experiment performed by measuring the sodium methoxide in the test tube 0.1 g. Then, 10 ml of the solvent was added into the test tube and starting a timer. The solution was stirred for 1 hour at room temperature and observed the dissolution of sodium methoxide in each solvent. Figure 1 shows an example of experimental results. The solution was measured pH and temperature after the dissolution experiment was finished.

The recrystallization of sodium methoxide performed by a preparation of saturated solution of sodium methoxide in methanol. The saturated solution was filtered by 0.45 micrometers membrane for separation of excess sodium methoxide. The anti-solvent was added into the saturated solution and then observed the crystalline product from anti-solvent crystallization.



Figure 1 Example of experimental results (sodium methoxide in methanol)

Results and Discussion

This work is a preliminary study of sodium methoxide property for designing the crystallization process. Anti-solvent or non-solvent addition crystallization needs dissolution property of the substance in the solvent for selecting an appropriate anti-solvent to use in the crystallization process design. The suitable anti-solvent should have the property that the solute cannot dissolve in it then the substance can easily separate from the solvent. From the experiments, the results of dissolution property of sodium methoxide are shown in table 1.

Table 1 Dissolution property of sodium methoxide in various solvent

Solvents	Dissolution property	pH	Temperature
Acetone	✓	4	increase
Benzyl alcohol	✓	10	-
2-Butanol	✓	5	decrease
Cyclohexane	✗	4	increase
Dicloromethane	✓	5	increase
Ethanol	✓	12	increase
Ethyl acetate	✗	5	-
Formic acid	✓	2	-
Glycerol	✓	6	-
Hexane	✗	5	-
Methanol	✓	12	increase
Phenol	✓	10	-

Remark: ✓ = dissolved, ✗ = non-dissolved, - = the temperature doesn't change

As shown in table 1, sodium methoxide was insoluble in three solvents, namely cyclohexane, ethyl acetate, and hexane. As a result of this, such solvents are suitable for using as an anti-solvent in the anti-solvent crystallization process of sodium methoxide. This property was the first which we have to consider. In the case of pH solution, we can separate the solvents into two groups. The first group is basic solution such as phenol, methanol, ethanol, and benzyl alcohol. As you can see in the table 1, sodium methoxide can dissolve in all solvents having the basic property. This is because sodium methoxide is also the basic substance. The second group is acid solution. The solvents in the second group are hexane, glycerol, formic acid, ethyl acetate, dicloromethane, cyclohexane, 2-butanol, and acetone. In the acid solution group, there are two phenomena observed. There are three solvents that sodium methoxide cannot dissolve of which the pH is around 4 to 5. For other solvents, the sodium methoxide can dissolve like the basic solution group and they have the pH around 4 to 5 as well. Thus, we cannot conclude that the sodium methoxide cannot dissolve in acid solution because there are two different results. So, we need more information about the property of the acid solution to explain about the dissolution of sodium methoxide.

The second parameter used to observe the dissolution of sodium methoxide in various solvents is the temperature. The temperature observation is conducted by comparing the temperature with the room temperature. If the temperature of the solution increases, it should have some reaction between sodium methoxide and the solvent called the exothermic reaction. If the temperature of the solution decreases, it is endothermic reaction. From the results of temperature in table 1, the relationship between dissolution property and the temperature of the solution was unreliability. This resulted from the differentiation of sodium methoxide dissolution.

Figure 2 shows the factors affecting dissolution rate. Solubility, dissolution, and dissolution rate are related but they have different definitions (Smith, 2015). The solubility is the thermodynamics process in which the amount of a solute dissolves in a pure solvent at the

endpoint of dissolution. The dissolution is a process that a solute dispersing in a solvent. It is different from the solubility because the solubility is the end point of the dissolution process.

The rate of dissolution is determined by Noyes-Whitney equation that shows how fast the solute can dissolve in the solvent. This work focuses on the dissolution because it is a preliminary study for selecting the anti-solvent of crystallization process. So, we need to know which solvent that sodium methoxide cannot dissolve in them. When we add the anti-solvent into the system of sodium methoxide in some solvent, we can separate the sodium methoxide from the solution by the crystallization.

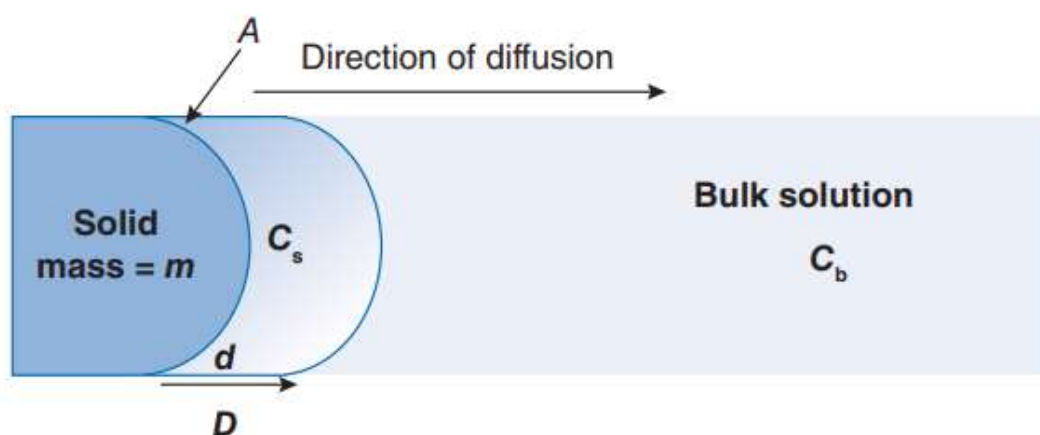


Figure 2 Noyes-Whitney parameters for dissolution rate (Smith 2015)



Figure 3 Recrystallization of sodium methoxide

From Figure 3, the recrystallization of sodium methoxide was performed to investigate the crystallization process. As you can see, the white crystal of sodium methoxide was generated by anti-solvent crystallization process by adding an anti-solvent into the saturated solution. Thus, we can use anti-solvent for separating the solute from saturated solution by crystallization process. This mechanism occurred when the anti-solvent was added into the saturated solution; the solvent will diffuse into the anti-solvent phase. So, the superstation of the solution phase will increase and then the solute can separate from the solution as crystalline product.

Conclusion

The dissolution of sodium methoxide in twelve solvents was studied. The suitable solvent for crystallization process is methanol and ethanol, whereas hexane, cyclohexane, ethyl acetate were used as anti-solvent for separation of sodium methoxide. For further investigation, this project will continue to study dissolution rate of the sodium methoxide in various solvents and the solubility of sodium methoxide. This is because sodium methoxide is an important catalyst in biodiesel production. If we can produce the sodium methoxide by using the process with low energy consumption, it will help the biodiesel production to reduce operating cost.

Acknowledgement

The authors are grateful to Faculty of Engineering, Rajamangala University of Technology Thanyaburi for financial support and fellowships.

References

- Bradley, D. C. 1958. A structural theory for metal alkoxide polymers. **Nature** 182: 1211-1214.
- Flood, A. E. 2009. **Industrial crystallization from solution: A primer** Suranaree University of Technology, Nakhon Ratchasima.
- Gao, Z., Sohrab, R., Junbo, G., and Jingkang, W. 2017. Recent Developments in the Crystallization Process: Toward the Pharmaceutical Industry. **Engineering** 3: 343-53.
- Granjo, J. F. O., and Oliveira, N. M. C.. 2016. Process Simulation and Techno-Economic Analysis of the Production of Sodium Methoxide. **Industrial & Engineering Chemistry Research** 55: 156-67.
- Guth, J., Holger F., Hans J. S., Gerd, K., Kirsten, B., and Elke, H. 2004. **Method for producing alkali methylates**. In Patent.
- Kai, T., Goon L. M., Shohei, W., Tsutomu, N., Hirokazu, T., and Yoshimitsu, U. 2014. Production of biodiesel fuel from canola oil with dimethyl carbonate using an active sodium methoxide catalyst prepared by crystallization. **Bioresource Technology** 163: 360-63.
- Karnis, D., and Chilari, D. 2013. A comparison between of sodium methoxide and sodium hydroxide catalysts for ethyl esters production. In **the 13th International Conference of Engviromental Science and Technology**. Athens, Greece.
- Nowee, M. S., Ali, A., and Jose, A. R. 2008. Antisolvent crystallization: Model identification, experimental validation and dynamic simulation. **Chemical Engineering Science** 63: 5457-67.
- Smith, B. T. 2015. **Remington Education: Physical Pharmacy** Remington.
- Tse, S. W. 1997. **Continuous process for sodium methylate**. In Patent.
- Wardlaw, W. 1955. Presidential address. A problem in structural chemistry. **J. Chem. Soc.**: 3569-76.
- Wardlaw, W. 1956. Presidential address. Alkoxides old and new. **J. Chem. Soc.**: 4004-14.

Poisson Regression Model for Predict Dengue Haemorrhagic Fever Prevalence in Kreang Sub-District, Cha-Uat District, Nakhon Si Thammarat, Thailand

Suppawan Promprao^{1*}

ABSTRACT

Dengue haemorrhagic fever (DHF), was a mosquito-borne viral disease that has rapidly spread in all regions of WHO in recent years. It was transmitted by *Aedes* mosquitoes, which breeding sites are nearby or in human households. An importance campaign for the prevention of DHF ought to start at studying the relationship between DHF cases and related variables involved the human behaviors' factors and mosquitoes breeding sites. To develop and validate a Poisson regression model to verify predictors of DHF patients in Kreang Sub-District, Cha-Uat District, Nakhon Si Thammarat, Thailand. DHF cases, types and number of mosquitoes breeding sites were collected from 160 households by surveying, starting from March - July 2016. DHF cases were counted data and were assigned to response variables. The mean of response variables was approximately equal to its variance. It was suggested that a Poisson regression model would be appropriate. Mosquitoes breeding sites factors were assigned to exploratory variables. Maximum likelihood method was used to parameter estimation. The results showed that the Poisson regression was statistical significant model (Omnibus Test: Likelihood Ratio $\chi^2_{(3)} = 13.849$, $p = 0.003 < 0.05$). The constant had suitable for model (constant; $\chi^2_{(1)} = 52.940$, $p = 0.000 < 0.05$). The significant predictor variables were number of cement tanks outdoor (CT: $\chi^2_{(1)} = 4.015$, $p = 0.045 < 0.05$), number of cement tanks for toilet (TCT: $\chi^2_{(1)} = 4.445$, $p = 0.035 < 0.05$) and number of water jars (WJ: $\chi^2_{(1)} = 6.589$, $p = 0.010 < 0.05$). The log of the DHF was predicted with a linear combination of the predictors: $\log(\text{DHF}) = -2.970 + 1.584(\text{CT}) + 2.277(\text{TCT}) + 1.386(\text{WJ})$. This implies: $\text{DHF} = \exp [-2.970 + 1.584(\text{CT}) + 2.277(\text{TCT}) + 1.386(\text{WJ})]$. Understanding a human's behaviors which causes mosquitoes breeding places related to the number of DHF patients, will be able to predict the occurrence of DHF and plan to prevent and control this disease.

Keywords: Dengue Haemorrhagic Fever, Mosquitoes, Poisson Regression, Likelihood Ratio

¹ Mosquitoes Operational Research Unit (MORU), Faculty of Science and Technology, Nakhon Si Thammarat Rajabhat University, Tha-Ngew, Mueang, Nakhon Si Thammarat 80280, Thailand

*Corresponding author, e-mail: spromprao@gmail.com

Introduction

Dengue and dengue hemorrhagic fever (DHF) result from infection by any of four serotypes of dengue viruses. Transmission occurs through the bite of infected *Aedes* mosquitoes, principally *Aedes aegypti* (Pinheiro, 1989). The majority of DHF cases, however, occur in Southeast Asia. From 1981 through 1986, 796 386 cases of DHF and 9774 deaths caused by dengue were reported to the World Health Organization (WHO) from countries in Southeast Asia (Halsread, 1990). Dengue viruses are spread by female *Aedes* mosquitoes through blood-feeding on human hosts. Patients suffering from dengue fever experience sudden onset of fever, rashes, muscle aches, joint pain, and leucopenia. A dengue patient usually recovers within 14 days. Nevertheless, some patients develop severe dengue which is a potentially lethal complication characterized by hemorrhagic manifestations, severe plasma leakage, and severe organ impairment (WHO, 2009). Globally, about 500,000 severe dengue cases with 12,500 deaths have been reported annually (WHO, 2012).

Dengue haemorrhagic fever was first reported in Thailand in 1950. In the beginning, about 50 to 100 cases were diagnosed annually until the first large outbreak of the disease in 1958 when 2158 cases and 300 deaths were reported. In earlier outbreaks, the disease was mainly found in Bangkok and surrounding areas. Since 1965, it has been reported from all regions of Thailand. (Rojanapithayakorn, 1998). The southern region had the highest incidence of dengue during this period, with 4,136 dengue incidences and a dengue incidence rate of 25.06 cases per 100,000 populations. There were 314 incidences in Nakhon Si Thammarat province, or 20.58 dengue incidences per 100,000 population (Bureau of Epidemiology, 2012)

During the years 2012 - 2016, the researcher (Promprao *et al.*, 2015; Promprao, *et al.*, 2016; Promprao, *et al.*, 2018) studied the dengue related issues in several related projects at Kreang Sub-District, Cha-Uat District, Nakhon Si Thammarat, Thailand. The result of these projects found that Dengue haemorrhagic fever has been reported in 10 villages out of 11 villages (Cha-Uat Hospital, 2016). Dengue hemorrhagic fever in each village was not repeated with consecutive years. Entomological Indices were the index to assess DHF risk areas of the latest 3-year were likely to the downward trend (House Index: HI=34.7,16.5,13.8; Container Index: CI=8.6,5.1,3.3; Breteau Index: BI=73.6,18.2,16.3) (Promprao *et al.*, 2015; Promprao, *et al.*, 2016; Promprao, *et al.*, 2018). There is no specific treatment for dengue, but appropriate medical care frequently saves the lives of patients with the more serious dengue haemorrhagic fever. The most effective way to prevent dengue virus transmission was to combat the disease-carrying mosquitoes (WHO, 2011). Knowing the trends and patterns of dengue disease will lead to sustainable disease prevention and control. An importance campaign for the prevention of DHF ought to start at studying the relationship between DHF patients and related variables that involved the human behaviors' factors, such as the changes in patterns of water storage in containers, which serve as breeding sites for the mosquitoes, may also affect disease transmission patterns (Gubler, 1998). **Objective of this study** was to develop and validate a Poisson Regression Model (PRM) to verify predictors of DHF patients in Kreang Sub-District, Cha-Uat District, Nakhon Si Thammarat, Thailand.

Materials and Methods

1. Study area

Khreng was one of Sub-District of Cha-Uat District, Nakhon Si Thammarat, Thailand. Seventy percentage of Khreng Sub-District was swamp forest. There was a forest in lowland flooding throughout the year. The natural river flow was Cha-Uat which flows into the sea at Pak Phanang River. Most people living along the flood plains, flat area without water flooding, and live in the hills known as "khuan", which has a total area of 110,016 Rai (hectares). Khreng Sub-District was divided into 11 villages with a local population 84,227 and a density of 101.1 /km² (Figure 1).

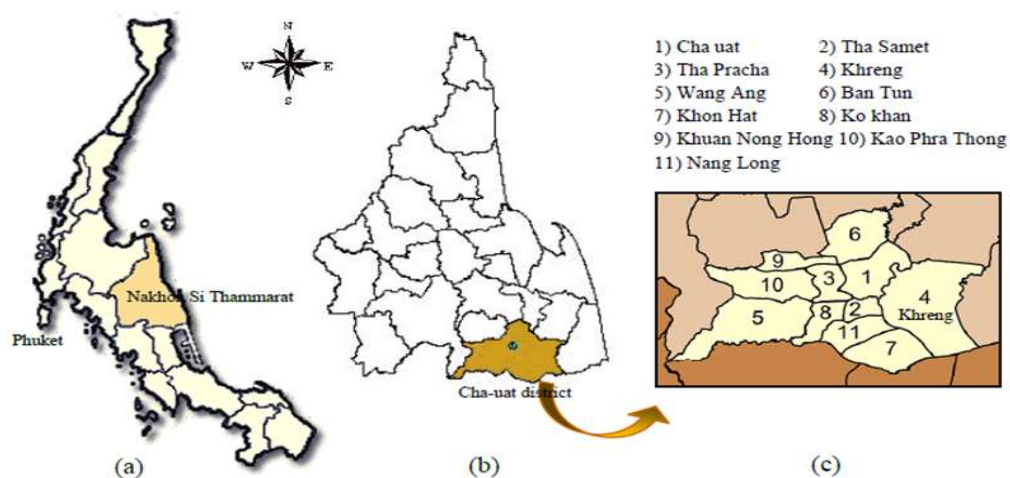


Figure 1 Study Area Khreng Sub-District, Cha-Uat District, Nakhon Si Thammarat, Thailand

2. Data collection

A questionnaire survey was conducted in Khreng Sub-District, in August-October 2016, covering 11 villages that composed of 1) Ban Hua Thanon 2) Ban Sai Hua Mar 3) Ban Khuan Yao 4) Ban Khuan Khreng 5) Ban Thung Krai 6) Ban Khuan Rab 7) Ban Yan Deang 8) Ban Samet Ngam 9) Ban Khuan Ching 10) Ban Bang Noi 11) Ban Sai Khanun. One hundred and sixty households in these areas were sampled by a systematic stratified random sampling technique. By a proportional allocation method, these 160 sample units were assigned to 11 villages that assigned as stratum (Fig. 2). One person per household in the collected household was identified as a sample unit. Breeding places (Katyal et al., 1997) were sampled both indoors and outdoors within 15 m of the houses. DHF cases and human behavior's factors were collected from 160 households by interview and survey.

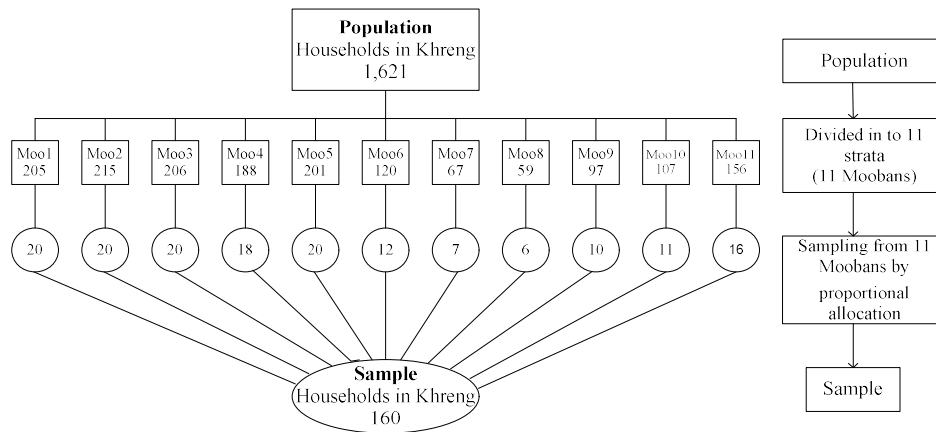


Figure 2 Sampling procedure

3. Poisson regression model (PRM)

PRM is commonly used for count data (MacDonald *et al.*, 2010). In modeling PRM, one of the major assumptions was the equality of the mean and variance. Poisson regression is similar to regular multiple regressions except that the dependent (Y) variable is an observed count that follows the Poisson distribution. Thus, the possible values of Y are the nonnegative integers: 0, 1, 2, 3, and so on. The Poisson regression analysis is used since the distribution of dengue cases data is in a form of Poisson distribution function. Poisson distribution appears to be appropriate when the response variable consists of nonnegative integers and is not normally distributed (Miaou and Lum, 1993; Kleinbaum *et al.*, 1998; Green, 2003). Furthermore, the occurrence must be random and independent of each other. Poisson regression is a regression technique available for modeling variables that describe count or discrete data of the occurrences of some event over a specified interval. This is a common process in clinical and epidemiological research (Pedan, 2001; Parodi and Bottarelli, 2006).

The Poisson probability distribution with parameter μ is given by the formula:

$$p(y) = P(Y = y) = \frac{e^{-\mu} \mu^y}{y!}, y = 0, 1, 2, \dots \quad (1)$$

where $\mu > 0$ is the mean of y. The logarithm of response variable is linked to a linear function of explanatory variables such that:

$$\ln(y) = \beta_0 + \beta_1 x_1 + \beta_2 x_2 + \beta_3 x_3 + \dots + \beta_p x_p \quad (2)$$

$$\text{and } y = (e^{\beta_0})(e^{\beta_1 x_1})(e^{\beta_2 x_2}) \dots (e^{\beta_p x_p}) \quad (3)$$

where the predictor variables $x_1, x_2, x_3, \dots, x_p$ are given, and the population regression coefficients $\beta_0, \beta_1, \beta_2, \beta_3, \dots, \beta_p$ are to be estimated (Zwilling, 2013). This formulation is popular because it allows the modeling of Poisson heterogeneity using a gamma distribution (Cameron and Trivedi, 2013; Hilbe, 2014). This program computes Poisson regression on both numeric and categorical variables. It reports on the regression equation as well as the goodness of fit, confidence limits, likelihood, and deviance. It performs a comprehensive residual analysis

including diagnostic residual reports and plots. It can perform a subset selection search, looking for the best regression model with the fewest independent variables.

DHF cases (patients) and human behavior's factors were collected from 160 households by interview and survey (Fig.3), starting from August - October 2016. DHF cases were count data and were treat as the response variables. The mean and variance of it was not significantly different. These suggested that a PRM would be appropriate. Human behavior's factors composed of number of cement tanks (CT), toilet cement tanks (TCT) and number of water jars were assigned to exploratory variables (Table 1).

Table 1 Mean, standard deviation and variance of number of DHF cases and behavior's factor of households

Name of variables	mean	standard deviation	variance
DHF cases	0.11	0.41	0.17
no. of cement tanks outdoor (CT)	0.01	0.11	0.01
no. of cement tanks for toilet (TCT)	0.01	0.11	0.01
no. of water jars (WJ)	0.26	0.44	0.19

Maximum Likelihood method was used to parameter estimation and Poisson regression technique was used to analysis method. The general model was as followed:

$$\log (\text{DHF}) = b_0 + b_1X_1 + b_2X_2 + b_3X_3 + \dots + b_k X_k$$

$$\text{DHF} = \exp[b_0 + b_1X_1 + b_2X_2 + b_3X_3 + \dots + b_k X_k]$$

$$\text{DHF} = e^{b_0} e^{b_1 x_1} e^{b_2 x_2} e^{b_3 x_3} \dots e^{b_k x_k}$$

where DHF was number of dengue haemorrhagic fever cases, $b_0, b_1, b_2, b_3, \dots, b_k$ were constants in model and $X_1, X_2, X_3, \dots, X_k$ were independent variables.

4. Significance Testing

This study used the maximum likelihood ratio statistics or commonly known as deviance (D) statistics to test for the goodness of fitted model for Poisson regression model. Deviance in the normal linear regression was similar to R^2 or coefficient of determination which was used to provide the descriptive information about the model fit and was calculated by:

$$R^2 = \frac{\sum(\hat{y} - \bar{y})^2}{\sum(y - \bar{y})^2}$$

where y was the observed value of y , \hat{y} was the value of y predicted from the model, and \bar{y} was the mean value of y . The log likelihood ratio statistic (deviance) was introduced to check the appropriateness of a chosen response distribution when explanatory variables were added or excluded from the model. The deviance value was defined as:

$$\text{Deviance (D)} = 2 \left\{ \sum_i [y_i \ln \left(\frac{y_i}{\hat{\mu}_i} \right) - (y_i - \hat{\mu}_i)] \right\}$$

For a well fitted model with appropriate link function, error distribution and functional form, the expected value of residual deviance should approximately be equal to the number of degree of freedom, regardless of the value of μ (Wan et al., 2010). SPSS were used to parameter estimation by considering from mean deviance that, the mean deviance close to 1 was the optimal model. (UCLA Academic Technology Services, 2012)

5. Residuals analysis

To fully assess model fit, residual can be thought of as the error associated with predicting or estimating outcomes using predictor variables. Residuals analysis was extremely important for meeting the linearity, normality and homogeneity of variance assumptions of poisson regression model.

Results and Discussion

This dataset of DHF cases contains 160 observations, with the smallest number being 0. The maximum number of 3, the mean is 0.110, the standard deviation is 0.414, the variance is 0.168, and the distribution index is $0.168 / 0.110 = 1.52 \sim 1$. The mean and variance of the variables were not significantly different. It is equal or at least roughly equal (Rodriguez, 2007). This model assumes that these values are independent variables. Poisson process occurred so the detailed creation steps are as follows:

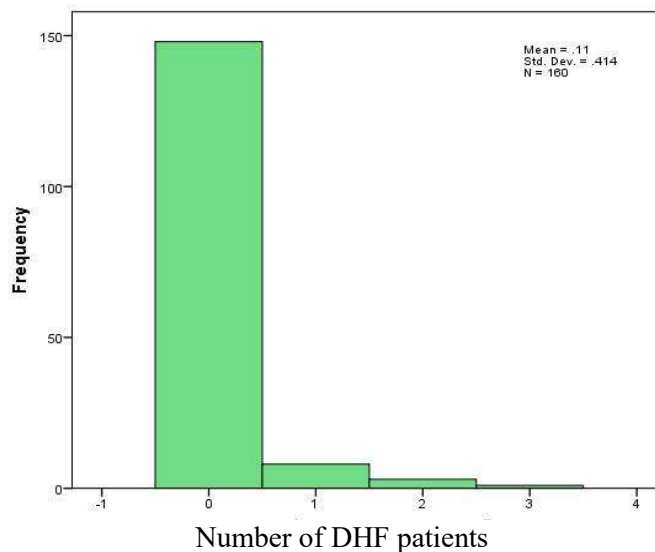


Figure 3 The distribution of the number of DHF patients in Khreng Sub-District

Table 2 Goodness of Fit for verifying the suitability of the data

Goodness of Fit			
	Value	df	Value/df
Deviance	77.287	156	0.495
Scaled Deviance	77.287	156	
Pearson Chi-Square	223.000	156	1.429
Scaled Pearson Chi-Square	223.000	156	
Log Likelihood	-52.060		

The goodness of fit table lists various statistics indicating model does the fit the data well (value/df of Pearson Chi-Square = 1.429 > 0.05). To assess the fit of the model, the goodness of fit chi-squared test was provided. The deviance (77.287) was evaluated as chi-squared distributed with the model degrees of freedom (156). A test of the model form fitted our data and concluded that the model fitted reasonably well because the goodness of fit chi-squared test was not statistically significant with 156 degrees of freedom.

Table 3 Chi-Square value of likelihood ratio

Omnibus Test		
Likelihood Ratio Chi-Square	Degree of freedom	p-value
13.849	3	0.003

Table 3 showed Omnibus Tests. This was test that all the estimated coefficients were equal to zero. From the p-value = 0.003 < 0.05, it had shown that the model suitable for data and was statistically significant at 0.05 level.

Table 4 Estimators of coefficients for Poisson regression model; CT = no. of cement tanks outdoor, TCT= no. of cement tanks for toilet, WJ= no. of water jars

Parameters	Degree of freedom	Coefficients (B)	Wald Chi-square	p-value	Exp(B)	95% Confidence Interval of Exp(B)	
						Lower	Upper
Constant	1	-2.970	52.940	0.000	0.051	0.023	0.114
CT	1	1.584	4.015	0.045	4.875	1.035	22.957
TCT	1	2.277	4.445	0.035	9.750	1.174	80.986
WJ	1	1.386	6.589	0.010	4.000	1.388	11.528

Table 4 included the regression coefficients for each of the variables along with p-value and 95% confidence intervals for the exponential of coefficients. Constant (constant; $\chi^2_{(1)} = 52.940$, $p = 0.000 < 0.05$) and three significant predictor variables were cement tanks outdoor CT: $\chi^2_{(1)} = 4.015$, $p = 0.045$) cement tanks for toilet (TCT: $\chi^2_{(1)} = 4.445$, $p = 0.035$) and water jar (WJ: $\chi^2_{(1)} = 6.589$, $p = 0.010$). Sometimes, we might want to present the results as incident rate ratios. These values were equal to our coefficients from the output above exponential column. The log of the DHF was predicted with a linear combination of the predictors: $\log(\text{DHF}) = -2.970 + 1.584(\text{CT}) + 2.277(\text{TCT}) + 1.386(\text{WJ})$. This implies: $\text{DHF} = \exp [-2.970 + 1.584(\text{CT}) + 2.277(\text{TCT}) + 1.386(\text{WJ})]$.

The significant predictor variables consisted of no. of cement tanks outdoor, no. of cement tanks for toilet and no. of water jars. The log of the DHF was predicted with a linear combination of the predictors: $\log(\text{DHF}) = -2.970 + 1.584(\text{CT}) + 2.277(\text{TCT}) + 1.386(\text{WJ})$. This implies: $\text{DHF} = \exp [-2.970 + 1.584(\text{CT}) + 2.277(\text{TCT}) + 1.386(\text{WJ})]$. These mean that the expected increase in logarithmic of count of DHF patients for a one unit increase in number of cement tanks outdoor, number of cement tanks for toilet and number of water jars were 1.584, 2.277 and 1.386, respectively.

Based on the above statement it can be explained that

$$\log(\text{DHF}) = -2.970 + 1.584(\text{CT}) + 2.277(\text{TCT}) + 1.386(\text{WJ})$$

$$\text{DHF} = \exp[-2.970 + 1.584(\text{CT}) + 2.277(\text{TCT}) + 1.386(\text{WJ})]$$

$$\text{DHF} = \exp[-2.970] \exp[1.584(\text{CT})] \exp[2.277(\text{TCT})] \exp[1.386(\text{WJ})]$$

$$\text{DHF} = [e^{-2.970}] [e^{1.584(\text{CT})}] [e^{2.277(\text{TCT})}] [e^{1.386(\text{WJ})}]$$

$$\text{DHF} = 0.051303 [e^{1.584(\text{CT})}] [e^{2.277(\text{TCT})}] [e^{1.386(\text{WJ})}]$$

The coefficient for the CT variant was 1.584, it meant that if the number of outdoor cement tanks were increased by 1 unit, log(DHF) would increase by 1,548 units (when other variables are fixed). That is, the DHF (dengue hemorrhagic fever) will increase by about 0.25 units (DHF = (0.051303)exp [1.584] = (0.051303)(4.875) = 0.250 estimates)

The coefficient for the TCT variant was 2.277, it meant that if the number of toilet cement tanks were increased by 1 unit, log (DHF) would increase by 2,277. That is, DHF (dengue hemorrhagic fever) would increase by approximately 0.50 units (DHF = (0.051303)exp [2.277] = 0.500 estimates). While the coefficient for the WJ variant was 1.386, it meant that if the amount of water jar were increased by 1 unit, log (DHF) would increase by 1.386. That is, the DHF (dengue fever) increase 0.205 units (DHF = (0.051303) exp[1.386] = 0.205 estimates)

Cement tanks and toilet cement tanks were important variable to explain the number of DHF patients. They were estimated to positively influence the number of DHF cases in Khreng Sub-District. One point three percentage and 31.9% of households used cement tanks and toilet cement tanks to store water for daily consumption. They were a common reservoir of water in this area as a cultural practice in Girardot (Columbia) and the practices of water storage were associated with being a housewife (García-Betancourt *et al.*, 2015). Cement tanks were *Aedes* positive containers in this study, this finding agreeable with the study of Kusumawathie and Fernando (2003), Wongkoon *et al.* (2007) and Promprao *et al.* (2015), founded that cement tanks have been infested with *Aedes* larvae, identified as the major breeding sites in the Kandy District of Sri Lanka, and preferred breeding site for *Ae. aegypti* and *Ae. albopictus* mosquito in Kreang Sub-District, Cha-Uat District, Nakhon Si Thammarat, respectively. However, cement tanks in the toilet or bathroom were more common than common cement tanks. High growth rate of larvae was found from these containers. It should be paid attention because it was a source of untamed water in the dark. Cleaning was not easy and was usually done in the bathroom (Chansang *et al.*, 1993).

Water jars were opened water-filled containers provided breeding sites for *Aedes* mosquitoes. All of them were found around the houses during the survey. This result was corresponded with the studies of Koopman *et al.* (1991). Khera and Sharma (1993) and Bhandari *et al.* (2008), indicated that uncovered water containers and pitchers were significantly associated with dengue infection. They were estimated to positively influence the number of DHF cases in Khreng Sub-District. 25.6% of households used these containers for storage rainwater for drinking and consuming in households. The study was in the same way as the study of Chansang *et al.* (1993) and Chang *et al.* (2009), revealed that the most positive container with *Aedes* larvae were the jars, the number per house was 0.58 in Southern Thailand (Chansang *et al.*, 1993). The majority of pupae were recovered either from large concrete water storage jars or concrete water storage tanks. There were small but significantly higher levels of dengue vector infestation in rural than urban areas (Chang *et al.*, 2009).

Conclusion

Cement tanks and water jars were important variables to explain the number of DHF patients. They were estimated to positively influence the number of DHF cases in Khreng Sub-District, Cha-Uat District, Nakhon Si Thammarat. Thus, mosquitoes control in water storage; cement tanks and water jars were important for mosquito borne disease control and prevention as well as for reduction for mosquito nuisance. Understandings the person's behaviors in relation to the number of DHF patients, will be able to predict the occurrence of DHF and plans to prevent and control this disease.

Acknowledgement

This study was financial supported by Nakhon Si Thammarat Rajabhat University, Office of the Higher Education Commission, Thailand.

References

- Bhandari, K.P., Raju, P.L.N. and Sokhi, B.S. 2008. Application of GIS modeling for dengue fever prone area based on socio-cultural and environmental factors –a case study of Delhi city zone. **Remote Sensing and Spatial Information Sciences**37: 165-170.
- Bureau of Epidemiology. 2012. DHF Situation in Thailand, Thailand: Ministry of Public Health.
- Cameron, A. C. and Trivedi, P. K. 2013. **Regression Analysis of Count Data**. 2nd Ed. Cambridge University Press. NewYork.
- Chansang, CH., Chansang, U., Thavara, U. and Phun-Urai, P. 1993. The distribution of *Aedes aegypti* in Rural Areas During 1989-1991. Bulltin of the department of medical sciences. 35(2): 85-102.
- Chang, M., Seng, C.M., Setha, T., Nealon, J. and Socheat, D. 2009. Pupal sampling for *Aedes aegypti* (L.) surveillance and potential stratification of dengue high-risk areas in Cambodia. **Tropical Medicine and International Health**14(10): 1233-1240.
- Cha-Uat Hospital. 2016. **Patient registration DHF-Kreang Sub-District**. Information from Cha-Uat Hospital.
- Green, W.H. 2003. **Econometric Analysis** 5th Ed. Prentice Hall.
- García-Betancourt, T., Higuera-Mendieta, D.R., González-Uribe, C., Cortés, S. and Quintero, J. 2015. Understanding Water Storage Practices of Urban Residents of an Endemic Dengue Area in Colombia: Perceptions, Rationale and Socio-Demographic Characteristics. PLOS ONE 10(6): e0129054. <https://doi.org/10.1371/journal.pone.0129054>
- Gubler, D.J. 1998. Dengue. In: Monath T.P., ed. **The arboviruses: epidemiology and ecology**. Boca Raton, FL: CRC Press, 1988: chap 23, 223-60.
- Halsread, S.B. 1990. Dengue. In: Warren, Mahmoud, eds. Tropical and geographic medicine. New York: McGraw-Hill.
- Hilbe, J.M. 2014. Negative Binomial Regression. In Modeling Count Data (pp. 126-161). Cambridge: Cambridge University Press.
- Katyal, R., Kumar, K. and Gill, K.S. 1997. Proceedings of *Aedes aegypti* and its impact on dengue/DHF in rural areas. WHO/SEARO. **Dengue Bulletin**21, 93–95.
- Khera, A., Sharma, R.S. 1993. Epidemiological investigations of an outbreak of dengue fever in Malikpur village under Najafgarh block, Delhi. **Dengue Newsletter**18: 1.

- Kleinbaum, D.G., Kupper, L.L. Muller and Nizam, K.E.A. 1998. **Applied Regression Analysis and Other Multivariate Methods 3rd Ed.** Duxbury Press.
- Koopman, J. S., Prevots, D. R., Vaca Marin, M. A., Gomez Dantes, H., Zarate Aquino, M. L., Longini Jr., I. M. and Sepulveda, A. J. 1991. Determinants and predictors of dengue infection in Mexico. **American Journal of Epidemiology**, 133 (11): 1168–1178.
- Kusumawathie, P.H.D. and Fernando, W.P. 2003. Breeding habitats of *Aedes aegypti* Linnaeus and *Ae. albopictus* Skuse in a dengue transmission area in Kandy, Sri Lanka. **Ceylon Journal of Medical Science** 46 (2): 51–60.
- MacDonald, J. and Lattimore, P. 2010. Count models in criminology. In Piquero A, Weisburd D, Eds. **Handbook of Quantitative Criminology**. Springer.
- Miaou, S.P. and Lum, H. 1993. Modeling Vehicle Accidents and Highway Geometric Design Relationships. **Accident Analysis and Prevention** 25(6): 689-709.
- Parodi, S. and Bottarelli, E. 2006. **Poisson Regression Model in Epidemiology -An Introduction, Annual Report of Faculty of Medicine**. Vet. di Parma (Vol. XXVI, 2006): 25-44.
- Pedan, A. 2001. Analysis of Count Data Using the SAS® System. SAS Proceedings, SUGI 26: 247-26.
- Pinheiro, F.P. 1989. Dengue in the Americas 1980-1987. **Epidemiology Bulletin** 10:1-8.
- Promprao, S., Ratmanee, Y. and Kaikaew, J. (2015). **Distribution of Aedes Mosquitoes at Kreang Sub-District, Cha-Uat District, Nakhon Si Thammarat**, Nakhon Si Thammarat Rajabhat University. (research report year 1)
- Promprao, S., Ratmanee, Y. and Kaikaew, J. (2016). **Distribution of Aedes Mosquitoes at Kreang Sub-District, Cha-Uat District, Nakhon Si Thammarat**, Nakhon Si Thammarat Rajabhat University. (research report year 2)
- Promprao, S., Ratmanee, Y. and Kaikaew, J. (2018). Ecology of Aedes Mosquitoes in Kreang Sub-District, Cha-Uat District, Nakhon Si Thammarat. **Taksin University Journal** 21(1): 9-21.
- Rodriguez, J. 2007. A constraint programming model for real-time train scheduling at junctions. *Transportation Research Part B*, 41:231–245.
- Rojanapithayakorn, W. 1998. Dengue Haemorrhagic Fever in Thailand. **Dengue Bulletin** 22: 60-72.
- UCLA: Academic Technology Services, Statistical Consulting Group. 2011. Available Source: <http://www.ats.ucla.edu/stat/r/dac/zinbreg.htm>
- Wan Fairos, W. Y., Wan Azaki, W. H., Mohamad Alias, L. and Bee Wah, Y. 2010. Modelling Dengue Fever (DF) and Dengue Haemorrhagic Fever (DHF) Outbreak Using Poisson and Negative Binomial Model. **World Academy of Science, Engineering and Technology** 38: 903-908.
- Wongkoon, S., Jaroensutasinee M. and Jaroensutasinee, K. 2007. Development sites of *Aedes aegypti* and *Ae. albopictus* in Nakhon Si Thammarat, Thailand. **Dengue Bulletin** 31: 141-152.
- WHO. 2009. Dengue: guidelines for diagnosis, treatment, prevention and control - New edition. Geneva: World Health Organization.
- WHO. 2011. Comprehensive guidelines for prevention and control of dengue and dengue haemorrhagic fever. Revised and expanded edition. India: World Health Organization.
- WHO. 2012. Dengue and dengue haemorrhagic fever. Fact sheet 117. World Health Organization. Available Source: <http://www.who.int/mediacentre/factsheets/fs117/en/>
- Zwilling, M.L. 2013. Negative binomial regression. **The Mathematica Journal**. [Dx.doi.org/10.3888/tmj.15-16](https://doi.org/10.3888/tmj.15-16).

Exploration of Aquatic Plants and Algae in Rajamangala University of Technology

Akhom Khatfan ^{1*} and Tassnapa Wongsansilp ¹

ABSTRACT

Natural water resources harbor several species of aquatic plant and algae. Two groups of organism were more or less linked to each other. In order to maintain a sufficiency and sustainable utilization of natural resources, a proximate exploration of aquatic plants in the areas of Rajmangala University of Technology Srivijaya, Trang Campus, was conducted. Several aquatic plants living in seasonal water pools were identified. Signal grass (*Brachiaria*), Bermuda grass (*Cynodon*) and sedge (*Cyperus*) were found everywhere in the area. Water hyacinth (*Eichhornia*), water pennywort (*Hydrocotyle*), pipewort (*Eriocaulon*), morning glory (*Ipomoea*), lotus (*Nelumbo*), and tridax daisy (*Tridax*) were less abundant. Water sprite (*Ceratopteris*), *Hydrilla*, and water snowflake (*Nymphoides*) were found in limited areas. The most common freshwater algae found living with these aquatic plants were *Oscillatoria*, *Chara*, *Closterium*, *Cosmarium*, and *Spirogyra*.

Keywords: Aquatic plants, Freshwater algae, Density

¹ Department of Biological Science Faculty of Science and Fisheries Technology, Rajamangala University of Technology Srivijaya, Sub-district Maifat, District Sikao, Province Trang 91150, Thailand

* Corresponding author, e-mail) : akhom.k@gmail.com

Introduction

Natural water sources such as pools and ponds harbor aquatic plants and algae. Both groups of living are producers of ecosystem. They are responsible for generating organic matters and stored it in their tissue. Fish and zooplanktons get benefit from these plants and algae not only directly as food but also indirectly as shelters (Dodds and Gudder, 1992). Algae also contribute to environment stabilization; *Cladophyta* and *Spirogyra* absorbed certain kinds of heavy metals such as lead and copper (Lee and Chang, 2011). *Cladophora* provides chemical for cosmetic uses. (Soltani *et al.*, 2011).

Plants and algae are affected by environmental changes such as global warming, water acidification, etc. The effects either positively or negatively exert on plants and algae; different ecological condition promotes certain kind of algae, such as, *Galdieria* (Hirooka *et al.*, 2017). On the other hand, management of plants and algae in ecological community might be a way to improve those environmental changes. The aim of this study was to explore and identify plants and algae. Information would be further used to manipulate plants and algae in ecological optimization to approach better condition for agriculture and better human living.

Materials and Methods

Exploration of the campus area was conducted on October, 2017 and April, 2018. Aquatic Plants were taken photograph. Plant's type was identified into three categories regarding to the report of Brown (2012). Plant densities were scored as “abundant and found everywhere” (++++), “abundant and found in certain area” (+++), “moderate and found in limited area” (++) and “few and found in limited area” (+). Water samples were examined under microscope. Algae, found under microscope, were identified regarding to description reported by Van Vuuren *et al.* (2006). Plants which were susceptible to lack of water, such as Water pennywort, water snowflake and hydrilla, were kept in artificial ponds, to be analyzed during dry season. Water samples from these ponds were examined for algae as well.

Results and Discussion

Thirteen genera of aquatic plants, in eight orders and 10 families, were found and identified. Nine genera were classified as “marginal” plants (Table 1). Signal grass (*Brachiaria*), Burmuda grass (*Cynodon*) and sedges (*Cyperus*) were considered abundant; these three genera were seen everywhere. Water hyacinth (*Eichhornia*), pipewort (*Eriocaulon*), water pennywort (*Hydrocotyle*), morning glory (*Ipomoea*) lotus (*Nelumbo*) and tridax daisy (*Tridax*) were less abundant and found in the certain areas (Figure 1 and 2). Water sprite (*Ceratopteris*), *Hydrilla* and water snowflake (*Nymphoides*) were found in a few number and only in the limited areas (Figure 3). Since water sources in the campus area were not permanent pools, when water dried out, three later genera were died or turned into dormant stage and were not seen.

The pool areas, once dominated by these plants, were outgrown by other land plants, including *Cyperus* and other grass plants during dry season. During flood season, grass plants were probably affected by lack of oxygen. Deplete of oxygen, in plant tissues, promoted anaerobic respiration which resulted in accumulation of anaerobic metabolites such as alcohol and lactic acid (Crawford, 2003) and grass probably less tolerate to these metabolite than aquatic plants.

Table 1 Classification and density of aquatic plants in Rajmangala University of Technology Srivijaya, Trang Campus

Genus	Type	Clade	Order	Family	Density
<i>Brachiaria</i>	Marginal	Monocots	Poales	Poaceae	++++
<i>Ceratopteris</i>	Marginal	Ferns	Polypodiales	Pteridaceae	+
<i>Cynodon</i>	Marginal	Monocots	Poales	Poaceae	++++
<i>Cyperus</i>	Marginal	Monocots	Poales	Cyperaceae	++++
<i>Eichhornia</i>	Floating	Monocots	Commelinales	Pontederiaceae	+++
<i>Eriocaulon</i>	Marginal	Monocots	Poales	Eriocaulaceae	++
<i>Hydrilla</i>	Submerged	Monocots	Alismatales	Hydrocharitaceae	+
<i>Hydrocotyle</i>	Marginal	Dicots	Apiales	Araliaceae	+++
<i>Ipomoea</i>	Marginal	Dicots	Solanales	Convolvulaceae	+++
<i>Nelumbo</i>	Marginal	Dicots	Proteales	Nelumbonaceae	+++
<i>Nymphaea</i>	Floating	Dicots	Nymphaeales	Nymphaeaceae	++
<i>Nymphoides</i>	Floating	Dicots	Asterales	Menyanthaceae	+
<i>Tridax</i>	Marginal	Dicots	Asterales	Asteraceae	+++

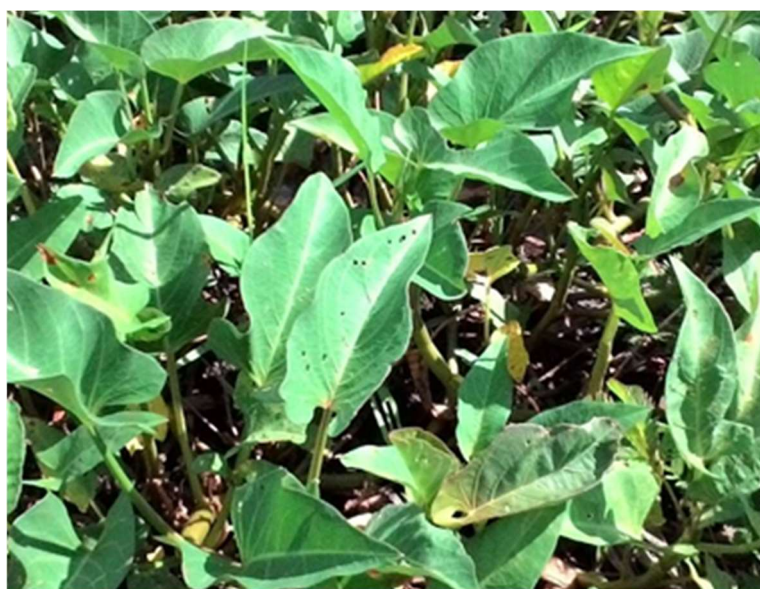


Figure 1 Morning glory (*Ipomoea aquatica* Forssk)



Figure 2 Water pennywort (*Hydrocotyle umbellata* L.) at flowering stage

Cyanobacteria were common to every water source in Rajmangala University of Technology Srivijaya, Trang Campus. *Oscillatoria* was dominant among other blue green bacteria in every pool directly contacted to sunlight and was grown in a form of green sludge floating on water surface; water snowflakes were also seen in the area (Figure 3). However *Oscillatoria* was not seen together with water pennywort which preferred shaded area. *Oscillatoria* was reported to be well adapted to sun light and able to tolerate to temperature fluctuation (Biddanda *et al.*, 2015).

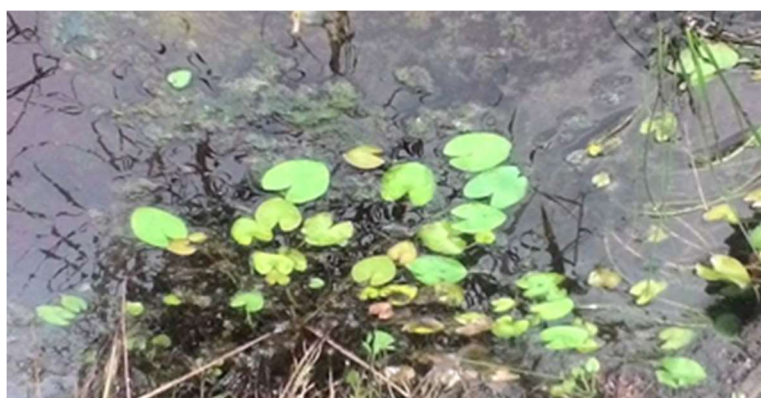


Figure 3 Water snowflake (*Nymphoides indica* (L.) Kuntze) in a natural water pool; *Oscillatoria* was also seen in the area as floating dark green patches

Green algae of Zygnematophyceae were abundant in the campus area. *Chara* grew well in area contact to sunlight. However *Oscillatoria* was not found in the area where *Chara* was seen. *Spirogyra* (Figure 4), on the other hand, was well adapted to shaded area (Krupek and Branco, 2012) and required soft water to grow (Cambra and Aboal, 1992). Hence this filamentous alga was easily seen in pools where water pennywort was grown.



Figure 4 *Spirogyra* observed under microscope (10x)

Other Zygnematophyceae algae, such as *Closterium* and *Cosmarium*, were also found in water canals and pools. *Closterium* was found in water bed under morning glory and was seen in two-celled crescent form. *Closterium* preferred shaded area, hence it was found on water bed and required light protection from aquatic plants (Van Vuuren *et al.*, 2006).

Cosmarium was observed in everywhere both shaded or sun lighted area (Stamenkovic and Hanelt, 2013). However, in this study *Cosmarium* was abundant in sun lighted area and was able to live well with *Oscillatoria*. *Cosmarium* itself produced mucilage substances as it was reported by Van Vuuren *et al.* (2006). The mucilage substances were able to cause trouble to some aquatic plants like water snowflake in this study.

Conclusions

Rajamangala University of Technology Srivijaya, Trang Campus harbored abundant of signal grass, Bermuda grass and sedges. Water pennywort, water hyacinth, pipewort, morning glory, lotus and tridax daisy were less abundant than the previous three. These nine genera of plants were able to survive as land plants during dry season. Several algae were found living with aquatic plants in the area. For the algae and cyanobacteria associated with these aquatic plants, most of algae belonged to Zygnematophyceae except *Oscillatoria*. *Oscillatoria*, *Chara* and *Cosmarium* preferred sun lighted area whereas *Closterium* and *Spirogyra* preferred shaded area.

References

- Biddanda, B.A., McMillan, A.C., Long, S.A., Snider, M.J. and Weinke, A.D. 2015. Seeking sunlight: Rapid phototactic motility of filamentous mat-forming cyanobacteria optimize photosynthesis and enhance carbon burial in Lake Huron's submerged sinkholes. **Frontiers in Microbiology** 6: 930.

- Brown, E. 2012. **Aquatic Plants**. Available Source: http://www.cowyafs.org/wp-content/themes/cowyafs/AquaticPlants/AquaticPlants_AFS_20120326.pdf, July 5, 2018
- Cambra, J. and Aboal, M. 1992. Filamentous green algae of Spain: Distribution and ecology. **Limnologia** 8: 213-220.
- Crawford, R.M.M. 2003. Seasonal difference in plant responses to flooding and anoxia. **Canadian Journal of Botany** 81: 1224-1246.
- Dodds, W.K. and Gudder, D.A. 1992. The ecology of *Cladophora*. **Journal of Phycology** 28: 415-427.
- Hirooka, S., Hirose, Y., Kanesaki, Y., Higuchi, S., Fujiwara, T., Onuma, R., Era, A., Ohbayashi, R., Uzuka, A., Nozaki, H., Yoshikawa, H. and Miyagishima, S. 2017. Acidophilic green algal genome provides insights into adaptation to an acidic environment. **PNAS** 114: E8304-E8313.
- Krupek, R.A. and Branco, C.C.Z. 2012. Ecological distribution of stream macroalgae in different spatial scales using taxonomic and morphological groups. **Brazilian Journal of Botany** 35: 273-280.
- Lee, Y.C. and Chang, S.P. 2011. The biosorption of heavy metals from aqueous solution by *Spirogyra* and *Cladophora* filamentous macroalgae. **Bioresource Technology** 102: 5297-5304.
- Stamenkovic, M. and Hanelt, D. 2013. Adaptation of growth and photosynthesis to certain temperature regimes is an indicator for the geographical distribution of *Cosmarium* strains (Zygnematophyceae, Streptophyta). **European Journal of Phycology** 48: 116-127.
- Soltani, S., Saadatmand, S., Khavarinejad R and Nejadstatti, T. 2011. Antioxidant and antibacterial activities of *Cladophora glomerata* (L.) Kütz. in Caspian Sea Coast, Iran. **African Journal of Biotechnology** 10: 7684-7689.
- Van Vuuren, S.J., Taylor, J., Van Ginkel, C. and Gerber, A. 2006. **Easy Identification of the Most Common Freshwater Algae**. North-West University and Department of Water Affairs and Forestry, Pretoria, South Africa.

Evaluation of Universal Pre-enrichment Medium for Multiple Foodborne Pathogen Detection in Milk by PCR Based Method

Chanida Kupradit^{1*}, Chompoonuch Khongla¹, Sumalee Musika¹, Araya Ranok¹,
Seksan Mangkalan¹ and Mariena Ketudat-Cairns²

ABSTRACT

Milk has been shown to be a natural reservoir for a number of pathogens. Therefore, specific, and sensitive methods such as polymerase chain reaction (PCR) have been considered for detecting and identifying pathogens. Foodborne pathogen detection in naturally contaminated milk by PCR has been performed under varying enrichment medium and protocols. Therefore, the aim of this research was to evaluate the effect of different pre-enrichment broth including, buffer peptone water (BPW), lactose broth (LB), trypticase soy broth (TSB) and Half-Fraser broth (HF), on the sensitivity and specificity of PCR to detect *Bacillus cereus*, *Escherichia coli*, *Listeria monocytogenes*, *Salmonella* spp., and *Staphylococcus aureus* in artificially contaminated milk samples when compared to conventional culture techniques. For conventional culture detections, the presumptive colonies of all five target pathogens were observed on their selective agar after 24 hours enrichment in LB. For enrichment culture of BPW, TSB, and LB, the minimum bacterial load that tested positive for *E. coli*, *S. aureus* and *Salmonella* by PCR had 30, 25, and 13 cells in milk, respectively. Artificially contaminated milk sample with initial concentration of *L. monocytogenes* at 8 cells showed positive PCR results after 24 hour enrichment in HF. Contamination of *B. cereus* at initial concentration lower than 10 cells in milk could not be detected by PCR after 24 hour enrichment in all media while conventional culture could be detected in LB cultures. These results indicated that the suitable pre-enrichment broth for the detection of *B. cereus*, *E. coli*, *Salmonella* spp. and *S. aureus* was LB and for *L. monocytogenes* was HF. By this reason, the enrichment of two bacterial groups in LB for enrichment of *Salmonella*, *E. coli*, *S. aureus*, *B. cereus* and HF for *L. monocytogenes* will be performed prior to total genomic DNA extraction followed by simultaneous detection using PCR based method.

Keywords: Foodborne Pathogens, Pre-enrichment Broth, PCR, Milk

¹ Department of Applied Biology, Faculty of Sciences and Liberal Arts, Rajamangala University of Technology Isan, Nakhon Ratchasima, 30000, Thailand

² School of Biotechnology, Institute of Agricultural Technology, Suranaree University of Technology, Nakhon Ratchasima, 30000, Thailand

*Corresponding author, e-mail : Lego7823@hotmail.com

Introduction

Amongst the food samples, milk has been shown to be a natural reservoir for a number of pathogenic strains and thus represents a significant health risk (Ramesh *et al.*, 2002). In Thailand and many other countries, the prevalence of foodborne pathogens especially *Bacillus cereus*, *Escherichia coli*, *Listeria monocytogenes*, *Salmonella* spp. and *Staphylococcus aureus* in raw milk and dairy products have been reported (Chye *et al.*, 2004; Van Kessel *et al.*, 2004; Padungtod and Kaneene, 2006; Chitov *et al.*, 2008; Bianchi, 2013; Kanungpean *et al.*, 2014; Ombarak *et al.* 2016). The conventional methods for detecting enteropathogens in food comprises of propagation in selective enrichment media followed by microbiological and biochemical tests. They are very laborious and time consuming (Boera and Beumer, 1999; Ramesh *et al.* 2002). For cultural based methods, processing of large numbers of samples is not easy in general, 10 or more tests may be necessary for differentiation of the species within a group (Settanni and Corsetti, 2007). Therefore, rapid, specific, and sensitive methods for detecting and identifying pathogens have been developed. Most methods of detecting bacteria, including nucleic acid-based, antibody-based, and biosensor-based methods, frequently require a bacterial enrichment step. The growth of target bacteria may be influenced by the co-existence of other unrelated bacteria when a nonselective enrichment broth is used (Xiao *et al.*, 2014). The highly selective medium, secondary enrichment media can be employed to help select the specific bacteria from a mixed bacterial background culture (Bailey and Cox, 1992). Although the two-step enrichment method can be selective, it is labor intensive and time consuming (Xiao *et al.*, 2014). Thus, the universal pre-enrichment broth for effective growth of the regulated target pathogenic bacteria in milk, particularly for the growth of *B. cereus*, *E. coli*, *L. monocytogenes*, *S. aureus*, and *Salmonella* spp., is needed. Several research have reported the novel pre-enrichment broth for detection of multiple pathogens (Zhao and Doyle, 2001; Oliveira *et al.*, 2003; Myint *et al.*, 2006; Suo and Wang, 2013; Xiao *et al.*, 2014). However, data information of universal pre-enrichment broth to support the growth of *B. cereus*, *E. coli*, *L. monocytogenes*, *S. aureus*, and *Salmonella* spp. are still limited. Therefore, the purposes of the present study were to evaluate a pre-enrichment broth suitable for the concurrent growth of *E. coli*, *B. cereus*, *L. monocytogenes*, *Salmonella* and *S. aureus*. The general non-selective media including buffer peptone water (BPW), lactose broth (LB), trypticase soy broth (TSB) were tested for the performance of bacterial enrichment from milk. The selective media, Half Fraser broth (HF), was also evaluated for the enrichment of *L. monocytogenes*. The detection of multiple target pathogens were performed by PCR based methods using total genomic DNA extracted from each enrichment cultures after 24 hours enrichment as templates. The sensitivity and specificity of the enrichment media were evaluated from the artificially contaminated milk samples.

Materials and methods

1. Bacterial strains and culture conditions

The bacterial reference strains, including *B. cereus* TISTR 1474, *E. coli* TISTR 887, *L. monocytogenes* DMST 1327, *S. aureus* TISTR 517, and *Salmonella* Typhimurium TISRT 292, were obtained from The Culture Collection for Medical Microorganism, Department of Medical Sciences, Thailand (DMST) and Thailand Institute of Scientific and Technology Research (TISTR). All strains were aerobically grown at 37 °C in TSB (United States Food and Drug Administration, 1998). After overnight incubation from single colony, bacterial cells were used for preparation of artificially contaminated milk.

2. Artificially contaminated milk preparation and pre-enrichment

The evaluation of universal pre-enrichment for simultaneous multiple pathogen detection was tested with total of 4 enrichment broths. In this experiment, pasteurized milk from supermarket in local area were tested as natural and bacteria spiked samples. To determine the sensitivity of conventional culture and PCR for detecting bacteria, *B. cereus* TISTR 1474, *E. coli* TISTR 887 and *L. monocytogenes* DMST 1327, *S. aureus* TISTR 517 and *S. Typhimurium* TISRT 292 were separately grown in TSB at 37°C for 18–24 h. A 10-fold dilution series of each bacterial culture were prepared using 0.85% sterile NaCl solution. At the same time, enumeration was done by spreading 100 µl dilutions onto TSA plates for viable count. For spiked samples, 10 ml of the milk samples were spiked with 100 µl of each cell dilution solution prior to separately adding of 90 ml of each pre-enrichment broth including BPW (United States Food and Drug Administration, 1998), LB (United States Food and Drug Administration, 1998), TSB (United States Food and Drug Administration, 1998), and HF (Himedia, Mumbai, India). Sample BC, TC, LC and HC were non-spiked milk samples. Concentrations of each pathogen spiked in milk are shown in **Table 1**. The enrichment steps were performed to increase target bacterial cells in all universal pre-enrichment broths under aerobic condition for 24 hours at 37°C. After 24 hours incubation, aliquot of each enrichment culture from spiked and non-spiked milk samples were subjected to the PCR and conventional culture analyses. Target bacterial detection from the enrichment cultures were evaluated using conventional culture and PCR technique.

Table 1 The initial cell concentration of target pathogenic bacteria in artificially contaminated milk

Enrichment medium	Sample name	Bacterial concentration (cells)				
		<i>B. cereus</i>	<i>E. coli</i>	<i>L. monocytogenes</i>	<i>S. aureus</i>	<i>S. Typhimurium</i>
BPW	B _c	0	0	0	0	0
	B ₁	10	130	83	25	123
	B ₂	5	30	8	20	13
TSB	T _c	0	0	0	0	0
	T ₁	10	130	83	25	123
	T ₂	5	30	8	20	13
LB	L _c	0	0	0	0	0
	L ₁	10	130	83	25	123
	L ₂	5	30	8	20	13
HalF Fraser	H _c	0	0	0	0	0
	H ₁	10	130	83	25	123
	H ₂	5	30	8	20	13

3. Pathogen detection by conventional culture methods

For pathogen detection by conventional culture methods, all enrichment culture were streaked on MYP agar (Himedia), EMB agar (Himedia), PALCAM agar (Himedia), XLD agar (Himedia) and Baird Parker agar (Himedia) for *B. cereus*, *E. coli*, *L. monocytogenes*, *Salmonella* and *S. aureus* detections, respectively. The isolation of *E. coli* and *Salmonella* were incubated at 37°C for 24 hours. For *L. monocytogenes* detection, the enrichment cultures were incubated at 37°C for 48 hours. The isolation of *B. cereus* on MYP agar and *S. aureus* on Baird Parker agar were carried out at 35°C for 48 h.

4. Pathogen detection by PCR technique

For detection of bacterial pathogens by PCR technique, 1 ml of milk enrichment cultures from BPW, LB, TSB, and HF of a total 12 samples (**Table 1**) were separately collected. Cell pellets were harvested by centrifugation and washed once in 0.85% sterile NaCl solution. The cell pellets were then extracted for the total genomic DNA using phenol-chloroform based method (Kupradit *et al.*, 2013). The total genomic DNA pellet was dissolved in 50 µl Tris-EDTA (TE), pH8. PCR assay were performed using gene specific primers as shown in Table 2. A total volume of 25 µl PCR reaction contained 1X GenTaq PCR buffer (Invitrogen), 0.2 mM dNTPs (Invitrogen), primers of 0.4 µM of each primer (**Table 2**), 0.5 U DNA polymerase (Invitrogen), and genomic DNA templates. One µl of the total genomic DNA solution obtained from each enrichment cultures were used as template for separate amplification of 16S rRNA, *entFM*, *uspA*, *prfA*, *fimY* and *eap* genes. The PCR reactions were heated at 95°C for 3 min and then, 35 cycles at 95°C for 30 s, 52°C for 45 s, and 72°C for 60 s followed by a final step of 5 min incubation at 72°C. The products of PCR were analyzed by electrophoresis on 1.5% agarose gel.

Table 2 Primers used for target gene amplifications by PCR

Target bacteria	Target gene	Primer name	Primer sequences (5'→3')	PCR product size (bp)	References
All bacteria	16S rRNA	16S_F 16S_R	AGACTCCTACGGGAGGC GGTAAGGTTCTTCGCGT	625-655	Kupradit <i>et al.</i> , 2013
<i>S. aureus</i>	<i>eap</i>	SA_ <i>eap</i> _F1 SA_ <i>eap</i> _R1	TTAAATCGATATCACTAAATACCTC TACTAACGAAGCATCTGCC	230	Hussain <i>et al.</i> , 2008
<i>B. cereus</i>	enterotoxin <i>FM</i>	BC_ <i>EntFM</i> _F200 BC_ <i>EntFM</i> _R713	TGCTGATGTATTAAATGTTTCGTTTC GCGTTGTATGTAGCTGGGCCT	513	Kupradit <i>et al.</i> , 2017
<i>E. coli</i>	<i>uspA</i>	EC_ <i>uspA</i> _F EC_ <i>uspA</i> _R	CCGATACGCTGCCAATCAGT ACGCAGACCGTAGGCCAGAT	884	Chen and Griffiths, 1998
<i>L. monocytogenes</i>	<i>prfA</i>	LM_ <i>prfA</i> _F LM_ <i>prfA</i> _R	CACAAGAATATTGTATTTTCTATATGAT CAGTGTAATCTTGATGCCATCA	398	Kupradit <i>et al.</i> , 2013
<i>Salmonella</i> spp.	<i>fimY</i>	SM_ <i>fimY</i> _F SM_ <i>fimY</i> _R	GCCTCAATACAGGAGACAGGTAGCG GCAGGGAAAGACACCGCCGTTTAA	315	Kupradit <i>et al.</i> , 2017

Results and Discussion

1. Pathogen detection using conventional cultures

The target pathogens in 8 artificially contaminated milk samples with initial cell concentration ranging from 5 to 130 cells were enriched using different universal pre-enrichment medium and isolated on isolation agar. Sensitivity results of pathogen detection using conventional methods are shown in **Table 3**. The contaminations of target pathogens were not detected in all 4 non-spiking pasteurized milk samples (**Table 3**). For *E. coli* detection, the presumptive colonies which were able to produce metallic green sheen on EMB agar (Himedia) were found after 24 hours enrichment in BPW, TSB and LB media with low initial concentration of 30 cells (**Table 3**). For detection of *Salmonella* in artificial contaminated milks, red colonies with black center on XLD agar (Himedia) were observed after 24 hours enrichment in BPW, TSB and LB with initial cell concentration ranged from 123 to 13 cells (**Table 3**). The presumptive *Listeria* colonies of dark or with dark halo were found on esculin containing medium (PALCAM) (Himedia) from 24 hours enrichment in BPW, TSB, LB and

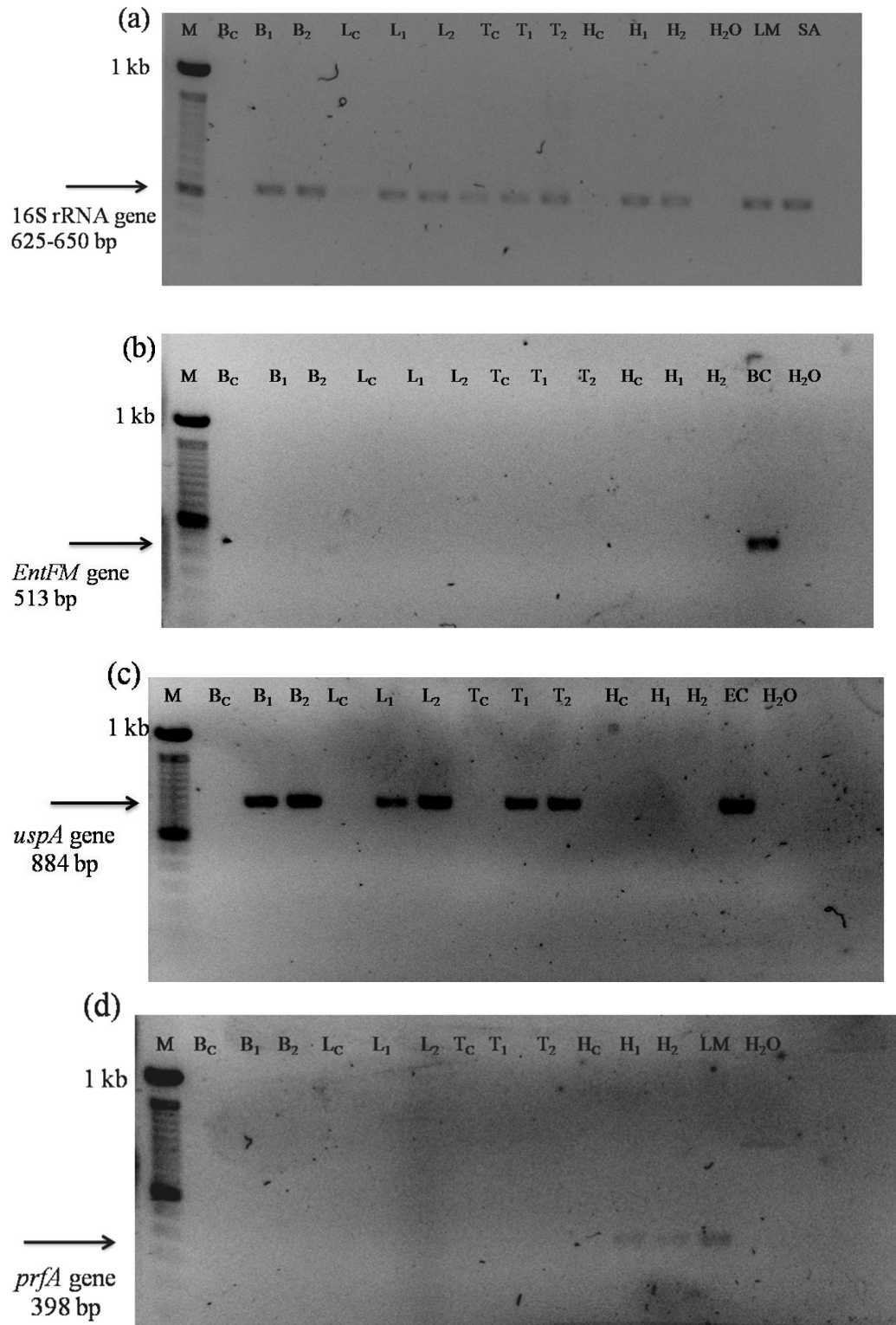
HF medium with initial concentration of 83-8 cells (**Table 3**). The black colonies with opaque zone of *S. aureus* were found on Baird Parker agar (Himedia) after 24 h enrichment in BPW, TSB, LB and HF with initial cell concentration of 20-25 cells. In case of *B. cereus*, low initial cell concentration as 5 cells in milks could be enriched only in LB media. The presumptive red colonies with opaque zone of *B. cereus* were found on MYP agar (Himedia) after 24 h enrichment in LB medium. Based on results of pathogen detection using conventional culture method, all target bacteria was isolated from artificially contaminated milk after 24 hours enrichment in LB with low initial concentration of 30 cells *E. coli*, 13 cells *Salmonella*, 8 cells *L. monocytogenes*, 20 cells *S. aureus*, and 5 cells *B. cereus*.

Table 3 Sensitivity of multiple target pathogen detections by conventional cultures from different pre-enrichment medium

Enrichment broth	<i>S. aureus</i> on Baird Parker agar	<i>L. monocytogenes</i> on PALCAM agar	<i>B. cereus</i> on MYP agar	<i>E. coli</i> on EMB agar	<i>Salmonella</i> spp. on XLD agar
HF +milk (control)	-	-	-	-	-
HF + milk spiked with bacteria	25 cells	8 cells	-	-	-
BPW + milk (control)	-	-	-	-	-
BPW + milk spiked with bacteria	25 cells	8 cells	-	30 cells	13 cells
LB + milk (control)	-	-	-	-	-
LB + milk spiked with bacteria	20 cells	8 cells	5 cells	30 cells	13 cells
TSB + milk (control)	-	-	-	-	-
TSB + milk spiked with bacteria	25 cells	8 cells	-	30 cells	13 cells

2. Multiple pathogen detection using PCR based methods

Multiple pathogen detection by PCR was performed using gene specific amplification as shown in **Table 2**. The 4 different pre-enrichment media, *E. coli*, *Salmonella* spp. and *S. aureus* were detected by PCR from artificial contaminated milk after 24 hours enrichment in BPW, TSB and LB (**Table 4**). Results of specific gene amplifications using total genomic DNA extracted from each enrichment cultures as templates are shown in **Figure 1**.



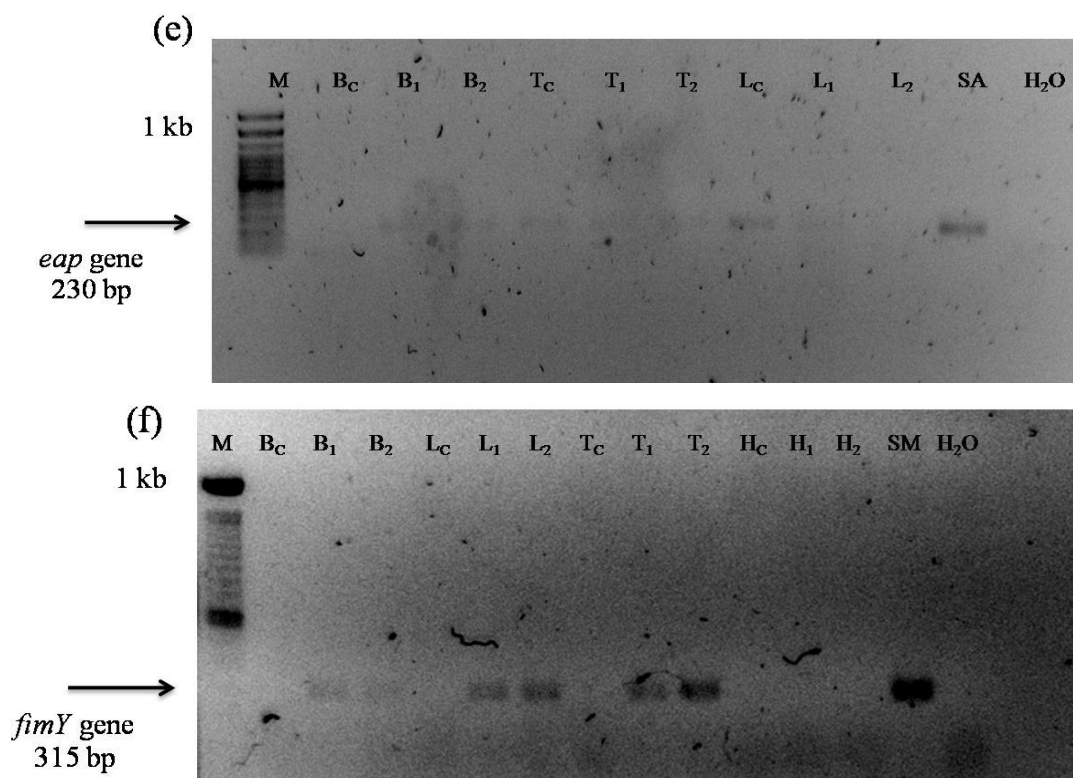


Figure 1 Sensitivity of pathogen detection from artificially contaminated milk with different cell concentrations (**Table 1**) by PCR after 24 hours enrichment in BPW (B), LB (L), TSB (T) and HF (H). The amplification of 16S rRNA with bacteria universal primers are shown in **Figure 1a**. The amplification of *EntFM*, *uspA*, *prfA*, *eap* and *fimY* genes with gene specific primers (**Table 2**) are shown in **Figure 1b-f**, respectively. M, DNA ladder 100 bp (Invitrogen). The genomic DNA of each target bacteria including, BC: *B. cereus*; EC: *E. coli*; LM: *L. monocytogenes*; SA: *S. aureus*; SM: *S. Typhimurium*, were used as templates of positive control for specific gene amplification of each specific primer.

The 16S rDNA PCR products were observed in agarose gel electrophoresis especially in the amplification of genomic DNA extracted from enrichment culture which target bacteria were spiked in milk samples (**Figure 1a**). In our research, the 16S rRNA gene which can be amplified from all target bacteria was used as an internal control of the presence of amplifiable bacterial DNA. These results indicated that the PCR reaction contained bacterial gDNA. The amplicons of gene specific were found from amplification of *uspA*, *eap*, and *fimY* using gDNA extracted from milk enrichment culture of BPW (B1, B2), LB (L1, L2), TSB (T1, T2) medium as templates for detection of *E. coli*, *S. aureus* and *Salmonella* spp. (**Figure 1c e, f**), respectively. These results indicated that BPW, LB and TSB could be used as the enrichment medium for simultaneous specific detection of *E. coli*, *S. aureus*, *Salmonella* spp. in milk by PCR methods. However, only the faint PCR product bands of *eap* and *fimY* were detected from amplification of specific gene using gDNA extracted from enrichment culture of BPW medium as template (**Figure 1e and f**). For enrichment culture of BPW, TSB and LB medium, the minimum initial concentration of bacterial load that tested positive for *E. coli*, *S. aureus* and *Salmonella* by PCR

had 30, 25, and 13 cells in sample, respectively. Similar results using the combination of enrichment step and PCR have been reported by Myint *et al.* (2006). Chicken meat samples from retail grocery stores were pre-enriched in buffered peptone water (BPW) and *Salmonella* specific primers ST 11 and ST 15 were used to amplify a 429 bp region of random fragment target specific to all *Salmonella* spp. Earlier researchers reported that both PCR and culture methods demonstrated increased sensitivity when pre-enrichment with BPW was followed with selective enrichment in TT-H (Myint *et al.*, 2006). For detection of *L. monocytogenes*, PCR products of *prfA* gene amplifications were observed in only the amplification of gDNA extracted from HF enrichment cultures (**Figure 1d**). Milk samples with initial *L. monocytogenes* concentration ranged from 83 to 8 cells showed positive results after 24 h enrichment using HF as enrichment medium. These results agree with the results observed by Joffe and colleagues in 2005. They reported that the enrichment of the samples only in BPW produced poor detection of *L. monocytogenes* due to the major growth of *Salmonella* in this broth. Another enrichment broth has been reported for enrichment of *Salmonella* spp., *S. aureus*, and *L. monocytogenes* in different food sources prior to detection by PCR based method. In 2001, Zhao and Doyle developed the universal pre-enrichment broth (UPB) for enrichment of injured foodborne pathogens of *E. coli* O157:H7, *S. Typhimurium*, *Salmonella* Enteritidis and *L. monocytogenes*. The researchers found that enrichment in UPB at 37°C of foods or environmental sponge samples containing heat-injured cells of *S. Typhimurium*, *S. Enteritidis*, *E. coli* O157:H7, or *L. monocytogenes* for 24 hours was sufficient cell population for detection by rapid immunoassay or PCR assay procedures (Zhao and Doyle, 2001). In 2003, Oliveira and colleagues reported that PCR with non-selective media (peptone water or in BHI) was less sensitive than PCR with selective media (RV broth) which could decrease the time necessary to detect and identify *Salmonella* (Oliveira *et al.* 2003). In 2008, Kim and Bhunia developed the SEL broth to allow the simultaneous growth of *Salmonella enterica*, *E. coli* O157:H7, and *L. monocytogenes*. Researcher investigated that SEL promoted the growth of all three pathogens in a mixture in ready-to-eat salami and in turkey meat samples. Moreover, each pathogen was readily detected by a pathogen-specific immune-chromatographic lateral-flow or multiplex PCR assay (Kim and Bhunia, 2008). In 2013, Suo and Wang evaluated the detection of *Salmonella*, *E. coli* O157:H7 and *L. monocytogenes* in artificially contaminated ground beef after 20 hours enrichment of sublethally injured cells in a selective enrichment broth SEL. The researcher reported that all the three injured pathogens could be simultaneously detected without discrimination by real-time PCR combined with SEL broth. However, when BPW was employed as the enrichment broth in the same detection procedure, injured *L. monocytogenes* could not be detected if the initially spiked level was below 10² CFU/10 g ground beef (Suo and Wang, 2013). In 2014, Xiao and colleagues developed novel enrichment broth (SSS broth) for detection of *S. Enteritidis*, *Shigella dysenteriae*, and *S. aureus*, by multiplex real-time PCR. A major characteristic of selective enrichment SSS broth suitable for the growth of multiple pathogens is that, in addition to the basic ingredients and promoters, it can be formulated by adding three antimicrobial agents. However, data showed that the SSS broth had little inhibitory effect on growth of these target pathogens (Xiao *et al.* 2014).

In this research, the target pathogens and food samples were different from the previous reports. The concentration of microbial background in pasteurized milks was very low when compared to meat sample. Thus, only non-selective media including BPW, LB, TSB media were evaluated for enrichment of *B. cereus*, *E. coli*, *Salmonella* spp., and *S. aureus* in pasteurized milk to avoid the inhibitory effect on growth of these target pathogens. However, *B. cereus* at initial concentration lower than 10 cells in milk could not be detected by PCR methods after 24 enrichments in all media tested while conventional culture could be detected

in only LB enrichment cultures (**Table 4**). These might be the amount of genomic DNA of Gram-positive bacteria, *B. cereus*, was lost during the DNA extraction step. Therefore, yield of the genomic DNA extracted from *B. cereus* was lower than that of other Gram-negative bacteria at the same level of cell concentration. Our finding results indicated that enrichment is necessary and extremely common for target bacteria detection. Based on the results of pathogen detection using conventional culture methods and PCR assay, the suitable pre-enrichment for detection of *B. cereus*, *E. coli*, *Salmonella* spp. and *S. aureus* was LB. The suitable pre-enrichment medium for detection of *L. monocytogenes* was HF.

Table 4 Comparison of pathogen detection by conventional and PCR techniques

Enrichment medium	Sample name	Conventional culture *					PCR technique*				
		BC MYP agar	EC EMB agar	LM PALCAM agar	SA Baird Parker agar	SM XLD agar	BC EntFM	EC uspA	LM prfA	SA eap	SM fimY
BPW	B _c	-	-	-	-	-	-	-	-	+	-
	B ₁	-	+	+	+	+	-	+	-	+	+
	B ₂	-	+	+	-	+	-	+	-	+	+
TSB	T _c	-	-	-	-	-	-	-	-	+	-
	T ₁	-	+	+	+	+	-	+	-	+	+
	T ₂	-	+	+	-	+	-	+	-	+	+
LB	L _c	-	-	-	-	-	-	-	-	+	-
	L ₁	+	+	+	+	+	-	+	-	+	+
	L ₂	+	+	+	+	+	-	+	-	-	+
HF	H _c	-	-	-	-	-	-	-	-	-	-
	H ₁	-	-	+	+	-	-	-	+	-	-
	H ₂	-	-	+	-	-	-	-	+	-	-

* Target bacterial pathogens including, BC: *B. cereus*; EC: *E. coli*; LM: *L. monocytogenes*; SA: *S. aureus*; SM: *S. Typhimurium*

Conclusion

The initial concentration of pathogen contamination in food samples is often at a very low level (Zhao and Doyle, 2001). Moreover, more than one species of bacterial pathogens could be contaminated in food. Thus, a multipathogen selective enrichment medium is essential to allow the concurrent growth of pathogens (Kim and Bhunia, 2008). In milk samples contaminated with *B. cereus*, *E. coli*, *L. monocytogenes*, *S. aureus*, and *Salmonella* spp. at very low initial of cell contamination, pre-enrichment for 24 h in the suitable pre-enrichment broth could increase sensitivity and accuracy of pathogen detections. In this research, the LB and HF was the most suitable pre-enrichment both for detection of these pathogens by both conventional culture and PCR methods. By these reasons, separate enrichment of two bacterial groups in LB for enrichment of *B. cereus*, *E. coli*, *S. aureus*, *Salmonella* and HF for enrichment of *L. monocytogenes* will be performed prior to total genomic DNA extraction. Then the detection of *Salmonella*, *E. coli*, *S. aureus*, *B. cereus* should be performed using total genomic DNA extracted from LB culture as template. For *L. monocytogenes* detection in milk sample, total genomic DNA were extracted from HF culture and were used as template alone for amplification of *prfA* gene by conventional PCR. By these techniques, all target bacteria will be simultaneously detected using DNA labeling of all PCR product and hybridized with their

specific probes on single array. Therefore, combining these methods with PCR-oligonucleotide array could increase detectability and accuracy of the detection systems which can be applied to detect multiple target pathogen species directly from milk after 24 hours enrichment in LB and HF.

Acknowledgment

This research project was supported by Rajamangala University of Technology Isan. Contract No. 2560/036. The authors would like to thank the Faculty of Science and Liberal Arts, Rajamangala University of Technology Isan and the Protein Engineering Laboratory, School of Biotechnology, Institute of Agricultural Technology, Suranaree University of Technology for providing some chemicals and instruments.

References

- Bailey, J. S. and Cox, N. A. 1992. Universal preenrichment broth for the simultaneous detection of *Salmonella* and *Listeria* in Foods. **Journal of Food Protection** 55(4): 256-259.
- Bianchi, D. M., Barbaro, A., Gallina, S., Vitale, N., Chiavacci, L., Caramelli, M. and Decastelli, L. 2013. Monitoring of foodborne pathogenic bacteria in vending machine raw milk in Piedmont, Italy. **Food Control** 32: 435–439.
- Boera, E. D. and Beumer, R. R. 1999. Methodology for detection and typing of foodborne microorganisms. **International Journal of Food Microbiology** 50: 119–130.
- Chen, J. and Griffiths, M. W. 1998. PCR differentiation of *Escherichia coli* from other gram-negative bacteria using primers derived from the nucleotide sequences flanking the gene encoding the universal stress protein. **Letters in Applied Microbiology** 27(6): 369-371.
- Chitov, T., Dispan, R. and Kasinrer, W. 2008. Incidence and diarrhegenic potential of *Bacillus cereus* in pasteurized milk and cereal products in Thailand. **Journal of Food Safety** 28(4): 467–481.
- Chye, F. Y., Abdullah, A. and Ayo, M. K. 2004. Bacteriological quality and safety of raw milk in Malaysia. **Food Microbiology** 21: 535–541.
- Hussain, M., Eiff, C. V., Sinha, B., Joost, I., Herrmann, M., Peters, G. and Becker, K. 2008. *eap* gene as novel target for specific identification of *Staphylococcus aureus*. **Journal of Clinical Microbiology** 46(2): 470-476.
- Jofré, A., Martin, B., Garriga, M., Hugas, M., Pla, M., Rodríguez-Lázaro, D. and Aymerich, T. 2005. Simultaneous detection of *Listeria monocytogenes* and *Salmonella* by multiplex PCR in cooked ham. **Food Microbiology** 22(1): 109-115.
- Kanungpean, D., Rujit, J., Chanda, J., Boonyaprapa, N., Tonchotiwech, P., Mahanil, W., Tain, A. and Intarapuk, A. 2014. The quality testing of raw goat's milk in Nongchok District, Bangkok. **Journal of Mahanakorn Veterinarian Medicine** 9(2): 83–88.
- Kim, H. And Bhunia, A.K. 2008. Sel, A Selective Enrichment Broth For Simultaneous Growth Of *Salmonella Enterica*, *Escherichia Coli* O157:H7, And *Listeria Monocytogenes*. **Applied And Environmental Microbiology** 74(15): 4853-4866.
- Kupradit, C., Rodtong, S. And Ketudat-Cairns, M. 2013. Development Of A Dna Macroarray For Simultaneous Detection Of Multiple Foodborne Pathogenic Bacteria In Fresh Chicken Meat. **World Journal Of Microbiology Biotechnology** 29(12): 2281–2291.

- Kupradit, C., Innok, S., Woraratphoka, J. And Ketudat-Cairns, M. 2017. Novel Multiplex Pcr Assay For Rapid Detection Of Five Bacterial Foodborne Pathogens. **Suranaree Journal Of Science And Technology** 24(1): 41–50.
- Myint, M. S., Johnson, Y. J., Tablante, N. L. And Heckert, R. A. 2006. The Effect Of Pre-Enrichment Protocol On The Sensitivity And Specificity Of Pcr For Detection Of Naturally Contaminated *Salmonella* In Raw Poultry Compared To Conventional Culture. **Food Microbiology** 23: 599–604.
- Oliveira, S. D., Rodenbusch, C. R., Ce', M. C., Rocha, S. L. S. And Canal, C. W. 2003. Evaluation Of Selective And Non-Selective Enrichment Pcr Procedures For *Salmonella* Detection. **Letters In Applied Microbiology** 36: 217–221.
- Ombarak, R. A., Hinenoya, A., Awasthi, S. P., Iguchi, A., Shima, A., Elbagory, A. R. And Yamasaki, S. 2016. Prevalence And Pathogenic Potential Of *Escherichia Coli* Isolates From Raw Milk And Raw Milk Cheese In Egypt. **International Journal Of Food Microbiology** 221: 69–76.
- Padungtod, P. and Kaneene, J. B. 2006. *Salmonella* in food animals and humans in northern Thailand. **International Journal of Food Microbiology** 108: 346–354.
- Ramesh, A., Padmapriya, B. P., Chandrashekar, A. and Varadaraj, M. C. 2002. Application of a convenient DNA extraction method and multiplex PCR for the direct detection of *Staphylococcus aureus* and *Yersinia enterocolitica* in milk samples. **Molecular and Cellular Probes** 16: 307-314.
- Settanni, L. and Corsetti, A. 2007. The use of multiplex PCR to detect and differentiate food- and beverage-associated microorganisms: A review. **Journal of Microbiology Methods** 69: 1–22.
- Suo, B. and Wang, Y. 2013. Evaluation of a multiplex selective enrichment broth SEL for simultaneous detection of injured *Salmonella*, *Escherichia coli* O157:H7 and *Listeria monocytogenes*. **Brazilian Journal of Microbiology** 44(3): 737-742.
- United States Food and Drug Administration. Bacteriological analytical manual / Food and Drug Administration, 8th ed, Gaithersburg, MD: AOAC International; 1998.
- Van Kessel, J. S., Karns, J. S., Gorski, L., McCluskey, B. J. and Perdue, M. L. 2004. Prevalence of *Salmonellae*, *Listeria monocytogenes* and fecal coliforms in bulk tank milk on US Dairies. **Journal of Dairy Science** 87: 2822–2830.
- Xiao, X-l., Zhai, J-x., Wu, H., Liu, D., Yu, Y-g. and Li, X-f. 2014. Development and evaluation of a selective enrichment broth for simultaneous growth of *Salmonella enterica* serovar Enteritidis, *Shigella dysenteriae* and *Staphylococcus aureus*. **Annals Microbiology** 64:1543–1551.
- Zhao, T. and Doyle, M. P. 2001. Evaluation of universal preenrichment broth for growth of heat-injured pathogens. **Journal of Food Protection** 64(11): 1751–1755.

Potential Use of Cashew Leaves Extract for the Quality Improvement in Chinese Sausage (Kun-Chiang)

Supasit Chooklin^{1*} and Parichat Ninup-patham²

ABSTRACT

The objective of this study was to assess the effect of cashew leaves extract (CLE) on the chemical and microbial qualities of Chinese sausage stored at 4°C for 21 days. The total phenolic and antioxidant activity of CLE were 219.58±2.35 mg GAE/g DW and 1,205.68±3.12 equivalent to vitamin C mg/g DW, respectively. CLE inhibited tested microorganisms (*L. monocytogenes* DMST 17003, *E. coli* TISTR 780 and *S. aureus* 1466) by agar well diffusion method. During refrigerated storage, sausages containing CLE showed lower L* values and higher a* value compared to the control. CLE tended to retard the increase in TBARS values. Moreover, microbial counts of the sausages with CLE were lower than control samples during storage. These results demonstrated that CLE are effective against microbial growth and lipid oxidation and showed potential as a natural antioxidant and antimicrobial in Chinese sausages.

Keywords: Cashew leaves, Extract, Chinese sausage, Antioxidant, Antimicrobial

¹ Department of Food Science and Technology, Faculty of Agro-Industry, Rajamangala University of Technology Srivijaya, Thungyai Campus, Nakhonsrithamarat 80240, Thailand

² Department of Biotechnology, Faculty of Agro-Industry, Rajamangala University of Technology Srivijaya, Thungyai Campus, Nakhonsrithamarat 80240, Thailand

*Corresponding author, e-mail: supasit.c2015@gmail.com

Introduction

Chinese sausage is a popular Chinese-style semi-dry sausage (Du and Ahn, 2001; Sun *et al.*, 2010) which is susceptible to quality deterioration due to their rich nutritional composition. The quality deterioration is due to chemical and microbial changes. Meat and poultry products have frequently been found to be contaminated with microorganisms during the butchering and manufacturing process. These microorganisms produce undesirable quality changes in meats, especially in relation to lactic acid bacteria, a major bacterial group associated with meat spoilage (Doulgeraki *et al.*, 2012). The most common form of chemical deterioration is the oxidation of meat lipids. Lipid oxidation is a complex process and depends on chemical composition of meat, light and oxygen access and storage temperature (Kanner, 1994). It would be useful if an additive in meat products could prevent lipid oxidation. One of the common strategies for retarding lipid oxidation is the use of antioxidants. The antioxidants can be of synthetic or natural origin. Synthetic antioxidants such as butylate hydroxyanisole (BHA), butylate hydroxytoluene (BHT), tert-butylhydroxylhydroquinone (TBHQ), and propyl gallate (PG) have been widely used in meat and poultry products (Formanek *et al.*, 2001; Biswas *et al.*, 2004; Jayathilakan *et al.*, 2007). Various plant materials containing phenolic compounds have been demonstrated to be effective antioxidants in meat products (Mielnik *et al.*, 2006). In recently year, the demand for natural antioxidants, especially of plant origin has increased due the growing concern among consumers about these synthetic antioxidants because of their potential toxicological effects (Juntachote *et al.*, 2006; Naveena *et al.*, 2008; Nunez de Gonzalez *et al.*, 2008).

Anacardium occidentale L. (family Anacardiaceae) or cashew is a small-sized tree with a dome-shaped crown. The bark is brown or grey with longitudinal fissures. Leaves are simple, alternate, narrowly to broadly obovate with a rounded apex. In the early stages, leave are pliable and reddish but turn to dark green and leathery with prominent yellow veins when mature. Traditionally, cashew leaves have also been used to treat rheumatic disorders and hypertension (Tan and Chan, 2014). Phenolic compounds are a large group phytochemicals derived from secondary metabolism in plants that serve as powerful antioxidant. Antioxidant properties based on phenolic content and antioxidant activity of fresh leaves of cashew was 3,890 mg GAE/100 g and 6,620 mg ascorbic acid/100 g (Tan and Chan, 2014). Moreover, the total polyphenol content of young cashew leaves, which is indigenous vegetables from southern Thailand, was 4,075.79 mg GAE/100 g (Kongkachuichai *et al.*, 2015).

However, to our knowledge, there is no information available regarding the effectiveness of the inclusion of cashew leaves to inhibit lipid oxidation and antimicrobial in Chinese sausage. Consequently, the objective of the present study was to investigate the effects of addition of CLE to Chinese sausage on retarding lipid oxidation and antimicrobial, as well as determining its impact on quality deterioration during of Chinese sausage storage.

Materials and Methods

Preparation of cashew leaves

Cashew leaves were thoroughly washed and drained on a screen. Then, fresh cashew leaves were cut and tray-dried at 60°C until moisture was less than 10%. Samples were ground and sieved through 0.25 mm mesh, and kept in aluminum foil laminated packaging at ambient temperature (28-30°C).

Preparation of cashew leaves extract (CLE)

Leaf powder (2 g) was mixed with 150 mL 60% (v/v) ethanol. The mixture was then placed in ultrasonic bath operating at a frequency of 45 MHz, an ultrasonic input power of 120 watt. The extraction was done at 30°C for 25 min (Chooklin *et al.*, 2015). Subsequently, the mixture was centrifuged (6000 rpm, 5°C, 5 min). The supernatant was collected and evaporated by rotary evaporator (100-150 mmHg, 40°C) then freeze-dried for complete solvent removal. Phenolic content was analyzed by a Folin Ciocalteu's method (Singleton, 1965) and expressed as mg gallic equivalent/g (dried weight). Anti-oxidants potency was analyzed through DPPH method and expressed as equivalent to vitamin C mg/g dried weight.

Determination of total phenolic content

Total phenolics were determined using the Folin-Ciocalteu reagent, adapted from Singleton and Rossi (1965). 2 mL of properly diluted sample extracts was transferred and reacted with 10 mL of Folin-Ciocalteu reagent (previously diluted 10-fold with distilled water) in 25 mL volumetric flask. After 30 s and before 8 min, 8 mL of 7.5% of sodium carbonate was added and mixed, and the contents of the flask made to volume with distilled water. Solutions were heated in a 40°C water bath for 30 min. The color was developed and absorbance was measured at 765 nm. The standard curve was prepared using 0, 0.5, 1.0 and 1.5 mL of gallate stock solution (8 mg/100 mL) in 25 mL volumetric flask. The regression line between absorbance (y) and gallic acid content (x) was $y = 0.0025x + 0.0064$. The results were expressed as mg gallic acid equivalent (GAE) /g dry weight.

DPPH radical scavenging activity

DPPH scavenging activity was determined using a modified method of Ohnishi *et al.* (1994). The free radical scavenging activity of crude extracts was tested, indicated by bleaching of the stable 1,1-diphenyl-2-picrylhydrazyl radical (DPPH). A diluted extract of the right concentration, 0.15 mL, was added to 0.9 mL of 0.1 mM ethanolic DPPH solution. The mixture was vortexed and allowed to stand at room temperature. After 20 min, the absorbance was recorded at 517 nm. A control consisted of 0.15 mL of 95% aqueous ethanol and 0.9 mL of 0.1 mM DPPH solution. DPPH % scavenging activity (%SA) was calculated $\%SA = (C-X)*100/C$, where C was absorbance of control and X was absorbance of the extract.

Impact of CLE on the quality of Chinese sausage during the storage

Chinese sausage was prepared in the meat processing plant of Faculty of Agro – Industry, Rajamangala University of Technology Srivijaya under strict hygienic conditions. Lean meat (5x5x5 mm³) was mixed with NaCl (2%), lard (26%), sugar (10%) and water (7%). To the mixture, CLE and BHT were added to obtain the final concentration of 0.2% (w/w). Control containing no antioxidants was also prepared. Then all the samples were ground using a silent cutter. Finally, samples were manually stuffed into the collagen casings. Raw sausages were roped into approximate 10 cm lengths manually and dried in a pre-heated oven at 65°C for 10 h. The sausages were then taken out and cooled to room temperature and then stored at 4°C. Each treatment of packaged sausage was randomly taken at days 0, 7, 14 and 21 to determine color L*, a* and b*, water activity (aw), thiobarbituric acid reactive substances (TBARS) and total bacteria value. All samples were prepared in triplicate.

Results and Discussion

Chemical and microbial properties of CLE

Table 1 shows the yields of CLE in each process. The results show that the yields of CLE in ultrasound assisted extraction and freeze dry process were 94.69% and 1.26%, respectively.

Table 1 Material balance of CLE.

Process	Input	Output
Drying -Cashew leaves -Moisture	1,000 g 74.9%	225 g (22.5%) 4.9%
Milling and sieving -Milled cashew leaves (mesh no.60)	225 g	63.68 g (28.3%)
Extraction (S/L ratio 1:50) -Ethanol (40%) -Milled cashew leaves -Crude extract	3,183.75 mL 63.68 g 846.88 g	2,336.87 mL (70.34%) 801.91 g (94.69%)
Freeze drying -Crude extract	801.91 g	10.10 g (1.26%)

Phenolic compounds are a large group of phytochemicals derived from secondary metabolite in plants that serve as effective antioxidants. Phenolic compounds are beneficial to humans, since they may play an important role as reducing agents for hydrogen atom or electron transfer to free radicals and metal chelating agents that can inhibit oxidative reactions, and particularly LDL oxidation that result in progressions of chronic diseases (Stagos *et al.*, 2012). Total phenolic content and antioxidant activity of CLE in this study was 219.58 ± 2.35 mg GAE/g DW and $1,205.68 \pm 3.12$ equivalent to vitamin C mg/g DW. Similarly, Chooklin *et al.* (2015) examined ultrasound-assisted extraction of phenolic compound from southern Thai indigenous vegetables, reported that CLE (281.98 mg GAE/g DW, 723.91 equivalent to vitamin C mg/g DW) showed the highest total phenolic content and antioxidant activity.

The antibacterial activity of CLE was measured using the agar well diffusion assay. CLE showed inhibition against the three meats pathogenic and spoilage organism (Figure 1). The susceptibility of the *L. monocytogenes* DMST 17003, *E. coli* TISTR 780 and *S. aureus* 1466 to CLE was determined by minimal inhibitory concentration (MIC). It was found that increasing extract concentration from 1 to 5%v/v increased the diameter of inhibition clear zone. The highest diameter of inhibition clear zone at 5%v/v extract concentration for *L. monocytogenes* DMST 17003, *E. coli* TISTR 780 and *S. aureus* 1466 was observed at 19.5 ± 0.71 , 17.5 ± 0.71 and 18.25 ± 0.35 mm, respectively (Table 2). The results show that *L. monocytogenes* (gram-positive) was the most sensitive among the three strains of bacteria used in the test. *L. monocytogenes* has emerged as a serious food-borne pathogen and is widely distribute in the environment. The pathogen survives and can grow over a wide temperature range, including refrigerator temperatures. *L. monocytogenes* poses a real threat as a post-process contaminant in ready-to-eat meat products. Zhang *et al.* (2016) determined effects of

antimicrobial and antioxidant activities of spice extracts on raw chicken meat quality found that spice extracts showed various degrees of inhibition against the four meat pathogenic and spoilages organism (*L. monocytogenes*, *E. coli*, *P. fluorescence*, *L. sake*). Moreover, the MIC of CLE to inhibit all the indicator strains was 2.5 mg/mL. Akash *et al.* (2009) similarly reported that the largest zone of inhibition was observed for ethanolic cashew leaf extract against *S. aureus* (20mm) and *E. coli* (11 mm).

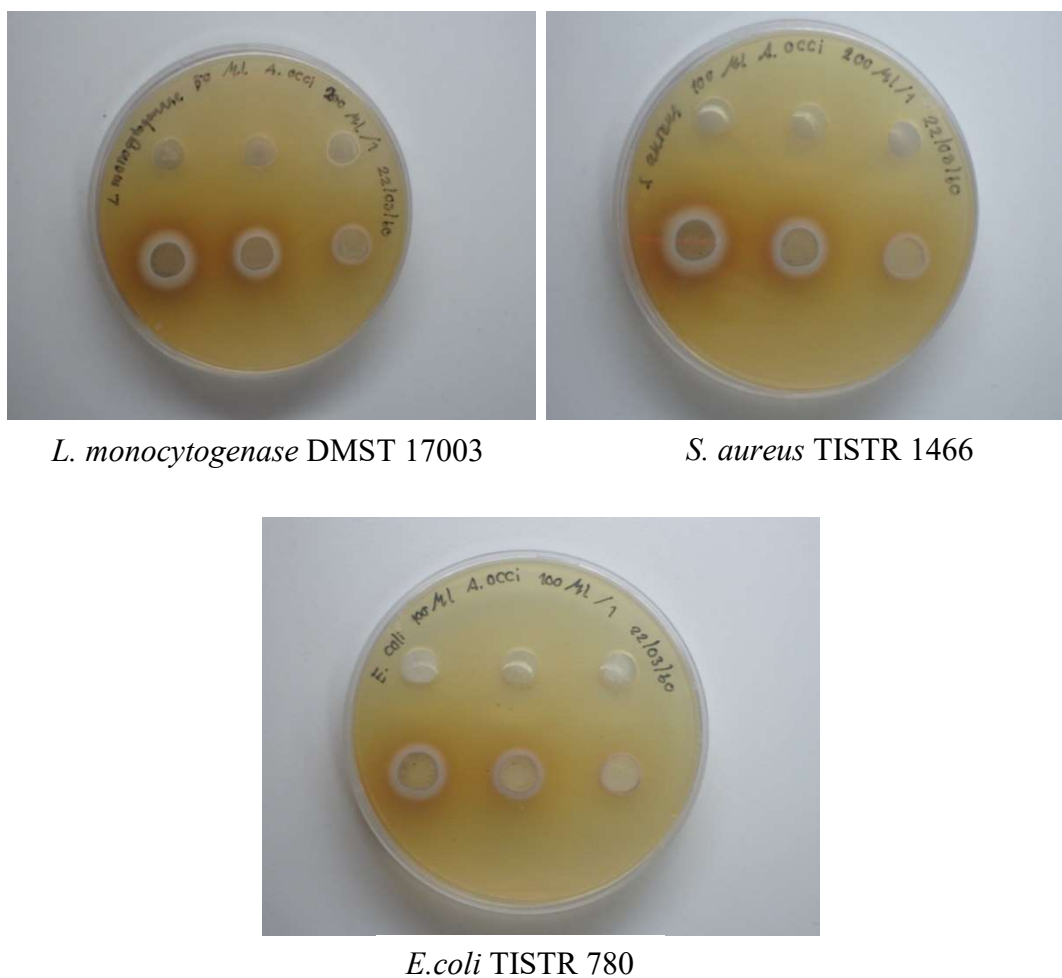


Figure 1 Antibacteria activities of CLE against chosen bacterial strains.

Table 2 Diameter of inhibition clear zone (mm) caused by CLE against chosen bacterial strain.

Microbial strain	Inoculum volume (μL)	Extract content (μL)	Diameter of inhibition clear zone (mm)		
			Concentration (%v/v)		
			1	3	5
<i>L. monocytogenes</i> DMST 17003	50	100	12.5±0.71 ^b	15.5±2.12 ^{ab}	17.5±3.54 ^a
		200	12.0±0.00 ^c	16.5±0.71 ^b	18.5±0.71 ^a
	100	100	12.0±0.00 ^b	14.0±0.00 ^a	15.0±0.00 ^a
		200	12.5±0.71 ^c	16.0±0.00 ^b	19.5±0.71 ^a
<i>S. aureus</i> TISTR 1466	50	100	12.0±0.00 ^b	14.0±0.00 ^a	15.5±0.71 ^a
		200	12.5±0.71 ^b	16.0±1.41 ^a	17.0±0.00 ^a
	100	100	12.0±0.00 ^b	14.0±0.00 ^a	15.5±0.71 ^a
		200	12.5±0.71 ^c	15.0±0.00 ^b	17.5±0.71 ^a
<i>E.coli</i> TISTR 780	50	100	12.0±0.00 ^c	14.0±0.00 ^b	16.0±0.00 ^a
		200	12.5±0.71 ^c	15.0±0.00 ^b	18.0±0.00 ^a
	100	100	12.0±0.00 ^c	14.25±0.35 ^b	16.0±0.00 ^a
		200	12.75±0.35 ^c	16.25±0.35 ^b	18.25±0.35 ^a

*a, b, c means that share different letters are significantly different (P<0.05)

Effect of CLE on quality of Chinese sausage during storage

Water activity and color values

The water activities of Chinese sausage were increased during refrigerated storage up to 21 days. All values obtained for the various group tested were between 0.62 - 0.68 (Figure 2).

The L* values of the sausage decreased during the refrigerated storage (Figure 3A). The sausages containing CLE showed lower L* values than the control. This might be due to the presence of leaf pigments, especially, chlorophylls (Li-wen *et al.*, 2012). The polyphenols in CLE were likely oxidized to corresponding quinones by polyphenol oxidases. Those quinones might condense to form darkened compounds, which resulted in an intense color of sausage (Lui *et al.*, 2009).

The a^* values of the sausage decreased during the refrigerated storage (Figure 3B). The a^* values with CLE and BHT were higher than the control at days 7, 14 and 21. It was observed that CLE showed a protective effect on the deterioration of color during refrigerated storage. The redness of meat products results from the presence of the heme proteins, hemoglobin and myoglobin. These proteins are red when they exist in the reduced forms and brown in the oxidized forms (Sabeena *et al.*, 2012). Lipid oxidation also contributes to deterioration of redness. Protective effect of natural antioxidants on color deterioration in meat products was reported. The phenolic compounds have been shown to inhibit lipid and protein oxidation in muscle foods (Zhang *et al.*, 2013). Therefore, it is likely that protective effect of CLE on color stabilizing of meat products might due to the present of phenolics.

Samples treated with CLE also showed decreased b^* values (Figure 2C) over the entire storage period. The b^* values of samples treated with CLE were higher than the value measured for the control throughout the entire storage period, which may have been caused by the presence of slight color compounds in the CLE.

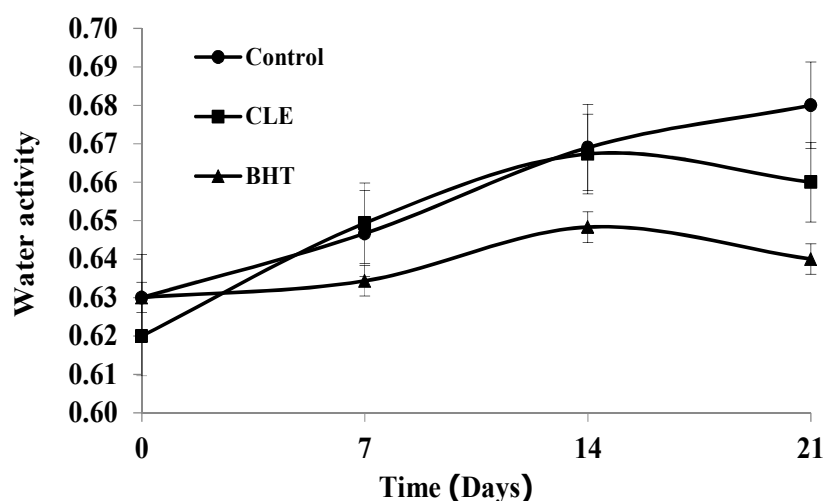


Figure 2 Effect of CLE on water activity of Chinese sausage during storage at 4°C.

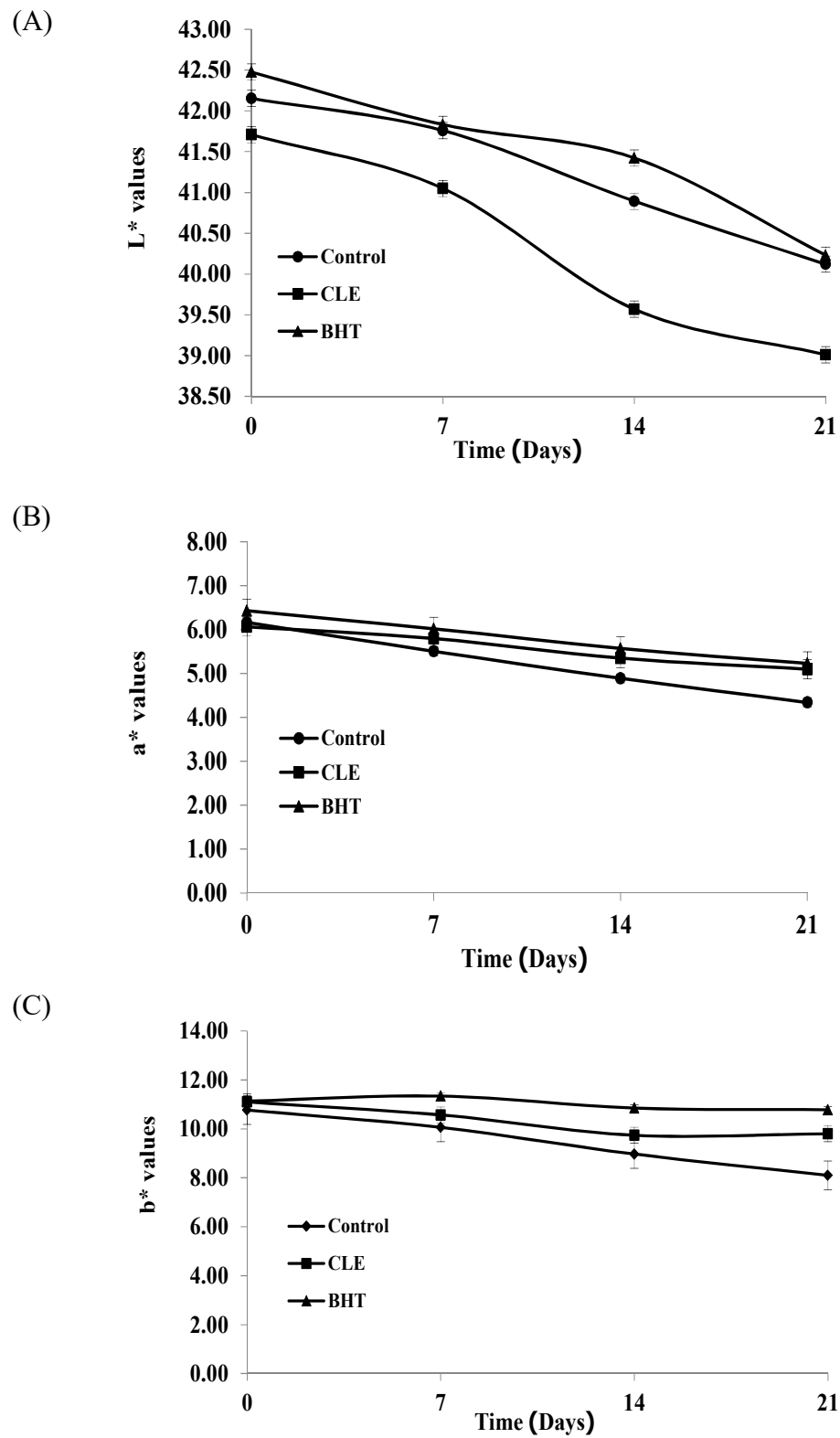


Figure 3 Effect of CLE and BHT on color parameters of Chinese sausage during storage at 4°C.

Thiobabutyric acid substance (TBARS)

TBARS analysis determines the formation of secondary products of lipid oxidation, mainly malondaldehyde, which may contribute to the off – flavor of oxidized fat. Figure 4 illustrate the antioxidant effects of CLE on the TBARS values of Chinese sausage during storage (4°C) for 21 days. The TBARS values of all samples increased with increasing storage. The TBARS values of all treated samples were lower than those of control and BHT during storage, showing that CLE had highly protective effect against lipid oxidation in Chinese sausage. Natural antioxidants are believed to interrupt free radical chains by offering hydrogen from the phenolic groups, resulting in the formation of a stable end product. This finding was in line with previous results showing that mustard leaf possesses antioxidant activity in foods because of its high content of phenolic compounds (Lee *et al.*, 2010). Similarly, Zhang *et al.* (2016) examined the effects of antimicrobial and antioxidant activities of spice extracts on raw chicken meat quality and reported that the antioxidant effects of extracts inhibited TBARS values in chicken meat. Zhang *et al.* (2013) reported that Chinese sausage containing sage showed retarded increases in TBARS during refrigerated storage.

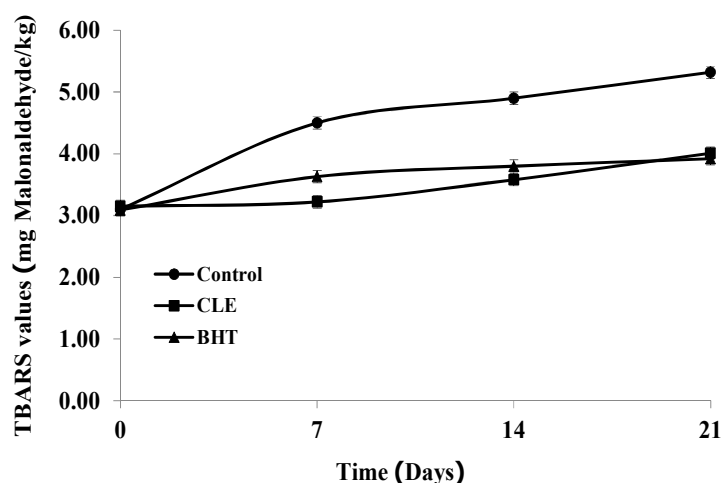


Figure 4 Effect of CLE on TBARS values of Chinese sausage during storage at 4°C.

Microbial load

In this study, the total plate counts of all samples increased during refrigerated storage (Figure 5). The total plate counts of Chinese sausage with CLE were between 0.99 to 3.53 log CFU/g, which were lower than that of the control (1.09 – 4.99 log CFU/g). Some researchers have reported that phenolic compounds from different plant sources could retard the growth of various food-borne pathogens, and total phenolic content has been strongly associated with antimicrobial activity (Shan *et al.*, 2007). The antimicrobial activities of phenolic compounds may involve multiple modes of action. For example, phenolic compounds can break down the cell wall, disrupt the cytoplasmic membrane, cause leakage of cellular components, alter fatty acid and phospholipid constituents, influence the synthesis of DNA and RNA and destroy protein translocation (Shan *et al.*, 2007).

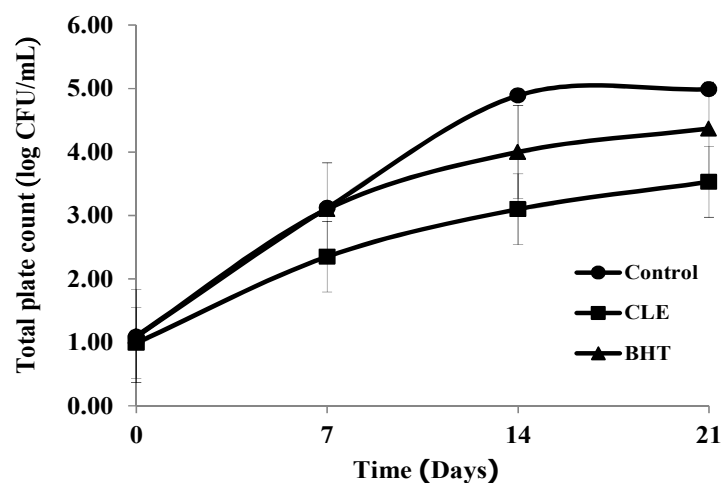


Figure 5 Effect of CLE on total plate count of Chinese sausage storage at 4°C.

Conclusion

Cashew leaf extract was prepared with the aid of ultrasound with higher yield. Total phenolic and antioxidant activity of CLE were 219.58 ± 2.35 mg GAE/g DW and $1,205.68 \pm 3.12$ equivalent to vitamin C mg/g DW, respectively. The results demonstrate the effectiveness of CLE in inhibiting microbial growth and reducing lipid oxidation of Chinese sausage during storage at 4°C for 21 days.

Acknowledgement

This work was supported by the Faculty of Agro-Industry, Rajamangala University of Technology Srivijaya, Nakhon Sri Thammarat, Thailand and Prof.Dr.Soottawat Benjakul proof reading the article.

References

- Akash, P.D., Vishal, D.J. and Arun, B.J. 2009. Antimicrobial Screening of Different Extract of *Anacardium occidentale* Linn. Leaves. **International Journal of Chemistry Technology Research** 4: 856-858.
- Biswas, A.K., Keshri, R.C. and Bisht, G.S. 2004. Effect of enrobing and antioxidants on quality characteristics of precooked pork patties under chilled and frozen storage conditions. **Meat Science** 66: 733-741.
- Chooklin, S., Bilmud, A., Tongboriboon, K. and Sriwilai, S. 2015. Ultrasound-assisted extraction of phenolic compound from southern Thai indigenous vegetables. International Conference of Thai Society for Biotechnology (TSB2015), 17-20 November, 2015, Mandarin Hotel, Bangkok, Thailand.
- Doulgeraki, A., Ercolini, D., Villani, F. and Nychas, G.E. 2012. Spoilage microbiota associated to the storage of raw meat in different conditions. **International Journal of Food Microbiology** 157: 177 – 188.

- Du, M and Ahn, D.U. 2001. Volatile substances of Chinese traditional jinhua ham and cantones sausage. **Journal of Food Science** 66: 827-831.
- Formanek, Z., Kerry, J.P., Higgins, F.M., Buckley, D.J., Morrissey, P.A. and Farkas, J. 2001. Addition of synthetic and natural antioxidants to alpha-tocopheryl acetate supplemented beef patties: Effects of antioxidants and packaging on lipid oxidation. **Meat Science** 58: 337-341.
- Jayathilakan, K., Sharma, G.K., Radhakrishna, K. and Bawa, A.S. 2007. Antioxidant potential of synthetic and natural antioxidants and its effect on warmed-over-flavour in different species of meat. **Food Chemistry** 105: 908-916.
- Juntachote, T., Berghofer, E., Siebenhandl, S. and Bauer, F. 2006. The oxidative properties of Holy basil and Galangal in cooked ground pork. **Meat Science** 72: 446-456.
- Kanner, J. 1994. Oxidative process in meat and meat products; Quality implications. **Meat Science**, 36: 169-174.
- Kongkachuichai, R., Chareonsiri, R., Yakoh, K., Kringkasemsee, A. and Insung, P. 2015. Nutrients value and antioxidant content of indigenous vegetables from southern Thailand. **Food Chemistry** 173: 838-846.
- Lee, M.A., Choi, J.H., Choi, D.J., Choi, Y.S., Han, D.J., Kim, H.Y. and Shim, S.Y. 2010. The antioxidative properties of mustard leaf (*Brassica juncea*) kimchi extracts on refrigerated raw ground pork meat against lipid oxidation. **Meat Science** 84(3): 498 – 504.
- Li-wen, Z., Guo-cheng, Z., Li, Z., Rui-wu, Y., Chun-bang, D. and Yong-hong, Z. 2012. A study on photosynthesis and photo-response charecteristics of three Salvia species. **Acta Prataculturae Sinica** 21(2): 70-76.
- Lui, D.C., Tsu, R.T., Lin, Y.C., Jan, S.S. and Tan, F.J. 2009. Effect of various levels of rosemary or Chinese mahogany on the quality of fresh chicken sausage during refrigerated storage. **Food Chemistry** 117(1): 106-113.
- Mielnik, M.B., Olsen, E., Vogt, G., Adeline, D. and Skrede, G. 2006. Grape seed extract as antioxidant in cooked, cold stored turkey meat. **LWT-Food Science and Technology** 39: 191-198.
- Naveena, B.M., Sen, A.R., Vaithiyanathan, S., Babji, Y. and Kondaiah, N. 2008. Comparative efficacy of pomegranate juice, pomegranate rind powder extract and BHT as antioxidants in cooked chicken patties. **Meat Science** 80: 304-308.
- Nunez de Gonzalez, M.T., Hafley, B.S., Boleman, R.M., Miller, R.K., Rhee, K. and Keeton, J.T. 2008. Antioxidant properties of plum concentrates and powder in precooked roast beef to reduce lipid oxidation. **Meat Science** 80: 997-1004.
- Ohnishi, M., Morishita, H., Iwahashi, H., Toda, S., Shirataki, Y., Kimura, M. and Kido, R. 1994. Inhibitory effects of chlorogenic acids on linoleic acid peroxidation and hemolysis. **Phytochemistry** 36: 579–583.
- Sabeena, F.K.H., Grejen, H.D. and Jacobsen, C. 2012. Potato peel extract as a natural antioxidant in chilled storage of minced horse mackerel (*Trachurus trachurus*): Effect on lipid and protein oxidation. **Food Chemistry** 131(3): 843-851.
- Singleton, V.L. and Rossi, J.A. 1965. Colorimetry of total phenolics with phosphomolybdcphosphotungstic acid reagents. **American Journal of Enology and Viticulture** 16: 144-158.
- Shan, B., Cai, Y.Z., Brooks, J.D. and Corke, H. 2007. The in vitrio antibacterial activity of dietary spice and medical herb extracts. **International Journal of Microbiology** 117: 112 – 119.
- Stagos, D., Amoutzais, G.D., Matakos, A., Spyrou, A., Tsatsakis, A.M. and Kouretas, D. 2012. Chemoprvention of liver cancer by plant polyphenols. **Food and Chemical Toxicology** 50: 2155-2170.

- Sun, W., Zhao, H., Zhao, M. and Yang, B. 2010. Volatile compounds of Cantonese sausage released at different stages of processing and storage. **Food Chemistry** 121: 319-325.
- Tan, Y.P. and Chan, E.W.C. 2014. Antioxidant, antityrosinase and antibacterial properties of fresh and processed leaves of *Anacardium occidentale* and piper betle. **Food Bioscience** 6: 17-23.
- Zhang, L., Lin, Y.H., Leng, X.J., Huang, M. and Zhou, G.H. 2013. Effect of sage (*Salvia officinalis*) on the oxidative stability of Chinese-style sausage during refrigerated storage. **Meat Science** 95: 145-150.
- Zhang, H., Wu, J. and Guo, X. 2016. Effects of antimicrobial and antioxidant activities of spice extracts on raw chicken meat quality. **Food Science and Human Wellness** 5: 39-48.

Development of Pasta from Riceberry Flour, Commercial Rice Flour and Mung Bean Flour

Arpathsra Sangnark¹, Natthaporn Subanmanee¹, and Thappasarn Jaikaew^{1*}

ABSTRACT

A mixture design of 3 components, namely, Riceberry flour (RBF 25-75%), commercial rice flour (CRF 12.5-37.5%) and mung bean flour (MBF 12.5-37.5%) were performed to investigate the optimum formulation of pasta using extrusion processing. The conditions of extrusion process were as follows: moisture content of each flour mixture was 30%, barrel and die temperature was 75-80 and 85-100°C, respectively and screw speed was 100 rpm. It was found that the best quality in terms of color, texture and cooking quality of pasta was produced from 25% of RBF, 37.5% of CRF and 37.5% of MBF. The optimum pasta consisted of 14.90% (db) protein, 0.01% (db) fat, 0.08% (db) crude fiber, 3.80% (db) ash and 81.21% (db) total carbohydrate.

Keywords: Riceberry Flour, Commercial Rice Flour, Mung Bean Flour, Extrusion, Pasta

¹Department of Food Technology and Nutrition, Faculty of Home Economics Technology, Rajamangala University of Technology Krungthep, Bangkok, 10120 Thailand

*Corresponding author, e-mail: thappasarn.j@mail.rmutk.ac.th

Introduction

Extrusion cooking is increasingly being used in the production of food products such as breakfast cereals, snacks and pasta. The extrusion process can modify flour to produce a variety of pasta products. Purple rice called ‘Riceberry’ (*Oryza sativa* L.) is reported to have high nutritional value and it provides some special characteristics that can be used as the raw material to produce pasta by extruder. Riceberry bran contains bioactive compounds and anthocyanins that are able to reduce inflammation and acts as an antioxidant (Leardkamolkarn *et al.*, 2011). Moreover, Riceberry is rich in fiber and minerals. Therefore, RBF was used in this study as a major ingredient to formulate into pasta. Wu *et al.* (2015) reported that when MBF was added to rice flour, it improved texture, appearance and nutritional value of pasta. Mixture design supports to design experiments with ingredient factors in mixture. The aim of this research was to use a mixture design to develop pasta formulation using extrusion processing. A mixture design of 3 components, namely, RBF, CRF and MBF were performed to identify the formulation achieving the optimum physical and chemical properties.

Material and Methods

1. Raw material preparation

Riceberry and mung bean, from general supermarket of Thailand, was coarsely and finely ground by FitzMill comminutor and Pin Mill, respectively. RBF and MBF were then passed through an 80-mesh sieve. Finally, the prepared samples were packed, sealed in polyethylene bags and kept at 4 °C until use. While, CRF (Erawan Brand, Thailand) was purchased from local market. A three-factor mixture design was applied to develop pasta formulation from RBF, CRF and MBF in the range of 25-75, 12.5-37.5 and 12.5-37.5%, respectively. Nine formulations of pasta provided by mixture design were detailed in Table 1. Each mixed formula was then adjusted moisture content to 30% by thoroughly mixing and spraying water in a kitchenAid. All flour mixtures were kept at chilled temperature of a refrigerator for 48 hr to reach the maximum water absorption.

Table 1 Formulations of pasta obtained from mixture design

Formulation	RBF (%)	CRF (%)	MBF (%)
1	75	12.5	12.5
2	62.5	18.75	18.75
3	50	37.5	12.5
4	50	31.25	18.75
5	50	25	25
6	50	18.75	31.25
7	50	12.5	37.5
8	37.5	31.25	31.25
9	25	37.5	37.5

2. Extrusion conditions

Pasta samples were produced with a laboratory scale single screw extruder. Screw length per diameter (L/D), screw diameter and length were 12:1, 25 and 300 mm, respectively. Diameter of die hole and barrel were 2 and 25 mm, respectively. The extruder barrel section was heated with band heater. The barrel temperature at transition and die zone was adjusted to 75-80 and 85-100°C, respectively and screw speed was 80-100 rpm. Feed rate was fixed at 20 g/ min. The condition of extrusion was brought to steady state before sampling. Each pasta

sample was cooled at room temperature for 30 min, cut manually into 25 cm long and dried in hot air oven at 40°C about 3 hr until the moisture content reached to approximately 10%. Finally, the pasta were placed in polyethylene bags and stored at room temperature for analysis.

3. Proximate analysis

The chemical composition (moisture, protein, ash and fiber) of pasta samples were determined according to the Association of Official Analytical Chemists standard (AOAC, 2005).

4. Pasta cooking quality

a) Cooking time

About 5 cm length of extruded pasta was cooked in boiling water. Optimum cooking time was defined as the required time for the core of cooked pasta strand to disappear when the cooked pasta was pressed between two transparent glass slides (Ritthiruangdej *et al.*, 2011).

b) Cooking loss

The Cooking loss, defined as the amount of solid substance lost into the cooking water (Lu *et al.*, 2009). The 5 g sample of pasta was placed into 200 mL of boiling distilled water. The cooking water and rinsed using 20 mL of distilled water. The cooking water and rinsing water were collected in a beaker and placed into an air oven at 105°C until dry. The residue was weighed and reported as a percentage of the starting material.

c) Cooking yield

Cooking yield was determined according to American Association of Cereal Chemists method (AACC 66-50, 2003) For each sample, 5 g of pasta was cooked until their optimal cooking time was reached in 200 mL boiling distilled water, drained and rinsed with another 50 mL of distilled water at room temperature for 1 min. Each of cooked pasta was weighed after reaching room temperature. Cooking yield of drained pasta was determined as follows:

$$\text{Cooking yield} = (\text{weight of cooked pasta})/(\text{weight of raw pasta}) \times 100$$

5. The color of the cooked pasta

Each cook pasta color was measured with Hunter Lab (Color Quest XE, USA) equipped with a D65 illuminant using the CIE L* a* b* system. L* value is a measurement of brightness (0-100); a* value represents the red-green coordinates (- is green while + is red); b* value indicates the blue-yellow coordinates (- is blue while + is yellow).

6. Pasta texture analysis

All pasta samples were cooked in boiling water for 6 min. Then, measurements were carried out at room temperature exactly 10 min after cooking (Lu *et al.*, 2009). Texture properties of pasta were measured using texture analyzer (TA. XT plus, Stable Microsystem, UK). Each cooked pasta was pulled at test speed 1 mm/s with the Spaghetti tensile grips probe (A/SPR) and resulted as tensile strength (maximum force; g force).

All data were done in triplicate independent analyses and analyzed using one-way ANOVA. The significant of mean difference were analysed at $p < 0.05$.

Results and Discussion

Increasing of MBF to 37.25% in the formula, caused protein of pasta increased to 14.9% (db) as formula 7 and 9 (Table 2). This might be due to MBF containing with 26% (db) protein while RBF and CRF composed of about 9% (db) protein as in the preliminary experiment. Cooking time was varied from 8 to 9 min (Figure 1). This might be due to the difference of gelatinization temperature RBF CRF and MBF. Cooking yield was varied inversely with cooking loss. Increase the amount of MBF from 12.5% (formula 1) to 37.5% (formula 7 and 9) resulting the increasing of cooking yield to maximum 212% while cooking loss was only 15%. Brightness of all formulated pasta was about 44-46 which indicated dim color of pasta due to dark-purple color of RBF (Table 3). Tensile strength of pasta was increased directly with MBF from 13.9 to 24.1 g force that was supported by Wu *et al.* (2015).

Table 2 Proximate composition of pasta developed from different formulation

Formulation	Chemical composition (% by dry basis)*				
	Protein	Fat	Crude fiber	Ash	Carbohydrate
1	11.67±0.03 ^f	0.03±0.01 ^{bc}	0.11±0.01 ^b	3.47±0.19 ^{cd}	84.71±0.21 ^b
2	12.05±0.36 ^c	0.02±0.01 ^c	0.09±0.01 ^c	3.79±0.03 ^{bc}	83.82±0.18 ^c
3	10.59±0.02 ^g	0.03±0.01 ^{bc}	0.05±0.01 ^e	2.91±0.18 ^e	86.42±0.17 ^a
4	11.70±0.07 ^f	0.03±0.01 ^{bc}	0.07±0.01 ^{cde}	3.21±0.14 ^{de}	84.98±0.18 ^b
5	13.09±0.13 ^d	0.05±0.01 ^a	0.07±0.01 ^{cd}	3.93±0.13 ^{bc}	82.86±0.04 ^d
6	14.11±0.01 ^b	0.04±0.01 ^b	0.08±0.01 ^c	4.04±0.32 ^b	81.74±0.32 ^e
7	14.92±0.32 ^a	0.03±0.01 ^{bc}	0.08±0.01 ^c	4.76±0.08 ^a	80.20±0.26 ^g
8	13.64±0.19 ^c	0.02±0.01 ^c	0.07±0.01 ^{cde}	3.59±0.35 ^{bcd}	82.68±0.42 ^d
9	14.89±0.03 ^a	0.01±0.01 ^d	0.08±0.01 ^c	3.80±0.52 ^{bc}	81.21±0.50 ^f

*Values are the mean±SD (replication=3); means that share different letters are significantly different ($p<0.05$)

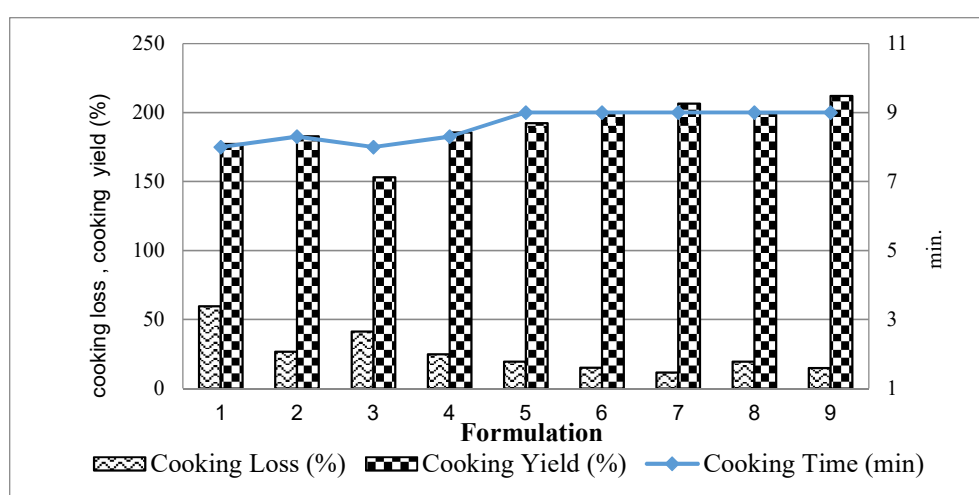


Figure 1 Cooking properties of different pasta

Table 3 Color values and tension force of pasta developed from different formulations

Formulation	Color values			Tension force (g force)
	L*	a*	b*	
1	37.36±0.13 ^c	4.32 ± 0.18 ^a	0.51±0.05 ⁱ	13.88±0.10 ^f
2	45.1±0.86 ^{ab}	3.90 ± 0.03 ^b	2.34±0.19 ^e	14.93 ±0.22 ^e
3	44.76±0.95 ^{ab}	3.26 ± 0.12 ^d	1.78±0.13 ^f	14.27±0.09 ^f
4	44.00±0.30 ^b	2.70 ± 0.08 ^f	1.56±0.15 ^g	17.08±0.06 ^d
5	44.51±1.15 ^{ab}	4.07 ± 0.21 ^b	3.07±0.08 ^c	20.40±0.07 ^c
6	43.35±0.62 ^b	2.5 ± 0.22 ^g	1.46±0.22 ^h	21.87±0.09 ^b
7	44.1±1.33 ^b	3.62 ± 0.17 ^c	2.64±0.24 ^d	22.01±0.21 ^b
8	46.34±0.93 ^a	3.05 ± 0.11 ^c	3.37±0.44 ^b	24.03±0.15 ^a
9	46.34±0.44 ^a	2.93 ± 0.07 ^c	5.03±0.12 ^a	24.14±0.04 ^a

Values are the mean±SD (replication=3); means that share different letters are significantly different (p<0.05)

Conclusion

The best quality pasta was produced from 25% of RBF, 37.5% of CRF and 37.5% of MBF. The pasta consisted of 14.90% (db) protein, 0.01% (db) fat, 0.08% (db) crude fiber, 3.80% (db) ash and 81.21% (db) total carbohydrate.

Acknowledgement

The authors would like to thank Rajamangala University of Technology Krungthep for financial support.

References

- AACC. 2003. **Approved methods of the American Association of Cereal Chemists**. St. Paul, MN: American Association of Cereal Chemists.
- AOAC. 2005. **Association of Official Analytical Chemists**. Official method of analysis. 18th ed. Gaithersburg, MD, USA: AOAC International.
- Leardkamolkarn, V., Thongthep, W., Suttiarporn, P., Kongkachuichai, R., Wongpornchai, S. and Wanavijitr, A. 2011. Chemopreventive properties of the bran extracted from a newly-developed Thai rice: The Riceberry. **Food Chemistry** 125(3): 978-985.
- Lu, Q., Guo, S. and Zhang, S. 2009. Effects of flour free lipids on textural and cooking qualities of Chinese noodles. **Food Research International** 42(2): 226-230.
- Ritthiruangdej, P., Parnbankled, S., Donchedee, S. and Wongsagonsup, R. 2011. Physical, chemical, textural and sensory properties of dried wheat noodles supplemented with unripe banana flour. **Kasetsart Journal (Natural Sciences)** 45(3): 500-509.
- Wu, F., Meng, Y., Yang, N., Tao, H. and Xu, X. 2015. Effects of mung bean starch on quality of rice noodles made by direct dry flour extrusion. **LWT - Food Science and Technology** 63(2): 1199-1205.

Harvesting Maturities Affecting Phenolic Compounds and Antioxidant Activities in ‘Sangyod Phatthalung’ Rice Cultivated at Upland

Uraiwan Wattanakul^{1*}, Nopparat Mahae¹ and Peerapong Puengyam²

ABSTRACT

This study aimed to determine the effect of harvesting maturity (35, 45 and 55 days after flowering) and storage times (1, 2, 4 and 6 months) of paddy on phenolic compounds and antioxidant activity of upland Sangyod brown rice (SBR). The results showed that harvesting maturity and storage time of paddy had affected on antioxidant activity by DPPH assay ($P < 0.05$) except in the first month. However, harvesting maturity and storage time of paddy affected to phenolic compounds and antioxidant activity by ABTS assay ($P < 0.05$). The phenolic content of SBR harvested at 45 days after flowering showed the highest values at all storage times. In particular, at 6 months of storage, the phenolic content reached the highest level at 36.68 mg gallic acid equivalent per gram of rice. Therefore, the results indicated that approximate harvested times of paddy rice was affected to increase bioactive compounds on these samples. As same as, the storage times of paddy rice was affected to increase bioactive compounds on upland Sangyod brown rice.

Keywords: Harvesting maturity, Phenolic compounds, Antioxidant Activity, Upland

¹ Faculty of Sciences and Fisheries Technology, Rajamangala University of Technology Srivijaya, Maifad, Sikao District, Trang 92150, Thailand

² Program in Chemistry, Faculty of Science, Phuket Rajabhat University, Phuket. Radsada, Mueang, Phuket 83000, Thailand

*Corresponding author, e-mail: uriwan16@gmail.com

Introduction

Thailand has a strong tradition of rice production. Rice (*Oryza sativa* L.) is a staple food for over half of the world's population (Roy, 2011). This is one of the main foods and sources of nutrition for most Thai citizens. Thailand can harvest three rice crops a year, but rice is water intensive: one calculation says rice requires 1,500 m³ of water per 1600 m² cultivated area. This is problem when due to the drought. During rice processing, rice grains produced from rice milling has a high nutritive value (Saunders, 1990) such as phenolic compounds (Liu, 2003) and antioxidative activity (Pietta, 2000).

Timely harvesting ensures good grain quality and high nutritional value. Harvesting too early will result in a higher percentage of immature grains, while, harvesting too late will lead to excessive losses and increased breakage in rice. Harvest time also affects the germination potential of rice seed and nutrients.

The rice quality depends on the time of harvesting as significant changes in bioactive compound contents occur during the grain development and maturation period (Lin and Lai, 2011). In general, harvesting time of rice is determined based on both, the head rice yield and the physicochemical and nutritional characteristics such as moisture content, protein content, milling suitability, and taste (Hossain *et al.*, 2009)

In some areas, immature rice is used for many rice products because of its nutritional and physicochemical properties (Lin and Lai, 2011). Evidence indicates that developing grains have higher contents of phytochemicals such as oryzanols, tocopherols, and phenolic compounds, than do fully mature grains (Chrastil, 1993). It is thus important to determine the changes in these physicochemical characteristics during the pre-harvest maturation period.

The yield and quality of brown rice obtained by paddy processing determine the income of rice producers. The variety, soil, climate conditions, applied technology in production and paddy processing are the main factors that affect on yield and quality of paddy and brown rice. Ilieva *et al.* (2009) reported that the optimum time for harvest is when the moisture content in grain is between 18 and 20 %.

Rice is known in a variety of colors including red, black, purple, and white. Colored rice has been used as food and medicine for sixty years (Katsura and Oiso, 1976). There are high in minerals and bioactive substances such as anthocyanin, flavonoid, phenolic compounds (Guerra and Jaffe, 1975). These bioactive compounds have been reported to have high potency as anticarcinogens agents. For example, Anthocyanins exert an inhibitory effect of cell invasion on various cancer cell lines (Chen *et al.*, 2006). Anthocyanin rich extract from black rice (AEBR) could suppress tumor growth and angiogenesis in nude mice (Hui *et al.*, 2010).

In Thailand, the Sangyod red rice (*Oryza sativa*, L., var. *indica*) is one of special red rice, originally planted in Pattalung, a province in the South for hundred years. It has been proposed as the protected rice variety under the law and registered as goods associated with geographical indications called Sangyod rice of Muang Pattalung since 2006 (Ministry of Commerce, 2011). Sangyod rice has a significantly lower yield rate than other types of rice, but it was normally sold at a higher price more than double the price of other strains on the market. High content of minerals, vitamin B complex and bioactive compounds have been reported (Banchuen *et al.*, 2010). In addition, the antioxidant activity of the water extract of Sangyod red rice were analyzed and found three times higher than that of Dawk Mali 105, the jasmine white rice (Srisawat *et al.*, 2010). The high activity was consistent with high content of phenolic compounds and flavonoids. The natural antioxidant activity is well known for protection against oxidative stress related chronic diseases (Wojcik *et al.*, 2010). Nevertheless, there was a few basic information regarding the antioxidant components and properties of upland Sangyod rice cultivars in Thailand.

The object of this study was to investigate the antioxidant components and Phenolic content of upland Sangyod brown rice, which are the most commonly cultivated in Phatthalung, to provide information on bioactive compounds for upland sangyod rices.

Materials and Methods

1. Preparation of Sangyod rice extracts

‘Sangyod Phatthalung’ rice cultivated on upland area in the wet season (September – February) at Phatthalung, Thailand (figure 1). Water management in this field was continuous irrigation during the period from the beginning of planting until 25 days before the harvest. This experiment used organic fertilizer 2 times but not pesticides. Sangyod brown rice powders were prepared from paddy harvested at 35, 45, 55 days after flowering (DAF) and stored for 1, 2, 4, 6 months, by grinding mill. Rice powder (50.0 g) was extracted with 100 ml absolute methanol for 24 h at room temperature. The extract was filtered through Whatman No.1 filter paper and the supernatant was collected. The residual rice powder was further extracted twice, with methanol. All the extracts were combined before evaporating under vacuum using a rotary evaporator. The residual crude methanolic rice extract was weighed and stored at -20 °C. until further use for bioactive compounds analysis.

2. Determination of total phenolic content

Total phenolic content of upland Sangyod rices extract was measured according to Folin-Ciocalteu colorimetric method (Wolfe *et al.*, 2003) with some modification. Rice extract was dissolved with methanol. An aliquot of rice extract (125 µl) at appropriate dilution was mixed with 500 µl of the freshly prepared Folin–Ciocalteu reagent and a further 125 µl of distilled water. The mixture was shaken for 6 min in the dark at room temperature and 1.25 ml of 7% sodium carbonate was added. The final volume was made up to 1 ml with distilled water. After 90 min of reaction at room temperature, the absorbance at 760 nm was determined by UV–vis spectrophotometer. Gallic acid was used as a standard and the total phenolic compounds were expressed as milligram gallic acid equivalents (GAE) per gram dry weight of extracts.

3. Determination of 2,2-diphenyl-1-picrylhydrazyl radical scavenging activity

The DPPH radical scavenging capacity of upland Sangyod rices extract was determined according to the method reported by Fenglin (2004) with some modification. Briefly, 0.1 ml of sample was mixed with 0.9 ml of a 1 mM methanolic solution of DPPH[•]. The mixture was kept for 30 min in the dark at room temperature. The absorbance was measured at 517 nm relative to the control(as 100%) using a UV–vis spectrophotometer. DPPH radical scavenging ability was calculated using the formula: scavenging ability (%)

$$= [\text{Absorbance}_{517\text{nm of control}} - \text{Absorbance}_{517\text{nm of sample}} / \text{Absorbance}_{517\text{nm of control}}] \times 100.$$

The scavenging activity of rice extract was expressed as 50% inhibitory concentration, IC₅₀ (mg/ml)

4. Determination of ABTS⁺ radical scavenging activity

Total antioxidant capacity of upland Sangyod rices extracts was followed out using the improved 2,2-azino-bis- (3-ethylbenzothiazoline-6-sulphonic acid) diammonium salt (ABTS) radical cation method as described by Bao *et al.* (2005) with some modification. Briefly, ABTS⁺ solution (1 mL, absorbance of 0.700) was added to 0.5 mL of the extracts and mixed thoroughly. The mixture was kept at room temperature for 5 min and the absorbance was immediately

recorded at 734 nm. Trolox standard solution was assayed under the same conditions. ABTS radical-scavenging ability was calculated by using the formula: scavenging ability (%)

$$= [\text{Absorbance}_{734\text{nm of control}} - \text{Absorbance}_{734\text{nm of sample}} / \text{Absorbance}_{734\text{nm of control}}] \times 100.$$

The scavenging activity of rice extract was expressed as 50% inhibitory concentration, IC₅₀ (mg/ml)

5. Statistical analysis

The experimental data were statistical analyzed using SPSS Program. The data of three replicate experiments were expressed as mean \pm standard deviation (SD) (n = 3). Duncan's multiple range test was used to compare means at probability level of 0.05.

Results and Discussions

The total phenolic content of upland Sangyod rice extracts in the first month, as determined by the Folin–Ciocalteu reagent, ranged from 2.93 to 9.86 mg GAE/g rice (Table 1). The harvesting time (35, 45 and 55 days after flowering) had an effect on the total phenolic content of Sangyod brown rice. The harvesting time at 45 days after flowering had the highest total phenolic content (9.86 mg GAE /g rice), while the lowest content was found at 35 days after flowering (p<0.05). ABTS scavenging activity of rice extracts was highest at 45- 55 days after flowering, showing IC₅₀ of 0.19-0.20 mg/ml. On the other hand, the harvesting time showed no effect on DPPH scavenging activity of Sangyod paddy stored for 1 month. As shown in table 1, IC₅₀, was between 0.31-0.65 mg/ml. By DPPH assay, differences in antioxidant activity of all the varieties were not significant while by ABTS⁺ significant differences in scavenging activity were observed. Similarly, antioxidant activity and total phenolic compounds (table 1) exhibited similar variations. Similar results were obtained by other researchers; Iqbal *et al.* (2005) found that the phenolic compounds may contribute directly to antioxidative action.

The total phenolic compounds in this study were similar to those of rice reported by Shen *et al.* (2009) have reported that the whole rice grain had phenolic contents ranging from 108.1 to 1244.9 mg GAE/100 g, depending on the color of grain (Choi *et al.*, 2007) Goffman and Bergman (2004) reported that the phenolic contents in the white, red and purple rice ranged from 25 to 246, 34 to 424, 69 to 535 mg GAE/100 g, which was a little lower than this study



Figure 1 (Left) upland Sangyod rice (Right) paddy harvested at 35, 45, 55 DAF

Table 1 IC₅₀ value (mg/ml) of DPPH and ABTS assay for radical scavenging activity and total phenolic content of rice extract at 1 month storage time

harvesting maturity of SBR (day)	DPPH free radical- scavenging (mg/ml)	ABTS free radical- scavenging (mg/ml)	Total phenolic content (mg GAE / g sample)
35	0.58±0.10 ^{ns}	0.30±0.04 ^b	2.93±0.29 ^c
45	0.38±0.13 ^{ns}	0.19±0.01 ^a	9.86±1.70 ^a
55	0.65±0.21 ^{ns}	0.20±0.01 ^a	7.28±1.32 ^b

Results represent means \pm SD (n = 3). In each column, different letters mean significant differences (p < 0.05).

The bioactive compound; the scavenging activity of methanolic rice extracts from Sangyod paddy with stored for two months was determined by DPPH and ABTS⁺ assays as shown in table 2. The phenolic compound contents of upland Sangyod rice extracts in the second months, ranked the samples in descending order, as follows: 45 days, 35 days and 55 days after flowering, the values of which were 12.43, 8.68 and 8.40 mg GAE/g rice, respectively. The highest was observed for harvesting time at 45 days after flowering. The total phenolic content was not significantly different between harvesting time at 35 days and 55 days (p > 0.05). This study was two times higher than the other studies, where phenolic compounds exhibiting effective antioxidant properties were found in washed water extract of Sangyod brown rice was 6.75 mg GAE/g of the extracts (Ratanavalachai *et al.*, 2012).

Maximum scavenging activity was observed for the harvesting time of 45 days after flowering, followed by 35 and 55 days, respectively. The ABTS assay was not significantly different between 35 and 45 days after flowering (p > 0.05). The shown IC₅₀ was 0.07, 0.06 and 0.32 mg/ml for harvesting time 35, 45 and 55 days after flowering, respectively. While, the highest DPPH scavenging activity was found in 45 days (0.29 mg/ml) and the lowest activity was in 55 days (0.65 mg/ml) (p < 0.05).

Table 2 IC₅₀ value (mg/ml) of DPPH and ABTS assay for radical scavenging activity and total phenolic content of rice extract at 2 month storage time

harvesting maturity of SBR (day)	DPPH free radical- scavenging (mg/ml)	ABTS free radical- scavenging (mg/ml)	Total phenolic content (mg GAE / g sample)
35	0.35±0.01 ^b	0.07±0.02 ^a	8.68±1.39 ^b
45	0.29±0.01 ^a	0.06±0.01 ^a	12.43±1.06 ^a
55	0.65±0.02 ^c	0.32±0.01 ^b	8.40±1.17 ^b

Results represent means \pm SD (n = 3). In each column, different letters mean significant differences (p < 0.05).

Table 3 IC₅₀ value (mg/ml) of DPPH and ABTS assay for radical scavenging activity and total phenolic content of rice extract at 4 month storage time

harvesting maturity of SBR (day)	DPPH free radical- scavenging (mg/ml)	ABTS free radical- scavenging (mg/ml)	Total phenolic content (mg GAE / g sample)
35	0.39±0.08 ^a	0.24±0.03 ^b	11.52±0.65 ^b
45	0.49±0.18 ^a	0.32±0.005 ^c	21.36±1.87 ^a
55	0.74±0.07 ^b	0.17±0.03 ^a	18.41±3.07 ^a

Results represent means \pm SD (n = 3). In each column, different letters mean significant differences (p < 0.05).

The total phenolic content of upland Sangyod rice extracts in the fourth month of storage ranged from 11.52 to 21.36 mg GAE/g rice (Table 3). It was found that the harvesting time affected the total phenolic content. The lower level of total phenolics was obtained from harvesting time at 35 days, while phenolic compounds were produced higher at 45 and 55 days after flowering. IC₅₀ value of DPPH assay of Sangyod rice extracts was highest at harvesting time at 35 and 45 days after flowering (0.39-0.49 mg/ml) and the lowest value was at 55 days (0.74 mg/ml) (p < 0.05). The harvesting time also had significant effect on ABTS antioxidant activity of Sangyod paddy stored at 4 month. The highest ABTS scavenging activity was found in paddy harvested at 55 days after flowering (0.17 mg/ml) followed by 35 and 45 days, respectively. The results were lower than the values reported by Shen *et al.* (2009) found that total phenolic content ranged from 108.1 to 1,244.9 mg GAE/100 g, with the lower values coming from the white rice, while the higher values were from red and black rice.

In the sixth month of this experiment. The results showed that harvesting maturity of paddy had no effect on antioxidant activity by ABTS assay (P > 0.05). Showing IC₅₀ of 0.16 - 0.23 mg/ml (Table 4). On the other way, harvesting maturity and storage time of paddy affected total phenolic content and antioxidant activity by DPPH assay (P < 0.05). The highest total phenolic compound was from 45 days after flowering (36.68 mg GAE/g rice). The harvesting time at 35 and 55 days after flowering had lower phenolic content (21.95 and 22.01 mg GAE/g rice, respectively). As the same results were obtained by Goffman and Bergman (2004) reported mean concentrations of 69, 213 and 274 mg GAE 100 g⁻¹ for light brown, red and black pericarp color rice grains, respectively. The whole rice grain had phenolic contents depending on the color of grain (Goffman and Bergman, 2004; Choi *et al.*, 2007). The highest DPPH scavenging activity was observed for rice harvested at 45 days after flowering with IC₅₀ of 0.40 mg/ml, followed by 35 days and 55 days after flowering, respectively. By ABTS assay, differences in antioxidant activity of all were not significant while by DPPH assay, there was a significant difference. According to Awika *et al.* (2003) the superiority of the ABTS assay over DPPH, is because of operable over a wide range of pH, inexpensive and more rapid than that of the DPPH assay.

This research indicated that the harvesting time and storage time affected the total phenolic content and antioxidant activity in upland Sangyod brown rice. The total phenolic contents of this experiment were higher than the values reported by Srisawat *et al.* (2010) reported that the total phenolic content of the washed water extract of brown rice and the water-soluble extract of rice bran from Dawk Mali 105 and Sangyod were in the range of 228.10-753.48 µg GAE/g rice extract. The content of phenolic compounds was the highest in the water-soluble extract of Sangyod rice.

Table 4 IC₅₀ value (mg/ml) of DPPH and ABTS assay for radical scavenging activity and total phenolic content of rice extract at 6 month storage time

harvesting maturity of SBR (day)	DPPH free radical- scavenging (mg/ml)	ABTS free radical- scavenging (mg/ml)	Total phenolic content (mg GAE / g sample)
35	0.43±0.2 ^{ab}	0.16±0.00 ^{ns}	21.95±1.69 ^b
45	0.39±0.02 ^a	0.19±0.02 ^{ns}	36.68±2.75 ^a
55	0.64±0.05 ^b	0.23±0.10 ^{ns}	22.01±4.36 ^b

Results represent means \pm SD (n = 3). In each column, different letters mean significant differences (p< 0.05)

Conclusion

In conclusion, harvesting maturity and storage times had a significant effect on the antioxidant properties and total phenolics content, Brown rice is a potent source of antioxidants suggesting its use in nutraceuticals and functional food industries. The phenolic content could be indirectly predicted by appropriate harvesting period. Their relationships with cultivated area, harvesting times and storage times of paddy can be used as a guideline for preservation and processing of rice at the appropriate time to maintain the value of the bioactive compound. The results from Sangyod rice could lead to understand more the upland rice cultivation. For harvesting maturity time of 45 days after flowering and paddy storage 6 month gave highest the antioxidant properties and total phenolics content in upland Sangyod brown rices.

Acknowledgement

The authors acknowledge the financial support granted by Rajamangala University of Technology Srivijaya. The authors thank Faculty of Sciences and Fisheries Technology for laboratory and equipments allowed.

References

- Awika, J. M., Rooney, L. W., Wu, X., Prior, R. L. and Zevallos, L. C. 2003. Screening methods to measure antioxidant activity of sorghum (*Sorghum bicolor*) and sorghum products. **Journal of Agricultural and Food Chemistry** 51: 6657–6662.
- Banchuen J., Thammarutwasik P., Ooraikul B., Wuttijumnong P. and Sirivongpaisal P. 2010. Increasing the bioactive compounds contents by optimizing the germination conditions of Southern Thai Brown Rice. **Songklanakarin Journal of Science and Technology** 3: 207- 326.
- Bao, J.S., Cai, Y., Sun, M., Wang, G.Y. and Corke, H. 2005. Anthocyanins, flavonols, and free radical scavenging activity of Chinese bayberry (*Myrica rubra*) extracts and their color properties and stability. **Journal of Agricultural and Food Chemistry** 53: 2327–2332.
- Choi, Y., Jeong, H.S., and Lee, J. 2007. Antioxidant activity of methanolic extracts from some grains consumed in Korea. **Food Chemistry** 103: 130–138.

- Chrastil, J. 1993. Changes of oryzenin and starch during pre-harvest maturation of rice grains. **Journal of Agricultural and Food Chemistry** 41:2242–2244.
- Chotimakorn, C., Benjakul, S., and Silalai, N. 2008. Antioxidant components and properties of five long-grained rice bran extracts from commercial available cultivars in Thailand. **Food Chemistry** 111:636–641.
- Chen, P.N., Kuo, W.H., Chiang, C.L., Chiou, H.L., Hsieh, Y.S. and Chu, S.C. 2006. Black rice anthocyanins inhibit cancer cells invasion via repressions of MMPs and u- PA expression. **Chem Biological Interaction Journal** 163: 218-29.
- Choi, Y., Jeong, H.S. and Lee, J. 2007. Antioxidant activity of methanolic extracts from some grains consumed in Korea. **Food Chemistry** 103: 130–138.
- Fenglin, H., Ruili, L., Bao, H. and Liang, M. 2004. Free radical scavenging activity of extracts prepared from fresh leaves of selected Chinese medicinal plants. **Fitoterapia**. 75: 14-23.
- Goffman, F.D. and Bergman, C.J. 2004. Rice kernel phenolic content and its relationship with antiradical efficiency. **Journal of the Science of Food and Agriculture** 84: 1235–1240.
- Guerra, M.J. and Jaffe, W.G. 1975. Nutritional studies with rice bran. **Archivos latinoamericanos de nutrición** 25: 401-17.
- Hossain, M.F., Bhuiya, M.S.U., Ahmed, M. and Mian, M.H. 2009. Effect of harvesting time on the milling and physicochemical properties of aromatic rice. **Thai Journal Agriculture Science** 42:91–96.
- Hui, C., Bin Y., Xiaoping, Y., Long, Y., Chunye, C. and Mantian M. 2010. Anticancer activities of an anthocyanin- rich extract from black rice against breast cancer cells in vitro and in vivo. **Nutrition and Cancer** 62: 1128-36.
- Iqbal, S., Bhangar, M.I. and Anwar, F. 2005. Antioxidant properties and components of some commercially available varieties of rice bran in Pakistan . **Food Chemistry** 93 :265–272.
- Katsura, E. and Oiso, T. 1976. Beriberi. **Monogr Ser World Health Organ**. 136-45.
- Lin PY and Lai HM. 2011. Bioactive compounds in rice during grain development. **Food Chemistry**. 127:86–93.
- Liu, R. H. 2003. Health benefits of fruit and vegetables are form additive and synergistic combinations of phytochemicals. **American Journal of Clinical Nutrition**78:517S–520S.
- Ministry of Commerce, Thailand. Department of Intellectual Property. 2011. **Sangyod muang Phatthalung Thailand rice (Geographical Indications: GI)**. Available Source : http://www.moc.go.th/opscenter/pt/Sangyod_index.htm, March 24, 2011.
- Moure, A., Cruz, J. M., Franco, D., Dominguez, J. M., Sineiro, J., Dominguez, H., *et al.* 2001. Natural antioxidants from residual sources. **Food Chemistry**72:145–171.
- Pietta, P. G. 2000. Flavonoids as antioxidants. **Journal of Natural Products** 63:1035–1042.
- Ratanavalachai, T., Thitiorul, S., Tanuchit, S., Jansom, C., Uttama, S., and Itharat, A. 2012. Antigenotoxic Activity of Thai Sangyod Red Rice Extracts against a Chemotherapeutic Agent, Doxorubicin, in Human Lymphocytes by Sister Chromatid Exchange (SCE) Assay In Vitro. **Journal of the Medical Association of Thailand**. 95 (1): S109-S114.
- Roy, P., Orikasa, T., Okadome, H., Nakamura, N., and Shiina, T. 2011. Processing conditions, rice properties, health and environment. **International Journal of Environment Research and Public Health** 8:1957–1976
- Saunders, R. M. 1990. The properties of rice bran as a food stuff. **Cereal Food World** 35: 632–636.

- Shen, Y., Jin, L., Xiao, P., Lu, Y. and Bao, J. 2009. Total phenolics, flavonoids, antioxidant capacity in rice grain and their relations to grain color, size and weight. **Journal of Cereal Science**. 49: 106-111.
- Srisawat, U., Panunto, W., Kaendee, N., Tanuchit, S., Ithara, t A. and Lerdvuthisopon, N. 2010. Determination of phenolic compounds, flavonoids, and antioxidant activities in water extracts of Thai red and white rice cultivars. **Journal of the Medical Association of Thailand**. 93(7): S83-91.
- Verica, I., Danica, A., Andov, D., Natalija, M. and Mirjan, a J. 2009. Dressing percentage of white rice in correlation with the harvest time of the rice. **Yearbook of the Faculty of Agricultural Sciences and Food**, Skopje. 5: 19-27.
- Wojcik, M., Burzynska-Pedziwiatr, I. and Wozniak, L.A. 2010. A review of natural and synthetic antioxidants important for health and longevity. **Current Medicinal Chemistry**. 17: 3262-88.
- Wolfe, K., Wu, X. and Liu, R.H. 2003. Antioxidant activity of apple peels. **Journal of Agriculture and Food Chemistry** 51: 609- 614.

Substitution of Soybean Meal with Fermented Palm Kernel Meal in Diet of Sex Reversed Red Tilapia (*Oreochromis niloticus* × *O. mossambicus*)

Wattana Wattanakul^{1*}, Uraiwan Wattanakul¹ and Jesada Ishaak²

ABSTRACT

The solid state fermentation of palm kernel meal (PKM) by effective microorganisms (EM) improved the nutritive values of PKM. Substitution of soybean meal (SBM) with fermented PKM (FPKM) as protein source was investigated for its effects in sex reversed red tilapia (*Oreochromis niloticus* × *O. mossambicus*). The two month old fish (14.85 ± 0.28 g initial weight) were randomly stocked into 20 cement ponds (1 m x 2 m x 0.6 m) at 40 fish/pond. The fish were fed by SBM based diets with replacement by FPKM at 25% (25FPKM), 50% (50FPKM), 75% (75FPKM) and 100% (100FPKM), while an FPKM free diet (0FPKM) was used as control. All these diets contained 30% protein. Four replicate experiments were conducted in a recirculating system for 6 months. At the end of the feeding trial, fish fed with the 50FPKM diet were superior in growth performance and feed utilization parameters (FCR and PER) ($P < 0.05$). No differences in carcass composition and no negative effects on hematological parameters at the 50% replacement level of SBM by FPKM also supports this alternative. Findings from the current study could be applied in a low-cost FPKM-containing diet for tilapia, and they suggest the potential feedstuff use of FPKM also with other aquatic animals.

Keywords: Palm kernel meal, Effective microorganisms, Carcass, Feed utilization, Red Tilapia (*Oreochromis Niloticus* × *O. Mossambicus*).

¹Department of Fisheries Technology, Faculty of Sciences and Fisheries Technology, Rajamangala University of Technology Srivijaya, Trang 92150, Thailand

²Department of Food Industry and Fisheries Products, Faculty of Sciences and Fisheries Technology, Rajamangala University of Technology Srivijaya, Trang 92150, Thailand

³Department of Fisheries Sciences, Faculty of Agricultural Technology and Agro-Industry, Rajamangala University of Technology Suvarnabhumi, Phranakhon Si Ayutthaya 13000, Thailand

*Corresponding author, e-mail: wattanakul67@gmail.com

Introduction

Nile Tilapia (*Oreochromis niloticus*) is a fish known worldwide because it's an economically important fish species that is widely cultured around the world (FAO, 2012). The production of tilapia (all species) increased from 1.5 million tonnes in 2003 to 2.5 million tonnes in 2010, with the sales value exceeding 5 billion USD (FAO, 2016). Red Tilapia (*O. niloticus* × *O. mossambicus*) is a fish improved from the breeding of tilapia. It is popular due to its attractive color and good taste, increasing its marketability. Similar to other economic fish species, the cost of producing the pellet diets is continuously increasing, and strongly depends on cost of the protein ingredients (El-Saidy and Gaber, 2003). Generally, the efficiency of various protein sources from plant by-products, as lower cost alternatives to replace fish meal, has been evaluated in fish diets as has been the replacement of fish meal by low-cost animal by-products (Wattanakul *et al.*, 2017).

Soybean meal (SBM) is the main plant protein in practical fish feed production. This feedstuff is moderately rich in protein, produced in great quantities, reasonably priced, and has relatively well-balanced amino acid profile among the plant by-product meals (Lim and Lee, 2009). High price and presence of anti-nutritional compounds (including goitrin, phytohemagglutinins, lectins, non-starch polysaccharides, phytate, phytoestrogens, protein antigens, saponins and trypsin inhibitor) are disadvantages of this plant by-product in aquafeed production (Drew *et al.*, 2007). Therefore, the replacement of SBM by low-cost plant protein sources is worth considering in the aquaculture sector.

Palm kernel meal (PKM), a by-product from palm oil production, is mainly produced in South-East Asian and African countries. This feedstuff is generally used in feeds for terrestrial animals (Saenphoom *et al.*, 2013) and as a component in fish feed formulations (Thongprajukaew *et al.*, 2015). Poor usability in aquafeed is due to the large amount of cell wall constituents, low protein content, and amino acid deficiencies (Ng *et al.*, 2002; Ng and Chen, 2002). Biological pretreatment of the PKM for improving its nutritive value appears to have potential, by enzyme supplementation and fermentation by cellulolytic or cocktail enzymes (Saenphoom *et al.*, 2013).

Effective microorganisms (EMs) are various blends of common predominantly anaerobic microorganisms, probably including lactic acid bacteria (LAB), photosynthetic bacteria, yeast, and naturally beneficial microorganisms. Worldwide the EM support sustainable practices in farming, composting, and mitigation of environmental pollution. In animal nutrition research, EMs have been applied to benefit economic terrestrial and aquatic animals. Therefore, the aim of this study was to investigate the effects of partial or full replacement of SBM protein by fermented PKM (FPKM) in the diet of sex reversed red tilapia. Findings from the current study may support the use of PKM in aquafeed production, providing a low-cost diet for tilapia farming and other aquatic animals.

Materials and Methods

Preparation of FPKM and the experimental diets

The PKM was obtained from a palm oil industry in Sikao District, Trang and the other feedstuffs were purchased from Phatthalung Livestock CO., LTD, Phatthalung, Thailand. This by-product was fermented with activated effective microorganisms (EM-Plus, Microbe for Life, Bangkok, Thailand) that contain photosynthetic bacteria, LAB, nitrogen fixing bacteria, yeast and bacillus. The solid-state fermentation was performed by mixing PKM with liquid EM (5% v/w), molasses (5% v/w), and then adding water (5% v/w). These mixtures were packed in polyethylene bags, sealed and incubated for 30 days in dark at ambient temperatures (30–31°C). The protein from SBM was replaced by FPKM at 25% (25FPKM), 50% (50FPKM), 75%

(75FPKM) and 100% (100FPKM), while an FPKM free diet (0FPKM) was used as the control. The solid feedstuff ingredients (fish meal, SBM, FPKM, corn meal, broken rice, and rice bran) were mixed together for 10 min, followed by adding soybean oil, fish oil, and vitamin-mineral premixes. Thirty percent water was then added. The glutinous mixture was passed through a meat mincer (4–6 mm sized hole), dried at 60°C for 24 h and then kept in polyethylene bags at 4°C until feeding.

Determination of diet proximate composition

All experimental diets were analyzed for moisture, crude protein (CP), crude lipid, crude ash and crude fiber, according to standard methods of AOAC (2005). All the analyses were performed in triplicates and are reported in g kg⁻¹ as fed. Nitrogen free extract (NFE, g kg⁻¹) and gross energy (GE, kcal kg⁻¹) were calculated from $1,000 - (CP + \text{crude lipid} + \text{crude ash} + \text{crude fiber})$ and $(CP \times 5.6) + (\text{crude lipid} \times 9.44) + (\text{crude fiber} \times 4.1) + (NFE \times 4.1)$, respectively. All the chemical analyses were performed in duplicates and are reported on % as fed basis.

Fish preparation and feeding trial

The two month old sex reversed red tilapia were obtained from Phatthalung Inland Fisheries Research and Development Center, Phatthalung, Thailand. The fish were acclimatized in cement pond (1 m × 4 m × 1 m) for 10 days. They were fed to satiation with the control diet (0FPKM) at 08.00 and 16.00 h daily. Subsequently, forty fish with similar weight (14.85 ± 0.28 g initial weight) were randomly distributed into each cement pond (1 m × 2 m × 0.6 m) with 40 cm water depth. There were five treatments with four replicates each. The experiment was conducted for 6 months. The fish were fed with the experimental diets at 10% of body weight (BW) per day, and the feed amount was adjusted weekly according to the actual feeding performance. The feed conversion ratio (FCR), and the protein efficiency ratio (PER). The measured growth (body weight) and the feed utilization were summarized monthly. At the end of the experiment, all the fish were starved for 24 h, anesthetized by quinadine and then body weight were measured for every fish. Samples of fish fillets and blood were collected from three fish in each replicate ($n = 12$ per treatment). Growth performance and feed utilization characteristics were calculated as follows:

$$\text{Survival (\%)} = 100 \times [\text{Final fish number}/\text{initial fish number}]$$

$$\text{Specific growth rate (SGR, \% day}^{-1}\text{)} = 100 \times [(\ln W_t - \ln W_0)/(t - t_0)]$$

$$\text{Weight gain (WG, \%)} = 100 \times [(W_t - W_0)/W_0]$$

$$\text{Average daily gain (ADG, g day}^{-1}\text{)} = (W_t - W_0)/t$$

$$\text{where } W_t = \text{mean weight (g) at day } t,$$

$$W_0 = \text{mean weight (g) at day } t_0.$$

$$t = \text{feeding duration (day)}$$

$$\text{Feed conversion ratio (FCR, g feed g gain}^{-1}\text{)} = \text{Dry feed consumed (g)}/\text{wet weight gain (g)}$$

$$\text{Protein efficiency ratio (PER, g gain g protein}^{-1}\text{)} = \text{Wet weight gain (g)}/\text{protein intake (g)}$$

Determination of water quality

Recirculating aquaculture system was used throughout the experiment and the quality of water was measured every other week. Overall the water quality parameters during the experiment were in the ranges $28.86 \pm 0.28^\circ\text{C}$, pH 7.80 ± 0.04 , 6.05 ± 0.21 mg L⁻¹ dissolved oxygen, 99.23 ± 1.85 mg L⁻¹ alkalinity, 0.57 ± 0.05 mg L⁻¹ ammonia, and 0.67 ± 0.04 mg L⁻¹ nitrite.

Carcass composition analysis and hematological determinations

Fish fillets were minced and analyzed for moisture, crude protein, crude lipid and crude ash, according to standard methods of AOAC (2005). Blood samples were collected from the caudal vessel after anesthetizing with 2-phenoxyethanol. Heparinized blood samples were used for analysis of hematological parameters. Plasma protein was determined according to Lowry et al. (1951). Red (RBC) and white (WBC) blood cells were counted from diluted samples, as described by Blaxhall and Daisley (1973). Hemoglobin (Hb) and hematocrit (Hct) were determined according to the method of Larsen and Snieszko (1961).

Statistical analysis

All the data were analyzed using SPSS program and are expressed as mean \pm standard error of mean (SEM). Variables that are percentages were subjected to arcsine transformation. Duncan's multiple range test was used to compare for significant differences between treatments at $P < 0.05$ in all statistical analyses.

Results and Discussion

Chemical compositions of PKM and FPKM, and the experimental diets

Fermentation of PKM with EM significantly improved the amount of crude protein (20.79%) and NFE (40.07%) while crude lipid (15.65%), crude fiber (36.45%) and ash (29.53%) were decreased (**Table 1**). GE was similar between PKM and FPKM. All the experimental diets were mutually isonitrogenous and isolipidic (**Table 2**).

Table 1 Proximate chemical compositions (% of dry weight) of PKM and FPKM. The data given are means from duplicate analysis.

Composition	PKM	FPKM	% Change
Crude protein (%)	13.13	15.86	20.79
Crude lipid (%)	9.14	7.71	-15.65
Crude fiber (%)	38.74	24.62	-36.45
Ash (%)	4.03	2.84	-29.53
NFE (%)	34.96	48.97	40.07
GE (kcal kg ⁻¹)	4,620	4,633	0.28

PKM, palm kernel meal; FPKM, fermented palm kernel meal; NFE, nitrogen free extract; GE, gross energy.

Fermentation of plant by-products with beneficial microorganisms has been adopted to improve the nutritional quality of feedstuffs by the action of enzymes from bacteria, yeasts and molds. Increased protein in FPKM in the current study could be due to the secretion of enzymes or to the release of bound proteins by breakdown of protein complexes (Lohlum *et al.*, 2014), attributed to bacterial growth and proliferation. In PKM, increased protein content and improved quality in terms of the amino acid profile have also been observed when fermented with *Trichoderma Reesei* (Cheah *et al.*, 1989). The cell wall constituents and non-starch polysaccharides (NSP) contribute 73% and 75% of raw PKM, respectively (Dusterhoft and Voragen, 1991). Significantly decreased crude fiber was not surprising since the EM contained cellulolytic microorganisms providing high cellulase activity (Halliwell *et al.*, 1985). Fluctuation in the amount of this indigestible element can increase the digestible carbohydrates, NFE. Fermentation of a medicinal plant with *Lactobacillus plantarum* and *Saccharomyces cerevisiae* can reduce the amount of saturated fatty acids (Ahmed *et al.*, 2016). Decreased lipid content in the current study is possible since the fatty acids in PKM are mainly in saturated forms.

Survival, growth and feed consumption

No differences in survival (90.50% on average) were observed across the five dietary treatments ($P>0.05$, **Table 3**). Fish fed 50FPKM were superior in final body weight, Feed utilization parameters (FCR and PER), were significantly different to those with the other treatments ($P<0.05$).

Various alternative protein source meals from plant by-products have been evaluated in fish diets as dietary replacement for SBM. The replacement of SBM by cottonseed meal was optimal at 60% in the diet for the hybrid tilapia, *O. Niloticus* × *O. Aurous* (Yue and Zhou, 2008). Thirty percent replacement of SBM by rubber seed meal was also suitable for the same species (Deng *et al.*, 2015), similar to the 24% replacement by faba beans in *O. niloticus* diet (Azaza *et al.*, 2009), while 50% replacement level was suitable by cottonseed meal in diets for channel catfish, *Ictalurus Punctatus* (Barros *et al.*, 2002). In the current study, sex reversed red tilapia fed with 50FPKM diet was superior in growth performance, While SGR, FCR and PER of 50FPKM treatment are significantly different with 100FPKM. Higher replacement levels than the optimal level tend to give poorer growth and feed utilization in several fish.

Table 2 Formulations and proximate compositions of experimental diets containing varying levels of FPKM.

Item	0FPKM	25FPKM	50FPKM	75FPKM	100FPKM
<i>Ingredient (%)</i>					
Fish meal	26.9	30.8	34.8	38.8	42.7
SBM	25.0	18.8	12.5	6.2	—
FPKM	—	6.2	12.5	18.8	25.0
Corn meal	15.9	14.2	12.5	10.8	9.1
Broken rice	12.7	11.4	10.0	8.6	7.3
Rice bran	8.5	7.6	6.7	5.8	4.9
Fish oil	2	2	2	2	2
Soybean oil	2	2	2	2	2
Alfa starch	4	4	4	4	4
Vitamin-mineral premix ^a	3	3	3	3	3
<i>Proximate composition (% fed basis)</i>					
Moisture	5.84	5.96	5.81	5.90	5.91
Crude protein	30.63	29.87	30.61	30.22	30.05
Crude lipid	10.13	10.90	10.11	9.54	9.50
Crude ash	13.28	14.50	15.37	17.22	18.78
Crude fiber	7.28	7.47	7.82	8.03	8.98
NFE	32.84	31.30	30.28	29.09	26.78
GE (kcal kg ⁻¹)	4,316	4,291	4,231	4,115	4,046

SBM, soybean meal; FPKM, fermented palm kernel meal; NFE, nitrogen free extract; GE, gross energy.

^a Vitamin-mineral premix, 1 kg contained 1,000 U vitamin A, 250 U vitamin D₃, 5 U vitamin E, 2,000 mg vitamin B₁, 800 mg vitamin B₂, 2,000 mg vitamin B₆, 1 mg vitamin B₁₂, 10,000 mg vitamin C, 300 mg pantothenic acid, 5,000 mg nicotinic acid, 200 mg folic acid, 2 mg biotin, 500 mg iron, 7,000 mg zinc, 2 mg biotin, 800 mg manganese, 10 mg selenium, 15,000 mg lysine, 3,000 mg methionine.

Carcass composition and hematological parameters

There were no significant differences in carcass moisture, crude protein, crude lipid and ash across the five dietary treatments at the end of experiment (**Table 4**). WBC was comparatively high in the fish fed with diets replacing at least 50% of SBM by FPKM, relative to the other treatment groups (**Table 5**). Except for the above parameters, the other hematological assays were very similar across the five dietary treatments. Three hematological parameters of the overall items were affected by the replacement of SBM with FPKM. At least 50% replacement can significantly increase WBC. Our results are in agreement with those from replacing SBM with 10–30% rubber seed meal in the diet of *Labeo rohita* fingerlings (Sharma *et al.*, 2014), or replacement with 15–30% cottonseed meal in the diet of hybrid tilapia (Yue and Zhou, 2008). Plasma protein also increased in a replacement level dependent manner. Fermentation by the EM might provide easily digested protein to the feed, or a high amount of fish meal can enhance protein digestibility (Hong *et al.*, 2004).

Table 3 Survival, growth performance and feed utilization of sex reversed red tilapia fed with experimental diets containing varying levels of FPKM for 6 months.

Parameter	0FPKM	25FPKM	50FPKM	75FPKM	100FPKM	<i>P</i> -value
Survival (%)	90.63 ± 3.15	89.38 ± 2.39	92.50 ± 2.88	90.00 ± 3.40	90.00 ± 2.04	0.930
Average initial weight (g)	14.66 ± 0.37	15.13 ± 1.23	14.60 ± 0.60	15.05 ± 0.25	14.81 ± 0.56	0.975
Average final weight (g)	208.41 ± 5.62 ^{ab}	215.99 ± 4.28 ^a	218.97 ± 3.29 ^a	203.44 ± 5.77 ^{ab}	187.73 ± 4.67 ^b	0.025
SGR (% BW day ⁻¹)	1.47 ± 0.08 ^{ab}	1.48 ± 0.10 ^a	1.51 ± 0.03 ^a	1.45 ± 0.03 ^{ab}	1.41 ± 0.03 ^b	0.015
WG (% BW)	1328.65 ± 86.18	1357.06 ± 69.07	1403.83 ± 77.20	1254.05 ± 76.14	1171.42 ± 73.94	0.093
ADG (g day ⁻¹)	1.07 ± 0.04 ^{ab}	1.12 ± 0.02 ^a	1.14 ± 0.06 ^a	1.04 ± 0.03 ^{ab}	0.96 ± 0.04 ^b	0.010
FCR (g feed g gain ⁻¹)	2.18 ± 0.12 ^{bc}	2.15 ± 0.18 ^{bc}	1.95 ± 0.08 ^{ab}	2.21 ± 0.09 ^{bc}	2.40 ± 0.16 ^c	< 0.001
PER (g gain g protein ⁻¹)	1.53 ± 0.02 ^{ab}	1.54 ± 0.11 ^{ab}	1.69 ± 0.06 ^a	1.51 ± 0.08 ^{ab}	1.41 ± 0.09 ^b	< 0.001

FPKM, fermented palm kernel meal; SGR, specific growth rate; WG, weight gain; ADG, Average daily gain; FCR, feed conversion ratio; PER, protein efficiency ratio.

Data are expressed as mean ± SEM of all fish in four replications.

Significant differences in each row are indicated by different superscripts ($P < 0.05$).

Table 4 Fish fillet composition (% of wet weight basis) of sex reversed red tilapia fed with experimental diets containing varying levels of FPKM for 6 months.

Composition (%)	0FPKM	25FPKM	50FPKM	75FPKM	100FPKM	P-value
Moisture	66.94 ± 0.63	67.35 ± 0.56	68.01 ± 0.75	68.43 ± 0.56	67.06 ± 0.67	0.723
Crude protein	20.04 ± 0.61	20.03 ± 0.45	20.53 ± 0.87	19.86 ± 0.65	18.72 ± 0.73	0.454
Crude lipid	5.94 ± 0.52	6.01 ± 0.58	6.20 ± 0.60	5.66 ± 0.49	5.71 ± 0.68	0.546
Ash	3.33 ± 0.49	3.65 ± 0.63	3.16 ± 0.50	3.54 ± 0.76	3.70 ± 0.45	0.682

FPKM, fermented palm kernel meal.

Data are expressed as mean ± SEM ($n = 12$).

Table 5 Hematological parameters of sex reversed red tilapia fed with experimental diets containing varying levels of FPKM for 6 months.

Hematological parameter	0FPKM	25FPKM	50FPKM	75FPKM	100FPKM	P-value
RBC ($\times 10^6$ cells μL^{-1})	2.33 ± 0.03	2.05 ± 0.10	2.14 ± 0.04	2.01 ± 0.05	2.11 ± 0.12	0.602
WBC ($\times 10^4$ cells μL^{-1})	49.02 ± 3.11 ^b	39.87 ± 4.05 ^b	56.10 ± 4.26 ^a	52.56 ± 5.38 ^a	58.43 ± 4.56 ^a	0.001
Hb (g dL^{-1})	8.73 ± 0.16	7.60 ± 0.58	7.98 ± 0.37	8.02 ± 0.52	7.64 ± 0.37	0.535
Hematocrit (%)	33.23 ± 0.71	30.63 ± 0.58	32.22 ± 0.87	31.20 ± 0.51	30.24 ± 0.91	0.579
Plasma protein (g %)	2.14 ± 0.04	2.01 ± 0.11	2.32 ± 0.18	2.20 ± 0.16	2.06 ± 0.15	0.735

FPKM, fermented palm kernel meal; RBC, red blood cells; WBC, white blood cells; Hb, hemoglobin

Data are expressed as mean ± SEM ($n = 12$).

Significant differences in each row are indicated by different superscripts ($P < 0.05$)

Conclusion

The nutritive value of PKM was significantly improved by solid state fermentation with EM. This pretreated feedstuff could be used to replace SBM at 50%, as indicated by superior growth performance and maintained feed utilization, while no negative effects on carcass composition, hematological parameters. Therefore, the results overall support a low-cost FPKM-containing diet as suitable for tilapia production. The findings of this research should be useful for fish farmers, especially in the Southern part of Thailand where there is plenty of palm-oil kernel.

Acknowledgement

This project was funded by Rajamangala University of Technology Srivijaya. The authors thank Assistant. Prof. Dr. Karun Thongprajukaew for the excellent technical help and for the advice in manuscript preparation, Research and Development Office.

References

- Ahmed, S.T., Mun, H-S., Islam, Md.M., Ko, S-Y. and Yang, C-J. 2016. Effects of dietary natural and fermented herb combination on growth performance, carcass traits and meat quality in grower-finisher pigs. **Meat Science**. 122: 7–15.
- AOAC. 2005. **Official Methods of Analysis** (18th ed). Association of Official Analytical Chemists, Washington, DC.
- Azaza, M.S., Wassim, K., Mensi, F., Abdelmouleh, A., Brini, B. and Kraïem, M.M. 2009. Evaluation of faba beans (*Vicia faba* L. var. *minuta*) as a replacement for soybean meal in practical diets of juvenile Nile tilapia *Oreochromis niloticus*. **Aquaculture** 287: 174–179.
- Barros, M.M., Lim, C. and Klesius, P.H. 2002. Effect of soybean meal replacement by cottonseed meal and iron supplementation on growth, immune response and resistance of channel catfish (*Ictalurus punctatus*) to *Edwardsiella ictaluri* challenge. **Aquaculture** 207: 263–279.
- Blaxhall, P.C. and Daisley, K.W. 1973. Routine haematological methods for use with fish blood. **Journal of Fish Biology** 5: 771–781.
- Cheah, S.C., Ooi, L.C.L. and Ong, A.S.H. 1989. Improvement in the protein content of palm kernel meal by solid state fermentation, pp. 96–99. In Applewhite, T.H., ed. **Proceedings of the World Congress on Vegetable Protein Utilization in Human Foods and Animal Feedstuffs**. AOCS, Champaign, IL.
- Deng, J., Mai, K., Chen, L., Mi, H. and Zhang, L. 2015. Effects of replacing soybean meal with rubber seed meal on growth, antioxidant capacity, non-specific immune response, and resistance to *Aeromonas hydrophila* in tilapia (*Oreochromis niloticus* × *O. aureus*). **Fish and Shellfish Immunology** 44: 436–444.
- Drew, M.D., Borgeson, T.L. and Thiessen, D.L. 2007. A review of processing of feed ingredients to enhance diet digestibility in finfish. **Animal Feed Science and Technology** 138: 118–136.
- Dusterhoft, E.M. and Voragen, A.G.J. 1991. Nonstarch polysaccharides from sunflower (*Helianthus annuus*) and palm kernel (*Elaeis guineensis*) meal: preparation of cell wall material and extraction of polysaccharide fractions. **Journal of the Science of Food and Agriculture** 55: 411–422.

- El-Saidy, D.M.S.D. and Gaber, M.M.A. 2003. Replacement of fish meal with a mixture of different plant protein sources in juvenile Nile tilapia, *Oreochromis niloticus* (L.) diets. **Aquaculture Research** 34: 1119–1127.
- FAO. 2012. **The state of world fisheries and aquaculture**. FAO, Rome.
- FAO. 2016. **Cultured aquatic species information programme *Oreochromis niloticus* (Linnaeus, 1758)**. FAO, Rome.
- Halliwell, G., Wahab, M.N.B.A. and Patel, A.H. 1985. The contribution of endo-1,4-β-D-glucanase to cellulolysis in *Trichoderma koningii*. **Journal of Applied Biochemistry** 7: 43–54.
- Hong, K.J., Lee, C.H. and Kim, S.W. 2004. *Aspergillus oryzae* 3.042GB-107 fermentation improves nutritional quality of food soybeans and feed soybean meals. **Journal of Medicinal Food** 7: 430–434.
- Larsen, H.N. and Snieszko, S.F. 1961. Comparison of various methods of determination of haemoglobin in trout blood. **Progressive Fish-Culturist** 23: 8–17.
- Lim, S.J. and Lee, K.J. 2009. Partial replacement of fish meal by cottonseed meal and soybean meal with iron and phytase supplementation for parrot fish *Oplegnathus fasciatus*. **Aquaculture** 290: 283–289.
- Lohlum, S.A., Forcados, E.G., Chuku, A., Agida, O.G. and Ozele, N. 2014. Corn cob as a feed component through fungal fermentation using *Aspergillus niger*. **CIBTech Journal of Microbiology** 3: 37–42.
- Lowry, O.H., Rosenbrough, N.J., Farr, A.L. and Randall, R.J. 1951. Protein measurement with the Folin phenol reagent. **Journal of Biological Chemistry** 193: 265–275.
- Ng, W.K. and Chen, M.L. 2002. Replacement of soybean meal with palm kernel meal in practical diets for hybrid Asian-African catfish, *Clarias macrocephalus* × *C. gariepinus*. **Journal of Applied Aquaculture** 12: 67–76.
- Saenphoom, P., Liang, J.B., Ho, Y.W., Loh, T.C. and Rosfarizan, M. 2013. Effects of enzyme treated palm kernel expeller on metabolizable energy, growth performance, villus height and digesta viscosity in broiler chickens. **Asian-Australasian Journal of Animal Sciences** 26: 537–544.
- Sharma, B.B., Saha, R.K. and Saha, H. 2014. Effects of feeding detoxified rubber seed meal on growth performance and haematological indices of *Labeo rohita* (Hamilton) fingerlings. **Animal Feed Science and Technology** 193: 84–92.
- Thongprajukaew, K., Rodjaroenc, S., Yoonram, K., Sornthong, P., Hutcha, N., Tantikitti, C. and Kovitvadi, U. 2015. Effects of dietary modified palm kernel meal on growth, feed utilization, radical scavenging activity, carcass composition and muscle quality in sex reversed Nile tilapia (*Oreochromis niloticus*). **Aquaculture** 439: 45–52.
- Wattanakul, W., Wattanakul, U., Thongprajukaew, K. and Muenpo, C. 2017. Fish condensate as effective replacer of fish meal protein for striped snakehead, *Channa striata* (Bloch). **Fish Physiology and Biochemistry** 43: 217–228.
- Yue, Y. and Zhou, Q. 2008. Effect of replacing soybean meal with cottonseed meal on growth, feed utilization, and hematological indexes for juvenile hybrid tilapia, *Oreochromis niloticus* × *O. aureus*. **Aquaculture** 284: 185–189.

Gamat (*Stichopushorrens*) Pickling with Different Sugar Media and Addition into Rice Porridge

Chutinut Sujarit^{1*}, and Luksamee Vittaya²

ABSTRACT

This study aimed to examine the effect of sugar pickling on the chemical characteristics of Gamat (*Stichopushorrens*) and to apply the pickled gamat as a food ingredient in instant rice porridge. Dried gamat was composed of 7.79%, 2.15%, 30.06% and 11.04% of protein, fat, ash and water, respectively. The amino acids present in the highest proportions were glycine and glutamic acid, at 8.63% and 7.85% by weight, respectively. Fresh gamat was pickled for three months in three sugar media namely, bee honey, palm syrup and sugar cane syrup. The results showed that bee honey was the best sugar source; post-pickled gamat became more transparent and the total sugar content in the pickled product was 61% w/w. The chemical composition by weight of pickled gamat that had used bee honey as the sugar source was 37.76%, 2.53%, 12.61% and 0.44% of water, ash, protein and fat, respectively. Honey-pickled gamat was applied as an ingredient in brown-rice porridge. The Formula II, containing 6% of dried pickled gamat, had the highest score for acceptance according to the 9-point hedonic scale, conducted on 30 customers, and the total score was significantly higher than the other formulas, at the statistical significance of $P \leq 0.05$. Regarding to the acceptance score, Formula II earned the sensory score of “like very much”.

Keywords: Sea cucumber, Sugar-pickling, Rice porridge

¹ Department of Food Industry and Fisheries Production, Faculty of Science and Fisheries Technology, Rajamanagala University of Technology Srivijaya, Trang, Thailand 92150

² Department of Physical, Faculty of Science and Fisheries Technology, Rajamanagala University of Technology Srivijaya, Trang, Thailand 92150

*Corresponding author, e-mail : s.chutinut58@gmail.com

Introduction

Gamat is a common name for the golden sea cucumber (*Stichopus horrens* Selenka, 1867), a marine invertebrate of the phylum Echinodermata. Other members of this phylum include sea star, feather star and sea urchin. Gamat is commonly found in deep seas across the coasts of the Andaman Sea in Malaysia and the Thai provinces of Phuket, Krabi, Trang, and Satun. Apart from the 70-89% of water content, the flesh of gamat consists of 10-12% protein and 0.002-0.04% fat, along with several natural chemicals including chondroitin sulfuric acid, a type of mucoprotein which promotes muscular function, and holotoxin (or holothurin), a biochemical which has been traditionally used for its antifungal and anticancer properties (Somchun, 2012). Gamat flesh is widely accepted as a folk remedy by Chinese traditional medicine (Sangjindawong, 1980). However, the flesh of gamat harbors several kinds of micro-organisms, leading to rapidly flesh decay after taken out of the water (Palomares and Pauly, 2017). Boiling is not recommended preservation for gamat flesh due to the texture damage and flesh loss (Li, 2004). Preferably, gamat is preserved in bee honey or distilled spirits after removing of the internal organs through incision on the ventral site (Li, 2004). Cured gamat products are renowned for their medical properties such as reducing the symptoms of aging-associated diseases, diabetes, paralysis, wound healing and anti-hypertension (Bussarawich and Thongthaem, 2000; Forghani *et al.*, 2012). In addition, gamat flesh has been utilized in a number of folk medicine traditions as an ingredient in several foods and remedies. However, there has been little scientific study on the use of gamat.

According to the folk medicine traditions, the method of preparation and pickling in this experiment is suitable for prolonging gamat shelf life; the products were remained suitable as a food or remedy for aches, stiffness and fatigue. Dried gamat was initially prepared by washing in filtrated sea water, and incisions were made to remove the innards. However, according to the method proposed by Xing *et al.* (2012), sea cucumber was rewashed in sea water before being boiled in clean water. The boiled sea cucumber was roasted with a charcoal grill until it was completely dried. Regarding to the local traders who sell sea cucumber to Chinese buyers, dried sea cucumber can be stored for as long as one year. After drying on the charcoal grill, the sea cucumber required sun drying. By this series of methods, the sea cucumber was shrunk. Its weight was reduced to one tenth of its original weight, which contradicted the results reported by Li (2004). The fresh weight to dry weight ratio ranged from 27:1 to 20:1. The dried sea cucumber was rather sticky and had a marine scent.

It would be useful to examine the change on chemical characteristics of gamat during preservation and use the preserved gamat as a food ingredient.

Materials and Methods

Gamats were collected from Ko Poo, Ko Si Boya Subdistrict, Nuea Khlong District, Krabi Province. The body of gamat was 16 cm. and weighed 149 g. by average.

Based on the traditional practice, harvested gamats were thoroughly washed with filtrated sea water, and then the internal organs were removed. The body was sliced into pieces of 2x4 cm, for further used in the next experiment.

The dried samples were sent to the Central Laboratory (Thailand) in Hat Yai District, Songkla Province, for examination of essential nutrient content based on the full nutrition information required by the Food and Drug Administration (FDA), including protein, fat, calcium, cholesterol, and vitamin A, B1 and B2. Amino acid analysis was conducted in the Central Instrument Facility (CIF), Faculty of Science, Mahidol University.

Gamat pickling in different sugar media

The sliced gamat fresh (110 g) was put in a glass jar (25 x 10 x 10 cm) and was immersed in 200 ml of sugar medium at room temperature for three month (Li, 2004).

After three months of pickling, the total sugar, in gamat sample, was measured and the gamat texture was evaluated as well. The pickled gamat with the highest sugar content was selected for further experiment.

The experiment was conducted using Completely Randomized Design (CRD). Data were tested by one way analysis of variance (ANOVA) and means were compared using Duncans Multiple Range Test (DMRT).

Gamat utilization as food ingredient

Gamat sample chosen from the result of the best sugar medium was utilized as food addition of instance rice porridge. Before utilization, the gamat was dried in 60°C for 24 hr and then was further sliced into cubes of 0.5x0.5x0.5 cm.

The instant rice porridge was prepared according to the method of Rueangthip (2001). Basic ingredients of rice porridge comprised of 300 g rice, 50 g dried green onion leaf, 70 g dried carrot and 70 g dried ginger. Dried gamat was added to the rice porridge at the rate of 3, 6 and 9 gram which were designed as the formula I, II and III, respectively.

Two main ingredients, rice and vegetable, were prepared separately. Rice was washed 2-3 times and soaked in water for two hours. The fully-saturated rice was rewashed 2-3 times and boiled into porridge. The water was drained from the porridge through a sieve and the porridge was evenly spread on a tray and frozen at -25 °C for two hours. The frozen porridge was thawed at room temperature, re-spread, baked in a hot air oven at 90 °C for nine hours and ground into powder. Fresh onion leaf, carrot, and ginger were cleaned and sliced into 0.3 cm length pieces. Each vegetable was boiled for 1 min, immediately cooled down and drained on a sieve. The vegetables were spread on a tray, frozen at -20 °C for two hours and baked in a hot air oven at 90 °C for three hours.

The porridge was prepared by adding 150 ml water to premixed instance rice (1:5 w/v). To ensure uniform dispersion, the mixtures were thoroughly stirring for 5-10 min was required.

The sensory analysis was evaluated using the “9-Point hedonic scale” basis, based on color, appearance, odor, taste, and texture. Thirty well-trained panelists were selected for the sensory analysis.

The experiment was conducted according to CRD design, with three replications. Data was analyzed by ANOVA and means were compared by DMRT.

Results and Discussion

Biology of gamat and nutritional value

The result of proximate analysis showed that, the protein, fat, ash and moisture contents of dried gamat were 7.79%, 2.15%, 30.06% and 11.04%, respectively. The analysis also indicated that the calcium and iron content of gamat was considerably high (1,870 and 9.98 mg/100g, respectively). Additionally dried gamat contained high sodium content (4,390 mg/100 g) as well. Protein content of gamat in this study was found to be comparable to the results reported by Bordbar *et al.* (2011), who showed that the fresh sea cucumber contained 10-12% of protein, 70-80% of moisture and 0.002-0.04% of fat on a weight basis. Moreover, Pangestuti and Arifin (2017) also reported that the protein content in sea cucumbers was found up to 64%. Hence gamat flesh provided high protein and very low fat content.

Dried gamat in this study contained 14 amino acids; six of these amino acids, threonine, leucine, valine, lysine, isoleucine and histidine, were essential. Glycine was present in the

highest proportion (8.63 mg per 100 mg of protein) followed by Glutamic acid (7.85 mg per 100 mg of protein). Among the essential amino acids, threonine was present in the highest amounts (2.48 mg per 100 mg of protein), followed by leucine (2.04 mg per 100 mg of protein). These findings were similar to the study reported by Widianingsih *et al.* (2016). Glycine is an amino acid that serves as a remedy for the treatment of underactive hypothalamus, muscular atrophy, and hypoglycaemia. Glutamic acid is neuro-transmitters in the central nervous system (Szpak, 2011) and is recently used in anticancer treatment (Dutta *et al.*, 2003). Threonine is one of the precursors for glycine synthesis (Razak *et al.*, 2017).

Comparison of the chemical compositions of fresh gamat and honey-pickled gamat showed that they differ in various aspects. The composition of the gamat flesh was comparable to the results reported by Sangjindawong (1980), which found that the flesh contained upto 84% moisture, as well as a higher level of protein (6.6%) and fat (1.7%).

The gamat pickling study showed that bee honey was the best pickling medium for gamat preservation. Bee honey was thoroughly absorbed by the gamat flesh and produced a jelly-like body, as described in Table 1. In this study gamat picked in natural honey bee was jelly-like and full of honey which was considered as the best texture. Whereas gamat pickled in palm syrup was swollen due to water absorption and gamat pickled in sugar cane syrup was remained unchanged. Although, after three months of pickling, the honey had become less thick and the color of the gamat was changed from its natural brown color into white or pale yellow. According to folk traditions, however, gamat at this stage is ready to be consumed as uncooked form either a remedy or a cosmetic.

Table 1 Chemical components found in gamat samples at different stages of pickling and with different media

Crude extracts	Nutritional value ^{1/} (% w/w)				
	Moisture	Ash	Protein	Fat	Total Sugar
- Honey Gamat	37.76±0.17 ^b	2.53±0.06 ^b	12.61±0.44 ^a	0.44±0.06 ^a	61
- Cane syrup Gamat	51.42±0.55 ^b	5.85±0.37 ^a	12.87±0.30 ^a	0.53±0.10 ^a	34
- Palm syrup Gamat	57.93±0.77 ^b	3.16±0.07 ^b	9.03±0.22 ^b	0.50±0.01 ^a	40

^{1/}Values shown in the same column with different small letter superscripts are significantly different ($P \leq 0.05$)

The chemical compositions of gamat at the beginning and after pickling in three different sugar media are indicated in Table 1. All three types of sugar resulted in significantly reduced moisture and ash content and increased protein content, while the fat content was unaffected to any significant degree. Bee honey was absorbed into gamat and reduced the moisture content to 37.76% and the ash content to 2.53%, while the protein content was increased to 12.61% w/w. In comparison, the moisture content of the samples pickled in cane syrup and palm syrup was reduced to 51.42% and 57.93% respectively.

Application of sugar-preserved gamat as a food ingredient

Honey-pickled gamat was utilized as a food ingredient in instant rice porridge. Porridge was prepared following three formulas. The proximate compositions of all three rice porridge formulas were 13.20% protein, 0.85% fat, 0.90% ash and 79.05% moisture, respectively.

Table 2. Sensory paneling scores of three gamat instant rice porridge formulas

Sensory Paneling Category	Score ¹		
	Formula I	Formula II	Formula III
Color	7.53±0.57 ^a	7.97±0.32 ^a	7.93±0.58 ^a
Odor	7.57±0.50 ^a	8.20±0.41 ^b	8.10±0.48 ^b
Taste	7.00±0.64 ^a	8.63±0.49 ^c	7.70±0.75 ^b
Texture	7.17±0.38 ^a	8.37±0.56 ^b	7.83±0.59 ^a
Overall acceptance score	7.00±0.53 ^a	8.63±0.49 ^b	7.83±0.53 ^a

¹/Values shown in the same row with different small letter superscripts are significantly different ($P \leq 0.05$)

The sensory panelling scores of three rice porridge formulas are shown in Table 2. The results of panelling test for color were not significantly different among three rice porridge formulas, while the odor and taste scores of formula II and formula III were significantly higher than that of formula I ($p < 0.05$). For the texture and overall acceptance score, the formula II had the highest scores ($p < 0.05$).

The instant porridge composed of roasted ground rice which was highly capable of water absorption (Office of Agricultural Research and Development, 2003; Thai Industrial Standards Institute, 2004). The property of dried rice enabled the porridge to be miscible with dried cured gamat flesh. Together with dried green onion leaf, carrot and ginger, the porridge scent and aroma was improved (Yai-eiam, *et al.*, 2010). The three formulas used the same weight ratio for almost all of the ingredients, with the exception of the gamat flesh.

However, the total acceptance score was considered “moderate”. Formula I received the lowest total acceptance score of the three. These results indicated that consumers would prefer the formula II to the other two formulas, owing to gamat improving food flavor. The food combinations affected the total acceptance score, similar to the results reported by Lim (2011) and Bastian (2015).

Acknowledgement

This research was financially supported by Rajamangala University of Technology Srivijaya.

References

- Bastian, M. 2015. **Effects of Panelist Participation Frequency and Questionnaire Design on Overall Acceptance Scoring for Food Sensory Evaluation in Consumer Central Location Test**. Available Source: <https://scholarsarchive.byu.edu/etd/4446>, January 23, 2018.
- Busarawich, S. and Thongthaem, N. 2000. Fishery and trade of sea cucumbers in Thailand. **Thai Fisheries Gazette** 53(2): 161-168.
- Dutta, S., Ray, S. and Nagarajanc, K. 2013. Glutamic acid as anticancer agent: An overview. **Saudi Pharmaceutical Journal** 21(4): 337–343.

- Forghani, B., Ebrahimpour, A., Bakar, J., Hamid, AA., Hassan, Z. and Saari, N. 2012. Enzyme hydrolysates from *Stichopus horrens* as a new source for angiotensin-converting enzyme inhibitory peptides. **Evidence-Based Complementary and Alternative Medicine**. Article ID 236384, 9 p.
- Li, X.M. 2004. **Fishery and resource management of tropical sea cucumbers in the islands of South China Sea**. Advances in Sea Cucumber Aquaculture and Management. Vol 463, pp 261-5, by FAO Corporate Document Repository.
- Lim, J. 2011. Hedonic scaling: A review of methods and theory. **Food Quality and Preference** 22: 733-747.
- Office of Agricultural Research and Development. 2003. **History of Rice**. Available Source: <http://www.arda.or.th/kasetinfo/rice/rice-histories.html#HisThai>, April 22, 2016,
- Palomares, M.L.D. and Pauly, D. 2017. **Sea Life Base**. World Wide Web electronic publication. Available Source: www.sealifebase.org, version (10/2017).
- Pangestuti, R. and Arifin, Z. 2017. Medicinal and health benefit effects of functional sea cucumbers. **Journal of Traditional and Complementary Medicine**. In Press.
- Razak, M.A., Begum, P.S., Viswanath, B. and Rajagopal, S. 2017. Multifarious Beneficial Effect of Nonessential Amino Acid, Glycine: A Review. **Oxidative Medicine Cell and Longevity**, Article ID1716701,8p. doi: 10.1155/2017/1716701.
- Ruangthip, N. 2001. Development of Tuna Precooked Rice Porridge. MS Thesis, Department of Fishery Products, Faculty of Fisheries, Kasetsart University. 103 p.
- Sangjindawong, M. 1980. Sea cucumber of Thailand. **Thai Fisheries Gazette** 33: (1). 25-32.
- Somchun, C. 2012. **Research on Gamat cell division**. Available Source: www.thairath.co.th., November 12, 2015.
- Szpak, P. 2011. Fish bone chemistry and ultrastructure: Implications for taphonomy and stable isotope analysis. **Journal of Archaeological Science** 38(12): 3358-3372.
- Thai Industrial Standards Institute. 2004. **Thai Community Product Standards: Instant Husked Rice Porridge**. (TCPS Number 689/2547).
- Widianingsiha, Zaenurib, M., Anggorob, S. and Kusumaningrum, H.P.S. 2016. Nutritional Value of Sea Cucumber [*Paracaudina australis* (Semper, 1868)]. **Aquatic Procedia** 7: 271-276.
- Xing, K., Liu, SL., Yang, HS., Zhang, MZ. and Zhou, Y. 2012. Southward transplanted cage-culture of sea cucumbers *Apostichopus japonicus* in China's Shensi Islands. **SPC Beche-de-mer Information Bulletin** 32: 33-38.
- Yai-eiam, S., Teangpook, S., Wirivutthikorn, W. and Siripanporn, J. 2010. Development of Instant Brown Fragrance Rice Porridge. Institute of Food Research and Product Development, Kasetsart University. Available Source: <http://anchan.lib.ku.ac.th/agnet/handle/001/5124>.

The Use of Boiled Liquid Waste as an Ingredient for Crab Sauce

Chutinut Sujarit^{1*}, Akhom Khatfan² and Amornrat Aungaudchariya²

ABSTRACT

Blue swimming crab (*Portunus armatus* Linn) provides a major source of crab meat. The meat is exported mostly in the form of frozen and canned products providing up to US\$ 80 million per year. In the process of meat separation from its shell and skeleton a large amount of boiled liquid becomes liquid waste required an appropriate treatment before releasing into environment, unless it can be utilized. The research was proposed of a fully utilization on the waste of crab products and turn it into a high value product for use as appetizer or food seasonings. Proximate analysis showed that the boiled liquid waste composed of 96.68% moisture, 3.06% ash, 1.12% protein and 0.13% fat content. The processing of blue swimming crab was started by concentrating the boiled liquid waste at 50 °C until the liquid was concentrated into 30 °brix. The condensed liquid was further utilized as an ingredient in commercial oyster sauce; three formulas were proposed. Formula I was found to be the most appropriate for crab sauce production and comprised of 44.21% crab broth, 37.41% oyster sauce, 6.80% cane sugar, 2.72% modified starch, 1.36% monosodium glutamate, 0.68% powdered chili and 6.80% water. Sensory paneling of consumer acceptability was found no statistically significant differences ($p \geq 0.05$) for three formulas. Proximate analysis of this crab product revealed that the overall compositions were 45.44% moisture, 15.29% ash, 1.28% protein and 0.34% fat. An examination of shelf life revealed that during 5-week storage, its overall quality still met the standard requirement of Thai Standard of Community's Product No. 1016/2548 (oyster sauce product).

Keywords: Agro-industrial waste, Waste utilization, Crab sauce, *Portunus armatus*

¹ Department of Food Industry and Fisheries Production, Faculty of Science and Fisheries Technology, Rajamangala University of Technology Srivijaya, Trang, Thailand 92150

² Department of Biological Science, Faculty of Faculty of Science and Fisheries Technology, Rajamangala University of Technology Srivijaya, Trang, Thailand 92150

*Corresponding author, e-mail : s.chutinut58@gmail.com

Introduction

Among Thai seafood, Blue Swimming crab (*Portunus armatus* Linn., 1758) is one of the most popular and widely consumed. Hence, the Blue Swimming crab is generally regarded as an economically important product for Thailand. It has been utilized as a raw material in food industry for more than 20 years, especially canned products. As 2004, the total export of the product was about 34,400 tonnes which was calculated to approximately US\$ 21.2 million (Songrak and Watcharintarachai, 2006). It is clearly that demand for blue swimming crab products in both domestic and international markets is increasing. The domestic market consists of many markets at various levels, from smaller, local markets with high raw material availability to larger and more distant markets. These markets include village markets, local district markets, and provincial and regional markets. Local and provincial aquatic animal markets play important roles as they act as a starting point for the purchase and transfer of raw materials from various aquacultural ponds to consumers and seafood processing factories. Various blue swimming crab products are available in domestic markets, such as fresh chilled crab, fresh iced crab, live crab, molted shell crab and ready-to-cook crab meat.

Now a day, the numbers of blue swimming crab and other crab are steadily increasing due to successfully implemented conservation programs. A particularly important conservation program has been the establishment of blue swimming crab banks, which have been established in various local areas in order to achieve rehabilitation and conservation objectives for mangrove forest and aquatic species. In addition to the sustainable conservation of mangrove and aquatic species, crab banks have also resulted in enhanced community food productivity, enhanced community resource self-reliance and the increased generation of income by villages and communities. All of the benefits mentioned above are critical for the creation of sustainable communities, as they contribute to a community's food security and create immunity against extreme economic changes such as internationally repercussive financial crises.

The community's crab bank played an essential role of blue swimming crab replenishment. Newly-bred crabs would be hatched, from crab eggs acquired from female crabs carrying fertilized eggs. The female crab, carrying fertilized eggs, is indicated by grayish sponge-like body attached to her abdomen. Eggs were acquired, from female crabs as described above, and were incubated in 30-liter tanks containing 20 liters of water. An aerator was required to be installed in each tank, to supply oxygen from air into water. Oxygenation by this method could promote larva hatching from eggs; the crab larva hatching rate was higher in a tank with aeration than a tank without aeration. Within two days, crab eggs turned from greyish black oval shaped into tiny louse-like larvae. Crab larvae lived on their yolk sacs which rapidly depleted; hence crab larvae would require to be released into natural water within eight hours after hatching, before their nutrient in yoke sac completely used up. Few days after hatching, crab larvae turned into zoea which gradually grown, along with several molting. The zoea eventually develops into mature crab.

The blue swimming crab bank in Songkhla serves as an example of how fishermen and farmers benefit from their contributions to the community crab bank. The blue swimming crab bank features many activities, such as releasing blue swimming crabs into their natural environment, crab catching and selling as a way for community residents to earn a living, and preliminary processing of crabs prior to their sale to food manufacturing plants.

During the crab processing, a huge amount of boiled water is utilized and released as liquid waste which required to be treated with appropriate methods before releasing into natural water. Treating waste water required larger area, much more resources and power consumption than utilization of the waste water as a newly precursor in food industry. Therefore, our research

staff was interested in making use of this liquid waste by converting it into usable, value-added products as an alternative way to generate income within communities.

Materials and methods

1. Raw materials for preparation of crab sauce using blue swimming crab boiled waste

Boiled extracted waste was kindly donated by the Crab Hatchery Learning Centre of Hua Kao Sub-district, Singhanakorn District, Songkhla Province, in the southern region of Thailand.

Ingredients for preparing crab sauce were as follows: commercial oyster sauce, cane sugar, refined starch, monosodium glutamate, powdered chilli and water.

2. Methods

2.1 Preliminary analysis of blue swimming crab boiled waste water

The boiled water waste acquired from the Crab Hatchery Learning Centre of Hua Kao Sub-district was chemically analysed for its moisture, ash, protein and fat content by the methods described by the AOAC Official Methods of Analysis (2000).

2.2 Preparation of the crab sauce

Boiled waste water of blue swimming crab was poured into vessels and was condensed by water-evaporation at a constant temperature of 50 °C until the liquid concentration reached 30°Brix of sugar. Evaporated liquid was used as an ingredient of crab sauce, as indicated in Table 1.

Table 1 Formula for crab sauce production from boiled water concentrates

Ingredients (%)	Formula		
	1	2	3
Evaporated crab waste	65	75	85
Commercial sauce	55	55	55
Cane sugar	10	10	10
Modified starch	4	4	4
Monosodium glutamate	2	2	2
Powdered chilli	1	1	1
Water	10	10	10

Formulas were scored by means of sensory paneling based on a 9-point hedonic scale in terms of appearance, colour, flavour and overall acceptability using 30 trained panelists.

2.3 A nutritional evaluation of crab sauce manufactured from boiled liquid waste concentrate

2.3.1 Nutritional values

The formula, of which earned the highest paneling score (in Section 2.2), was further inspected for the nutrition values such as moisture, ash, protein and fat content, using the methods provided by AOAC (2000). The pH was also evaluated by pH meter.

2.3.2 Microbiological examination

The crab sauce with the highest paneling score was packed in 200-ml bottles and kept in ambient temperature, while waiting for microbiological evaluation. Total colony counts of bacteria, yeast and mould were carried out every week for five weeks (weeks 0, 1, 2, 3, 4 and 5) using the method indicated by AOAC (2000).

2.4 Investigation of production costs of crab sauce made from blue swimming crab boiled liquid waste concentrate

Preliminary production costs were calculated based only on the cost of raw materials and the total costs were evaluated by summation of all calculable material prices.

Results and Discussion

1. Qualities and composition of boiled liquid waste from blue swimming crab

Boiled waste water extracted from the processing of blue swimming crab, provided by the Crab Hatchery Learning Centre of Hua Kao Sub-district, was slightly brownish with a fishy odor as typical crab meat. The process of crab boiling was initiated by putting the whole bodies of washed blue swimming crab into a boiling vessel using an equal proportion of crab to water (1:1, w/w) at 150 °C for 15 min. The proximate analysis of boiled crab liquid is shown in Table 2.

The boiled water was analysed in terms of moisture, ash, protein and fat content. It was found to consist of 96.68 % moisture, 3.06% ash, 1.12% protein and 0.13% fat content. These figures corresponded to the results of Pornchaloempong and Rattanapanont (2010), who reported that the chemical composition of general aquatic waste comprised 74.6% moisture, 1.6% ash, 19.8% protein, 4.0% fat and no carbohydrate detected.

Table 2 Proximate chemical constituents of boiled liquid waste from blue swimming crab

Constituents	Contents (%)
Moisture	96.68 ± 0.02
Ash	3.06 ± 0.35
Protein	1.12 ± 0.02
Fat	0.13 ± 0.06

2. Acceptant score of crab sauces

Sauce products from boiled liquid waste of blue swimming crab were manufactured by concentrating boiled liquid waste by evaporation at a constant temperature of 50 °C until a final concentration of 30°Brix was achieved. This solution was incorporated into three different formulas and organoleptically evaluated using a 9-point hedonic scale by 30 trained panelists in terms of color, odor, flavor, appearance and overall acceptability. Results of sensory evaluation are presented in Table 3.

Table 3 Sensory evaluation scores of 3 different formulations of crab sauce made from boiled liquid waste concentrate.

Qualities	Sensory Scores		
	Formulation 1	Formulation 2	Formulation 3
Colour	8.16 ^b	7.90 ^a	7.73 ^a
Odour	8.10 ^a	7.93 ^b	7.56 ^a
Flavour	8.16 ^a	7.90 ^b	7.30 ^a
Appearance	8.40 ^{NS}	7.80 ^{NS}	7.80 ^{NS}
Overall acceptance	8.15 ^b	7.90 ^b	7.36 ^a

Note: different letters in the same column indicate statistically significant difference ($P < 0.05$)

Colour score evaluation

It was found that the average colour scores of sauce produced from boiled liquid waste concentrate fell into the range of moderate to high acceptability (7.73-8.16). The formula of which earned the maximum colour score was the formula I (8.16), with a statistically significant difference ($P>0.05$) from the other two formulas. Colour scores of formula II (7.90) and III (7.73) did not show a statistically significant difference ($P>0.05$). However those two scores were considered as “moderate” acceptable.

Odour score

The average odour scores of crab sauce produces ranged from moderate to high acceptability (7.56-8.10). The formula I was the highest (8.10) of three; however the score was not different to the other two, the formula II and III, indicating by the significant notation higher than 0.05 ($P>0.05$). The formula I was considered the high acceptant, whereas the formula II (7.93) and III (7.56) were considered moderately acceptable.

Flavor score

Based on the flavour scores, crab sauce produces were considered moderate to high acceptable (7.30-8.16). The formula I got the highest of three (8.16), but the score did not show a statistically significant difference ($P>0.05$) to the formula II's score which was 7.90.

Overall acceptance score

It was found that overall acceptance score fell into the range of moderate to high acceptability (7.36-8.15). The overall acceptance score of formula I was the highest (8.15) of the three formulations, and it had no statistically significant difference ($P<0.05$) compared to the overall acceptance score of formula II (7.90). However, the overall acceptance score of formula III (7.36) was significantly different ($P<0.05$).

This investigation of blue swimming crab sauce manufactured with boiled liquid waste concentrate, using a modification of the publicly available oyster sauce formulation that is generally used as a fundamental formula for commercially manufactured sauce, clearly demonstrated that all three formulations resulted in a brownish viscous and homogeneous texture property without the occurrence of syneresis or too thick or too thin a texture. The 9-scale hedonic sensory evaluation, using 30 trained panelists, revealed that the colour, odour, flavour, appearance and overall acceptability of the sauce were consistent and conformed to Community Product Standard No. 1016/2005. The most acceptable formulation was formula I, as shown in Table 4. The formula I would be used in further experiment.

3. Nutritional values of blue swimming crab sauce made from boiled liquid waste concentrate

3.1 Nutritional values of crab sauce made from boiled liquid waste concentrate

The nutritional values of blue swimming crab sauce made from boiled liquid waste concentrate were investigated by analysis of moisture, ash, protein and fat content (AOAC, 2000). The results are shown in Table 4.

Table 4 Proximate analysis of crab sauce made from boiled liquid waste concentrate

Components	Contents (%)
Moisture	45.44 ± 0.30
Ash	15.29 ± 0.09
Protein	1.28 ± 0.02
Fat	0.34 ± 0.03

The nutritional values of crab sauce, using condensed liquid waste of blue swimming crab, are indicated in table 3. Its moisture, ash, protein and fat content were 45.44, 15.29, 1.28, and 0.34%, consecutively. The chemical components were similar to the report of Yeneng (2001), who studied on shrimp sauce. In his report, shrimp sauce was made by using condensed liquid waste from boiled shrimp; its ash and fat content were reported to be 6.29% and 0.03% respectively. However, the physical and chemical properties of crab sauce, produced from blue swimming crab liquid waste, indicated that the produced was considered acceptable according to The Community Product Standard No. 1016/2005.

3.2 Microbiological changes during storage

Crab sauce formula III was packed in 250-ml bags and kept at room temperature for five weeks, with sampling for quality checks performed at weeks 0, 1, 2, 3, 4 and 5. Microbiological evaluations were Total Bacteria Count(TBC) and Total Yeast Mold Count (TYMC); the examination results are presented in Table 5.

Table 5 Microbiological changes during 5-week storage at room temperature

Storage period (weeks)	Microbiological parameters	
	TBC (CFU/g)	TYMC (CFU/g)
0	< 30	< 10
1	< 30	< 10
2	< 30	< 10
3	< 30	< 10
4	< 30	< 10
5	960	< 10

Four week of storage at room temperature, TBC and TYMC were constant at <30 and <10/g, respectively. However in the fifth week, TBC abruptly rose to 960 CFU/g, while TYMC remained less than 10 CFU/g, indicating that the crab sauce product was able to be kept at room temperature for at least four weeks and crab sauce was considered “acceptable” regarding to Community Product Standard No. 1016/2005. The results were similar to those reported by Wannaphuak (2015) who studied in shrimp sauce storage at room temperature; the TBC were less than 3 CFU/g on the first three weeks and TBC rose into 685 and 776 CFU/g on the following weeks. The TYMC was also less than 10 CFU/g. during five-weeks of storage. In addition, sensory acceptability of shrimp sauce was still acceptable as the product was kept in the room temperature for 10 weeks.

3.3 pH

The pH of crab sauce, made from blue swimming crab liquid waste, was similar to the commercial oyster sauce which was stable at 6.7 as well. Therefore, based on pH, the crab sauce product was still at the acceptable value according to Community Product Standard No. 1016/2005, which states that the optimal pH of commercial oyster sauce and related products ought to be in the range of 6.5-7.5 (Ueprasertsak, 1996).

4. Proximate cost of production for crab sauce from crab liquid waste

Cost of production was evaluated based only on the raw materials at the time. Price of individual raw material used for making crab sauce from boiled liquid waste was listed in table 6, as the product was sold in a 150 ml-bottle.

Table 6 Preliminary cost of production for crab sauce made from boiled liquid waste

Constituents	Cost (baht/g)	Cost per Unit	Quantities (g)	Cost/bottle (Thai-baht)
Boiled liquid waste	-	-	65	-
Commercial sauce	23 baht/200 ml	0.11	55	6.32
Cane sugar	28 baht/1000 g	0.02	10	0.28
Modified starch	48 baht/1000 g	0.04	4	0.19
Monosodium glutamate	10 baht/85 g	0.11	2	0.23
Powdered chilli	27 baht/50 g	0.54	1	0.54
Water	-	-	10	-
Total				7.56

Consequently, the proximate production cost for a 150 ml-bottle of crab sauce, made from boiled liquid waste, was 7.56 baht, which 1.24 baht /bottle was added up by using crab liquid waste. As the boiled liquid waste, used in the production process was free of charge as it was considered as waste, and therefore did not contribute to the cost. Moreover, the crab sauce was much cheaper when compared to the original oyster sauce of the same volume (150 ml) which was about 17.24 baht.

Conclusion

1. The proximate analysis of boiled liquid waste, from boiling blue swimming crab, prior to be concentrated to 30 °Brix, were 96.68% moisture, 3.06% ash, 1.12% protein and 0.13% fat.

2. The waste was concentrated to 30°Brix and was utilized as an ingredient to crab sauce, a new product proposed in this experiment. The formula I was the most accepted and composed of 44.21% concentrated waste, 37.41% commercial sauce, 6.80% cane sugar, 2.72% modified starch, 1.36% monosodium glutamate, 0.68% powdered chili and 6.80% water. The product acceptance scores were considered “acceptable” regarding to the Community Product Standard No. 1016/2005.

3. Crab sauce, made from concentrated liquid waste, was further evaluated for chemical compositions and microbial assessment. The result shows it composed of moisture, ash, protein and fat at 45.44%, 15.29%, 1.28% and 0.34%, respectively. Microbiological examination was conducted using total bacteria count (TBC) and total yeast&mold count (TYBC). TBC remained <10 CFU/g in the first-four week and was increased to 960 CFU/g in last week of storage, while the TYMC was constant at <10 CFU/g throughout the storage period. This indicated the crab sauce was qualified according to the Community Product Standard No. 1016/2005

4. Proximate evaluation for cost of production, the crab sauce, made from concentrate liquid waste, was 7.56 baht per 150 ml bottle compared to 17.24 baht per bottle for the original oyster sauce of the same volume. Therefore, this product was able to be a cheap product to make a great income for the community.

References

- A.O.A.C. 2000. **Official methods of analysis**. 17th edition. Association of Official Analytical Chemists. Arlington, VA, USA.
- Chitchuen, A. 2000. The production of seasoning sauce from sesame extracted protein. MS Thesis, Chulalongkorn University.
- Pornchaloempong, P and Rattanapanont, N. 2010 .Comparison of Chemical in Aquatic Fish. Available Source: <http://www.foodnetworksolution.com>, April 24, 2016.
- Songrak, A. and Watcharintarachai, K. 2006. **Cage culture of blue swimming crab (*Portunuspelagicus* Linnaeus, 1758) at Bathuputae village, Kholibong subdistrict, Kantang district, Trang province, Thailand**. Faculty of Science and Fisheries Technology, Trang Campus, Trang, Thailand.
- Thai Industrial Standards Institute. 2005. **Thai Community Product Standards: Oyster Sauce** (TCPS Number 1016/2548). Ministry of Industry, Bangkok, 5 p
- Ueprasertsak, R. 1996.. Development of condiment with low sodium and low sugar. MS Thesis Mahidol University
- Wannaphuak, S. 2015. **Development of Hard Clam (*Meretrixcasta*) sauce from Hard Clam water extract**. Project by Rajamangala University of Technology Srivijaya.
- WWF. 2017. **Thailand Blue Swimming Crab**. Available Source: <http://seafoodsustainability.org>, 30 June 30, 2018.
- Yeneng, S. 2001. Production of shrimp flavour sauce from shrimp cooking water. MS Thesis, Kasetsart University

Development of Shellfish Soup Enhanced with Herbs and Nutritional Value

Chompunooch Somalee^{1*} Suprewpan Lohaluksadat¹ and Sirinad Jongrak²

ABSTRACT

The purpose of this study was to development of formula of shellfish soup enhanced with herbs and study the nutritional value of shellfish soup products. The results of the development of soup product from 3 formula of soup stocks; fish stock, chicken stock and vegetable stock. Found that the consumers have accepted the most was the vegetable stock with the score 8.53 ± 0.91 . The results on the acceptability of stock to shellfish species were 3 types; hard clam (*Meretrix casta*), bicolored pinna and mussel. Sensory evaluation of consumers test were accepted of vegetable stock to hard clam with score 8.16 ± 1.20 . The study of quantities of herbs used in soup products which were galangal, lemongrass, basil leaves and onion were 2, 4, 6, 8 percent of soup. The results showed that the total of herbs enhanced in the product was acceptable at 6 percent. The results of nutritional value of the shellfish soup products found that contained the total energy (k.cal) 10.69, energy of fat (k.cal) 0.09, carbohydrates (grams) 1.86 , protein (grams) (%Nx6.25) 0.79 , total fat (grams) 0.01 , cholesterol (mg) 0.99, sugar (grams) 1.74 , vitamin B2 (mg) 0.15 , sodium (mg) 189.35, calcium (mg) 0.47 , moisture (grams) 96.60 , ash (grams) 0.74 per 100 ml.

Keywords: Shellfish-soup, Herbs , Shellfish, Nutritional value of soup

¹ Department of Food Industry and Fishery Product, Faculty of Science and Fishery Technology , Rajamangala University of Technology Srivijaya, Sikao, Trang. 92150 Thailand

² Community Enterprise Ban Pak-klong. M9 Bohin, Sikao, Trang. 92150 Thailand

* Corresponding author, e-mail : so_chompunooch@hotmail.com

Introduction

Many types of shellfish can be eaten and they also have different tastes, odor and flavor. There are about 50 species of shellfish found in the coastline provinces. They are divided into two groups. The first group is the commercial shellfish that is intensively farmed for high yield. They can also be found in medium-sized and large-sized fisheries. The second group is natural shellfish collected by local people in the areas. They are for consumption in the household or for selling in the local markets and the seafood restaurants. There are seven species of shellfish that are for eating; cockle, mussel, oyster, spotted babylon snail, abalone, razor clam, and horse mussel. Each species has a different nutrient. 100 grams of shellfish meat contain protein 6.9-22.3 grams, carbohydrate 0.8-6.1 grams, total fat 0.4-1.4 grams, and calcium 15-98 milligrams. Mussels contain a lot of minerals needed for our bodies such as Vitamin B 1, 2, 3, 4, 5, 6 and 12 which help prevent many diseases such as anemia, numbness and peripheral neuropathies to not make us feel weak. They also help cope with stress, help with blood circulation and relieve arthritis symptoms (ASTV,2015). Bicoloured pinna shell (Chalemwat, 2011) said this type of shellfish is popular for cooking various types of delicious sweet taste. *Meretrix casta* found on the Andaman coast. Samut Songkhram, Chon Buri, shellfish is a good seafood.

Soup is a type of food that has more water than meat and meant to be the first appetizer before eating the main dish. Soup plays an important role in health, making the body healthy, not fatigue, nutrient absorption system. The digestive tract better keep warm. (Janvikul, 2013). It can make us strong and may help prevent us from feeling tired or exhausted. Food absorption system and digestion in the body will function better. However, the way to make the soup more delicious is not only the time spent on simmering, but also choosing the raw materials which will be put together in the soup. (Suvanbol, 1981) said that about stock; There are many stocks example stocks from chicken bones; from beef; from fish and made of vegetables. Nowadays, many people in the family have changed their way of life because they have to go out and work against the time in order to get more money. They don't have time to make the soup and care of themselves. Ready to eat foods are popular options for the people nowadays.

Study the formula of shellfish soup products enhanced with herbs to be accepted by the consumers. The development of shellfish soup is one ways to bring natural shellfish which have nutrition and easy to find in community, to make shellfish soup products and enhance with herbs. These are healthy products for consumers who care about their health. Study the nutritional value of the shellfish soup products. Analysis of shellfish soup enhanced with herbs to know the nutritional value and may help the consumers able to select these healthy products for consumption.

Materials and Methods

1. Study the formula of shellfish soup enhanced with herbs products that are accepted by the consumers.

1.1 Raw materials preparation

Prepare 3 species meat of shellfish ; hard clam (*Meretrix casta*), bicolored pinna and mussel by rinsing them with clean water. Then boiling in water 3-7 minutes (Krasachol et al,

2010). Next, remove the meat from the shells and put it in a basket. Finally, rinse the meat in the clean water for 1-2 times and drain the water out.

1.2 Study the formula of soup stocks and select to produce for shellfish soup.

1.2.1 Study the formula of three soup stocks were fish stock, chicken stock, and vegetable stock. Then develop these stocks to have good tastes. Sensory evaluation focusing on the color, odor, taste, appearance and Total sensory and 9-point hedonic scale is used for the evaluation with 30 people in order to select the formula of a soup stock that consumers prefer and select to used with meat shellfish for produce shellfish soup further.

Fish Stock Formula (Hongvivat, 2003)

water	2	litters
fish bones (salmon)	300	grams
roughly chopped coriander	7	grams
black pepper	1	gram
garlic	25	grams
salt	3	grams
roughly chopped carrots	200	grams
onion	100	grams

Chicken Stock Formula (Hongvivat, 2003)

water	2	litters
chicken skeleton	0.5	kilogram
chopped coriander	7	grams
black pepper	1	gram
garlic	25	grams
salt	3	grams

Vegetable Stock Formula

water	2	litters
black pepper	1	gram
garlic	25	grams
salt	3	grams
roughly chopped carrots	200	grams
onion	100	grams
Bouquet garni	1	bouquet
celery	100	grams
sweet corn	300	grams
radish	150	grams

ginger	10	grams
Chinese cabbage	200	grams

1.2.2 Study the acceptance of soup stocks with each type of shellfish.

Get the shellfish meat prepared from No. 1.1 and measure the ratio at 10 g. per 100 ml of the soup stock from No. 1.2.1. Then study the acceptance of three types of shellfish; hard clam (*Meretrix casta*), bicolored pinna and mussel with the soup stocks. After that, Sensory evaluation focusing on the color, odor, taste, appearance and Total sensory and 9-point hedonic scale is used for the evaluation with 30 people in order to select the formula. Randomized Complete Block Design is used as the experiment plan and the mean scores are compared by using Duncan's New Multiple Rang Test. The data is analyzed using SPSS for Windows.

1.3 Develop the formula of shellfish soup products

Making shellfish consommé soup products from the original formula
(Adapted from http://wealthyfood.blogspot.com/2011/10/blog-post_20.html)

shellfish meat	180	grams
stock	2	cups
chopped red onion	2	tablespoons
chopped garlic	1	tablespoon
roughly chopped basil	2	tablespoons
sliced cayenne pepper	1	pepper
chopped peeled canned tomato	200	grams
tomato paste	1	tablespoon
white wine	¼	cup
olive oil	1½	tablespoons
salt	¼	teaspoon
grounded black pepper	¼	teaspoon
white sugar	¼	teaspoon

1.4 Study on quantity of herbs enhanced in shellfish soup products

The herbs used in the product are basil, lemongrass, galangal, and onion mixed together and added in the ratio of 2,4,6,8 percent of soup. Then, start making the soup by following the instruction in No.1.3 and add the mixed herbs. After that, Sensory evaluation focusing on the color, odor, taste, appearance and Total sensory and 9-point hedonic scale is used for the evaluation with 30 people in order to select the formula.

2. Analyzing the nutritional values of shellfish soup enhanced of herbs products

Collect the samples in order to analyze the nutritional values of the shellfish soup products such as the total energy, energy from fat, carbohydrates, fiber, protein, total fat, cholesterol, sugar, vitamins, sodium, calcium, iron, moisture, and ash (A.O.A.C.2016)

Results and Discussion

1. The results of the study the formula of shellfish soup enhanced with herbs products that are accepted by the consumers.

1.1 The result of the formula of soup stocks for making shellfish soup

The results of the acceptance sensory evaluation of soup stock formulas; fish stock, chicken stock, and vegetable stock were evaluated by 30 tasters as shown in Table 1.

Table 1 The results of sensory evaluation of the consumers test to 3 types of soup stock

Types of soup stock	The score of sensory acceptance				
	Color	Odor	Taste	Appearance	Total sensory
Fish	7.36 ^b ±0.65	6.36 ^b ±0.68	6.63 ^b ±0.45	6.93 ^b ±0.71	6.86 ^b ±0.63
Chicken	7.43 ^b ±0.71	7.36 ^b ±0.65	7.40 ^b ±0.74	7.33 ^a ±0.61	7.43 ^b ±0.85
Vegetable	8.60 ^a ±0.96	8.63 ^a ±0.76	8.10 ^a ±0.79	8.16 ^a ±0.78	8.53 ^a ±0.91

Remark : The mean score with the same in the vertical showed that there was non-significant ($P>0.05$)

The results of the sensory evaluation among three types of stock (Fig. 1); fish stock, chicken stock, and vegetable stocks indicated that the first stock accepted by the consumers. Total sensory of vegetable stock was score 8.53±0.91. It is because the vegetable stock had a good odor and sweet taste more than other types of stock. The appearance and color of the stock were more desirable than fish stock and chicken stock. It is because in chicken skeletons and fish bones, there were still fat ; even though, they were scalded. The second stock was chicken stock with the score 7.43±0.85. The least was fish stock with the score 6.86±0.63. In conclusion select vegetable stock for further experiment.



Fish



Chicken



Vegetable

Figure 1 Types of soup stock

1.2 The results of the acceptance the formula of soup stock with type of shellfish.

The results of the stock toward the types of shellfish were shown in Table 2-4

Table 2 The results of sensory evaluation of the consumers test to the stock with hard clam (*Meretrix casta*)

Types of stock	Score of sensory acceptance				
	Color	Odor	Taste	appearance	Total sensory
Fish	7.16 ^a ±0.73	6.83 ^b ±0.43	6.83 ^b ±0.48	6.70 ^b ±0.54	6.90 ^b ±0.69
Chicken	7.50 ^a ±0.77	7.20 ^b ±0.68	7.33 ^b ±0.71	7.36 ^{ab} ±0.56	7.36 ^{ab} ±0.56
Vegetable	8.20 ^a ±1.30	8.03 ^a ±0.91	7.90 ^a ±0.97	7.76 ^a ±1.02	8.16 ^a ±1.20

Remark : The mean score with the same in the vertical showed that there was non-significant (P>0.05)

Table 3 The results of sensory evaluation of the consumers test to the stock with bicolored pinna

Types of soup stock	Score of sensory acceptance				
	Color	Odor	Taste	appearance	Total sensory
Fish	7.26 ^a ±0.63	7.06 ^b ±0.54	7.20 ^a ±0.69	7.10 ^b ±0.68	7.00 ^b ±0.71
Chicken	7.63 ^a ±0.68	7.50 ^a ±0.62	7.56 ^a ±0.64	7.50 ^b ±0.62	7.46 ^b ±0.61
Vegetable	7.80 ^a ±0.73	7.80 ^a ±0.73	7.90 ^a ±0.77	7.93 ^a ±0.77	7.90 ^a ±0.77

Remark : The mean score with the same in the vertical showed that there was non-significant (P>0.05)

Table 4 The results of sensory evaluation of the consumers test to the stock with mussel

Types of soup stock	Score of sensory acceptance				
	Color	Odor	Taste	Appearance	Total sensory
Fish	6.80 ^c ±0.77	6.93 ^c ±0.61	6.33 ^c ±0.72	6.16 ^c ±0.59	6.26 ^c ±0.64
Chicken	7.70 ^b ±0.73	7.30 ^b ±0.69	7.40 ^b ±0.70	7.76 ^b ±0.60	7.46 ^b ±0.61
Vegetable	7.86 ^a ±0.81	7.56 ^a ±0.76	7.73 ^a ±0.71	9.00 ^a ±0.92	7.80 ^a ±0.67

Remark : The mean score with the same in the vertical showed that there was non-significant (P>0.05)

The results of meat shellfish prepared using the ratio of 10 percent of soup stock to investigate the acceptance of three types of shellfish; hard clam (*Meretrix casta*), bicolored pinna and mussel with each stock. (Fig. 2) The sensory evaluation doing the preference evaluation on the color, odor, taste, appearance and total sensory. The results found that total sensory of consumers preferred vegetable soup stock with hard clam the most with the score 8.16 ± 1.20 due to the taste of sweetness and no fishy odor of the shellfish. Moreover, the appearance including with the color and odor of the stock made it more desirable than the stock with bicolored pinna and the stock with mussel. The second acceptance of the vegetable stock was with bicolored pinna the score 7.90 ± 0.77 . It is because the stock with bicolored pinna wasn't clearer than with the hard clam. However, the tastes of the stock with bicolored pinna and stock was with hard clam were the same with the score $7.90^a \pm 0.97$ and $7.90^a \pm 0.77$ respectively. The vegetable stock with mussel was the least accepted by the consumers with the score 7.80 ± 0.67 . Although it looked the same as the stock with bicolored pinna, the fishy odor and the taste of it were not acceptable with the score $7.56^a \pm 0.76$ and $7.73^a \pm 0.71$ respectively. In conclusion, the results of the acceptance of the soup stock toward each type of shellfish indicated that most consumers preferred the soup stock with hard clam the most. Therefore, it was chosen for further experiment.



Figure 2 Types of meat shellfish

1.3 The development of shellfish soup enhanced with herbs products

The results of developing shellfish soup enhanced with herbs to soup products from the original formula (Table 5) and using herbs at the ratio of 2,4,6,8 percent of soup produced from No.1.3. Sensory evaluation was shown in Table 6.

Table 5 The ingredients and the amount of raw materials used in shellfish soup products

Ingredients	Quantity
water	1000 grams
onion	50 grams
carrot	100 grams
celery	50 grams
sweet corn	150 grams
radish	75 grams
coriander	5 grams
pounded garlic	25 grams
ginger	5 grams
black pepper	1 gram
coriander root	3.5 grams
Chinese radish	200 grams
Hard clam meat	250 grams
chopped red onion	30 grams
sliced cayenne pepper	30 grams
salt	12 grams
peeled fresh tomato	100 grams
white wine	65 grams
white sugar	8 grams

Table 6 The score of the sensory evaluation on the consumers test to the amount of herbs added in shellfish soup.

The amount of herbs	Score of sensory acceptance				
	Color	Odor	Taste	Appearance	Total sensory
2 grams	7.33 ^b ±0.71	7.66 ^b ±0.54	7.43 ^b ±0.93	7.30 ^b ±0.65	7.23 ^b ±0.77
4 grams	7.53 ^b ±0.71	7.70 ^b ±0.69	7.60 ^b ±1.00	7.60 ^a ±0.89	7.30 ^b ±0.97
6 grams	8.22 ^a ±0.89	8.32 ^a ±0.54	8.12 ^a ±0.89	7.96 ^a ±0.90	8.22 ^a ±0.80
8 grams	7.60 ^b ±0.81	7.93 ^b ±0.65	7.40 ^b ±0.71	7.30 ^b ±0.83	7.53 ^b ±0.65

Remark : The mean score with the same in the vertical showed that there was non-significant (P>0.05)

The result of the sensory evaluation test on the consumers to the amount of herbs (onion, lemongrass, galangal, basil) added in shellfish soup indicated that the amount of 6 grams of herbs was the most acceptable from consumers. It showed the scores of the color, odor, taste, appearance and total sensory at 8.22±0.89, 8.32±0.54, 8.12±0.89, 7.96±0.90, 8.22±0.80 respectively which were different other quantities. Moreover, these herbs are beneficial to reducing the fishy odor and enhancing the taste of shellfish to be better. So that selected to 6 % of herbs enhance in shellfish soup product.(Fig 3)



Figure 3 Shellfish soup enhanced with herbs

2. The result of the nutritional values of shellfish soup enhanced with herbs analysis

Table 7 The nutritional values of shellfish soup enhanced with herbs products

Lists	Per 100 ml.	Per serving size	%RDI	Reference Method
Total energy (Kcal)	10.69	0.00	-	In-house method TE-CH-169 based on Compendium of Methods for Food Analysis Thailand, 1 st Edition,2003
Energy from fat (Kcal)	0.09	0.00	-	Journal of AOAC INTERNATIONAL;1993.p.106
Carbohydrate (gram)	1.86	less than 1	0	Journal of AOAC INTERNATIONAL;1993.p.106
Fiber (gram)	0.00	0.00	0	AOAC (2016) 985.29
Protein (gram)(%Nx6.25)	0.79	0.00	-	AOAC (2016) 981.10
Total fat (gram)	0.01	0.00	0	AOAC (2016) 948.15
Saturated fat (gram)	0.00	0.00	0	In-house method TE-CH—208 by GC Technique
Cholesterol (mg.)	0.99	0.00	0	In-house method TE-CH-143 based on AOAC (2016)976.26
Sugar (gram)	1.74	less than 1	-	AOAC (2016) 925.35(B)
Vitamin A (microgram)	Not found	0.00	0	In-house method TE-CH-022 based on Bull.Dept.Med.Sci.1995;37(1):57-64
Vitamin B1(mg.)	Not found	0.00	0	In-house method TE-CH-311 based on Journal of AOAC International, vol.85, No.4,2002
Vitamin B2(mg)	0.15	0.06	4	In-house method TE-CH-225 base on Journal of Agriculture Food Chemistry(1984)32,p.1326-1341

Sodium (mg)	189.35	75.00	3	In-house method TE-CH-134 based on AOAC (2016)984.27
Calcium (mg)	15.80	6.32	0	In-house method TE-CH-134 based on AOAC (2016)984.27
Iron (mg)	0.47	0.19	0	In-house method TE-CH-134 based on AOAC (2016)999.10
moisture	96.60	-		In-house method TE-CH-180 based on AOAC (2016)950.46
Ash (gram)	0.74	-		AOAC (2016) 938.08

Nutritional analysis of shellfish soup enhanced with herbs. It found that total energy at 10.69 kcal ,Energy from fat 0.09, carbohydrate 1.86 g , protein 0.79 g, total fat 0.01 g, cholesterol 0.99 mg., sugar 1.74 g, vitamin B2 0.15 mg, sodium 189 mg, calcium 15.80 mg, Iron 0.47 mg.

Conclusion

Development of shellfish soup enhanced with herbs. The results of stock soup found that consumers have accepted the most was the vegetable stock formulation with the score 8.53 ± 0.91 . The results of the acceptability of stock soup to shellfish species was hard clam (*Meretrix casta*) with score of total sensory 8.16 ± 1.20 . The results of quantities of herbs used in soup products which were galangal, lemongrass, basil leaves and onion mix were 6 percent of soup. The result of the nutritional values of shellfish soup enhanced with herbs products were total energy at 10.69 kcal ,Energy from fat 0.09, carbohydrate 1.86 g , protein 0.79 g, total fat 0.01 g, cholesterol 0.99 mg., sugar 1.74 g, vitamin B2 0.15 mg, sodium 189 mg, calcium 15.80 mg, Iron 0.47 mg.

Acknowledgement

This study wouldn't be completed without the support of many people. Therefore, the researchers would like to express the special gratitude and thanks to Rajamangala University of Technology Srivijaya, Trang Campus for supporting the budget for this study, assistant researchers and students who helped in this research.

References

- AOAC. 2016.**Official methods of analysis of AOAC INTERNATIONAL**, 20th Edition (2016) Association of official Analytical Chemist. Washington DC, USA.
- ASTV . 2015. **Eat the shell is so good and have high nutritional value** .Online Manager. Available Source : <http://www.mana>, July 22, 2017.
- Chalemwat, K. 2011. **Shrimp culture**. Bangkok : Green Fence. 16 p.
- Hongvivat, T. 2003. **Soup from western soup to Tom Yum curry and healthy soup**. Sunshine Publishing. Bangkok, Thailand. 111 p.

- Janvikul, N. 2013. **Soup for bodies**. (online)) Available Source: <http://rakya-2k.blospot.om>, August 23, 2017.
- Krasachol, N., Yenyongputakal, V. and Noypan, P. 2010. **Development of style chinese shells soup product**. Academic Conference of Kasetsart University. 48th. Fisheries. Bangkok. 466-474 p.
- Nutaman, N. and Pinratampai, C. 2008. **Effect of leafy leaves and tween 80 on sensory acceptance of Western shellfish soup products**. Special issue. Food Science. Burapa university. Chonburi.
- Suvanbol, S. 1981. **Recipe of Thai and foreign curries**. Thai Wattana Panich Co., Ltd.

Effects of Fermented Bioextracts on Yield Potential and Growth of Rice RD 49 Variety

Sujitra Ruengdechawiwat¹* Pornwipa Sanawong² and Chutharat Aimkham²

ABSTRACT

The main objective of this research aimed to test the effectiveness of various fermented bioextracts on growth and yields of rice RD 49 variety. The experiment was set as randomized complete block design RCBD with 4 treatments and 4 replications; treatment 1) control, treatment 2) bioextract from fresh fruits, treatment 3) bioextract from banana shoot and treatment, 4) bioextract from microbial activators PD2 (ARDA2) at Plant Science Field, Faculty of Science and Agricultural Technology, Rajamangala University of Technology Lanna, Phitsanulok. Field study was conducted from June – October 2017. The results showed that 14 – 98 days after planting treatment 2 could produce the highest growth and yield, as well as, plant height in rice RD 49 variety. For the chemical grain qualities of rice RD 49 variety, the results found that the treatment 2 and the treatment 3 could produce the highest 2.17 phosphate contents and 1.48 nitrogen contents respectively and were significantly different ($P > 0.05$). It can be concluded that the using fermented bioextracts from both fresh fruits and banana shoot had efficiency on yield components of rice RD 49 variety.

Keywords: Fermented bioextracts, Rice RD 49 variety, Growth, Yield

¹ Science Majors, Faculty of Sciences and Agricultural Technology, Rajamangala University of Technology Lanna, Phitsanulok 65000, Thailand

² Plant Science Majors, Faculty of Sciences and Agricultural Technology, Rajamangala University of Technology Lanna, Phitsanulok 65000, Thailand

*Corresponding author, e-mail : sujitra5000@gmail.com

Introduction

The agricultural sector is one of the most important sectors of Thailand economy that has generated food and living incomes for most of the Thai citizens. Thailand has exported various kinds of agricultural products, such as rice, vegetables, tropical fruits, industrially processed foods and, etc., to many countries around the world. Forty percent of Thais works in agriculture, 16 million of them are rice farmers by one estimate. Thailand has a strong tradition of rice production. It has the fifth-largest amount of land under rice cultivation in the world and is the world's second largest exporter of rice [1,9] .

Rice (*Oryza Sativa L.*) is an annual cereal grain and it is the most important staple food for a large part the world's human population, especially in East and South Asia [1,3,9]. The rice RD 49 variety (RD49) is one of the most quality rice and very famous on the world market because of its unique, long, slender grain and white color. Moreover, it tastes soft and smells like a natural fragrance after cooking. The potential yield of this variety is 733 Kg/rai. To prevent crop losses to the agricultural pests, pesticides are then used to control insect and to increase agricultural products. However, pesticide intoxication is one of the major public health problems in Thailand and it is caused by intensive use and exposure to pesticides. These pesticides do not only raise production cost but in long term they also deteriorate soil qualities [2].

Currently, many imported plant growth promoters or fertilizers are found to be bio-extracts. Some of them are produced by fermentation, as this procedure enhances output qualities. Bio-extract fertilizer becomes one of the alternatives which minimizes chemical treatments [5-8,10]. The aim of this study was to investigate the benefit of fermented bioextracts in the growth of the rice RD 49 variety.

Materials and Method

1. Treatments and Experimental Design

One variety of rice namely, the rice RD 49 variety was selected based on its yielding potential. The experiment consisted of four treatments with 4 replications set as randomized complete block design (RCBD). A field experiment was conducted at the same time, between June - October 2017. The pot experiment was undertaken in an open air environment at plant science field, Faculty of Science and Agricultural Technology, Rajamangala University of Technology Lanna, Phitsanulok. Three formulas of fermented bioextracts for growth in treatment 2-4 (shown as Figure 1) bioextract from on treatment 2, were on used banana shoot (treatment 3) and from bioextract from microbial activators PD2 (treatment 4) to compare with control treatment (without bioextracts) (treatment 1).



Figure 1 (a) bioextract from fresh fruits (b) from banana shoot
(c) from microbial activators PD2

2. Determinations and data analysis

Growth Parameters

At the growth stages ten plants from each of the plots (shown as Figure 2) were selected randomly to determine grain growth parameters such as plant height and number of tillers.

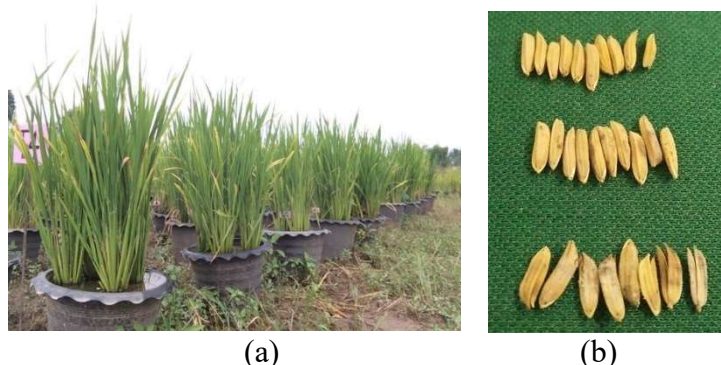


Figure 2 Growth of (a) the tillering stage (b) grain of the rice RD 49 variety

Chemical composition

Both the used fermented bioextracts and the obtained grain of the rice RD 49 variety at differences condition were assayed according to the AOAC method.

Grain Yield, Yield Components

Grain yield was adjusted to less than 12.5% moisture content. The plants were randomly selected to determine yield and yield components, which consisted of number of tillers per plant, number of seeds per spike and seeds weight.

3. Statistical Analysis

To determine statistical difference between means ($p < 0.05$), ANOVA and Duncan's Multiple Range Test (DMRT) were calculated using SPSS statistical software.

Results and Discussion

The fermented bioextract chemical compositions

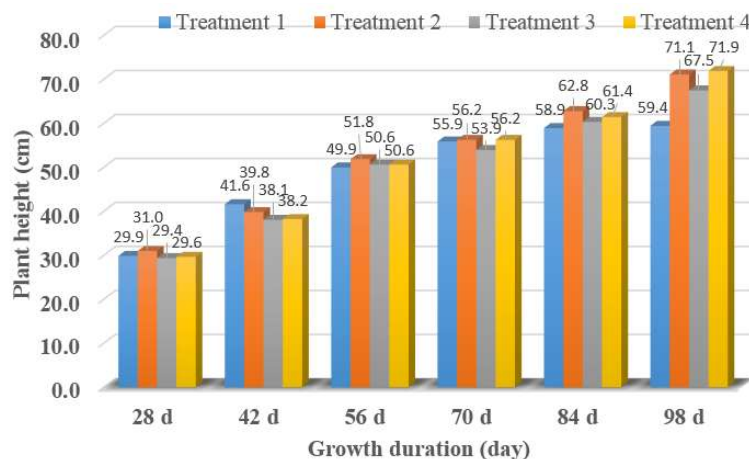
The used fermented bioextracts were collected for chemical analysis before planting. From the results, it had indicated that the fermented bioextract from microbial activators PD2 gave the highest total nitrogen and phosphorous (P_2O_5) content as 0.23 and 0.010 % respectively. While the fermented bioextracts from fresh fruits and banana shoot gave the highest total potassium (K_2O) as 0.22-0.23 %. All the fermented bioextracts pH was between 3.7 and 4.1 because of organic acid occur after fermentation (Table 1).

Table 1 Some Chemical composition of the various fermented bioextracts.

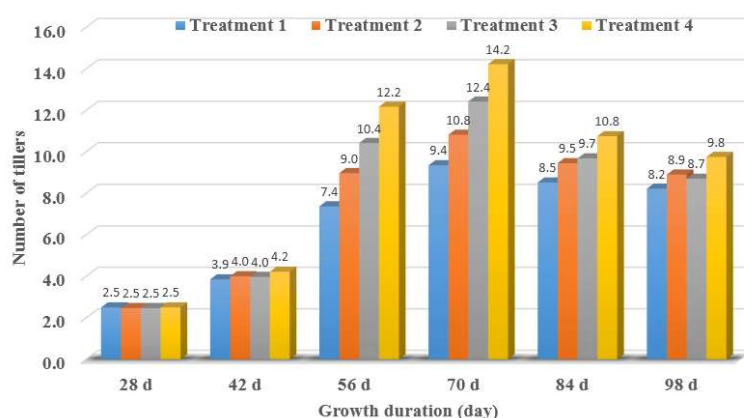
Parameters	Formula of fermented bioextracts		
	Fresh fruits	Banana shoot	Microbial activators PD2
Total Nitrogen content (%N)	0.110±0.002	0.040±0.001	0.230±0.004
Phosphorous content (% P_2O_5)	0.001±0.000	0.002±0.000	0.010±0.000
Potassium content (% K_2O)	0.230±0.004	0.220±0.004	0.190±0.003
pH	4.06	3.99	3.73
Electrical Conductivity; EC (mS/cm)	15.13	13.68	11.55

Grain Yield, Yield Components

The analysis of variance exhibited that bioextract used had significantly influenced days to planting. From the results, it was indicated that treatment 2, 3 and 4 (bioextracts from fresh fruits, banana shoot and microbial activators PD2 respectively) showed a significantly higher plant height and number of tillers than treatment 1 (without bioextract) (Figure 3).



(a)



(b)

Figure 3 Effect of growth duration, aboveground fermented bioextracts on growth of rice at various planting day at maturity, of the obtained rice RD 49 variety grown (a) plant height (b) number of tillers.

Planting at 70 days, treatment 1-4 gave number of tillers per plant as 9.4, 10.8, 12.4 and 14.2 respectively. However, it was found that number of tillers per plant decrease tendency after planting 70 day in various treatment. This could possibly be due to the enhanced tillering capacity of the existing plant population associated with the adequate availability of bioextract nutrients for the lower population.

After harvest, the result showed that all the phenological and growth parameters (grain yield and yield components) at various treatments (Table 2). From this result, the used bioextracts for plant could be appropriate for rice production.

Table 2 Grain yield and yield components of the obtained rice RD 49 variety at various treatments.

Treatment	Number of seeds per spike	Grain weight (mg)	Grain length (cm)	Grain yield (Kg rai ⁻¹)
Treatment 1	20.04±0.40	2.45±0.04	0.98±0.02	101.05±9.10
Treatment 2	29.18±0.60	2.41±0.04	1.01±0.02	468.88±11.10
Treatment 3	24.65±0.40	2.28±0.02	0.97±0.02	441.89±11.10
Treatment 4	28.21±0.50	2.30±0.02	1.00±0.02	311.58±10.20

Grain chemical compositions

After harvest, the obtained grain were collected for chemical analysis. From the results, it had indicated that the treatment 2 and the treatment 3 could produce highest 2.17 % phosphate contents and 1.48 % nitrogen contents respectively (Table 3).

From the data in table 1, the fermented bioextract from Microbial activators PD2 in treatment 4 had the highest total nitrogen content as 0.230 %, whereas the fermented bioextract from banana shoot in treatment 3 had total nitrogen content only 0.040 %. However, it was found that the obtained grain in treatment 3 gave highest nitrogen contents. This could possibly be due to the molecular aggregation in nitrogen compound on adsorption of nutrient for rice growth.

Table 3 Chemical properties of the obtained grain in various treatments.

Treatment	Nitrogen content (%)	Phosphate content (%)	Potassium content (%)
Treatment 1	1.44±0.10	1.60±0.18	2.69±0.01
Treatment 2	1.43±0.10	2.17±0.25	0.73±0.01
Treatment 3	1.48±0.11	1.72±0.18	0.46±0.01
Treatment 4	1.45±0.10	1.50±0.17	0.35±0.01

Conclusion

In summary, we confirmed that utilization of 3 formulas bioextract would make rice be possibly increase grain yield and yield components. The suggestions of this study are to promote production and utilization of bioextract in order to increase yield of the rice RD 49 variety including reducing chemical fertilizer conservation. Therefore, campaigning of production and utilization of the 3 formulas bioextract mentioned earlier is very necessary.

Acknowledgement

The authors wish to thank Faculty of Sciences and Agricultural Technology, Rajamangala University of Technology Lanna (RMUTL), Phitsanulok province for providing the facilities used in this research.

References

- Apiwat I. *et al.* 2016. Comparison on Quality of Rice var. Khao Dawk Mali 105 Planted by Using Chemical and Organic Fertilizers in Surin Province. **Journal of Science and Technology** 24 (5): 767-769.
- Apiwat T. 2015. Pesticides used in Thailand and toxic effects to human health. **Medical Research Archives** 3: 1-8.
- Boonhong C. *et al.* 2016. Physical and Chemical Grain Qualities of Thammasat Aromatic Rice Variety. **Thai Journal of Science and Technology** 5 (1): 37-41.
- Ganghua L 2009. Comparison of yield components and plant type characteristics of high-yield rice between Taoyuan, a ‘special eco-site’ and Nanjing, China. **Field Crops Research** 112: 214–221.
- Nisit K. 2008. Role of Fermented Bio-extracts Produced by Farmers on Growth, Yield and Nutrient Contents in Cowpea (*Vigna unguiculata* (L.) Walp.) in Northeast Thailand. **Biological Agriculture & Horticulture** 25 (4): 353-368.
- Phakpen P. *et al.* 2017. Effect of High Quality Organic Fertilizer on Production of Suphan Buri 1 Rice. **Journal of science and technology** 25 (2): 248-257.
- Renoo T. 2013. Effect of fertilizers application on growth and yield of some vegetable crops. **Prawarun Agricultural Journal** 10 (1): 19-27.
- Saowapa C. 2011. Study the Processing and Quality of Liquid Fertilizer of Swine Manure Fermentation for Organic Agriculture, Tambon Kongtool, Amphor Nongphai, Phetchabun Province. Phetchabun Rajabhat University.
- Tekle Y. 2014. Determination of optimum seed rate for productivity of rice (*Oryza Sativa L.*), at Woito, Southern Ethiopia. **Agriculture, Forestry and Fisheries** 3(3): 199-202.
- Thanaporn K. *et al.* 2016. Effect of Bio-Extract on Growth and Flower Yield in Jasmine (*Jasminum sambac* (L.) Ait.). **Thai Agricultural Research Journal** 32 (2): 129-138.

In vitro* Gas Production of Leucaena (*Leucaena leucocephala*) Silage Added with Xylanase and Cellulase from Dried Tomato Pomace by *Aspergillus niger

Smerjai Bureenok^{1*}, Niracha Phasuk¹, Chalermpon Yuangklang¹, Benya Saenmahayak¹, Kraisit Vasupen¹ and Nittaya Pitiwittayakul¹

ABSTRACT

This study aimed to determine the effects of xylanase and cellulase from dried tomato pomace treated by *Aspergillus niger* addition to leucaena silage on total gas production, organic dry matter digestibility (OMD) and metabolizable energy (ME) by using *in vitro* gas techniques. Xylanase and cellulase were added at 0, 0.2, 0.4, and 0.8% of dry matter leucaena silage. Commercial cellulase enzyme from *Aspergillus niger* were also used at 0.2% (w/w of dry matter). Gas production (GP) were measured by the syringe at distinct incubation times (0, 1, 2, 4, 6, 8, 12, 18, 24, 36, 48, 60, 72, 84, and 96 h). At 96 h, total gas production increased by addition of enzyme level at 0.4 and 0.8% and these value were not different from the addition of commercial cellulase. Gas production obtained from the insoluble fraction (b), gas potential extent of gas production (a+b) and cumulative gas production were improved by increasing the enzyme levels. The organic matter digestibility (OMD) was not different in all silages. Addition of xylanase and cellulase from dried tomato pomace produced by *Aspergillus niger* at 0.4% can improve the nutrient digestibility of leucaena silage.

Keywords: Cellulase, Gas production, *Leucaena leucocephala*, Xylanase

¹Department of Agricultural Technology and Environment, Faculty of Sciences and Liberal Arts, Rajamangala University of Technology Isan, Nakhon Ratchasima, 30000, Thailand

*Corresponding author, e-mail : asmerjai@hotmail.com

Introduction

Xylanases and cellulase are used in several industrial processes such as bioconversion of lignocellulosic waste into their constituent sugars (Shah and Madamwar, 2005), improvement of the digestibility of animal feed, etc. (Tapingkae *et al.*, 2008). The use of abundant and low cost agricultural by-products as fermentation substrates for the production of xylanases is one of the ways to substantially reduce enzyme production cost. Solid state fermentation is a microbial process in which the microorganisms grow under conditions closer to their natural habitat and produce larger amounts of extra cellular enzymes (Sato and Sudo, 1990). Among existing technologies in the fermentation, solid state fermentation (SSF) shows many advantages over fermentation in submerged culture, such as lower cost and much lower reactor volumes (Rodriguez-Couto and Sanroman, 2006). In this way, xylanolytic enzymes have been successfully produced in SSF using solid substrates such as corn cobs, rice bran, rice husk (Badhan, 2007), sunflower head, grape pomace (Diaz, 2007) or wheat bran. For these reasons, tomato pomace is a waste abundantly available and its chemical composition contains proteins, lipids, carbohydrates, amino acids, carotenoids and minerals (Al-Wandawi *et al.*, 1985). *Aspergillus niger* have been reported to be the main sources of cellulase, hemicellulase, pectinase and xylanase products on the non-starch polysaccharides including cellulose (Hamlyn, 1998). *Leucaena leucocephala*, the widely propagated species, is nitrogen fixing and drought resistant with a high productivity rate and the leaves of the plant are potentially excellent source of crude protein for livestock. Fibrolytic enzymes such as cellulase and hemicellulase have also been used and improved the nutrient digestibility. The addition of cellulase increased the apparent digestibility of dry matter, organic matter, and neutral detergent fiber of dairy cows (Ballard *et al.*, 2003). Therefore, the aim of this study was to evaluate the effect of cellulase and xylanase on the nutrient digestibility of leucaena silage by *in vitro* gas production method.

Materials and Methods

Microorganism and inoculum preparation

The fungal culture of *Aspergillus niger* was obtained from the National Center for Genetic Engineering and Biotechnology (BIOTEC, Pathum Thani, Bangkok). Inoculum of *A. niger* was maintained on potato dextrose agar (PDA) at 30°C for 5 d and stored at 4°C until being used. The spores from PDA plates were harvested by using sterile 0.01% Tween 80 (w/v) to obtain 1×10^7 spores/mL.

Culture conditions

The culture medium used for solid-state fermentation was dried tomato pomace (residue from the extraction of tomato sauce). The moisture content of dried tomato pomace was adjusted to about 50% and autoclaved. The substrate was cooled and mixed with 10% of an *A. niger* spore suspension (1×10^7 spores/mL) (w/w). The solid-state culture was incubated at 30°C for 72 h. Then, the substrate was dried at 50°C for 3-5 days before using as fibrolytic enzyme.

Enzyme activity test

Dried tomato pomace treated by *A. niger* was milled through a 1 mm sieve. The moisture content of the culture medium was determined by drying in a hot-air oven at 80°C to derive a constant weight. The xylanase and cellulase enzyme activity were examined by adapted method of Bailey *et al.* (1992) and Mandels *et al.* (1976), respectively. Moisture content was determined by AOAC method.

***In vitro* gas production**

The ruminal fluid used as inoculant was obtained from 2 adult goats. The animal was fed Napier grass silage diet and supplemented daily with concentrate for 1 week. Kinetics of degradation and gas production were evaluated in the samples of ensiling opened after 30 days of fermentation by the semi-automatic *in vitro* gas production. Evaluating the digestibility of forage silage by *in vitro* gas production technique method was performed according to Menke and Steingass (1988).

Briefly, samples of each leucaena silage (0.2 g DM) were accurately weighed into 100 ml syringe with 4 different levels of xylanase and cellulase (0, 0.2, 0.4, and 0.8% (w/w)) in four replicates. Commercial cellulase were also added at 0.2% (w/w) (Sigma-aldrich, 1.21U/mg). Subsequently, a mixture composed of 20 ml of anaerobic buffer solution and 10 ml of ruminal fluid was added to each syringe. Blank (rumen fluid without sample) were run in triplicate in each series. Then, the syringes were placed into water bath which were automatically stirred at 39°C. Gas production (GP) were measured the syringe at distinct incubation times (0, 1, 2, 4, 6, 8, 12, 18, 24, 36, 48, 60, 72, 84, and 96 h). Total gas production were collected for blank incubation. Cumulative gas production data were fitted to model of Ørskov and McDonald (1979);

$$y = a + b(1 - e^{-ct})$$

Where: a= the gas production from the immediately soluble fraction (ml), b= the gas production from the insoluble fraction (ml), c= the gas production rate constant for the insoluble fraction b (h), t = the incubation time (h), a+b = the potential gas production (ml), gas production at the time “t”.

The effective degradability (ED) was calculated by $ED (\%) = (a + b/0.02) + c / 100$. The organic matter digestibility (OMD) was calculated by $OMD (\%) = 16.149 + (gas24h * 0.9042) + (CP * 0.0492) + (EE * 0.0387) + (Ash * 0.0387)$. Metabolizable energy (ME) content of the silage at 24 h (ME MJ/kg DM) was calculated using equation of Menke et al. (1979) as follows: $ME (MJ/kg DM) = 2.2 + (0.136 * gas24h) + (0.057 * CP) + (0.002859 * EE)$. Where GP = 24 h net gas production (ml/200mg), CP = crude protein and EE = ether extract.

Statistical analysis

Statistical analyses were performed using the Statistical Analysis System (SPSS). After analysis of variance (ANOVA), the differences between treatment means were compared using Duncan's New Multiple Range Test (DMRT).

Results and Discussion

Composition of enzymes used in this experiment prepared from the fermentation of dried tomato pomace by *Aspergillus niger* are shown in Table 1. There was a gradually increasing of cumulative gas production on 0-60 h after incubation time (Figure 1). Then, the gas production was quite stable from 72 h until the end of the incubation time (96 h). At 24 h incubation, the gas production was not significantly different among the treatment groups (Table 2). However, increasing enzyme levels tended to increase the total gas production at 96 h ($p = 0.0115$). As can be seen from the result, the immediately soluble fractions (a) and the gas production rate (c) were not significant differences among treated silages. Gas production from slowly fermentable fraction (b), potential gas production (a+b) and effective degradability (ED) tended to increase with the increasing level of enzyme levels. Nagadi et al. (2000) suggested that the *in vitro* gas production is highly dependent on the availability of fermentable carbohydrate and nitrogen. This may cause by high in water soluble fraction that might be

degraded by a higher level of enzyme addition. The organic matter digestibility (OMD) were not different in all silages.

Table 1 Enzymes composition and activities from *Aspergillus niger* incubated with dried tomato pomace

Composition	
Moisture content (%)	6.57±0.63
pH	6.25±0.08
Amylase activity (Unit/ g dry weight)	55,658±9,836
Protease activity (Unit/ g dry weight)	3,706±1,021
Cellulase activity (Unit/ g dry weight)	46,144±13,079
Xylanase activity (Unit/ g dry weight)	34,299±9,085
Total aflatoxin (µg/kg)	1.42

Table 2 Effect of enzymes addition to leucaena silage on in vitro total gas, effective degradability (ED), organic matter digestibility (OMD) and metabolizable energy (ME)

	Cellulase		Xylanase + Cellulase						SEM	P-value	Linear*		
	0.20%		0%		0.20%		0.40%		0.80%				
Total gas production													
24h (ml/200 mg DM)	24.02	a	21.08	ab	18.36	b	22.14	ab	21.04	ab	0.58	0.0861	0.5350
96h (ml/200 mg DM)	36.49	a	31.91	bc	30.93	c	35.48	ab	35.19	ab	0.58	0.0455	0.0115
Gas kinetics													
a	11.13		9.87		9.73		11.79		10.19		0.34	0.2824	0.4166
b	42.96	a	39.58	ab	39.06	b	41.49	ab	42.91	a	0.47	0.0543	0.0039
c	0.05		0.051		0.047		0.046		0.044		0.00	0.2960	0.1655
a+b	54.08	a	49.46	b	48.78	b	53.28	ab	53.1	ab	0.62	0.0490	0.0080
ED (%)	27.04	a	24.73	b	24.39	b	26.64	ab	26.55	ab	0.31	0.0490	0.0080
OMD (%)	39.47	a	36.82	ab	34.35	b	37.78	ab	36.78	ab	0.52	0.0861	0.5350
ME (MJ/kg DM)	6.59	a	6.29	ab	5.92	b	6.43	ab	6.28	ab	0.08	0.0861	0.5350

^{a-c} Means with different superscripts within columns significantly differed (P<0.05).

*Commercial cellulase enzyme. Cellulase + Xylanase enzyme from dried tomato pomace treated by *Aspergillus niger*. **Linear effect of cellulase + xylanase enzyme level.

a = soluble fraction; b = insoluble fraction, but degradable; c = degradation rate of fraction; a+b = potential gas production.

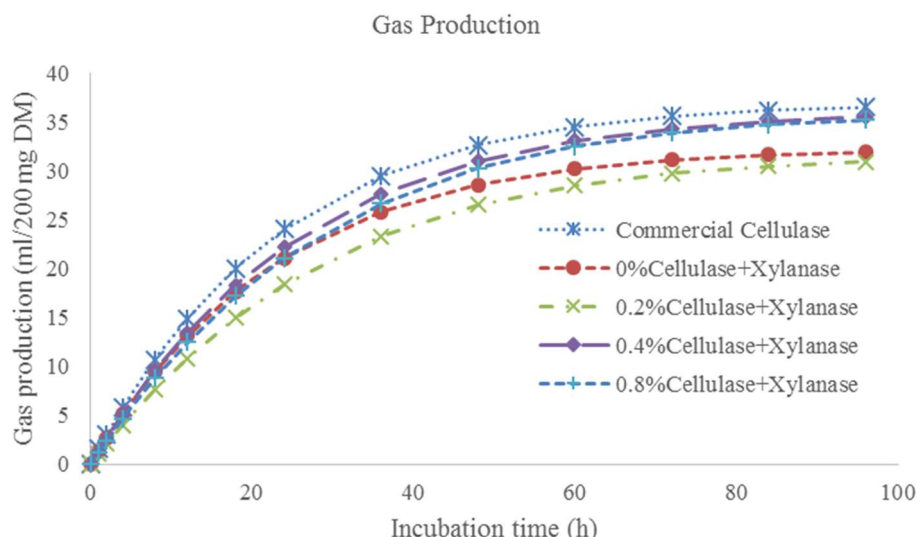


Figure 1 Cumulative gas production (ml /0.2g DM) from *in vitro* fermentation of leucaena silages added with enzymes

Conclusion

The results of present study indicated that addition of xylanase and cellulase from dried tomato pomace produced by *Aspergillus niger* at 0.4% can improve the *in vitro* gas production of luecaena silage.

Acknowledgment

This study was financially supported by Rajamangala University of Technology Isan.

References

- Al-Wandawi, H, Abdul-Rahman, M. and Al-Shaikhly, K. 1985. Tomato processing waste as essential raw materials source. **Journal of Agricultural and Food Chemistry** 33:804-807.
- Badhan, A.K., Chadha, B.S., Kaur, J., Saini, H.S. and Bhat, M.K. 2007. Production of multiple xylanolytic and cellulolytic enzymes by thermophilic fungus *Myceliophthora* sp. IMI 387099. **Bioresource Technology** 98: 504-510.
- Bailey, M. J., Biely, P. and Poutanen, K. 1992. Interlaboratory testing of methods for assay of xylanase activity. **Journal of Biotechnology** 23: 257-270.
- Ballard, C.S., Carter, M.P., Tach, K.W.C, Sniffen, C.J., Sato, T., Uchida, K., Teo, A., Nhan, U.D. and Meng, T.H. 2003. Feeding fibrolytic enzymes to enhance DM and nutrient digestion and milk production by dairy cows. **Journal of Dairy Science** 86: (Suppl 1):150. (Abstr.).
- Díaz, A.B., Caro, I., de Ory, I. and Blandino, A. 2007. Evaluation of the conditions for the extraction of hydrolitic enzymes obtained by solid state fermentation from grape pomace. **Enzyme and Microbial Technology** 41: 302–306.
- Hamlyn, P.F. 1998. Fungal Biotechnoly. British Mycological Society Newsletter, ISSN 1465-8054.

- Mandels M., Andreotti, R. and Roche, C. 1976. Measurement of accharify in cellulose. **Biotechnology and Bioengineering Symposium** 6: 21-33.
- Menke, K. H., Raab, L., Salewski, A., Steingass, H., Fritz, D. and Schneider, W. 1979. The estimation of the digestibility and metabolizable energy content of ruminant feeding-stuffs from the gas production when they are incubate with rumen liquor in vitro. **The Journal of Agricultural Science** 93: 217-222.
- Menke, K. H. and Steingass, H. 1988. Estimation of energetic feed value obtained from chemical analysis and gas production using rumen fluid. **Animal Research and Development** 28: 7-55.
- Nagadi, S., Herrero, M. and N.S. Sessop, N.S. 2000. The effect of fermentable nitrogen availability on in vitro gas production and degradability of NDF. **Animal Feed Science and Technology** 87: 214-251.
- Ørskov, E. R. and McDonald, P. 1979. The estimation of protein degradability in the rumen from incubation measurements weighed according to rate of passage. **The Journal of Agricultural Science** 92: 499-503.
- Rodriguez-Couto, S. and Sanroman, M.A. 2006. Application of solid-state fermentation to food industry-A review. **Journal of Food Engineering** 76: 291-302.
- Sato, K. and Sudo S. 1990. Small scale solid state fermentation, pp. 61-79. *In* L. D. Arnold, and E. D. Jullian, eds. **Manual of Industrial microbiology and Biotechnology**. ASM press, Washington, D.C.
- Shah, A. and Madamwar, D. 2005. Xylanase production by a newly isolated *Aspergillus foetidus* strain and its characterization. **Process Biochemistry** 40: 1763–1771.
- Tapingkae, W., Yachai, M., Visessanguan, W., Pongtanya, P. and Pongpiachan, P. 2008. Influence of crude xylanase from *Aspergillus niger* FAS128 on the in vitro digestibility and production performance of piglets. **Animal Feed Science and Technology** 140: 125-138.

Optimization of Culture Condition for Biomass Production and Starch Accumulation of Cyanobacteria, *Nostoc* sp.

Somrak Rodjaroen^{1,*}, Sujaree Kaewkong¹, Thirarat Kaewchamnon¹, Usa Nuichan¹ and Watcharee Kunyalung²

ABSTRACT

The cyanobacteria, *Nostoc* spp. has been investigated for its potential use as algal biomass in hydrogen production. In this work, we investigated cultivation media (CHU medium, Bold medium, BGA medium and BG-11 medium), K₂HPO₄ concentrations (0.00, 0.02, 0.04, 0.06 and 0.08 g/L), NaNO₃ concentrations (0.00, 0.75, 1.50, 2.25 and 3.00 g/L), pH (5, 6, 7, 7.4, 8, 9 and 10) and temperature (25, 28, 30, and 35°C) effects on biomass production and starch accumulation of cyanobacteria, *Nostoc* sp., under laboratory conditions. Algal cells were grown at 28±1°C under illumination at 60 µmol photon/m²/s and shaken at 150 rpm on orbital shaker for 20 days. *Nostoc* sp. showed the highest biomass production and starch accumulation in BG-11 medium with added 0.04 g/L K₂HPO₃ and under other conditions of pH 8 and 28°C. The results of starch accumulation showed that the highest amount of starch was achieved without any addition of NaNO₃ in BG-11 medium while biomass production was the highest at 2.25 g/L. These results should be taken into consideration when evaluating the biomass and starch value of these microalgae for hydrogen production.

Keywords: Optimization, Biomass Production, Starch Accumulation, *Nostoc* sp.

¹ Agriculture Program, Faculty of Sciences and Technology, Nakhon Si Thammarat Rajabhat University, Nakhon Si Thammarat, 80280, Thailand

² Department of Bioscience, Thailand Institute of Scientific and Technological Research (TISTR), Pathum Thani, 12120, Thailand

*Corresponding author, e-mail : Somrak_25@hotmail.co.th

Introduction

Cultivation microalgae could be an alternative process to produce biomass for a wide range of applications, including a human and animal food, and a possible way to obtain other products like proteins, carbohydrates, lipids, vitamins and pigments (Spolaore *et al.*, 2006, Cai *et al.*, 2007; Markou and Georgakakis, 2011). Studies of environmental factors that affect biomass production by microorganisms are essential since they contribute to understanding the control of metabolic activities and the optimising of yields. Temperature and pH are among the environmental factors that play a significant role in the metabolic activities of microalgae (Bhatia and Srivastava, 1995; Rafiqul *et al.*, 2005). Many researchers have been developed for biomass production and starch accumulation by microalgae for hydrogen production (Kawaguchi *et al.*, 2001, Kim *et al.*, 2006; Rodjaroen *et al.*, 2011). However, the wide use of microalgae hydrogen production is restricted by its high production cost. This problem could be solved by developing the process technologies in biomass production, carbohydrate content, extraction and so on (Kim *et al.*, 2006; Rodjaroen *et al.*, 2011). And the key to microalgae hydrogen production and industrialization is to increase the biomass productivity.

The aims of this work were to determine the biomass production and starch accumulation of *Nostoc* sp. grown on different of cultivation media, K₂HPO₄ concentrations, NaNO₃ concentrations, pH and temperature. The final purpose was to evaluate the starch accumulation for use as biomass for hydrogen production

Materials and Methods

1. Algae strain and culture condition

The cyanobacterial strain, *Nostoc* sp. was obtained from the Thailand Institute of Scientific and Technological Research (TISTR). It was preserved in BG-11 medium. Algae were inoculated at an initial concentration of 0.20 at OD₁₀₀₀ in 250 mL Erlenmeyer flasks containing 100 mL liquid medium (Wang *et al.*, 2010). The culture flasks were incubated under stationary condition at an illumination of 60 $\mu\text{mol photon m}^{-2}\text{s}^{-1}$ from cool white fluorescence lamps with a cycle of 12 h dark and 12 h light (Guan *et al.*, 2004), and shaken at 150 rpm on an orbital shaker at 28 \pm 1°C (Kawaguchi *et al.*, 2001; Kim *et al.*, 2006).

2. Optimization of cultivation conditions for biomass production and starch accumulation

This experiment was set up to examine the effects of cultivation media on algal biomass and starch accumulation by *Nostoc* sp. Then, the physical factors (pH and temperature) and chemical factors (various concentrations of NaCl, K₂HPO₄ and NaNO₃) were optimized.

2.1. Effects of culture media on biomass production and starch accumulation

The effects of cultivation media on biomass production and starch accumulation by *Nostoc* sp. was investigated with 4 cultivation media (as treatments) namely, CHU medium, Bold medium, BGA medium and BG-11 medium. This experiment was set up to study the physiological characterization of *Nostoc* sp. grown in various cultivation media. For algal calls, 200 ml culture medium in 500 ml flask was used and grown at temperature 28 \pm 1°C and continuously shaken at 150 rpm on orbital shaker, and cultured under illumination at 60 $\mu\text{mol photon m}^{-2}\text{s}^{-1}$ using cool white fluorescence lamps with 12 h dark and 12 h light cycles for 20 days. The biomass (g) was collected for starch analysis (% DW).

2.2. Effects of K₂HPO₄ concentration on biomass production and starch accumulation

To examine the effects of K₂HPO₄ concentrations at 0.00, 0.02, 0.04, 0.06 and 0.08 g/L in BG-11 medium (as treatments) on biomass production and starch accumulation, algal cells were cultured using the same cultivation conditions as explained in 2.1.

2.3. Effects of NaNO₃ concentration on biomass production and starch accumulation

To examine the effects of NaNO₃ concentrations at 0.00, 0.75, 1.50, 2.25 and 3.00 g/l in BG-11 medium (as treatments) on biomass production and starch accumulation, algal cells were cultured using the same cultivation conditions as explained in 2.1.

2.4. Effects of pH on biomass production and starch accumulation

To examine the effects of pH at 5, 6, 7, 8, 9 and 10 in BG-11 medium (as treatments) on production and starch accumulation, algal cells were cultured using the same conditions as explained in 2.1.

2.5. Effects of temperature on biomass production and starch accumulation

To examine the effects of temperature at 25, 28, 30, and 35°C in BG-11 medium (as treatments) on production and starch accumulation, algal cells were cultured using the same cultivation conditions as explained in 2.1.

3. Analysis

Algal growth curves were monitored by spectrophotometer. The strains were sampled every 2 days for determination of cell growth by a spectrophotometer at OD₁₀₀₀. Algae were harvested at stationary growth stages. After 20 days of cultivation, algal biomass was determined as total dry weight. Starch accumulation was analyzed for glucose content using Kochert's method (1978) after hydrolysis in 2M HClO₄ for 2 h at 100°C, using glucose (VWR International Ltd., England) as a standard. Percent dry weight was calculated as a percentage of starch per algal biomass dried weight.

Statistical analyses were performed using SPSS for Windows version 12.0, using analysis of variance (ANOVA) and Tukey's multiple comparison tests to examine between different cultivation media, K₂HPO₄ concentrations, NaNO₃ concentrations, pH and temperature.

Results and Discussion

1. Effects of various media on biomass production and starch accumulation

The results showed that cultivation of *Nostoc* sp. in BG-11 medium produced the highest biomass production and starch accumulation with significant difference ($p \leq 0.05$) to CHU and Bold medium but no significant difference to BGA medium. However, Bold medium cultivation gave the lowest biomass production with significant difference to others while BGA media was the lowest starch accumulation with significant difference to all medium ($p \leq 0.05$), as shown in Table 1. Thippasuksri (2007) was reported that *N. commune* produced the highest biomass in CHU and BG-11 medium. Similarly, Mahakhant *et al.* (2006) reported that *N. commune* cultivated in BGA, BGA+N and BG-11 media produced the highest biomass production. Das and Sarma (2015) were reported that *Anabaena spiroides* and *Nostoc punctiformae* were showed optimum growth on BG-11 Modified 5 culture medium. Nevertheless, other cyanobacterial strains provided similar results on the highest biomass production in BG-11 medium such as *Oscillatoria* sp., *Synechocystis aquatilis* and *Anabaena* sp. (Katircioglu *et al.*, 2006) and *N. muscorum* (Panda *et al.*, 2005). The advantage of BG-11 medium is that it contains nitrogen source (but not in BGA medium) which is the limited factor for growth of all general algae (Peerapornpisal, 2006).

Table 1 Biomass production and starch accumulation of *Nostoc* sp. cultured in various medium types for 20 days.

Medium types	Biomass (g DW/L; Mean±SE)	Starch (% DW; Mean±SE)
CHU	0.25±0.01 ^b	18.87±0.28 ^b
Bold	0.20±0.02 ^a	18.07±0.36 ^b
BGA	0.27±0.01 ^{bc}	11.81±1.51 ^a
BG-11	0.30±0.00 ^c	30.66±0.58 ^c

Note: Means in the column followed by the same letters are not significantly different as determined by means of Tukey's multiple comparison tests ($\alpha=0.05$, $n=3$).

2. Effects of K₂HPO₄ concentration on biomass production and starch accumulation

As nitrogen and phosphorous are a limited factor for algal growth, the main chemical constituents in BG-11 medium, NaNO₃ and K₂HPO₄, were investigated. The highest biomass production of *Nostoc* sp. was obtained at 0.04 g/L K₂HPO₄ concentration with no significant difference to that of 0-0.02 g/L and would decrease with increasing K₂HPO₄ concentration from 0.06-0.08 g/L, as shown in Table 2. Similar to biomass production, starch accumulation was the highest at 0.04 g/L K₂HPO₄, which is a normal concentration in BG-11. The experimental result was different from Thippasuksri (2007) who found that *N. commune* grew well in 0.02 and 0.09 g/L K₂HPO₄ concentrations in liquid BG-11 and CHU media, respectively. From other study, the optimum phosphate concentrations for *D. salina* and *D. viridis* growth were about 0.02-0.025 g/L K₂HPO₄ and the algal growth was inhibited at higher concentrations (>5 g/L) (Borowitzka and Borowitzka, 1989). Furthermore, Panda *et al.* (2005) reported that *N. muscorum* was grown under phosphate deficiency. *N. muscorum* showed a rise in biomass production for the first 7 days and was able to maintain only up to 15 days. Finally, a complete death of the organism was evidently observed after 21 days.

Table 2 Biomass production and starch accumulation of *Nostoc* sp. cultured in different K₂HPO₄ concentration in BG-11 medium for 20 days.

K ₂ HPO ₄ (g/L)	Biomass (g DW/L; Mean±SE)	Starch (% DW; Mean±SE)
0.00	0.31±0.01 ^b	13.63±1.27 ^{ab}
0.02	0.29±0.02 ^b	13.16±3.41 ^a
0.04	0.30±0.00 ^b	30.66±0.58 ^c
0.06	0.21±0.03 ^a	25.45±2.06 ^{abc}
0.08	0.17±0.01 ^a	27.75±8.61 ^{bc}

Note: Means in the column followed by the same letters are not significantly different as determined by means of Tukey's multiple comparison tests ($\alpha=0.05$, $n=3$).

3. Effects of NaNO₃ concentration on biomass production and starch accumulation

The highest amount of algal biomass was produced at 2.25 g/L NaNO₃ concentration in BG-11 medium and was not significantly different to those at other NaNO₃ concentrations ($p \geq 0.05$) (except at 0 and 3.00 g/L) as shown in Table 3. These results suggested that algal biomass decreased with increasing and decreasing K₂HPO₄ concentration to 0 and 3.00 g/L, respectively. These experimental results were not in accordance with Thippasuksri (2007) who found that *N. commune* produced the highest amount of biomass in BG-11 medium without the addition of NaNO₃.

Table 3 Biomass production and starch accumulation of *Nostoc* sp. cultured in different NaNO₃ concentration in BG-11 medium for 20 days.

NaNO ₃ (g/L)	Biomass (g DW/l; Mean±SE)	Starch (%DW; Mean±SE)
0.00	0.24±0.02 ^{ab}	36.08±3.57 ^b
0.75	0.33±0.02 ^c	32.77±2.23 ^b
1.50	0.30±0.01 ^{bc}	30.66±0.58 ^b
2.25	0.34±0.02 ^c	14.29±0.09 ^a
3.00	0.22±0.02 ^a	12.41±2.19 ^a

Note: Means in the column followed by the same letters are not significantly different as determined by means of Tukey's multiple comparison tests ($\alpha=0.05$, $n=3$).

The results of starch accumulation from these experiments showed the highest in BG-11 medium without NaNO₃ but no significant difference with 0.75 and 1.50 g/L NaNO₃. This might be due to the decreased growth of algal cells and polysaccharide mucous matters, which are formed under stress condition, were observed. Therefore, this would increase the amount of starch accumulation in this experiment. These results suggested that 0.75 g/L NaNO₃ in BG-11 medium would be the optimal NaNO₃ concentration for biomass production and starch accumulation by *Nostoc* sp. TISTR 8872.

In general, cyanobacteria require the minimal nitrogen concentrations of 0.5-0.6 g/L (Vonshak, 1986). A shortage of nitrogen affects the reduced production of pigments. Consequently, this will reduce the photosynthesis process (Allen, 1969). Therefore, the amount of biomass produced is decreased.

4. Effects of pH on biomass production and starch accumulation

The experimental results showed that the highest amounts of biomass production and starch accumulation were obtained at pH 8 and pH 7.4, respectively (Table 4). The algal biomass production of *Nostoc* sp. significantly declined when pH reduced to 5 and increased to 11. These results suggested that pH 8 would be the optimal for biomass production and starch accumulation by *Nostoc* sp. These experimental results were in agreement with Thippasuksri (2007) for that *N. commune* provided the high biomass in BG-11 medium of pH 7.5. Moreover, *C. applanata* exhibited wide tolerance at pH range of 3.4-8.4, with optimal growth obtained at 7.4 (Visviki and Santikul, 2000).

It has been shown by previous studies (Danesi *et al.*, 2001) that the optimal growth temperature for *S. platensis* is between 30°C and 35°C, with 40°C definitely being deleterious to this cyanobacterium. However, Mahakhant (1998) reported that most freshwater algae could only survive in temperature range of 15-30°C and most of them could not survive beyond 35°C. As the results indicated, it could be concluded that the optimal temperature for *Nostoc* sp. TISTR 8872 cultivation was at 28°C under the conditions used in these experiments.

Table 4 Biomass production and starch accumulation in *Nostoc* sp. cultured in different pH in BG-11 medium for 20 days.

pH	Biomass (g DW/l; Mean±SE)	Starch (%DW; Mean±SE)
5	0.13±0.00 ^{ab}	24.50±0.17 ^c
6	0.14±0.01 ^{ab}	14.91±0.61 ^a
7	0.13±0.01 ^a	19.95±1.35 ^b
7.4	0.21±0.02 ^d	31.06±0.19 ^d
8	0.30±0.00 ^f	30.66±0.58 ^d
9	0.25±0.01 ^e	25.98±0.11 ^c
10	0.18±0.02 ^{cd}	12.65±0.68 ^a
11	0.17±0.01 ^{bc}	15.08±3.85 ^a

Note: Means in the column followed by the same letters are not significantly different as determined by means of Tukey's multiple comparison tests ($\alpha=0.05$, $n=3$).

5. Effects of temperature on biomass production and starch accumulation

The results are shown in Table 5. The biomass production and starch accumulation of *Nostoc* sp. at 28°C were the highest and without significant differences at 25°C ($p \geq 0.05$), but significantly different ($p \leq 0.05$) with that of 20°C. These results indicated the effects of temperature on biomass production and starch accumulation as also reported by Araujo and Garcia (2005) that temperature was the main factor influencing *Chaetoceros* cf. *wighamii* composition and higher lipid and carbohydrate were obtained at 20°C and 25°C than at 30°C.

Table 5 Biomass production and starch accumulation in *Nostoc* sp. cultured in different temperature in BG-11 medium for 20 days.

Temperature (°C)	Biomass (g DW/l; Mean±SE)	Starch (%DW; Mean±SE)
20	0.16±0.02 ^a	18.37±1.30 ^a
25	0.29±0.02 ^b	28.72±0.49 ^b
28	0.30±0.00 ^b	30.65±0.58 ^b
30	0.20±0.02 ^a	24.51±2.63 ^{ab}

Note: Means in the column followed by the same letters are not significantly different as determined by means of Tukey's multiple comparison tests ($\alpha=0.05$, $n=3$).

Conclusion

In conclusion, in order to achieve the highest biomass production and starch accumulation, *Nostoc* sp. was the best cultured in BG-11 medium with other chemical additions such as 0.04 g/L K₂HPO₃, 0.75 g/L NaNO₃, and under other conditions of pH 8 and 28°C for the period of 20 days.

References

- Allen, M.M. and Smith, A.J. 1969. Nitrogen chlorosis in blue-green algae. **Archives of Microbiology** 69 (114): 45-48.
- Araujo, S.C. and Garcia, V.M.T.. 2005. Growth and biochemical composition of the diatom *Chaetoceros* cf. *wighamii* bright well under different temperature, salinity and carbon dioxide level. I. Protein, carbohydrates and lipids. **Aquaculture**. 246: 405-412.

- Bhatia, R., and Srivastava, P. 1995. Optimisation of culture conditions for *Spirulina labyrinthiformis* : Light and temperature. **Journal of Phytological Research** 8(2): 185-189.
- Borowitzka, M.A. and Borowitzka, L.J. 1989. *Dunaliella*, pp. 27-58. In Borowitzka, M.A. and Borowitzka, L.J. eds. **Micro-algal biotechnology**. Cambridge Univ. Press Publ.
- Cai, S.Q., Hu, C.Q. and Du, S.B. 2007. Comparisons of growth and biochemical composition between mixed culture of alga and yeast and monocultures. **Journal of Bioscience and Bioengineering** 104(5): 391-397.
- Danesi, E.D.G., Rangel, C.O., Pelizer, L.H., Carvalho, J.C.M., Sato, S. and Moraes, I.O. 2001. Production of *Spirulina platensis* under different temperatures and urea feeding regimes for chlorophyll attainment. In **Proceedings of the Eighth International Congress on Engineering and Food** 2:1978-1982.
- Das, K., and Sarma, G.C. 2015. Optimization of culture media for the growth of *Anabaena spiroides* and *Nostoc punctiforme* of Jorhat district, Assam. **IOSR J. Pharmacy and Biological Sciences** 10(2): 37-41.
- Guan, Y., Deng, M., Yu, X. and Zhang, W. 2004. Two-stage photo-biological production of hydrogen by marine green alga *Platymonas subcordiformis*. **Biochemical Engineering Journal** 19:69-73.
- Katircioglu, H., Beyatli, Y., Aslim, B., Yuksekdog, Z. and Atici, T. 2006. Screening for antimicrobial agent production of some microalgae in freshwater. **Journal of Microbiology** 71:718-723.
- Kawaguchi, H., Hashimoto, K., Hirata, K. and Miyamoto, K. 2001. H₂ production from algal biomass by a mixed culture of *Rhodobium marinum* A-501 and *Lactobacillus amylovorus*. **Journal of Fermentation and Bioengineering** 91(3):277-282.
- Kim, M.S., Baek, J.S., Yun, Y.S., Sim, S.J., Park, S. and Kim, S.C. 2006. Hydrogen production from *Chlamydomonas reinhardtii* biomass using a two-step conversion process: Anaerobic conversion and photosynthetic fermentation. **International Journal of Hydrogen Energy** 31:812-816.
- Kochert, A.G. 1978. Carbohydrate determination by the phenol-sulphuric acid method, In **Handbook of phycological and biochemical methods**, edited by Hellebust, J.A. and Craigie, J.S. Cambridge Univ. Press Publ., pp. 95-97.
- Mahakhan, A. 1998. **Fresh water algal culture**. Microbiological Resources Centre (MIRCEN), Thailand Institute of Scientific and Technological Research (TISTR). Bangkok. 25 p.
- Mahakhan, A., Klinhom, U., Tugthanuwat, M., Thippayasuksri, C., Kunlayalung, W., Phatomyothin, W., Srinorakutara, P., Bunyaphak, P., Sae-khow, K., Srisawas, S., Arunpairojana, V. and Nutalai, S. 2006. **Research and Development on Food Products from “Hed Lab” Alga (*Nostoc commune*, Cyanophyta)**. Thailand Institute of Scientific and Technological Research (TISTR). Bangkok. 75 p.
- Markou, G. and Georgakakis, D. 2011. Cultivation of filamentous cyanobacteria (blue-green algae) in agro-industrial wastes and wastewaters: A review. **Applied Energy** 88: 3389-3401.
- Panda, B., Sharma, L. and Mallick, N. 2005. Short communication: Poly-b-hydroxybutyrate accumulation in *Nostoc muscorum* and *Spirulina platensis* under phosphate limitation. **Journal of Plant Physiology** 162:1376-1379.
- Peerapornpisal, Y. 2006. **Phycology**. Department of Biology, Faculty of Science, Chiang Mai University, Chiang Mai. 545 p.
- Rafiqul, I.M., Jalal, K.C.A. and Alam, M.Z. 2005. Environmental factors for optimization of *Spirulina* biomass in laboratory culture. **Biotechnology** 4:19-22.

- Rodjaroen, S., Juntawong, N., Mahakhant, A., Kanghae, H. and Miyamoto, K. 2011. Production of hydrogen from wastewater by a three-step microbial hydrogen producing system. **The fourth international fisheries conference climate change: Impact on aquatic resources and fisheries**. Maejo University 74 p.
- Spolaore P., Joannis-Cassan, C., Duran, E., and Isambert, A. 2006. Commercial applications of microalgae. **Journal of Bioscience and Bioengineering** 101:87-96.
- Thippayasuksri, C. 2007. Laboratory and optimization and outdoor cultivation of “Het Lap” alga (*Nostoc commune* Voucher). M.S. Thesis, Mahasarakham University.
- Visviki, I. and Santikul, D. 2000. The pH Tolerance of *Chlamydomonas applanata* (Volvocales, Chlorophyta). **Archives of Environmental Contamination and Toxicology** 38:147-151.
- Vonshak, A. 1986. Laboratory techniques for the cultivation of microalgae, pp. 117-145. *In* Richmond, A., ed. **CRC handbook of microalgal mass culture**. CRC Press, Florida.

Effect of Mixed Enzyme Produced from Tomato Pomace by *Aspergillus niger* on Meat Quality Attributes of Broiler Chickens

Benya Saenmahayak^{1*}, Chalermpon Yuangklang¹, Smerjai Bureenok¹, Kraisit Vasupen¹ and Sukanya Saithi²

ABSTRACT

The influence of mixed enzyme produced from tomato pomace treated with *Aspergillus niger* (TP) in solid-state fermentation on meat quality of broiler chickens was assessed at 49 days of age. A total of 240 mixed-sex broilers (1-day old) were fed with corn-soybean meal diets with 6 inclusion levels of enzyme supplementation; 0, 0.1, 0.2, 0.3, 0.4, 0.5 and 0.6% TP. The birds were arranged in a Completely Randomized Design (CRD; 4 replicates/treatment and 10 birds/pen). A 2-stage feeding program was provided to each treatment. At the age of 42 days old, birds were processed and chilled in static slush ice. Meat quality attributes (color, cooking loss, drip loss, tenderness and lipid oxidation) were determined on skinless breast fillets (30 fillets/treatment). Results indicated no differences ($P>0.05$) in color, cook loss, drip loss, and lipid oxidation because of dietary treatments. However, adding enzyme on top of the feed at 0.1% TP had increased ($P<0.05$) the tenderness of the meat compared to those fed control diet. The improvement is achieved through the lowest inclusion level of enzyme produced from tomato pomace treated by *Aspergillus niger* on meat tenderness.

Keywords: Solid-state fermentation, By-products, Tomato pomace, Meat quality attributes, Broilers

¹ Department of Agricultural Technology and Environment, Faculty of Sciences and Liberal Arts, Rajamangala University of Technology Isan, Muang, Nakhon Ratchasima, 30000, Thailand

² Department of Food Sciences and Technology, Faculty of Natural Resources, Rajamangala University of Technology Isan, Sakon Nakhon Campus, Phangkhon, Sakon Nakhon, 47160, Thailand

* Corresponding author, e-mail : sbenya@hotmail.com

Introduction

By-products is defined as leftover feedstuffs from agricultural industries. However, large amounts of industrial waste had been released to the environment, and required special treatment to dispose. The use of by-products as animal feedstuffs would reduce environmental pollutions and reduce the cost of feed production. Many of by-products have contained high level of mineral and trace elements. Those may have high potential to use as animal feed (Xu *et al.*, 2007). Feed ingredients for broiler chickens are based on corn-soybean meal. However, the problem always occurs when birds fed those feedstuffs which contain high levels of non-starch polysaccharides, the digesta viscosity increase and nutrient digestibility reduce. Enzymes has been introducing to the broiler diets to improve nutrient digestibility and increase the energy value of diets. The feed enzyme has greatly beneficial to reduce the excretion of those nutrients to the environment (Bedford *et al.*, 2016). To increase value added of those agricultural by-products, solid-state fermentation is one of the inexpensive methods to produce enzyme in which microbial growth and product formation occur on the surfaces of solid substrates. Various agricultural by-products such as tomato pomace is the leftover product from the tomato processing plant in Thailand. Tomato pomace contains various mineral and trace elements which needed for microorganism development. *Aspergillus niger* have been reported to be the main sources of cellulase, hemicellulase, pectinase and xylanase products on the non-starch polysaccharides including cellulose (Hamlyn, 1998). The objective of this study was to evaluate meat quality attributes (color, cooking loss, drip loss, tenderness and lipid oxidation) of broilers fed enzyme supplementation produced from tomato pomace by *Aspergillus niger* at 42 d of age.

Materials and Methods

1. Feed preparation

The tomato pomace was separated and obtained from the processing plant in Northeastern part of Thailand. The pomace was dried until the moisture content reached 40-60%. Then, the pomace was fermented with *Aspergillus niger* (1×10^7 spores/mL) at 30°C for 72 hours. The enzyme activity of mixed enzyme produced from tomato pomace by *Aspergillus niger* is shown in Table 1.

Table 1 Enzyme activity of enzyme produced from tomato pomace by *Aspergillus niger*

Enzyme	Enzyme Activity (Unit/g total substrate dry weight)
Cellulase	123,164.70
Xylanase	469,633.07
Amylase	70,932.62
Proteinase	7,409.85

2. Dietary treatments

A total of 240 (1-day old) mixed-sex broilers were raised in an open-sided, naturally ventilated house with 24 floor pens to 42 day of age, pens bedded with new rice husk (4 pens/diet; 10 birds/pen) using a two-stage feeding program. The starter feed was fed on days 1-21, and the grower feed on days 22-42. Birds were fed *ad libitum* with six dietary treatments from tomato pomace treated by *Aspergillus niger* (TP): 1) Basal diet (control); 2) 0.1% TP; 3) 0.2% TP; 4) 0.3% TP; 5) 0.4% TP, and 6) 0.5% TP. The proximate analysis of tomato pomace were measured dry matter and protein content according to the standard methods of AOAC (1995) (Table 2). Feed were formulated according to NRC (1994) recommendation. All birds were processed at 42 day of age. Breast fillet from 5 birds per pen were randomly selected for

meat quality attributes. Deboned breast fillets (skinless *Pectoralis major* muscle) were individually bagged and stored at 4°C for meat quality measurements.

Table 2 Composition of dried tomato pomace and dried tomato pomace treated by *Aspergillus niger*

Treatments	Dry matter (DM, %)	Crude Protein (% DM)
Dried tomato pomace	93.6	19.9
Dried tomato pomace treated with <i>Aspergillus niger</i>	95.0	24.5

3. Color measurement

The left fillets were measured for color using a Portable Colorimeter (CR-410 Chroma Meter, Konica Minolta). The CIE system color profile of L* a* b* was used to express the lightness, redness, and yellowness values, respectively. The cranial breast area (3 replicates/fillet, 30 fillets/treatment) were selected for color measurement and avoided obvious defects such as bruises and discolorations due to possible over-scalding during processing.

4. Drip loss

Weight of individual right fillets (30 fillets/treatment) were recorded immediately after deboning, placed in plastic bags, stored for 24 h and 48 h at 4°C, and then reweighed. Fillets were lightly blotted before re-weighing. Fillet drip loss (%) was calculated as the difference between deboned and stored fillet weights divided by deboned weight.

5. Cooking loss

The right fillets were weighed and placed on a rack and then baked in an air-convection oven at 177°C to attain an internal temperature of 77°C. After fillets had been removed and cooled to room temperature, the fillets were weighed again and cooking loss was calculated as cooked fillet weight divided by raw fillet weight x 100 (Northcutt et al, 1994).

6. Shear force

The cooked pieces of meat were cut to the size on each breast sample cylindrical metal that measures 1.25 cm in diameter to determine shear force of meat according to Bratcher et al. (2005), (Warner-Bratzler Meat Shear Apparatus/Brookfield Texture Analyzer). This apparatus measures the maximum strength in kg force.

7. Thiobarbituric acid reactive substances (TBARS)

The breast meat samples (10 g) were homogenized with 30 mL of distilled water for 2 min. The homogenate (2 mL) was then mixed with 4 mL of thiobarbituric acid/trichloroacetic reagent and 100 µL of 10% butylated hydroxyanisole in a glass test tube. The mixture was incubated for 15 min in a 100°C water bath, allowed to cool in the cold water and centrifuged at 4,000 rpm for 10 min. The absorbance of the supernatant was then read against a blank containing the same reagents at 531 nm using a spectrophotometer. The TBARS values were calculated from a standard curve of malondialdehyde (MDA) and expressed as mg MDA/kg sample (Buege and Aust, 1978).

8. Statistical Analysis

The data were analyzed by Statistical Analysis System (SPSS). All percentage data was transformed to arcsine values prior to analysis. The Tukey's test was used to compare and separate means when main effects were significant ($P < 0.05$).

Results and Discussion

The effect of mixed enzyme produced from tomato pomace treated by *Aspergillus niger* on meat quality attributes is shown in Table 3. No differences on color (L^* , a^* , b^*), drip loss, cook loss, and lipid oxidation (TBARS) were detected ($P>0.05$) due to dietary treatments in this study. Average pH of the meat was 6.13 (data not shown). The result was in the agreement with the study of Werner et al. (2009) and Zakaria et al. (2010), enzymes supplementation did not affect the different meat quality attributes such as pH, cooking loss, water holding capacity, and color which are mainly affected by the haem concentration and cooking loss. However, tenderness (shear force) of the meat was increased ($P<0.05$) when birds fed 0.1% TP enzyme dietary treatment in the study. There was a numerical trend of improvement in cook loss and TBARS with enzyme supplementation from tomato pomace by *Aspergillus niger* compared to the control diets. On the other hands, according to Omojola and Adesehinwa (2007), the shear force was not significantly different ($P>0.05$) when birds fed exogenous enzyme. Despite the non-significance, indicating that less force was required to shear through the meat as the enzyme level increased. The reason for this effect of TP enzyme dietary treatment on meat tenderness is still unclear and needs further investigation. Tenderness is one of the most important quality attribute affecting meat acceptability. The meat tenderization is a multifactorial process depending on a number of biological and environmental factors (Quali, 1990).

Table 3 The effect of mixed enzyme produced from tomato pomace treated by *Aspergillus niger* on meat quality attributes

Factors	Color			Drip loss (%)		Cook loss (%)	Shear force (kgf)	TBARS (mg MDA/kg of meat)
	L^*	a^*	b^*	24 h	48 h			
	NS ¹	NS	NS	NS	NS	NS	*	NS
Control	63.43	6.51	15.80	0.87	0.65	28.17	2.72 ^a	1.55
0.1%TP	64.75	6.37	14.44	0.96	0.46	22.48	1.89 ^b	0.89
0.2%TP	63.23	6.80	14.67	0.73	0.51	25.69	2.54 ^a	1.41
0.3%TP	62.14	6.42	15.14	0.68	0.54	24.08	2.33 ^{ab}	0.99
0.4%TP	62.31	6.54	14.51	1.58	0.74	26.93	2.43 ^a	1.01
0.5%TP	62.24	6.22	12.29	1.01	0.70	23.84	2.43 ^a	1.23
SEM ²	1.343	0.635	0.846	0.344	0.126	2.961	0.126	0.232

¹Not significant ($P>0.05$); ²SEM = Pooled Standard Error of the Mean;

^{abc}Means within a column with difference superscripts differ significantly;

*($P<0.05$)

Conclusion

The application of mixed enzyme produced from tomato pomace by *Aspergillus niger* may affect on meat quality attributes of broiler chickens. The improvement may be achieved through the lowest inclusion level of enzyme (0.1% TP) produced from tomato pomace treated by *Aspergillus niger* on meat tenderness.

Acknowledgement

This study was financially supported by Rajamangala University of Technology Isan, Nakhon Ratchasima, Thailand.

References

- AOAC. 1995. Official methods of analysis, 16th ed. **Association of official analytical chemists**. Washington. D.C.
- Bedford, M. R., Walk, C. L. and Masey O'Neill, H. V. 2016. Assessing measurements in feed enzyme research: Phytase evaluations in broilers. **The Journal of Applied Poultry Research**. 25(2): 305-314.
- Bratcher, C. L., Johnson, D. D., Litell, R. C. and Gwartney, B.L. 2005. The effects of quality grade, aging and location within muscle on Warner-Bratzler shear force in beef muscles of locomotion. **Meat Science**. 70: 279-284.
- Buege, J. A. and Aust, S.D. 1978. Assay of lipid oxidation in muscle samples. **Methods in Enzymology**. 54: 305.
- Hamlyn, P.F. 1998. Fungal Biotechnology. **British Mycological Society Newsletter**. ISSN 1465-8054.
- National Research Council (NRC). 1994. **Nutrient requirements of poultry**, 9th ed. National Academic Science. Washington, D.C.
- Northcutt, J. K., Foegeding, E. A. and Edens, F. W. 1994. Water-holding properties of thermally preconditioned chicken breast and leg meat. **Poultry Science**. 73: 308-316.
- Omojola, A. B. and Adeschinwa, A.O. K. 2007. Performance and carcass characteristics of broiler chickens fed diets supplemented with graded levels of Roxazyme G®. **International Journal of Poultry Science**. 6(5): 335-339.
- Quali, A. 1990. Post-mortem Changes in Muscles Tissue. **Journal of Muscles Foods**. 1: 129-134.
- Werner, C., Janisch, S., Kumbet, U. and Wicke, M. 2009. Comparative study of the quality of broiler and Turkey meat. **British Poultry Science**. 50: 318-324.
- Xu, C., Cai, Y., Moriya, N. and Ogawa, M. 2007. Nutritive value for ruminants of green tea grounds as a replacement of brewers' grains in totally mixed ration silage. **Animal Feed Science and Technology**. 138: 228-238.
- Zakaria, H. A. H., Jalal, M. A. R. and Ishmais, M. A. A. 2010. The influence of supplemental multi-enzyme feed additive on the performance, carcass characteristics and meat quality traits of broiler chickens. **International Journal of Poultry Science**. 9(2): 126-133.

Isolation and Screening of Acetic Acid Producing Microorganisms from Fruits in the Northeastern Region (Isan) of Thailand

Nittaya Pitiwittayakul^{1*}, Yaowapa Kwamman¹ and Smerjai Bureenok¹

ABSTRACT

Acetic acid bacteria are Gram negative aerobic bacteria capable of oxidizing ethanol to acetic acid. They are used in the industrial production of vinegar. Moreover, this group of bacteria is also used in cellulose production. The aim of this study was to isolate acetic acid bacteria from several kinds of local rotten fruits in Nakhon-Ratchasima province, the northeastern region of Thailand. Glucose Ethanol Yeast extract (GEY) broth supplemented with 5% ethanol was used as an enrichment medium. Sixteen isolates were obtained from 10 varieties of fruits; Rambelh, Java plum, Monkey jack, Mulberry, Korlan, Gold apple, Cashew nut, *Flacourtia indica* (Burn.f.) Merr and *Polyalthia cerasoides* (Roxb.) Benth. ex Bedd. All isolates are capable of producing acetic acid as show the halo zone on the selective Glucose/ Ethanol/ Calcium carbonate Agar (GECA) medium containing 5% ethanol. Eleven isolates were obtained when incubated at 37°C and five isolates were obtained when incubated at room temperature. All isolates are Gram negative and microscopic observation of the strains showed rod small round shape. In addition, one isolate obtained from cashew nut could produce cellulose.

Keywords: Acetic acid bacteria, Cellulose production, Local rotten fruits, Vinegar

¹ Department of Agricultural Technology and Environment, Faculty of Sciences and Liberal Arts, Rajamangala University of Technology Isan, Nakhon Ratchasima campus, Nakhon Ratchasima 30000, Thailand

* Corresponding author, e-mail : pitiwittayakul_n@hotmail.com

Introduction

Acetic acid bacteria (AAB) belong to the family *Acetobacteraceae* of the *Alphaproteobacteria* (De Ley *et al.*, 1984; Sievers *et al.*, 1994). They are obligate aerobic Gram-negative bacteria, which are commonly widespread in nature such as fruit, flower, honey, sugarcane, fruit juice, soil and water (Maal and Shafiee, 2010; Sharafi *et al.*, 2010). AAB are important microorganisms in food industry because of their ability to oxidize many types of sugars and alcohols to organic acids as end products during fermentation process. Therefore, these AAB are widely applied for vinegar production. Furthermore, these bacteria can produce some polysaccharides such as cellulose, apart from acetic acid (Hibbert and Barsha, 1931). Thailand is a tropical country with a large biodiversity of fruits and microbial resources. This is a good source for isolation of acetic acid bacteria. This research, we aimed to isolate AAB from local rotten fruits in Nakhon-Ratchasima province, the northeastern region of Thailand.

Materials and Methods

Sample collection and isolation of AAB: Different rotten fruits (Rambelh, Java plum, Monkey jack, Mulberry, Korlan (*Nephelium hypoleucum*), Gold apple (*Diospyros decandra* Lour.), Cashew nut (*Anacardium occidentale* L.), *Flacourtia indica* (Burn.f.) Merr, *Polyalthia cerasoides* (Roxb.) Benth. ex Bedd.) were collected from several local places in Northeastern region of Thailand for isolation of acetic acid producing microorganisms. Some pieces of rotten fruits were submerged in Glucose Ethanol Yeast Extract (GEY) broth containing 5% ethanol and incubated at room temperature or 37°C for 7-10 days. Afterwards, the samples were streak-plated on Glucose Ethanol Calcium carbonate Agar (GECA) media containing 5% ethanol and incubated at room temperature or 37°C for 2-3 days. This selective media normally shows halo zone around organism's colony if the organism is capable of producing acetic acid. Suspected acetic acid bacteria isolated from selective medium were further identified by morphological characters of colonies. Gram staining was performed.

Results and Discussion

AAB were successfully isolated from several kinds of local rotten fruits (Figure 1). All colonies were screened on the basis of their morphological and cultural properties.



Figure 1 Several local rotten fruit samples were collected at Nakhon-Ratchasima for isolating acetic acid bacteria for vinegar and cellulose production

All sixteen isolates were primarily screened and detected as AAB because they produced halos zone around their colonies in the selective GECA medium. As incubation condition at 37°C, four isolates were obtained from Rambelh. Three isolates were obtained from Lakoocha or Monkey jack. Each one isolate was obtained from these local fruits; Java Plum, Mulberry, Korlan and gold apple. In case of incubation condition at room temperature, two isolates were obtained from *Flacourtia indica* (Burn. f.) Merr. Each one isolate was obtained from different local fruits as follows: *Polyalthia cerasoides* (Roxb.) Benth. ex Bedd, *Oxyceros horridus* and cashew nut. (Table 1). All isolates are Gram negative and showed rod small round shape. Klawpiyapamornkun *et al.* (2015) obtained ninety-nine isolates of AAB from various kinds of fruits and fermented fruit juices from the northern and eastern areas in Thailand. Diba *et al.* (2015) also screened and isolated AAB from various decomposed fruit available in Bangladeshi local markets. They have successfully isolated 15 Gram negative bacterial acetic acid producing bacteria. In addition, we found that one isolates from cashew nut is able to produce bacterial cellulose (Figure 2). According to Neera *et al.* (2015), cellulose producing bacteria were isolated from fruit samples such as apple, mango, banana, orange, watermelon and kombucha tea. Six bacterial strains showing cellulose production were identified as *Komagataeibacter xylinus*, *K. oxydans*, *Acetobacter orientalis* and *K. intermedius*. Two hundred and four strains of biocellulose (BC)-producing AAB were isolated from 48 rotten tropical fruits collected in Thailand (Suwanposri *et al.*, 2013). The results supported that tropical fruits collected in Thailand are a rich source of bacterial cellulose producers.

Table 1 Acetic acid bacterial strains isolated from fruit samples

Source	Isolation temperature	Total of isolates
Rambelh (<i>Baccaurea ramiflora</i>)	37°C	4
Java Plum (<i>Syzygium cumini</i>)	37°C	1
Lakoocha or Monkey jack (<i>Artocarpus lacucha</i>)	37°C	3
Mulberry (<i>Morus alba</i> Linn.)	37°C	1
Korlan (<i>Nephelium hypoleucum</i>)	37°C	1
Gold apple (<i>Diospyros decandra</i> Lour.)	37°C	1
Cashew nut (<i>Anacardium occidentale</i> L.)	Room temperature	1
<i>Flacourtia indica</i> (Burn. f.) Merr	Room temperature	2
<i>Polyalthia cerasoides</i> (Roxb.) Benth. ex Bedd	Room temperature	1
<i>Oxyceros horridus</i>	Room temperature	1

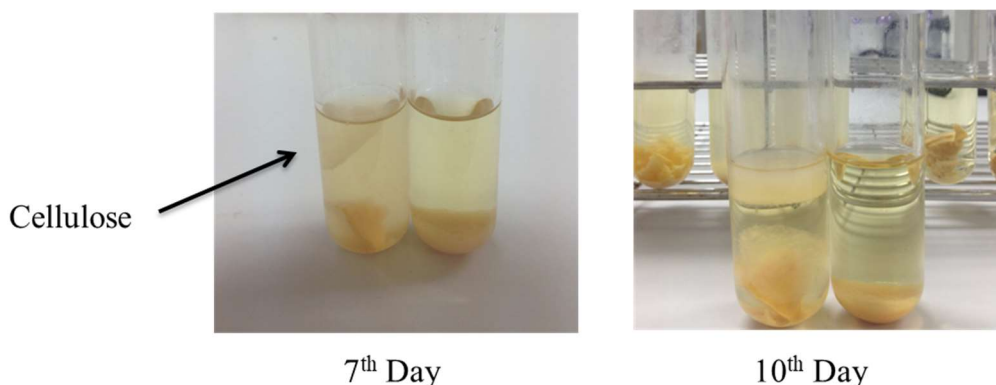


Figure 2 Cellulose producing acetic acid bacteria isolated from cashew nut

The further study is required to use genomic methods such as 16S rRNA sequencing in combination with phenotypic and chemotaxonomic test for AAB identification. Moreover, characterization of acetic acid production and cellulose production will be performed.

Conclusion

This present study also showed that AAB are associated with various kinds of local fruit which supported the view that local fruits are also good source for AAB isolation.

Acknowledgement

This work was financially supported by Rajamangala University of Technology Isan.

References

- De Ley, J., Gillis, M. and Swings, J. 1984. Family VI. *Acetobacteraceae*, pp. 267-278. In Krieg, N.R., Holt, J.G., eds. 1th Ed. **Bergey's Manual of Systematic Bacteriology**, Vol. 1. Baltimore, Maryland: Williams and Wilkins Co.
- Diba, F., Alam, F., and Talukder, A.A. 2015. Screening of acetic acid producing microorganisms from decomposed fruits for vinegar production. **Advances in Microbiology** 5: 291-297.
- Hibbert, H. and Barsha, J. 1931. Structure of the cellulose synthesized by the action of *Acetobacter xylinus* on glucose. **Canadian Journal of Research** 5: 580-591.
- Klawpiyapamornkun, T., Bovonsombut, S. and Bovonsombut, S. 2015. Isolation and characterization of acetic acid bacteria from fruits and fermented fruit juices for vinegar production. **Food and Applied Bioscience Journal** 3(1): 30-38.
- Maal, K.B. and Shafiee, R. 2010. Isolation and characterization of an *Acetobacter* strain from Iranian white-red cherry as a potential strain for cherry vinegar production in microbial biotechnology. **Asian Journal of Biotechnology** 2(1): 53-59.
- Neera, Ramana, K.V. and Batra, H.V. 2015. Occurrence of Cellulose-Producing *Gluconacetobacter* spp. in Fruit Samples and Kombucha Tea, and Production of the Biopolymer. **Applied Biochemistry and Biotechnology** 176(4): 1162-1173.
- Sharafi, S.M., Rasooli, I. and Beheshti-Maal, K. 2010. Isolation, characterization and optimization of indigenous acetic acid bacteria and evaluation of their preservation methods. **Iranian Journal of Microbiology** 2(1): 41-48.
- Sievers, M., Ludwig, W. and Teuber, M. 1994. Phylogenetic positioning of *Acetobacter*,

Gluconobacter, *Rhodopila* and *Acidiphilium* species as a branch of acidophilic bacteria in the α -subclass of *Proteobacteria* based on 16S ribosomal DNA sequences. **Systematic and Applied Microbiology** 17: 189-196.

Suwanposri, A., Yukphan, P., Yamada, Y. and Ochaikul, D. 2013. Identification and biocellulose production of *Gluconacetobacter* strains isolated from tropical fruits in Thailand. **Maejo International Journal of Science and Technology** 7(1): 70-82.